ACTA CHIMICA

ACADEMIAE SCIENTIARUM HUNGARICAE

ADIUVANTIBUS

V. BRUCKNER, GY. DEÁK, K. POLINSZKY,
E. PUNGOR, G. SCHAY, Z. G. SZABÓ

REDIGIT

B. LENGYEL

TOMUS 85 FASCICULUS 1

AKADÉMIAI KIADÓ, BUDAPEST

1975

ACTA CHIM. (BUDAPEST) ACASA 2 85 (1) 1–124 (1975)

ACTA CHIMICA

A MAGYAR TUDOMÁNYOS AKADÉMIA KÉMIAI TUDOMÁNYOK OSZTÁLYÁNAK IDEGEN NYELVŰ KÖZLEMÉNYEI

SZERKESZTI

LENGYEL BÉLA

TECHNIKAI SZERKESZTŐK

DEÁK GYULA és HARASZTHY-PAPP MELINDA

Az Acta Chimica német, angol, francia és orosz nyelven közöl értekezéseket a kémiai tudományok köréből.

Az Acta Chimica változó terjedelmű füzetekben jelenik meg, egy-egy kötet négy füzetből áll. Évente átlag négy kötet jelenik meg.

A közlésre szánt kéziratok a szerkesztőség címére (Budapest 112/91 Műegyetem) küldendők.

Ugyanerre a címre küldendő minden szerkesztőségi levelezés. A szerkesztőség kéziratokat nem ad vissza.

Megrendelhető a belföld számára az „Akadémiai Kiadó"-nál (1363 Budapest Pf 24. Bankszámla 215 11488), a külföld számára pedig a „Kultúra" Könyv- és Hírlap Külkereskedelmi Vállalatnál (1389 Budapest 62, P.O.B. 149 Bankszámla: 218 10990) vagy annak külföldi képviseleteinél és bizományosainál.

Die Acta Chimica veröffentlichen Abhandlungen aus dem Bereich der chemischen Wissenschaften in deutscher, englischer, französischer und russischer Sprache.

Die Acta Chimica erscheinen in Heften wechselnden Umfanges. Vier Hefte bilden einen Band. Jährlich erscheinen 4 Bände.

Die zur Veröffentlichung bestimmten Manuskripte sind an folgende Adresse zu senden

Acta Chimica
Budapest 112/91 Műegyetem

An die gleiche Anschrift ist auch jede für die Redaktion bestimmte Korrespondenz zu richten. Abonnementspreis pro Band: $ 32.00.

Bestellbar bei dem Buch- und Zeitungs-Außenhandels-Unternehmen »*Kultúra*« (1389 Budapest 62, P.O.B. 149 Bankkonto Nr. 218 10990) oder bei seinen Auslandsvertretungen und Kommissionären.

ACTA CHIMICA

ACADEMIAE SCIENTIARUM HUNGARICAE

ADIUVANTIBUS

V. BRUCKNER, GY. DEÁK, K. POLINSZKY,
E. PUNGOR, G. SCHAY, Z. G. SZABÓ

REDIGIT

B. LENGYEL

TOMUS 85

AKADÉMIAI KIADÓ, BUDAPEST

1975

ACTA CHIM. (BUDAPEST)

ACTA CHIMICA

TOMUS 85

FASCICULUS 1: 1975
FASCICULUS 2: 1975
FASCICULUS 3: 1975
FASCICULUS 4: 1975

INDEX

ABD-ALLAH, M. M. s. SAMMOUR, A.
ACKERMANN, G., LÖWE, W., KADEN, W.: Anwendungsmöglichkeiten der Remissionsphotometrie in der quantitativen Analyse (On the Possible Applications of Remission Photometry in Quantitative Analysis) 1
AFIFY, A. A. s. SAMMOUR, A.
AGARWAL, S. K., TANDON, J. P.: Schiff Base Derivatives of Lanthanons. Synthesis of Polymeric Derivatives of La(III), Pr(III) and Nd(III) from the Schiff Bases Derived from the Condenzation of Benzaldehyde with Hydroxy Alkylmines or Hydroxy Arylmines 71
AHMAD, N. s. FAROOQ, O.
AMERIA, R. L. s. KHADIKAR, P. V.
ANANTHAKRISHNAN, T. R., ARULDHAS, G.: Parametric Approach to theAnalysis of Infrared Intensities 269
ARULDHAS, G. s. ANANTHAKRISHNAN, T. R.
BAJUSZ, S. s. TURÁN A.
BAKÓ, P. s. FENICHEL, L.
BARCZA, L. s. PAÁL, T.
BARTÓK, M. and FELFÖLDI, K.: Study of the Transformation of Diols and Cyclic Ethers, XXXVII. Isomerization of Oxetanes to Unsaturated Alcohols on GC Columns 339
BASYOUNI, M. N. s. OMAR, M. T.
BENES, J. s. MEZŐ, I.
BOKSAY, Z., BOUQUET, G. and BUSHUEVA, I. M.: Variation of the Composition of Glasses Under the Effect of Molten Salts 439
BOUQUET, G. s. BOKSAY, Z.
BULACOVSCHI, V. and SIMIONESCU, CR.: Copolymerization of 3-Methyl-1-pentyn-3-ol with *p*-Diethynylbenzene 221
BUSHUEVA, I. M. s. BOKSAY, Z.
CSER, F., PÁRKÁNY, L., HENCSEI, P.: Lattice Dynamics Study of Crystalline Tetraphenylsilane 289
CSŰRÖS, Z. s. FENICHEL, L.
CZIRA, G. s. POZSGAY, V.
DEÁK, GY. s. FENICHEL, L.
DÖRING, C. E., STEVENZ, D., GEYER, R. und HÖPFNER, J.: Bsetimmung von Ameisensäure und ihren Derivaten mittels Reaktions-Gaschromatographie (Determination of of Traces of Formic Acid by Reaction Gas Chromatography) 47
EL-FEYEY, S. A. s. FARAH, M. Y.
FARAH, M. Y. and EL-FEKEY, S. A.: Studies on the Calcination of Ammonium Uranate with Special Reference to Surface Area 385
FAROOQ, O. and MALIK, A.: Interaction of Transition Metals with Some Alkaloids, Metal Complexes of Quinaldine, Quinine, Brucine and Codeine 391
FAROOQ, O. and AHMAD, N.: Metal–Amino Acid Interaction, II. A Study of the Complex Compounds of Trivalent Rare Earths with Glutamic Acid 397
FELFÖLDI, K. s. BARTÓK, M.

FENICHEL, L., DEÁK, GY., HOLLY, S., BAKÓ, P. and CSŰRÖS, Z.: Preparation and Investigation of Lewis Acid Complexes, X. Investigation of the Titanium Tetrachloride and Ethoxytitanium Trichloride Complexes of Triacetyllevoglucosan 299
FENICHEL, L., DEÁK, GY., BAKÓ, P., HOLLY, S. and CSŰRÖS, Z.: Preparation and Investigation of Lewis Acid Complexes, XI. Investigation of the Mechanism of the Ring Cleavage Reaction of Tryacetyllevoglucosan 313
FÖLDIÁK, G. s. HORVÁTH, ZS.
FÜLÖP, J. s. POLINSZKY, K.
GAÁL, J. and INCZÉDY, J.: Investigations on Metal Complexes Containing Optically Active Ligands, I. Complexes of D: and L-threo-1-(*p*-nitrophenyl) 2-amino-propanediol-1,3 Formed with Palladium(II)-ions 261
GEYER, R. s. DÖRING, C. E.
GERGELY, A. s. SÓVÁGÓ, I.
GHANDOUR, M. A. s. ISSA, I. M.
HABERLANDT, R. s. SCHMIDT, R.
HAMMAN, A. M. s. ISSA, I. M.
HAMMOUDA, F. M. s. RIZK, A. M.
HANKOVSZKY, O. H., HIDEG, K., POLGÁR, K. and LLOYD, D.: Reaction of α,β-Unsaturated Ketones with bis-Nucleophilic Reactants. Further Studies with Polyolefinic ($\alpha,\beta,\gamma,\delta$-unsaturated) Ketones and β-Heteroaryl (furyl and thienyl) α,β,-Unsaturated Ketones 333
HASSAN, M. K. s. ISSA, I. M.
HAVRÁNEK, M. s. MEZŐ, I.
HENCSEI, P s. CSER, F.
HIDEG, K. s. HANKOVSZKY, O. H.
HOLLY, S. s. FENICHEL, L.
HORVÁTH, ZS. and FÖLDIÁK, G.: Influence of Cyclic Structure on the Radiolysis of Hydrocarbons, III. Radiolysis of Cyclopropane, Cyclobutane and Cyclobutene 777
HÖPFNER, J. s. DÖRING, C. E.
HUNEK, J. s. TETTAMANTI, K.
INCZÉDY, J. s. GAÁL, J.
ISSA, I. M., GHANDOUR, M. A., HASSAN, M. K. and HAMMAN, A. M.: Polarographic Behaviour of Uranyl Ion in Citrate Solutions 447
ISMAIL, S. I. s. RIZK, A. M.
JAIN, P. C. s. SWAMI, M. P.
KADEN, W. s. ACKERMANN, G.
KAMMER, H. s. RÜGER, C.
KAPOSI, O., RIEDEL, M., ROBERTO SÁNCHEZ, G.: Mass-Spectrometric Study of Electron-impact and Heterogeneous Pyrolytic Decomposition of Methyl Bromide 363
KHADIKAR, P. V. and AMERIA, R. L.: Studies on Some 5-Nitrosalicylate Complexes.... 131
KISS, L. and VARSÁNYI, M. L.: Investigation of Anodic Dissolution of Copper in Anhydrous Acetic Acid Solutions, III. The Combined Effect of Chloride and Perchlorate Ions 401
LAKATOS, I. s. PAKSY, L.
LEMPERT-SRÉTER, M., OSZBACH, GY., RUFF, F. and VAJDA, M.: Isobenzpyrylium Salts, V. Polarographic and Spectrophotometric Investigation of Some Hydroxy-Substituted 1-Arylisobenzpyrylium Salts 79
LENGYEL, T.: Investigations on Ion-Exchange Equilibria with Radioactive Tracer Method, XVIII. Determination of the Stability Constant of $Cd_2(OH)_2^{2+}$ with the Acid of Ion Exchange Technique 125
LÉVAY, B. s. NAGY, S.
LLOYS, D. s. HANKOVSZKY, O. H.
LÖWE, W. s. ACKERMANN, G.
MALIK, A. s. FAROOQ, O.
MANCZINGER, J. s. TETTAMANTI, K.
MEZŐ, I., HAVRÁNEK, M., TEPLÁN, I., BENES, J. and TANÁCS, B.: Labelled Amino Acids and Their Derivatives, VI. Preparation of L-Ornithine-[5-^{3}H] and L-Lysine-[6-^{3}H] 201
NAGY, S., LÉVAY, B. and VÉRTES, A.: Investigations on the Correlation Between the Optimum Thickness of Mössbauer-Absorbents and Certain Experimental Parameters 273
OMAR, M. T. and BASYOUNI, M. N.: Cleavage of 2-Thiono-4-oxo-dihydro-5,6-benzo-1,3-thiazones with Amines 89
OSZBACH, GY. s. LEMPERT, K.

PAÁL, T. and BARCZA, L.: The Formation of Ethylene Glycol–Borates in Aqueous Medium, I 139
PADMAKAR, V., KHADIKAR, RAMESHANDRA L. AMERIA: Studies on Some 5-Nitrosalycylate Complexes 139
PÁRKÁNY, L. s. CSER, F
PAKSY, L. and LAKATOS, I.: Effect of the Axial Injection of Argon on an Analytical Light Source, II. Comparative Study of Self-Absorption 233
PAKSY, L. and LAKATOS, I.: Effect of the Axial Injection of Argon on an Analytical Light-Source, III. Variation of Self-Absorption in the Electrode Space and with the Gas Rate and Concentration 249
PATHY, A. s. TURÁN, A.
POLGÁR, K. s. HANKOVSZKY, O. H.
POLINSZKY, K., FÜLÖP, J., SEITZ, K. and VAJDA, T.: Approximate Analytical Determination of the Average Values of Potential Functions Occurring in Chemical Transport Phenomena 161
POSTA, J. s. SÓVÁGÓ, I.
POZSGAY, V., TAMÁS, J. and CZIRA, G.: The Structure of Cogomycin, a Polyene Antibiotic (Short Communication) 215
RAMESHCHANDRA, L. AMERIA s. PADMAKAR, V. K.
RANA, V. B. s. SWAMI, M. P.
Recensiones 117
RIEDEL, M. s. KAPOSI, O.
RIZK, A. M., HAMMOUDA, F. M. and ISMAIL, S. I.: Phytochemical Investigation of Thymelea Hirsuta, III. Coumarins 107
ROBERTO SANCHEZ, G. s. KAPOSI, O.
RODER, M.: Radiolysis of Cyclohexane–Hexamethylbenzene Mixtures, I. Pure Substances 55
RUFF, F. s. LEMPERT, K.
RULDHAS, G. s. ANANTHAKRISHNAN, T. R.
RÜGER, C., SCHWETLICK, K. and KAMMER, H.: Thermodynamische Berechnung von Reaktionsgleichgewichten aliphatischer Stickstoffverbindungen (Thermodynamic Computation of Reaction Equilibria of Aliphatic Nitrogen Compounds) 349
RYTTER, E.: On the Classification of Normal Modes of Vibration, II. The Interaction Terms in Energy Distributions 147
SAHNI, S. K. s. SWAMI, M. P.
SAMMOUR, A., AFIFY, A. A., ADB-ALLAH, M. M., SOLIMAN, E. A.: Michael Reaction with β-*p*-Toluoyl- and *p*-Chlorobenzoyl-acrylic Acids and their Amides 457
SEITZ, K. s. POLINSZKY, K.
SIMIONESCU, CR. s. BULACOVSCHI, V.
SOLIMAN, E. A. s. SAMMOUR, A.
SÓVÁGÓ, I., GERGELY, A. and POSTA, J.: Equilibria of Alfa-aminoacid Complexes of Transition Metal Ions, VII. Effect of the Aliphatic Carbon Chain on the Thermodynamics and Structure of Ni(II)-aminoacid Complexes 153
SRIVASTAVA, A. K. s. SWAMI, M. P.
STEVENZ, D. s. DÖRING, C. E.
STILLER, W. s. SCHMIDT, R.
STOMFAI, R. s. TETTAMANTI, K.
SWAMI, M. P., JAIN, P. C., RANA, V. B., SAHNI, S. K. and SRIVASTAVA, A. K.: *o*-Hydroxy--4-benzamidothiosemicarbazide as a Chelating Reagent, IV. Magnetospectral Studies on its Ti(III), V(IV), Fe(II), Pd(II), Ce(III) and U(VI) Complexes 411
SCHMIDT, R., STILLER, W. and HABERLANDT, R.: Collision-Kinetic Calculation of Reaction Rate Coefficients of Ion-Molecule Reactions, I. 63
SCHWETLICK, K. s. RÜGER, C.
SZABÓ, V. and ZSUGA, M.: Cleavage of the Heterocyclic Ring of Isoflavonoids by Nucleophilic Reagents, I. Kinetics Equilibrium Conditions of the Cleavage of the Pyrone Ring of Isoflavone (3-Phenylchromone) in Aqueous Alkaline Medium 179
SZABÓ, V. and ZSUGA, M.: Cleavage of the Heterocyclic Ring of Isoflavonoids by Nucleophilic Reagents, II. Transformations of 2-Hydroxyisoflavonone 191
SZABÓ, Z. L.: Some Chemical Reaction of the Electrode Gap and Their Role in Spectrochemical Analysis, XXII. Role of the Chemical Reactivity of the Material of the Metal Electrodes 13
SZAMMER, J.: Thermal Transcarboxylation Reactions, V. Study of the Relative Reactivities of the Aromatic Hydrogen in the Thermal Transformation of Potassium Benzoate 97

Tamás, J. s. Pozsgay, V.
Tanács, B. s. Mező, I.
Tandon, J. P. s. Agarwall, S. K.
Teplán, I. s. Mező, I.
Tettamanti, K., Manczinger, J., Hunek, J. and Stomfai, R.: Calculation of Countercurrent Solid–Liquid Extraction 27
Turán, A., Pathy, A. and Bajusz, S.: Removal of the Nitro Group from Nitroarginine and Nitroarginine Peptides 327
Vajda, M. s. Lempert, K.
Vajda, T. s. Polinszky, K.
Varsányi, M. L. s. Kiss, L.
Vértes, A. s. Nagy, S.
Zsuga, M. s. Szabó, V.

Acta Chimica Academiae Scientiarum Hungaricae, Tomus 85 (1), pp. 1–12 (1975)

ANWENDUNGSMÖGLICHKEITEN DER REMISSIONS-PHOTOMETRIE IN DER QUANTITATIVEN ANALYSE

G. ACKERMANN, W. LÖWE [1] und W. KADEN [2]

(Bergakademie Freiberg, Sektion Chemie—Lehrstuhl für Analytische Chemie Freiberg (Sachs.), Deutsche Demokratische Republik

Eingegangen am 17. Mai 1974

Nach einigen prinzipiellen Erörterungen über die Anwendbarkeit der Remissionsphotometrie in der quantitativen Analyse wird über einige spezielle Möglichkeiten berichtet. Unter Verwendung geeigneter Trägermaterialien läßt sich die Menge eines gebildeten Niederschlags remissionsphotometrisch erfassen. Dieses Prinzip ist für die Bestimmung der Zusammensetzung schwerlöslicher Komplexverbindungen ebenso geeignet wie für die indirekte quantitative Analyse. Weiter wird gezeigt, daß Spurenbestandteile nach deren Anreicherung mittels farbloser oder schwach gefärbter Harzaustauscher und Umsetzung mit einem geeigneten Komplexbildner direkt quantitativ erfaßt werden können. Auch in Verbindung mit Kollektorfällungen lassen sich remissionsphotometrische Verfahren einsetzen.

Einleitung

Die Anwendung remissionsphotometrischer Messungen in der quantitativen Analyse hat besonders im Zusammenhang mit der Auswertung von Papier- und Dünnschichtchromatogrammen in den letzten Jahren steigende Bedeutung erlangt. Da die Isolierung der schichtchromatographisch getrennten Substanzen meist sehr aufwendig ist, werden die *in situ*-Methoden bevorzugt, obwohl sie mit relativ großen Meßfehlern behaftet sind [3].

Es hat deshalb nicht an Versuchen gefehlt, die Präzision durch eine geeignete Arbeitstechnik zu erhöhen. Ein besonders zweckmäßiger Weg, der allerdings keine reine *in situ*-Technik mehr darstellt, wurde von FREI und Mitarb. [4, 5, 6] empfohlen. Er besteht darin, daß man den farbigen Substanzfleck einschließlich Trägermaterial von der Dünnschichtplatte abkratzt, mit weißem Träger auf eine definierte Masse auffüllt und dann die Remission mißt. Im Zusammenhang mit einer eingehenden Untersuchung und Weiterentwicklung dieses Verfahrens ergab sich die Frage, in welchem Umfange remissionsphotometrische Messungen außerdem noch für die quantitative Analyse einsetzbar sind.

Prinzipiell kann man überall dort quantitativ-analytische Aussagen aus Remissionsmeßwerten ableiten, wo es gelingt, eine farbige Substanz aus einer Lösung auf einer definierten Menge eines geeigneten — in der Regel weißen — Trägermaterials abzuscheiden. Diese Arbeitsweise hat KORTÜM [7] als Ver-

dünnungsmethode bezeichnet. Der Autor benutzte das Verfahren besonders zum Studium der Wechselwirkung zwischen Sorbens und Sorbat.

Arbeitstechnik

Das mit dem zu bestimmenden Stoff in der Lösung beladene Trägermaterial wird in geeigneter Weise (z. B. durch Filtration, durch Zentrifugieren, aber auch durch Verdampfen der Reaktionslösung) abgetrennt und getrocknet. Dem Trockenprozeß ist dabei besondere Aufmerksamkeit zu schenken, da sowohl die Lage des Extinktionsmaximums wie auch der Extinktionskoeffizient durch die Trockenbedingungen deutlich beeinflußt werden können [1, 8]. Von dem so erhaltenen Pulver wird nach dem Homogenisieren in einem Achatmörser in üblicher Weise die Remission bestimmt.

Die Ergebnisse, über die hier berichtet werden soll, wurden mit dem Universalspektralphotometer VSU 2 bzw. dem Spektralkolorimeter »Spekol« des VEB Carl Zeiss, Jena, unter Verwendung der entsprechenden Remissionsansätze erhalten.

Wie KORTÜM [9] ausführlich dargelegt hat, genügt es bei der Remissionsphotometrie nicht, die Messungen auf eine Vergleichsprobe (z. B. das reine Trägermaterial) zu beziehen. Man muß vielmehr einen Weiß-Standard mit bekannten optischen Eigenschaften verwenden, m. a. W. man muß zur Berechnung der KUBELKA—MUNK-Funktion $F(R_\infty)$ anstelle des relativen Remissionsgrades R'_∞ dessen Absolutwert R_∞ einsetzen.

Trägermaterial

Die Fixierung des zu bestimmenden Stoffes auf dem Trägermaterial erfolgt durch Adsorption, durch Ionenaustausch, durch Mischkristallbildung usw. In jedem Falle wird man das Sorbens so auswählen, daß es neben einem guten Haftvermögen für den interessierenden Stoff eine möglichst hohe Remission aufweist, d. h. man wird weißen Substanzen den Vorzug geben.

In Abb. 1 sind die Remissionsspektren einiger Trägermaterialien im Vergleich zu Magnesiumoxid dargestellt. Besonders fällt dabei die hohe Remission des Calciumfluorids (Hersteller VEB Fluorwerk Dohna) auf. Da man prinzipiell auch im ultravioletten Spektralbereich messen kann, ist in Abb. 2 auch noch das Verhalten der Träger im Bereich zwischen 250 und 400 nm dargestellt. Man erkennt, daß mit Ausnahme des Calciumfluorids bei den anderen Sorbentien unterhalb 350 nm eine starke Eigenabsorption auftritt, die natürlich Messungen in diesem Gebiet stark beeinträchtigt.

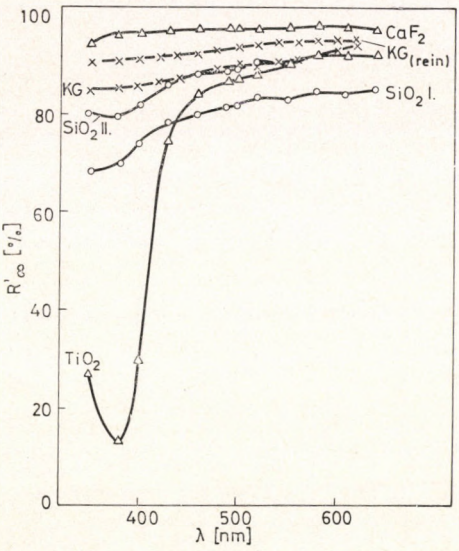

Abb. 1. Remissionsspektren von Trägermaterialien. Standard: MgO. KG (rein): gereinigtes Kieselgel, KG: ungereinigtes Kieselgel, SiO_2I: Quarzpulver (Korngröße 25÷40 μm), SiO_2II: Quarzpulver (Korngröße 10÷25 μm)

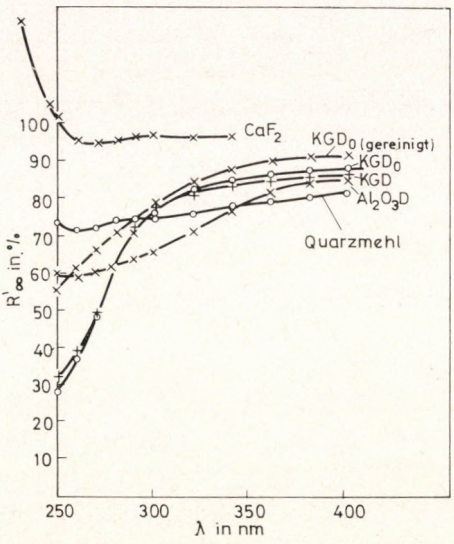

Abb. 2. Remissionsspektren von Trägermaterialien im ultravioletten Spektralbereich Standard: MgO

Weiterhin ist zu beachten, daß die Trägermaterialien ein möglichst enges Korngrößenspektrum aufweisen sollen. Das ist wichtig, um beim Lagern eine Entmischung zu vermeiden, weil der Streukoeffizient und der Anteil der regulären Reflexion von der Korngröße beeinflußt werden.

Erwartungsgemäß übt auch die Teilchengröße des Trägermaterials über die damit zusammenhängende Oberfläche einen signifikanten Einfluß auf die Meßwerte aus.

Wie Tabelle I zeigt, gehen die Remissionswerte mit der Teilchengröße zurück, d. h. man erhält bei Verwendung einer relativ groben Kornfraktion eine steilere Eichkurve. Bei der Auswahl für den praktischen Einsatz ist aller-

Tabelle I

Einfluß der Korngröße auf die Remission

15 μg Nickel-Diacetyldioxim-Komplex je 100 mg Quarzpulver

Korngröße in μm	$F(R_\infty)$
100÷40	0,334
40÷25	0,183
<25	0,113

dings zu berücksichtigen, daß mit der Teilchengröße auch der Anteil der regulären Reflexion zunimmt, daß die Eigenabsorption (vgl. Abb. 1) wächst und daß außerdem beim Homogenisieren des aus der Lösung abgetrennten Feststoffs im Mörser eine merkliche Änderung der Korngröße möglich ist. Als optimal erwiesen sich Pulver mit Korngrößen zwischen 40 und 25 μm.

Anwendungsbeispiele

Im Folgenden sind einige Beispiele für die Anwendung remissionsphotometrischer Methoden zusammengestellt, die die Vielfalt der Möglichkeiten zeigen sollen.

Bestimmung von Nickel mit Diacetyldioxim

Die Bestimmung kleiner Nickelmengen erfolgt in der Regel photometrisch, da die mikro-gravimetrische Methode mit ziemlichem Aufwand verbunden ist. Hier soll gezeigt werden, daß man den abgeschiedenen Komplex auch über eine Remissionsmessung quantitativ auswerten kann.

Arbeitsvorschrift

Zu 5 bis 15 ml der zu untersuchenden Nickellösung werden 250,0 mg Calciumfluoridpulver bzw. 200,0 mg Quarzmehl (Korngröße 40 ÷ 25 μm) gegeben und der Komplex in ammoniakalischem Medium mit Diacetyldioxim gefällt. Die erhaltene Suspension wird mit Hilfe eines Heißluftstroms eingedampft und dann noch 1 Std. an der Luft belassen. Nach dem Homogenisieren im Achatmörser wird die Remission bei 540 nm gemessen.

Bei Vorversuchen ergab sich, daß scharfes Trocknen (Trockenschrank $>$100 °C; Exsikkator über Phosphorpentoxid) zu einer Entfärbung des Niederschlags führt. Nach dem Aufbewahren der Probe an der Luft kehrt jedoch die Rotfärbung des Nickelkomplexes wieder zurück. Um aber definierte Ausgangsbedingungen zu gewährleisten, müssen die oben angeführten milden Trocknungsbedingungen eingehalten werden.

Die Eichkurve verläuft bei Verwendung von Quarzpulver als Träger im Bereich von 0 bis 50 μg und bei Calciumfluorid im Bereich von 0 bis 25 μg geradlinig, wobei deren Anstieg bei Verwendung von CaF_2 wesentlich steiler ist. Die bei der statistischen Auswertung erhaltenen Ergebnisse sind in Tabelle II zusammengestellt.

Man erkennt, daß die Meßfehler bei Verwendung von Calciumfluorid als Träger wesentlich geringer sind. Für dieses Verdünnungsmittel ergab sich als

Tabelle II

Statistische Kenndaten zur Bestimmung von Nickel mit Diacetyldioxim $\lambda = 540$ nm

Träger	Konzentration µg Ni/mg Träger	n	$F(R_\infty)$	v in %
Quarzpulver	40/200	11	0,224	5,09
Calciumfluorid	18/250	11	0,232	3,64

n = Anzahl der Messungen, v = Variationskoeffizient, $F(R_\infty)$ = KUBELKA—MUNK-Funktion

Nachweisgrenze [10] $c = 0{,}093$ µg Ni/250 mg CaF_2. FEIGL [11] gibt als Erfassungsgrenze bei der Tüpfelanalyse 0,16 µg an.

Bestimmung von Germanium mit Phenylfluoron

Bei der üblichen photometrischen Germaniumbestimmung mit Phenylfluoron muß ein Schutzkolloid zugesetzt werden, da der schwerlösliche Metallkomplex nach relativ kurzer Zeit ausflockt. Das führt zu ungenauen Meßwerten. Andererseits konnte festgestellt werden, daß die Remissionswerte über mindestens 5 Tage unverändert blieben.

Arbeitsvorschrift

Zu 5 bis 15 ml der zu untersuchenden Lösung (pH = 1,8), die maximal 15 µg Germanium enthalten kann, gibt man 200,0 mg Kieselgel und 1,5 ml Phenylfluoronlösung (0,05 g Reagens in 75 ml Äthanol und 25 ml konz. Salzsäure gelöst). Die Suspension bleibt 45 min stehen. Dann wird über eine G 4-Glasfritte abgesaugt, mit 6 ml 1 *N* Salzsäure sowie mit 1,5 ml Wasser gewaschen und anschließend im Exsikkator 2 *h* über Calciumchlorid getrocknet. Vor der Messung bei 500 nm wird im Achatmörser homogenisiert.

Tabelle III

Statistische Kenndaten zur Bestimmung von Germanium mit Phenylfluoron $\lambda = 500$ nm

Konzentration µg Ge/100 mg Kieselgel	n	$F(R_\infty)$	v in %
0 (Blindwert)	21	—	—
3,5	11	0,551	5,12

Eine Trocknung bei erhöhter Temperatur ist nicht zu empfehlen, da sich unter diesen Bedingungen die Lage des Absorptionsmaximums irreversibel verlagert.

Die Eichkurve ist unter den genannten Versuchsbedingungen im Bereich 0 bis 15 μg Ge eine Gerade. Die statistischen Kenndaten für die Bestimmung sind in Tabelle III zusammengefaßt.

Die Nachweisgrenze wurde zu $\underline{c} = 0{,}077$ μg Ge/100 mg Kieselgel ermittelt. FEIGL [11] gibt als Erfassungsgrenze für die Tüpfelreaktion 0,13 μg an.

Bestimmungen unter Verwendung eines Ionenaustauschers als Trägermaterial

Ausführliche Untersuchungen über das Remissionsverhalten farbiger Schwermetallkomplexe und über das Methylenblaukation, die an einen Ionenaustauscher gebunden sind, wurden von FUJIMOTO und KORTÜM [12] durchgeführt. Die beiden Wissenschaftler prüften auch die Möglichkeit der quantitativen Auswertung mittels Eichkurve. ERMOLENKO *et al.* [13] berichteten über ein remissionsphotometrisches Verfahren zur Bestimmung von Nickel und von Mangan nach deren Anreicherung mit Hilfe eines Zellulose-Ionenaustauschers. TISCHER [14] konnte zeigen, daß man auch farblose bzw. schwach gefärbte Metallionen, die an einen Harzaustauscher gebunden sind, unter Verwendung geeigneter Reagenzien direkt auf dem Austauscher remissionsphotometrisch bestimmen kann. Da dieser Autor nur die prinzipielle Seite geklärt hat, schien es sinnvoll, diese Frage noch etwas näher zu studieren. Voraussetzung für die remissionsphotometrische Auswertung ist ein möglichst schwach gefärbter Harzaustauscher mit einem hohen Remissionsgrad. Aus der Produktion des VEB Chemiekombinat Bitterfeld eignen sich besonders die Sorten Wofatit KS 10, Wofatit SBK, Wofatit SBW und Wofatit CP für diese Zwecke. Die folgenden Versuche wurden mit Wofatit KS 10 (Korngröße 10÷50 μm) durchgeführt und Nickel(II) als Testkation ausgewählt. Als Reagens diente Rubeanwasserstoff. Um eine gleichmäßige Verteilung der Kationen auf dem Harz zu erreichen, wurde das batch-Verfahren angewandt.

Arbeitsvorschrift

Zu der zu untersuchenden ammoniakalischen Nickelsalz-Lösung gibt man 100,0 mg des lufttrockenen Austauschers (z. B. Wofatit KS 10) und rührt 5 min. Nach dieser Zeit ist das Gleichgewicht eingestellt, der Austauscher kann über eine G 4-Glasfritte abgesaugt und mit einer 0,1%igen Lösung von Rubeanwasserstoffsäure in Äthanol »entwickelt« werden. Das farbige Material wird im Exsikkator getrocknet und anschließend bei 620 nm gemessen.

Abb. 3 ist zu entnehmen, daß die Eigenfärbung des Harzes die Nikkelbestimmung praktisch nicht stört. Der noch vorhandenen geringe Einfluß wird dadurch eliminiert, daß man als Standard metallionenfreien Austauscher verwendet.

Aus den Untersuchungen ergab sich, daß die Eichkurve im Bereich von 0 bis 45 μg Nickel je 100 mg Ionenaustauscher linear verläuft. In Tabelle IV sind die statistischen Kenndaten zusammengestellt.

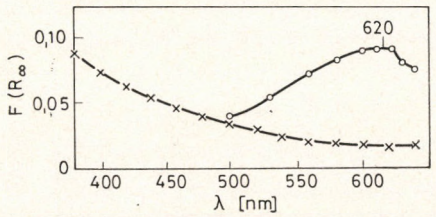

Abb. 3. Remissionsspektren von Wofatit KS 10. x———x Remissionsspektrum des Wofatit KS 10, o———o Remissionsspektrum des Wofatit KS 10 beladen mit Nickel-Rubeanwasserstoff-Komplex

Tabelle IV

Statistische Kenndaten zur Nickelbestimmung nach Anreicherung an einen Harzaustauscher (Wofatit KS 10) $\lambda = 620$ nm

Konzentration μg Ni/100 mg Harz	n	$F(R_\infty)$	v in %
0 (Blindwert)	21	0,050	—
19,5	11	0,310	6,9

Die Nachweisgrenze wurde zu $\underline{c} = 0{,}61$ μg Ni/100 mg Wofatit KS 10 bestimmt.

Tabelle V ist zu entnehmen, daß man das geschilderte Verfahren auch zur Anreicherung und Bestimmung aus hochverdünnten Lösungen anwenden kann.

Tabelle V

Remissionsgrade R'_∞ für 60 μg Ni bei der Anreicherung von Nickelionen mit Hilfe des Austauschers Wofatit KS 10

Konzentration der Ausgangslösung in mol l^{-1}	R'_∞ in %
$1{,}02 \cdot 10^{-4}$	56,5
$1{,}02 \cdot 10^{-5}$	55,7
$5{,}11 \cdot 10^{-6}$	55,9

Bestimmungen nach Anreicherung mittels Kollektoren

Bei Verwendung von Kollektoren für die Anreicherung von Spurenbestandteilen wird man das zu bestimmende Element in der Regel zu dessen Bestimmung vom Sammler abtrennen müssen. Wie gezeigt werden konnte [2, 15], läßt sich jedoch in besonderen Fällen auch hier durch Einsatz der Remissionsphotometrie der Arbeitsaufwand verringern.

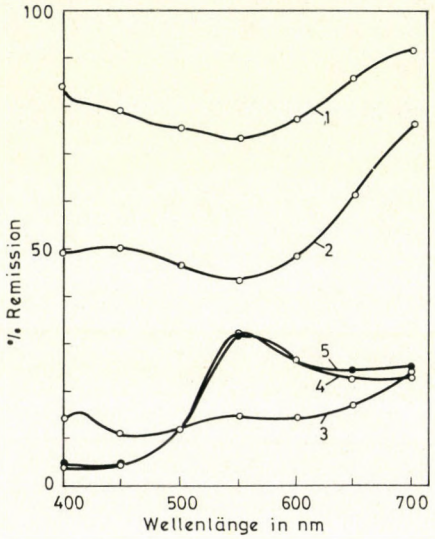

Abb. 4. Remissionsspektren von Tetrathiocyanato-mercurat(II)-Mischkristallen mit $Zn[Hg(SCN)_4]$. Standard: $Zn[Hg(SCN)_4]$, $\lambda = 550$ nm, 1: 0,1 Atom-% Cu, 2: 1,0 Atom-% Cu, 3: 45,0 Atom-% Cu, 4: 90,0 Atom-% Cu, 5: 100,0 Atom-% Cu

Zur Anreicherung von Kupferspuren kann man z. B. dessen Mitfällung mit Zink-tetrahiocyanato-mercurat(II) verwenden, das mit Kupfer violette Mischkristalle bildet, falls der Kupfergehalt in dem gebildeten Niederschlag den des Zinks nicht übersteigt. Bei einem Kupfer–Zink-Verhältnis $>1:1$ tritt dann deutlich die grüne Farbe des Kupfer-tetrathiocyanato-mercurat(II) auf, wie das den Spektren in Abb. 4 zu entnehmen ist.

Obwohl, wie Abb. 5 zeigt, bei den Messungen keine Eichgerade erhalten werden kann, läßt sich das Verfahren doch in einem recht großen Konzentrationsbereich anwenden. Für die Bestimmung von 35 μg Kupfer unter Verwendung von 2,0 g des Zinkkomplexes ergab sich ein Variationskoeffizient von ca. 4%. Die Nachweisgrenze konnte zu 6 μg Cu je 1 g Zink-tetrathiocyanatomercurat(II) ermittelt werden. Die Erfassungsgrenze für den mikrochemischen Nachweis als Kristallfällung wird zu 5 μg angegeben [16].

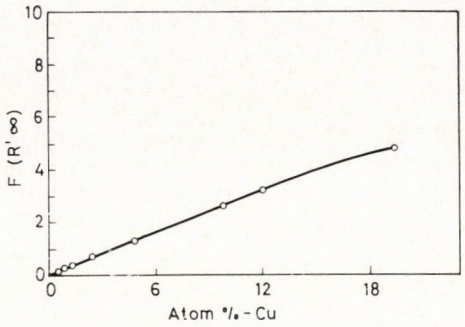

Abb. 5. Eichkurve zur Kupferbestimmung mittels Zink-tetrathiocyanato-mercurat(II) als Kollektor. Standard: $Zn[Hg(SCN)_4]$, $\lambda = 550$ nm

Indirekte Bestimmungen

Wie bei den Transmissionsmethoden kann auch bei Einsatz der Remissionsphotometrie Bestimmungsverfahren anwenden, die auf der stöchiometrischen Umsetzung des zu bestimmenden Ions mit einer farbigen Substanz zu einem farblosen oder andersfarbigen Reaktionsprodukt beruhen.

Man geht dabei zweckmäßigerweise so vor, daß man sich von dem das Reagens enthaltenden Trägermaterial eine größere Menge herstellt und eine definierte Menge davon zur Gewinnung der Eichkurve bzw. zur eigentlichen Messung mit dem zu bestimmenden Ion umsetzt.

Es ist zu sichern, daß das Reagens genügend fest auf dem Trägermaterial haftet und auch beim Filtrieren und Waschen keine nennenswerten Verluste im Hinblick auf die Farbintensität auftreten.

Als Beispiel soll hier eine Methode zur indirekten Bestimmung von Fluorid durch Entfärbung des Zirkonium-Alizarin S-Farblacks angeführt werden.

Arbeitsvorschrift

Das Farblack-Träger-Verhältnis muß der zu bestimmenden Fluoridmenge angepaßt und durch Vorversuche festgelegt werden. Allgemein versetzt man einige Gramm Kieselgel D (mit Salzsäure gewaschen) mit einem passenden Volumen einer 0,5%igen Lösung von Zirkoniumoxidchlorid und dampft zur Trockne ein. Zum Rückstand gibt man einen Überschuß an 1%iger Lösung von Alizarin S, saugt ab und wäscht mit Wasser nach. Das Präparat wird abschließend an der Luft getrocknet.

Bei der Bestimmung wird zur schwach salzsauren, fluoridhaltigen Probelösung eine definierte Menge des Reagens-Träger-Materials (z. B. 300 mg) gegeben und die Suspension genau 4 min gerührt. Anschließend wird über eine G 4-Fritte abgesaugt, mit sehr verdünnter Salzsäure und dann mit dest. Wasser

gewaschen und schließlich über Phosphorpentoxid getrocknet. Die Bestimmung der Remission erfolgt bei 500 nm.

Als Vergleichssubstanz wird ein durch Umsetzung mit überschüssigem Fluorid entfärbtes Kieselgel verwendet.

Auch im vorliegenden Fall darf nicht bei erhöhter Temperatur getrocknet werden, da bei 120 °C eine Verschiebung des Absorptionsmaximums von 500 auf 480 nm beobachtet werden konnte.

Die Auswertung der erhaltenen Meßergebnisse kann man durch Dehnung der Eichkurve verbessern. Dazu setzt man den Remissionsgrad des als Standard verwendeten Trägers gleich 100% ($R_{\infty_{so}}$) und den Remissionsgrad des Reagens-Träger-Gemisches gleich 0% ($R_{\infty_{su}}$). In beiden Fällen muß man die durch Vergleich mit Magnesiumoxid erhaltenen Absolutwerte verwenden (Differentielle Methode).

Zur Aufstellung der Eichkurve und auch bei der Messung an der unbekannten Probe verfährt man so, daß zunächst gegen den entfärbten Träger der Remissionsgrad R_{∞_d} gemessen wird. Daraus berechnet man unter Verwendung von $R_{\infty_{su}}$ den absoluten Remissionsgrad R_{so} nach

$$R_\infty = R_{\infty_d}(1 - R_{\infty_{su}}) + R_{\infty_{su}}.$$

Daraus erhält man die KUBELKA—MUNK-Funktion $F(R_\infty)$ nach

$$F(R_\infty) = \frac{(1 - R_\infty)^2}{2 \cdot R_\infty}.$$

Im vorliegenden Falle lagen die Meßwerte für $R_{\infty_{so}}$ bei 77% $F(R_\infty) = 0{,}034$ und für $R_{\infty_{su}}$ bei 26,9% $F(R_\infty) = 0{,}987$.

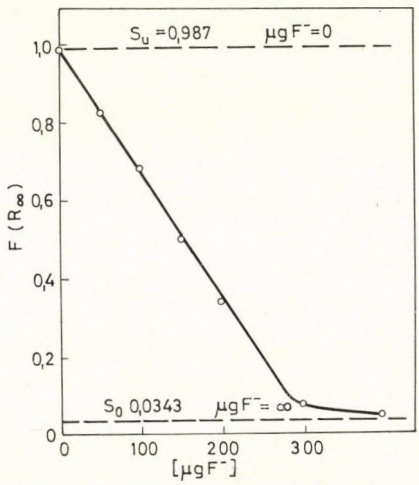

Abb. 6. Eichkurve zur Bestimmung von Fluorid. Reagens: Zirkonium-Alizarin S-Lack, Träger: Kieselgel D, $\lambda = 500$ nm, Standard: Kieselgel D

Abb. 6 zeigt die unter den angegebenen Bedingungen aufgestellte Eichkurve. Man erkennt eine gute Linearität im Bereich von 0 bis ca. 300 μg Fluorid. Für die Bestimmung von 200 μg Fluorid ergab sich ein Variationskoeffizient $v = 4{,}5\%$.

Ermittlung der Komplexzusammensetzung nach der Methode der kontinuierlichen Variation

Die Bestimmung der Zusammensetzung eines schwerlöslichen gefärbten Komplexes nach der Methode von Job [17] ist im Prinzip durch Auswägen des gebildeten Niederschlags möglich [18]. Die Wägung kann man bei Einsatz der Remissionsmethode durch eine photometrische Messung ersetzen und so Fehler, die z. B. bei der Trocknung und der Massebestimmung kleiner Mengen auftreten, ausschalten. Obendrein wird das Verfahren prinzipiell vereinfacht.

Als Modelle sollen hier die Nickelkomplexe mit Diacetyldioxim und mit Rubeanwasserstoff verwendet werden.

Arbeitsvorschrift

Zu einem definierten Volumen einer 10^{-3} *M* Nickelsalzlösung werden 500 mg Calciumfluorid (bzw. 300 mg Kieselgel D) gegeben und dann ein dem Versuchsprogramm entsprechendes Volumen der Reagenslösung zugesetzt. Die Lösung wird mit Hilfe eines Warmluftstroms eingedampft und nach dem Homogenisieren die Remission des Rückstands (für den Diacetyldioximkomplex bei 540 nm, für den Rubeanwasserstoffkomplex bei 610 nm) gemessen.

Die erhaltenen Job-Kurven sind in Abb. 7 wiedergegeben. Man sieht, daß die bekannte Zusammensetzung der beiden Verbindungen eindeutig aus den Diagrammen abgeleitet werden kann.

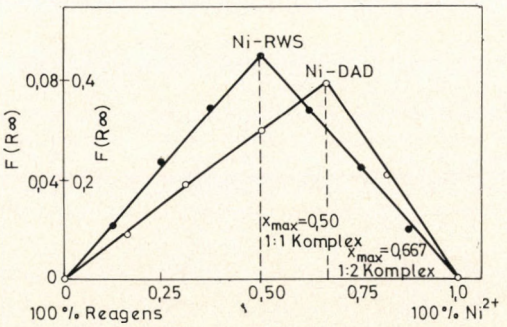

Abb. 7. Job-Kurven für die Nickel-Komplexe mit Diacetyldioxim und mit Rubeanwasserstoff

LITERATUR

[1] Löwe, W.: Dissertation Bergakademie Freiberg 1970
[2] Kaden, W.: Dissertation Bergakademie Freiberg 1970
[3] Ackermann, G., Wiesner, H.-J.: J. Chromatogr. **33** (1968) 53
[4] Frei, R. W., Zeitlin, H.: Analyt. chim. Acta **32** (1965) 32
[5] Frodyma, M. M., Lieu, V. T., Frei, R. W.: J. Chromatogr. 15 (1965) 520
[6] Frei, R. W., Frodyma, M. M.: Analyt. chim. Acta **32** (1965) 501
[7] Kortüm, G., Elkrug, D. O.: Naturwiss. **53** (1966) 600
[8] Ackermann, G., Löwe, W.: J. Chromatogr. **78** (1973) 175
[9] Kortüm, G.: Reflexionsspektroskopie, Berlin 1969
[10] Kaiser, H.: Z. analyt. Chem. **216** (1966) 80
[11] Feigl, F.: Spot tests in inorganic analysis, 5. Aufl. Amsterdam 1958
[12] Fujimoto, M., Kortüm, G.: Ber. Bunsenges. physik. Chem. **68** (1964) 488
[13] Ermolenko, J. N., Longin, M. L., Gavrilov, M. Z.: Ž. analitičeskoj Chim. **17** (1962) 1035
[14] Tischer, W.: Z. Chemie **10** (1970) 156
[15] Ackermann, G., Kaden, W.: Jenaer Rdsch. 14 (1969) 168
[16] Ackermann, G.: Einführung in die qualitative anorganische Halbmikroanalyse 5. Aufl. Leipzig 1968
[17] Job, P.: Ann. Chimie **9** (1928) 113
[18] Asmus, E.: Z. analyt. Chem. 210 (1965) 401

Gerhard Ackermann
Wolfgang Löwe
Werner Kaden

Bergakademie Freiberg, Sektion Chemie — Lehrstuhl für Analytische Chemie, Freiberg (Sachs.), Deutsche Demokratische Republik.

Acta Chimica Academiae Scientiarum Hungaricae, Tomus 85 (1), pp. 13–25 (1975)

SOME CHEMICAL REACTIONS OF THE ELECTRODE GAP AND THEIR ROLE IN SPECTROCHEMICAL ANALYSIS, XXII

ROLE OF THE CHEMICAL REACTIVITY OF THE MATERIAL OF THE METAL ELECTRODES

Z. L. SZABÓ

(Department of Inorganic and Analytical Chemistry, L. Eötvös University, Budapest)

Received March 1, 1974

The evolved heat of reactions proceeding at the electrode surface increases the evaporation of the sample. With more reactive partners this effect is more important. At electrodes connected as anode an oxidation tendency, promoting this reaction, can be observed, while the reduction tendency manifested at the cathode tries to diminish the oxidation reactions. The effect of the heat of oxidation depends also on the volatility properties of the metal electrodes.

In the first parts of our communication series, experiments were reported in which cylindrical aluminium electrodes with larger mass were connected against the carbon counter-electrodes [1, 2]. During the burning of the arc, the aluminium electrodes were rotated helically to reduce thereby the warming up of the sample and the arcing-off effects, and to facilitate the investigation of the phenomena studied. It has been found in these experiments that the behaviour of aluminium in the arc is greatly controlled by its high chemical reactivity. On the other hand, experiments with copper counter-electrode [3, 4] gave some information on the behaviour of this chemically less active metal in the arc. These results called our attention to the fact that the role of the substance of the metal electrodes ought to be investigated more extensively. Therefore, experiments were carried out with five kinds of electrode materials, which in the order of increasing reactivity were as follows: silver, copper, iron, aluminium and magnesium.

Our earlier results were obtained on one hand by changing the intensities and the intensity ratios of the spectral lines under changing some of the parameters of the a.c. polarized arc, primarily the current strength and the polarity of the electrodes. However, it is well known that line intensities and intensity ratios depend also on several other conditions, such as e.g. the thermal and excitation characteristics of the electrode material, the gas atmosphere used, etc. Until the role of these factors has not been cleared, at least partly, in our earlier communications, results discussed now could not be evaluated satisfactorily. Therefore, relevant earlier experiments and conclusions to be drawn from them, are reported only now, in the following.

Experimental

The cylindrical (20 mm ⌀ and 80 mm long) metal electrodes were rotated helically in the gas cell apparatus described earlier [5] at a speed of 5 rpm, so that the arc should always burn on a new surface. The counter-electrode was an RW II carbon electrode with a conical end of 60°, while the electrode distance was 3 mm. The material of the metal electrodes was a relatively pure metal, permitting to neglect the role of the secondary components. The silver electrode was prepared by the electrodeposition of silver in several portions from a cyanide bath on the surface of a pure copper cylinder used also otherwise. After each deposition, the new surface obtained was turned to give a continuous, uniform silver layer of more than 1 mm final thickness, which is not burned through by the arc.

Experiments were carried out in 1% O_2 + 99 N_2, 20% O_2 + 80% N_2 (air) and 99% O_2 + 1% N_2 gas atmospheres. With the first and the last gas mixtures, oxygen-free and nitrogen-free atmospheres, respectively, were approached without the necessity of flushing out completely the gas cell of large dimensions. Similarly, the large dimensions of the gas cell permitted to neglect the effect of the carbon dioxide, formed in the arc from the carbon electrode.

The average current of the a.c. polarized arc, ignited at maximum voltage, was varied in general between 3 and 12 A, but a few experiments were carried out also at a current of 1.5 and 24 A. The slit of the spectrograph was illuminated directly from a distance of 320 mm. The spectra were photographed on Orwo type "blau rapid" plates. The blackening values measured were converted by $P_\varkappa$-transformation and background correction to $Y = \log I$ values (results in the tables represent 100-fold values). The higher intensity values were calculated in knowledge of the filter constant of the step filter, and in the case of wider intensity limits an exposition of 4, 16 and 32 sec was used, resp. instead of the illumination time of 8 sec, used generally. The use of these exposition times and the conversion of the values to 8 sec did not cause an error, because the electrodes of larger mass were rotating during the investigation, so that neither their warming up nor arcing-off effects were considerable.

The following spectral lines were measured in the case of the single electrode materials:

Ag I	338.29 nm	Ag II	243.78 nm
Cu I	324.75	Cu II	236.99
Fe I	272.09	Fe II	259.84
Al I	305.01	Al II	266.92
Mg I	277.67	Mg II	292.87

Results and discussion

Surface of the electrodes after arc excitation

Fig. 1 shows metal microscopic photos* of 6× linear magnification of, the surface of the rotated electrodes connected as cathode. Fig. 2 presents the surface of the electrodes connected as anode at an identical magnification, similarly after the burning of the arc. The rotation of the electrodes and the direction of progression of the arc at the surface agree with the (horizontal) direction of the surface stripes formed during the turning of the electrodes. The average current used was in all cases about 12 A, and changed only a few tenth amperes with the various electrode materials and gas atmospheres.

It can be seen from the pictures that in the case when there is no possibility or only a very slight one for a chemical reaction, the arc migrates in a wide area at the surface, but causes evaporation only in a very small depth,

* The metal microscopic pictures were taken by János SÜLE, mech. engr., department leader of the Erőmű Javító és Karbantartó Vállalat, for whom I wish to express my thanks.

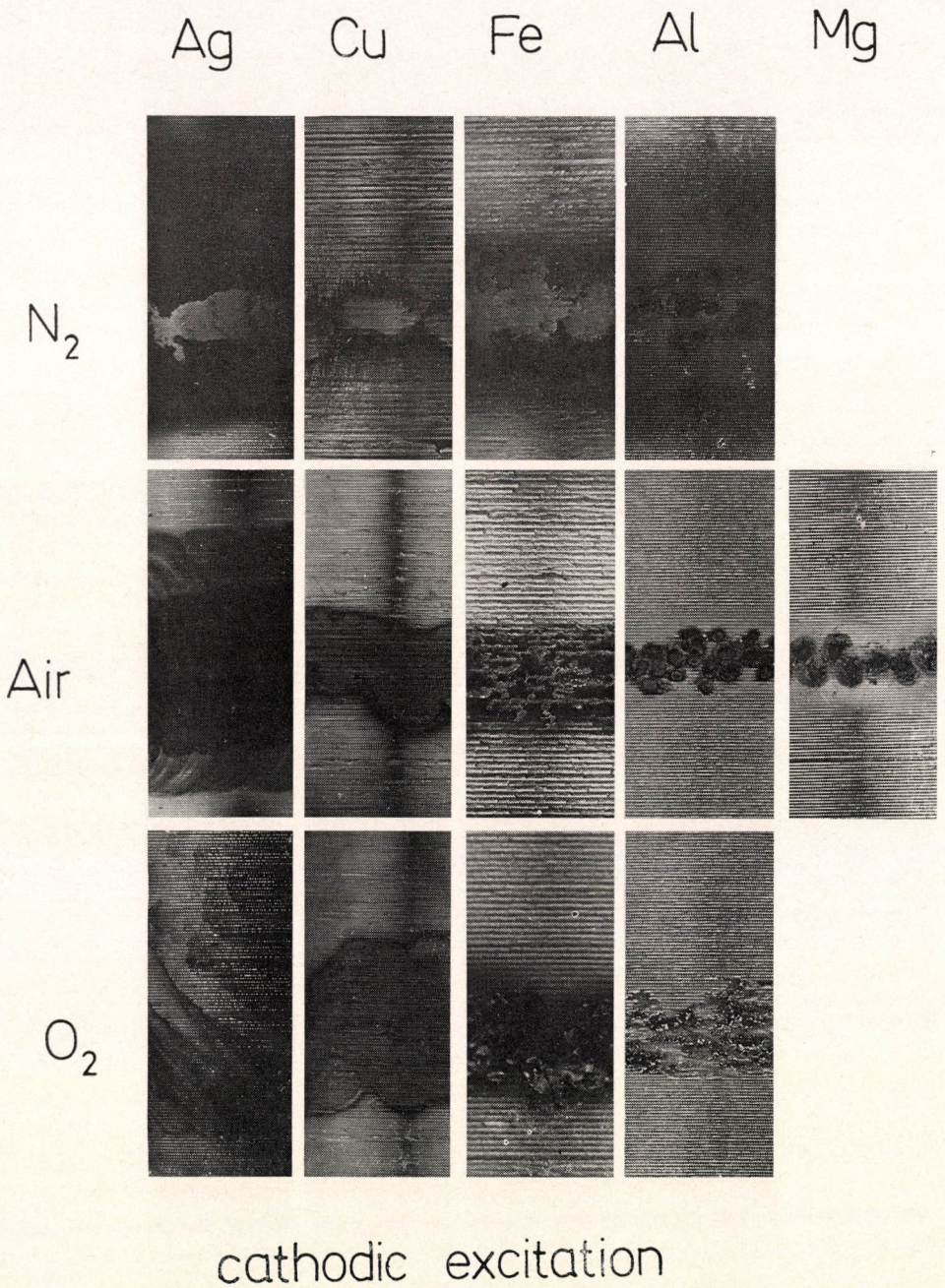

Fig. 1. The surface of metal electrodes connected as cathode in nitrogen, air and oxygen atmospheres

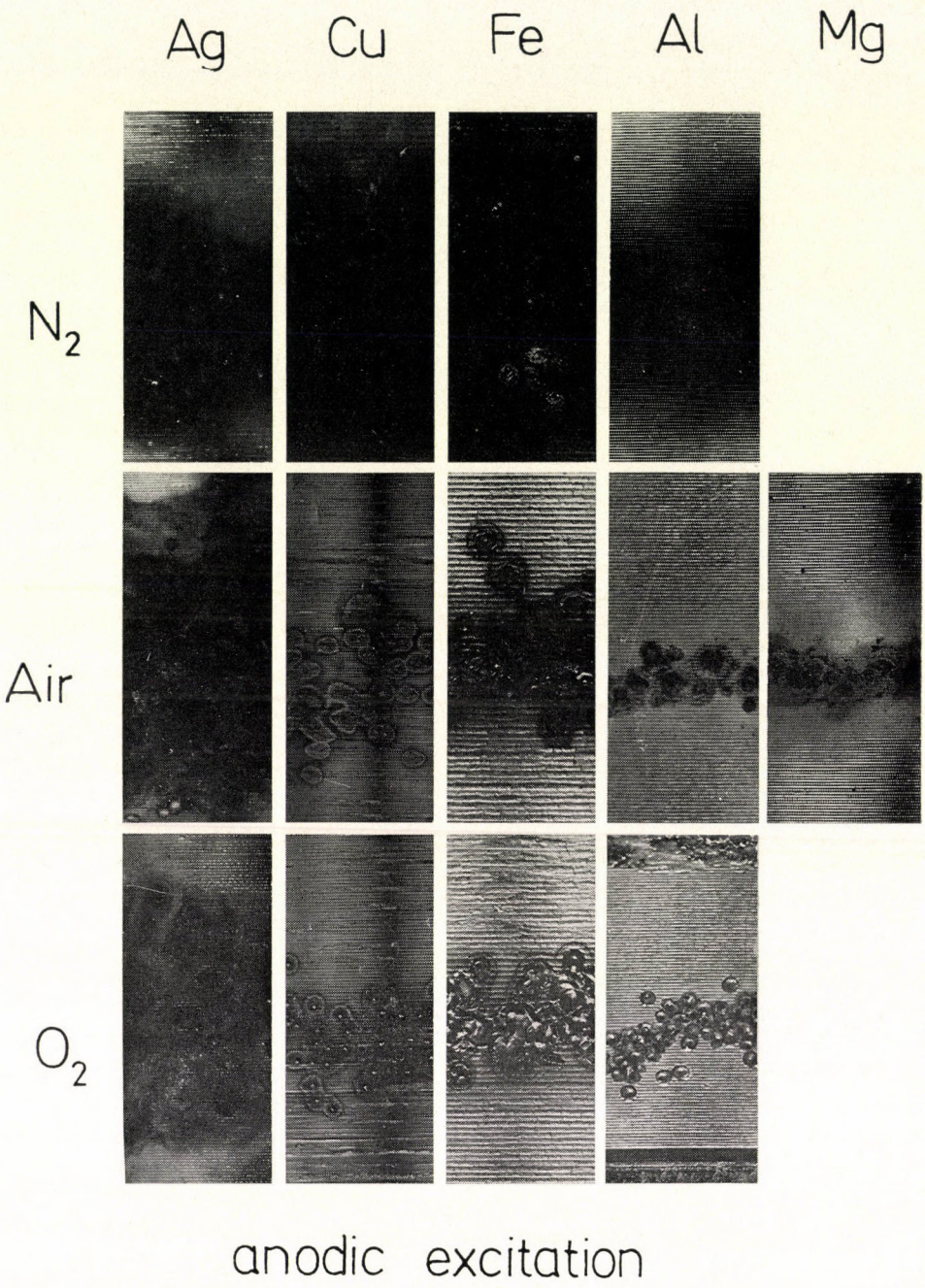

Fig. 2. The surface of metal electrodes connected as anode in nitrogen, air and oxygen atmospheres

This can be observed in the cases of chemically scarcely reacting copper and silver of more positive character, particularly in cathodic connection. Cathodic excitation, as has been proved already by several approaches [3, 5—10], results a reduction tendency at the electrode surface. This suppresses so strongly in the case of silver and copper even in the most reactive atmosphere, in practically pure oxygen, the oxidation during the burning of the arc, that there is nothing which would fix the arc to one spot. Naturally, as the arc migrates with time, even during one discharge, the surface cooled to an appropriate temperature is subsequently oxidized. This causes the broadly protracted black oxide band on the photo of the surface.

In the case of iron of medium reactivity, cathodic connection and the insufficiently reactive atmosphere (nitrogen) with low oxygen content produce a similar picture. In air and particularly in oxygen atmosphere, burning-in becomes increasingly distinct. In the environment of the discharges an increasing oxide deposition can be observed. The surface of the aluminium electrode shows even in the slightly reacting atmosphere, similar to nitrogen, distinct burning-in, which phenomenon is still increased in air. Owing to the high reactivity of aluminium, here discharge craters with sharp outline are formed in spite of the oxidation diminishing effect of cathodic excitation, with a resolidified melt drop in their center and an already easily observable oxide deposit in their environment. In oxygen atmosphere, as has been reported already earlier [2, 5], evaporation is again less than that observed in air, due to the physical properties of oxygen. Local surface parts warm up less and are also less oxidized. Thus, the thermal energy evolved is lower, and the craters are less deep. The lower amount of oxide deposit does not seal well the discharge environment, the arc begins to slip again during the single discharges.

Magnesium, of which regrettably pictures were taken only in air atmosphere, follows immediately aluminium in the series of reactivity and its behaviour is also similar to that of aluminium.

In pictures taken in nitrogen atmosphere, carbon deposit originating from carbon used as counter-electrode is also readily observable, as the carbon could not burn in oxygen deficiency. The same is valid to a still larger extent for metal electrodes connected as anode, because on account of the higher temperature of the cathode spot, the carbon ejection by the carbon cathode is of a larger extent for metal electrodes connected as anode, because on account of the higher temperature of the cathode spot, the carbon ejection by the carbon cathode is of a larger extent [7]. Thus, it is difficult to observe the tracks of the discharge under the carbon deposits. In air atmosphere, the arc continues to slip at the surface of the least reactive silver, however, already a few more dictinct burning-in tracks can be observed. At the surface of the other metals, already distinctly separated discharge craters can be observed in air or oxygen atmospheres, with oxide deposit in the environment of the craters.

This can be seen best on the pictures of the silver, copper and iron surfaces, giving dark oxides. Moreover, that distance from the center of the burning-in, that place at the surface can be observed in these pictures, at which after the single arc discharges of about 0.005 sec the optimal temperature develops, at which oxidation can still proceed or already proceeded. Here, naturally, the fact must also be taken into consideration that the supply of the gaseous reactant by diffusion is limited by the diffusion rate.

Oxidation tendencies exhibited at the anode [3, 5—10] can exert themselves increasingly with increasing reactivity of the metals and with increasing oxygen content of the atmosphere. Craters to be observed at the surfaces of aluminium and magnesium become deeper, and a larger amount of oxide is deposited in their environment. Naturally, here too, the fact must be taken into consideration that though oxygen has a very high reactivity, owing to its physical role in evaporation, the local heating up, evaporation and oxidation of the electrodes is relatively lower [2, 5]. The diameter of the burning spot is smaller, and consequently also the surface part of optimal reaction temperature in its environment. Thus, relatively less heat of reaction will be evolved, which evaporates less further substance, and this again affects the oxidation in a decreased measure.

All the aforesaid seems to indicate that the occurrence of chemical reactions stabilizes, localizes the arc for two reasons, and does not permit the migration of the arc even within a single arc discharge. One of these reasons is that the oxide of lower electrical conductivity, deposited in ring form in the environment of the discharge, localizes the arc. On the other hand, due to the heat of reaction evolved, the electrode is locally overheated at a small place, so that the arc so to speak "burns on". Here, evaporation, and thereby the chemical reaction becomes more intensive.

Conclusions to be drawn from the spectrum

The further figures show the logarithm-intensity values calculated from the blackening of the spectral lines as a function of the current. Though it has been shown earlier that in investigations of this character, curves plotted from values calculated back on the intensities proper are more illustrative [4, 6], in the present given case the changes of certain very small intensity values and their mutual relation can be followed easier in logarithmic representation.

Phenomena to be discussed can clearly be seen also from experimental results shown in Fig. 3. These experiments were carried out in air atmosphere, representing a gas atmosphere of medium reactivity, so that the results obtained can be considered as a basis of comparison. As has been often done earlier, the intensities of the spectral lines, primarily those of the atomic lines, have been taken in good approximation as proportional to evaporation, though

knowing well that plasma parameters play also an important part in their development.

On comparing the shape of the curves and the relative position of the pairs of curves obtained by anodic (a) and cathodic (c) excitation, the following can be established.

The chemically less reactive silver and copper give at arc excitation in cathodic connection a more intensive spectrum. This is in good agreement with our own earlier findings [3, 4] and results of other authors [11], according to which cathodic excitation is the more light-intensive in the absence of chemical reactions (or at a limited extent of reaction), and owing to the cathode spot of higher temperature, though of smaller diameter, evaporation, and proportional to it, excitation is also higher.

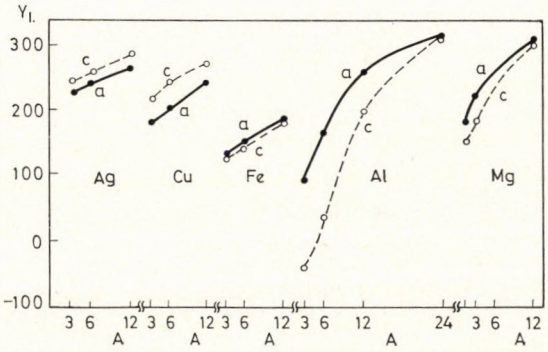

Fig. 3. The log intensities of the atomic lines measured as a function of current. Air atmosphere, anodic (a) and cathodic (c) excitations

In the case of iron of medium activity, the position of the intensity curves obtained by excitation of the two kinds of polarity is already opposite. However, there is no great difference between the two curves. Here the not too large heat of reaction evolved at the anode can just compensate by its excess energy the intensity conditions developed between the cathode and the anode.

The relative increase of the anodic values can still more clearly be seen in the cases of the most reactive aluminium and magnesium. However, the oxidation of both of the very reactive metals occurs also at cathodic excitation, though to a slighter extent, as compared to anodic excitation. Thus, with increasing current both the curves plotted for excitation with the two polarities ascend more rapidly than those discussed earlier.

On comparing our results with data in Table I [12, 13], out of the data listed there, this phenomenon can be explained (besides by the order of the atomic weight and the density) by the given order of the heats of oxide formation alone.

Table I

Some physical data of the metals investigated

Metal electrode	Melting point °C	Boiling point °C	Heat of oxide formation kcal/equiv. O_2	Excitation potential of the atomic line measured eV	First ionization potential eV	Excitation potential of the ionic line measured eV
Silver	961	1950	3.5	3.66	7.57	9.93
Copper	1083	2436	17.5	3.82	7.72	8.84
Iron	1535	3000	32.5	4.61	7.86	4.82
Aluminium	660	2057	68.0	7.67	5.99	4.64
Magnesium	651	1107	72.0	7.18	7.65	8.65

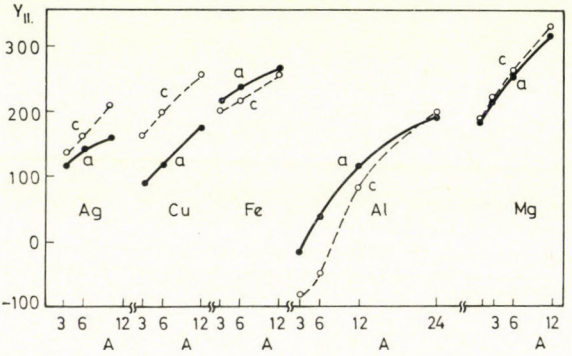

Fig. 4. The log intensities of the ionic lines measured as a function of current. Air atmosphere, anodic (a) and cathodic (c) excitations

Similar conditions are exhibited in Fig. 4 concerning the ionic lines. However, ratios change somewhat, due to the different energy requirements of the individual spectral lines. Thus, the magnesium line is here still more intensive at cathodic excitation.

The role of the volatility data (melting and boiling points) can also be seen from the curves, and is in our case for pure metals similar as has been found earlier for the alloying elements of aluminium [14]. The difference between the excitations at the two polarities is smaller in the case of the more volatile silver, than in that of the less volatile copper, and is also for the more volatile magnesium smaller than for the relatively less volatile aluminium. The oxidations investigated proceed predominantly at the electrode surface, thus, evidently they do influence more decisively the evaporation. With more volatile substances, smaller effects occurring at the cathode can also be well-seen, and change (in our case, increase) easier the evaporation. With electrode materials evaporating more difficultly, only larger effects manifested at the anode

can produce substantial changes. Therefore, differences between excitation with the two kinds of polarities are more distinct here.

Naturally, in addition to these factors, the shape of the curves is influenced also by the parameters of the arc plasma (the effective ionization potential of the plasma, which, however in a given gas atmosphere is not independent of the evaporation of the sample; the electron pressure and the arc temperature and their distribution; the excitation potentials, etc.). However, these parameters have not yet been taken into account in this first approximation.

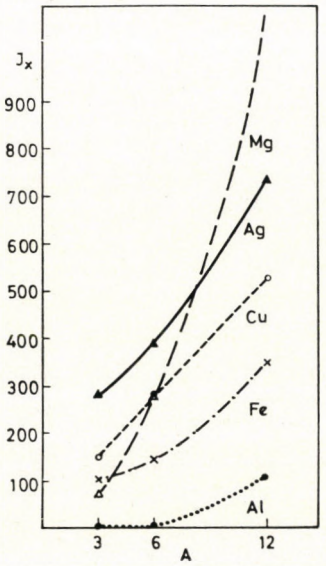

Fig. 5. Intensity — current curves obtained with metal cathodes in air atmosphere

The role of the volatility data is well reflected also by the slope of the curves, converted to intensity values, primarily in cathodic excitation, which is less influenced by oxidation (Fig. 5). The curve for magnesium is the steepest, and this element is the most volatile out of those investigated, though its high reactivity slightly exceeds that of aluminium. At the same time, the intensity curve of the least volatile iron is the flattest. The comparison of the two less reactive metals, of silver and copper, seems to give the same results, though not as distinctly. Out of the curves of these metals, that of silver is somewhat steeper. The situation is the same for the intensity curves obtained for the metals connected as anodes, not presented here. The difference is only that the individual curves are shifted relative to each other, obviously on account of the different physical properties of the electrode materials, and the curves of the two chemically active metals become steeper. This latter indicates that evaporation increases with increased chemical reaction. This means that

the evaporation of the more volatile compounds is more dependent on the circumstances (current, chemical reactions).

Similar differences as above, but more emphasized in certain cases, can be observed in the less active nitrogen atmosphere (Fig. 6). Here, the largest difference to the credit of cathodic values is shown by silver in the case of atomic lines, and the difference is much smaller for the somewhat more active copper. Moreover, the changed gas atmosphere modifies also on account of its physical role considerably the intensity values, obviously in a different extent with electrode materials of different physical properties.

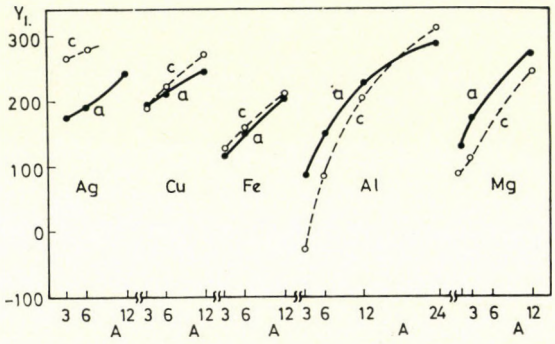

Fig. 6. Log intensities of the atomic lines measured as a function of current. Nitrogen atmosphere, anodic (a) and cathodic (c) excitations

In the case of iron, the heat of reaction evolved in a diminished extent on account of the low oxygen content, is still insufficient to invert or even to compensate the difference between the excitations at the two kinds of polarities. As it can only diminish this difference, cathodic excitation remains the more intensive.

Magnesium reacts intensively also with the small amount of oxygen. Thus, though cathodic values increase too with the slight increase in evaporation produced by the reaction heat evolved also here, though to a slighter extent, this and the initially higher evaporation at the cathode is surpassed in the anodic case by the effect of the excess energy from the chemical reaction at the anode. The situation is the same for aluminium, for which measurements were carried out also at 24 A. Owing to the relatively lower diffusion rate of oxygen than necessary, at the high current the effect of oxidation is already dwarfed. Thus, cathodic excitation gives higher line intensities, as was found already earlier [16]. Therefore, the two curves intersect each other, which is to be expected also for magnesium, when working also at a higher current.

The curves for ionic lines obtained in nitrogen atmosphere containing 1 per cent of oxygen are shown in Fig. 7. Here it can clearly be seen again that owing to the higher energy requirement of ionic lines, the increase in anodic values is also smaller. The intersection of the curves for aluminium

occurs already at 12 A, and the difference between the two curves of magnesium is also much smaller. In the same way, the anodic curves of the two more positive metals lie also substantially lower.

It is interesting to compare the four preceding figures with those obtained in oxygen atmosphere (Figs 8 and 9).

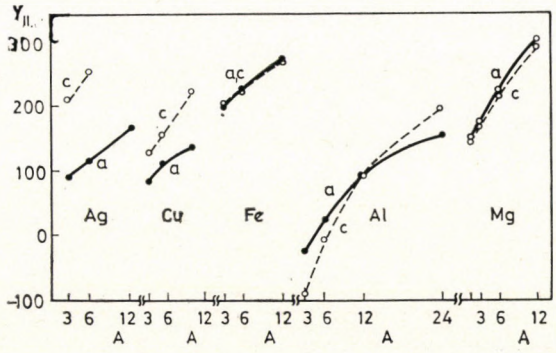

Fig. 7. Log intensities of the ionic lines measured as a function of current. Nitrogen atmosphere, anodic (a) and cathodic (c) excitations

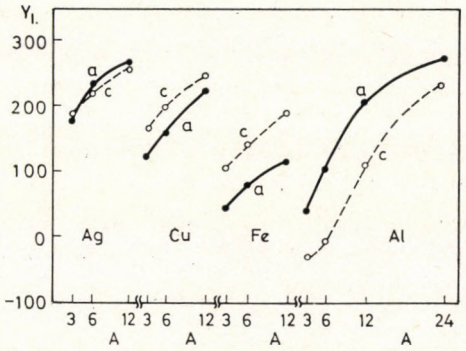

Fig. 8. Log intensities of the atomic lines measured as a function of current. Oxygen atmosphere, anodic (a) and cathodic (c) excitations

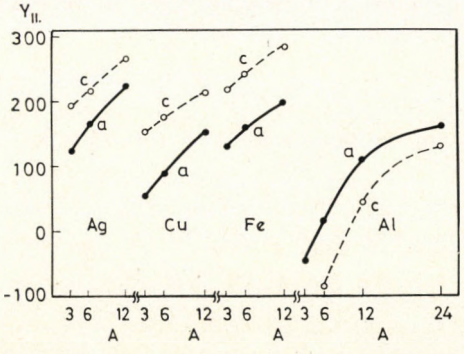

Fig. 9. Log intensities of the ionic lines measured as a function of current. Oxygen atmosphere anodic (a) and cathodic (c) excitations

Owing to the high oxygen excess and the resulting high reactivity of the gas atmosphere, the anodic values of aluminium lie even in the case of 24 A considerably above the cathodic values. It is true, on the other hand, that according to our earlier experiments the evaporation of the electrode is lower in oxygen atmosphere, as has been mentioned repeatedly also in the present communication. Thus, the "percentually" higher heat of reaction between anodic and cathodic excitation results a difference, equal to that observed at about 13 A in air atmosphere. This indicates also partly that the evaporation of the electrode material in oxygen atmosphere at 24 A can only be — according to coarse estimation — about the same as in air at about 13 A. Naturally, here too plasma parameters, influencing considerably the line intensities, have not been taken into consideration. However, the importance of these parameters is reflected most probably in the curve obtained for the atomic line of silver. Here, the higher line intensity in the case of atomic lines has been obtained for silver electrode connected as anode, obviously not on account of chemical energy. However, this can be considered as an exception, because at the same time ionic lines, which appear in a much larger number in the spectrum, have a blackening easier to measure and are less sensitive to side effects, were in each case at cathodic excitation more intensive. Without venturing into a more detailed explanation of the phenomenon, it should be mentioned that in the given case the intensities of such broadened lines had to be compared on account of the identical currents, in the measurement of which uncertainties are already considerable. Neither are we certain that experiments have been carried out in a current region, which is most favourable for silver. In the case of aluminium it has been found already earlier [6, 15] under the given experimental conditions that at a low extent of evaporation the effect of the chemical reactions is slightly noticeable. Therefore, in certain cases aluminium too gives in cathodic connection higher line intensities, in spite of the fact that aluminium is a very active reaction partner.

In oxygen atmosphere there are differences also in the case of iron. Here too, electrodes connected as cathode give the spectral lines of higher intensity. As an explanation, only the different plasma parameters can be mentioned again. In addition, the iron particles sparkled during several experiments with such intensity that our gas cell with luxite walls twice caught fire. Possibly, this sparkling caused the very different energy conditions in the arc. This is indicated by the very low line intensity values. Anyway, it seems probable that in the given current range the excess of oxygen changes after a certain value rather the physical effect of the gas atmosphere, while it contributes only slightly to a further increase of the chemical reactions.

However, under consideration of the behaviour of several other spectral lines not discussed here, according to our opinion, these two exceptions do

not disprove the facts established in the aforesaid. Curves for copper, shown in the last figures, also support our opinion expounded above.

Similar experiments with magnesium were omitted here, owing to the violent reaction to be expected in practically pure oxygen.

All these results agree well with the surface photographs shown in the first part of the present communication. When the arc burns at one point, even if only for the duration of one to two discharges, the local temperature of the surface is higher, particularly if heated also by the heat of chemical reaction, or it extends to larger local surfaces. Thus, the evaporation of the sample increases, and parallel to it, the extent of oxidation, which acts back again on evaporation, and *vice versa*.

In summary, it can be established again that the extent and effect of the chemical reactions, proceeding in the electric arc at the surface of the electrodes, depends on the relative reactivity of the reactants (the material of the electrode and the gas atmosphere) and on the polarity of the electrode. Anodic connection promotes oxidation, while cathodic connection endeavours to diminish it by providing for more reducing circumstances. However, in the exertion of these oxidative and reductive tendencies, the evaporation properties of the electrode material play also, among others, a role. Indeed, the heat of the chemical reactions evolved at the surface of the electrode increases primarily the evaporation of the sample, and only through this the line intensities.

REFERENCES

[1] Szabó, Z. L., Szakács, O.: Acta Chim. (Budapest) **73,** 143 (1972)
[2] Szabó, Z. L., Török, T.: *ibid.* **73,** 153 (1972)
[3] Szabó, Z. L., Tóth, I.: *ibid.* **73,** 373 (1972)
[4] Szabó, Z. L., Tóth, I.: *ibid.* **73,** 387 (1972)
[5] Szabó, Z. L., Tóth, I.: Spectrochim. Acta **27/M,** 107 (1972)
[6] Szabó, Z. L., Tóth, I.: *ibid.* **27/M,** 117 (1972)
[7] Szabó, Z. L., Pöppl, L.: Acta Chim. (Budapest) **77,** 125 (1973)
[8] Szabó, Z. L., Pöppl, L.: *ibid.* **77,** 137 (1973)
[9] Pöppl, L., Szabó, Z. L.: *ibid.* **79,** 27 (1973)
[10] Szabó, Z. L.: Spetrochim. Acta (in print)
[11] Anderman, G., Kemp, J. W.: ASTM Techn. Publ. 259 (1959)
[12] Hodgman, C. D., Weast, R. C., Selby, S. M.: Handbook of Chemistry and Physics, Chemical Rubber Publ. Co., Cleveland, 1958
[13] Zaidel, A. N., Prokofev, V. K., Raiskii, S. M.: Tablitsi spectralnih linii, Izdatelstvo "Nauka", Moskow, 1969
[14] Szabó, Z. L., Pöppl, L.: Acta Chim. (Budapest) **79,** 119 (1973)
[15] Szabó, Z. L., Pöppl, L.: *ibid.* **79,** 237 (1973)
[16] Szabó, Z. L., Tóth, L.: *ibid.* **73,** 267 (1972)

Zoltán László Szabó; 1088 Budapest, Múzeum krt. 4/b, Hungary.

Acta Chimica Academiae Scientiarum Hungaricae, Tomus 85 (1), pp. 27—45 (1975)

CALCULATION OF COUNTERCURRENT SOLID-LIQUID EXTRACTION

K. TETTAMANTI,* J. MANCZINGER,* J. HUNEK* and R. STOMFAI**

*(*Department of Chemical Unit Operations, Technical University, Budapest and **L. Eötvös Institute of Geophysics, Budapest)*

Received March 15, 1974

Based on the solution of Fick's IInd differential equation, and assuming that comminuted vegetable particles are plates, cylinders or spheres, a general method has been evolved for the design of continuous and discontinuous, countercurrent solid–liquid extraction. The complex mathematical expressions have been evaluated by computer and are tabulated for easy use in engineering calculations.

The determination of unknown parameters required for design work is carried out according to a simple laboratory method based upon the experimental determination of the constants characteristic of the resistance against diffusion within the solid phase.

The simplifying assumptions are shown to be justified by experimental data.

In the literature there is relative little information on the design of apparatus for solid–liquid extraction and no correlations generally applicable for calculating the number of stages or the solvent requirement in countercurrent operations have been established. The well-known correlations for liquid–liquid extraction are not applicable here.

Starting from the differential equations for diffusion, we have elaborated a method suitable for both rapid calculations and design of the apparatus.

The solutions of Fick's second equation for the various cases of diffusion are well known from the literature, its mathematical formulation, however, is not suitable for rapid calculations. A problem is posed by the irregular shapes of the particles of comminuted vegetable matter, which are difficult to describe geometrically, and by the inner inhomogeneity of these vegetable grains. Diffusion within these particles can only be treated mathematically by introducing several simplifying assumptions and the accuracy of the results thus calculated must be checked by experiment. Experimental results, to be presented later, have shown that in the studied cases the simplifications are admissible and the solutions of the differential equations allow the formulation of general correlations. The "ideal drug-extraction system" corresponding to the simplifying assumptions is defined as follows:

1. In the case of dry drugs, soluble ingredients are instantaneously dissolved at steeping.

2. The liquid ratio, *i.e.* the specific quantity of the extracting liquid per unit mass of cell liquor, does not change during extraction.

3. After infinite time, the concentrations in the cell liquor and in the extracting liquid are the same, *i.e.* the vegetable skeletal matter has no adsorptive properties.

4. The concentration of the cell liquor is initially the same throughout the drug.

5. The drug area available for mass transfer does not change with time.

6. The interior of the drug is isotropic in the direction of diffusion, thus a constant "apparent" diffusion coefficient can be defined for the given material.

7. The solid phase consists of regular particles of the same shape and size: minced leaves, stems or seed are regarded as plates, infinitely long cylinders (relative to their axis) or to spheres, respectively.

8. In the extract the concentration gradient is zero in every direction within a closed system; in a flowing system this gradient is zero in the direction perpendicular to that of flow.

9.The densities of the liquids remain practically constant during extraction.

Countercurrent extraction can be implemented in various ways.

The methods most frequently practised are the following.

1. Continuous operation

a) both phases are kept in countercurrent motion (*e.g.* J-extractor, U-extractor),

b) with a high number of vessels, the so-called continuous juice-draught diffuser system allows practically continuous operation. The liquid phase is in continuous movement and the batchwise charge and discharge of the vegetable phase, *i.e.* its direction, represent the countercurrent feature of the operation.

2. Batch operation

carried out in such a way that in the intervals between extract removals, the solvent is circulated through layers of the solid phase.

For the calculation of any of the operations mentioned we may start from Fick's IInd differential equation

$$\frac{\partial^2 x}{\partial r^2} + \frac{G-1}{r}\frac{\partial x}{\partial r} = \frac{1}{D}\frac{\partial x}{\partial t} \tag{1}$$

where G is a geometrical symmetry factor.

The initial and boundary conditions are only formally the same for cases 1a, 1b and 2; the mathematical solution is presented as an infinite series totally unsuitable for rapid calculations. For the simplest case of a single step, closed extraction system, the time dependence of average concentrations of the raffinate and extract are given by the equation

$$\bar{x}(t) = \frac{x_0 + f y_0}{1+f} + (x_0 - y_0)\, 2 f^2 \sum_{k=1}^{\infty} \frac{G}{f^2 \mu_k^2 + G^2 (1+f)} \exp\left(-\frac{D}{r_0^2}\mu_k^2 t\right) \tag{2}$$

$$y(t) = \frac{x_0 + fy_0}{1+f} - (x_0 - y_0)\, 2f \sum_{k=1}^{\infty} \frac{G}{f^2\mu_k^2 + G^2(1+f)} \exp\left(-\frac{D}{r_0^2}\mu_k^2 t\right) \quad (3)$$

The expressions for the concentration in a continuous countercurrent operation (Cases 1a and 1b) are formally very similar

$$\bar{x}(t) = \frac{x_0 - fy_1}{1-f} + (x_0 - y_1)\, 2f^2 \sum_{k=1}^{\infty} \frac{G}{f^2\lambda_k^2 + G^2(1-f)} \exp\left(-\frac{D}{r_0^2}\lambda_k^2 t\right) \quad (4)$$

$$y(t) = \frac{x_0 - fy_1}{1-f} + (x_0 - y_1)\, 2f \sum_{k=1}^{\infty} \frac{G}{f^2\lambda_k^2 + G^2(1-f)} \exp\left(-\frac{D}{r_0^2}\lambda_k^2 t\right) \quad (5)$$

The batchwise countercurrent extraction (Case 2; *cf.* Fig. 1) consists, essentially, of several simple, closed-system extraction steps, thus for its description we sought a correlation by utilizing the suggestion of PÁL [1], on the basis of Eqs. (2) and (3). (Derivation omitted.)

The relationships have been written in such a way that they included the relative losses characteristic of countercurrent extraction from the aspects of chemical engineering.

Using abbreviated symbols for the terms containing infinite sums and assuming the concentration of the entering solvent to be zero, these correlations can be written as follows.

For a continuous countercurrent extraction:

$$\frac{x_n}{x_0} = \frac{1 - f\dfrac{1+B_T}{f+B_T}}{1-f} + 2f^2\left[1 - \frac{1+B_T}{f+B_T}\right]\frac{B_T}{2f(1-f)} \quad (6)$$

where

$$B_T = 2f(1-f)\sum_{k=1}^{\infty} \frac{G}{f^2\lambda_k^2 + G^2(1-f)} \exp\left(-\frac{D}{r_0^2}\lambda_k^2 T\right) \quad (7)$$

and T is the residence time of the drug in the extractor.

For batch-type countercurrent operation

$$\frac{x_n}{x_0} = \Psi^n \frac{f-1}{f-\Psi^n} \quad (8)$$

where

$$\Psi = \frac{1 + f \cdot P(t_c)}{f + P(t_c)} \quad (9)$$

and

$$P(t_c) = 2f(1+f)\sum_{k=1}^{\infty} \frac{G}{f^2\mu_k^2 + G^2(1+f)} \exp\left(-\frac{D}{r_0^2}\mu_k^2 t_c\right) \quad (10)$$

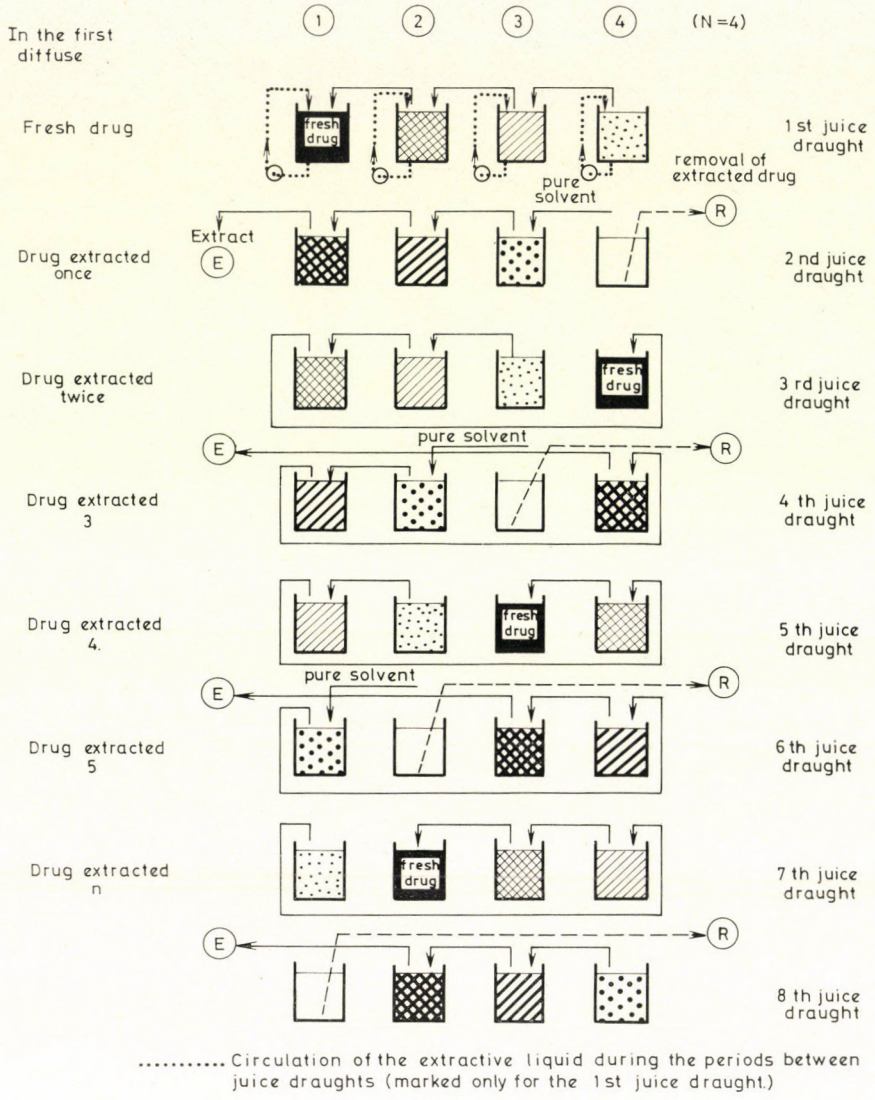

Fig. 1

Equations (6)—(10), which describe the correlations between the operational parameters of extractions are not suitable for rapid calculations, therefore, they have been evaluated and tabulated, and are given in the form of diagrams.

As a function of the Fourier number (Fo)

$$\frac{Dt}{r_0^2} = Fo \tag{11}$$

figuring in the exponential terms of the correlations, we present, for continous countercurrent extraction (Tables I, II and III) the relative losses $\frac{x_n}{x_0}$ directly, whereas for batch-type countercurrent extraction (Tables IV, V and VI) the $P(t)$ values are listed. The liquid ratio is the parameter used in the Tables. On the basis of these Tables the diagrams shown in Figs. 2—7 can be constructed.

The value of the $P(t)$ function for batch-type countercurrent extraction gives, at the same time, the concentration in a closed system for a simple, single-step extraction, because from the material balance and the criterion of $x_\infty = y_\infty$, it follows that

$$y_\infty = \frac{x_0 + f y_0}{1 + f} \tag{12}$$

and from Eqs. (3) and (10) we have

$$P(t) = \frac{y_\infty - y_t}{y_\infty} \left[1 + (1 + f) \frac{y_0}{x_0 - y_0} \right] \tag{13}$$

For the calculation of the operations only the constant

$$\frac{D}{r_0^2} = \varkappa \tag{14}$$

in the Fourier number must be known, which includes the parameters characteristic of the material properties and structures. According to our suppositions, $\varkappa$ is independent of time and the liquid ratio, and is only slightly affected by the flow characteristics at liquid speeds linear velocity 0.5—2 cm/sec prevailing in commercial drug extraction apparatus. (This effect generally remains within the limits of experimental error even if this velocity is changed by one order of magnitude.)

We have devised a simple method for the experimental determination of the constant $\varkappa$. Known quantities of the solvent and the drug to be extracted were placed into the apparatus shown in Fig. 8, and the solvent was circulated in a suitable way (*e.g.* by a gear pump). If extraction is carried out with a boiling solvent, a flask provided with a reflux condenser may be used as the extraction vessel. The rate of circulation should be chosen so as to approximate the relative velocity of liquid transport in the commercial apparatus to be designed.

The change of concentration in the extract and the initial concentration of the diffusing substance are determined by chemical analysis; the amounts of the extracting solvent and that retained by the substrate are measured

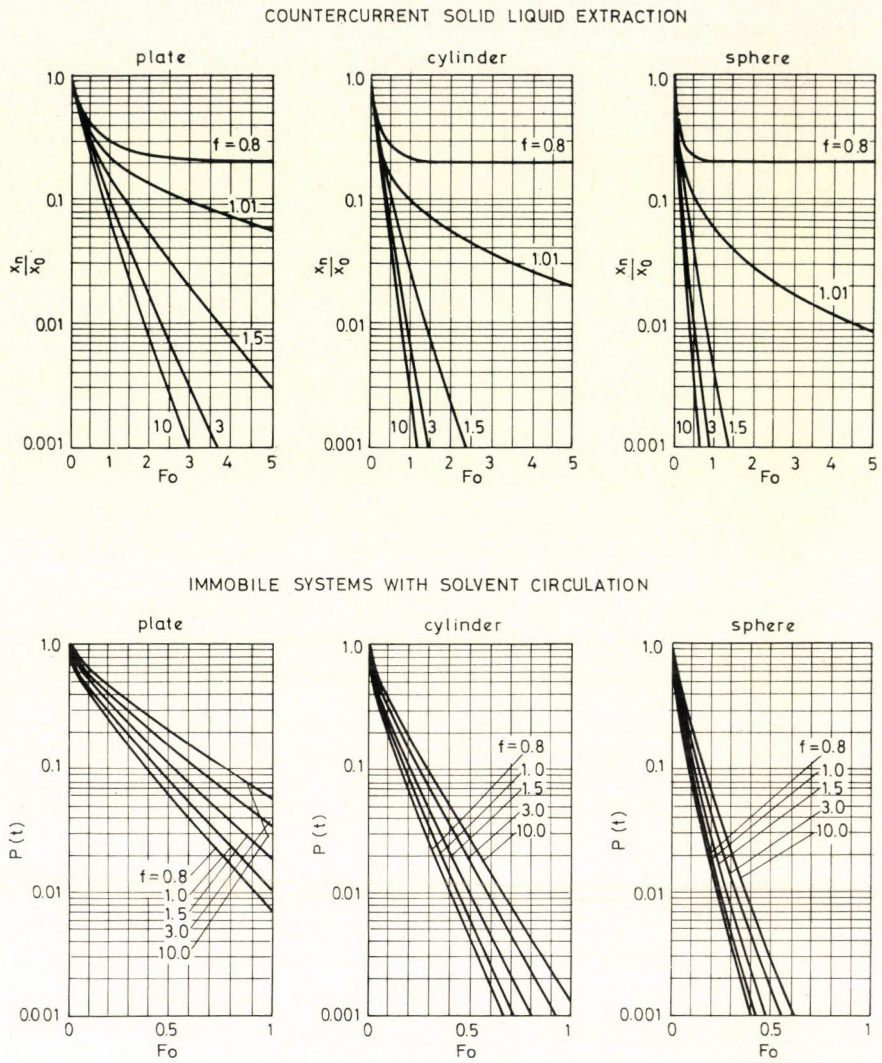

Fig. 2—7

(the latter is determined by the weight loss upon drying the extracted drug). The liquid ratio and the $P(t)$ function for various times are calculated.

On the basis of the shape of the substrate particles one finds the Fourier numbers in Tables IV, V or VI; from this and the pertinent extraction time the value of $\varkappa$ can be calculated.

In Figs. 9—14 some experimental results are shown. Figures 9—12 present results of model tests where the geometrical homodispersity of the drug particles was artificially assured. These experiments prove that the values

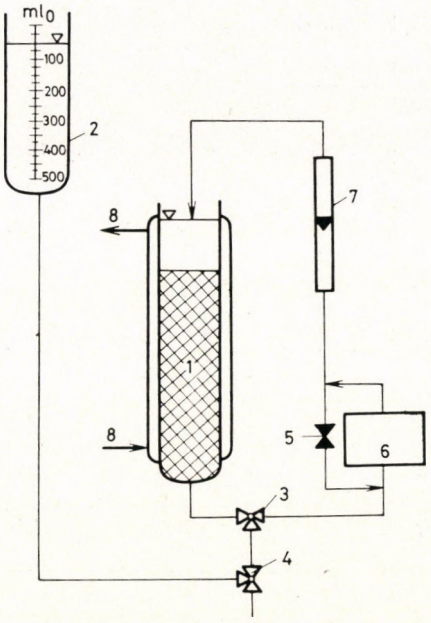

1 Thermostated extraction column
2 Solvent feed
3 Three-way stop cock
4 Three-way stop cock
5 Throttle valve
6 Gear pump
7 Flowmeter
8 Thermostated water

Fig. 8

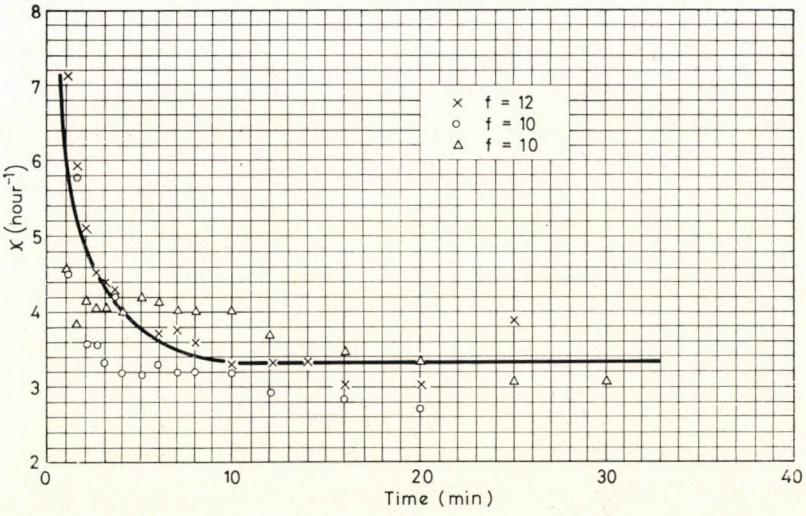

Fig. 9

Table I

Countercurrent solid–liquid extraction

$\frac{x_n}{x_0}$ values for diffusion from a plane sheet

f \ Fo	0.01	0.02	0.04	0.06	0.08	0.10	0.20	0.40	0.60	0.80	1.00	2.00	5.00	10.00
0.80	.8907	.8476	.7888	.7456	.7105	.6806	.5728	.4501	.3806	.3363	.3059	.2373	.2030	.2001
0.90	.8903	.8467	.7871	.7430	.7070	.6761	.5634	.4314	.3541	.3033	.2675	.1803	.1191	.1030
1.01	.8899	.8460	.7857	.7408	.7040	.6723	.5554	.4154	.3315	.2756	.2356	.1355	.0576	.0277
1.10	.8897	.8455	.7847	.7393	.7020	.6698	.5502	.4049	.3168	.2577	.2153	.1094	.0305	.0065
1.20	.8895	.8451	.7838	.7380	.7001	.6674	.5453	.3952	.3035	.2417	.1974	.0883	.0155	.0013
1.30	.8893	.8447	.7831	.7368	.6986	.6654	.5412	.3872	.2925	.2286	.1830	.0730	.0083	.0003
1.40	.8891	.8444	.7824	.7358	.6972	.6638	.5377	.3804	.2832	.2178	.1713	.0616	.0048	.0001
1.50	.8890	.8442	.7819	.7350	.6961	.6623	.5348	.3746	.2754	.2088	.1616	.0530	.0029	.0000
1.60	.8889	.8439	.7814	.7342	.6951	.6611	.5322	.3696	.2687	.2011	.1535	.0463	.0019	.0000
1.70	.8888	.8437	.7809	.7336	.6942	.6600	.5299	.3652	.2629	.1945	.1466	.0411	.0013	.0000
1.80	.8887	.8435	.7806	.7330	.6935	.6590	.5279	.3614	.2579	.1888	.1407	.0369	.0009	.0000
1.90	.8886	.8434	.7802	.7325	.6928	.6581	.5262	.3580	.2534	.1838	.1356	.0335	.0007	.0000
2.00	.8885	.8432	.7799	.7320	.6922	.6574	.5246	.3549	.2494	.1794	.1311	.0307	.0005	.0000
3.00	.8881	.8423	.7780	.7292	.6883	.6525	.5147	.3363	.2256	.1537	.1058	.0176	.0001	.0000
5.00	.8877	.8415	.7765	.7269	.6853	.6487	.5070	.3221	.2081	.1357	.0890	.0112	.0000	.0000
10.00	.8874	.8410	.7754	.7253	.6830	.6459	.5014	.3119	.1959	.1236	.0782	.0081	.0000	.0000

Table II

Countercurrent solid–liquid extraction

$\frac{x_n}{x_0}$ values for diffusion from a cylinder

f \ Fo	0.01	0.02	0.03	0.04	0.06	0.08	0.10	0.20	0.40	0.60	0.80	1.00	2.00	5.00
0.80	.7971	.7257	.6756	.6363	.5762	.5309	.4948	.3834	.2897	.2502	.2298	.2184	.2019	.2000
0.90	.7956	.7228	.6712	.6306	.5679	.5200	.4815	.3594	.2501	.1996	.1709	.1527	.1159	.1009
1.01	.7944	.7203	.6676	.6258	.5608	.5108	.4703	.3394	.2181	.1600	.1259	.1035	.0536	.0198
1.10	.7935	.7187	.6651	.6226	.5562	.5049	.4630	.3266	.1983	.1366	.1005	.0771	.0274	.0027
1.20	.7928	.7171	.6629	.6197	.5519	.4994	.4563	.3151	.1811	.1171	.0805	.0574	.0135	.0003
1.30	.7921	.7159	.6610	.6172	.5484	.4948	.4508	.3057	.1676	.1025	.0663	.0442	.0071	.0000
1.40	.7915	.7148	.6595	.6151	.5454	.4910	.4462	.2979	.1568	.0913	.0559	.0352	.0041	.0000
1.50	.7911	.7138	.6581	.6134	.5429	.4878	.4423	.2914	.1480	.0825	.0482	.0288	.0025	.0000
1.60	.7906	.7130	.6569	.6118	.5407	.4849	.4389	.2858	.1406	.0755	.0423	.0242	.0016	.0000
1.70	.7903	.7123	.6559	.6105	.5388	.4825	.4360	.2810	.1345	.0698	.0377	.0207	.0011	.0000
1.80	.7899	.7117	.6550	.6093	.5371	.4803	.4334	.2768	.1292	.0651	.0340	.0181	.0008	.0000
1.90	.7896	.7111	.6541	.6083	.5356	.4784	.4311	.2731	.1248	.0612	.0310	.0160	.0006	.0000
2.00	.7894	.7106	.6534	.6073	.5342	.4767	.4291	.2699	.1209	.0579	.0286	.0143	.0005	.0000
3.00	.7877	.7075	.6489	.6015	.5260	.4663	.4167	.2505	.0992	.0409	.0172	.0073	.0001	.0000
5.00	.7864	.7050	.6454	.5969	.5196	.4583	.4073	.2366	.0851	.0314	.0117	.0043	.0000	.0000
10.00	.7855	.7032	.6428	.5936	.5150	.4526	.4006	.2269	.0762	.0259	.0088	.0030	.0000	.0000

Table III

Countercurrent solid–liquid extraction

$\frac{x_n}{x_0}$ values for diffusion from a sphere

f \ Fo	0.01	0.02	0.03	0.04	0.05	0.06	0.08	0.10	0.20	0.40	0.60	0.80	1.00	2.00
0.80	.7169	.6278	.5689	.5248	.4899	.4613	.4165	.3829	.2917	.2316	.2126	.2053	.2023	.2000
0.90	.7138	.6220	.5604	.5139	.4767	.4459	.3971	.3597	.2537	.1746	.1431	.1270	.1176	.1027
1.01	.7111	.6170	.5533	.5048	.4657	.4331	.3810	.3407	.2235	.1314	.0922	.0706	.0568	.0275
1.10	.7094	.6138	.5487	.4989	.4586	.4249	.3707	.3286	.2049	.1070	.0660	.0441	.0308	.0068
1.20	.7078	.6108	.5444	.4935	.4522	.4174	.3615	.3179	.1889	.0877	.0474	.0273	.0163	.0015
1.30	.7065	.6083	.5409	.4891	.4468	.4113	.3540	.3091	.1764	.0740	.0354	.0179	.0093	.0004
1.40	.7054	.6062	.5380	.4853	.4424	.4062	.3477	.3019	.1663	.0638	.0276	.0125	.0057	.0001
1.50	.7044	.6044	.5354	.4821	.4386	.4019	.3425	.2958	.1581	.0562	.0222	.0091	.0038	.0000
1.60	.7035	.6028	.5332	.4794	.4354	.3982	.3380	.2907	.1514	.0503	.0183	.0069	.0026	.0000
1.70	.7028	.6015	.5313	.4770	.4325	.3950	.3341	.2863	.1457	.0456	.0155	.0054	.0019	.0000
1.80	.7021	.6003	.5297	.4749	.4301	.3922	.3307	.2825	.1409	.0419	.0134	.0044	.0015	.0000
1.90	.7015	.5992	.5282	.4730	.4279	.3897	.3277	.2791	.1367	.0388	.0118	.0037	.0011	.0000
2.00	.7010	.5983	.5269	.4714	.4259	.3875	.3251	.2761	.1332	.0363	.0105	.0031	.0009	.0000
3.00	.6978	.5924	.5187	.4613	.4141	.3742	.3094	.2586	.1131	.0240	.0053	.0012	.0003	.0000
5.00	.6952	.5878	.5125	.4537	.4053	.3644	.2980	.2461	.1001	.0177	.0032	.0006	.0001	.0000
10.00	.6933	.5845	.5080	.4482	.3990	.3574	.2900	.2375	.0918	.0143	.0023	.0004	.0001	.0000

Table IV

Immobile systems with solvent circulation

$P(t)$ values for diffusion from a plansheete

f \ Fo	0 01	0.02	0.03	0.04	0.05	0.06	0.08	0.10	0 20	0 40	0 60	0.80	1.00	2.00
0.80	.7718	.6905	.6326	.5866	.5480	.5147	.4586	.4125	.2568	.1052	.0433	.0178	.0073	.0001
0.90	.7834	.7050	.6488	.6038	.5658	.5329	.4773	.4312	.2736	.1162	.0495	.0211	.0090	.0001
1.00	.7929	.7170	.6621	.6180	.5808	.5482	.4931	.4472	.2884	.1261	.0553	.0243	.0107	.0002
1.10	.8008	.7270	.6734	.6301	.5934	.5613	.5067	.4609	.3013	.1351	.0608	.0274	.0123	.0002
1.20	.8075	.7355	.6830	.6405	.6043	.5726	.5184	.4729	.3128	.1433	.0659	.0303	.0139	.0003
1.30	.8132	.7428	.6913	.6495	.6138	.5824	.5287	.4834	.3230	.1508	.0706	.0331	.0155	.0003
1.40	.8182	.7492	.6985	.6573	.6220	.5910	.5377	.4927	.3322	.1576	.0751	.0357	.0170	.0004
1.50	.8225	.7548	.7049	.6642	.6294	.5986	.5458	.5010	.3404	.1639	.0792	.0383	.0185	.0005
1.60	.8263	.7597	.7106	.6704	.6359	.6054	.5530	.5084	.3479	.1697	.0830	.0406	.0199	.0006
1.70	.8297	.7641	.7156	.6759	.6417	.6115	.5594	.5151	.3547	.1750	.0866	.0429	.0212	.0006
1.80	.8328	.7681	.7201	.6808	.6470	.6170	.5653	.5211	.3609	.1800	.0900	.0450	.0225	.0007
1.90	.8355	.7716	.7242	.6853	.6518	.6220	.5706	.5267	.3666	.1845	.0932	.0471	.0238	.0008
2.00	.8380	.7749	.7280	.6894	.6561	.6266	.5754	.5317	.3718	.1888	.0962	.0490	.0249	.0009
3.00	.8539	.7958	.7522	.7160	.6846	.6566	.6076	.5654	.4076	.2191	.1180	.0636	.0343	.0016
5.00	.8670	.8132	.7725	.7385	.7088	.6822	.6354	.5947	.4400	.2481	.1403	.0793	.0448	.0026
10.00	.8770	.8266	.7883	.7561	.7279	.7024	.6575	.6182	.4668	.2734	.1605	.0942	.0553	.0039

Table V

Immobile systems with solvent circulation

$P(t)$ values for diffusion from a cylinder

f \ Fo	0.01	0.02	0.03	0.04	0.05	0.06	0.07	0.08	0.10	0.20	0.40	0.60	0.80	1.00
0.80	.6028	.4874	.4127	.3576	.3142	.2787	.2489	.2234	.1818	.0704	.0112	.0018	.0003	.0000
0.90	.6195	.5057	.4311	.3755	.3315	.2952	.2646	.2383	.1951	.0776	.0130	.0022	.0004	.0001
1.00	.6334	.5211	.4467	.3909	.3464	.3096	.2784	.2514	.2070	.0843	.0148	.0026	.0005	.0001
1.10	.6452	.5343	.4602	.4043	.3594	.3222	.2905	.2630	.2176	.0904	.0165	.0030	.0005	.0001
1.20	.6552	.5456	.4719	.4160	.3709	.3334	.3013	.2734	.2271	.0961	0181	.0034	.0006	.0001
1.30	.6639	.5556	.4823	.4263	.3811	.3433	.3109	.2827	.2356	.1013	.0197	.0038	.0007	.0001
1.40	.6716	.5644	.4914	.4355	.3902	.3522	.3195	.2910	.2434	.1061	.0212	.0042	.0008	.0002
1.50	.6783	.5721	.4996	.4438	.3984	.3602	.3273	.2986	.2504	.1106	.0226	.0046	.0009	.0002
1.60	.6842	.5791	.5069	.4512	.4058	.3674	.3344	.3055	.2569	.1147	.0240	.0050	.0010	.0002
1.70	.6896	.5853	.5135	.4579	.4124	.3740	.3409	.3118	.2627	.1186	.0252	.0054	.0011	.0002
1.80	.6943	.5909	.5194	.4640	.4185	.3801	.3468	.3175	.2682	.1221	.0265	.0058	.0012	.0003
1.90	.6987	.5961	.5249	.4695	.4241	.3856	.3522	.3228	.2731	.1255	.0276	.0061	.0013	.0003
2.00	.7026	.6007	.5298	.4746	.4292	.3906	.3572	.3277	.2778	.1286	.0288	.0064	.0014	.0003
3.00	.7284	.6316	.5631	.5090	.4639	.4253	.3915	.3614	.3100	.1513	.0374	.0093	.0023	.0006
5.00	.7501	.6582	.5921	.5393	.4950	.4566	.4227	.3924	.3401	.1739	.0470	.0127	.0034	.0009
10.00	.7670	.6793	.6155	.5640	.5204	.4824	.4487	.4184	.3656	.1941	.0564	.0164	.0048	.0014

Table VI

Immobile systems with solvent circulation

$P(t)$ values for diffusion from a sphere

f \ Fo	0.01	0.02	0.03	0.04	0.05	0.06	0.07	0.08	0.09	0.10	0.20	0.40	0.60	0.80
0.80	.4755	.3497	.2749	.2232	.1848	.1549	.1310	.1115	.0953	.0817	.0187	.0010	.0001	.0000
0.90	.4937	.3673	.2910	.2378	.1979	.1666	.1415	.1209	.1037	.0892	.0212	.0012	.0001	.0000
1.00	.5092	.3825	.3051	.2506	.2095	.1771	.1509	.1294	.1113	.0961	.0234	.0015	.0001	.0000
1.10	.5224	.3957	.3175	.2620	.2198	.1865	.1595	.1371	.1183	.1024	.0256	.0017	.0001	.0000
1.20	.5338	.4073	.3284	.2721	.2291	.1950	.1672	.1441	.1247	.1081	.0277	.0019	.0001	.0000
1.30	.5438	.4175	.3382	.2812	.2375	.2027	.1742	.1505	.1305	.1134	.0296	.0021	.0001	.0000
1.40	.5526	.4267	.3470	.2894	.2451	.2097	.1806	.1564	.1358	.1183	.0314	.0023	.0002	.0000
1.50	.5604	.4348	.3548	.2968	.2520	.2160	.1865	.1617	.1408	.1228	.0332	.0025	.0002	.0000
1.60	.5674	.4422	.3620	.3036	.2583	.2219	.1919	.1667	.1453	.1270	.0348	.0027	.0002	.0000
1.70	.5737	.4488	.3685	.3097	.2641	.2272	.1968	.1713	.1495	.1309	.0363	.0029	.0002	.0000
1.80	.5794	.4549	.3744	.3154	.2694	.2322	.2014	.1755	.1534	.1345	.0378	.0031	.0003	.0000
1.90	.5846	.4604	.3798	.3205	.2742	.2367	.2057	.1794	.1571	.1378	.0392	.0033	.0003	.0000
2.00	.5893	.4654	.3848	.3253	.2788	.2410	.2096	.1831	.1605	.1410	.0405	.0035	.0003	.0000
3.00	.6205	.4997	.4190	.3585	.3104	.2708	.2376	.2093	.1849	.1636	.0505	.0050	.0005	0000
5.00	.6475	.5300	.4500	.3890	.3399	.2991	.2644	.2347	.2088	.1861	.0612	.0068	.0008	.0001
10.00	.6689	.5547	.4757	.4146	.3650	.3234	.2878	.2569	.2299	.2061	.0716	.0089	.0011	.0001

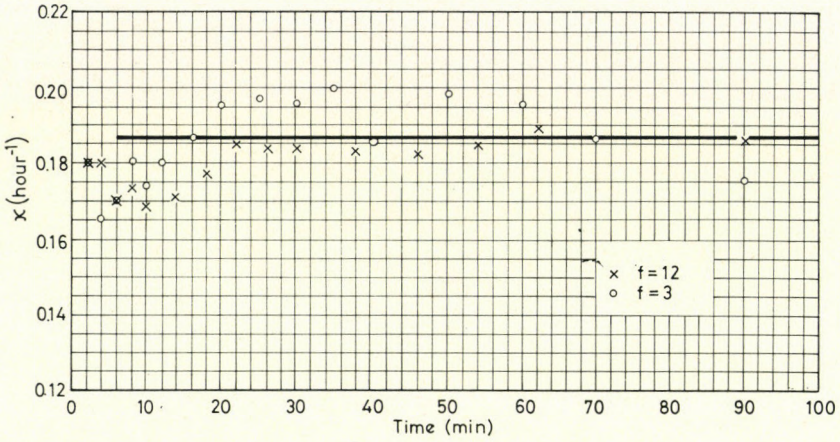

Fig. 10

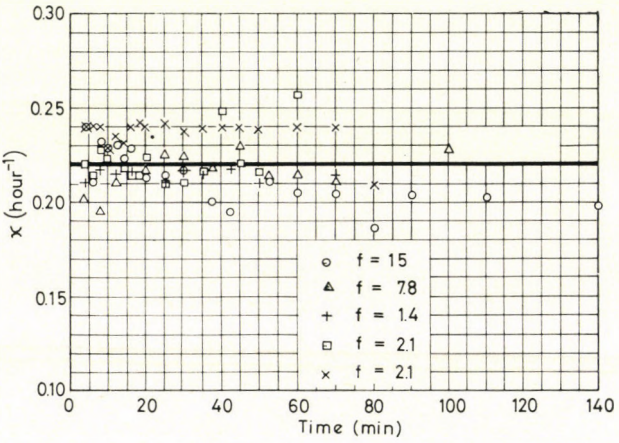

Fig. 11

of $\varkappa$ are unaffected by liquid ratios. The diffusing substance was sodium chloride and phenol in aqueous solution. Figures 13 and 14 show results of experiments with commercial drug substances: these data prove if the heterodispersity is not too large, it may be left out of consideration.

These findings confirm that the simplifying assumptions made at the definition of an "ideal drug-extraction system" are correct. In all model tests the relatively high $\varkappa$-values for short extraction times are presumably due to the rapid dissolution of the adhering liquid layer. If the dimensions of the solid particles vary over wide limits, as in industrial extractions of vegetable drugs, the values decrease with time (*cf.* Fig. 15) because diffusion is initially very rapid from the small particles thus these soon become exhausted and slower diffusion from larger particles will be dominant. We have found that

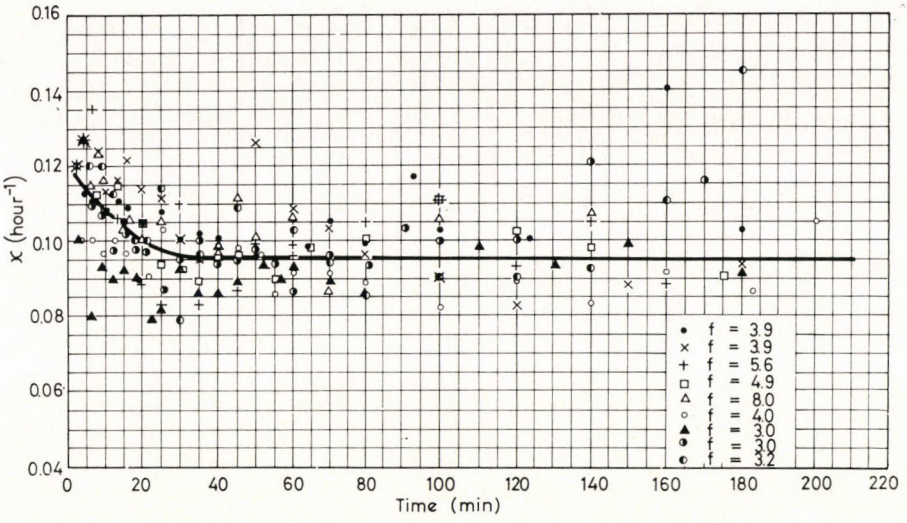

Fig. 12

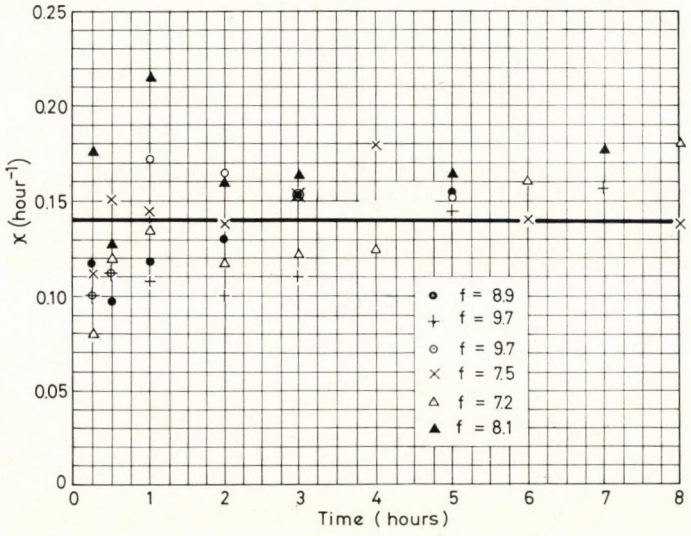

Fig. 13

also in these cases calculations of sufficient accuracy can be carried out provided that we use integral average $\varkappa$-values for the extraction time in the relevant equations. However, if extraction time is the unknown parameter, its determination requires iteration consisting of experimental and calculation steps.

The accuracy of the results obtained with the average $\varkappa$-values mentioned is supported by the study of an extractor operated on an industrial scale for

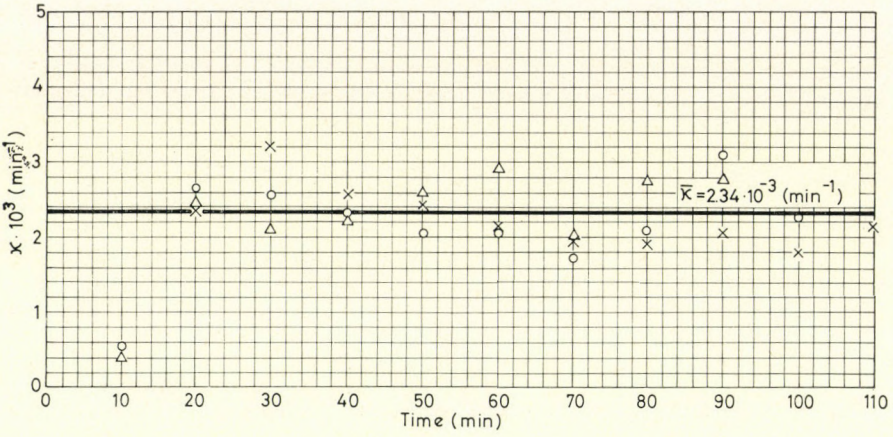

Fig. 14

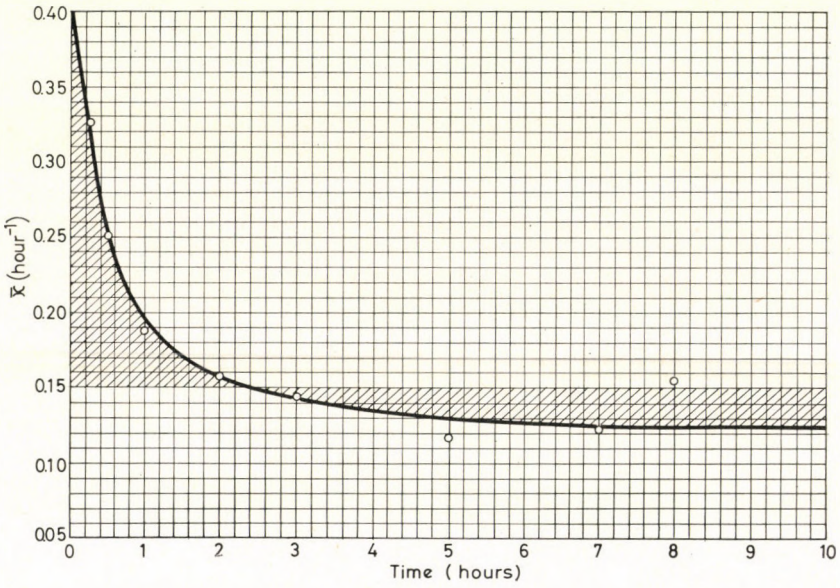

Fig. 15

the production of solasodine: the losses calculated according to our method amount to 6.6% whereas the analytically determined losses in the plant correspond to be 5.6%.

For industrial extraction a plant composed of six diffusers is used. The principle of operation is shown in Fig. 1 and involves double transfer of the liquid. In the one-hour intervals between transfers the liquid is forced by centrifugal pumps through the substrate in the diffusers.

Owing to uncertainties in sampling, the concentration parameters for these commercial diffusers were calculated from an average over a prolonged time (50 days). If the total solasodine introduced with the drug over these 50 days is equal to 100%, 93.37% of the solasodine was found in the extract recovered during the same time and 5.59% was retained in the substrate, thus the error in the material balance amounted to −1.0%.

According to the method described, calculation of the relative loss should be started with the determination of $\varkappa$. Figure 15 shows the results of averaging the experiments; according to this $\bar{\varkappa} = 0.15$. (Owing to the crushed state of the vegetable drug, this value is somewhat higher than that for unbroken leaves (*cf.* Fig. 13), the deviation, however, is not more than 10%.)

The calculation of relative losses is carried out on the basis of Eqs. (8)—(11) and (14). The Fourier number calculated for the one-hour interval of liquid circulation is 0.15. In order to calculate the value of $P(t_c)$, the liquid ratio must be known. This is obtained from actual plant data: if in one vessel the total of the extracting liquid is taken as 100%, the extract removed from one vessel is 61%, *i.e.* the substrate retains 39% of the liquid; the liquid ratio is $f = 1.56$.

From Table IV (or from Fig. 5) at Fo = 0.15 and $f = 1.56$ we find $P(t_c) = 0.42$; from Eq. (9) this gives $\Psi = 0.835$.

In the extraction system we have $N = 6$ diffusers, thus, according to Fig. 1, the number of juice draughts is

$$n = 2(N - 1) = 10 \tag{15}$$

With these values the relative losses calculated according to Eq. (8) amount to $\frac{x_n}{x_0} = 0.0663$ and this is in a very good agreement with the figure of 0.0559 calculated from actual plant operation data.

Thus as proved by expriment and calculations, the proposed simplified method accurately describes industrial extraction operations. It seems now that the design of solid–liquid extraction apparatus or the optimization of existing plants is feasible, to the necessary degree of confidence, without costly pilot-plant investment and experiments. The expressions allow optimization by computer.

A further possibility of utilizing the equations and tables involves calculation of the Fo number or the constant $\bar{\varkappa}$ characteristic of the raw drug or extractive solvent for past operations, provided that recorded data are available for the loss factor $\frac{x_n}{x_0}$, liquid ratio f, residence time t_c or T. With Fo numbers and $\bar{\varkappa}$ values thus established, the changes in loss due to variation of parameters n, f and t_c of an extraction can be predicted without any model

tests. The routine handling of these calculations is illustrated by the following scheme.

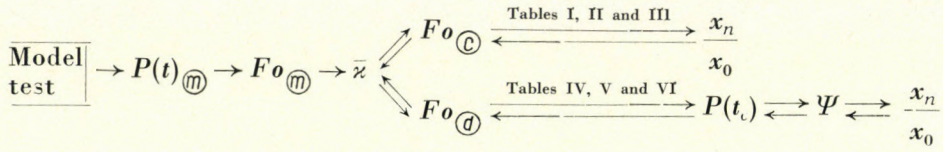

ⓜ model, ⓒ continuous, ⓓ discontinuous

Optimization of the operation is feasible since the expressions are easily adapted for computer evaluation.

Symbols

x = concentration of cell liquor, w/w%
y = concentration in the extractive liquid, w/w%
r = coordinate relative to the axis of symmetry
G = factor of geometrical symmetry
$G = 1$ for plates
$G = 2$ for cylinders
$G = 3$ for spheres
D = diffusivity
T = residence time of the solid phase in the continuous countercurrent apparatus
t = time
t_c = time of circulation (batch-type countercurrent operation)
f = liquid ratio
x_0, y_0 = initial concentrations
y_1 = concentration of the extract
x_n = concentration of the cell liquor in the extracted vegetable drug
μ_k = k-th root of the characteristic equation relevant to the given geometrical shape,
$\operatorname{tg} \mu_k = -f\mu_k$ for plates,
$J_1(\mu_k) = -\frac{1}{2} f\mu_k J_0(\mu_k)$, for cylinders, ($J_0$, J_1 = Bessel functions),
$\operatorname{tg} \mu_k = \frac{3\mu_k}{3 + f \cdot \mu_k^2}$, for spheres.
λ_k = characteristic roots of the solutions of FICK's IInd equation relevant to continuous countercurrent extraction; the equations are formally the same as the ones above but with reversed sign for f, *cf.* Eq. (14)
r_0 = half diameter of solid particles *cf.* Eq. (9)
$P(t)$ = *cf.* Eq. (10)
Fo = Fourier number
n = number of juice draught's
N = number of extraction units

REFERENCES

[1] PÁL, S.: Countercurrent Diffusion Systems (in Hungarian). Fiz. és Alk. Mat. Előadások. MTA Mat. és Term. Tud. Oszt. Közl. **1,** 143 (1949)
[2] OPLATKA, GY.: Magy. Kém. Lapja, **4** (10—11. sz.) 573, 645 (1949)
[3] PÁL, S.: 1. Magyar Mat. Kongr. Közl. 693 (1952)
[4] R. E. TREYBAL: Mass Transfer Operations. 2nd ed., McGraw Hill 1968
[5] WILSON, A. H.: Phil. Mag., Ser. 7., **39,** 48 (1948)
[6] BERTHIER, G.: J. Chim. Phys., **49,** 527 (1942)
[7] J. CRANK: The Mathematics of Diffusion. pp. 52, 70 88. Clarendon Press, Oxford 1956
[8] CRANK, J.:Phil. Mag. Ser. 7., **39,** 130, 362 (1948)

[9] PIRET, E. L., EBEL, R. A., KIANG, C. T., ARMSTRONG, W. P.: Chem. Eng. Progress, **47,** 628 (1951)
[10] ROMANKOV, P. G., CHZHI-TSYUAN BAO, KUROCHKINA, M. I.: Khim. Nauka i Prom., **3,** 506 (1958)
[11] AKSEL'RUD, G. A.: Teoria Diffuzionnovo Izvlechenia Veshcestv iz Porystykh Tel. Lvov Ministerstvo Vyshego Obrazovania, USSR; Lvov Polytech. Inst. 1959
[12] KASAOKA, S., SAKATA, Y., NITTA, K.: J. Chem. Eng. Japan, **1,** 32 (1968)
[13] DRONOV, S. F.: Sakharnaya Prom., **23** (10), 15 (11), 24 (1949)
[14] OPLATKA, GY.: Cukoripari Kut. Int. Évk. pp. 5—64 (1950)
[15] TEGZE, M.: Cukoripari Kut. Int. Évk. p. 123 (1951—52)
[16] SZÁSZ, K., GRACZA, L., LŐRINCZ, CS.: Acta Pharmac. Hung., **31,** 211 (1961)

Károly TETTAMANTI
József MANCZINGER
József HUNEK
Róbert STOMFAI; 1111 Budapest, Müegyetem rkp. 3.
1440 Budapest, POB 35, Hungary

Acta Chimica Academiae Scientiarum Hungaricae, Tomus 85 (1), pp. 47—54 (1975)

BESTIMMUNG VON AMEISENSÄURE UND IHREN DERIVATEN MITTELS REAKTIONS-GASCHROMATOGRAPHIE

C. E. Döring, D. Stevenz, R. Geyer und J. Höpfner

(VEB Leuna-Werke »Walter Ulbricht«, Leuna und Technische Hochschule für Chemie »Carl Schorlemmer«, Merseburg, DDR)

Eingegangen am 8. April, 1974

Ameisensäure im Konzentrationsbereich <100 ppm wird an BPO_4-Katalysatoren unter reaktions-gaschromatographischen Bedingungen dehydratisiert und das gebildete CO an einem nachgeschalteten Hydrierreaktor in CH_4 überführt, das mit einem Flammenionisationsdetektor angezeigt wird. Die Nachweisgrenze liegt bei 3 ppm. Die relative Standardabweichung im Bereich bis 20 ppm liegt bei ±20%, im Bereich bis 100 ppm bei ±5%. Die Selektivität der Bestimmung wird untersucht.

Einleitung und Aufgabenstellung

Die gaschromatographische Analyse von Ameisensäure im Konzentrationsbereich <100 ppm bereitet aus verschiedenen Gründen besondere Schwierigkeiten. Neben der durch die Carboxylgruppe bedingten Adsorptionsaktivität sind dies ihre leichte Zersetzlichkeit an den Metalloberflächen des Gerätes (Verdampfer, Trennsäule, Detektor) und an den oxidischen Oberflächen des Trägermaterials bei erhöhter Temperatur sowie die Tatsache, daß der zur Analyse von Spurenkonzentrationen eingesetzte Flammenionisationsdetektor gegenüber Ameisensäure keinen Response zeigt. Offenbar haben diese Gründe dazu geführt, daß in zahlreichen Arbeiten über die gaschromatographische Analyse von niederen Carbonsäuren die Ameisensäure nicht einbegriffen ist [1], [2], [3], [4], [5].

In der vorliegenden Arbeit wird über Versuche berichtet, die erwähnten Schwierigkeiten mit Hilfe einer reaktions-gaschromatographischen Methode zu umgehen. Als Reaktion wurde die katalytische Zersetzung der Ameisensäure ausgewählt. Ameisensäure läßt sich, wie weiter unten ausgeführt wird, in Abhängigkeit von den gewählten Bedingungen zu CO oder CO_2 zersetzen. Da hiermit das Problem der Detektierbarkeit von Spurenkonzentrationen mit Hilfe des Flammenionisationsdetektors noch nicht gelöst ist, muß sich in einer zweiten Stufe die Konvertierung des Reaktionsproduktes zu Methan anschließen. Schließlich ist zu überlegen, welches Maß an Spezifität mit einer so charakterisierten Arbeitsweise hinsichtlich der Bestimmung von Ameisensäure erreichbar ist.

Die Zersetzung der Ameisensäure unter reaktions-gaschromatographischen Bedingungen

Die katalytische Zersetzung der Ameisensäure in der Gasphase ist bereits an sehr verschiedenartigen Katalysator-Systemen untersucht worden [6, 7]. Während die Zersetzung an metallischen Katalysatoren wie Pd, Pt, Cu, Ni, Cd vorwiegend unter Dehydrierung verläuft

$$HCOOH \rightarrow H_2 + CO_2, \tag{1}$$

erfolgt an oxidischen Katalysatoren daneben auch die Zersetzung unter Dehydratisierung

$$HCOOH \rightarrow H_2O + CO. \tag{2}$$

Das Vorherrschen der einen oder anderen Zersetzungsreaktion wird von der Art des gewählten Metalloxids bestimmt. Auch die Zersetzung der Ameisensäure in flüssiger Phase in Gegenwart starker Mineralsäuren verläuft als Dehydratisierungsreaktion.

Für den vorliegenden Fall kam es darauf an, Bedingungen zu finden, unter denen die Zerfallsreaktionen der Ameisensäure zur reaktions-gaschromatographischen Analyse genutzt werden können. Wesentlich ist eine ausreichende Aktivität des Katalysators, um unter den gaschromatographisch möglichen Verweilzeiten, die durch Trägergasmengenstrom und Länge der Reaktorsäule in Grenzen variiert werden können, die Ameisensäure weitgehend quantitativ zu zersetzen. Da die gasförmigen Zersetzungsprodukte nur mit der Ameisensäure-Konzentration korrelieren sollen, müssen schließlich die Zersetzungsbedingungen sehr spezifisch gestaltet werden. Es ergibt sich somit die Frage, welche der beiden Reaktionen (1) bzw. (2) hierfür besser geeignet ist. Rein von der Stöchiometrie her betrachtet ist auch gegen ein Katalysatorsystem, an dem beide Reaktionen gleichzeitig ablaufen, nichts einzuwenden, da im folgenden Schritt CO und CO_2 gemeinsam zu CH_4 konvertiert und analytisch erfaßt werden können [8]. Vom Standpunkt der Spezifität ist es jedoch vorteilhaft, wenn nur ein Reaktionsprodukt auftritt, das unter den Reaktionsbedingungen nur aus der Ameisensäure gebildet werden kann. Ein Vergleich der Möglichkeiten deutet darauf hin, daß dies am ehesten durch die dehydratisierende Zersetzung der Ameisensäure unter Einfluß starker Mineralsäuren zu erreichen ist. Unter diesen Bedingungen ist CO ein nur für die Ameisensäure und ihre Derivate typisches Reaktionsprodukt. Die Aktivierungsenergien ΔE der HCOOH-Zersetzung in Gegenwart verschiedener Mineralsäuren liegen zwischen 20—28 kcal/mol [9]. Die Aktivierungsenergien thermischer Zersetzungsreaktionen organischer Stoffe, die unter CO-Bildung verlaufen, liegen rund um das Doppelte höher, z. B.

$$CH_3CHO \rightarrow CO + CH_4;\ \Delta E = 48 \text{ kcal}$$
$$(C_2H_5)_2O \rightarrow CO + 2CH_4 + 1/2C_2H_4;\ \Delta E = 53 \text{ kcal}$$

[12]. Die an verschiedenen Dehydrierungskatalysatoren für Reaktion (1) erhaltenen Aktivierungsenergien überstreichen den Bereich von 21—52 kcal/Mol [9], innerhalb dessen beispielsweise auch die ΔE-Werte von Decarboxylierungsreaktionen anderer Carbonsäuren liegen [13].

Die Untersuchung geeigneter Katalysator-Systeme erfolgte folgendermaßen:

An den Probeneinlaßstutzen eines Gaschromatographie-Gerätes GCHF 18/3.1 (VEB Chromatron Berlin) ist ein beheizbarer Reaktor (l = 150 mm, d = 3 mm) angeschraubt, in den am Eingang durch eine Silikonmembran

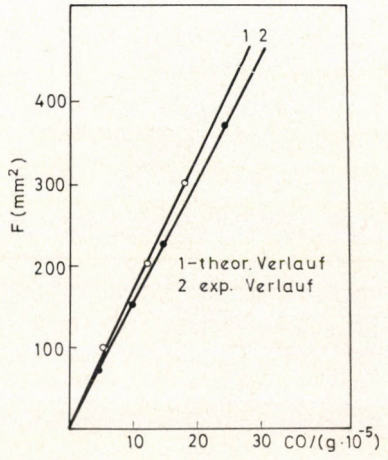

Abb. 1. Umsatz am H_3PO_4/H_3BO_3 Katalysator

hindurch Proben wäßriger Ameisensäurelösungen injiziert werden konnten. Die gebildeten Zersetzungsprodukte wurden an verschiedenen nachgeschalteten Trennsäulen (Porapak Q, Molsieb 5 A, Supergel) identifiziert und CO bzw. CO_2 durch Absoluteichung quantitativ bestimmt. Als Trägergas fand Wasserstoff, als Detektor eine Wärmeleitfähigkeitsmeßzelle Verwendung.

Versuche mit Pd auf Al_2O_3 als Träger (Werkskontakt 7748) sowie mit H_3PO_4-imprägnierter A-Kohle (15—21 Masse % P) im Temperaturbereich von 200—300 °C brachten keine befriedigenden Resultate. Im ersteren Falle wurde CO_2, im zweiten CO als alleiniges Produkt erhalten. In beiden Fällen jedoch betrug der Umsetzungsgrad trotz Erhöhung der Verweilzeit, die mittels einer Bypass-Schaltung realisiert wurde, sowie Übergang zu der aktiveren Diphosphorsäure [10] durch Erhitzen der beladenen A-Kohle bei 255—260 °C im Muffelofen nicht mehr als 30%. Am Pd-Kontakt traten außerdem unübersichtliche Adsorptions-Desorptions-Verhältnisse auf. Dosierung von H_2O im unmittelbaren Anschluß an eine Ameisensäure-Probe führte zur abermaligen Elution eines CO_2-Peaks. In Bestätigung der oben geführten Diskussion zeigte

sich, daß bei der Dosierung von Buttersäure durch Decarboxylierung ebenfalls CO_2-Peaks gebildet wurden.

Gute Ergebnisse wurden jedoch mit dem von GIORGINI *et al.* [11] sowie von anderen beschriebenen Borsäure-Phosphorsäure-Katalysator erhalten. Zu seiner Herstellung wurden kristalline Borsäure und 85%ige H_3PO_4 im Molverhältnis 1 : 1,2 vermischt und bei 100 °C bis zur Gewichtskonstanz getrocknet. Nach Zerkleinern und Sieben wurde bei 300 °C im Muffelofen calziniert. Nach GIORGINI [11] hat die weiße, kristalline Substanz eine tetragonale, bipyramidale Kristallstruktur, in der B^{3+} und P^{5+} tetraedrisch von O^{2-} umgeben ist. Die Zusammensetzung entspricht der formalen Summenformel BPO_4.

Abb. 1 zeigt, daß die mit diesem Katalysator bei 300 °C experimentell gemessenen CO-Werte nahezu mit den theoretischen Werten übereinstimmen. Der Umsetzungsgrad der Ameisensäure beträgt danach 96%.

Die reaktions-gaschromatographische Apparatur

Abb. 2 zeigt das Schema der gesamten reaktions-gaschromatographischen Anordnung.

Der BPO_4-Katalysator ist in einem Glasrohr (180×9 mm) angeordnet, das sich in einem auf 260 °C beheizten Röhrenofen befindet. Im allgemeinen wurden 10 µl der ameisensäurehaltigen Probe direkt auf die Katalysatorschicht aufgegeben. Das Trägergas Wasserstoff strömt mit einer Geschwindigkeit von 3 l/h über den Katalysator und führt das nach Gl. (2) gebildete CO sowie weitere, bei dieser Temperatur flüchtige Bestandteile oder Umsetzungsprodukte der Probe mit. Eine nachgeschaltete Adsorptionsschicht gewährleistet, daß außer CO kein weiterer Bestandteil in die nächste Reaktionszone gelangt, in der die Konvertierung zu CH_4 erfolgt. Als optimal erwies sich die

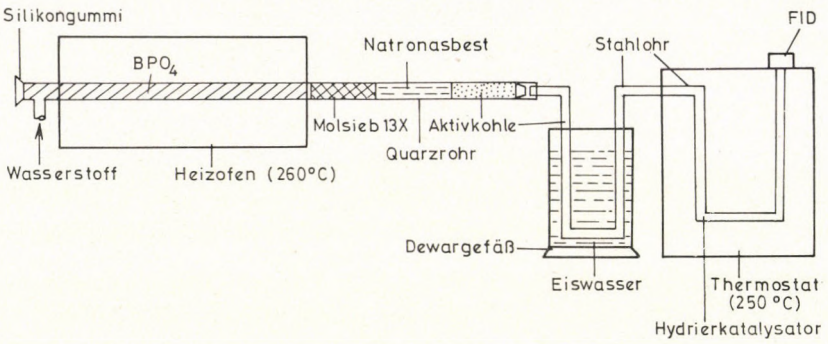

Abb. 2. Schematische Darstellung der Apparatur zur Ameisensäurebestimmung

Anordnung aufeinanderfolgender Adsorptionsschichten von Molsieb 13X, Natronasbest und Aktivkohle. Die letztere wurde auf 0 °C gehalten. Eine solche Adsorptionsstrecke konnte bis zu 50 Dosierungen bei jeweils 10 μl Probelösung, deren Hauptbestandteil Methanol war, aufnehmen ohne daß Störkomponenten auf den Konvertierungskontakt gelangten.

Die Konvertierung des CO zu Methan erfolgte an einem Ni-Katalysator (Werkskontakt 6540), der sich in einer 1 m-Trennsäule innerhalb des Thermostaten des GCHF 18/3-Gerätes befand. Der frische Kontakt wurde im Wasserstoffstrom aktiviert, wobei vom Start bei 50 °C an die Temperatur stündlich um 20 °C bis zur Endtemperatur bei 250 °C erhöht wurde.

Ergebnisse

Abb. 3 zeigt Chromatogramme von Ameisensäureproben verschiedener Konzentration, die nach der beschriebenen Arbeitsweise erhalten wurden. Die Abhängigkeit der Peakfläche des gebildeten Methans von der Ameisensäurekonzentration ist im untersuchten Konzentrationsbereich linear (Abb. 4) und dient als Eichkurve für die Bestimmung der Ameisensäurekonzentration in den zu untersuchenden Proben. Die Bestimmung des Korrelationskoeffizienten r für verschiedene in dieser Weise aufgestellte Eichkurven ergab Werte von 0,999; 0,998; 0,998; 0,997, d. h. die Linearität ist sehr gut. Die relative Standardabweichung im Bereich von 20 ppm liegt bei $\pm 20\%$, im Bereich von 100 ppm bei $\pm 5\%$. Die Nachweisgrenze liegt bei 3 ppm.

Zur Überprüfung der Selektivität der Methode wurden Verbindungen mit verschiedenen funktionellen Gruppen eindosiert: primäre Alkohole (C_1-*n*-C_4; *i*-C_4, 3-Methylbutanol-(1)); sekundäre Alkohole (C_3, C_4, Di-*i*-propylcarbinol, Dimethylphenylcarbinol), tertiäre Alkohole (C_4, C_5, Diacetonalkohol), Äther (C_2, C_4), Ester (Essigsäuremethyl- und äthylester, Buttersäurebutyl-

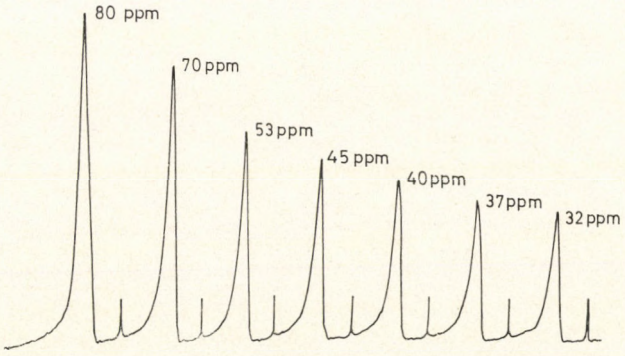

Abb. 3

ester), Carbonsäuren (C_2-C_4), Ketone (Aceton, Methyläthyl-, Methylisopropyl-, Methylisobutyl-, Diisopropyl-Keton, Acetophenon, Mesityloxid), Aldehyde (2%ige Lösung von HCHO in Methanol, C_2, C_3, Acrolein), Kohlenwasserstoffe (Paraffine, Olefine, Aromaten verschiedener C-Zahlen), Propylenoxid. Das Ausbleiben eines Meßeffektes in allen Fällen zeigte in Übereinstimmung mit den eingangs geäußerten Erwartungen, daß diese Verbindungen keine Störeffekte ausüben. Die Methode ist somit zur Bestimmung von Ameisensäure in Gemischen anwendbar, in denen die vorstehend aufgeführten Verbindungsklassen enthalten sind. Wie ersichtlich ist die Selektivität der beschriebenen Arbeitsweise recht beträchtlich. So wurde der Gehalt an Ameisensäure in Phenolgemischen der Cumolphenolsynthese als auch der Gehalt an Ameisensäure und dem entsprechenden Methylester in Produkten der Methanolsynthese routinemäßig bestimmt. Phenole, die bei Zimmertemperatur fest waren, wurden in Methanol gelöst.

Die Untersuchung von Derivaten der Ameisensäure, wie des Methyl-, Äthyl-, *n*-Propyl-, *n*- und *i*-Butyl-Esters sowie von Na-Formiat-Lösungen

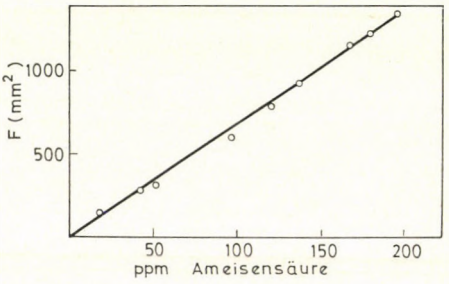

Abb. 4

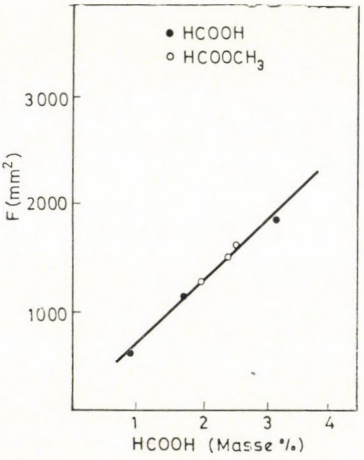

Abb. 5. Umsetzung von HCOOH und $HCOOCH_3$

ergab jedoch, daß sich diese in derselben Weise wie die freie Säure unter CO-Bildung zersetzen. Abb. 5 zeigt, daß man eine Gerade erhält, wenn man bei der Zersetzung von Ameisensäure und von Ameisensäuremethylester die gebildeten CO-Mengen auf die Säure bezieht. Das bedeutet, daß in Proben, in denen neben der Ameisensäure auch mit der Anwesenheit ihrer Ester oder ihrer Salze zu rechnen ist, mit der beschriebenen Methode nur die Summe der die $HC\begin{matrix}\diagup O \\ \diagdown O-\end{matrix}$-Gruppierung tragenden Verbindungen erfaßt wird.

Erweist sich die gesonderte Erfassung von Ameisensäure und ihrem Methylester als erforderlich, so besteht eine Möglichkeit darin, den Ester durch direkte gaschromatographische Analyse an einer geeigneten Trennsäule zu erfassen und die Ameisensäure durch Differenzbildung zu ermitteln.

Eine andere Möglichkeit besteht darin, dem BPO_4-Kontakt eine Trennsäule vorzuschalten, so daß beide Komponenten nacheinander die Zersetzungs- und Konvertierungszone durchlaufen und im Chromatogramm als zwei sepa-

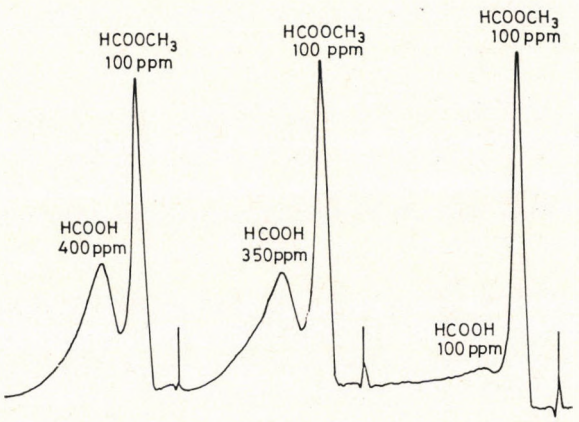

Abb. 6

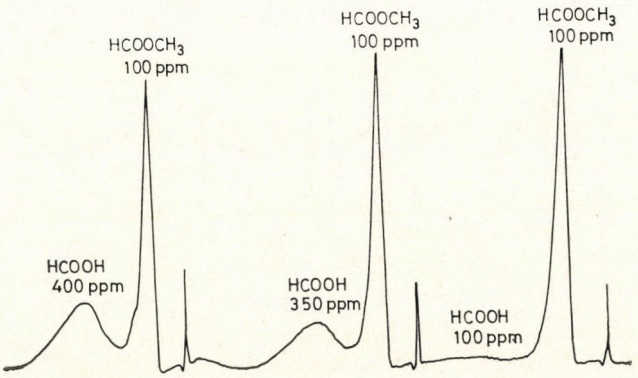

Abb. 7

rate CH_4-Peaks registriert werden. Abb. 6 zeigt ein in dieser Weise erhaltenes Chromatogramm. Die vorgeschaltete Trennzone besaß eine Länge von 100 mm und enthielt Chromosorb 102 als stationäre Phase. Die Temperatur betrug 130 °C. Der erste Peak entspricht dem Ester, der zweite, mit einem Tailing behaftete Peak der Säure. Allerdings liegt bei dieser Arbeitsweise die erreichbare Nachweisgrenze mit 100 ppm wesentlich schlechter. Temperaturerhöhung auf 150 °C (Abb. 7) führt zu verbesserten Peakformen bei gleichzeitiger Verschlechterung der Auflösung beider Peaks.

LITERATUR

[1] Emery, E. W., Koerner, W. E.: Anal. Chem. **33** (1961), 1., 146—147
[2] Mahadevan, V., Stenroos, L.: Anal. Chem. **39** (1967), 1652—1654
[3] Hamid, H. A., Saffle, R. L.: J. Food Sci. **30** (1965), 4, 697
[4] Nakae, T., Nakanishi, T.: J. Agric. Chem. Soc. Japan **37** (1963) 5, 302—305
[5] Saburov, M. A., Demarina, V. F., Cechanskaja, K. L.: Neftepererabotka i Neftechim. 1970, 4, 46—48
[6] Mars, P., Scholten, J. J. F., Zwieterling, H.: Advances in Catalysis, New York and London, Academic Press, 1963, S. 35—109
[7] Sabatier, P., Finkeistein, H.: Die Katalyse in der organischen Chemie 1. Auflage, Leipzig, Akademische Verlagsgesellschaft, 1964, S. 209—220
[8] Williams, F. W., Woods, F. J., Umsteads, M. E.: J. Chromatogr. Sci. **10**(1972) 570—572
[9] Höpfner, J.: Diplomarbeit, TH Merseburg, 1972
[10] Gelbstein, A. J., Ceglova, G. G., Tenikin, M. J.: Ž. fiz. Khim. (Moskva) **30** (1956) 2267—2274
[11] Giorgini, M., Marconi, P. F., Monzani, G., Simula, R.: J. of Catalysis **22** (1971) 521—528
[12] Laidler, K. J.: Chemical Kinetics, Mc Graw-Hill New York, Toronto, London 1950 S. 260 u. S. 268
[13] Pande, G. S.: J. Sci. Ind. Res. **26** (1967) 3939

C. E. Döring, D. Stevenz, R. Geyer, J. Höpfner
VEB Leuna-Werke „Walter Ulbricht" DDR-422 Leuna
Lilienweg 24
Technische Hochschule für Chemie „Carl Schorlemmer"
DDR-42 Merseburg.

Acta Chimica Academiae Scientiarum Hungaricae, Tomus 85 (1), pp. 55–62 (1975)

RADIOLYSIS OF CYCLOHEXANE–HEXAMETHYLBENZENE MIXTURES, I

PURE SUBSTANCES

M. RODER

(Central Research Institute for Physics, Budapest)

Received April 18, 1974

The ^{60}Co gamma radiolysis of cyclohexane–hexamethylbenzene (HMB) mixtures of different compositions has been investigated in liquid and solid phases. The radiation chemical yields of the main products were determined as a function of the mixture composition and temperature.

On the basis of these results it is concluded that HMB exerts a protective effect in cyclohexane decomposition in the liquid phase and this effect can be understood in terms of some kind of physical interaction.

It is a well known observation that aromatic hydrocarbons exhibit, in general, a lower sensitivity to radiation damage than their saturated counterparts. Furthermore, the addition of relatively small amounts of an aromatic substance to a saturated hydrocarbon frequently results in a reduction of radiation sensitivity of the mixture to a much larger extent than would have been predicted under the assumption that each component in the mixture absorbs energy proportional to its electron fraction (*i.e.* the mixture law is violated) [1]. Although there are some conceptions that the non-additivity can be explained by the difference in the primary transfer of energy, it is assumed that the mixture law is valid for primary energy transfer in the hydrocarbon systems and therefore an attempt is made to explain the drop in the radiolysis yields in terms of secondary physical and chemical interactions between the components. The physical interaction consists in the scavenging of the electrons and the positive charge and in the transfer of excitation energy from solvent to solute. The chemical interaction usually means the scavenging of hydrogen or of some other radicals.

Although the nature of both types of interaction in hydrocarbons has been extensively investigated and discussed, especially for cyclohexane–benzene mixtures, their relative importance is far from being resolved. The purpose of the present work has been to study the intermolecular effect of aromatic and saturated molecules in the cyclohexane–hexamethylbenzene (HMB) system. It has been established [2] that in the case of HMB, unlike with other aromatics, the addition of an H-atom to the aromatic ring of the molecule is an unimportant process, and if we find a protective effect toward cyclohexane decomposition, this cannot be attributed to H-atom scavenging. The studies were

carried out on liquid and solid systems and were aimed at the determination of the principal gaseous and liquid radiolysis products (hydrogen, methane, cyclohexene, bicyclohexyl).

Experimental

Hexamethylbenzene ("Fluka" reagent grade) was purified by recrystallization from ethanol followed by threefold sublimation in vacuum. Gas chromatographic analysis of the repurified HMB revealed an impurity concentration less than 0.07%. Cyclohexane ("Merck" spectroscopic grade) was purified by passage through silica gel and was degassed and distilled under vacuum in a greaseless system and stored in an evacuated vessel fitted with break-seal.

Solutions of low HMB concentration were prepared in bulk and aliquots were placed into irradiation vessels fitted with break-seals and were degassed by the freeze-thaw method on a vacuum line and sealed. Blank runs in which the reaction mixtures were not irradiated were carried out to determine any loss of solute during the degassing procedure. Solutions of higher HMB concentrations were made up by weight. The HMB was weighed in the irradiation cell, which was then connected to the vacuum line. After evacuation of the cell a storage vessel of liquid solvent was attached to the vacuum line, its break-seal was opened and a known quantity of solvent was distilled into the cell which was then sealed off. The appropriate choice of the volumes of sample vessels and that of the solutions assured that each solution was in the liquid phase at a temperature of 170°C.

The samples for solid phase irradiation were prepared similarly, they were heated until melting and then were frozen by rapid immersion into liquid nitrogen.

Irradiations were performed in ^{60}Co gamma sources. Dose rates were measured by the Fricke and the Cu-modified Fricke dosimeters, taking $G(Fe^{III}) = 15.6$ and 0.66, respectively, and allowing for the different electron densities of the dosimeter and of the system studied. Higher than ambient temperatures were maintained by a furnace regulated to within ± 2°C. For solid phase irradiations a Dewar vessel containing liquid nitrogen was used.

After irradiation the samples were connected to a vacuum line combined with a Toepler pump and the total volume of the gaseous products volatile at -196°C was measured with a McLeod gauge. The collected gaseous fraction was analyzed by gas chromatography on a 6 m silica gel column at 150°C with nitrogen as carrier gas, using thermal conductivity and flame ionization detectors. Liquid products were analyzed by gas-liquid chromatography using an 8 m polypropylglycol adipate column at 75°C for cyclohexene and a 2 m

silicone grease column at 150°C for bicyclohexyl separation. Individual yields were determined by calibration of the detectors.

Results

Figure 1 shows the number of observed molecules of H_2, $G(H_2)_{obs.}$ and CH_4, $G(CH_4)_{obs.}$ formed per 100 eV of absorbed energy in the cyclohexane–HMB system irradiated at 170°C (melting point of HMB 166°C) plotted as a function of the electron fraction of HMB, in the full range of composition. Since $G(H_2)$ for pure cyclohexane decreases with increasing dose, each sample was irradiated with the same dose of 1.2×10^{20} eV/g. The dashed lines in Fig. 1 represent the yields of hydrogen and methane that would be expected ($G_{expect.}$) if the mixture law were valid. For H_2, the straight line fits the relationship

$$G(H_2)_{expect.} = \varepsilon_{C_6H_{12}} G(H_2)^{\circ}_{C_6H_{12}} + \varepsilon_{HMB} G(H_2)^{\circ}_{HMB} \qquad (1)$$

(and correspondingly for methane) where $G(H_2)^{\circ}_{C_6H_{12}}$ and $G(H_2)^{\circ}_{HMB}$ are the hydrogen yields for pure cyclohexane and pure HMB, respectively, and $\varepsilon_{C_6H_{12}}$ and ε_{HMB} are the electron fractions of the respective components. From Fig. 1 where each point corresponds to the average of three measurements, it can be seen that the yields never obey the mixture law. At low HMB concentrations the observed $G(H_2)$ decreases very rapidly.

The observed $G(CH_4)$ exhibits a positive deviation from the mixture law and this deviation is especially significant in mixtures with low HMB concentrations and shows a maximum at $\varepsilon_{HMB} = 0.1$.

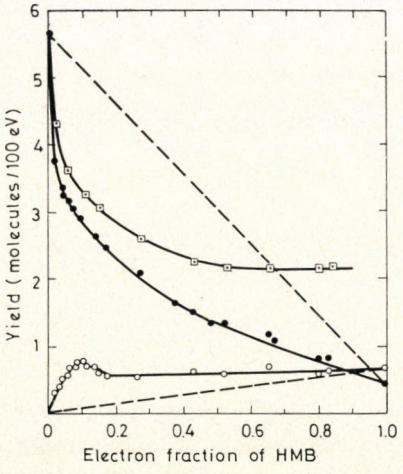

Fig. 1. Dependence of $G(H_2)$, $g(H_2)$ and $G(CH_4)$ on the electron fraction of hexamethylbenzene in cyclohexane–hexamethylbenzene solutions irradiated at 170°C. ● $G(H_2)$, ⊡ $g(H_2)$, ⊙ $G(CH_4)$

A plot of $g(H_2)$, equal to the number of hydrogen molecules formed from cyclohexane per 100 eV dose absorbed by cyclohexane, is also displayed in Fig. 1. The relationship between $G(H_2)_{obs.}$ and $g(H_2)$ is given by Eq. (2) for cyclohexane-HMB

$$G(H_2)_{obs.} = \varepsilon_{C_6H_{12}} g(H_2)_{C_6H_{12}} + \varepsilon_{HMB} g(H_2)_{HMB} \qquad (2)$$

It is assumed that the yield of hydrogen from HMB is unaffected by the presence of cyclohexane, *i.e.* $g(H_2)_{HMB} = G(H_2)^{\circ}_{HMB}$ for all values of ε_{HMB} and, consequently, the observed differences between $G(H_2)_{expect.}$ and $G(H_2)_{obs.}$ can be attributed to a decrease in $g(H_2)$ with increasing HMB concentration.

In order to elucidate the role of the temperature in methane evolution and to compare our results with those for cyclohexane–benzene mixtures with regard to $G(H_2)$, irradiations were performed at different temperatures in the

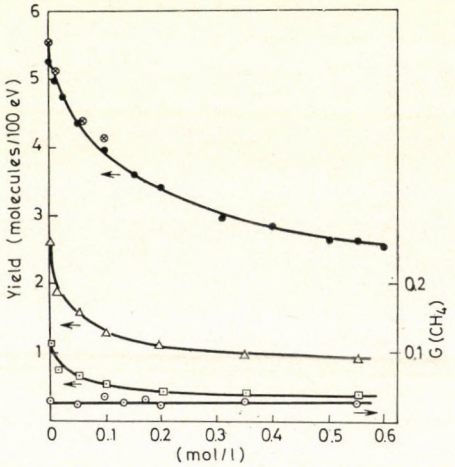

Fig. 2. Dependence of $G(H_2)$, $G(C_6H_{10})$, $G(C_{12}H_{10})$ and $G(CH_4)$ on the solute concentrations; irradiation at 70°C. ● $G(H_2)$, △ $G(C_6H_{10})$, □ $G(C_{12}H_{10})$ and ⊙ $G(CH_4)$ in cyclohexane–hexamethylbenzene solutions, ⊗ $G(H_2)$ in cyclohexane–benzene solutions [3]

liquid phase. The radiolytic hydrogen and methane yields are plotted in Fig. 2 against the HMB concentration in cyclohexane for samples irradiated at 70°C. The temperature dependence of $G(H_2)$ was checked for 10^{-2}—10^{-1} M solutions and was found to remain unchanged between 20°C and 70°C. Results obtained by STONE and DYNE [3] for cyclohexane–benzene mixtures are also presented in this Figure. These data are consistent with the results of MAINON BURTON [4], FREEMAN [5], and KLOTS *et al.* [6]. The plots show that the effect of HMB on $G(H_2)$ is very similar to that observed for cyclohexane–benzene solutions, and that in the concentration range investigated the yield of methane does not change with the HMB concentration.

The *G*-values of the main liquid radiolytic products of cyclohexane, *viz.* cyclohexane and bicyclohexyl, are also shown in Fig. 2 as a function of the HMB concentration.

In Figure 3, $G(H_2)$ is plotted against the electron fraction of HMB for cyclohexane–HMB mixtures irradiated at —196°C, resulting in an approximately linear dependence.

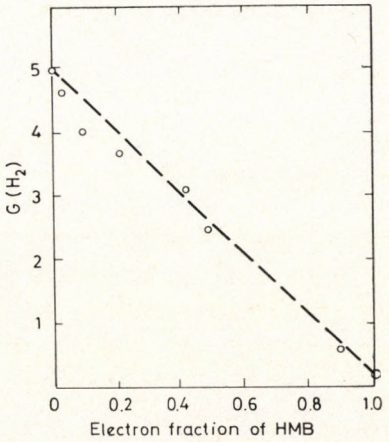

Fig. 3. Dependence of $G(H_2)$ on the electron fraction of hexamethylbenzene irradiated a —196°C

Discussion

Since the curve for $G(H_2)_{obs.}$ in Fig. 1 runs below that for $G(H_2)_{expect.}$, HMB inhibits the formation of hydrogen in the radiolysis of cyclohexane. The extent of the effect of HMB is shown by the decrease in $g(H_2)$ from 5.7 to 2.15. The latter value is that part of $G(H_2)$ for cyclohexane, which is unaffected by the presence of HMB. It can be seen from Fig. 2 that the yield of cyclohexene and bicyclohexyl, the other main radiolytic product of cyclohexane, also decreases with increasing HMB concentration. From the above facts one can conclude that cyclohexane decomposition is reduced owing to a protective effect exerted by HMB; this is roughly of the same magnitude as that observed for benzene. This effect is present in the liquid phase, at least within the temperature range of 20—170°C. The observed product yields — with the sole exception of $G(CH_4)$ — change rapidly with HMB concentration below 0.1 *M*. At higher concentrations the changes are less rapid. It can be seen from the concentration dependence of the yields that the protective effect cannot be a result of a single process.

The following reactions are assumed [7] to contribute to the formation of the main radiolytic products from cyclohexane

$$C_6H_{12} \rightsquigarrow \begin{cases} \rightarrow C_6H_{12}^{+} + e & (1a) \\ \rightarrow C_6H_{12}^{*} & (1b) \end{cases}$$

$$C_6H_{12}^{+} + e \longrightarrow C_6H_{12}^{*} \qquad (2)$$

$$C_6H_{12}^{*} \begin{cases} \rightarrow C_6H_{10} + H_2 & (3a) \\ \rightarrow \dot{H} + \dot{C}_6H_{11} & (3b) \end{cases}$$

$$\dot{H} + C_6H_{12} \longrightarrow H_2 + \dot{C}_6H_{11} \qquad (4)$$

$$\dot{C}_6H_{11} + \dot{C}_6H_{11} \begin{cases} \rightarrow C_6H_{10} + C_6H_{12} & (5a) \\ \rightarrow C_{12}H_{22} & (5b) \end{cases}$$

The initial steps are ionization (1a) and direct excitation (1b). Recombination of an electron and a positive ion leads to an excited molecule (2) too. The excited molecules from reactions (1a) and (2) decompose to give cyclohexene and H_2 (3a) or to give a cyclohexyl radical and an H-atom (3b), the latter having presumably an excess energy (hot H-atom). The H-atom can react further (4) to produce H_2 and another cyclohexyl radical. The cyclohexyl radical can disproportionate (5a) or recombine (5b).

Since it has been shown [2] that H-atom addition to the aromatic ring of HMB is an unimportant process, the observed protective effect of HMB in cyclohexane decomposition can be assumed to be due to a certain physical interaction. This means that the protective effect has to be attributed to some characteristic effect during the moderation of the intermediates of reactions (1) and (2). The values of the ionization potentials in the gas phase are 9.88 eV for cyclohexane [8], 7.85 eV for HMB [9]; the lowest known electronic excited states are characterized by $\sim$7 eV for cyclohexane [10] and $\sim$4 eV for HMB [11]. Thus a protective effect of HMB on cyclohexane by energy transfer in the form of electronic excitation and by charge transfer, are feasible.

HMB may scavenge electrons formed in (1a) giving a negative ion

$$HMB + e \rightarrow HMB^{-} \qquad (6)$$

which alters the recombination process (2) to an ion–ion recombination without the formation of products [12]. Since electron capture reduces the recombination energy by an amount equal to the electron affinity of the negative ion and the remaining energy distributed between the two product molecules, ASMUS *et al.* [13] have concluded from his experimental results that in "$C_6H_{12}^{+}$ + negative ion" type recombination processes the H_2 yield is about zero.

It is assumed that HMB can also scavenge positive charge from the product of reaction (1a)

$$HMB + C_6H_{12}^+ \rightarrow HMB^+ + C_6H_{12} \qquad (7)$$

changing the recombination process (2) to one not yielding $C_6H_{12}^*$. The other possibility for the reduction of the number of excited cyclohexane molecules by HMB is the excitation energy transfer

$$C_6H_{12}^* + HMB \rightarrow C_6H_{12} + HMB^* \qquad (8)$$

This excitation energy transfer is possible from both types of excited molecules produced in direct excitation reaction (1b) and in recombination process (2).

Since all these processes diminish the concentration of excited cyclohexane molecules and they can lead to the reduction of the product yield of cyclohexane radiolysis, as the main products — according to the decomposition scheme — are derived from excited $C_6H_{12}^*$ through subsequent chemical reactions. Thus all these processes may be involved in the protective effect of HMB in cyclohexane decomposition.

The dependence of $G(CH_4)$ on the concentration of mixtures irradiated at 170°C is different from that obtained for systems irradiated at 70°C. At 170°C the observed $G(CH_4)$ value increase with increasing electron fraction of HMB whenever $\varepsilon_{HMB} \leq 0.1$; if, however, $\varepsilon_{HMB} > 0.1$, the yield diminishes with the further increase of ε_{HMB}. In mixtures of low HMB concentration irradiated at 70°C, the $G(CH_4)$ value corresponds to $G(CH_4)$ found for pure cyclohexane. It is likely that HMB at 170° shows some additional chemical effect. At this temperature — in contrast to lower temperatures — reaction (9) of the H-atoms derived from cyclohexane in reaction (3b) may probably occur to a certain extent

$$\dot{H} + C_6(CH_3)_6 \rightarrow CH_4 + \dot{C}_6(CH_3)_5 \qquad (9)$$

This results in a decrease in $G(H_2)$ and an increase in $G(CH_4)$. With increasing concentration of HMB, the probability of reaction (9) decreases as a result of the decreasing amount of H-atoms owing to the increasing probability of reactions (6—8). This qualitative explanation will have to be checked quantitatively in mixtures containing deuterated HMB.

No protective effect of HMB on cyclohexane was observed in mixtures irradiated at —196°C. During freezing a liquid mixture may have formed separating the molecules of cyclohexane and HMB and thus preventing energy and charge transfer [14].

The present investigation shows that HMB exerts a protective effect on cyclohexane in the liquid phase and that this effect can be understood in terms of some kind of physical interaction. In future studies we shall make an attempt to establish the relative probabilities of these interactions by the scavenger technique.

*

Thanks are due to Dr. R. SCHILLER for a critical discussion and to Dr. L. WOJNÁROVITS for his helpful advice regarding gas chromatography.

REFERENCES

[1] KROH, J.: Rad. Res. Rev., **1,** 411 (1969)
[2] RODER, M.: Acta Chim. (Budapest) **73,** 443 (1972)
[3] STONE, J. A., DYNE, P. J.: Rad. Res., **3,** 353 (1963)
[4] MAINON, J. P., BURTON, M.: J. Phys. Chem. **56,** 560 (1952)
[5] FREEMAN, G. R.: J. Chem. Phys., **33,** 71 (1960)
[6] KLOTS, C. E., RAEF, Y., JOHNSEN, R. H.: J. Phys. Chem., **68,** 2040 (1964)
[7] GAUMANN, T., HOIGNE, J.: Aspects of Hydrocarbon Radiolysis, Academic Press, London 1968, p. 159
[8] WATENABLE, K.: J. Chem. Phys. **26,** 542 (1957)
[9] VILESEV, F. I.: Zh. Fiz. Khim. **35,** 2010 (1961)
[10] R. A. HOLROYD: Fundamental Processes in Radiation Chemistry, Interscience Publishers, New York 1968, p. 448
[11] VINOGRADOV, I. P., ALESIN, I. V., DODONOVA, N. JA.: Optika i Spectroskopia, **28,** 477 (1970); **28** 170 (1970)
[12] VOLTZ, R.: International Discussion on Progress and Problems in Contemporary Radiation Chemistry, Prague **1,** 1939 (1971)
[13] ASMUS, K. D., WARMAN, J. M., SCHULER, R. H.: J. Phys. Chem., **74,** 246 (1970)
[14] DYNE, P. T., DENHARTOG, T.: Nature, **1106** (1964)

Magda RODER; 1525 Budapest, 114 P. O. B. 49, Hungary.

Acta Chimica Academiae Scientiarum Hungaricae, Tomus 85 (1), pp. 63—70 (1975)

COLLISION-KINETIC CALCULATION OF REACTION RATE COEFFICIENTS OF ION–MOLECULE REACTIONS, I

EVALUATION OF QUANTUM EFFECTS ON THE BASIS OF A POLARIZATION POTENTIAL

R. SCHMIDT, W. STILLER and R. HABERLANDT

(Zentralinstitut für Isotopen- und Strahlenforschung der Akademie der Wissenschaften der DDR, Leipzig)

Received April 28, 1974

For the r^{-4} interaction potential describing ion–molecule reactions, the classical and quantum-mechanical reactive capture cross-sections σ_{cl} and σ_{qu}, respectively, are compared using an asymptotic expression $\underline{\sigma}_{qu}$ for σ_{qu} (valid for relative energies of $E > E_0$) derived by VOGT and WANNIER. Assuming the velocity distribution functions of ions and molecules to have Maxwellian forms and neglecting internal degrees of freedom of the reactants, partial rate coefficients $\underline{k}_{cl}$ and $\underline{k}_{qu}$ are calculated by a collision-kinetic treatment. Comparison of $\underline{k}_{cl}$ with $\underline{k}_{qu}$ under the assumptions made above results in the conclusion that $\underline{k}_{qu} \approx k_{cl}$ in most physical situations. This is demonstrated by the reaction $CH_4^+ + CH_4 \rightarrow$ products.

Introduction

The reaction rate coefficient k of a homogeneous bimolecular ion–molecule reaction (IMR) between an ion A^+ and a neutral species M according to

$$A^+ + M \rightarrow \text{products} \tag{1}$$

is given on the basis of kinetic gas theory by the relation

$$k = \int_6 v\sigma_{IM}(v) f_I(\vec{v}_I) f_M(\vec{v}_M)\, \mathrm{d}\vec{v}_I\, \mathrm{d}\vec{v}_M \tag{2}$$

where

$\sigma_{IM}(v)$ microscopic reactive ion–molecule cross-section of the reactants A^+ and M,

$f_I(\vec{v}_I), f_M(\vec{v}_M)$ velocity distribution function of the ion and molecule, respectively, and

$v = |\vec{v}_I - \vec{v}_M|$ relative velocity of the reactants.

In the framework of this paper, Eq. (2) represents a satisfactory special case of a more general statistical definition of rate coefficient k, taking into account internal degrees of freedom of reactants, too [1]. Assuming Maxwellian forms for both distribution functions and changing over from the system of

laboratory velocities $\vec{v}_I$, $\vec{v}_M$ to the center-of-mass system, the following expression for k is obtained by integration:

$$k(T) = \left(\frac{8\beta^3}{\pi m}\right)^{1/2} \int_0^\infty E\sigma_{IM}(E)\, e^{-\beta E}\, \mathrm{d}E \tag{3}$$

where

$E = \frac{m}{2} v^2$ relative translational energy;

$m = \frac{m_I m_M}{m_I + m_M}$ reduced mass;

$\beta = \frac{1}{k'T}$; k' is Boltzmann's constant and T the absolute temperature.

As can be seen from Eq. (3), rate coefficient k can be easily calculated if information on the ion–molecule reaction cross-section $\sigma_{IM}(E)$ is available. If gaseous molecules have no permanent dipole moment and the ions are larger than the molecules, then the interaction between the reacting species may be described in the simplest case by the potential

$$V(r) = -\frac{1}{2} e^2 \alpha r^{-4} \tag{4}$$

which takes into account the charge-induced dipole attraction between ions A^+ (charge e) and molecules M (polarizability α) leading to a (classical) capture cross-section [2] of

$$\sigma_{cl}(E) = \pi e \left(\frac{2\alpha}{E}\right)^{1/2} \tag{5}$$

Upon insertion of Eq. (5) into (3), the well-known result is

$$k_{cl} = 2\pi e \left(\frac{\alpha}{m}\right)^{1/2} \tag{6}$$

Now the problem to be treated in this paper is:

(1) what expression would provide a quantum mechanical derivation of the cross-section $\sigma_{qu}(E)$, considering the same potential as in Eq. (4);

(2) what modification of the rate coefficient k according to Eq. (3) would permit the use of $\sigma_{qu}(E)$ in place of $\sigma_d(E)$ in Eq. (3)?

With respect to the first question it must be pointed out that potentials of the form $V \sim r^{-n}$ and the resulting cross-sections were considered by several authors *e.g.* in Refs. [3, 4, 5].

BERNSTEIN [3] has investigated the properties of scattering cross-section σ_{qu} on the basis of a $\{12.6\}$ potential of Lennard–Jones type and explained especially the undulatory behaviour of σ_{qu} obtained by a partial wave treat-

ment of the quantum mechanical cross-section. Resorting to the general case of $V \sim r^{-n}$, CASE [4] studied the difficulties arising in quantum mechanics when the potential is singular. He solved the problem by introducing a fixed phase factor for all the wave functions at the origin.

VOGT and WANNIER [5] calculated the quantum mechanical expression σ_{qm} of the cross-section on the basis of the polarization potential $V(r) \sim r^{-4}$ as in Eq. (4). In what follows the differences between the rate coefficients k_{cl} and k_{qu} for some ion–molecule reactions will be estimated using σ_{cl} and σ_{qu} in Eq. (3) (according to Ref. [5]).

Comparison between the classical and quantum mechanical rate coefficients

VOGT and WANNIER [5] have derived the following expression for the quantum mechanical scattering cross-section $\sigma_{qu}(E)$:

$$\sigma_{qu} = \pi \frac{A^2}{q^2} \sum_{l=0}^{\infty} \frac{2l+1}{1+e^{2\Phi}} \tag{7}$$

where

$$A = \left(\frac{e^2 \alpha m}{\hbar^2}\right)^{1/2} \tag{8}$$

$$q = A \frac{mv}{\hbar} = \left(\frac{2\, e^2 \alpha m^2 E}{\hbar^4}\right)^{1/2} = \varkappa^2 \tag{9}$$

$$\Phi = \Phi\left(l + \frac{1}{2},\ q\right) \tag{10}$$

This function Φ is "exactly defined, but only approximately known". A lower limit Φ_0 and an upper limit Φ_1 bracket this function Φ closely for large l and q.

Φ is used in the approximation $\Phi \approx \frac{1}{2}(\Phi_0 + \Phi_1)$.

As a consequence of the lack of an appropriate representation of the function in Φ Ref. [5], an asymptotic expansion σ_{qu} is given. Considering Eq. (9) for larger $q > q_0$, and retaining only the first 3 terms, the asymptotic expression assumes the form

$$\underline{\sigma}_{qu} = \underline{\sigma}^{(1)}_{qu} + \underline{\sigma}^{(2)}_{qu} + \underline{\sigma}^{(3)}_{qu} =$$

$$= \frac{2\pi e^2 \alpha m}{\hbar^2} \left\{ \frac{1}{\varkappa^2} - \frac{4}{\varkappa^3} e^{-\sqrt{2}\pi} \sin\left[2\pi\sqrt{2}\,\varkappa + \frac{\sqrt{2}\,\pi + 1}{8\varkappa}\right] + \right.$$

$$\left. + \frac{4}{\varkappa^3} e^{-2\pi\sqrt{2}} \sin\left[4\pi\sqrt{2}\,\varkappa + 0\left(\frac{1}{\varkappa}\right)\right] \right\} \text{ for } \varkappa > \varkappa_0 \tag{11}$$

while the classical counterpart is

$$\sigma_{cl} = \frac{2\pi e^2 \alpha m}{\hbar^2} \cdot \frac{1}{\varkappa^2} \qquad \text{for } \varkappa > 0 \tag{12}$$

Therefore

$$\frac{\sigma_{qu}}{\sigma_{cl}} = 1 - \frac{4}{\varkappa} e^{-\sqrt{2}\pi} \sin\left[2\pi\sqrt{2}\,\varkappa + \frac{\sqrt{2}\,\pi + 1}{8\pi}\right] + \\ + \frac{4}{\varkappa} e^{-2\pi\sqrt{2}} \sin\left[4\pi\sqrt{2}\,\varkappa + 0\left(\frac{1}{\varkappa}\right)\right] \quad \text{for } x > x_0 \tag{13}$$

Using Eq. (9) again, Eq. (3) yields

$$k = 8\beta^{3/2}\sqrt{\frac{2}{\pi m}} R^2 \int_{\varkappa=0}^{\infty} \sigma(\varkappa)\,\varkappa^7\, e^{-\beta R\varkappa^4}\,\mathrm{d}\varkappa \tag{14}$$

with

$$R = \frac{\hbar^4}{2\,e^2\alpha m^2} \tag{15}$$

To compare k_{qu} with k_{cl}, it has to be considered that $\underline{\sigma}_{qu}$ is valid for $\varkappa > \varkappa_0$ only. Hence it is only possible to compare the "partial" rate coefficients

$$\underline{k}_{qu} = \underline{k}_{qu}^{(1)} + \underline{k}_{qu}^{(2)} + \underline{k}_{qu}^{(3)} \\ = 8\beta^{3/2}\sqrt{\frac{2}{\pi m}} R^2 \int_{\varkappa_0}^{\infty} \underline{\sigma}_{qu}^{(1)}\,\varkappa^7 e^{-\beta R\varkappa^4}\,\mathrm{d}\varkappa + \\ + 8\beta^{3/2}\sqrt{\frac{2}{\pi m}} R^2 \int_{\varkappa_0}^{\infty} \underline{\sigma}_{qu}^{(2)}\,\varkappa^7 e^{-\beta R\varkappa^4}\,\mathrm{d}\varkappa + \\ + 8\beta^{3/2}\sqrt{\frac{2}{\pi m}} R^2 \int_{\varkappa_0}^{\infty} \underline{\sigma}_{qu}^{(3)}\,\varkappa^7 e^{-\beta R\varkappa^4}\,\mathrm{d}\varkappa \tag{16}$$

and

$$\underline{k}_{cl} = 8\beta^{3/2}\sqrt{\frac{2}{\pi m}} R^2 \int_{\varkappa_0}^{\infty} \sigma_{cl}\,\varkappa^7 e^{-\beta R\varkappa^4}\,\mathrm{d}\varkappa\,, \tag{17}$$

respectively.

$$\underline{k}_{qu}^{(1)} = 16\sqrt{\frac{\pi e^2\alpha}{m}}\,(\beta R)^{3/2} \int_{\varkappa_0}^{\infty} \varkappa^5 e^{-\beta R\varkappa^4}\,\mathrm{d}\varkappa = \\ = 4\sqrt{\frac{\pi e^2\alpha}{m}}\left\{\sqrt{\beta R}\;\varkappa_0^2 e^{-\beta R\varkappa_0^4} + \frac{\sqrt{\pi}}{2}\,erfc\left(\sqrt{\beta R}\;\varkappa_0^2\right)\right\} = \underline{k}_{cl} \tag{18}$$

As to be seen from Eq. (18), the $\underline{k}_{qu}^{(1)}$ part of the quantum mechanical partial rate coefficient $\underline{k}_{qu}$ corresponds with the partial classical value $\underline{k}_d$, i.e. the contributions $\Delta\underline{k}_{qu} = \underline{k}_{qu}^{(2)} + \underline{k}_{qu}^{(3)}$ represent the quantum mechanical

corrections of the classical partial rate coefficient $\underline{k}_d$.

$$\underline{k}_{qu}^{(2)} = -64 \sqrt{\frac{\pi e^2 \alpha}{m}}\, e^{-\sqrt{2}\,\pi}\, (\beta R)^{3/2} \int_{\varkappa_0}^{\infty} \varkappa^4 e^{-\beta R \varkappa^4} \sin\left[2\pi\sqrt{2}\,\varkappa + \frac{\sqrt{2}\,\pi + 1}{8\varkappa}\right] \mathrm{d}\varkappa$$

In further calculations the term $\dfrac{\sqrt{2}\pi + 1}{8\varkappa}$ will be omitted.

$$\underline{k}_{qu}^{(2)} = -64 \sqrt{\frac{\pi e^2 \alpha}{m}}\, e^{-\sqrt{2}\,\pi}\, (\beta R)^{3/2} \int_{\varkappa_0}^{\infty} \varkappa^4 e^{-\beta R \varkappa^4} \sin\left(2\pi\sqrt{2}\,\varkappa\right) \mathrm{d}\varkappa =$$

$$= -\frac{1}{2} \sqrt{\frac{\pi e^2 \alpha}{m}} \frac{e^{-\sqrt{2}\,\pi}}{\pi^5} (\beta R)^{3/2} \int_{x = 2\pi\sqrt{2}\,\varkappa_0}^{\infty} x^4 \exp\left(-\frac{\beta R}{64\pi^4} x^4\right) \cdot \sum_{\nu=0}^{\infty} \frac{(-1)^\nu}{(2\nu+1)!}\, x^{2\nu+1}\, \mathrm{d}x$$

$$= -\frac{1}{2} \sqrt{\frac{\pi e^2 \alpha}{m}} \frac{e^{-\sqrt{2}\,\pi}}{\pi^5} (\beta R)^{3/2} \sum_{\nu=0}^{\infty} \frac{(-1)^\nu}{(2\nu+1)!} \int_{2\pi\sqrt{2}\,\varkappa_0}^{\infty} x^{2\nu+5} \exp\left(-\frac{\beta R x^4}{64\pi^4}\right) \mathrm{d}x =$$

$$= -\frac{1}{4\pi^5} \sqrt{\frac{\pi e^2 \alpha}{2m}}\, e^{-\sqrt{2}\,\pi}\, (\beta R)^{3/2} \sum_{\mu=2}^{\infty} \frac{(-1)^\mu}{(2\mu-3)!} \left(\frac{8\pi^2}{\sqrt{\beta R}}\right)^{\mu+1} \int_{\xi = \sqrt{\beta R}\,\varkappa_0^2}^{\infty} e^{-\xi^2} \xi^\mu \,\mathrm{d}\xi$$

$$\underline{k}_{qu}^{(2)} = -\frac{1}{4\pi^5} \sqrt{\frac{\pi e^2 \alpha}{2m}}\, e^{-\sqrt{2}\,\pi}\, (\beta R)^{3/2} \times$$

$$\times \sum_{\mu=2}^{\infty} \frac{(-1)^\mu}{(2\mu-3)!} \left(\frac{8\pi^2}{\sqrt{\beta R}}\right)^{\mu+1} \left\{ e^{-\beta R \varkappa_0^4} \sum_{\nu=0}^{r-1} \frac{(\mu-1; -2; \nu)}{2^{\nu+1}} \left(\sqrt{\beta R}\,\varkappa_0^2\right)^{\mu-2\nu-1} + \right.$$

$$\left. + (1-s) \frac{(1; 2; r)}{2^{r+1}} \sqrt{\pi}\, erfc\left(\sqrt{\beta R}\,\varkappa_0^2\right) \right\} \qquad (19)$$

where

$\mu = 2r - s$ ($s = 0$ or 1),

$(m; d; \nu) = m(m+d)(m+2d) \ldots (m + (\nu-1)d)$
for m and d real and ν natural,

$(m; -d; \nu) = (m - (\nu-1)d; d; \nu)$,

$(m; d; 0) = 0$.

$$\underline{k}_{qu}^{(3)} = 64 \sqrt{\frac{\pi e^2 \alpha}{m}}\, e^{-2\sqrt{2}\,\pi}\, (\beta R)^{3/2} \int_{\varkappa_0}^{\infty} \varkappa^4 e^{-\beta R \varkappa^4} \sin\left(4\pi\sqrt{2}\,\varkappa\right) \mathrm{d}\varkappa =$$

$$= \frac{1}{64\pi^5} \sqrt{\frac{\pi e^2 \alpha}{2m}}\, e^{-2\sqrt{2}\,\pi}\, (\beta R)^{3/2} \int_{x_0 = 4\pi\sqrt{2}\,\varkappa_0}^{\infty} x^4 \exp\left(-\frac{\beta R x^4}{1024\pi^4}\right) \times$$

$$\times \sum_{\nu=0}^{\infty} \frac{(-1)^\nu}{(2\nu+1)!}\, x^{2\nu+1}\, \mathrm{d}x =$$

$$= \frac{1}{64\pi^5} \sqrt{\frac{\pi e^2 \alpha}{2m}}\, e^{-2\sqrt{2}\,\pi}\, (\beta R)^{3/2} \sum_{\nu=0}^{\infty} \frac{(-1)^\nu}{(2\nu+1)!} \int_{x_0}^{\infty} x^{2\nu+5} \exp\left(-\frac{\beta R x^4}{1024\pi^4}\right) \mathrm{d}x =$$

$$= \frac{1}{128\pi^5} \sqrt{\frac{\pi e^2 \alpha}{2m}}\, e^{-2\sqrt{2}\,\pi}\, (\beta R)^{3/2} \sum_{\mu=2}^{\infty} \frac{(-1)^\mu}{(2\mu-3)!} \left(\frac{32\pi^2}{\sqrt{\beta R}}\right)^{\mu+1} \int_{\xi_0 = \sqrt{\beta R}\,\varkappa_0^2}^{\infty} e^{-\xi^2} \xi^\mu \,\mathrm{d}\xi$$

$$\underline{k}_{qu}^{(3)} = \frac{1}{128\,\pi^5}\sqrt{\frac{\pi e^2\alpha}{2\,m}}\,e^{-2\sqrt{2}\,\pi}\,(\beta R)^{3/2}\times$$

$$\times\sum_{\mu=2}^{\infty}\frac{(-1)^{\mu}}{(2\,\mu-3)!}\left(\frac{32\,\pi^2}{\sqrt{\beta R}}\right)^{\mu+1}\left\{e^{-\beta R\varkappa_0^4}\sum_{\nu=0}^{r-1}\frac{(\mu-1;\,-2;\,\nu)}{2^{\nu+1}}\left(\sqrt{\beta R}\;\varkappa_0^2\right)^{\mu-2\nu-1}+\right.$$

$$\left.+\,(1-s)\,\frac{(1;\,2;\,r)}{2^{r+1}}\sqrt{\pi}\;erfc\left(\sqrt{\beta R}\;\varkappa_0^2\right)\right\} \qquad (20)$$

where $\mu = 2r - s$ ($s = 0$ or 1).

Thus the quantum mechanical "partial" rate coefficient $\underline{k}_{qu}$ is given by $\underline{k}_{qu} = \underline{k}_{qu}^{(1)} + \underline{k}_{qu}^{(2)} + \underline{k}_{qu}^{(3)}$.

Numerical results

The equations presented above are used in the following notation:

$$\underline{k}_{qu}^{(1)} = 16\sqrt{\frac{\pi e^2\alpha}{m}}\int_{x_0=\sqrt[4]{\beta R}\;\varkappa_0'}^{3} x^5 e^{-x^4}\,dx$$

$$\underline{k}_{qu}^{(2)} =$$

$$= -64\sqrt{\frac{\pi e^2\alpha}{m}}\,e^{-\sqrt{2}\,\pi}\sqrt[4]{\beta R}\int_{x_0=\sqrt[4]{\beta R}\;\varkappa_0'}^{3} x^4 e^{-x^4}\sin\left(\frac{2\,\pi\sqrt{2}\;x}{\sqrt[4]{\beta R}}+\frac{\sqrt{2}\,\pi+1}{8}\cdot\frac{\sqrt[4]{\beta R}}{x}\right)dx$$

$$\underline{k}_{qu}^{(3)} = 64\sqrt{\frac{\pi e^2\alpha}{m}}\,e^{-2\sqrt{2}\,\pi}\sqrt[4]{\beta R}\int_{x_0=\sqrt[4]{\beta R}\;\varkappa_0}^{3} x^4 e^{-x^4}\sin\left(\frac{4\,\pi\sqrt{2}\;x}{\sqrt[4]{\beta R}}\right)dx$$

Remarks on the integrals:

a) Lower limit:

The lower limit must be sufficiently large to reach the range of validity of the asymptotic expansion. Taking $\varkappa = \varkappa_0 = \sqrt{0.5}$ the asymptotic expansion is accurate to within less than 0.8% in the neighbourhood of $\varkappa_0$ (see Fig. 3 in Ref. [5]). A slightly different value $\varkappa_0'$ is used for calculation making the integral to a relative extremum.

b) The upper limit should be ∞, but it is quite sufficient for our purposes to choose $x = 3$. At this point the integrand is already smaller than 10^{-33}.

Examples:

A hypothetical reaction is first examined. The parameters of this reaction (m, α) are selected to give corrections as large as possible in comparison with the classical value $\underline{k}_{cl}$.

The second example is the reaction $CH_4^+ + CH_4 \rightarrow$ products.

Table I

Hypothetical ion–molecule reaction $A^+ + B \rightarrow$ *products*
$m = 5 \times 10^{-25}$ g
$\alpha = 10^{-25}$ cm^3

(K) T	($cm^3 s^{-1}$)		
	$\underline{k}_{qu}^{(1)} = k_{cl}$	$\lvert \underline{k}_{qu}^{(2)} \rvert$	$\lvert \underline{k}_{qu}^{(3)} \rvert$
0.1	1.21×10^{-9}	$< 4 \cdot 10^{-11}$	$< 10^{-12}$
1	2.88×10^{-9}	$< 10^{-11}$	$< 10^{-14}$
10	2.99×10^{-9}	$< 10^{-13}$	$< 10^{-15}$
300	3.00×10^{-9}	$< 10^{-15}$	$< 10^{-17}$

Note: A temperature dependence exists for $\underline{k}_{qu}^{(1)}$ (resulting from the variable lower limit of integration) but not, of course, for the classical constant k_{cl}.

Table II

Ion–molecule reaction $CH_4^+ + CH_4 \rightarrow$ *products*

$m = 1.336 \times 10^{-23}$ g
$\alpha = 2.6 \times 10^{-24}$ cm^3

(K) T	($cm^3 s^{-1}$)		
	$\underline{k}_{qu}^{(1)} = k_{cl}$	$\lvert \underline{k}_{qu}^{(2)} \rvert$	$\lvert \underline{k}_{qu}^{(3)} \rvert$
0.1	1.32×10^{-9}	$< 10^{-15}$	$< 10^{-18}$
1	1.32×10^{-9}	$< 10^{-17}$	$< 10^{-19}$
10	1.32×10^{-9}	$< 10^{-18}$	$< 10^{-21}$
300	1.32×10^{-9}	$< 10^{-19}$	$< 10^{-22}$

Conclusions

For ion–molecule reactions described by an r^{-4} interaction potential the classical and quantum mechanical reactive capture cross-sections σ_d and σ_{qu}, respectively, were compared using an asymptotic expression $\underline{\sigma}_{qu}$ for σ_{qu} (valid for relative energies of $E > E_0$) derived by VOGT and WANNIER [5]. Assuming that the velocity distribution functions of both reactants have Maxwellian forms and neglecting internal degrees of freedom of the reactants, partial rate coefficients $\underline{k}_d$ and $\underline{k}_{qu}$ were calculated by a collision-kinetic treatment.

As may be seen from the numerical results, it is sufficient for a wide range of the parameters m, α T to use the classical value $\underline{k}_d$ instead of its quantum mechanical version $\underline{k}_{qu} = \underline{k}_d + \Delta \underline{k}_{qu}$ because of the smallness of quantum mechanical corrections $\Delta \underline{k}_{qu}$.

However, for full comparison between k_{qu} and k_{cl}, it would be necessary to calculate the contributions $\bar{k}_{qu}$ and $\bar{k}_{cl}$, too; these terms could be obtained according to Eq. (3) by integration from 0 to E_0, *i.e.* up to the energy value, E_0, where is the begining of validity of the asymptotic formula of σ_{qu}. By the owing to the uncertainty of the mathematical form of the function Φ in the exact σ_{qu} expression, Eq. (7), it is impossible to make full comparison between the total values $k_{qu} = \bar{k}_{qu} + \underline{k}_{qu}$ and $k_{cl} = \bar{k}_{cl} + \underline{k}_{cl}$.

REFERENCES

[1] ELIASON, M. A., HIRSCHFELDER, H. O.: J. Chem. Phys., **30,** 1426 (1959)
[2] GIOUMOUSIS, G., STEVENSON, D. P.: J. Chem. Phys., **29,** 294 (1958)
[3] BERNSTEIN, R. B.: J. Chem. Phys., **36,** 1403 (1962); **37,** 1880 (1962); **38,** 2599 (1963)
[4] CASE, K. M.: Phys. Rev., **80,** 797 (1950)
[5] VOGT, E., WANNIER, G. H.: Phys. Rev., **95,** 1190 (1954)

R. SCHMIDT
W. STILLER
R. HABERLANDT

Zentralinstitut für Isotopen- und Strahlenforschung der Akademie der Wissenschaften der DDR, 705 Leipzig, Permoserstr. 15. DDR.

Acta Chimica Academiae Scientiarum Hungaricae, 85 (1), pp. 71—78 (1975)

SCHIFF BASE DERIVATIVES OF LANTHANONS

SYNTHESIS OF POLYMERIC DERIVATIVES OF La(III), Pr(III) AND Nd(III) FROM THE SCHIFF BASES DERIVED FROM THE CONDENZATION OF BENZALDEHYDE WITH HYDROXY ALKYLAMINES OR HYDROXY ARYLAMINES

S. K. AGARWAL and J. P. TANDON

(Department of Chemistry, University of Rajasthan, Jaipur, India)

Received July 17, 1974

Compounds characterized by the formula $Ln(O\text{-}i\text{-}C_3H_7)_{3-n}(C_6H_5C(H){:}NR)_n$ (where Ln = La(III), Pr(III) or Nd(III); $n = 1$ or 2; and R = $—CH_2CH_2O$, $—CH_2CHCH_3O$ and $—C_6H_4O$) have been synthesized by the reaction of the isopropoxides of lanthanides with the Schiff bases, $C_6H_5C(H){:}NCH_2CH_2OH$, $C_6H_5C(H){:}{:}NCH_2CH(OH)CH_3$ and $C_6H_5C(H){:}NC_6H_4OH$ in different stoichiometric ratios in dry benzene. The resulting derivatives tend to polymerize as shown by their change into almost insoluble and higher melting materials on standing. On the basis of elemental analyses, molecular weights of freshly prepared samples, IR spectra and exchange reactions, the plausible structures of the resulting derivatives are indicated.

Introduction

In recent years, there has been a renewed interest in the synthesis of a variety of polymeric derivatives of transitional as well as non-transitional elements, as these are now assuming increased industrial importance [1—4]. Syntheses of products with polymeric Schiff bases have also been reported [5]. In earlier work in these laboratories, syntheses of a variety of Shiff base derivatives of some of the lanthanons have been studied [6, 7]. However, polymeric derivatives of lanthanides with the Schiff bases do not seem to have been prepared so far, and in the present paper the synthesis of some such derivatives, which appear to polymerize on standing is reported.

Experimental

Materials

Lanthanum(III), praseodymium(III) and neodymium(III) isopropoxides were prepared from their oxides (Schuchardt, Germany) by the sodium alkoxide method and analyzed before use [8].

Benzene (B. D. H.) was refluxed over sodium wire for several hours and finally distilled azeotropically with ethanol. Isopropanol (B. D. H.) was dried by distilling first from sodium metal and finally from aluminium isopropoxide.

Preparation of Schiff bases

(i) *Benzylidine-2-hydroxyethylamine* ($C_9H_{11}ON$)

Benzaldehyde (15.9 g) and 2-hydroxyethylamine (9.1 g) were taken up in benzene. A highly exothermic reaction took place resulting in a clear reddish solution. This was refluxed

Table 1

Reactions of La(III), Pr(III) and Nd(III) isopropoxides with the Schiff bases

$Ln(O-i-C_3H_7)_3$ (g)	Schiff base (g)	Molar ratio	Refluxing time (hrs.)	Product and characteristics	Isopropanol in the azeotrope, Found (Calcd.)	Analysis %		Molecular weight	Molecular association
						Ln Found (Calcd.)	N Found (Calcd.)	Found (Calcd.)	
$La(O-i-C_3H_7)_3$	$C_9H_{11}ON$	1:1	8	$La(O-i-C_3H_7)_2(C_9H_{10}ON)$	0.21 (0.24)	34.28 (34.28)	3.37 (3.45)	852 (405)	2.1
1.28	0.60			Light yellow solid, soluble in benzene					
$La(O-i-C_3H_7)_3$	$C_9H_{11}ON$	1:2	11	$La(O-i-C_3H_7)(C_9H_{10}ON)_2$	0.57 (0.60)	27.58 (28.09)	5.58 (5.63)	692 (494)	1.4
1.58	1.49			Light yellow solid, soluble in benzene					
$La(O-i-C_3H_7)_3$	$C_{10}H_{13}ON$	1:1	8	$La(O-i-3_3H_7)_2(C_{10}H_{12}ON)$	0.08 (0.08)	33.10 (33.14)	3.37 (3.33)	876 (419)	2.0
0.44	0.22			Light yellow solid, soluble in benzene					
$La(O-i-C_3H_7)_3$	$C_{10}H_{13}ON$	1:2	11	$La(O-i-C_3H_7)(C_{10}H_{12}ON)_2$	0.20 (0.20)	26.62 (26.61)	5.35 (5.36)	748 (522)	1.4
0.54	0.56			Light yellow solid, soluble in benzene					
$La(O-i-C_3H_7)_3$	$C_{13}H_{11}ON$	1:1	10	$La(O-i-C_3H_7)_2(C_{13}H_{10}ON)$	0.09 (0.09)	30.61 (30.65)	3.12 (3.08)	—	—
0.48	0.30			Blackish solid, insoluble in benzene					
$La(O-i-C_3H_7)_3$	$C_{13}H_{11}ON$	1:2	15	$La(O-i-C_3H_7)(C_{13}H_{10}ON)_2$	0.17 (0.17)	23.52 (23.53)	4.75 (4.74)	—	—
0.45	0.57			Blackish solid, insoluble in benzene					
$Pr(O-i-C_3H_7)_3$	$C_9H_{11}ON$	1:1	8	$Pr(O-i-C_3H_7)_2(C_9H_{10}ON)$	0.14 (0.14)	34.66 (34.59)	3.40 (3.41)	830 (407)	2.0
0.76	0.36			Yellow solid, soluble in benzene					
$Pr(O-i-C_3H_7)_3$	$C_9H_{11}ON$	1:2	11	$Pr(O-i-C_3H_7)(C_9H_{10}ON)_2$	0.23 (0.24)	28.36 (28.38)	5.60 (5.64)	750 (496)	1.5
0.65	0.61			Yellow solid, soluble in benzene					
$Pr(O-i-C_3H_7)_3$	$C_{10}H_{13}ON$	1:1	8	$Pr(O-i-C_3H_7)_2(C_{10}H_{12}ON)$	0.11 (0.11)	33.42 (33.45)	3.36 (3.32)	848 (421)	2.0
0.59	0.30			Yellow solid, soluble in benzene					

$Pr(O\text{-}i\text{-}C_3H_7)_3$	$C_{10}H_{13}ON$	1:2	11	$Pr(O\text{-}i\text{-}C_3H_7)(C_{10}H_{12}ON)_2$	0.18	26.82	5.30	800	1.5
0.49	0.51			Yellow solid, soluble in benzene	(0.18)	(26.85)	(5.34)	(524)	
$Pr(O\text{-}i\text{-}C_3H_7)_3$	$C_{13}H_{11}ON$	1:1	10	$Pr(O\text{-}i\text{-}C_3H_7)_2(C_{13}H_{10}ON)$	0.11	30.96	3.00	—	—
0.60	0.37			Blackish solid, insoluble in benzene	(0.11)	(30.94)	(3.07)		
$Pr(O\text{-}i\text{-}C_3H_7)_3$	$C_{13}H_{11}ON$	1:2	15	$Pr(O\text{-}i\text{-}C_3H_7)(C_{13}H_{10}ON)_2$	0.20	23.80	4.77	—	—
0.54	0.67			Blackish solid, insoluble in benzene	(0.20)	(23.79)	(472).		
$Nd(O\text{-}i\text{-}C_3H_7)_3$	$C_9H_{11}ON$	1:1	8	$Nd(O\text{-}i\text{-}C_3H_7)_2(C_9H_{10}ON)$	0.18	35.10	3.38	835	2.0
0.98	0.45			Yellow solid, soluble in benzene	(0.18)	(35.13)	(3.41)	(410)	
$Nd(O\text{-}i\text{-}C_3H_7)_3$	$C_9H_{11}ON$	1:2	11	$Nd(O\text{-}i\text{-}C_3H_7)(C_9H_{10}ON)_2$	0.27	28.78	5.65	750	1.5
0.75	0.70			Deep yellow solid, soluble in benzene	(0.28)	(28.86)	(5.60)	(499)	
$Nd(O\text{-}i\text{-}C_3H_7)_3$	$C_{10}H_{13}ON$	1:1	8	$Nd(O\text{-}i\text{-}C_3H_7)_2(C_{10}H_{12}ON)$	0.11	33.99	3.26	862	2.0
0.63	0.32			Yellow solid, soluble in benzene	(0.11)	(33.96)	(3.29)	(424)	
$Nd(O\text{-}i\text{-}C_3H_7)_3$	$C_{10}H_{13}ON$	1:2	11	$Nd(O\text{-}i\text{-}C_3H_7)(C_{10}H_{12}ON)_2$	0.20	26.70	5.34	802	1.5
0.56	0.57			Deep yellow solid, soluble in benzene	(0.21)	(26.71)	(5.30)	(527)	
$Nd(O\text{-}i\text{-}C_3H_7)_3$	$C_{13}H_{11}ON$	1:1	10	$Nd(O\text{-}i\text{-}C_3H_7)_2(C_{13}H_{10}ON)$	0.10	31.49	2.99	—	—
0.53	0.33			Blackish solid, insoluble in benzene	(0.10)	(31.44)	(3.05)		
$Nd(O\text{-}i\text{-}C_3H_7)_3$	$C_{13}H_{11}ON$	1:2	15	$Nd(O\text{-}i\text{-}C_3H_7)(C_{13}H_{10}ON)_2$	0.20	24.24	4.68	—	—
0.58	0.71			Blackish solid, insoluble in benzene	(0.21)	(24.22)	(4.70)		

at 120°C for 3—4 hrs., water was then azeotropically removed with benzene, and finally the product was distilled at 99—100°C/0.1—0.2 mm.

Calcd. C 72.46; H 7.43; N 9.38.
Found C 72.32; H 7.38; N 9.29%.

(ii) *Benzylidine-2-hydroxy-n-propylamine* ($C_{10}H_{13}ON$)

This was prepared similarly, by refluxing benzaldehyde (18.3 g) and 2-hydroxy-*n*-propylamine (12.9 g) in benzene. The product was distilled at 95—97°C/0.3—0.4 mm.

Calcd. C 73.58; H 8.03; N 8.57.
Found C 73.45; H 7.98; N 8.52%.

(iii) *Benzylidine-o-aminophenol* ($C_{13}H_{11}ON$)

Benzaldehyde (8.8 g) and *o*-aminophenol (9.1 g) were dissolved in absolute alcohol and the solution was heated on a water bath for 2—3 hrs. On cooling, fine, yellow, needlelike crystals were obtained, which were purified by distillation at 156—158°C/2.5—2.7 mm.

Calcd. C 79.16; H 5.61; N 7.10.
Found C 79.04; H 5.55; N 7.12%.

Synthesis of lanthanide (III) Schiff base complexes

The reactions of the lanthanide isopropoxides with the Schiff base were effected in anhydrous benzene. The experimental technique and the azeotropic removal of isopropanol were the same as described earlier. [6, 7] Adequate precautions were taken to exclude moisture at all stages of the reaction and its course was ascertained by estimating the isopropanol liberated in the azeotrope due to replacement by the ligand. The experimental details of all these reactions are recorded in Table I.

Exchange reaction of Schiff base derivatives of lanthanides with an excess of t-butyl alcohol

Excess of *t*-butyl alcohol was added to the freshly prepared lanthanide derivative in benzene. The contents were refluxed and the ternary azeotrope, *t*-butyl alcohol–isopropanol–benzene was distilled until the boiling point rose to the constant temperature of 80°C. The volatile fraction was then stripped off under reduced pressure (60°C/0.5 mm) for 2—3 hrs. The details of these reactions are given in Table II.

Analytical methods and physical measurements

Lanthanum, praseodymium and neodymium determined by EDTA titration using Eriochrome Black T as an indicators, [9], and nitrogen was measured by the Kjeldahl method. The isopropanol was determined by the oxidimetric method using 1 *N* $K_2Cr_2O_7$ in 12.5% H_2SO_4 [10]. Molecular weights were determined ebullioscopically in boiling benzene and the IR spectra were recorded within the range 4000—400 cm^{-1} on a Perkin—Elmer 337 grating infrared spectrophotometer using KBr optics.

Results and discussion

The reactions with 1 : 1 and 1 : 2 molar ratios of lanthanides: Schiff bases, yielded the bis- and monoisopropoxy Schiff base derivatives, respectively, as shown by the following general equation:

$$Ln(O\text{-}i\text{-}C_3H_7)_3 + n\ C_6H_5C(H){:}NRH \rightarrow$$

$$\rightarrow Ln(O\text{-}i\text{-}C_3H_7)_{3-n}\,(C_6H_5C(H){:}NR)_n + n\ i\text{-}C_3H_7OH$$

Table II

Reactions of mono- or diisopropoxy Schiff base derivatives of Ln(III) with t-butyl alcohol

Compound (g)	*t*-Butyl alcohol (in excess) (g)	Product and characteristics	Isopropanol in the azeotrope, Found (Calcd.)	Analysis %	
				Ln Found (Calcd.)	N Found (Calcd.)
$La(O\text{-}i\text{-}C_3H_7)_2(C_{10}H_{12}ON)$ 0.62	2.52	$La(O\text{-}t\text{-}C_4H_9)_2(C_{10}H_{12}ON)$ Light yellow solid, soluble in benzene	0.16 (0.17)	31.08 (31.07)	3.08 (3.13)
$La(O\text{-}i\text{-}C_3H_7)(C_{10}H_{12}ON)_2$ 0.75	2.64	$La(O\text{-}t\text{-}C_4H_9)(C_{10}H_{12}ON)_2$ Light yellow solid, soluble in benzene	0.07 (0.08)	25.86 (25.92)	5.26 (5.22)
$Pr(O\text{-}i\text{-}C_3H_7)_2(C_{10}H_{12}ON)$ 0.72	2.44	$Pr(O\text{-}t\text{-}C_4H_9)_2(C_{10}H_{12}ON)$ Yellow solid, soluble in benzene	0.20 (0.20)	31.31 (31.37)	3.15 (3.12)
$Pr(O\text{-}i\text{-}C_3H_7)(C_{10}H_{12}ON)_2$ 0.94	2.32	$Pr(O\text{-}t\text{-}C_4H_9)(C_{10}H_{12}ON)_2$ Yellow solid, soluble in benzene	0.10 (0.11)	26.12 (26.17)	5.13 (5.20)
$Nd(O\text{-}i\text{-}C_3H_7)_2(C_{10}H_{12}ON)$ 0.66	2.84	$Nd(O\text{-}t\text{-}C_4H_9)_2(C_{10}H_{12}ON)$ Yellow solid, soluble in benzene	0.18 (0.18)	31.84 (31.86)	3.11 (3.09)
$Nd(O\text{-}i\text{-}C_3H_7)(C_{10}H_{12}ON)_2$ 0.86	3.24	$Nd(O\text{-}t\text{-}C_4H_9)(C_{10}H_{12}ON)_2$ Yellow solid, soluble in benzene	0.09 (0.09)	26.66 (26.62)	5.12 (5.16)

(where Ln = La(III), Pr(III) or Nd(III); $n = 1$ or 2; and

$$R = -CH_2CH_2O, \ -CH_2CHCH_3O \text{ or } -C_6H_4O).$$

The reactions with 1:3 molar ratio did not appear to proceed beyond the formation of $Ln(O\text{-}i\text{-}C_3H_7)(C_6H_5C(H):NR)_2$ even on prolonged refluxing and continuous removal by fractionation of the isopropanol liberated in the reaction.

The resulting products of the type

$$Ln(O\text{-}i\text{-}C_3H_7)_2(C_6H_5C(H):NR) \text{ and } Ln(O\text{-}i\text{-}C_3H_7)(C_6H_5C(H):NR)_2$$

are non-volatile, light to deep yellow or blackish in colour, and crystalline in nature. It was observed that the 1 : 1 and 1 : 2 lanthanide derivatives of benzylidene-*o*-aminophenol were insoluble in benzene, while the freshly prepared derivatives of benzylidene-2-hydroxyethylamine and benzylidene-2-hydroxy-*n*-propylamine were soluble. Their bis- and monoisopropoxy Schiff base derivatives have been shown to have the molecular association of ~2.0 and ~1.5, respectively, and on heating they begin to decompose at about 245°C. However, on standing for a few days these compounds appear to polymerize as shown by their change into almost insoluble products, also having higher thermal stability. Even when heated up to 320°C they do not appear to decompose. The lower solubility can probably be ascribed to the formation of higher polymeric units as shown below (**I** and **II**).

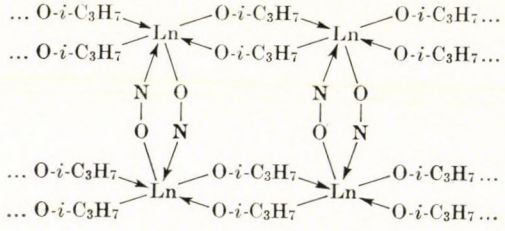

I

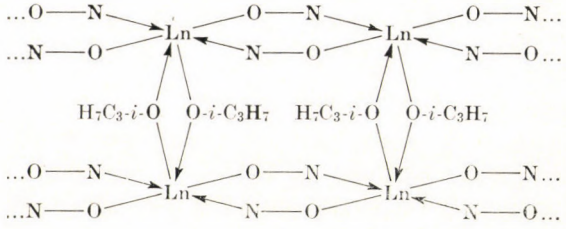

II

(where Ln = La(III), Pr(III) or Nd(III) and —N—OH represents the Schiff base molecule).

In order to study the nature of the isopropoxy groups in the soluble as well as in insoluble products, exchange reactions with an excess of *t*-butyl alcohol were attempted. The soluble compounds were found to undergo exchange reactions and yield the *bis*- or monobutoxy derivatives, as shown by the following general equations:

$$\mathrm{Ln(O\text{-}i\text{-}C_3H_7)_{3-n}(C_6H_5C(H){:}NR)_n + 3 - n\ t\text{-}C_4H_9OH \rightarrow}$$

$$\rightarrow \mathrm{Ln(O\text{-}t\text{-}C_4H_9)_{3-n}(C_6H_5C(H){:}NR)_n + 3 - n\ i\text{-}C_3H_7OH}$$

(where Ln = La(III), Pr(III) or Nd(IIII); $n = 1$ or 2; and

$$\mathrm{R = -CH_2CHCH_3O).}$$

However, in the case of the insoluble derivatives such exchange reactions were not possible, and this is probably due to the immobilized nature of the isopropoxy groups in these products due to polymerization.

The resulting butoxy derivatives are non-volatile, light yellow, crystalline products. These also tend to behave like their parent isopropxy derivatives, as shown by their higher thermal stability.

WILKINS and WITTBECKER, were the first to report the preparation of beryllium *bis*-(β-diketone) polymers [3]. PATTERSON *et al.* [4], have prepared some polymeric chelates of aluminium by the condenzation of diisopropoxy-aluminium monoacetylacetone with *bis*-acetoacetate. The stability and the insolubility of the products has been explained by the rigidity of the polymer chain backbone. Recently, some polymeric glycol derivatives of lanthanides have been prepared, the polymerization occurring by intermolecular co-ordination through oxygen atoms [11—13].

Infrared spectra

1. In the spectra of the Schiff bases, such as benzylidene-2-hydroxyethylamine, benzylidene-2-hydroxy-*n*-propylamine and benzylidene-*o*-aminophenol, bands of strong intensities are observed in the region 3300—3100 cm^{-1}, due to the presence of OH and NH groups [14—15].

2. On comparing the infrared spectra of the Schiff bases and their lanthanide derivatives, it can be inferred that chelate formation probably takes place through the oxygen (phenolic or alcoholic) and the nitrogen of the azeomethine group $\diagdown\!\!\diagup C = N-$. This is evidenced by the disappearence of the —OH frequency band in the range 3300—3100 cm^{-1} and appearence of some new bands in the region 700—600 cm^{-1} in the metal complexes.

3. The C = N absorption band at about 1630 cm^{-1} in the Schiff bases remains almost unaffected in the case of the metal derivative of benzylidene-2-hydroxyethylamine and benzylidene-2-hydroxy-*n*-propylamine [16]. However, in the case of metal derivatives of benzylidene-*o*-aminophenol it is shifted to a lower region (about 1600 cm^{-1}).

4. In the isopropoxy derivatives, the characteristic bands of the isopropoxy group appear at 1375, 1130 and 990 cm^{-1}. The strong peak at 1375 cm^{-1} may be assigned to the *gem*-dimethyl structure and bridged C—O stretching [17].

5. The bands around 675 cm^{-1} may be attributed to ring deformation coupled with both the Ln—O stretching and C—CH_3 stretching modes [18].

*

Thanks are due to Prof. R. C. MEHROTRA and Prof. K. C. JOSHI, Chemistry Department, Rajasthan University, for providing all the laboratory facilities. One of us (S. K. A.) is also thankful to the C. S. I. R., New Delhi, for an award of J. R. F.

REFERENCES

[1] KLUIBER, R. V., LEWIS, J. W.: J. Am. Chem. Soc. **82,** 5777 (1960)
[2] CHARLES, R. G.: J. Phys. Chem. **64,** 1747 (1960)
[3] WILKINS, J. P., WITTBECKER, E. L.: U. S. Pat. 2, 659, 711 (1953)
[4] PATTERSON, T. R., PAVLIK, F. J., BALDOMI, A. A., FRANK, R. L.: J. Am. Chem. Soc. **81,** 4213 (1959)
[5] DRINKARD, W. C. JR., CHAKRAVORTY, D. N.: Wadc Tech. Rept., 59/761, 232 (1960)
[6] AGARWAL, S. K., TANDON, J. P.: Syn. Inorg. Metal-org. Chem. **4**, 387 (1974)
[7] AGARWAL, S. K., TANDON, J. P.: J. Inorg. Nucl. Chem. (In press)
[8] MISRA, S. N., MISRA, T. N., KAPOOR, R. N., MEHROTRA, R. C.: Chem. & Ind. **1963** 120
[9] LYLE, S. J., RAHMAN, MD. M.: Talanta **10, 1963** 1177
[10] BRADLEY, D. C., HALIM, F. M., WARDLAW, W.: J. Chem. Soc. **1950** 3450
[11] MISRA, S. N.: Ph. D. Thesis, Rajasthan University, 1964
[12] MISRA, T. N.: Ph. D. Thesis, Rajasthan University, 1963
[13] BATWARA, J. M.: Ph. D. Thesis, Rajasthan University, 1969
[14] RASMUSSEN, R. S., TUNNICLIFF, D. D., BRATTAIN, R. R.: J. Am. Chem. Soc. **71,** 1068 (1949)
[15] FREEDMAN, H. H.: J. Am. Chem. Soc. **83,** 2900 (1961)
[16] SHARMA, B. D., BAILER, J. C. JR.: J. Am. Chem. Soc. **77,** 5476 (1955)
[17] MEHROTRA, R. C., BATWARA, J. M.: Inorg. Chem. **9,** 2505 (1970)
[18] LIANG, C. Y., SCHIMITSCHEK, E. J., TRIAS, J. A.: J. Inorg. Nucl. Chem. **32,** 811 (1970)

S. K. AGARWAL
J. P. TANDON
University of Rajasthan, Jaipur-302 004 India.

Acta Chimica Academiae Scientiarum Hungaricae, 85 (1), pp. 79—87 (1975)

ISOBENZPYRYLIUM SALTS, V

POLAROGRAPHIC AND SPECTROPHOTOMETRIC INVESTIGATION OF SOME HYDROXY-SUBSTITUTED 1-ARYLISOBENZPYRYLIUM SALTS

M. LEMPERT-SRÉTER, GY. OSZBACH, F. RUFF and M. VAJDA

(Institute of Organic Chemistry, L. Eötvös University, Budapest)

Received April 26, 1974

The transformations of hydroxyisobenzpyrylium salts in aqueous alcoholic solutions of various pH values have been studied. Differences in the transformations of 7- and 6-hydroxy compounds are discussed and evidence is given for the probable structure of the unstable intermediates.

In earlier communications [1, 2, 3] we have reported that the spectroscopic and polarographic behaviour of some hydroxy-substituted 1-arylisobenzpyrylium salts of the general formula **I**, derived from the oxidative degra-

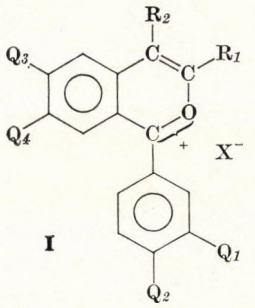

I

$R_1 = CH_3$

$R_2 = C_2H_5$

	Q_1	Q_2	Q_3	Q_4	ref.
a	OCH_3	OH	OCH_3	OH	[1, 2, 3]
b	H	OCH_3	OCH_3	OH	[2, 3, 4]
c	H	OH	OCH_3	OCH_3	[2, 3, 4]
d	OCH_3	OH	OH	OH	[5]
e	H	OH	OH	OH	[6]
f	OCH_3	OC_2H_5	OH	OC_2H_5	[6]
g	H	OCH_3	OH	OC_2H_5	[6]
h	OH	OCH_3	OH	OCH_3	[6]
i	H	OH	OH	H	[7]
k	H	H	OH	H	[7]
l	H	OH	H	H	[2, 3, 4]

dation of dimeric propenyl phenol ethers, differs from that of the corresponding alkoxy derivatives. This points to the fact that the pH-dependent transformations involve different intermediates in hydroxy and alkoxy compounds. Further synthetic work has now made it possible to make a more detailed investigation of the equilibria involved.

Experimental

Polarograms were recorded using an LP 55 photo recording and a Radelkis OH 102 type pen recording polarograph and a Kalousek type polarographic cell with a thermostating jacket. The temperature was maintained with an ultrathermostat at 25.00 ± 0.1. Buffers used were phosphoric acid–monosodium phosphate; formic acid–sodium formate; acetic acid–sodium acetate; monosodium hydrogen phosphate–disodium hydrogen phosphate; dimethylglycine–sodium dimethylglycinate. Depolarizer-concentrations studied were $(0.1—2) \times \times 10^{-4}$ *M*. A saturated calomel electrode or a 0.1 *N* silver–silver chloride electrode was used as reference electrode. Half-wave potentials are given against the saturated calomel electrode. All solutions contained 50% v/v alcohol.

As some solutions — mostly those with pH values above 5 — were unstable, polarograms of these compounds were recorded in the following manner: the alcoholic solution of the compound was deaerated in the Kalousek vessel, while the buffer was deaerated in a jacketed separatory funnel which was fitted into a seperate hole in the stopper of the Kalousek vessel. This separatory funnel was equipped with a rubber stopper containing the deaerating glass tube and an exit tube with a stopcock. After deaeration had been complete, the buffer solution was added to the alcoholic solution of the compound by opening the stopcock of the separatory, funnel and closing the stopcock on the exit tube. The buffer solution was forced into the Kalousek vessel, mixed by nitrogen gas for 10 sec and the polarogram recorded in the usual way.

UV-Vis spectra were recorded using a UNICAM SP 700 spectrophotometer in Britton—Robinson buffers or the buffers listed above. Concentrations of the compounds were $0.5 \times 10^{-5} M$.

Results and discussion

All compounds show well defined one-electron reduction waves in solutions of strong acids but, contrary to the behaviour of the alkoxy compounds, the waves of the hydroxy compounds show pronounced maxima which can be suppressed by gelatine.

The UV-visible spectra of all compounds in acid solutions are also similar to each other and to the spectra of the alkoxy compounds.

In buffers above pH 2.0 the structure differences of the hydroxy compounds are shown by differences in their polarographic and spectroscopic behaviour.

The first group comprises the compounds which have hydroxy groups in the 4'- and/or 7-position and an alkoxy group in the 6-position. The first of these compounds studied, 4',7-dihydroxy-3',6-dimethoxy-3-methyl-4-ethylisobenzpyrylium perchlorate (**Ia**) shows the following behaviour [1]. The half-wave potential is constant up to pH 4.5, than the $E_{1/2}$/pH function acquires a slope of 30 mV/pH and the wave height diminishes. A very small wave (about 10% of the one-electron cathodic wave) appears between pH 4.0 and

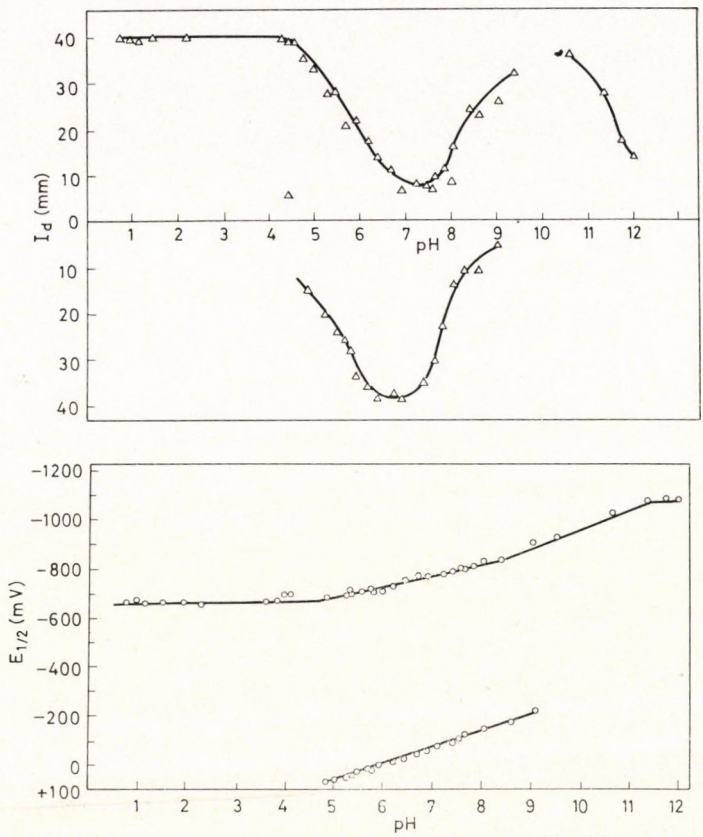

Fig. 1. pH dependence of the wave height and half wave potential of 4',7-dihydroxy-3',6--dimethoxy-3-methyl-4-ethylisobenzpyrylium perchlorate

4.5 with an $E_{1/2}$ of about —400 mV. Concurrently with the diminishing of the first wave an anodic wave appears with an $E_{1/2}$ value of about +70 mV at pH 4.8 and a slope of 60 mV/pH. This anodic wave grows as the cathodic wave diminishes, their sum being approximately constant. At pH 7.0 the anodic wave reaches its maximum height and then again diminishes. It cannot be observed above pH 9.0. The cathodic wave, on the other hand, grows again and acquires a slope of 60 mV/pH, almost reaching its previous height at pH 11. It decreases up to pH 12 but is still easily discernible at this pH value which was the highest studied.

The character of the anodic wave seemed to deserve some further study as the most probable assumption is that the wave is due to the oxidation of an intermediate phenolic inner salt but the possibility of a mercurous salt formation had to be taken into account. In the first case the half-wave potential should be independent of the concentration and it should produce a revers-

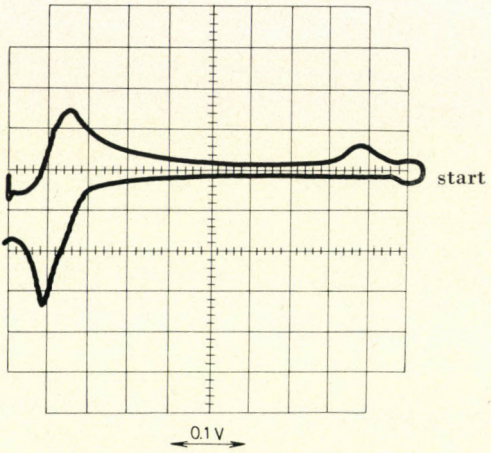

Fig. 2. Cyclic voltamogramm of a 1×10^{-4} *M* solution of 4',7-dihydroxy-3',6-dimethoxy-3--methyl-4-ethylisobenzpyrylium perchlorate in Britton—Robinson buffer (pH = 6.83) The scan was started from —0.9 V towards positive potentials. Time of scan 4 sec (full cycle). Electrode: hanging mercury drop

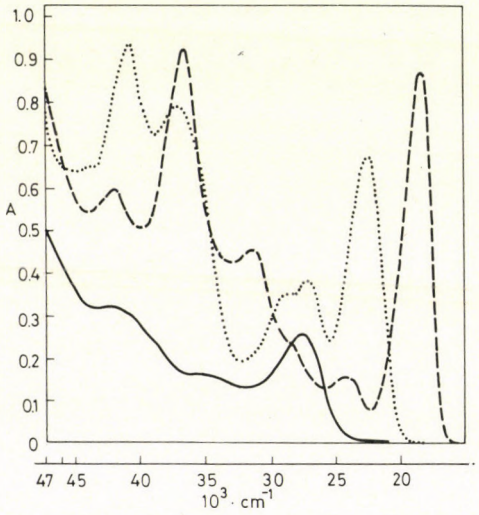

Fig. 3. UV-Vis spectra of 4',7-dihydroxy-3',6-dimethoxy-3-methyl-4-ethylisobenzpyrylium perchlorate at various pH values. $c = 4\times10^{-5}$ *M*; pH values: ..... 1.18; --------- 10.28; ——— 10.28 after warming to 50°C

ible peak in a cyclic voltametric experiment if the voltage scan starts with the oxidation half cycle. Experiments showed that this is indeed the case and this lends strong support to the assumption mentioned above.

1-(4'-methoxy-phenyl)-3-methyl-4-ethyl-6-methoxy-7-hydroxy-isobenzpyrylium perchlorate behaves very similarly to the above compounds. The only difference is that the anodic wave splits into two waves at pH 8 and a new

cathodic wave appears at high negative potentials at pH values above 10. The sum of the wave heights in this case is also practically constant.

4-Hydroxy-6,7-dimethoxyisobenzpyrylium perchlorate also behaves analogously to the above compounds but the analogy is not as strong as that between the other two compounds mentioned. The cathodic wave splits into two waves at pH values above 2.5. The second wave is not purely diffusion controlled but has some kinetic character as its $I_d = k \cdot h^n$ function has an exponent of less than 1/2. The anodic wave can only be seen in a very small pH interval and the very negative wave $E_{1/2} > 1400$ mV appears at pH values above 9.

The UV-visible spectra show changes occurring in parallel with the changes in polarographic behaviour. The 7-hydroxy- and 4',7-dihydroxy compounds show a red colour which appears in the spectra taken between 4.8 and 9.0 as a separate absorption maximum. This red colour is not very stable and the two compounds show markedly different stability. The colour produced in the 4',7-dihydroxy compound is stable for more than 12 hrs (approximate half life at room temperature), while that of the 7-hydroxy compound is only stable for about 2 or 3 hrs. Because of this, great care had to be taken to ensure reproducibility of the spectra by recording the spectra as fast as possible after mixing the solutions. The colour change in 4'-hydroxy-6,7-dimethoxy-3-methyl-4-ethylisobenzpyrylium perchlorate (**IIIc**) solutions is transient and the colour can only be seen for a few minutes after mixing. It was therefore impossible to record the spectrum. Qualitative tests show that the colour appears at pH 8.5, reaches its maximum intensity at pH 9.2 and does not appear at pH 10 and above.

In earlier communications [1, 3] we suggested structure **II** or **III** for the intermediate red compounds.

These formulae show inner salt structures. Although no direct structural proof exists for this suggestion, the following data seem to be in accordance with it:

(1) Although a quinoidal structure (**IV**) can be written for compound **Ia** if the 4-hydroxy group enters into the quinoidal structure, no analogous formula is conceivable in the case of **Ib**. A transient formation of very small amounts of this quinoidal compound may be the reason for the appearance of the small wave around 400 mV at pH 4—4.5 on the polarograms of **Ia**. The quinoidal structure could be stable in the case of **Ia** and **Ic** but no evidence was found in the case of **Ic**.

(2) If the red compound derived from **Ia** is extracted with chloroform, dried rapidly, and an infrared spectrum recorded, no bands assignable to a quinoidal carbonyl can be found. The spectrum shows only the carbonyl bands of diketone **V** which is the decomposition product of **IIIa**.

(3) The 6-hydroxy-isobenzpyrylium salts are transformed to quinoidal compounds of structure **VII** [5]. These compounds undergo addition with

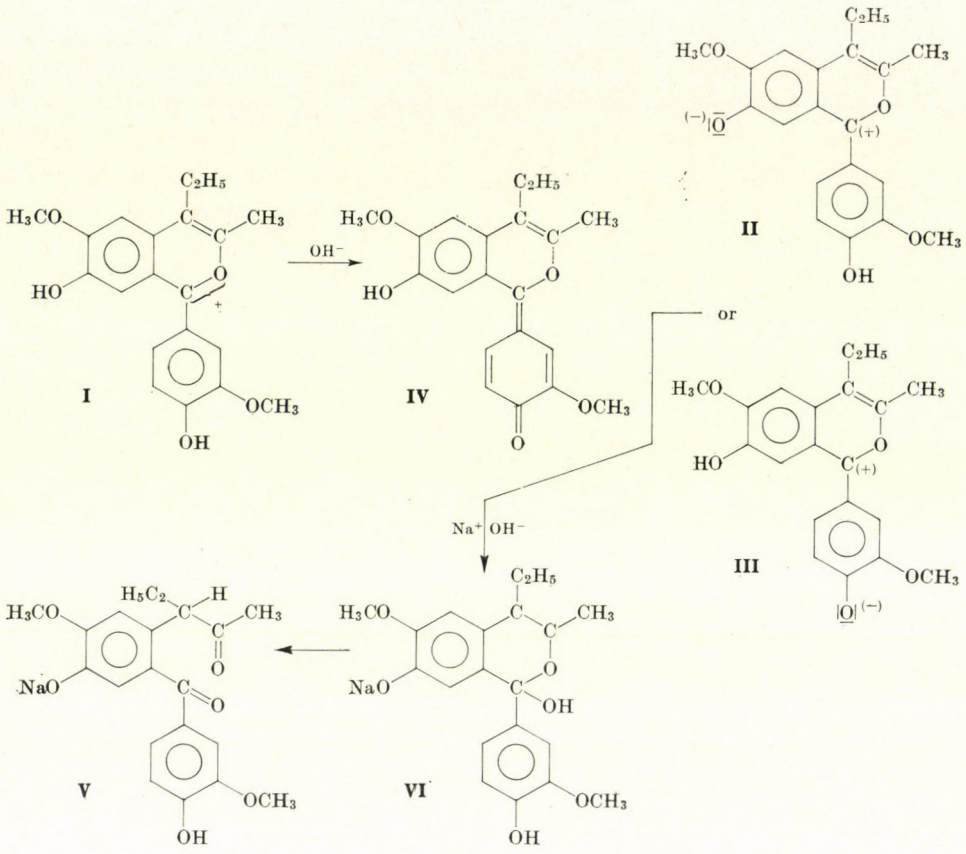

mineral acids and the isobenzpyrylium salt is reformed. The longest wavelength band of these quinoidal compounds appears at a much lower wavelength than that of the compounds of type **II** or **III** (see Figs. 3, 5).

(4) The relatively high stability of the red derivatives of compounds **Ia** and **Ib** and the very low stability of compound **Ic** also points to an inner-salt structure.

(5) A free radical structure is improbable as no ESR signal could be observed in a solution of **IIIa** in chloroform.

(6) The appearance of an oxidation wave is in accordance with the inner-salt structure proposed.

The slight differences in the polarographic behaviour of **Ic**, *i.e.* the splitting of the cathodic wave at pH 2.7 show that this compound is partly transformed to the isobenzpyrylium base **VI** before the formation of the inner-salt. This shows that formation of the quinone (structure **IV**) is not favoured. The probable reason for this is that, according to a study of models, the aromatic ring attached to C_1 of the heterocyclic system cannot be coplanar with the heterocyclic ring. This also means that there can be no conjugative inter-

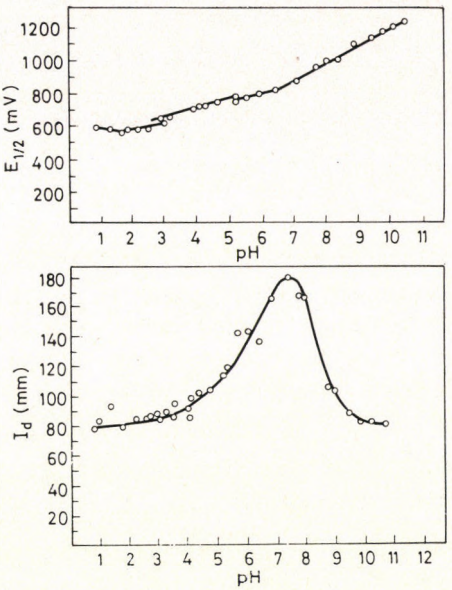

Fig. 4. pH dependence of the half wave potential and wave height of 6-hydroxy-4-methoxy-7-ethoxyisobenzpyrylium perchlorate

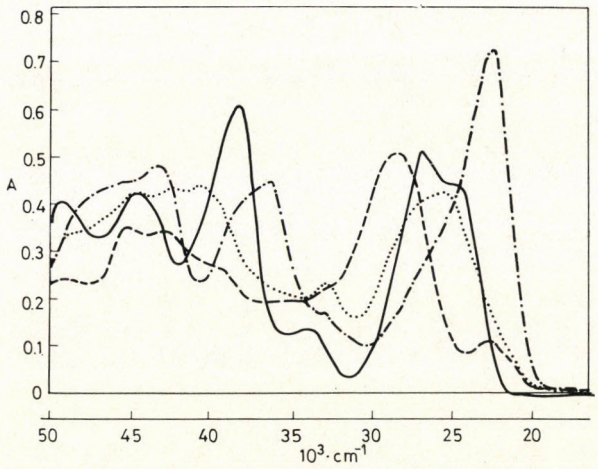

Fig. 5. UV-Vis spectra of 4',6-dihydroxy-3-methyl-4-ethylisobenzpyrylium perchlorate at various pH values: ——— pH = 1.3; . . . . . pH = 7.0; -.-.-.-.-.- pH 10.0; -------- pH > 12 (0.1 *N* NaOH solution)

action between C_1 and the para-position of the aromatic ring which explains that the inner-salt structure is much less stable in this case than in the case of **Ia** and **Ib**.

The second group of compounds are those which have a hydroxy group in 6-position. OH groups in the other positions cause much less significant

variations in the behaviour of the compounds, although the differences are of some interest.

The polarographic properties are as follows. The single cathodic wave which also shows a maximum in the absence of gelatine starts to grow in height at about pH 4. Concurrently, the slope of the $E_{1/2}$/pH function changes from 0 to about 60 mV/pH. The maximum wave height is reached at about pH 8 and is approximately double the height observed in acid solution. The wave is diffusion-controlled. In the case of 6,7-dihydroxy salts a second, very negative cathodic wave can also be observed on the polarograms above pH 8.

The height of the first wave diminishes very suddenly at about pH 8, its height being reduced to a one-electron wave.

The UV spectra of the 6-hydroxy compounds also show two major transitions with variation of pH. In strong acid solution the compounds show spectra which are completely analogous to those of alkoxy substituted isobenzpyrylium salts. At pH values above 4 a different UV spectrum appears, superimposed on that of the isobenzpyrylium salts. This spectrum is best observed at pH values around 7. A further change of the spectra can be observed at pH above 9 but the changes observed here depend very strongly on the number and position of other hydroxy groups in the molecule.

Both the polarographic and the UV spectroscopic behaviour of this group of compounds are in accordance with the transformations suggested previously [5, 6].

The isobenzpyrylium salt is reduced in a one-electron wave.

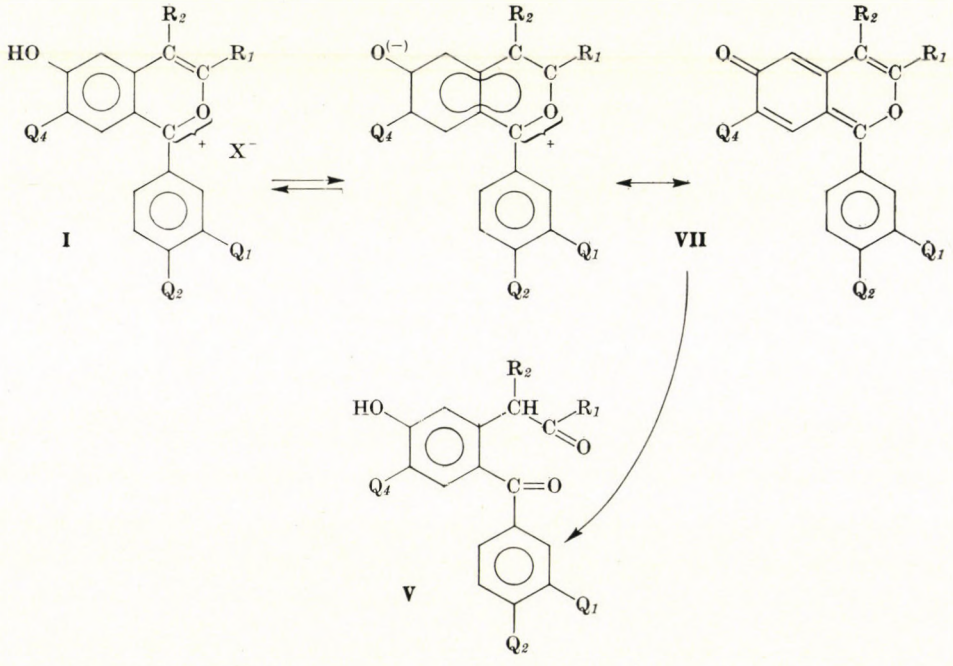

Concurrently with the transformation of the ion (**I**) to the anhydro base **VII**, the wave is transformed to a two-electron wave and the UV spectrum of the salt is also transformed to that of the base. As a two-electron reduction is only possible if a proton adds fast enough to a radical form and the phenolate anion is stabilized in alkaline solution, the height of the wave is again reduced to that of the one-electron wave at higher pH values. The second wave at high negative potentials is probably due to the phenolate anion form of the compound (**VII**).

The study of the UV spectrum of the various compounds of group two (6-hydroxy compounds) at higher pH values and preparative evidence also show that the compounds differ in their stability in alkaline solution. If the compounds contain a free hydroxyl group in position 7, the heterocyclic ring is not cleaved in alkaline buffers or sodium hydroxyde solutions. If, on the other hand, hydroxyl groups are present in the 3'- or 4'-position of the 1-aryl ring, the heterocyclic ring is cleaved by sodium hydroxide with the formation of the diketone. This was partly shown by preparative evidence [6] and also by reneutralizing solutions of the compounds in alkaline buffers or alkali hydroxide solutions and recording the UV spectra. In the case of compound **Ie** the cleavage to the diketone occurs already in a Britton–Robinson buffer of pH 10.

The only compound among those studied, which falls into group (3), is 1-(4'-hydroxy-phenyl)-3-methyl-4-ethylisobenzpyrylium perchlorate. This compound behaves exactly like the alkoxy substituted compound which has no alkoxy substituent in position 6, *i.e.* the cathodic wave appearing in acid solutions shows a break in the half-wave potential/pH function that diminishes in height, disappearing at higher pH values [1]. The obvious reason for this is that the pK value of this isobenzpyrylium ion is very low and therefore the transformation to the diketone is already complete at pH values which would favour the other transformations of the ion.

REFERENCES

[1] VAJDA, M.: Polarographic investigation of isobenzpyrylium salts, in LONGMUIR: Advances in Polarography, Vol. 2., 746. Pergamon Press, London 1960
[2] VAJDA, M., GELLÉRI, A.: Ann. Univ. Sci. Rol. Eötvös nom., Sectio Chim., **3,** 107 (1961)
[3] VAJDA, M., RUFF, F.: Acta Chim. Acad. Sci. Hung., **40,** 225 (1964)
[4] VAJDA, M.: Acta Chim. Scad. Sci. Hung., **40,** 295 (1964)
[5] MÜLLER, A., LEMPERT-SRÉTER, M.: Monatshefte, **96,** 369 (1965)
[6] LEMPERT-SRÉTER, M., BÁRDY, M.: Acta Chim. Acad. Sci. Hung., **57,** 181 (1968)
[7] VAJDA, M., SZÖRÉNYI, M., RUFF, F.: Acta Chim. (Budapest) (In press)

Magda LEMPERT-SRÉTER
György OSZBACH
Ferenc RUFF
Miklós VAJDA

1088 Budapest, Múzeum krt. 4/b, Hungary.

Acta Chimica Academiae Scientiarum Hungaricae, 85 (1), pp. 89–95 (1975)

CLEAVAGE OF 2-THIONO-4-OXO-DIHYDRO-5,6-BENZO-1,3-THIAZANES WITH AMINES

M. T. OMAR and M. N. BASYOUNI

(Faculty of Science, Ain Shams University, Cairo, Egypt)

Received April 28, 1974

The reaction of 2-thiono-4-oxo-dihydro-5,6-benzo-1,3-thiazines 1 with primary and secondary amines depends on both the molarity and the substituent present at the 3-position. The route through which the ring cleaved is discussed. The cleavage seems to occur at 1,2- as well as 3,4-bonds.

Alkaline cleavage of 2-thiono-4-oxo-dihydro-5,6-benzo-1,3-thiazines with potassium hydroxide and alkoxides [1] gives 2-thiobenzoic acid and its ester, respectively. In the present paper the reaction of a variety of organic bases with **1** is studied to obtain more information about the mode of cleavage. It is observed that both the molarity and the substituent present at 3-position have profound effects on the type of products obtained.

Thus, refluxing 2-thiono-3-methyl-(**1a**) and 2-thiono-3-ethyl-(**1b**)4-oxo-dihydro-5,6-benzo-1,3-thiazine with 1 mol of benzylamine gives 2-benzylimino-3-methyl- and 2-benzylimino-3-ethyl-4-oxo-dihydro-5,6-benzo-1,3-thiazines, **3a** and **3b**, respectively, with evolution of hydrogen sulfide gas. The structure of **3a** is substantiated by analytical data, infrared spectroscopy and its hydrolysis. Thus, the infrared spectrum shows a band at 1620 cm^{-1} characteristic of the stretching frequency of the carbonyl group in disubstituted amides [2]. The structure receives further support from the fact that boiling in alcoholic hydrochloric acid leads to the corresponding 1,3-thiazin-2,4-dione. The structure of **3b** is deduced from the analogy of its electronic spectrum (*cf.* Table I) to that of **3a**.

Formation of **3a** and **b** indicates that the amine attacks primarily the carbon atom at position 2.

However, refluxing each of **1a** and **b** with excess benzylamine yields a product which gives spot test [3] characteristic of disulfides. It is identical with an authentic specimen [4] of N,N'-dibenzyl-2,2'-dithiobisbenzamide (**5a**). Its formation indicates that the cleveage occurs at C-2 and C-4.

WAGNER *et al.* [5] reported the formation of 2-imino-4-oxo-2H-1,3-benzothiazines upon treatment of the corresponding 2-thiono derivatives with ammonia and primary amines in the presence of mercuric oxide. However, treating each of **1a** and **b** with excess anhydrous ethylamine at room temper-

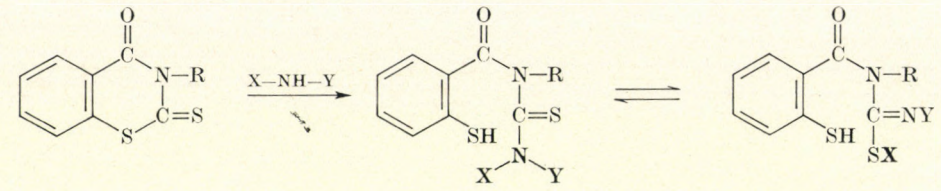

1 **2** **2'**

a: R = CH_3
b: R = C_2H_5
c: R = H

a: X, Y = $(CH_2)_5$

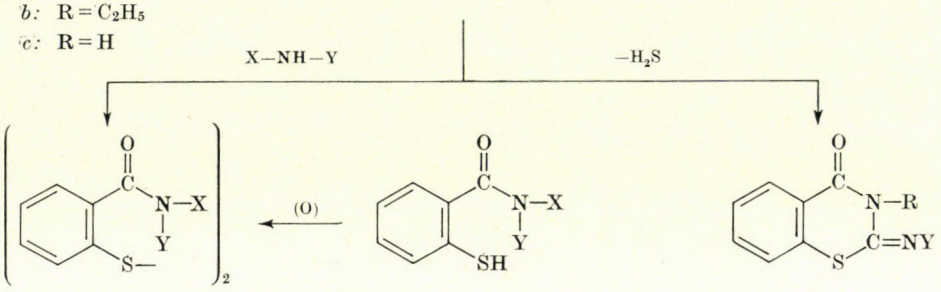

5 **4** **3**

	X	Y
a:	H	CH_2Ph
b:	H	C_2H_5
c:	$-(CH_2)_5-$	

X = H, Y = C_2H_5

	R	Y
a:	CH_3	CH_2Ph
b:	C_2H_5	CH_2Ph
c:	CH_3	C_2H_5
d:	C_2H_5	C_2H_5
e:	H	C_2H_5
f:	H	CH_2Ph

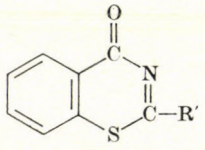

6

a: R′ = Piperidyl
b: R′ = Morpholyl

ature gives a mixture of 2-thiol-N-ethylbenzamide (**4**) and the 2-ethylimino-3-methyl- and 2-ethylimino-3-ethyl-4-oxo-dihydro-5,6-benzo-1,3-thiazines, **3c** and **3d**, respectively, with the former predominating. If the reaction mixture is worked up after two days, disulfide **5b** is obtained instead of thiol **4**, most probably by oxidation in air.

The structure of **4** is substantiated by its solubility in dilute alkali and by its easy oxidation to the disulfide **5b**. The disulfide nature of the oxidation product is confirmed by a spot test [3] and by the analogy of its electronic

Table I

Electronic spectral data in absolute methanol

Product	Electronic spectra					
	λ_{max}	ε_{max}	$\lambda_{max.}$	ε_{max}	λ_{max}	ε_{max}
3a	227	32580	~238—240	24480	315	720
3b	223	31480	~238—240	23340	313	1854
3c	227	25470	~236—240 ~280	20470 1290	317	900
3d	229	27700	~238—242 ~280	22120 1900	317	1075
3e	228	34200	~240—245 270	25320 8770	~300—310	2330
3f	228	31150	~240—245 ~270	24980 11070	~300—307	2840
5b	248	16845	305	4370		
5c	240	18860	~270—290	2320		
6a	228	20255	244 279	21065 11345	~305	3405
6b	230—234	21640	244 253 278	22995 22995 12850	~300	4510
2a	220	19530	250	8580	311	4625

~ Shoulder

spectrum to that of **5a**. The structure of **3c** is confirmed by m.p. and mixture m.p. with authentic sample [6]. **3d** has an electronic spectrum analogous to that of **3b** (*cf.* Table I) which supports its structure.

The formation of **5** when using an excess amine cannot be explained by the intermediate formation of **3** since attempted cleavage of **3a** and **b** with benzylamine or ethylamine is unsuccessful. Furthermore, the formation of **3** and **4** on treating **1** with ethylamine implies that the cleveage occurs *via* intermediate **2** formed by 1,2-cleavage (not isolated in these cases). However, **2a** has been isolated on using piperidine. Thus, the refluxing of **1a** with 1 mol of piperidine gives N-methyl-N-(2-thiobenzoyl)-piperidylthioformamide, **2a**.

The structure of **2a** is substituated by analytical data, the negative colour reaction for disulfides [3] and by degradation. Thus, refluxing of **2a** with aqueous potassium hydroxide or piperidine gives 2-thiolbenzoic acid and 2,2'-dipiperidylcarbonyldiphenyl disulfide **5c**, respectively. The latter product is also obtained on treating **1a** with 2 mol of piperidine and its structure is confirmed by m.p. and mixture m.p. with an authentic sample obtained by treating the acid chloride of 2,2'-dithiobisbenzoic acid with piperidine.

From the above observations it is concluded that the cleavage of 2-thiono-3-alkyl-4-oxo-dihydro-5,6-benzo-1,3-thiazines occurs at the 1, 2-as well as at the 3,4- bonds. The route through which the cleavage occurs involves rupture of the 1,2- bond with the amine by attack at the 2-carbon atom to give **2**. In the absence of excess primary amine, cyclization of **2** *via* the enolized form **2'** occurs with evolution of hydrogen sulfide to give **3**. In the presence of excess amine, cleavage of the 3,4- bond takes place by further attack at C-4 to give disulfides **5** most probably *via* their thiols. Isolation of **4** under relatively mild conditions supports this view.

The attempted cleavage of 3-unsubstituted benzo-1,3-thiazines, however, leads to cyclic products both with 1 mol or an excess amine. Thus, the treatment of 2-thiono-4-oxo-dihydro-5,6-benzo-1,3-thiazine **1c** with excess ethylamine and benzylamine gives 2-ethylimino- and 2-benzylimino-4-oxo-dihydro-5,6-benzo-1,3-thiazine, **3e** and **3f**, respectively, with the evolution of hydrogen sulfide gas.

The structure of **3e** is confirmed by its identity m.p. and IR with an authentic sample [4]. The structure of **3f** is deduced from the analogy of its electronic spectrum with that of **3e** (*cf.* Table I). Furthermore, its infrared spectrum shows a broad absorption band between 2300—3200 cm^{-1} which may be attributed to interbonded NH and/or OH groups arising from a possible lactam-lactim tautomerism. The lack of absorption bands above 1520 cm^{-1} (for $\nu_{C=O}$) supports this view. Similar treatment with 1 mol or excess piperidine or morpholine gives 2-piperidino- and 2-morpholino-4-oxo-5,6-benzo-1,3-thiazines, **6a** and **6b**, respectively, with evolution of hydrogen sulfide gas. The structure of **6a** is confirmed by comparison (m.p. and IR) with an authentic sample [7]. The structure of **6b** is deduced from the analogy of its electronic spectrum with that of **6a**.

The formation of cyclic products on treating **1c** with primary and secondary amines shows the increased stability of the ring in 3-unsubstituted 2-thiono-4-oxo-dihydro-5,6-benzo-1,3-thiazines towards such reagents, as compared to the corresponding 3-alkyl derivatives. A possible explanation is that in the former compounds the amine displaces directly the 2-SH group, which is formed by 3—2 tautomerization with evolution of hydrogen sulfide gas. A parallelism to this situation is observed in the displacement of the 2-SH groups in rhodanines by amines [8].

Experimental

All melting points are uncorrected. Infrared spectra were recorded on a Unicam SP 1200 Infrared spectrophotometer. Ultraviolet spectra were measured on a Perkin—Elmer Spectracord 4000 A spectrophotometer in absolute methanol.

2-Thiono-4-oxo-dihydro-5,6-benzo-1,3-thiazine (1c)

To a solution of 2-thiolbenzoic acid (0.1 mol) in glacial acetic acid (100 ml,) ammonium thiocyanate (0.2 mol) is added portionwise and the mixture is refluxed until precipitation occurs. The filtered solid product is washed successively with water, aqueous sodium hydrogen carbonate and again with water. The dried product is crystallized from glacial acetic acid to give the title compound in faint yellow needles, m.p. 232—234°C, undepressed on admixture with an authentic sample [4].

Action of benzylamine on 1a, b and c

a) Using 1 mol of amine

A mixture of each of **1a**—**c** (0.01 mol) and benzylamine in ethanol is refluxed until all the hydrogen sulfide gas ceased to evolve. The solids precipitated after cooling are filtered off and recrystallized from a suitable solvent.

1a gives 2-benzylimino-3-methyl-4-oxo-dihydro-5,6-benzo-1,3-thiazine **3a** (80%), m.p. 86—88°C from ethanol.

$C_{16}H_{14}N_2OS$. Calcd. C 68.08; H 2.98; S 11.34.
Found C 67.80; H 3.10; S 11.50%.

1b gives 2-benzylimino-3-ethyl-4-oxo-dihydro-5,6-benzo-1,3-thiazine **3b** (78%), m.p. 91—93°C from ethanol.

$C_{17}H_{16}N_2OS$. Calcd. C 68.90; H 5.40; S 10.90.
Found C 68.90; H 5.50; S 11.40%.

1c gives 2-benzylimino-4-oxo-dihydro-5,6-benzo-1,3-thiazine, **3f** (85%), m.p. 220—222°C from *n*-butanol.

$C_{15}H_{12}N_2OS$. Calcd. C 67.16; H 4.44; S 11.94.
Found C 67.50; H 4.30; S 12.20%.

b) Using excess amine

The reaction is carried out as under *a)*. However, the concentration of the solution followed by dilution with water gives semisolids which are solidified when triturated several times with ether.

1a or **b** gives N,N'-dibenzyl-2,2'-dithiobisbenzamide, **5a** (50%) m.p. 202—204°C from ethanol, undepressed on admixture with an authentic sample [4].

1c, however gives **3f** as confirmed by m.p. and mixture m.p. with the product obtained on treating with 1 mol of benzylamine.

Reaction of excess ethylamine with 1a, b and c

Excess anhydrous ethylamine is added to powdered **1a**, **b** or **c** and the solution is allowed to stand for two days at room temperature. The residue is dissolved in alcohol, warmed on a boiling water-bath to remove hydrogen sulfide gas, and diluted with water. The precipitated solids are filtered off and crystallized from methanol.

1a or **b** gives N,N'-diethyl-2,2'-dithiobisbenzamide, **5b** (50%), m.p. 202—204°C, Ref. [7], m.p. 204°C.

1c, however, gives 2-ethylimino-4-oxo-dihydro-5,6-benzo-1,3-thiazine **3e** (70%), m.p. 168—170°C.

$C_{10}H_{10}N_2OS$. Calcd. C 58.25; H 4.85; S 15.53.
Found C 58.60; H 4.90; S 15.70%.

Evaporation of the original mother liquors gives semi-solids which are fractionally crystallized from dilute methanol.

1a gives 2-ethylimino-3-methyl-4-oxo-dihydro-5,6-benzo-1,3-thiazine **3c** (5%), m.p. 100—102°C, undepressed on admixture with an authentic sample [5].

1b gives 2-ethylimino-3-ethyl-4-oxo-dihydro-5,6-benzo-1,3-thiazine **3d** (7%), m.p. 95—97°C.

$C_{12}H_{14}N_2OS$. Calcd. C 61.54; H 6.00; S 13.67.
Found C 61.20; H 5.85; S 13.80%.

2-Thiol-N-ethylbenzamide (4)

Excess ethylamine is added to powdered **1a** and the mixture is allowed to stand for 2 hrs. The solution is warmed on a boiling water-bath, the residue dissolved in dilute sodium hydrox-

ide solution, treated with charcoal and filtered. Acidification of the alkaline filtrate gives a faint viscous oil, which is extracted with ether. Evaporation of the ethereal extract gives the title compound 80% as a viscous syrup which fails to solidify. When an alcoholic solution of it is allowed to stand for two days at room temperature, a quantitative conversion to N,N'-diethyl-2,2'-dithiobis benzamide **5b** occurs as confirmed by m.p. with the product obtained previously.

Hydrolysis of 3a, e and f

To an alcoholic solution (50 ml) of each of **3a**, **e** and **f** (0.01 mol), concentrated hydrochloric acid 3 ml is added and the mixture refluxed for 3 hrs. The solid which precipitates after cooling is filtered off, washed with water, dried and crystallized from ethanol.

3a gives 3-methyl-dihydro-5,6-benzo-1,3-thiazine-2,4-dione (80%), 120-122°C. Ref. [4], m.p. 119—121°C.

3e and **f** give 5,6-benzo-dihydro-1,3-thiazin-2,4-dione (83%), m.p. 212—214°C. Ref. [5], m.p. 212—214°C.

Reaction of piperidine with 1a and b

a) Using 1 mol of amine

To a solution of **1a** (0.01 mol) in ethanol (20 ml), piperidine (0.01 mol) is added and the solution refluxed for 1 hr. The solution is concentrated, diluted with water and the solid precipitated is filtered off. Crystallization from methanol gives N-methyl-N-2-thiobenzoyl-piperidyl thioformamide **2a** (30%), m.p. 146—148°C.

$C_{14}H_{18}N_2OS_2$. Calcd. C 57.14; H 6.12; S 21.77.
Found C 57.50; H 6.30; S 21.80%.

b) Using excess amine

Piperidine is added to the alcoholic solution of each of **1a** and **b** and the reaction is continued as under **a**. Crystallization from dilute methanol gives 2,2'-dipiperidylcarbonyldiphenyl disulfide **5c** (40%), m.p.136—138°C.

$C_{24}H_{28}N_2O_2S_2$. Calcd. C 65.45; H 6.36; S 14.54.
Found C 65.20; H 6.50; S 14.50%.

2,2'-Dipiperidylcarbonyldiphenyl disulfide (5c)

The acid chloride of 2,2'-dithiobisbenzoic acid (0.01 mol) in tetrahydrofuran (10 ml) is treated portionwise, under stirring, with piperidine (0.03 mol) and stirring is continued for 2 hrs at room temperature. Evaporation of the solvent followed by addition of water gives a semisolid product which is crystallized from dilute methanol to give the title compound (70%), m.p. 136—138°C.

Reaction of aqueous potassium hydroxide or piperidine with 2a

A solution of **2a** (0.5 g) in ethanol (10 ml) is refluxed with piperidine (0.5 ml) for 4 hrs. The solvent is concentrated, diluted with water and allowed to stand overnight. The solid which precipitates is filtered off and recrystallizes from dilute methanol to give **5c**.

However, refluxing of **2a** with aqueous potassium hydroxide for 1 hr, working up the solution as usual, gives 2-thiolbenzoic acid.

2-Ethylimino-3-ethyl-4-oxo-dihydro-5,6-benzo-1,3-thiazine (3d)

To a solution of **3e** (0.01 mol) in dry acetone (15 ml) are added powdered anhydrous potassium carbonate 0.02 mol and ethyl iodide (0.02 mol), then the reaction mixture is refluxed on a boiling water-bath for 24 hrs. The solids are filtered off and washed several times with acetone. The combined filtrate is evaporated, the residual semi-solid is triturated several times with light petroleum (b.p. 60—80°C) and the remaining solid is crystallized from benzene–light petroleum (b.p. 60—80°C) to give the title compound (70%), m.p. 95—97°C.

$C_{12}H_{14}N_2OS$. Calcd. C 61.54; H 6.00; S 13.67.
Found C 61.20; H 5.80; S 13.50%.

Attempted cleavage of 3a and b with benzylamine and ethylamine

To a solution of either **3a** or **b** (0.5 g) in ethanol (20 ml), excess benzylamine or ethylamine is added and the mixture refluxed for 4 hrs. The solid products obtained after cooling are filtered off and crystallized from alcohol to give the unchanged starting materials **3a** and **b** (ca. 90% recovery).

REFERENCES

[1] WAGNER, G., RICHTER, P.: Z. Chem., **6,** 220 (1966)
[2] BELLAMY, L. J.: The Infrared Spectra of Complex Molecules, Methuen & Co. Ltd. New York N. Y., John Wiley and Sons, (1960) p. 213.
[3] FEIGL, F.: Spot Tests in Organic Analysis, Elsevier Publishing Company (1966) p. 225
[4] WAGNER, G., RICHTER, P.: Pharmazie, **22,** 611 (1967)
[5] WAGNER, G., GUENTHER, RICHTER, P., PETER.: Pharmazie **24,** 100 (1969)
[6] BOESHAGEN, H.: Chem. Ber., **99,** 2566 (1966)
[7] MILTON, W., JOHN, S., U. S. Patent 3 470 168; Chem. Abst., **71,** 112949 **P** (1969)
[8] RAOUF, A. R. A., OMAR, M. T., EL-BAYOUMY, K. E.: Unpublished results

M. T. OMAR, M. N. BASYOUNI } Chemistry Department, Faculty of Science, Ain Shams University, Abbassia, Cairo, Egypt.

Acta Chimica Academiae Scientiarum Hungaricae, 85 (1), pp. 97—105 (1975)

THERMAL TRANSCARBOXYLATION REACTIONS, V*

STUDY OF THE RELATIVE REACTIVITIES OF THE AROMATIC HYDROGENS IN THE THERMAL TRANSFORMATION OF POTASSIUM BENZOATE

J. SZAMMER

(Central Research Institute for Chemistry of the Hungarian Academy of Sciences, Budapest)

Received June 28, 1974

The relative rate of abstraction of the *o*-, *m*- and *p*-hydrogens in the thermal transformation of potassium benzoate was studied with the use of compounds specifically labelled with deuterium. It was found that the reactivity of the hydrogens of the aromatic ring exhibits the position-dependence *o*-H > *m*-H > *p*-H, the extent of which is more significant for the reaction occurring in the solid phase than for that in the melt.

Introduction

The aromatic potassium carboxylates are known to rearrange to symmetric dicarboxylic acid salts at higher temperature [1]. In the case of potassium benzoate this transformation results in the terephthalate (Fig. 1), the industrial importance of which is well known.

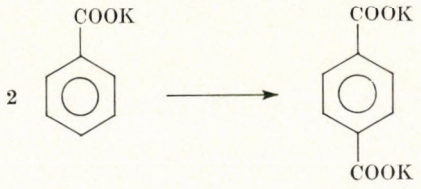

Fig. 1

In the thermal transformation process frequently referred to as the Henkel reaction in the literature, observations have been made on the formation of many aromatic carboxylates and the changes in the relative amounts of these with the advance of the reaction [2—5]. Dipotassium terephthalate appears and becomes predominant in the later stages of the reaction.

The composition of the products present at a given stage of the Henkel reaction is determined by the relative formation (kinetic) and conversion, (stability) characteristics of the individual components. On the above basis terephthalate is the product of a process the relative kinetic characteristics of which are not favourable. It appears of interest to examine the reaction from this aspect.

* Part IV: Radiochem. Radioanal. Lett. *20*, 151 (1974)

From the experimental results reported [6—9] the intermolecular nature of the thermal transcarboxylation reaction is generally accepted, and in essence it can be described by decarboxylation, hydrogen abstraction and recarboxylation reaction-steps (Fig. 2).

$$C_6H_5COOK \rightarrow [C_6H_5]^- + K^+ + CO_2$$

$$C_6H_5COOK + [C_6H_5]^- \rightarrow [C_6H_4COOK]^- + C_6H_6$$

$$[C_6H_4COOK]^- + K^+ + CO_2 \rightarrow C_6H_4(COOK)_2$$

Fig. 2

On this basis the terephthalate may form directly in a carboxylation reaction at the *para*-position of the benzoate.

The relative rates of formation of the dicarboxylates in the transcarboxylation process, *i.e.* the frequencies of carboxylation at given positions in the potassium benzoate molecule, are determined by the rate constants of the carboxylation reactions and the formation and stability constants of the carbanion $[C_6H_4COOK]^-$.

According to the intermolecular reaction scheme presented in Fig. 2, the carbanion is formed *via* hydrogen abstraction in some position of the benzoate molecule (Fig. 3). The frequency of carbanion formation in a given position can, thus, be characterized by the frequency of hydrogen splitting in that position. The present paper gives an account of the results of experiments carried out to study the position-dependence of hydrogen splitting.

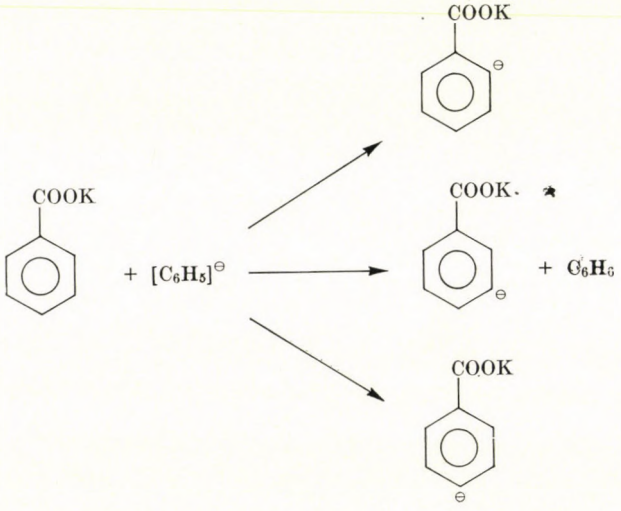

Fig. 3

Results and discussion

In earlier studies [10] it was found that under the experimental conditions employed the exchange of the hydrogens of the potassium benzoate molecule is a slow process; it cannot be detected in the initial stage of the reaction, even when a 1 : 1 molar mixture of $C_6H_5COOK + C_6D_5COOK$ is used. Thus, with the application of potassium benzoate specifically labelled with deuterium, a possibility arises for the study of the relative rate of aromatic hydrogen abstraction. For this purpose, benzoic acids and their potassium salts monodeuterated in *ortho*-, *meta*- and *para*-positions (Fig. 4) were prepared.

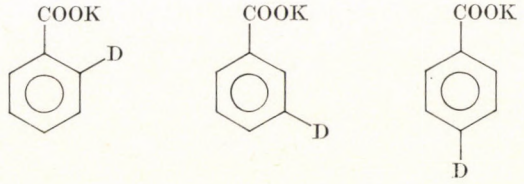

Fig. 4

All three labelled benzoates were subjected to thermal decomposition under identical conditions, at 430°C in the solid phase and at 450°C in the melt. The deuterium contents of the initial salts and of the benzene samples formed were determined mass-spectrometrically. The mole fractions (X_H, X_D and Y_n) calculated from the intensities relating to the individual mass numbers were used to characterize the various compositions. The experimental results are given in Table I.

Table I

Mass-spectrometric data on deuterated compounds

Position of labelling	Composition of starting salt		Temp. °C	Time min	Composition of benzene formed		
	X_H	X_D			Y_0	Y_1	Y_2
$o-d_1$	0.18	0.82	430	10	0.16	0.71	0.13
			450	3	0.15	0.75	0.10
$m-d_1$	0.18	0.82	430	10	0.16	0.78	0.06
			450	3	0.16	0.77	0.07
$p-d_1$	0.16	0.84	430	10	0.14	0.81	0.05
			450	3	0.14	0.79	0.07

From the data in the Table the frequency of the abstraction of the deuteriums in the different positions is given by the quotients of the Y_2 values. The deuterium mobility values referred to $o-d_1$ are listed in Table III. How-

ever, these data only correspond to the actual deuterium or hydrogen relative reactivity values if the H—D primary kinetic isotope effect demonstrated previously [10] is the same in all three positions. The appropriate experimental data are not available for this assumption. From the results in the Table, however, the following considerations provide a possibility for the determination of the relative hydrogen reactivity and the position dependence of the isotope effect.

In the thermal transformation of monodeuterated potassium benzoate, there are several possibilities for the formation of benzene molecules with different deuterium contents (Fig. 5).

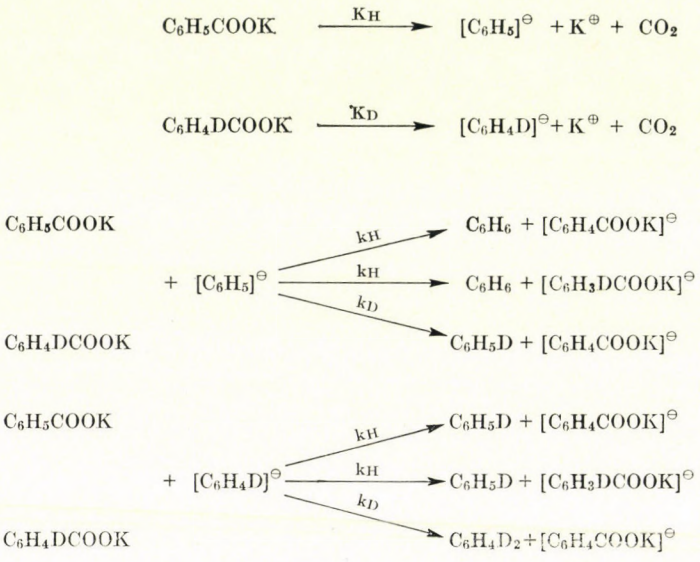

Fig. 5

The rate equations for these are as follows:

$$w_0^z = [C_6H_5^-]^z\{5k_H[C_6H_5COOK]^z + (5k_H - k_H^z)[C_6H_4DCOOK]^z\}$$
$$w_1^z = [C_6H_4D^-]^z\{5k_H[C_6H_5COOK]^z + (5k_H - k_H^z)[C_6H_4DCOOK]^z\} + \quad (1)$$
$$+ k_D^z[C_6H_5^-]^z[C_6H_4DCOOK]^z$$
$$w_2^z = k_D^z[C_6H_4D^-]^z[C_6H_4DCOOK]^z$$

where $5k_H = 2k_H^o + 2k_H^m + k_H^p$, and z is the position labelled with deuterium in the initial salt (Fig. 4).

Equations (1) can be written for the rates of formation of the benzene molecules with different deuterium contents in the processes of thermal transformation of all three specifically deuterated potassium benzoates, and in this

way we obtain a system of equations consisting of nine equations. If these equations are divided by one of them (in this case w_2^p), we arrive at equations (2)

$$\frac{w_0^z}{w_2^p} = \frac{[C_1H_5^-]^z}{[C_6H_4D^-]^p}\left\{\frac{5\,k_H}{k_D^p}\,\frac{[C_6H_5COOK]^z}{[C_6H_4DCOOK]^p} + \frac{5\,k_H - k_H^z}{k_D^p}\,\frac{[C_6H_4DCOOK]^z}{[C_6H_4DCOOK]^p}\right\}$$

$$\frac{w_1^z}{w_2^p} = \frac{[C_6H_4D^-]^z}{[C_6H_4D^-]^p}\left\{\frac{5\,k_H}{k_D^p}\,\frac{[C_6H_5COOK]^z}{[C_6H_4DCOOK]^p} + \frac{5\,k_H - k_H^z}{k_D^p}\,\frac{[C_6H_4DCOOK]^z}{[C_6H_4DCOOK]^p}\right\} + \tag{2}$$

$$+ \frac{k_D^z}{k_D^p}\,\frac{[C_6H_5^-]^z}{[C_6H_4D^-]^p}\,\frac{[C_6H_4DCOOK]^z}{[C_6H_4DCOOK]^p}$$

$$\frac{w_2^z}{w_2^p} = \frac{k_D^z}{k_D^p}\,\frac{[C_6H_4D^-]^z}{[C_6H_4D^-]^p}\,\frac{[C_6H_4DCOOK]^z}{[C_6H_4DCOOK]^p}$$

From these, if the simplifying conditions hold, the quotients of the rate constants referred to k_D^p for the abstraction of the hydrogens and deuteriums in the different positions (k_H^z/k_D^p and k_D^z/k_D^p) can be calculated from the data in Table I on the basis of the following considerations.

1. The low amount of material required for mass-spectrometric analysis means that experiments can be carried out up to an optionally low conversion. Calculations involving the above equations can the be made with the initial molar values.

2. The rate constant (K) of the decarboxylation reaction (Fig. 5) is not appreciably affected by monodeuterium substitution, *i.e.*

$$K_D^o = K_D^m = K_D^p = K_H$$

3. If the potassium benzoates specifically labelled with deuterium are subjected to thermal decomposition under exactly the same conditions, then the amount of benzene formed (B) is identical in the three cases, and

$$B = \sum_{i=0}^{2} B_i^o = \sum_{i=0}^{2} B_i^m = \sum_{i=0}^{2} B_i^p$$

Thus, from the above equations the following formula is obtained for the amount of benzene (B_i) containing i deuteriums formed in time t from potassium benzoate deuterated in position z:

$$B_i^z = Y_i^z B = \int_0^t W_i^z \cdot dt$$

4. The phenyl anion is formed in the decarboxylation step (Fig. 5), and reacts further in the step involving hydrogen abstraction, discussed above.

Accordingly, the stationary concentration of the phenyl anion can be given by the following formulas:

$$[C_6H_5^-]^z = \frac{K_H\,[C_6H_5COOK]^z}{5\,k_H - (k_H^z - k_D^z)\,[C_6H_4DCOOK]^z}$$

$$[C_6H_4D^-]^z = \frac{K_D\,[C_6H_4DCOOK]^z}{5\,k_H - (k_H^z - k_D^z)\,[C_6H_4DCOOK]^z}$$

The further reaction of the phenyl anion is represented by the expression in the denominator. It may be assumed that this latter is not affected appreciably by monodeuterium substitution, and that the following simplification does not lead to serious error:

$$\frac{5\,k_H - (k_H^p - k_D^p)\,[C_6H_4DCOOK]^p}{5\,k_H - (k_H^o - k_D^o)\,[C_6H_4DCOOK]^o} = \frac{5\,k_H - (k_H^p - k_D^p)\,[C_6H_4DCOOK]^p}{5\,k_H - (k_H^m - k_D^m)\,[C_6H_4DCOOK]^m} = 1$$

5. The quotients of the starting concentrations and the quotients of the amounts of benzene formed can be replaced by the following mole fractions as the coefficients in the above equation system:

$$\frac{[C_6H_5COOK]^z}{[C_6H_4DCOOK]^p} = \frac{X_H^z}{X_D^p};\quad \frac{[C_6H_4DCOOK]^z}{[C_6H_4DCOOK]^p} = \frac{X_D^z}{X_D^p};\quad \frac{\int_0^t W_i^z \cdot dt}{\int_0^t W_2^p \cdot dt} = \frac{B_i^z}{B_2^p} = \frac{Y_i^z}{Y_2^p}$$

Substitution of these expressions into equations (2) leads to the over-defined system of equations (3):

$$\begin{aligned}
\frac{Y_o^z}{Y_2^p} &= \frac{X_H^z}{X_D^p}\left(\frac{5\,k_H}{k_D^p\,X_D^p} - \frac{X_D^z}{X_D^p}\,\frac{k_H^z}{k_D^p}\right)\\
\frac{Y_1^z}{Y_2^p} &= \frac{X_D^z}{X_D^p}\left(\frac{5\,k_H}{k_D^p\,X_D^p} - \frac{X_D^z}{X_D^p}\cdot\frac{k_H^z}{k_D^p}\right) + \frac{X_H^z\,X_D^z}{(X_D^p)^2}\cdot\frac{k_D^z}{k_D^p} \qquad (3)\\
\frac{Y_2^z}{Y_2^p} &= \frac{(X_D^z)^2}{(X_D^p)^2}\cdot\frac{k_D^z}{k_D^p}
\end{aligned}$$

Solution of this system for the quotients of the rate constants gives the values reported in Table II. These data were used to calculate the hydrogen reactivity values referred to the *o*-hydrogen, and also the H–D primary kinetic isotope effect values for the various positions. These are given in Table III. It can be seen from the tabulated data that the frequency of hydrogen abstraction shows the position-dependence *o*-H > *m*-H > *p*-H; the extent of this for

Table II

Hydrogen and deuterium reactivity values referred to k_D^p

Temperature	k_H^o/k_D^p	k_H^m/k_D^p	k_H^p/k_D^p	k_D^o/k_D^p	k_D^m/k_D^p
430 °C	4.27	2.55	1.92	2.39	1.21
450 °C	2.78	1.96	1.83	1.47	0.96

Table III

Relative hydrogen reactivity values and H–D isotope effect values

z	Temp. °C	Y_2^z/Y_2^o	k_H^z/k_H^o	k_H^z/k_D^z
o	430	1.00	1.00	1.79
	450			1.89
m	430	0.46	0.60	2.11
	450	0.70	0.70	2.04
p	430	0.38	0.45	1.92
	450	0.70	0.66	1.83

the transformation in the solid phase at 430°C is more significant than for that in the melt at 450°C.

The reason for the greater mobility of the *o*-hydrogen is almost certainly a spatial one; the orientation of the potassium benzoate molecules results in the spatial proximity of the carboxyl groups [11]. Thus, the phenyl anion is formed in the close vicinity of the *o*-hydrogens, and thereby increases the frequency with which they split off.

According to the data in Table III, the phenyl anion abstracts a proton from the different positions with the frequencies given in Table IV. At the same time these values signify the frequency of formation of the carbanion at the corresponding positions. This latter, however, presumably plays a considerable controlling role in determining the relative amounts of the dicarboxylic acid salts formed in the thermal transcarboxylation reaction. In this way the experi-

Table IV

Frequency of abstraction of hydrogen in the different positions

Temperature	*o*	*m*	*p*
430 °C	0.55	0.33	0.12
450 °C	0.49	0.35	0.16

mental method described can also provide valuable information in research aimed at the preparation of a certain end-product of the transcarboxylation reaction.

The averages of the primary kinetic isotope effects in Table III, weighted in accordance with the frequencies of splitting-off, are: at 430°C 1.93, and at 450°C 1.91. If these values are compared with the effects found for the thermal decomposition of a 1 : 1 molar mixture of perdeuterated and non-deuterated potassium benzoates, the values of which are 2.20 at 430°C [13] and 2.15 at 450°C [10], it turns out that the following secondary effect (Fig. 6) is also appreciable in the step involving of hydrogen abstraction.

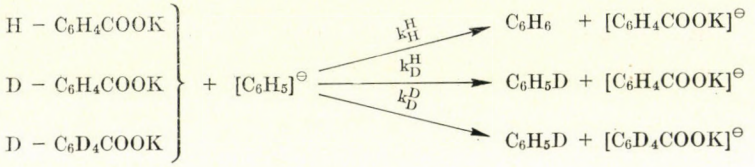

	k_H^H/k_D^D	k_H^H/k_D^H	k_D^H/k_D^D
430°C-on	2,20	1,93	1,14
450°C-on	2,15	1,91	1,12

Fig. 6

Experimental

Materials

The potassium salts were prepared by neutralizing the benzoic acid with an aqueous KOH solution. The aqueous solution of the salt was evaporated to dryness, and the residue was dried at 200°C at 1 mm Hg. The purities of the potassium salts thus obtained were checked through their potassium content.

Preparation of specifically deuterated benzoic acids

The 2-d_1, 3-d_1 and 4-d_1 benzoic acids were prepared by a literature procedure [14]. Deuterium oxide, and then deuterosulphuric acid, were added to an ether solution of tolylmagnesium bromide prepared from the corresponding bromotoluene. The specifically deuterated toluene formed was oxidized to the benzoic acid with an alkaline $KMnO_4$ solution. The deuterium content of the benzoic acid, in the form of the methyl benzoate, was determined by mass spectrometry.

Procedure

The thermal reactions were carried out in a metal-bath thermostat, thermostated within ± 1°C.

The specifically deuterium-labelled potassium benzoates were subjected to thermal decomposition at 1 mm Hg. The examinations were carried out on 20 mmole salt in identical

quartz tubes. The benzene formed was frozen out with liquid air. The amount of residual potassium benzoate was determined by isotope dilution, using ^{14}C-benzoic acid. The conversions were between 0 and 3% in the experiments reported above.

The deuterium contents of the methyl esters formed from the starting benzoic acids, and of the benzene samples produced in the thermal decomposition process, were determined on an Ms 902 mass spectrometer. The accuracy of these determinations was $\pm 1\%$.

REFERENCES

[1] RAECKE, B.: Angew. Chem. **70,** 1 (1958)
[2] KRAUS, M., KOCHLOEFL, K., SETINEK, K., BERÁNEK, L., ŠORM, F.: Chem. Ind. 1060 (1961)
[3] OGATA, Y., NAKAJIMA, K.: Tetrahedron **21,** 2393 (1965)
[4] RATUSKY, J., ŠORM, F.: Chem. Ind. 1798 (1966)
[5] RATUSKY, J.: Coll. Czech. Chem. Commun. **33,** 2346 (1968)
[6] RATUSKY, J., ŠORM, F.: Coll. Czech. Chem. Commun. **24,** 2553 (1959)
[7] RIEDEL, O., KIENITZ, H.: Angew. Chem. **72,** 738 (1960)
[8] MCNELIS, E.: J. Org. Chem. **30,** 1209 (1965)
[9] FURUYAMA, S.: Bull. Chem. Soc. Japan **40,** 1212 (1967)
[10] SZAMMER, J., NOSZKÓ, L.: Chem. Ind. 1540 (1970)
[11] FURUYAMA, S., EBARA, N.: Bull. Chem. Soc. Japan **39,** 1617 (1966)
[12] RATUSKY, J., TYKVA, T., ŠORM, F.: Coll. Czech. Chem. Commun, **32,** 1719 (1967)
[13] SZAMMER, J. *et al.:* unpublished results
[14] TAKAHASI, M.: Bull. Chem. Soc. Japan **33,** 808 (1960)

János SZAMMER; MTA Központi Kémiai Kutató Intézet
1525 Budapest, P. O. B. 17. Hungary.

Acta Chimica Academiae Scientiarum Hungaricae, 85 (1), pp. 107—115 (1975)

PHYTOCHEMICAL INVESTIGATION OF THYMELEA HIRSUTA, III*

COUMARINS

A. M. Rizk, F. M. Hammouda and S. I. Ismail

(Pharmaceutical Sciences Laboratory, National Research Centre, Dokki, Cairo, Egypt)

Received March 1, 1974

In revised form August 17, 1974

The study of the coumarins of *Thymelea hirsuta* revealed the presence of daphnorin, daphnoretin, daphnin, daphnetin, daphnetin-β-glucoside, umbelliferone, scopoletin and esculetin. The previously reported unidentified lactone was proved to be daphnoretin. The R_f values of 30 coumarins in several solvents are reported.

Introduction

Certain species of the family Thymelaceae (mostly *Daphne* spp.) have been reported to contain coumarins [1—10]. In addition to daphnetin which was found to be present as daphnin in several *Daphne* species, the presence of some other coumarins *viz.* daphnorin, daphnoretin, daphnetin, daphnoside and umbelleriferone was reported. The presence of daphnetin and its glycoside was stated to be restricted to Thymelaceae and Euphorbiaceae.

The only mention in the literature about the coumarins of *Thymelea hirsuta* the only representative of the Thymelaceae family in Egypt, was that stated by some of us [10] which revealed that the reportedly "new" constituent (thymelol) [12] isolated by Saleh and Haddad from the plant, is daphnoretin. Reinvestigation of the lipid fraction of *T. hirsuta* and the identification of another unidentified component mentioned by the latter authors [13] were recently reported by us [14].

This work deals with the study of the coumarins of the plant as well as the identification of the substance reported by Gharbo *et al.* [13] as an unidentified lactone.

Results and discussion

The substance reported by Gharbo *et al.* [13] as an unidentified lactone (m.p. 229—230°C) was prepared following the same reported procedure. The substance obtained (m.p. about 232°C) gave, after repeated crystallization

* For Part II see Ref. [14].

from ethanol, yellowish white needles which melted at 249—251°C both alone and upon admixture with authentic daphnoretin and had the same R_f as the authentic sample in different solvent systems. The IR, UV, MS and NMR spectra were identical with those of the authentic material: 2 doublets (each

Table I

NMR data of daphnoretin (in DMSO-d_6; 60 MHz)

H	cps	ppm	Multiplicity	J(cps)	System
H—4	473	7.88	s		—
H—5	434	7.25	s		—
H—8	413	6.90	s		—
H—3′	383	6.40	d	9	AB
H—4′	484	8.08	d	9	
H—5′	465	7.77	d	$J_{5',6'} = 9$	ABC
H—6′	420—433	7.01—7.23	m	$J_{7',8'} = 2.5$	
H—8′				$J_{5',8'} < 1$	ABX
H_3—C—O—	230	3.84	s	—	approximation

1 H, J = 9) at $\delta = 8.08$ (H-4) and 6.40 (H-3) ppm; a singlet at $\delta = 7.88$ (ppm) (1 H), which may be an olefinic proton in β-position of an α,β-unsaturated γ-lactone (position 4 of coumarins). The presence of at least two aromatic rings in the molecule (NMR: 1 ABC system and 2 singlets) shows that it is a dicoumarin derivative.

Moreover, the acetate and methyl ether derivatives prepared show no m.p. depression upon admixing with the corresponding authentic daphnoretin derivatives.

The coumarins were prepared using the procedure adopted by TSCHESCHE *et al.* [4] for the preparation of the coumarins of *Daphne*. TLC, using silica gel G and applying different solvent systems, revealed the presence of about 14 components.

Column chromatography, using silica gel, permitted only the isolation of daphnoretin (m.m.p., IR, MS) in a pure form (fractions 26—28 eluted with chloroform–acetone 98 : 2). On the other hand, the residue obtained from fractions 245—247 (eluted with acetone–methanol–water 90 : 10 : 1) gave daphnorin upon crystallization from benzene–methanol. Hydrolysis of daphnorin gave daphnoretin (R_f, m.m.p., MS) and glucose (paper chromatography).

Preparative TLC, using silica gel G, was successfully used for the fractionation of some other coumarins obtained as mixtures in the column chromatographic procedure. From fractions 29—43 (eluted with chloroform–acetone 98 : 2) scopoletin and umbelliferone were separated, while from the combined

fractions 127—149 (eluted with chloroform–acetone 50 : 50) daphnetin was isolated. Scopoletin was also obtained in the same manner from fractions 150—177 (eluted with chloroform–acetone 50 : 50). Sometimes purification of the isolated coumarins was achieved by further preparative TLC. The identity of the above coumarins was proved by m.m.p., UV, IR and MS.

The presence of esculetin, daphnin (daphnetin-7-glucoside) and daphnetin-8-glucoside was only proved by TLC, using different solvents.

Experimental

Plant material

Flowering plants of *Thymelea hirsuta* Endl. were collected from Burg El-Arab in December.

Thin-layer chromatography

Adsorbent: Silica gel G.
Solvent systems: Several solvents (4.14—19) were applied (Tables II, III).
For preparative TLC: Benzene–acetic acid–water 2 : 2 : 1.
Ether–petroleum ether–methanol 60 : 40 : 3.
Chloroform–methanol–formamide 80 : 19 : 1.

Detection (20.21): Visualization of the coumarins was carried out by examining the plates under the UV (before and after exposure to ammonia vapours) or by spraying with either 5% phosphomolybdic acid in ethanol or diazotized *p*-nitroaniline or 2% aqueous $FeCl_3$.

Identification of the unidentified lactone

About 100 g of the powdered leaves were extracted with ether; the marc was air-dried and then exhausted with ethanol. The alcoholic extract was evaporated *in vacuo* and the residue was refluxed for 5 min with successive portions of water. The aqueous extract was then cooled and shaked several times with ether. The ethereal extract was washed with water, dehydrated over anhydrous sodium sulfate and the solvent evaporated. The residue was then crystallized from ethanol.

The acetate (acetic anhydride–pyridine) melted at 242°C (undepressed) and the methyl ether derivative (diazomethane in ether) at 238°C (undepressed).

Preparation of the coumarins

The defatted powdered leaves (1.5 kg) were extracted, in Soxhlet, with methanol. The methanolic extract was concentrated in vacuum to about 700 ml, diluted with water (500 ml) and then extracted with 5 successive portions of chloroform (1 l each). The chloroform extract was evaporated in vacuum at 40°C, the residue was dissolved in about 650 ml benzene–chloroform mixture (1 : 3) and then left overnight at room temperature. The deposited precipitate (4.5 g) was separated by centrifugation, then washed with chloroform.

Column chromatography

The pale brown residue (4.5 g) was charged on a column (4.3 × 60 cm) packed with silica gel in chloroform. Elution was carried out with chloroform, chloroform–acetone mixtures, acetone and acetone–methanol–water (90 : 10 : 1); and fractions (100 ml) were then collected (Table IV).

Table II

R_f of some coumarins

Coumarin	R_f						UV				
	A	B	C	D	E	F	DL	NH_3	I	II	III
Angelicin	0.39	0.53	0.71	0.74	0.69	0.63	dB	dB	—	fY	V
Bergapten	0.36	0.42	0.72	0.72	0.69	0.59	Y	YG	—	—	—
Daphnetin	0.30	0.59	0.12	0.02	0.17	0.15	RBr	YBr	Br	iO	B
Daphnoretin	0.05	0.07	0.40	0.06	0.38	0.43	B	SB	Y	Y	—
Esculetin	0.02	0.03	0.18	0.11	0.07	0.34	BG	BG	YBr	Br	—
Felamedin	0.28	0.35	0.73	0.70	0.74	0.63	iV	iV	—	—	—
Herniarin	0.33	0.48	0.71	0.75	0.70	0.60	V	V	—	fY	—
Hydrangetin	0.18	0.31	0.61	0.10	0.60	0.54	YG	BrYG	YG	Y	—
Imperatorin	0.35	0.51	0.71	0.71	0.71	0.61	YG	YG	dG	RBr	fBr
Isobergapten	0.45	0.50	0.48	0.76	0.70	0.63	Y	YG	—	fY	—
Isoimperatorin	0.45	0.49	0.74	0.73	0.74	0.76	YG	Y	Gy	YBr	fBr
Isopimpinellin	0.31	—	0.71	0.70	0.70	0.51	O	dO	—	—	—
Marmesin	0.05	0.07	0.60	0.37	0.58	0.39	iBV	brV	Gy	YBr	—
Methyldalbergin	0.23	0.42	0.76	0.70	0.71	0.61	SB	brSB	—	—	—
Nordalbergin	0.03	0.06	0.17	0.03	0.18	0.48	iY	YG	dYBr	YBr	Br
Oxypeucedanin	0.22	0.29	0.73	0.69	0.74	0.59	YG	YG	—	fBr	—
(+) Oxypeucedanin (hydrate)	0.89	0.12	0.49	0.24	0.52	0.50	B	B	Gy	iBRr	—
Pimpinellin	—	0.45	—	—	0.70	—	Br	dBr	—	—	—
Prantscimgin	0.27	0.34	0.72	0.67	0.74	0.61	V	brV	—	—	—
Psoralen	0.33	0.46	0.71	0.66	0.69	0.57	B	B	—	fBr	—
Rutamarin	0.42	0.51	0.76	0.79	0.71	0.64	V	brV	—	fY	—
Scopoletin	0.08	0.11	0.48	0.07	0.48	0.42	iB	iB	Y	RBr	fBr
Sphondin	0.26	0.34	0.69	0.67	0.67	0.57	SB	BG	Gy	YBr	
Umbelliferone	0.12	0.23	0.64	0.15	0.60	0.49	iB	iB	—	YBr	—
Xanthotoxin	0.28	0.43	0.96	0.63	0.68	0.45	YG	YG	—	fY	—

Adsorbent: Silica gel G

Solvents:
A— Benzene–ether–acetic acid (89 : 10 : 1)
B— Benzene–ethyl acetate (9 : 2)
C— Chloroform–acetone (1 : 1)
D— Benzene–ethanol (85 : 15) (NH_3 atmosphere)
E— Chloroform–acetone–methanol (50 : 50 : 1)
F— Toluene–ethyl acetate–formic acid (5 : 4 : 1)

Detection:
I — 5% Phosphomolybdic acid in ethanol
II — Diazotid *p*-nitroaniline
III — 2% aqueous $FeCl_3$

Colours: B = blue; Br = brown; G = green; Gy = grey; O = orange; R = red; S = sky; V = violet; Y = yellow; br = bright; d = dull; f = faint; i = intense

Table III

R_f of the coumarin components of T. hirsuta and some coumarin glycosides

Component	R_f^*	UV				
		DL	NH_3	I	II	III
I	0.14	BG	G	fYG	YBr	fYBr
II	0.20	iB	YG	B	YBr	fYBr
III	0.24	B	V	B	YBr	fY
IV	0.30	—	—	B	P	—
V	0.40	G	brG	fY	Y	—
VI	0.45	iB	BV	B	YBr	—
VII	0.49	brB	brB	B	YBb	fYBr
VIII	0.55	B	B	B	fY	fYBr
IX	0.60	B	V	B	fY	—
X	0.65	B	V	B	fY	—
XI	0.80	YBr	O	YBr	iO	dG
XII	0.87	B	B	B	YBr	Br
XIII	0.90	YBr	YBr	fY	YBr	Br
Scopolin	0.32	iB	BV	—	—	—
Esculin	0.38	brB	brBG	fYG	Br	fB
Daphnin	0.31	—	—	B	P	—
Daphnetin-β-glucoside	0.40	G	brG	fY	Y	—
Daphnorin	0.45	iB	BV	B	fY	—

* Adsorbent: silica gel G
Solvent: ethyl acetate–methyl ethyl ketone–formic acid–water (5 : 3 : 1 : 1)
Colours: see Table II

Daphnorin

Daphnorin crystallized from the residue (obtained from fractions 245—247) melted at 200—203°C, Ref. [3]: 202—204°C). Hydrolysis of the glycoside (50 mg), in ethanol with 2 *N* H_2SO_4 (5 ml) for 6 hrs, gave daphnoretin (m.m.p., R_f). The IR spectra showed ν = 1720, 1610, 1570, 1555, 1510 cm^{-1}. The UV spectrum showed λ_{max} at 225 (ε = 7200), 267 (ε = 3400), 325 (ε = 7400), 345 (ε = 8300); λ_{min} at 252 nm. The MS showed m/e at 352 which corresponds to the molecular ion M^+ (100), 337 (2.7), 324 (2.7), 179 (2.7) and 145 (6.8). The NMR spectra (Table I) have confirmed the identity of the compound.

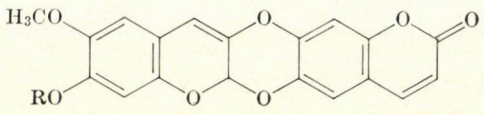

R = H: Daphnoretin
R = Glucose: Daphnorin

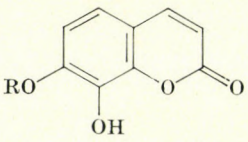

R = H: Daphnetin
R = Glucose: Daphnin

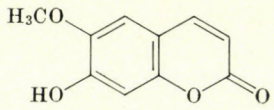

Scopoletin

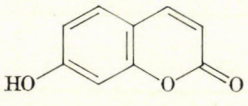

Umbelliferone

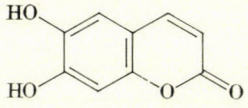

Esculetin

Daphnoretin

It crystallized from chloroform–petroleum ether and melted at 250—251°C (undepressed).

Scopoletin

Scopoletin (obtained from fractions 29—43), crystallized from methanol, melted at 204—205°C (Ref. [22]: 205°C), and had the same R_f and fluorescence as the authentic material. λ_{max} at 253, 300, 349 nm (Ref. [23, 24]: 255, 300, 350). Its MS agreed with that of scopoletin.

Umbelliferone

Umbelliferone (obtained from fractions 29—43 and 150—177), crystallized from methanol, melted at 220—223°C (Ref. [25]: 223—224°C). λ_{max} at 240, 300, 305, 325 nm (Ref. [25]: 240, 300, 325). MS showed M^+ 162 which corresponds to the molecular ion of umbelliferone; and the fragmentation agreed with it.

Daphnetin

Daphnetin (obtained from fractions 127—149), crystallized from methanol, melted at 254—256°C (Ref. [20]: 256°C). UV showed λ_{max} at 264, 329 nm (Ref. [20]: 265.5, 330 nm). The MS showed M^+ at 178 which corresponds to the molecular ion and the fragmentation is typical for daphnetin.

Table IV

Column chromatography of the coumarins

Solvent	Fractions (100 ml)	R_f^*	Detection in UV	
			$-NH_3$	$+NH_3$
Chloroform	1— 12	—	—	—
Chloroform–acetone	13— 25	—	—	—
(98 : 2)	26— 28	0.83	B	SB
	29— 43	0.79	iB	iB
		0.83	B	B
Chloroform–acetone	44— 76	0.18	G	YB
(90 : 10)		0.81	B	B
Chloroform–acetone	77—106	0.11	O	iO
(75 : 25)		0.25	G	YG
		0.76	Br	YBr
		0.82	B	B
	107—122	0.01	B	B
		0.24	G	YG
		0.66	V	V
		0.73	B	iB
		0.80	V	V
		0.89	Y	Y
	123—126	0.01	B	B
		0.15	YG	Y
		0.21	—	—
		0.68	—	—
		0.73	B	iB
		0.76	Br	YBr
		0.81	V	V
Chloroform–acetone	127—149	0.18	Y	Y
(50 : 50)		0.24	G	G
		0.66	YBr	YBr
		0.72	Br	Br
		0.81	BV	B
	150—177	0.81	B	iB
Chloroform–acetone	178—194	0.06	B	B
(25 : 75)		0.10	G	YG
		0.44	YBr	YBr
		0.49	SB	BG
	195—126	0.01	G	G
		0.18	B	BG

Table IV continued

Solvent	Fractions (100 ml)	R_f^*	Detection in UV	
			$-NH_3$	$+NH_3$
		0.24	YBr	YBr
		0.33	RBr	YBr
		0.38	V	V
		0.44	YBr	Y
		0.49	B	B
		0.60	BV	B
		0.81	V	V
Acetone	217—242	0.02	G	G
		0.06	BG	BG
		0.15	YG	G
		0.25	B	B
		0.33	RBr	YBr
		0.45	B	B
		0.60	Br	B
		0.76	G	G
Acetone–methanol–water	243—252	0.02	G	G
(90 : 10 : 1)		0.14	B	iB
		0.18	BG	BG
		0.24	B	BG
		0.43	V	V

* Adsorbent: silica gel G; solvent: chloroform–methanol–formamide 80 : 19 : 1.

*

The authors are grateful to Professors S. A. Brown (USA), A. Chaterjee (India) A. G. Gonzalez (Spain), R. K. Ibrahim (Canada), R. G. Kelsey (USA), P. Schersahl (W. Germany), W. Steck (Canada), I. R. Seshadri (India) and I. Ognyanov (Bulgaria) for kindly supplying the authentic samples.

REFERENCES

[1] Rindl, M.: African J. Sci., **30,** 455 (1963); Chem. Zbl., **1,** 715, 1991 (1934)
[2] Zwenger, C.: Liebigs Ann. Chem., **115,** 1 (1960)
[3] Tschesche, R. Schacht, U., Legler, G.: Liebigs Ann. Chem., **662,** 113 (1963)
[4] Tschesche, R., Schacht, U., Legler, G.: Naturwiss., **15,** 521 (1963)
[5] Kosheleva, L. I., Nikonov, G. K., Perel'son, M. E.: Khim. Prir. Soedin., **4,** 133 (1968)
[6] Kosheleva, L. I., Nikonov, G. K., Pimenov, M. G.: Lek. Aromat. Rast., **15,** 140 (1969)
[7] Kosheleva, L. I., Nikonov, G. K.: Tr. Vses. S'ezda Farm. I*st.*, 245 (1967); C. A. **75,** 126577 (1971)
[8] Kosheleva, L. I., Nikonov, G. K.: Farmatsiya Moscow, **17,** 40 (1968); C. A. **70,** 103683 (1969)
[9] Majumder, P. L., Sengupta, C. C.: J. Indian Chem. Soc., **45,** 1058 (1968)
[10] Rizk, A. M., Rimpler, H.: Phytochem. **11,** 473 (1972)

[11] PARIS, R.: The Distribution of Plant Glycosides, in "Chemical Plant Taxonomy", Edited by T. Swain, Academic Press, London, New York 1963
[12] SALEH, M. R. I., HADDAD, D. Y., SARG. T. M.: J. Pharm. Sci. U. A.R., **4,** 49 (1963)
[13] GHARBO, S. A., KHAFAGY, S. M., SARG, T. M.: U. A. R. J. Pharm. Sci., **11,** 101 (1970)
[14] RIZK, A. M., HAMMOUDA, F. M., ISMAIL, S. I.: Planta Medica **26,** 346 (1974)
[15] ABDEL-HAY, F. M., ABOU-MUSTAFA, E. A., EL-TAWIL, B. A. H., FAYEZ, M. B. E.: Planta Medica, **13,** 91 (1965)
[16] NOVAK, I., BUZÁS, G., MINKER, E., KOLTAI, M., SZENDREI, K.: Planta Medica, **14,** 151 (1966)
[17] IBRAHIM, R. K.: J. Chromatog., **42,** 544 (1969)
[18] SHAFIZADKH, F., MELINKOFF, A. B.: Phytochem., **9,** 1311 (1970)
[19] STAHL, E., SCHORN, P. J.: Z. Physiol. Chem., **325,** 306 (1961)
[20] SATŐ, M., HASEGAWA, M.: Phytochem., **8,** 1211 (1969)
[21] STAHL, E.: Dünnschicht-Chromatographie, Springer-Verlag, Berlin—Heidelberg—New York 1967
[22] MORS, W. B., RIBEIRO, O.: J. Org. Chem., **22,** 978 (1957)
[23] RICHARD, H. G., BRUCE, M. P.: Arch. Biochem. Biophys., **49,** 1 (1954)
[24] CINGOLANI, E.,: Ann. Chem. (Rome), **47,** 557 (1957)
[25] MANGINI, A., PASSERINI, R. Gazz. Chim. Ital., **87,** 243 (1957)

ABDEL-FATTAH M. RIZK
F. M. HAMMOUDA
S. I. ISMAIL

Pharmaceutical Sciences Lab., National Research Centre, Dokki, Cairo, Egypt.

RECENSIONES

D. BROOKS: *Student guide to chemistry — a modern introduction*

W. B. Saunders Company, Philadelphia—London—Toronto, pp. 233

Although this book is especially recommended as a guide to "Chemistry: A Modern Introduction", by BRESCCIA, MEHLMAN, PELLEGRINI and STAMBLER, in itself it lends the reader a comprehensive survey about the basic principles of chemistry. It contains the fundamental definitions and summaries briefly the chapters of the cited work. The brevity associated with lucidity should be mentioned as a mean value of the book. A list at the beginning of each chapter which enumerates what the student should be able to perform after studying the given chapter, focuses attention to the mean points. A great variety of problems along with solutions is presented in each chapter. Some pages are devoted to advices how to learn chemistry. Considering the inherent merits of this book, the reviewer thinks it can be a useful guide to other works than the one by BRESCIA, MEHLMAN, PELLEGRINI and STUMBLER. As for the subjects of the book here are some chapter titles of the 24: Gases (2), Liquids and Solids (3), Atoms and Molecules (4), Nomenclature — Chemical Arithmetic (5), Regularities in the Properties of Elements (7), The Covalent Bond: The Shape of Molecules (9), Energy Changes in Chemical Reactions (10), Chemical Equilibrium (11), Ionic Solutions: Oxidation and Reduction (13), Ionic Equilibrium (15), Chemical Kinetics (17), Nuclear Chemistry (18), The Chemistry of Several Common Nonmetallic Elements (19), The Chemistry of Some Representative Metals (20), The Chemistry of Carbon Compounds (22), Polymers and Proteins (23), Instrumental Analyses (24).

Z. BOKSAY

Structure and Bonding, Vol. 17, Metal Bonding in Proteins

Springer Verlag, 1973, 268 pp.

The 17th volume of this series consists of four independent chapters, and it is most expedient to consider these separately.

The first chapter (66 pp.), "*Structural Aspects and Biochemical Function of Erythrocuprein*", was written by U. WESER (Institute of Physiological Chemistry, University of Tübingen). The structural characteristics and catalytic properties of copper-containing proteins have become known recently, and these results are discussed in many review articles. In this small monograph the author gives an account of the most thoroughly studied copper-containing protein, erythrocuprein, isolated from erythrocytes. This low-molecular weight protein (M. W. 35,000) contains 0.34% copper. Other, closely related copper-containing proteins are also to be found in different parts of the organism. A detailed description is presented of the isolation and characterization of erythrocuprein, of the study of its chemical composition, of its spectroscopic properties and immunological features. Its enzymatic nature is manifested not only in its metal-transporting ability, but also in redox reactions. This review (with 226 literature references) covers the publications on erythrocuprein up to the middle of 1972.

The second chapter of the volume, on ferritin, contains 68 pages, and was written by R. R. CRICHTON (Max-Planck-Institut für Molekulare Genetik, Berlin—Dahlem). The iron-containing proteins of the living organism (*e.g.* haemoglobin, myoglobin) play an extremely

important role in the functioning of the organism. The present review deals with ferritin (M. W. 444,000), which contains 13% of the iron content of the human organism, and in one molecule of which there may be several thousand iron atoms. The assumed function of the protein is to act as a store of iron reserve not participating actively in the metabolism. The author discusses the isolation of the protein, the still fairly limited amount of material known in connection with its chemical structure, the manner of binding of the iron atoms, the ferritin–apoferritin transformation, and many other features of importance from a biochemical aspect.

The review is completed with 238 literature references, which deal with the results achieved in this field up to the beginning of 1973.

The title of the third small monograph is "*Metal-Polypeptide Interactions: The Conformational State of Iron Proteins*" (85 pp.), and its author is M. LLINÁS (Department of Biochemistry, University of California, Berkeley). This chapter differs in its structure from the previous two, for it is not a review of one definite metal-containing protein, but deals with the changes in conformation of a whole series of peptides and proteins containing relatively little iron (siderochrome, transferrin, rubredoxin, haemerythrin, etc.), in connection with complex-formation with the metal. The 320 literature references treat the relevant material up to the beginning of 1973.

The concluding chapter of the volume discusses the calcium-binding proteins (44 pp.) (F. L. SIEGEL, Departments of Pediatrics and Physiological Chemistry, The University of Wisconsin Center for Health Sciences, Madison, Wisconsin). This is the shortest of the four chapters and perhaps the most important; it certainly deals with the protein-binding of the most extensively utilized cation, calcium. The introduction reviews those biological processes in which calcium plays a role, and this is so comprehensive that even a mere listing is not possible here. Rereading of the chapter leads to the impression that the very succinctly outlined material would have deserved a much more detailed treatment. The 209 references again cover the literature up to the beginning of 1973.

K. MEDZIHRADSZKY

E. JUCKER (editor): *Progress in Drug Research.* Authors: M. W. ANDERS, A. L. BASSET and A. L. WIT, L. BOLIS, R. B. BURROWS, J. J. HLAVKA and J. H. BOOTHE, P. J. ISLIP, J. A. MONTGOMEYY and R. F. STRUCK, J. S. BINDRA and R. BINDRA, F. KRATZ

Birkhäuser Verlag, Basel and Stuttgart, 1973, 532 pp.

This series, which has been edited by Ernst JUCKER for 14 years, truly reflects the changes in the development of pharmacology and medicinal chemistry during this period. The chapters, written by eminent specialists, well show the present state of knowledge in the domains selected for discussion. This statement also applies to the present volume of the series, which comprehensively reviews nine important fields of drug research.

The first chapter by M. W. ANDERS deals with the factors promoting or inhibiting microsomal drug metabolism. The literature of agents acting directly on enzymes are only discussed. First a survey is given of the reports dealing with drugs affecting microsomal aromatic hydroxylation; among them well-known substances such as acetone, gaseous narcotics and Metyrapone are also considered. A detailed discussion is given of the problems connected with the explanation of the inhibition of microsomal drug metabolism. Data on the *in vitro* and *in vivo* inhibition, on factors causing changes in the microsomal drug metabolism and their importance in clinical therapy are included.

The next chapter by BASSET and WIT is concerned with recent results in the electrophysiology of antiarrythmic drugs. This chapter is of particular interest for the reviewer, since the literature of antiarrythmic agents was reviewed by him in the same series in 1968. The authors of the present survey are well-known researchers of the field with the proper personal experience for selecting and evaluating the problems to be discussed. First a summary on the present state of knowledge is given on the electrophysiology of the cell membrane and on the genesis of cardiac rhythm disturbances, followed by a treatment of the electrophysiological aspects of the mechanism of action of quinidine and procainamide.

The next subdivision is devoted to a very important topic, recent possibilities in further development of the technique of recording by means of microelectrodes. This method has led to new models for the examination of cardiac rythm disturbances and to a new approach in analyzing the genesis of the disease. The research on slow potentials, detected first partly by the authors, changes in the electrophysiology of the distal A—V system, the origin of supraventricular arrythmias and the evaluation of electrophysiological results obtained on blood-perfused isolated organs are mentioned here. A subdivision deals with the voltage clamp technique and the mechanism o action of cardioactive drugs; detailed discussion is given of the electrophysiological effects of some antiarrythmic agents, such as Diphenylhydantoin Lidocaine and Phentolamine. The excellent chapter is concluded by a survey of the much discussed problem of classifying antiarrythmic drugs.

L. BOLIS gives, in the third chapter, a comprehensive and very well illustrated summary on researches in connection with the red blood cell membrane being the model of the site of attack of drug action. Nearly fifty pages with 200 references are devoted to the transport and diffusion processes in red blood cells and the regulation of the ion transport, including potassium and sodium ions, and ion selectivity. Drug effects on the cation transport, the transport of non-electrolytes, passive ion transport, membrane stabilization and the simultaneous combined action of drugs are also treated. Separate sections deal with the chemical composition and molecular structure of red blood cells, and with some biophysical factors of influence; *e.g.* haemolysis and counteracting processes are mentioned.

The chapter written by R. B. BURROWS comprises more than 100 pages, giving a very detailed review of the literature between 1965 and 1971 on new anthelmintics in human and veterinary use. Classification is done according to the illness, i.e. the pathogenic worm to be destroyed or expelled, thus different sections deal with the drugs effective against trematodes, cestodes and nematodes. Clinical experiences with these agents in different pathological states are described in detail. The usefulness of this chapter is greatly enhanced by the large number (676) of references cited, and by a collection of synonyms and trade names.

There is a further review by P. J. ISLIP, also dealing with researches on anthelmintics, concentrating mainly on the experimental chemotherapy of helminthiasis; considering the wide sprading of such illnesses, this additional chapter does not seem to be excessive. The summary, in nearly 70 pages, discusses only drugs to be used against trematodes and cestodes; owing to its experimental character, this chapter is concerned with a larger number of compounds (including some inevitable repetitions) than the previous one that focussed mainly on practical experiences.

A relatively short, concise chapter has been written by HLAVKA and BOOTHE on recent developments in the group of tetracyclines. After a brief historical review, semisynthetic tetracyclines are discussed with the aid of many structural formulae and schemes. This is followed by descriptions of total syntheses, problems of manufacture and biosynthesis; it is only on the last two pages where the mechanism of action of tetracyclines, the question of bacterial resistance and clinical indications for the use of these drugs are dealt with. It appears that the latter few years contributed littleto the knowledge accumulated in this field during the previous period.

An extremely interesting and, in the reviewer's opinion, very timely chapter is devoted to the relationships between the activity and metabolism of anticancer agents. Both the volume (90 pages) of the paper and the number of references (794) are sufficient to afford a comprehensive review of the subject. After an introduction analysing the proper definition of the term metabolism, the parts which follow deal with antimetabolites, nitrogen mustard derivatives, DNA complexing agents, mitosis inhibitors and hormones. An excellent survey in tabular form summarizes anticancer agents, the enzymes playing a part in their metabolism, the reactions which occur, and the positive or negative effects on the activity due to the metabolism of the drug.

Discovery of the biological actions of prostaglandins has been one of the great "hits" in pharmacology in the recent years. Accordingly, J. S. BINDRA and R. BINDRA undertook a difficult job in attempting to introduce order in the rapidly growing, vast and ramifying literature of prostaglandins, in order to give a lucid survey of the field in keeping with the style and purpose of the present series. In the reviewer's opinion, the task has been solved successfully. The great amount of work behind this chapter is shown not only by its volume of 80 pages with 524 references, but also by the successful arrangement of the huge material into a clear-cut and well readable review. It is stated in the introduction that completeness of the bibliography was not even considered, as the number of publications exceeds 600 a year.

The isolation and structure of prostaglandins, problems in their nomenclature, their occurrence and liberation are the subjects of the first part. An important section deals with

the biological assay of prostaglandins, with their determination by spectrometry, enzymatic methods, gas chromatography and radio-immunoassay.

Further sections are concerned with the biosynthesis and metabolism of prostaglandins, with special reference to the properties of the various species of animals. This is followed by a discussion of the effects of prostaglandins on the living organism and systems of organs, such as the reproductive system, digestive system, lungs, circulation, renal function, platelets and metabolic functions.

Prostaglandin antagonists are described in another section; the connections between prostaglandins and anti-inflammatory agents are then discussed, and finally possible ways of synthesizing prostaglandins are reviewed, with many formulae, in the concluding part.

The last chapter of the book, written by F. KRATZ, deals with the oxidative metabolism of drugs and other foreign substances. The short chapter describes the part-processes playing a part in drug oxidation and reviews the literature on the inducement of hydroxylating enzyme action by drugs.

To sum up, the topics treated in Volume 17 of "Progress in Drug Research" have been selected very successfully and the problems of current interest in drug research are discussed. Therefore, the volume is greatly recommended to all chemists, pharmacologists, biologists and physicians who are interested in the development of new drugs.

L. SZEKERES

JAMES A. MOORE: Experimental Elementary Organic Chemistry

W. B. Saunders Company, 1974, 243 pp.

This workbook, intended to serve for one semester as a guide to laboratory experiments in organic chemistry, is closely connected, both topically and conceptually, to the author's textbook "Elementary Organic Chemistry". The plan of the book under review is consistent: starting with an exposition on laboratory instruments and operations, in Chapters 1 . . 6, it arrives at the discussion of methods used for the identification of unknown organic compounds in Chapter 21. Beside the treatment of classical types of reactions (aromatic substitution, Grignard reaction, synthesis of dyes) which still are rather useful for a practical instruction in organic chemistry, also the application of TLC (Chapt. 7), IR, and NMR spectroscopy (Chapt. 20) are explained on simple yet interesting examples.

Like the textbook, also this workbook is intended first and foremost for the use in the laboratory courses of undergraduates in medicine and biology. This is evidenced principally by the large number of chapters that deal with carbon compounds important from biological point of view. In the course of experimenting, the students will learn much about the chemistry of carbohydrates, amino acids, and lipids (Chapts. 16–18) and will become acquainted with some novel and spectacular organic chemical operations (*e. g.* the heat sensing of liquid crystals). Chapter 10, about substitution reaction, allows a glimpse into the study of the correlations between chemical structure and reactivity.

While the treatment of IR and NMR spectroscopies, perhaps the two spectroscopic methods most used in organic chemistry, should be mentioned as one of the best in this book, the lack of a discussion, however short, of chiroptical methods (ORD, CD) at least of specific rotation in the study of natural carbon compounds is very much regretted.

The instructions about the experiments are very thorough and detailed so that their execution will not have to depend on any previous training of the students. Most of the experiments described can be done with 100 mg samples, as test tube reactions; when laboratory training is to be provided for a high number of students this leads to significant economies in chemicals. Very instructive drawings and tables help understanding; the leaves being easily detachable allows, if need be, the use of them instead of a notebook.

In the era of rapid progress of biological sciences, first of all of biochemistry, the level of the practical knowledge and experimental training of future biochemists is a fundamentally important issue. "Experimental Elementary Organic Chemistry" is a book that can serve also within the framework of the present training of physicians and biologists as a basis for a more up-to-date education of practical organic chemistry.

Á. KUCSMAN

Cosmochemistry (Fortschritte der chemischen Forschung) Topics in Current Chemistry, Vol. 44.

Springer Verlag, Berlin—Heidelberg—New York, 1974, 176 pp.

The sci-fi authors have nowadays a hard job, indeed. The fast development of sciences overtakes the run of the boldest fantasy. In the last one and half decades the space is the stage of most sci-fi-imaginations and the center of researches sponsored by the largest sums, as well.

And what is the output? Data of measurements which could by far not been achieved in terrestial laboratories.

"Cosmochemistry", Vol. 44 of the Series "Topics in Current Chemistry" of Springer Verlag brings in four chapters the recent results from the fields of "Interstellar Molecules", "Carbon Chemistry of the Apollo Lunar Samples", "Chemistry of the Moon" and finally an extremely concised summary on "Advances in Inorganic Geochemistry".

The compilers of the chapters are themselves engaged in the research dealt with, thus providing as authentic reports of the topics concerned as possible.

In order to demonstrate the conditions under which space chemistry is to be practised, may some results be mentioned here:

The interstellar space is not so empty at all, there are some 0.2—10 molecules in each cubic cm. This matter still accounts for about 10% of the total mass of the Galaxy. Dust particles of typical size 0.02 μ to 0.15 μ of unknown composition are mixed in this gas. H and ^{4}He account for 98% of the total mass of the gas which is rather uniform throughout the Galaxy. In this gas different kinds of cloudlets are embedded representing the region where stars are born. The space here is filled with radiation, both high energy particles and photons whose spectrum ranges from γ rays to the microwaves.

It is surprising how many — over 30 — different molecules have been identified in this Galaxy gas and such ones which can be regarded as precursors of amino acids and thus the origin of life. The movements of these molecules were determined from the Doppler shifts. Reactions between molecules are sometimes heterogeneous ones taking place on the surface of dust grains. The residence time, and thus the reaction time, is of the order of seconds.

Perhaps the most interesting element on the Moon is carbon. Samples by the Apollo missions were collected from igneous rocks, breccias and fine grained soils. Quite a big number of carbon compounds were isolated by extremely sophisticated procedures. In the formation of these materials the impact of meteorites should have played a role although the terrestrial contamination by previous landings may be deceiving. Another source of carbon is the solar wind and the carbides can be regarded as intermediates.

As concerns the abundance of other elements of the Moon, the ratios found deviate considerably from that determined on the Earth. This rules out the idea that the Moon might be a primitive object; on the contrary, the Moon, like the Earth, is a highly differentiated object. The europium anomaly, *i.e.* the occurrence of its 2+ state, *e.g.* indicates a low particle pressure of oxygen (10^{-13} atm).

Correlations between pairs or groups of elements are of extraordinary significance, as from a limited number of samples collected at the surface elemental ratios can be determined for a whole planet. The seismic experiments indicate that the Moon is solid down to a depth of 800 km around a small molten core. All these statements present the ground to explain the origin of the Moon. The author of the chapter supports the hypothesis of the independent formation of the Moon somewhere in the solar system followed by capture by the Earth.

The book excels in a rather clear formulation and in its references, of which the most recent is from August 1973, thus making it a uniquely up to date publication.

Z. G. SZABÓ

John McDERMOTT: *Plating of Plastics with Metals*

Noyes Data Corp., Park Ridge, New Jersey, London, 1974, 278 pp.

Electroplating of plastics steadily gains in importance in industry. Besides those about ABS polymers that could be electroplated and were marketed in the sixties and thus gave impetus to this method, more and more communications and patent specifications have appeared on the plating of an ever growing number of plastics. Originally, these aimed at the production of decorative finishes; later, the deposits that perform technical duties, especially in the field of electronics, have come to the fore. Patent literature deals very extensively with the plating of plastics, therefore this book: a collection of copious extracts of 250 relevant patent specifications published in the U.S.A. between 1966 and 1973, offers a very valuable review of this field.

Patent literature makes available quite an amount of information that cannot be found in books or in periodicals. Its knowledge is indispensable for applied and industrial research, because patent specifications inform not only about the actual state of technology but also about its trends of progress and development. Since patent specifications are very thorough in their discussions of the disadvantages of known processes and of the most important features of the new, they offer a very good basis for industrial development work.

The first chapter contains extracts of patent specifications concerning the first operation in the electroplating of plastics, *i.e.* etching, respectively pre-treatment of surfaces. The second chapter is devoted to the so-called activation processes. Activation consists in the formation of crystal nuclei on the surface of the plastic body, this being one of the most important steps in the plating process. The next two chapters deal with the deposition of the metal on the activated surface, notably with copper- and nickel-baths for chemical plating (without external electric source).

Since various plastics demand various pre-treatments, separate chapter review the methods applied to polyolefins, ABS-, polyethylene terephthalates, polyamides, and polyimides, halogenated plastics, polystyrenes and other, thermoplastic or thermosetting, substances.

The last chapter considers the field of applications for plated plastics. Besides decorative finishes, printed circuits constitute the widest field. The importance of this technique is greatly stressed by the use of such plated sheets in fuel cells.

Indexes which list companies to which patents have been issued, names of inventors, and numbers of registration, facilitate the handling of the material collected.

This book represents a new tendency in publishing, by the special technique of its production, by the very easily readable set of type used, and the surprisingly short time within which its printing seems to have been carried out.

F. HASKÓ

J. M. COXON and B. HALTON: *Organic Photochemistry*

Cambridge Chemistry Texts (General Editors: E. A. V. Ebsworth, D. T. Elmore, P. J. Padley and K. Schofield)

Cambridge University Press, London and New York, 1974, VII + 196 pages, ISBN: 0521 09824 6 paperback

The still growing importance of, and interest in, organic photochemistry are, amongst others, reflected in the number of recently published short texts of and introductions to this particular field of organic chemistry. It is clearly impossible to cover, in a volume of the present size, even the basic principles of organic photochemistry, and the authors have to decide which of the many important points and concepts they wish to elaborate more deeply at the cost of others; the latter, as a consequence, must be treated rather briefly.

The authors of the present text have chosen the chemical aspects of the interaction of light and matter as the topic to be treated in detail, and after an 18-page introduction dealing with excitation, the excited state and excitation energy transfer, the rest of the book (more than 90% of the available space) has been reserved for covering the more important types of organic photochemical transformations, such as intramolecular reactions of the olefinic bond,

intramolecular reactions of the carbonyl group, intermolecular cycloaddition reactions and, finally, oxidation, reduction, substitution and elimination reactions. A list of references is added at the end of each chapter for the more interested reader. In the opinion of the reviewer, this selection of material is perhaps fortunate because emphasizing the chemical (rather than the physical) aspects of photochemistry is certainly the way of arousing the interest of the chemistry major student in photochemistry, as these aspects are easier to master for him: in addition, such a selection should make it easily possible in the future to integrate the introductory organic photochemistry courses with organic chemistry courses in general.

The main characteristic of the present text is the consistent application of the WOODWARD—HOFFMANN orbital symmetry conservation rules as the theoretical background for the rationalization of the experimental results described.

The printing is clear, the drawings are very good and the number of misprints is low. (However, "electrolytic reactions" in the index should correctly read electrocyclic reactions.)

In summary, the text of COXON and HALTON is, in the reviewer's opinion, a good introduction to organic photochemistry. Its use will be profitable both for chemistry students and young scientists starting organic photochemical research.

K. LEMPERT

Dennis G. PETERS, John M. HAYES, Gary M. HIEFTJE: *Chemical Separations and Measurements*

Theory and Practice of Analytical Chemistry

W. B. Saunders Company, Philadelphia, 1974, 790 pp.

Recently, several analytical handbooks and textbooks have been published. The change which has by now become permanent in the field of analysis is reflected by the increase in the number of books published. Perhaps the structure of no branch of science has changed to such a degree as that of analytical chemistry. The development and spreading of the most various methods of high-performance instrumental analysis and the differentiation of the demands on analysis, on the other hand, causes increasing concern to university lecturers teaching analytical chemistry. In addition to the fact that methods of instrumental analysis predominate today in practice by far over the classical methods of chemical analysis, the importance of the various methods is also changing as a result of the demands of the often digressing directions of research, characteristic of our time. Space research, biochemical research, solid state research, and recently, environmental problems represent all different requirements to the analyst.

The book written in collaboration by the three authors is a university textbook, which contains, in an up-to-date form, the fundamental analytical methods and their theories. The subjects of the introductory chapters are the processing of analytical data and the equilibria of the reactions in solution.

The structuring of the contents of the book and the mode of discussion of the single chapters are very modern and excellent also from the didactical point of view. Evidently, when compiling the chapters, the authors condensed their teaching experience of several years or decades. A better understanding of theoretical relationships is facilitated by cleverly selected, expressive figures and worked-out examples. Each chapter ends with many instructive "questions and problems". The solution of the numerical examples is to be found at the end of the book. In addition, each chapter closes with a detailed list of recommended literature.

The aim of the book, as mentioned, is to make the reader acquainted with the fundamental analytical methods. Therefore, it can be recommended primarily to freshmen or sophomores studying chemistry or some similar discipline at the university.

The book gives a suitable basis for the students in the course of their later studies to acquire further knowledge in other important fields of analysis (*e.g.* thermal analysis, mass spectrometry, NMR spectroscopy, electron spectroscopy, X-ray spectroscopy, neutron activation analysis, etc.), which are not discussed or only briefly mentioned in the book.

It should be mentioned that the rather detailed, schoolish mode of discussion of the single chapters is somewhat unusual for us. Indeed, the authors discuss also such general chemical relationships and fundamental phenomena in detail, which are learned by the students in the course of their studies of general or inorganic chemistry or physical chemistry.

Some remarks are as follows:

On page 117, the formula of Methyl Red, on page 118 the formula of phenolphthalein is erroneous. On page 471, ion exchange chromatography is to be found under the heading of thin-layer phase. This classification is objectionable, if ion exchanger resin packing is considered.

The chapters of the book deal with the following subjects:

The introduction is followed by the chapter "Treatment of analytical data", discussing he precision and accuracy of measurements, error, error statistics, propagation of error and regression analysis. Chapter 3 deals with the structure of water, the concepts of concentration and activity, and with chemical equilibrium. Chapters 4 and 5 treat the pH-calculations and acid-base titrations, while Chapter 6, the concept of complexes, complex equilibria and chelatometric titrations. Chapters 7 and 8 discuss the mechanism of precipitate formation, the purity of precipitates and precipitation from homogeneous solution, gravimetric determinations and precipitation titration.

Chapters 9 and 10 discuss in detail the theory of redox reactions, and describe the practically more important redox titration methods (permanganometry, chromatometry, iodometry, bromatometry, etc.).

Chapter 11 contains the fundamental theoretical problems and methods of direct potentiometric measurements and potentiometric titrations, Chapter 12 those of electrogravimetric and coulombmetric titrations, and Chapter 13 of polarographic and amperometric titrations. Chapters 14, 15, 16 and 17 deal with methods of chemical separation. After general principles and phase equilibria, the theoretical and practical problems of liquid-liquid extraction and chromatographic methods are discussed in detail. Among the chromatographic methods, thin-layer chromatography, gas-liquid chromatography, ion exchange and gel chromatography are discussed.

Chapters 18, 19, 20 and 21 treat spectrochemical methods. The discussion of the general principles of light absorption, luminescence, emission and scattering phenomena is followed by sub-chapters on ultraviolet and visible absorption spectrophotometry, spectrofluorimetry, emission flame spectrometry, atom absorption spectrometry, atom fluorescent flame spectrometry, and emission spectrography. The chapter on spectrochemical methods ends with the discussion of infrared and Raman spectroscopic methods.

The Appendix of the book contains the usual tabular collection of equilibrium, solubility, redox potential, etc., data. Finally, the book ends with an index of about 2500 key-words, facilitating learning and orientation.

The book gives a clear picture on what is taught today and how it is taught at the Indiana University in the USA, and is therefore very useful for every analyst teaching at universities. Owing to its subject, compiled with a good didactic sense, to its style affording good reading and to the very large collection of exercises, the book is to be recommended to both students learning and teachers teaching analytical chemistry at universities.

J. INCZÉDY

INDEX

ANALYTICAL CHEMISTRY – ANALYTISCHE CHEMIE – АНАЛИТИЧЕСКАЯ ХИМИЯ

ACKERMANN, G., LÖWE, W., KADEN, W.: Anwendungsmöglichkeiten der Remissionsphotometrie in der quantitativen Analyse (On the Possible Application of Remission Photometry in Quantitative Analysis) 1

PHYSICAL AND INORGANIC CHEMISTRY – PHYSIKALISCHE UND ANORGANISCHE CHEMIE – ФИЗИЧЕСКАЯ И НЕОРГАНИЧЕСКАЯ ХИМИЯ

SZABÓ, Z. L.: Some Chemical Reactions of the Electrode Gap and their Role in Spectrochemical Analysis, XXII. Role of the Chemical Reactivity of the Material of the Metal Electrodes 13

TETTAMANTI, K., MANCZINGER, J., HUNEK, J. and STOMFAI, R.: Calculation of Countercurrent Solid-Liquid Extraction 27

DÖRING, C. E., STEVENZ, D., GEYER, R. und HÖPFNER, J.: Bestimmung von Ameisensäure und ihren Derivativen mittels Reaktionsgaschromatographie (Determination of Traces of Formic Acid by Reaction Gas Chromatography) 47

RODER, M.: Radiolysis of Cyclohexane—Hexamethylbenzene Mixtures, I. Pure Substances 55

SCHMIDT, R., STILLER, W. and HABERLANDT, R.: Collision-Kinetic Calculation of Reaction Rate Coefficients of Ion-Molecule Reactions, I..... 63

AGARWAL, S. K., TANDON, J. P.: Schiff Base Derivatives of Lanthanons. Synthesis of Polymeric Derivatives of La(III), Pr(III) and Nd(III) from the Schiff Bases Derived from the Condenzation of Benzaldehyde with Hydroxy Alkylamines or Hydroxy Arylamines 71

ORGANIC CHEMISTRY – ORGANISCHE CHEMIE – ОРГАНИЧЕСКАЯ ХИМИЯ

LEMPERT-SRÉTER, M., OSZBACH, GY., RUFF, F. and VAJDA, M.: Isobenzpyrylium Salts, V. Polarographic and Spectrophotometric Investigation of Some Hydroxy-Substituted 1-arylisobenzpyrylium Salts 79

OMAR, M. T. and BASYOUNI, M. N.: Cleavage of 2-Thiono-4-oxo-dihydro-5,6-benzo-1,3-thiazanes with Amines 89

SZAMMER, J.: Thermal Transcarboxylation Reactions, V. Study of the Relative Reactivities of the Aromatic Hydrogens in the Thermal Transformation of Potassium Benzoate..... 97

RIZK, A. M., HAMMOUDA, F. M., ISMAIL, S. I.: Phytochemical Investigation of *Thymelea Hirsuta*, III. Coumarins 107

RECENSIONES 117

Printed in Hungary

A kiadásért felel az Akadémiai Kiadó igazgatója. Műszaki szerkesztő: Zacsik Annamária

A kézirat nyomdába érkezett: 1975. I. 7. — Terjedelem: 11,2 (A/5) ív, 53 ábra

75.1285 Akadémiai Nyomda, Budapest Felelős vezető: Bernát György

ACTA CHIMICA

ТОМ 85 – ВЫП. 1

РЕЗЮМЕ

Применение реэмиссионной фотометрии в количественном анализе

Г. АКЕРМАНН, В. ЛЕВЕ и В. КАДЕН

Обуждаются теоретические основы применимости реэмиссионной фотометрии в количественном анализе, а также описываются некоторые специальные возможности ее применения. Используя соответствующие носители, путем реэмиссионной фотометрии можно определить количество полученного осадка. Этот принцип может быть применен как для определения состава трудно растворимых комплексных соединений, так и для количественного анализа косвенным путем. Показано, что после обогащения неокрашенными или слабо окрашенными ионообменными смолами и превращения соответствующим комплексообразователем, можно непосредственно качественно и количественно определить компоненты, присутствующие в следах. Реэмиссионную фотометрию можно также применять вместе с собирательным осаждением.

Некоторые химические реакции в электродной щели и их роль в спектрохимическом анализе, XXII

Роль химической реакционной способности материала металлических электродов

З. Л. САБО

Теплота реакции, освобождающаяся при процессах на электродных поверхностях, увеличивает умтучивание образца. В случае более активных реакционных партнеров это влияние более значительно. Окисительная тенденция появляется на электродах, присоединенных в качестве анода, благоприятствует этой реакции, а восстанавливающая тенденция на катоде уменьшает окислительные реакции. Влияние теплоты окисления изменяется также согласно условиям летучести металлических электродов.

Расчет противоточной твердо-жидкостной экстракции

К. ТЕТТАМАНТИ, Й. МАНЦИНГЕР, Й. ХУНЕК и Р. ШТОМФАИ

Геометрически упрощая сложную форму зерен мола растительного происхождения (до параллельных пластин, цилиндров и шаров), был разработан общий метод непрерывного и стадийного измерения противоточной твердожидкостной экстракции на основе решения дифференциального уравнения Фика II. Полученные, сложные математические зависимости были рассчитаны с помощью ЭВМ. Результаты приводятся в виде таблиц, пригодных для непосредственного и быстрого инженерного расчета.

Для определения неизвестных параметров зависимостей, используемых в проектировании, был разработан простой лабораторный метод, который основан на экспериментальном определении константы, характеризующей диффузионное сопротивление во внутри твердого вещества.

Справедливость применения упрощений подтверждается экспериментальными данными.

Определение муравьиной кислоты и ее производных с помощью реакционной газовой хроматографии

Ц. Е. ДЁРИНГ, Г. Д. ШТЕВЕНЦ, Р. ГЕЙЕР и Й. ХЁПФНЕР

Муравьиную кислоту, в области концентраций ниже 100 мкг/мл, подвергали дегидратации на катализаторе BPO_4 в условиях реакционной газовой хроматографии. Образующийся CO пропускали через последовательно включенный гидрирующий реактор, где окись углерода превращалась в метан, а последний определяли с помощью пламенного детектора. Граница определения составляет 3 мкг/мл. Относительная стандартная погрешность метода в области концентраций до 20 мкг/мл равна $\pm 20\%$, а в области до 100 мкг/мл уже $\pm 5\%$. Была исследована селективность метода.

Радиолиз смесей циклогексан-гексаметилбензол, I

Чистые соединения

М. РОДЕР

Смеси циклогексан-гексаметилбензол с различным составом подвергались γ-радиолизу Co^{60} в жидкой и твердой фазах. Радиационно-химические выходы основных продуктов были определены в зависимости от состава смеси и температуры.

На основе этих результатов было заключено, что гексаметилбензол оказывает защитное действие на разложение циклогексана в жидкой фазе, и этот эффект может быть интерпретирован на основе физических взаимодействий.

Определение констант скоростей реакций ионов с молекулами с помощью расчета кинетики столкновений, I

Определение квантовых эффектов на основе поляризационного потенциала

Р. ШМИДТ, В. ШТИЛЛЕР и Р. ХАБЕРЛАНДТ

Для основания реакций между ионами и молекулами и потенциала взаимодействия r^{-4}, сравниваются сечения реакционного захвата по классической и квантовомеханической теориям σ_{Cl} и σ_{qu}, соответственно, прибегая к асимптотическому выражению σ_{qU}, т. е. σ_{au} (действительному при относительных энергиях $E > E_0$), выведенному Вогтом и Ванниером. Полагая то, что функции распределения скоростей ионов и молекул имеют максвелловскую форму и пренебрегая внутренними степенями свободы реактантов парциальные константы скоростей k_{Cl} и k_{qu} были рассчитаны, используя обработку кинетики столкновений. Сравнение k_{Cl} и k_{qu} на основе положений, сделанных выше, приводит к заключению, что $k_{Cl} \approx k_{qu}$ в почти всех физических положениях. Это демонстрируется на примере реакции $CH_4^+ + CH_4 \rightarrow$ продукты.

Шиффовы основания лантанонов

Синтез полимерных производных La(III), Pr(III) и Nd(III) из оснований Шиффа, полученных конденсацией бензальдегида с гидроксиалкиламинами и гидроксиариламинами

С. К. АГАРВАЛ и Дж. П. ТАНДОН

Приводится синтез производных типа $Ln(o\text{-изо-}C_3H_7)_{3-n}(C_6H_5CH = NR)_n$ (где Ln = = La(III), Pr(III) и Nd(III); n = 1 или 2 и R = $-CH_2CH_2O$, $-CH_2CHCH_3O$ и $-C_6H_4O$). Они были синтезированы путем взаимодействия изопропоксидов лантанидов с основаниями Шиффа $C_6H_5CH = NCH_2CH_2OH$, $C_6H_5CH = NCH_2CH(OH)CH_3$ и $C_6H_5CH = NC_6H_4OH$, применяемых в различных стехиометрических отношениях, в среде сухого бензола. Полученные производные обладают способностью полимеризоваться, о чем свидетельствует тот факт, что при стоянии они становятся почти нерастворимыми и обладают более высокими температурами плавления. На основе элементарного анализа, молекулярных весов свеже приготовленных образцов, ИК спектров и реакций обмена были сделаны заключения относительно структуры образующихся производных.

Соли изобензпирилия, V

Полярографическое и спектрофотометрическое исследование некоторых гидроксильных замещенных 1-арил изобензпирилиевых солей

М. ЛЕМПЕРТ-ШРЕЙТЕР, ДЬ. ОСБАХ, Ф. РУФФ и М. ВАЙДА

Были исследованы превращения гидрокси-изобензпирилиевых солей в водно-спиртовых растворах, при различных pH. Обсуждаются различия в превращениях 7- и 6-гидрокси-соединений, а также приводятся доводы в пользу возможных структур промежуточного соединения низкой стабильности.

Взаимодействие 2-тионо-4-оксодигидро-5,6-бензо-1,3-тиазинов с аминами

М. Т. ОМАР и М. Н. БАСИОНИ

Протекание реакции 2-тионо-4-оксодигидро-5,6-бензо-1,3-тиазинов (*1*) с первичными и вторичными аминами зависит как от молярности, так и от заместителя в положении *3*. Был обсужден ход реакции, согласно которому протекает расщепление кольца. Это расщепление, вероятно, протекает как по 1,2-, так и по 3,4-связям.

Реакции термического перекарбоксилирования, V

Исследование относительной реакционной способности ароматических водородов в процессе термического превращения бензоата калия

Я. САММЕР

Относительная способность отрыва о-, м- и п-водородов в процессе термического превращения бензоата калия была исследована на моделях со специфически дейтерированным кольцом. Было установлено, что реактивность водородов ароматического кольца соответствует следующему порядку о—Н > м—Н > п—Н. Степень этого изменения, в случае реакций в твердой фазе значительнее, чем в случае расплавов.

Фотохимическое исследование THYMELEA HIRSUTA, III

Кумарины

А. М. РИЗК, Ф. М. ХАММОУДА и С. И. ИЗМАИЛ

Исследование кумаринов *Thymelea hirsuta* указало на присутствие дафнорина, дафноретина, дафнина, дафнетина, дафнетин-8-глюкозида, умбеллиферона, скополетина и эскулетина. Неидентифицированный лактон, о котором сообщали ранее, оказался дафноретином. Приводятся величины R_f для 30 кумаринов в различных растворителях.

ANALYTICAL CHEMISTRY OF ORGANIC HALOGEN COMPOUNDS

by L. Mázor

Organic halogen compounds are important chemicals in the manufacture of drugs, insecticides and plant-protecting agents. This book deals with the main features of the production and chemical reactions of these compounds. The detection and quantitative determination of organic fluoro-, chloro-, bromo- and iodo-compounds are described, using chemical and instrumental analytical methods. Both the qualitative and the quantitative analytical chemistry of the fluoro-compounds are presented. Possible sources of interference and the problems of determining several halogen compounds in the presence of one another are described. An Appendix tabulates about 1000 organic halogen compounds giving those physical properties and constants required for the identification of the substances.

In English · Approx. 320 pages · Cloth

A co-edition — distributed in the socialist countries by Kultura, Budapest, ISBN 963 05 0450 2; in all other countries by Pergamon Press, Oxford

---

AKADÉMIAI KIADÓ
Budapest

PERGAMON PRESS
Oxford

ANALYTICAL APPLICATIONS OF COMPLEX EQUILIBRIA

by J. Inczédy

The introductory part of the book reviews the chemistry of complexes, complex-formation equilibria, and those functions with the help of which the composition of the solutions containing complexes as well as the concentration of the individual components can be calculed simply.
The simplest methods of determining the protonation and complexformation constants are described together with worked examples.

In its main chapters the book discusses all those analytical methods gravimetric potentiometric and polarograph methods; spectro photometry, ion-exchange and other methods in which complexes are utilized. By using equilibrium correlations and worked examples it is demonstrated how the most suitables parameters of analytical determination can be designed in a given case. The book contains a tabulated collection of equilibrium constants necessary for the analytical calculations. A useful bibliography is given and a table of logarithms to complete the book.

In English · Approx. 370 pages · 74 figures · Cloth

A co-edition — distributed in the socialist countries by Kultura, Budapest, ISBN 963 05 0513 4, in all other countries by Van Nostrand Reinhold Co., London

AKADÉMIAI KIADÓ
Budapest

VAN NOSTRAND REINHOLD CO.
London

The Acta Chimica publish papers on chemistry in English, German, French and Russian.

The Acta Chimica appear in volumes consisting of four parts of varying size, 4 volumes being published a year.

Manuscripts should be addressed to

Acta Chimica
Budapest 112/91 Műegyetem

Correspondence with the editors should be sent to the same address.

The rate of subscription is $ 32.00 a volume.

Orders may be placed with "*Kultúra*" Foreign Trade Company for Books and Newspapers (1389 Budapest 62, P.O.B. 149. Account No. 218 10990) or with representatives abroad.

Les Acta Chimica paraissent en français, allemand, anglais et russe et publient des mémoires du domaine des sciences chimiques.

Les Acta Chimica sont publiés sous forme de fascicules. Quatre fascicules seront réunis en un volume (4 volumes par an).

On est prié d'envoyer les manuscrits destinés à la rédaction à l'adresse suivante:

Acta Chimica
Budapest 112/91 Műegyetem

Toute correspondance doit être envoyée à cette même adresse.

Le prix de l'abonnement est de $ 32.00 par volume.

On peut s'abonner à l'Entreprise pour le Commerce Extérieur de Livres et Journaux «*Kultúra*» (1389 Budapest 62, P.O.B. 149. Compte-courant No. 218 10990) ou à l'étranger chez tous les représentants ou dépositaires.

«*Acta Chimica*» издают трактаты из области химической науки на русском, французском, английском и немецком языках.

«*Acta Chimica*» выходят отдельными выпусками разного объема. 4 выпуска составляют один том. 4 тома публикуются в год.

Предназначенные для публикации рукописи следует направлять по адресу:

Acta Chimica
Budapest 112/91 Műegyetem

По этому же адресу направлять всякую корреспонденцию для редакции.

Подписная цена — $ 32.00 за том.

Заказы принимает предприятие по внешней торговле книг и газет «*Kultúra*» (1389 Budapest 62, P.O.B. 149. Текущий счет № 218 10990) или его заграничные представительства и уполномоченные.

Reviews of the Hungarian Academy of Sciences are obtainable at the following addresses:

AUSTRALIA

C. B. D. Library and Subscription Service
Box 4886, G. P. O.
Sydney N. S. W. 2001

Cosmos Bookshop
145 Acland St.
St. Kilda 3182

AUSTRIA

Globus
Höchstädtplatz 3
A–1200 Wien XX

BELGIUM

Office International de Librairie
30 Avenue Marnix
1050–Bruxelles

Du Monde Entier
162 Rue du Midi
1000–Bruxelles

BULGARIA

Hemus
Bulvar Ruszki 6
Sofia

CANADA

Pannonia Books
P. O. Box 1017
Postal Station "B"
Toronto, Ont. M5T 2T8

CHINA

CNPICOR
Periodical Department
P. O. Box 50
Peking

CZECHOSLOVAKIA

Mad'arská Kultura
Národní třida 22
115 66 Praha

PNS Dovoz tisku
Vinohradská 46
Praha 2

PNS Dovoz tlače
Bratislava 2

DENMARK

Ejnar Munksgaard
Nörregade 6
DK–1165 Copenhagen K

FINLAND

Akateeminen Kirjakauppa
P. O. Box 128
SF–00101 Helsinki 10

FRANCE

Office International de Documentation et Librairie
48 Rue Gay Lussac
Paris 5

Librairie Lavoisier
11 Rue Lavoisier
Paris 8

Europeriodiques S. A.
31 Avenue de Versailles
78170 La Celle St. Cloud

GERMAN DEMOCRATIC REPUBLIC

Haus der Ungarischen Kultur
Karl-Liebknecht-Strasse 9
DDR–102 Berlin

Deutsche Post
Zeitungsvertriebsamt
Strasse der Pariser Kommüne 3–4
DDR-104 Berlin

GERMAN FEDERAL REPUBLIC

Kunst und Wissen
Erich Bieber
Postfach 46
7 Stuttgart S

GREAT BRITAIN

Blackwell's Periodicals
P. O. Box 40
Hythe Bridge Street
Oxford OX1 2EU

Collet's Holdings Ltd.
Denington Estate
London Road
Wellingborough Northants NN8 2QT

Bumpus Haldane and Maxwell Ltd.
5 Fitzroy Square
London W1P 5AH

Dawson and Sons Ltd.
Cannon House
Park Farm Road
Folkestone, Kent

HOLLAND

Swets and Zeitlinger
Heereweg 347b
Lisse

Martinus Nijhoff
Lange Voorhout 9
The Hague

INDIA

Hind Book House
66 Babar Road
New Delhi 1

India Book House
Subscription Agency
249 Dr. D. N. Road
Bombay 1

ITALY

Santo Vanasia
Via M. Macchi 71
20124 Milano

Libreria Commissionaria Sansoni
Via Lamarmora 45
50121 Firenze

JAPAN

Kinokuniya Book-Store Co. Ltd.
826 Tsunohazu 1-chome
Shinjuku-ku
Tokyo 160–91

Maruzen and Co. Ltd.
P. O. Box 5050
Tokyo International 100–31

Nauka Ltd.–Export Department
2–2 Kanda
Jinbocho
Chiyoda-ku
Tokyo 101

KOREA

Chulpanmul
Phenjan

NORWAY

Tanum-Cammermeyer
Karl Johansgatan 41–43
Oslo 1

POLAND

Węgierski Instytut Kultury
Marszalkowska 80
Warszawa

BKWZ Ruch
ul. Wronia 23
00–840 Warszawa

ROUMANIA

D. E. P.
Bucureşti

Romlibri
Str. Biserica Amzei 7
Bucureşti

SOVIET UNION

Sojuzpechatj – Import
Moscow
and the post offices in each town

Mezhdunarodnaya Kniga
Moscow G–200

SWEDEN

Almqvist and Wiksell
Gamla Brogatan 26
S–101 20 Stockholm

A. B. Nordiska Bokhandeln
Kunstgatan 4
101 10 Stockholm 1 Fack

SWITZERLAND

Karger Libri AG.
Arnold-Böcklin-Str. 25
4000 Basel 11

USA

F. W. Faxon Co. Inc.
15 Southwest Park
Westwood, Mass. 02090

Stechert-Hafner Inc.
Serials Fulfillment
P. O. Box 900
Riverside N. J. 08075

Fam Book Service
69 Fifth Avenue
New York N. Y. 10003

Maxwell Scientific International Inc.
Fairview Park
Elmsford N. Y. 10523

Read More Publications Inc.
140 Cedar Street
New York N. Y. 10006

VIETNAM

Xunhasaba
32, Hai Ba Trung
Hanoi

YUGOSLAVIA

Jugoslovenska Knjiga
Terazije 27
Beograd

Forum
Vojvode Mišića 1
21000 Novi Sad

ACTA CHIMICA

ACADEMIAE SCIENTIARUM HUNGARICAE

ADIUVANTIBUS
V. BRUCKNER, GY. DEÁK, K. POLINSZKY,
E. PUNGOR, G. SCHAY, Z. G. SZABÓ

REDIGIT
B. LENGYEL

TOMUS 85 FASCICULUS 2

AKADÉMIAI KIADÓ, BUDAPEST
1975

ACTA CHIM. (BUDAPEST) ACASA 2 85 (2) 125–232 (1975)

ACTA CHIMICA

A MAGYAR TUDOMÁNYOS AKADÉMIA KÉMIAI TUDOMÁNYOK OSZTÁLYÁNAK IDEGEN NYELVŰ KÖZLEMÉNYEI

SZERKESZTI

LENGYEL BÉLA

TECHNIKAI SZERKESZTŐK

DEÁK GYULA és HARASZTHY-PAPP MELINDA

Az Acta Chimica német, angol, francia és orosz nyelven közöl értekezéseket a kémiai tudományok köréből.

Az Acta Chimica változó terjedelmű füzetekben jelenik meg, egy-egy kötet négy füzetből áll. Évente átlag négy kötet jelenik meg.

A közlésre szánt kéziratok a szerkesztőség címére (Budapest 112/91 Műegyetem) küldendők.

Ugyanerre a címre küldendő minden szerkesztőségi levelezés. A szerkesztőség kéziratokat nem ad vissza.

Megrendelhető a belföld számára az „Akadémiai Kiadó"-nál (1363 Budapest Pf 24. Bankszámla 215 11488), a külföld számára pedig a „Kultúra" Könyv- és Hírlap Külkereskedelmi Vállalatnál (1389 Budapest 62, P. O. B. 149. Bankszámla: 218 10990) vagy annak külföldi képviseleteinél és bizományosainál.

Die Acta Chimica veröffentlichen Abhandlungen aus dem Bereich der chemischen Wissenschaften in deutscher, englischer, französischer und russischer Sprache.

Die Acta Chimica erscheinen in Heften wechselnden Umfanges. Vier Hefte bilden einen Band. Jährlich erscheinen 4 Bände.

Die zur Veröffentlichung bestimmten Manuskripte sind an folgende Adresse zu senden:

Acta Chimica
Budapest 112/91 Műegyetem

An die gleiche Anschrift ist auch jede für die Redaktion bestimmte Korrespondenz zu richten. Abonnementspreis pro Band: $ 32.00.

Bestellbar bei dem Buch- und Zeitungs-Außenhandels-Unternehmen »*Kultúra*« (1389 Budapest 62, P. O. B. 149 Bankkonto Nr. 218 10990) oder bei seinen Auslandsvertretungen und Kommissionären.

Acta Chimica Academiae Scientiarum Hungaricae, 85 (2), pp. 125—130 (1975)

INVESTIGATIONS ON ION-EXCHANGE EQUILIBRIA WITH RADIOACTIVE TRACER METHOD, XVIII

DETERMINATION OF THE STABILITY CONSTANT OF $Cd_2(OH)_2^{2+}$ WITH THE AID OF ION-EXCHANGE TECHNIQUE

T. LENGYEL

(Institute of Isotopes, Hungarian Academy of Sciences, Budapest)

Received May 21, 1973

Using di-2-ethylhexyl phosphoric acid as liquid ion-exchanger, the formation of the dinuclear hydroxo complex of cadmium has been studied.

It was found that at higher cadmium concentrations, in the pH region 3—4, the uncomplexed metal and the dinuclear species predominate and with certain simplifications the overall stability constant of $Cd_2(OH)_2^{2+}$ could be calculated which proved to be $\lg \beta_{22} = 23.9$.

Introduction

Reviews and monographs dealing with the determination of complex stability constants generally agree that ion-exchange technique is unapt to investigate polynuclear complexes [1—3]. The main reason for that is that the concentration region in which polynuclear species may exist is disadvantageous from the experimental point of view, *i.e.* the loads on the ion-exchanger are rather high, approaching the theoretical capacity values thereof and that activity coefficients can hardly be controlled. According to these objections, the interpretation of the experimental data is possible for very simple polynuclear systems only, by taking into account that the distribution ratio is a function of the concentrations both of the free ligand and the central group [4].

Some attempts have been made to investigate the dimeric species formed in the system iron–thiocyanate by using liquid anion-exchanger [5]. Within the scope of this paper an approach is presented which proved to be suitable for the determination of the stability constant of the [di-μ-hydroxo -bis(cadmium)] complex starting out from experimental data obtained with a liquid cation-exchanger.

Experimental

Equilibrium measurements were performed, using sealed glass ampoules containing the aqueous and organic phases which were shaken for 24 hours at room temperature. According to preliminary experiments — in spite of

the presumed inertness of cadmium complexes — the distribution ratio did not vary after some hours of shaking.

In order to facilitate analytical assay, ^{115}Cd tracer (half life 2.3 hours) of high specific activity was used. The relative intensities of aliquot samples were determined with the aid of a well-type scintillation detector coupled to a single channel pulse height analyser type MÉV, set to the 0.52 MeV photopeak of radiocadmium, so to avoid the discrepancies possibly caused by the presence of the $^{115}In^{m}$ daughter.

Reagents of spectrochemical or at least analytical purity were used all over the experiments.

Di-2-ethylhexyl phosphoric acid (DEHPA) dissolved in toluene was applied as ion-exchanger, while the aqueous phase was set to I = 1 ionic strength with perchloric acid as background electrolyte.

The pH was measured on Radiometer PH-4, using a glass–calomel electrode pair.

Theoretical

In the hydroxo complexes the valency orbitals of oxygen are in sp^2 hybrid state and as a result of colligative σ- and π-bonding the hydroxo groups are capable to form bridges which in turn favour the formation of dinuclear species of cadmium with μ-hydroxo and terminal aqua ligands.

The dinuclear hydroxo complex of cadmium is formed according to the reaction

$$2\ Cd^{2+} + 2\ OH^{-} \rightleftharpoons Cd_2(OH)_2^{2+} \qquad (1)$$

Determining the distribution of cadmium at constant (and relatively high) ionic strength and at constant ligand concentration (constant pH) but at different cadmium concentrations and plotting these data as a function of T_{Cd} (total concentration of cadmium), the curve extrapolated to $T_{Cd} = 0$ value yields D_0^*, *i.e.* the distribution ratio for the system in which only mononuclear species exist.

Presuming that at higher T_{Cd} values a concentration region can be found in which out of the possible polynuclear species only the dinuclear one exists or at least predominates, and postulating that this does not partition between the phases, the following relation can be written:

$$D = D_0^*(1 - Q) \qquad (2)$$

where Q denotes the ratio of the amount of the dinuclear species to all species (both mono- and dinuclear) present.

The overall stability constant of the dinuclear complex is, omitting symbols of charge

$$\beta_{22} = \frac{[Cd_2(OH)_2]}{[Cd]^2 [OH]^2} \tag{3}$$

The concentration of the dinuclear complex can be expressed as

$$[Cd_2(OH)_2] = 0.5\, QT'_{Cd} \tag{4}$$

where T'_{Cd} denotes the total concentration of cadmium in the aqueous phase which can be calculated from T_{Cd} and the corresponding D distribution ratio.

[OH] is calculated directly from the pH measured, while the concentration of the mononuclear species can be expressed according to the well-known relation modified because of the presence of dinuclear species as

$$[Cd] = \frac{T'_{Cd}(1 - Q)}{1 + \sum_{i=1}^{N} \beta_i [OH]^i} \tag{5}$$

Using proper sets of data, the overall stability constant of the dinuclear complex can be calculated, provided that the individual β_i values are known or are determined from independent measurements.

Results and discussion

In principle, the plot of D *vs.* T'_{Cd} can be obtained directly but practically the constant ligand concentration (constant pH) cannot be assured without using proper buffer. The use of such kind of reagent is, however, bound to occasional complex formation which may interfere with the accurate interpretation of the experimental data. In order to avoid such possibilities plots of lg D *vs.* pH at constant T_{Cd}, values were used which are presented in Fig. 1.

As it can be seen, linear correlations exist and at very low T_{Cd} values the slope of the straight line equals 2, while at higher cadmium concentrations the slopes are between 1 and 2 indicating the presence of the dinuclear species.

Starting out from the smoothed values of the experimental data, Fig. 2 was constructed which presents the relationship being necessary for calculation of β_{22} values according to Eqs (3), (4) and (5).

β_i values were taken from literature data [6] according to which lg β_1 = = 4.3 and lg β_2 = 7.7.

It is to be mentioned, however, that at the given pH values the concentration of mononuclear complexes can be neglected and practically only the

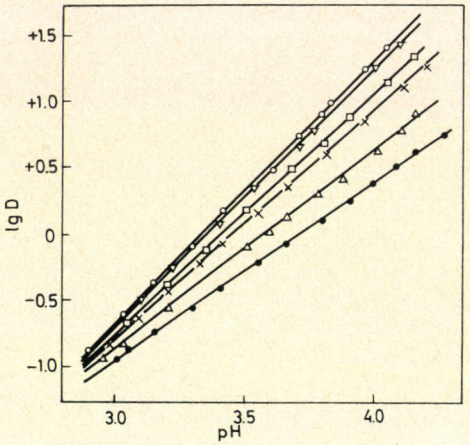

Fig. 1. Change of the distribution ratio as a function of pH at various T_{Cd} values
$I = 1\ M\ HClO_4$, DEHPA = 0.1 F

○ $T_{Cd} = 1\times10^{-5}\ M$ ▽ $T_{Cd} = 2\times10^{-4}\ M$
□ $T_{Cd} = 1\times10^{-3}\ M$ × $T_{Cd} = 2\times10^{-3}\ M$
△ $T_{Cd} = 5\times10^{-3}\ M$ ● $T_{Cd} = 1\times10^{-2}\ M$

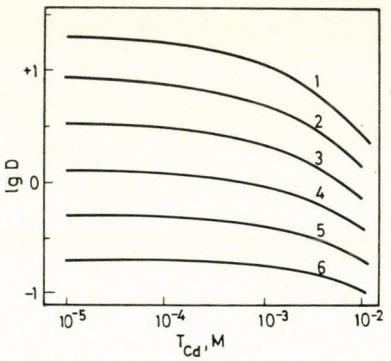

Fig. 2. Distribution ratio as a function of total cadmium concentration at constant pH values of the aqueous phase

1: pH = 4.0 2: pH = 3.8 3: pH = 3.6
4: pH = 3.4 5: pH = 3.2 6: pH = 3.0

uncomplexed metal and the dinuclear complex is to be taken into account. This has the consequence that Eq. (5) can be reduced to

$$[Cd] = T'_{Cd}(1 - Q) \tag{6}$$

The calculations performed yielded the value $\lg \beta_{22} = 23.9 \pm 0.15$ all over the experimental conditions studied, the deviations being less at higher pH values.

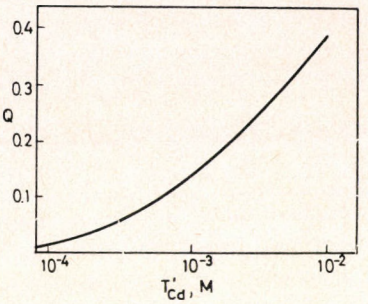

Fig. 3. Fraction of the dinuclear hydroxo complex as a function of total cadmium concentration in the aqueous phase at pH = 3.0

Based on the results obtained, the fraction of the dinuclear complex as a function of T'_{Cd} was calculated; data for pH = 3.0 are shown in Fig. 3.

It is striking that the amount of $Cd_2(OH)_2^{2+}$ is considerably high, even at concentrations less than $T'_{Cd} = 10^{-2}$ *M*. Obviously, the Q values increase at higher T'_{Cd} values but investigations with more concentrated solutions are burdened with greater errors both from experimental and theoretical points of view.

Anyhow, the question arises whether the decrease of the distribution ratio at higher T_{Cd} values is due to the formation of dinuclear species only or other reasons are also to be taken into account. Accepting that the assumptions made in the theoretical treatment are valid only, the consequences of the ion-exchange process are to be considered.

If only the uncomplexed metal is present in the aqueous solution the ion-exchange reaction is simply

$$2\ RH + Cd^{2+} \rightleftharpoons R_2Cd + 2\ H^+ \tag{7}$$

for which the mass-action law yields

$$K' = \frac{[H]^1\,[R_2\,Cd]}{[RH]^2\,[Cd]} = D\left(\frac{[RH]}{[H]}\right)^2 \tag{8}$$

or

$$D = K'\left(\frac{[RH]}{[H]}\right)^2 \tag{9}$$

However, in the course of ion-exchange the decrease of [RH] and increase of [H] can by no means cause an effect comparable with that experimentally observed, *i.e.* the ion-exchange process itself is not responsible for the decrease of D at higher T_{Cd} values, though in a small extent it may contribute at moderate cadmium concentrations.

*

The author's thanks are due to Prof. J. INCZÉDY for valuable discussions.

REFERENCES

[1] ROSSOTTI, F. J. C., ROSSOTTI, H.: The Determination of Stability Constants, McGraw-Hill Book Co., New York 1961
[2] BECK, M. T.: Chemistry of Complex Equilibria, Van Nostrand Reinhold Co., London 1970
[3] MARCUS, Y., KERTES, A. S.: Ion Exchange and Solvent Extraction of Metal Complexes. Wiley-Interscience, London 1969
[4] INCZÉDY, J.: Analytical Application of Complex Equilibria. Műszaki Könyvkiadó, Budapest 1970. (In Hungarian)
[5] RICE, N. M.: Thesis, University of London, London, 1966
[6] DYRSSEN, D., LUMME, P.: Acta Chem. Scand. **16,** 1785 (1962)

Tamás LENGYEL; 1525 Budapest, P. O. B. 77. Hungary.

Acta Chimica Academiae Scientiarum Hungaricae, 85 (2), pp. 131—137 (1975)

STUDIES ON SOME 5-NITROSALICYLATE COMPLEXES

*P. V. KHADIKAR and R. L. AMERIA

(School of Studies in Chemistry, Vikram University, Ujjain (M. P.) and Madhav Science College, Ujjain (M. P.) India)

Received October 25, 1973
In revised from November 6, 1974

The formation constants of Cu(II), Ni(II), Co(II), Mn(II), Zn (II) and Fe(II) complexes with 5-nitrosalicylic acid have been determined by the CALVIN—BJERRUM method. Approximate values of the formation constants are obtained from half-integral values of $\bar{n}$ and their refinement is done by the method of least-squares. The order of stability is found to be Cu(II) > Zn(II) > Ni(II) > Co(II) > Fe(II) > Mn(II). The bonding in the complexes has been discussed on the basis of the infrared spectra of the isolated complexes and the stereochemistry on the basis of the magnetochemical studies.

Introduction

Although the co-ordination chemistry of salicylic acid is well documented, the study of its derivative, the 5-nitrosalicylic acid (5 NSA), remained neglected until quite recently. ERNST and MENASHI [1, 2] have determined the protonation constants of 5 NSA and the formation constants of its complexes with Fe(III) employing spectrophotometric technique. Very recently KHADIKAR and AMERIA [3] have determined the proton-ligand formation constants of this compound and the formation constants of its complexes with Zn(II). KHADIKAR and BHAGWAT [4] have shown the formation of the 1 : 1 complex of Tl(I) and the 1 : 1, 1 : 2 and 1 : 3 complexes of In(III) with 5 NSA. KHADIKAR and SARWATE [5] have used 5 NSA as a colorimetric reagent for the determination of uranium. Formation of 1 : 1 complexes of 5 NSA with Cu(II), Ni(II) and Co(II), employing conductometric method, has also been reported in the literature [6]. In the present communication we report on the I R spectra, magnetochemical studies and the formation constants of the 5 NSA complexes of Cu(II), Ni(II), Co(II), Mn(II), Fe(II) and Zn(II).

Results and discussion

Formation constants

The interaction of M(II) with 5 NSA causes a considerable decrease in pH and a pH-metric titration of 1 : 1 metal–ligand system has revealed an

*Present address: 1. Jawahar Road N°. 1, Vyayamshala Gali, Ujjain — 456006 (M. P.) India

inflection at two equivalents of alkali. This obviously indicates that both carboxylic and phenolic protons of 5 NSA are liberated as a result of chelate formation. The reaction is the following:

$$M^{2+} + C_7H_5O_5N \rightleftharpoons M(C_7H_3O_5N)^{2+} + 2\ H^+,$$

where M^{2+} stands for Cu(II), Ni(II), Co(II), Zn(II), Mn(II) or Fe(II).

pH-metric titrations of 1 : 2 and 1 : 3 mixtures of metal and ligand with alkali show inflections at four equivalents of alkali which corresponds to the formation of 1 : 2 complex between metal and 5 NSA in accordance with the reaction:

$$M^{2+} + 2\ C_7H_5O_5N \rightleftharpoons M[C_7H_3O_5N]_2^{2-} + 4\ H^+.$$

The inflection at four equivalents of alkali for 1 : 2 and 1 : 3 metal–ligand pH-metric titrations indicates the absence of polynuclear species.

In calculating the stepwise formation constants by the CALVIN—BJERRUM method [7], solutions containing perchloric acid (0.01 *M*) + 5 NSA (0.01 *M*), and perchloric acid (0.01 *M*) + 5 NSA (0.01 *M*) + metal perchlorate (0.001 *M*), of constant volume (50.0 ml) and constant ionic strength (0.1 *M*) due to the addition of neutral salt $NaClO_4$, were titrated against standard alkali (0.1 *M*) at a temperature of 30±0.2°. The pK_a values of the ligand (pK_{a1} 2.33, pK_{a2} 10.40), as reported by KHADIKAR and AMERIA [3] under the same experimental conditions, were used for the calculation of formation constants. All the calculations were made for solutions below the pH at which the hydrolysis of the metal starts.

The values of stepwise formation constants were determined by the half-integral method as described by BJERRUM [8]; these are recorded in Table I. The refined values of $\log K_1$, $\log K_2$ and $\log \beta_2$ were obtained by the method of least squares and are given in the same table in parantheses. The values of $\log K_1$, $\log K_2$ and $\log \beta_2$ are accurate within the range of ±0.05, ±0.06 and ±0.10, respectively.

Table I

Stepwise formation constants of 5 NSA complexes

Complex	$\log K_1$	$\log K_2$	$\log \beta_2$
Cu(II)-5 NSA	7.65 (7.60)	7.05 (7.00)	14.70 (14.60)
Ni(II)-5 NSA	6.12 (6.12)	5.80 (5.80)	11.92 (11.92)
Co(II)-5 NSA	5.38 (5.35)	5.04 (5.00)	10.42 (10.40)
Zn(II)-5 NSA	6.70 (6.68)	6.32 (6.30)	13.04 (12.98)
Mn(II)-5 NSA	4.80 (4.80)	4.68 (4.68)	9.48 (9.48)
Fe(II)-5 NSA	5.05 (5.00)	4.70 (4.70)	9.75 (9.70)

A perusal of Table I shows that the order of stability is Cu(II) > Zn(II) > > Ni(II) > Co(II) > Fe(II) > Mn(II). This is found to be in accordance with the IRVING—WILLIAMS rule [9].

The parallelism between log K_n and second ionization potential is also observed in the present case. Except for Zn(II), this potential is a measure of the energy required for the removal of *d*-electrons. This observation indicates the involvement of *d*-orbitals in chelation. The higher values of formation constants of Zn(II) complexes than those of Ni(II) complexes, in case of phenolic-ligands, has also been observed earlier [10].

It will be interesting to compare our results with the corresponding salicylic acid complexes reported by PERRIN [11]. Though, because of different experimental conditions, exact comparison is not possible, yet it can be said that the 5 NSA complexes are relatively less stable as compared to the corresponding salicylic acid complexes. This is in accordance with the results obtained by ERNST and MENASHI [1].

Infrared spectra

All the complexes were isolated by the method described by KHADIKAR *et al.* [12]. The composition of the complexes was found to be $Na_2ML_2.2\,H_2O$. The characteristic absorption bands of the ligand and the complexes are given in Table II. The infrared spectra of the complexes show bands corresponding to the vibrational modes of the ligand present and also the M–O stretching vibrations.

The antisymmetric stretching frequency of the COO^- group is found to be at about 1600 cm^{-1} in all the complexes studied in the present investigation. This suggests that the extent of ionic (or partly covalent) interaction of the metal with the carboxylate oxygen is more or less the same in all the complexes. Shift of carboxyl group frequency from about 1700 cm^{-1} (ligand) to about 1600 cm^{-1} (complex) provides the evidence of metal–oxygen bonding in these complexes. If the structure of the complexes were $-\overset{\overset{O}{\|}}{C}-O-M$, we should observe the characteristic C=O frequency (1720 cm^{-1}) in place of the carboxylate frequency (about 1600 cm^{-1}) observed in the present investigation. No absorption band was observed in the region 1720 cm^{-1}. The absence of the absorption band near 1700 cm^{-1} and the presence of very strong band at about 1600 cm^{-1} indicates that the carboxylate to metal bond is essentially ionic and that the carboxylate resonance in the ligand is maintained.

There has been observed a considerable overlapping near 3300 cm^{-1} and 1600 cm^{-1}, due to H_2O bands as a result of co-ordinated water. As indicated by dehydration and deuteration studies [13, 14], bands in the region 3500—

Table II

Characteristic infrared frequencies in cm^{-1}

5 NSA 1	Cu(II)-5 NSA 2	Ni(II)-5 NSA 3	Zn(II)-5 NSA 4	Co(II)-5NSA 5	Mn(II)-5NSA 6	Fe(II)-5 NSA 7
2700—	3200—	3000—	3100—	3540s	3520s	3000—
3300sb	3600sb	3450sb	3600sb			3500sb
1940w	1610s	1600s	1600s	3440s	2910vw	1595s
1839vw	1575w	1535s	1580vw	2920vw	2840vw	1565w
1805vw	1530w	1510s	1480s	1632s	1595s	1470s
1655s	1475s	1475w	1432s	1595s	1485vw	1430s
1620s	1435s	1425s	1375vw	1555s	1460s	1390w
1575s	1320s	1380s	1320s	1510s	1430s	1300s
1505s	1195w	1300s	1270vw	1470vw	1345s	1132s
1470s	1105s	1140s	1110s	1420s	1320s	1065s
1430s	970s	1090w	830s	1375vw	1255vw	955vw
1330s	920s	975s	775vw	1300s	1180s	920s
1280w	825s	930vw	740vw	1135s	1140vw	830s
1225s	778w	910w	705vw	1065s	1106vw	780w
1185s	740s	830s	670vw	955w	1075vw	740s
1140s	710s	785w	—	925s	980s	700s
1110s	690w	745s	—	910s	930vw	650s
1065s	645w	695s	—	830s	920s	—
970w	—	—	—	780w	835s	—
922s	—	—	—	742s	740s	—
910s	—	—	—	690s	710s	—
875s	—	—	—	650w	670w	—
845s	—	—	—	—	—	—
815s	—	—	—	—	—	—
790s	—	—	—	—	—	—
780s	—	—	—	—	—	—
740s	—	—	—	—	—	—
715s	—	—	—	—	—	—
690s	—	—	—	—	—	—
620s	—	—	—	—	—	—

s: sharp sb: sharp and broad w: weak vw: very weak

3150 cm^{-1} and near 1600 cm^{-1} are attributed to ν-OH and ν-OH vibrations, respectively. In addition to these, FUJITA *et al.* [15] have observed bands in the 1000—800 cm^{-1} region when water is held in co-ordination. A band at 850 cm^{-1} observed in the present investigation shows the presence of co-ordinated water in the complexes [15].

BELLAMY and BRANCH [16] have shown a linear relationship between carboxyl group frequency and formation constants of the chelates of salicylaldehyde with different bivalent metal cations. BELLAMY and BEECHER [17] have shown that in acids also there should be a linear relationship between carboxyl group frequency and the formation constants of the complexes. A perusal of Table II shows that no direct relation could be traced between carboxyl group frequencies and formation constants. The absence of a linear relationship is not entirely unexplained. In comparing the complexes formed by a particular ligand with various metal cations, the action of the ligand is essentially the same in each case and except for the differences in the masses of metals any effect that strengthens the metal–oxygen bond weakens the carbon–oxygen bond to the same extent. The differences in resonance, inductive and mass effects between the various chelates must be attributed, essentially all, to the ligand.

Magnetic studies

Magnetic susceptibilities were measured by the Gouy method at room temperature. The apparatus used was similar to that described by FIGGIS and NYHOLM [18]. The Gouy tube was calibrated to $HgCo(CNS)_4$ (X_a 16.44×10^{-6}). Triplicate determinations were made, and the molar susceptibilities of all the complexes were corrected for the diamagnetism of all the constituent atoms. The results obtained are recorded in Table III.

Table III

Magnetic data of 5 NSA complexes

Complex	Magnetic moment (μ_{eff})
Cu(II)-5 NSA	2.15 B. M.
Ni(II)-5 NSA	3.31
Co(II)-5 NSA	5.33
Zn(II)-5 NSA	diamagnetic
Mn(II)-5 NSA	6.24 B. M.
Fe(II)-5 NSA	5.44

The room-temperature moment of Cu(II)—5 NSA complex lies within the range expected for Cu(II) in a pseudo-octahedral environment [19]. The magnetic moment of Ni(II)—5 NSA complex (3.31 B. M.) is in the range generally observed for octahedral Ni(II) complexes and is consistent with the values reported by LEVER [20] for octahedral Ni(II) complexes. The value of 5.33 B. M., measured for the Co(II)—5 NSA complex, indicates unequivocally

that the geometry in the environment of Co(II) is octahedral [21]. The higher moment value, which is observed in the present case may be attributed to incomplete quenching of the orbital contribution to the magnetic moment and it may be a consequence of inverted multiplet levels in this ion.

Most of Mn(II) complexes with weak-field ligands, possessing octahedral structure, have a magnetic moment about 6.0 B. M., whereas the corresponding moment value for the strong-field ligands is 2.0 B. M. It is clear, therefore, that Mn(II)—5 NSA complex possesses an octahedral structure.

Owing to the d^{10} configuration of Zn, the Zn(II) complexes are all diamagnetic; so that the stereochemistry of Zn(II)—5 NSA complex is by no means cleared by the magnetochemical investigations.

In case of Fe(II) complexes of regular octahedral symmetry, the works of GRIFFITH [22] and FIGGIS [23] are relevant. By an extension of KOTANI's method [24] they have calculated the magnetic moment at room temperature. The ground state of Fe(II) in O_h symmetry is $5_{T_{2g}}$ and μ_{eff} is expected to have a value of 5.6 B. M. at room temperature. Experimentally, magnetic moments between 5.1 and 5.7 B. M. have been observed [25]. The magnetic moment value (5.4 B. M.) obtained for Fe(II)—5 NSA complex indicates unequivocally that the geometry in the environment of Fe(II) is octahedral.

Experimental

Materials

All chemicals used were either of B. D. H. 'AnalaR' or of an equivalent quality.

Physical measurements and analyses

The presence of the ligand and the water molecules in the complexes was identified by infrared spectroscopy, using a 'Perkin—Elmer Model 237' spectrophotometer, in KBr matrix.

The magnetic moments were measured by the Gouy method at room temperature. The pH of the solutions was measured by employing a 'Polymetron CL-41' pH-meter.

Copper was determined volumetrically and other metals gravimetrically by the usual methods.

Preparation of the complexes

The complexes were prepared by the direct reaction of hydrated metal salts with 5NSA at 7.0 pH; the solvent used was either ethanol or an ethanol–water mixture (1 : 1 v/v). In all cases the crystals formed were removed by filtration, washed with ethanol and ether and then dried in a vacuum desiccation.

*

Thanks are due to Prof. R. D. PATEL for the magnetochemical data and to Dr. V. S. MEHTA for providing the infrared spectra.

REFERENCES

[1] ERNST, Z. L., MENASHI, J.: Trans. Faraday Soc., **58,** 2838 (1963)
[2] ERNST, Z. L., MENASHI, J.: Trans. Faraday Soc., **59,** 230 (1963)
[3] KHADIKAR, P. V., AMERIA, R. L.: J. Indian Chem. Soc. **49,** 1049 (1972)

[4] KHADIKAR, P. V., BHAGWAT, W. V.: J. Indian Chem. Soc. **47,** 478 (1970)
[5] KHADIKAR, P. V., SARWATE, A. G.: Curr. Sci. **38,** 511 (1969)
[6] KHADIKAR, P. V., PANDE, A. V., AMERIA, R. L.: Curr. Sci. **37,** 137 (1968)
[7] CALVIN, M., WILSON, K. W.: J. Am. Chem. Soc. **67,** 2003 (1945)
[8] BJERRUM, J.: Metal Ammine Formation in Aqueous Solution, P. Haase and Son, Copenhagen 1941
[9] IRVING, H., WILLIAMS, R. J. P.: J. Chem. Soc. **1953** 3192
[10] KHADIKAR, P. V., KAKKAR, S. N., POONIA, N. S.: Indian J. Chem. **11,** 709 (1973)
[11] PERRIN, D. D.: Nature **182,** 741 (1958)
[12] KHADIKAR, P. V., AMERIA, R. L., KEKRE, M. G., CHAUHAN, S. D.: J. Inorg. Nucl. Chem. **35,** 4301 (1973)
[13] BOLARD, J.: J. Chem. Phys. **1965** 900
[14] BISWAS, A. B., PANDE, A. V.: J. Indian Chem. Soc. **44,** 315 (1967)
[15] FUJITA, J., NAKAMOTO, K., KOBAYASKI, M.: J. Am. Chem. Soc. **78,** 3963 (1956)
[16] BELLAMY, L. J., BRANCH, R. F.: J. Chem. Soc. **1954** 4491
[17] BELLAMY, L. J., BEECHER, L.: J. Chem. Soc. **1954** 4487
[18] FIGGIS, B. N., NYHOLM, R. S.: J. Chem. Soc. **1959** 331
[19] NICHOLLS, D., WARBURTON, B. A.: J. Inorg. Nucl. Chem. **33,** 1041 (1971)
[20] LEVER, A. B. P.: Inorg. Chem. **4,** 765 (1965)
[21] LEWIS, J., WILKINS, R. G.: Modern Coordination Chemistry, Interscience, New York 1960
[22] GRIFFITH, J. S.: Trans. Faraday Soc. **54,** 1109 (1958)
[23] FIGGIS, B. N.: Nature, **182,** 1567 (1958)
[24] KOTANI, M.: J. Phys. Soc. (Japan) **4,** 293 (1949
[25] BAREFIELD, KENT E., BUSH, D. H.: Quart. Revs., **22,** 457 (1968)

Padmakar V. KHADIKAR; 1, Jawahar Road No. 1, Vyayamshala Gali, Ujjain (M. P.) 456006, India
Rameshchandra L.AMERIA; Vikram University, Ujjain (M. P.) India.

Acta Chimica Academiae Scientiarum Hungaricae, 85 (2), pp. 139—146 (1975)

THE FORMATION OF ETHYLENE GLYCOL–BORATES IN AQUEOUS MEDIUM, I

T. PAÁL and L. BARCZA*

*(CHINOIN Pharmaceutical and Chemical Works, Budapest. *Institute of Inorganic and Analytical Chemistry, L. Eötvös University, Budapest)*

Received May 9, 1974

Equilibria set up in solutions containing 0.010—0.020 *M* boric acid, 0.100—2.000 *M* ethylene glycol and 1.000 *M* $NaClO_4$ inert salt were studied at 25 °C by pH-metry. Borate–glycol anion complexes of 1 : 1 and 1 : 2 compositions and of $\beta_{011} = 1.78 \pm 0.03$ and $\beta_{012} = 0.12 \pm 0.03$ stability constants are formed. Since the acids corresponding to the two anions are at least hundred times stronger than boric acid, their formation can be disregarded.

As a result of the activity of the SILLÉN school [1], the formation of ion associates in aqueous salt solutions are well-known. Fewer data are available in the case of organic O-donor solvents, as *e.g.* alcohols, because in absolute solvents problems in the measuring technique arise, while in water–alcohol mixtures water is generally the dominant ligand. An exception is formed by ions, from the hydrate water of which two or more protons dissociate, because here the stability of the complex formed with *cis* vicinal glycols may be increased also in aqueous solution by the chelate effect.

Among the cyclic diol compounds, glycol–borate complexes, called also boric acid esters, are of industrial importance. Several organic chemical catalyses can be explained by their formation [2—6], they can be used for the protection of alcohol groups in syntheses [7], they are suitable as lubricants [8], as components of electroluminescent amalgams and flame-resistant varnishes, and possess bactericide and fungicide properties [9]. The analytical application of glycol borates is also well-known, for example in the electrophoresis of sugars [10], in the separation of steroid glycol epimers [11], in the determination of acetoacetyl decarboxylase [12], further in the photometric [13] and volumetic [14] analyses of boric acid proper.

In spite of many-sided application, no exact methods of investigation are reported in the literature for glycol borates utilized industrially, but mostly only practical values are given, such as *e.g.* the oxidability of diols, the pH of the solution or its conductivity [15]. Several communications report on the investigation of model compounds, but data in the literature show several inconsistencies.

Most of the glycol–boron compounds known are anionic complexes, but certain authors [16—20] report from neutral adducts. Though it is an ex-

perimental fact that the pH of boric acid complexes decreases on the addition of vicinal diols, according to the review paper of INGRI *et al.* [1], the neutral complexes are weaker acids than boric acid. An argued problem is also the formation of 1 : 1 and 1 : 2 complexes and their stability relationship. According to ANTIKAINEN [21] and CAMPBELL [22], only the 1 : 2 borate–mannit complex exists in concentrated solutions, TORSSELL [23] found 1 : 1 and (the more stable) 1 : 2 complexes, while BURGE [24] only the 1 : 1 compound. Similar discrepancies can be noted also in the description of the boric acid–fructose [23, 25, 26] and the boric acid–tartaric acid [27, 28] systems. According to ROY *et al.* [25], in pyrocatechol complexes $\beta_2 > \beta_1$, and on the basis of the measurements of ANTIKAINEN [29] in the case of the 2,3-naphthalene–diol ligand the 1 : 1 compound is more stable. A further problem is, whether more than one boron is linked to one ligand with polyhydroxy compounds. In the case of ascorbic acid and trioxyglutaric acid such complexes have been described [28], while in that of mannitol [29] not. The known tetrahedral co-ordination of boron makes it difficult to accept results involving mononuclear boron complexes containing more than two glycols [14, 19].

The ethylene glycol–boron interaction is described by KALACHEVA *et al.* [16] by the formation of a 1 : 1 neutral complex acid, by ROY *et al.* [25] by the formation at 25 °C of anionic complexes with $\beta_1 = 1.85$ and $\beta_2 = 0.1$, by CONNER and BULGRIN [30] with $\beta_1 = 2.15$ and $\beta_2 = 1.15$, while by OERTEL [37] with $\beta_1 = 1.8$ and $\beta_2 = 0.65$.

On account of the contradictions listed and in consideration of the practical importance of the theme, we started to study the complex formation reaction between glycol and borate. The present communication reports on the investigation of mononuclear ethylene glycol–borates.

Experimental

Boric acid recristallized several times from water, and ethylene glycol purified by distillation were used. The other chemicals were of analytical purity. 50% sodium hydroxide was stored in a plastic container under nitrogen atmosphere, and was diluted before titration under nitrogen atmosphere.

The perchloric acid, sodium hydroxide and sodium perchlorate stock solutions were prepared and checked as described in the literature [1].

Boric acid was used at 0.010 and 0.020 *M*, and ethylene glycol at 0.100, 0.200, 0.500, 1.000 and 2.000 *M* concentrations. The systems were titrated with sodium hydroxide at 25 ± 0.1 °C in the presence of 1.000 *M* $NaClO_4$. The composition of the titrating solution provided for a constant borate, glycol and Na^+ concentration during the measurements.

On a Radiometer pHm4d instrument, Radiometer G200B glass electrode

and an Ag/AgCl reference electrode with a Wilhelm bridge, the electromotiv force of the following cell was measured.

Glass electrode | test solution | 1.000 *M* $NaClO_4$ | 0.990 *M* $NaClO_4$, 0.010 *M* NaCl | Ag/AgCl

Measurements were carried out in the range from 7.0 to 9.5 pH. In this range the diffusion potential can be neglected in the presence of 1 *M* sodium perchlorate [31]. Thus, the relationship

$$E = E_0 - 59.15\ pH \qquad (1)$$

describes the pH dependence of the electromotive force. For the determination of E_0, perchloric acid of known concentration was titrated before each measurement with 0.01 *M* sodium hydroxide in the presence of 1.000 *M* $NaClO_4$. Without taking out of the electrodes, *i.e.* without changing the solution, the required quantities of boric acid, ethylene glycol and sodium perchlorate stock solutions were added to the titrated perchloric acid solution to make up the test solution.

Titration curves were recorded in several parallels, with 12—14 measuring points in each case. The reproducibility was ± 0.01 pH.

After alkaline titration, it was proved by the back-titration of the solutions with perchloric acid that the formation of the complexes was a rapid reversible process and not a time reaction. According to our control measurements, the E_0 value characteristic of the system in the presence of 1 *M* $NaClO_4$ did not change on the addition of ethylene glycol even at a glycol concentration as high as 2.000 *M*.

Calculations were carried out on a Hewlett—Packard Model HP 9100A calculator.

Symbols used for the descriptions of the equilibria

Symbols

HB	boric acid: $B(OH)_3$
B^-	the mononuclear borate ion: $B(OH)_4^-$
D	the ethylene glycol ligand
C_B	analytical concentration of boron in the system
C_A	total concentration of boron-containing anions
C_D	concentration of the weighed-in ethylene glycol
$H_pBD_r^{(1-p)-}$	symbol of the mononuclear glycol–borate complex
p	number of dissociable protons to be assigned to the complex, its value can be 0 and 1
r	number of the glycol ligands in the complex; on the basis of the tetrahedral configuration of borate, its value can be 0, 1 and 2.

Equilibria and constants

$B^- + H^+ \rightleftharpoons HB$

the protonation equilibrium of boric acid, corresponding to the process:

$$B(OH)_4^- + H^+ \rightleftharpoons B(OH)_3 + H_2O$$

$\beta_{110} = [HB]\ [H^+]^{-1}\ [B^-]^{-1}$

the protonation constant of boric acid (symbols in square brackets represent molar concentrations)

$$B^- + p\,H^+ + r\,D \rightleftharpoons H_pBD_r^{(1-p)-}$$

$$\beta_{p1r} = [H_pBD_r^{(1-p)-}]\,[B^-]^{-1}\,[H^+]^{-p}\,[D]^{-r}$$

the equilibrium of the formation of mononuclear glycol–borate and the corresponding equilibrium constant

K_w the ion product of water

Auxiliary functions

Z simulating boric acid as HB, Z is the average number of dissociable protons to be assigned to one boron

$Y = V(V+1)^{-1} = f(\log V)$
equation of SILLÉN's curve normalization [32], where V is an arbitrary variable

$Y = V(V+k)^{-1} = f(\log V)$
a curve normalization procedure similar to the preceding, where V is a variable, k a constant

$V^* = C_A(C_B - C_A)^{-1}$
ratio of the total concentration of anions and protonated forms

$W = V^*[H^+]$
auxiliary function for the calculation of the equilibrium constants.

Discussion

Protonation constant of the mononuclear borate ion

The function of formation to be constructed from measuring data is:

$$Z = \frac{C_B - C_A}{C_B} = \frac{[HB]}{[HB] + [B^-]} \tag{2}$$

because the concentration of the perchlorate ions does not change during the measurement, and the hydroxide ion concentration can be neglected in the pH range investigated, thus $C_A \approx [B^-]$.

The function of formation of 0.010 *M* (Fig. 1) and of 0.020 *M* boric acid,

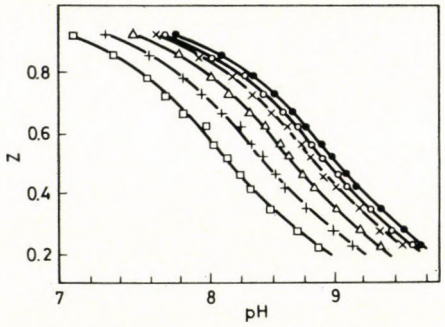

Fig. 1. The function of formation of 0.010 *M* boric acid in the presence of various quantities of ethylene glycol. Glycol concentrations: • 0; ○ 0.100; × 0.200; △ 0.500; + 1.000; □ 2.000 *M*

$Z = f(pH)$, can be fitted with SILLÉN's $Y = V(V + 1)^{-1} = f(\log V)$ normalized curve [32]. The protonation constant obtained is given in Table I.

Table I

Stability data of mononuclear complexes formed in solutions containing boric acid and ethylene glycol, measured at 25 °C in 1.000 M $NaClO_4$ medium

The accuracy of the results is expressed by the standard error of mean

Protonation constant of boric acid:

HB	$\log \beta_{110} = 8.84 \pm 0.01$

Stability constants of the ethylene glycol–borate complex:

BD^-	$\beta_{011} = 1.78 \pm 0.03$
BD_2^-	$\beta_{012} = 0.12 \pm 0.03$

If the data of INGRI [1] are recalculated with $\log K_w = -14.22$ relevant to the medium used by him (3.000 M $NaClO_4$, 25 °C) for the equilibrium formulated by us, $\log \beta_{110} = 8.95$ is obtained. According to our opinion, this deviation is due primarily to uncertainty in K_w, and not to the different media.

The stability of mononuclear ethylene glycol–borates

Is can be seen from Fig. 1, representing well the measuring data, that on the addition of glycol the $Z = f(pH)$ curves shift in the acid direction, but remain also further on parallel to the normalized curve $Y = V(V + 1)^{-1} = f(\log V)$. Thus, the systems behave as if monovalent acids with different protonation constants were investigated. Owing to the low stability of the complexes and to the high ligand excess, [D] remains practically constant during one titration. The formation function can be written in the following form:

$$Z = \frac{\sum_{r=0}^{2} \beta_{11r} [H^+] [D]^r}{1 + \sum_{r=0}^{2} \beta_{11r} [H^+] [D]^r + \sum_{r=1}^{2} \beta_{01r} [D]^r} = \frac{V}{V + k} \qquad (3)$$

However, curves of the type $Y = V(V + k)^{-1} = f(\log V)$ are parallel, if k is an arbitrary but constant value. Hence, SILLÉN's curve normalization [32] is the special case for the value $k = 1$ of the more general normalization (3), and may give even more information on the systems, than the determination of the stability constant of the 1 : 1 complexes.

The constants of the glycol complexes were not calculated on the basis of the Z functions, since another, more simple and at the same time highly descriptive auxiliary function: V* can be defined, which gives the ratio of the

concentrations of the borate anions and the protonated forms. This value, on multiplication with the hydrogen ion concentration, gives a simple function, the value of which in the case of mononuclear ethylene glycol borates is as follows:

$$W = V^* [H^+] = \frac{1 + \beta_{011} [D] + \beta_{012} [D]^2}{\beta_{110} + \beta_{111} [D] + \beta_{112} [D]^2} \tag{4}$$

It can be seen that calculation along the $W = f([D])$ plane curve is much simpler than with the aid of the curved surface $Z = f([H^+], [D])$.

An analysis of the experimental data according to Eq. (3) showed that for given C_B and C_D values the value of [D] is constant independently of C_A, so that W is also constant. Owing to the large excess of the ligand, the quantity of glycol bound in the ligand is only a very small ratio of the total quantity of ethylene glycol, so that $[D] \simeq C_D$ is also valid. Thus, the constants can be calculated on the basis of the deficient second-order equation $W = f(C_D)$. The shape of this function depends on the relative value of the equilibrium constants. It can be shown that under the following conditions:

$$\beta_{011} \text{ and } \beta_{110} > 0;\ \beta_{012} \leqq 0.01\, \beta_{011};\ \beta_{111} \text{ and } \beta_{112} \leqq 0.01\, \beta_{110}$$

the curve has a linear shape, in the case of

$$\beta_{012} > 0.01\, \beta_{011}$$

it deflects 'upwards', while in the case of

$$\beta_{111} \text{ or } \beta_{112} > 0.01\, \beta_{110}$$

'downwards' from the straight line. In principle, a linear relationship may be obtained also in the case when these two effects just counterbalance each other. However, an analysis of the experimental results on a computer (using the C_B, C_D, C_A, $[H^+]$ data, the assumed β_{p1r} constants and the program realizing the iteration of [D]) [33] show that experimental data in Fig. 2 prove only the existence of the 1 : 1 and 1 : 2 boron–glycol anion complexes. (Written similarly as above, the following variation can be proved mathematically)

$$\beta_{011} \text{ and } \beta_{110} > 0;\ \beta_{012} > 0.01\, \beta_{011};\ \beta_{111} \text{ and } \beta_{112} \leqq 0.01\, \beta_{110} \tag{5}$$

It can be seen from the Figure that the 1 : 2 complex is formed only at higher glycol concentrations. For the stability of the HBD and the HBD_2 forms only the information contained in (5) can be obtained from the measuring data, their formation can be neglected.

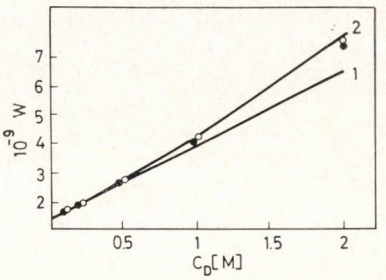

Fig. 2. The change in value of the auxiliary function W, calculated from measuring results, as a function of the ligand concentration. Data measured in • 0.100 *M* and ○ 0.020 *M* boric acid. Curves 1 and 2 in the figure represent the $W = f(C_D)$ functions calculated under the assumption of $\beta_{012} = 0$ and $\beta_{012} = 0.20$, respectively

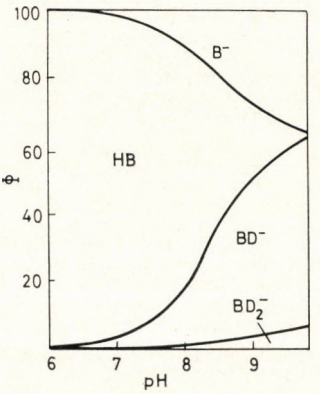

Fig. 3. The percentage distribution (Φ) of the ions formed in a solution containing 0.010 *M* boric acid and 1.000 *M* ethylene glycol as a function of pH. (The Φ value is obtained as the length of the given section of the vertical line of intersection)

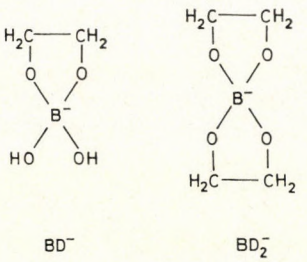

Fig. 4. The assumed structure of the ethylene glycol–borate anionic complexes

If the $W = f(C_D)$ curve is extrapolated to $C_D = 0$ value, the value $\beta_{110} = 8.85$ is obtained in good agreement with the constant measured in the absence of glycol.

Table I gives the constants, and in Fig. 3 the distribution of the ions formed in dependence on the pH are shown.

As a result of the equilibrium investigations, only the boron:glycol:OH^- ratio for the complexes formed and the stability constants are obtained. The method does not give any information on the number of the water molecules or perchlorate ions linked to the complex. However, it can be assumed on the basis of literature data [13, 18, 34—36] that also in aqueous medium the cyclic compounds shown in Fig. 4 are formed.

In our next paper the equilibrium investigations on ethylene glycol–polyborate systems will be discussed.

REFERENCES

[1] INGRI, N., FRYDMAN, M., LAGERSTRÖM, G., SILLÉN, L. G.: Acta Chem. Scand. **11,** 1034 (1957); INGRI, N.: Svensk. Kemisk Tidskrift **75,** 4 (1963)
[2] CAPON, B., GHOSH, B. CH.: Tetrahedron Lett. **25—26,** 1707 (1964)
[3] EMRICH, D. D., DARLING, S. M.: U.S.P. 3,104,255
[4] GEIGY, J. R.: Brit P. 969,059
[5] KULEV, L. P., KOJAIN, V. V.: Izv. Tomsk. Polytechn. Inst. **102,** 48 (1959)
[6] MORIZUR, J. P.: Bull. Soc. chim. France 1964, (7) 1625
[7] BACZEWSKI, A.: J. Electrochem. Soc. **112,** 243 (1965)
[8] DADURA, J. G., SIEGART, W. R., ODELL, N. R., HENRY, C.: U.S. Pat. 3,108,966
[9] BENGELSDORF, I. S.: FRENCH P. 1,315,567; DEBREY, R. J., FITZGIBBONS, W. O.: Belg. P. 630,109; WOODS, W. G.: U.S. Pat. 3,131,208
[10] FOSTER, A. B., STACEY, M.: J. Appl. Chem. **3,** 19 (1953)
[11] SCHNEIDER, J. J., LEWBART, M. L.: Tetrahedron Lett. **24,** 943 (1964)
[12] NEECE, S., FRIDOVICH, I.: Arch. Biochem. Biophys. **108,** 240 (1964)
[13] ROTH, H. J., MILLER, B.: Arch. Pharm. **297,** 660 (1964)
[14] BELCHER, R., TULLY, G. W., SVEHLA, G.: Anal. Chim. Acta **50,** 261 (1970)
[15] ICHIRO SAKURADA, ZENYA SHIHI, YASUOSHI SAKAGUCHI: Kobunski Kagoku **21,** 289 (1964)
[16] KALACHEVA, V. G., BEN'KOVSKII, V. G., SVARCS, E.: Latvijas PSR Zinatnu Akad. Vestis, Kim. Ser. 1969 (2), 149
[17] DRYSSEN, D., UPPSTRÖM, L., ZANGEN, M.: Anal. Chim. Acta **46,** 55 (1969)
[18] FISCHER, F., LOCKNER, S.: Z. chem. **4,** 301 (1964)
[19] MATEROVA, E. A., ROZHANSKAYA, T. I.: Zh. Neorg. Khim. **6,** 425 (1961)
[20] PESETSKY, B., ELDRED, N. R.: Tetrahedron **25,** 4137 (1969)
[21] ANTIKAINEN, P.: Ann. Acad. Sci. Fennicae, Ser. A. »». **56,** 8 (1954)
[22] CAMPBELL, G. W. JR.: J. Inorg. Nucl. Chem. **31,** 2625 (1969)
[23] TORSSELL, K.: Arkiv Kemi. **3,** 571 (1952)
[24] BURGE, D. E.: J. Phys. Chem. **67,** 2590 (1963)
[25] ROY, L. G., LAFERRIERE, A. L., EDWARDS, J. O.: J. Inorg. Nucl. Chem. **4,** 106 (1957)
[26] SWANN, W. B., MCNABB, W. M., HASEL, J. F.: Anal. Chim. Acta **28,** 441 (1963)
[27] GREKOVICH, A. L., MATEROVA, E. A.: Zh. Neorg. Khim. **15,** 187 (1970)
[28] SVARCS, E., IEVINS, A.: Latvijas PSR Zinatnu Akad. Vestis, Khim. Ser. 1961 (1), 19; 1969 (2), 131; 1969 (6), 667
[29] ANTIKAINEN, P.: Suomen Kem. B**43,** 31 (1970)
[30] CONNER, J. M., BULGRIN, V. C.: J. Inorg. Nucl. Chem. **29,** 1953 (1967)
[31] BARCZA, L., STRÓBL, L., LEHOCZKY, B.: Magy. Kém. Folyóirat **76,** 25 (1970)
[32] SILLÉN, L. G.: Acta Chem. Scand. **10,** 186 (1956)
[33] PAÁL, T.: Dissertation. L. Eötvös University, Budapest, 1972
[34] BALABAN, A. T., RENTEA, C. N., MOCANU, M.: Tetrahedron Lett. **29—30,** 2049 (1964)
[35] FINCH, A., PEARN, H. K.: Spectrochim. Acta **19,** 1621 (1963)
[36] ZIMMERMANN, H. K.: Advan. Chem. Ser. **42,** 23 (1964)
[37] OERTEL, R. P.: Inorg. Chem. **11,** 544 (1972)

Tamás PAÁL; 1045 Budapest, Tó utca 1—3. Hungary
Lajos BARCZA; 1088 Budapest, Múzeum krt. 4/b. Hungary.

Acta Chimica Academiae Scientiarum Hungaricae, 85 (2), pp. 147–151 (1975)

ON THE CLASSIFICATION OF NORMAL MODES OF VIBRATION, II

THE INTERACTION TERMS IN ENERGY DISTRIBUTIONS*

E. RYTTER

(Institutt for uorganisk kjemi Norges tekniske hogskole Universitetet i Trondheim)

Received May 30, 1974

Potential, kinetic and total energy distributions of twelve molecules where "exact force fields" are known have been compared. All these distributions become equal if the interaction terms are shared equally by the corresponding symmetry co-ordinates as suggested by PULAY and TÖRÖK [4]. However, it has been shown that this procedure fails for several of the molecules. It is proposed that the total energy-distribution method, with separate calculation of the interaction terms, should be used in the classification of normal modes of vibration.

The potential energy distribution [2] has become a standard tool in the classification of normal modes of vibration. In terms of symmetry coordinates the potential energy is given [3] by

$$2V = \sum_{ij} F_{ij} S_i S_j \tag{1}$$

Using the transformation to the normal co-ordinates, $\mathbf{S} = \mathbf{LQ}$, the values of the symmetry co-ordinates for the normal mode corresponding to $Q_k (Q_i = 0, i \neq k)$ are

$$S_i = L_{ik} Q_k \quad i = 1, 2, \ldots \tag{2}$$

This yields

$$2V^{(k)} = Q_k^2 \sum_{ij} F_{ij} L_{ik} L_{jk} \tag{3}$$

and the distribution

$$V_{ij}^{(k)} = F_{ij} L_{ik} L_{jk} \tag{4}$$

or, when normalized,

$$V_{ij}^{(k)} = F_{ij} L_{ik} L_{jk} \Big/ \sum_{ij} F_{ij} L_{ik} L_{jk} = F_{ij} L_{ik} L_{jk} \Big/ \lambda_k \tag{5n}*$$

and

$$\sum_{ij} V_{ij}^{(k)} = 1 \tag{6n}$$

* For Part I, see Reference [1].

* The *n* indicates that the distribution in the given equation is normalized.

The term $V_{ii}^{(k)}$ is associated with the symmetry co-ordinate S_i and the terms $V_{ij}^{(k)} = V_{ji}^{(k)}$ $(i \neq j)$ are the mixed contributions from the symmetry co-ordinates S_i and S_j to the potential energy. The latter terms are the off-diagonal or interaction terms. Usually the diagonal terms $F_{ii}L_{ik}^2$ are the largest and the vibration may be associated with the greatest of these.

However, the interaction terms may be important and a more distinct interpretation of these would be of great value. PULAY and TÖRÖK [4] proposed that the total contribution from the symmetry co-ordinate S_i to the potential energy may be written as

$$V_i^{(k)} = \sum_j F_{ij} L_{ik} L_{jk} / \lambda_k = L_{ik} L_{ki}^{-1} \tag{7n}$$

i.e.

$$2V^{(k)} = \lambda_k Q_k^2 \sum V_i^{(k)} \quad \sum_i V_i^{(k)} = 1 \tag{8n}$$

In this distribution the interaction terms $V_{ij}^{(k)} = V_{ji}^{(k)}$, totally $2\ F_{ij}L_{ik}L_{jk}$, are shared equally by S_i and S_j. The above distribution has been used by several authors [4—12]. Nevertheless, the fact that this distribution *does not* give a true picture of the normal mode of vibration is illustrated by the following.

(i) The kinetic energy distribution is given in exactly the same way [4], namely

$$T_i^{(k)} = \sum_j G_{ij}^{-1} L_{ik} L_{jk} = \sum_j T_{ij} = L_{ik} L_{ki}^{-1} \tag{9n}^*$$

Although it is not quite clear what $V_i^{(k)} = T_i^{(k)}$ implies, it seems strange, and suggests a kind of independence of each symmetry co-ordinate in the normal vibration.

(ii) For the two-dimensional case Eqs. (7*n*) and (9*n*) yield $M_1^{(1)} = M_2^{(2)}$ and $M_2^{(1)} = M_1^{(2)}$, where $V_i^{(k)} = T_i^{(k)} = M_i^{(k)}$ has been introduced.
In other words, for all two-dimensional cases the relative contribution from the second symmetry co-ordinate to the first vibration is equal to the relative contribution from the first co-ordinate to the second vibration, and *vice versa*. No justification has been given for this odd restriction and, moreover, it is certainly not correct for a triangular **L**-matrix.

(iii) An upper or lower triangular **L**-matrix implies $V_i^{(i)} = 1$ and $V_i^{(k)} = 0$ for $i \neq k$, *i.e.*, all vibrations are completely characteristic. However, Eq. (2) shows that, except for one of the vibrational modes, several symmetry co-ordi-

* The kinetic energy distributions are always normalized.

nates have values different from zero. Thus they should give a contribution to the potential energy or, at least, to the kinetic energy. It may be argued that a triangular **L**-matrix is physically impossible, but this approximation has given results very close to those obtained from additional information for many molecules [13—16]. For the examples given in Table I, $|L_{12}|$ is less than 0.01 for $GeCl_4$, RuO_4, OsO_4, SeF_6, TeF_6, RhF_6 and IrF_6, while L_{22} is in the range 0.30 to 0.41 [17].

(iv) With the definition given in Eq. (7*n*), it is possible that the contribution from a symmetry co-ordinate to the potential, as well as the kinetic energy, is negative. For the two-dimensional case this physically impossible situation occurs for $M_2^{(1)}$ and $M_1^{(2)}$ when L_{21} and L_{12} have the same signs. It is assumed that standard definitions and ordering of the co-ordinates are used [18]. Examples of negative $M_i^{(k)}$ values are given in Table I.

Table I

Energy distributions normalized to one hundered for the F_2 vibrations of tetrahedral, and the $F_{1\mu}$ vibrations of octahedral molecules, where 'exact force fields' are known. Data are taken from MÜLLER, KEBABCIOGLU *and* CYVIN [17] *and the standardized symmetry co-ordinates of* CYVIN [18] *have been used*

Molecule and mode		$V_{11}^{(k)}$	$2V_{12}^{(k)}$	$V_{22}^{(k)}$	$M_1^{(k)}$	$M_2^{(k)}$	$T_{11}^{(k)}$	$2T_{12}^{(k)}$	$T_{22}^{(k)}$	$E_{11}^{(k)}$	$2E_{12}^{(k)}$	$E_{22}^{(k)}$
$SiCl_4$	$\nu 1$	98	−12	14	92	8	192	−200	108	145	−106	61
	$\nu 2$	4	7	89	8	92	1	14	85	3	10	87
$GeCl_4$	$\nu 1$	104	−8	4	100	0	129	−57	28	116	−32	16
	$\nu 2$	0	0	100	0	100	0	0	100	0	0	100
$SnCl_4$	$\nu 1$	107	−7	1	103	−3	113	−20	7	110	−14	4
	$\nu 2$	14	−33	119	−3	103	1	−9	107	8	−21	113
RuO_4	$\nu 1$	99	0	1	99	1	105	−12	7	102	−6	4
	$\nu 2$	1	0	99	1	99	0	1	99	0	1	99
OsO_4	$\nu 1$	99	0	0	100	0	102	−5	3	101	−2	2
	$\nu 2$	1	−1	100	0	100	0	0	100	0	0	100
SF_6	$\nu 1$	97	−44	47	75	25	151	−153	102	124	−99	75
	$\nu 2$	15	20	65	25	75	10	30	60	12	25	62
SeF_6	$\nu 1$	106	−12	6	100	0	118	−36	18	112	−24	12
	$\nu 2$	0	0	100	0	100	0	0	100	0	0	100
TeF_6	$\nu 1$	103	−4	1	101	−1	109	−17	8	106	−11	5
	$\nu 2$	0	−2	102	−1	101	0	−1	101	0	−2	102
WF_6	$\nu 1$	102	−2	0	101	−1	105	−9	4	104	−6	2
	$\nu 2$	1	−3	102	−1	101	0	−2	102	0	−2	102
UF_6	$\nu 1$	97	2	1	98	2	102	−9	7	100	−4	4
	$\nu 2$	5	−7	102	2	98	0	3	97	3	−2	99
RhF_6	$\nu 1$	101	−3	2	100	0	113	−27	14	107	−15	8
	$\nu 2$	0	1	99	0	100	0	1	99	0	1	99
IrF_6	$\nu 1$	102	−2	1	100	0	105	−10	5	103	−6	3
	$\nu 2$	1	−2	102	0	100	0	0	100	0	−1	101

(v) The origin of the terms $L_{ik}L_{ki}^{-1}$ may be visualized by the transformation $\mathbf{Q} = \mathbf{L}^{-1}\mathbf{S}$ or

$$Q_k = L_{k1}^{-1} S_1 + \ldots L_{ki}^{-1} S_i + \ldots \tag{10}$$

Introduction of the values of the symmetry co-ordinates for the k'th normal mode of vibration (Eq. 2) gives

$$Q_k = L_{k1}^{-1} L_{1k} Q_k + \ldots L_{ki}^{-1} L_{ik} Q_k + \ldots \tag{11}$$

and there might seem to exist some connection between $L_{ik}L_{ki}^{-1}$ and the contribution of S_i to Q_k. However, L_{ki}^{-1} in Eq. (10) is not a measure of the 'weight' of S_i in Q_k, but is the contribution from the Q_k vector to the S_i vector [19].

In Table I $V_{ij}^{(k)}$, $M_i^{(k)}$, $T_{ij}^{(k)}$ and the total energy distribution [1],

$$E_{ij}^{(k)} = (F_{ij} + \lambda_k G_{ij}^{-1}) L_{ik} L_{jk} = V_{ij}^{(k)} + \lambda_k T_{ij}^{(k)} \tag{12}$$

or, when normalized distributions are used,

$$E_{ij}^{(k)} = (F_{ij} + \lambda_k G_{ij}^{-1}) L_{ik} L_{jk} / 2\lambda_k = \frac{1}{2}(V_{ij}^{(k)} + T_{ij}^{(k)}) \tag{13n}$$

are summarized for thirteen $XY_4(T_d)$ and $XY_6(O_h)$ type molecules where 'exact force fields' are known [17]. It is demonstrated that $M_1^{(1)} - M_2^{(2)}$, $M_2^{(1)} = M_1^{(2)}$ and that negative $M_i^{(k)}$ values may occur. An interesting case is represented by the $GeCl_4$ vibrations which are completely characteristic in terms of $M_i^{(k)}$. Examination of the other distributions confirms that $\nu_2(L_{12} = = -0.001, L_{22} = 0.317)$ is a pure S_2 vibration. On the other hand, while the potential energy distribution indicates a rather characteristic $\nu_1(L_{11} = 0.216, L_{21} = 0.169)$, the kinetic energy distribution shows contributions from both S_1 and S_2 as well as a large interaction term. A splitting of the latter term, giving $M_1^{(1)} = 100$ and $M_2^{(1)} = 0$, is an oversimplification. This is clearly recognized from the fact that the velocity in the S_2 direction is almost as great as in the S_1 direction.

A good method for the classification of normal modes of vibration should be simple, but at the same time contain all the essential information. The splitting of the interaction terms into equal parts in the method of PULAY and TÖRÖK [4] fulfils the first requirement, but the results may be misleading. The total energy distribution method [1], preferably with claculation of the interaction terms, seems to be the most suitable compromise at present. It is an open question whether it is at all possible to assign a part of an interaction term to a given co-ordinate.

*

The author wishes to thank Professor S. J. CYVIN and Professor H. A. ØYE for reading the manuscript of this paper and for suggesting several improvements. The author gratefully acknowledges the financial support from The Norwegian Research Council for Science and the Humanities.

REFERENCES

[1] RYTTER, E.: J. Chem. Phys., 1974 **60,** 3882 (1974)
[2] MORINO, Y., KUCHITSU, K.: J. Chem. Phys., **20,** 1809 (1952)
[3] WILSON, E. B., DECIUS, J. C. and CROSS, P. C.: Molecular Vibrations. McGraw-Hill, New York 1955
[4] PULAY, P., TÖRÖK, F.: Acta Chim. Acad. Sci. Hung., **47,** 273 (1966)
[5] ALIX, A., BERNARD, L.: C. R. Acad. Sci. Paris, B **269,** 812 (1969)
[6] ALIX, A., BERNARD, L.: C. R. Acad. Sci. Paris, **270,** 66, 151 (1970)
[7] ALIX, A., BERNARD, L.: C. R. Acad. Sci. Paris, B **272,** 528 (1971)
[8] ALIX, A., FREEMAN, D. E., BERNARD, L.: C. R. Acad. Sci. Paris, B **273,** 247 (1971)
[9] KERESZTURY, G., JALSOVSZKY, G.: J. Molec. Struc., **10,** 304 (1971)
[10] ALIX, A., BERNARD, L.: Z. Naturf., A **27,** 593 (1972)
[11] ALIX, A., MOHAN, N., MÜLLER, A.: Z. Naturf., A **28,** 1158 (1973)
[12] ALIX, A., MÜLLER, A., MOHAN, N., FREEMAN, D. E.: J. Molec. Struc., 1974 (In press)
[13] MÜLLER, A.: Z. phys. Chem., **238,** 116 (1968)
[14] MÜLLER, A., CYVIN, S. J., BRUNVOLL, J.: J. Molec. Spectrosc., **30,** 157 (1969)
[15] PEACOCK, C. J., HEIDBORN, U., MÜLLER, A.: J. Molec. Spectrosc., **30,** 338 (1969)
[16] MÜLLER, A., MOHAN, N., HEIDBORN, U.: Z. Naturf., A **27,** 129 (1972)
[17] MÜLLER, A., KEBABCIOGLU, R., CYVIN, S. J.: J. Molec. Struct., **3,** 507 (1969)
[18] CYVIN, S. J.: Molecular Vibrations and Mean Square Amplitudes. Elsevier, New York 1968
[19] RYTTER, E.: To be published

Erling RYTTER; Argonne National Laboratory 9700 S. CASS AV.
Argonne, Illinois 60439 USA.

Acta Chimica Academiae Scientiarum Hungaricae, 85 (2), pp. 153—159 (1975)

EQUILIBRIA OF ALFA-AMINO ACID COMPLEXES OF TRANSITION METAL IONS, VII

EFFECT OF THE ALIPHATIC CARBON CHAIN ON THE THERMODYNAMICS AND STRUCTURE OF Ni(II)–AMINO ACID COMPLEXES

I. Sóvágó, A. Gergely and J. Posta

(Institute of Inorganic and Analytical Chemistry, L. Kossuth University, Debrecen)

Received June 6, 1974

pH-metric equilibrium measurements were made to determine the stability constants of the Ni(II) complexes of glycine, α-alanine, α-aminobutyric acid, norvaline and norleucine. The relevant enthalpy and entropy values were obtained from calorimetric studies. The complexes of glycine are of marked stability; this is associated with a higher enthalpy change. A periodic variation dependent on the even–odd carbon atom number can be observed in the corresponding thermodynamic data in the series from alanine to norleucine. It can be established from a consideration of the spectra of Ni(α-amino acid)$_2$. 2 H_2O type complexes that the structures of the species present in the solid state and in aqueous solution may be significantly different. In the solid state the lengthening of the carbon chain results in an enhanced distortion of the structure; this is similarly manifested *via* a periodic change dependent on the carbon atom number.

Introduction

Many authors have already dealt with the equilibrium and thermodynamic conditions of the transition metal complexes of glycine and α-alanine [1, 2]. Earlier investigations tended to concentrate on the comparison of the complex-forming properties of the various metal ions. In connection with the equilibrium study of C-substituted glycine complexes, Irving and Pettit [3] pointed out the role of steric factors in complex formation. Sharma and Mathur [4] dealt with the effect of the aliphatic carbon chain in various amino acid complexes. On the basis of the data relating to the copper(II), nickel(II), cobalt(II) and zinc(II) complexes of glycine, α-alanine and α-aminobutyric acid, it was established that although the lengthening of the carbon chain does cause a slight decrease of stability, the thermodynamic data remain practically unchanged. At the same time, the significant effect of the alkyl chain complex formation was pointed out, among others, by Sacconi *et al.* [5] with regard to the N-alkyl-substituted salicylaldimine complexes of the Ni(II) ion, and by Császár [6] with regard to alkylamine and diamine complexes of Ni(II). It was found that a peridocity dependent on the even–odd carbon–atom number characteristic of the ligands can be demonstrated in the magnetic and spectral data for the metal complexes.

In an earlier equilibrium study of amino acid–amino acid mixed complexes, we have reached conclusions similar to those of the above authors [7]. Our results indicated that the previous findings of SHARMA and MATHUR [4] could be regarded as only partially valid. Thus, the complexes of glycine are of marked stability. In the series from α-alanine to norleucine, however, lengthening of the carbon chain no longer results in a further stability decrease. The data also permit the conclusion that there may be some periodicity dependent on the carbon atom number. This periodicity appears more strongly in the thermodynamic data, as supported by studies relating to the mixed complexes copper(II)–amino acid–histamine [8].

Appropriate thermodynamic data for the Ni(II) complexes of norvaline and norleucine are not available in the literature. At the same time, the elucidation of the small changes caused by the aliphatic carbon chain, necessitates the availability of as many data as possible, determined under identical conditions, for each of the complexes.

In accordance with the foregoing, the aim of this work is the termodynamic and spectral study of the complexes of nickel(II) with aliphatic α-amino acids.

Experimental

The chemicals used were products of Reanal. The DL-amino acids were purified by recrystallization from water–ethanol mixtures. The concentration of $NiCl_2$ solutions was determined gravimetrically, *via* the oxinate.

The pH-metric and calorimetric measurements were performed with a Radiometer PHM-4 pH-meter and an LKB-8700 solution calorimeter, as described previously [8].

The $\log \beta_1$ and $\log \beta_2$ values corresponding to the equilibrium processes

$$M + A \rightleftharpoons MA + \Delta H_1 \quad (1)$$

$$M + 2\,A \rightleftharpoons MA_{21} + \Delta H_{12} \quad (2)$$

together with the related enthalpy changes, were calculated as reported earlier [8].

For the spectrophotometric measurements, samples of the composition Ni(amino acid)$_2$.2 H_2O were employed; these were prepared by addition of excess $NiCO_3$ to an aqueous solution of the amino acid [9]. Both the spectra of aqueous solutions of the complexes and the reflection spectra of the solid materials were recorded, using a Beckmann DU spectrophotometer. MgO was employed as reference material in the measurement of the reflection spectra.

Results and discussion

The stability constants of the nickel(II)–amino acid parent complexes are listed in Table I, together with the values of $\log K_1/K_2$ and $2pK_2 - \log \beta_2$. The protonation constants, and the heats of proton dissociation necessary for the evaluation of the calorimetric results were reported earlier [10].

It is clear from the data in Table I that the complexes of glycine are of marked stability, but the increase of the carbon atom number in the series from alanine to norleucine results in only a very slight further stability decrease. At the same time, both the $\log \beta_2$ and the $2pK_2 - \log \beta_2$ values suggest a periodicity dependent on the carbon atom number. This is in agreement with earlier observations on mixed complexes [7].

Table I

Stability constants of the Ni (II)–α-amino acid parent complexes
$t = 25$ °C; $I = 0.2$ mol/dm³ KCl

Amino acid	$\log K_1$	$\log K_2$	$\log \beta_2$	$\log K_1/K_2$	$2pK_2 - \log \beta_2$
Glycine	5.65	4.75	10.40	0.90	8.70
Alanine	5.32	4.42	9.74	0.90	9.62
α-Aminobutyric acid	5.22	4.31	9.53	0.91	9.69
Norvaline	5.28	4.34	9.62	0.94	9.66
Norleucine	5.27	4.34	9.61	0.93	9.69

Table II

Thermodynamic data for the Ni (II)–aliphatic α-amino acid parent complexes

Amino acid	I	$-\Delta H_1$	$-\Delta H_{12}$	ΔS_1	ΔS_{12}	Reference
		kjoule/mol		joule/mol K		
Glycine	0	20.5	40.2	49.8	81.6	[11][a]
	0	17.1	36.7	60.7	89.1	[12][b]
	0.2	18.0	36.4	53.1	83.7	[4][b]
	0	18.3	39.1	56.1	80.3	[13][a]
	0.2	21.1	42.0	37.7	58.2	this work[a]
α-Alanine	0.2	18.4	38.5	50.2	83.7	[4][b]
	0.2	16.8	36.3	45.2	62.8	this work[a]
α-Aminobutyric acid	0.2	20.1	40.2	37.2	53.6	[4][b]
	0.2	17.2	33.9	42.3	68.6	this work[a]
Norvaline	0.2	17.9	35.6	41.0	64.9	this work[a]
Norleucine	0.2	16.7	32.7	44.8	74.5	this work[a]

[a] Calorimetric value
[b] Determined by the temperature coefficient method

The enthalpy and entropy changes measured for the formation of the nickel(II)–aliphatic α-amino acid complexes are given in Table II. Some recently determined literature data are also tabulated.

On the basis of the data in Table II it may be established that, allowing for the different ionic strengths, our data for nickel(II)–glycine agree fairly well with the values of other authors. A comparatively larger difference is observed between our data and those of SHARMA and MATHUR [4]. The data of these authors for the complexes of alanine also differ significantly from the more recent literature data, and thus it is probable that their other values obtained with the temperature coefficient method were not of sufficient accuracy either. Thus, their finding that the aliphatic carbon chain has practically no effect on the thermodynamic conditions cannot be considered valid either.

It emerges from our data that, similarly as with the corresponding copper(II) complexes, the high stability of the glycine complexes is associated with a larger enthalpy change. The data relating to the Ni(II) complexes of the amino acids with higher carbon atom numbers primarily indicate a periodicity dependent on the even–odd carbon atom number.

The effect of the aliphatic carbon chain on complex formation, and its periodic variation with the carbon atom number, are also confirmed by our spectral studies. It has been reported [14, 15] that the Ni(II) complexes of the amino acids studied can be described by a transplanar structure of D_{2h} symmetry. Naturally, upon co-ordination of two additional H_2O molecules it forms an octahedral structure:

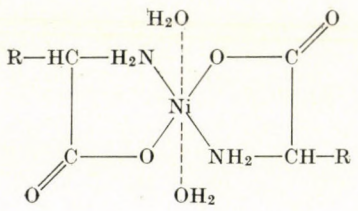

Accordingly, these complexes should give spectra containing the three absorption maxima characteristic of octahedral geometry in the wavelength range $300 < \lambda < 1200$ nm.

Our data obtained by evaluation of the solution and reflection spectra are listed in Table III.

The most striking observation to be made from the data in Table III is the extremely large difference between the solution and reflection spectra. This is confirmed by Fig. 1 and 2.

Figures 1 and 2 show a comparison of the spectra of the Ni(II) complexes of glycine and α-aminobutyric acid recorded in the two ways. The above differ-

Table III

Spectral data for Ni (amino acid)$_2$.2H$_2$O complexes in aqueous solution and in reflection

Amino acid	R	In aqueous solution					In reflection			
		ν_1 (kK)	ν_2 (kK)	ν_3 (kK)	B (cm^{-1})	$f.10^5$ (mole^{-1} cm^{-2})	ν_1 (kK)	ν_2 (kK)	ν_3(I) (kK)	ν_3(II) (kK)
Glycine	H	9.8	16.1	27.0	913	4.11	11.1	16.9	26.8	—
Alanine	CH_3	9.9	16.1	27.0	893	4.00	11.3	16.9	26.4	—
α-Aminobutyric acid	C_2H_5	9.9	16.1	27.0	893	4.80	11.7	17.0	26.2	28.6
Norvaline	C_3H_7	9.9	16.1	27.1	900	4.55	11.4	16.0	26.2	27.6
Norleucine	C_4H_9	9.9	16.1	27.0	893	5.73	11.7	17.1	26.1	28.6

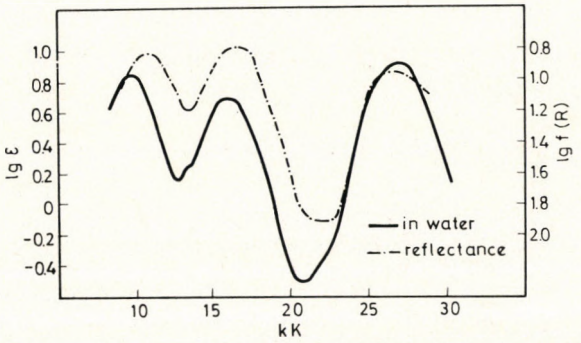

Fig. 1. Reflection spectrum and aqueous solution spectrum of Ni(glycine)$_2 \cdot 2\ H_2O$

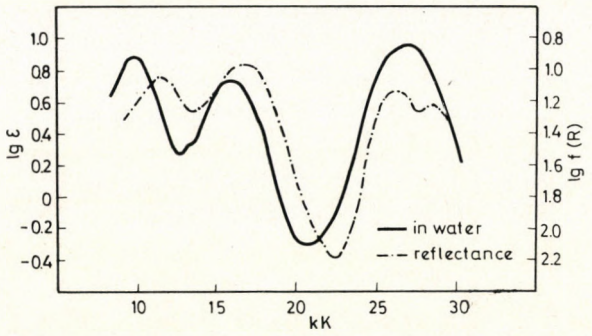

Fig. 2. Reflection spectrum and aqueous solution spectrum of Ni(α-aminobutyric acid)$_2 \cdot 2\ H_2O$

ence is also indicated by the fact that in spite of the D_{2h} symmetry actually present in solution, the Racah 'B' parameter can be well calculated with the known relations for O_h symmetry [16]. This calculation cannot be carried out for the reflection spectrum, however, because of the greater distortion of the molecule.

It emerges from Table III that the differences between the spectra of the various amino acid complexes in aqueous solution are very slight, though both the 10Dq and B parameters differ a little in the glycine complexes from those of the other amino acid complexes, which are practically the same. (This is in good agreement with the findings already mentioned in connection with the thermodynamic data.) In the series from alanine to norleucine, on the other hand, the spectral differences between the various complexes can no longer be measured, and thus the periodicity too is expressed only in the oscillator strength '*f*' [16]. At the same time, analysis of the reflection spectra clearly reveals that in the solid state there is a close relation between the length of the carbon chain and the extent of distortion from the octahedral symmetry. As shown in Fig. 1, in the case of the glycine complexes the only difference to be observed is in the positions of the spectral bands of the aqueous solution and the reflection spectrum. In the reflection spectrum of $Ni(alanine)_2 \cdot 2\ H_2O$, however, the third band is slightly split; in the case of the α-aminobutyric acid complex this splitting is well measurable. In the solid state, therefore, the lengthening of the carbon chain results in an ever more pronounced distortion of the structure. As shown by the data of Table III, this also involves a variation of a periodic nature.

As regards the effect of the aliphatic carbon chain, therefore, it can be established that the change of the carbon atom number is expressed both in the thermodynamic data and in the structures of the compounds. This is a fairly surprising experimental fact, for group R in the structural formula given above is attached to the chelate ring only as a side-chain. On the other hand, the outstanding behaviour of glycine (R=H) can readily be explained in comparison with the amino acid chelates containing alkyl groups as side-chains. In aqueous solution the increase of the length of the alkyl chain generally results in a variation of a periodic nature only. Naturally, these effects are very small. In the solid state, however, as a consequence of less freedom of movement, they are considerably larger.

*

The authors express their thanks to Dr. József CSÁSZÁR for valuable assistance in the evaluation of the spectral data.

REFERENCES

[1] SILLÉN, L. G., MARTELL, A. E.: Stability Constants, Special Publication No. 17, Chemical Society, London 1964
[2] CHRISTENSEN, J. J., IZATT, R. M.: Handbook of Metal Ligand Heats. Marcel Dekker, Inc., New York 1970
[3] IRVING, H., PETTIT, L. D.: J. Chem. Soc., **1546** (1963)
[4] SHARMA, V. S., MATHUR, H. B.: Indian J. Chem. Soc. **3,** 475 (1965)
[5] SACCONI, L., PAOLETTI, P., DEL RE, G.: J. Amer. Chem. Soc. **79,** 4062 (1957)

[6] CSÁSZÁR, J.: D. Sc. Thesis, Szeged 1971
[7] GERGELY, A., SÓVÁGÓ, I., NAGYPÁL, I., KIRÁLY, R.: Inorg. Chim. Acta, **6,** 435 (1972)
[8] GERGELY, A., SÓVÁGÓ, I.: J. Inorg. Nucl. Chem. **35,** 4355 (1973)
[9] SEGNINI, D., CURRAN, C., QUAGLIANO, J. V.: Spectrochim. Acta, **16,** 540 (1960)
[10] GERGELY, A., SÓVÁGÓ, I.: Magyar Kém. Foly., **78,** 578 (1972)
[11] ANDERSON, K. P., GREENHALG, W. O., BUTLER, E. A.: Inorg. Chem. **6,** 1056 (1967)
[12] BRANNAN, J. R., DUNSMORE, H. S., NANCOLLAS, G. H.: J. Chem. Soc., **304** (1964)
[13] IZATT, R. M., JOHNSON, H. D. CHRISTENSEN, J. J.: J. Chem. Soc. Dalton Transaction, 1152 (1972)
[14] NAKAMOTO, K., MORIMOTO, Y., MARTELL, A. E.: J. Amer. Chem. Soc., **83,** 4528 (1961)
[15] MAKI, G.: J. Chem. Phys., **29,** 162 (1958)
[16] CSÁSZÁR, J. BÁN, M.: Optical Spectra, Ligand-Field Theory, Complex Structure. Akadémiai Kiadó, Budapest 1972

Imre SÓVÁGÓ
Arthur GERGELY
József POSTA
4010-Debrecen, Hungary.

Acta Chimica Academiae Scientiarum Hungaricae, 85 (2), pp. 161—177 (1975)

APPROXIMATE ANALYTICAL DETERMINATION OF THE AVERAGE VALUES OF POTENTIAL FUNCTIONS OCCURING IN CHEMICAL TRANSPORT PHENOMENA

K. Polinszky, J. Fülöp, K. Seitz and T. Vajda

(Research Institute for Technical Chemistry, Hungarian Academy of Sciences)

Received June 17, 1974

A relatively simple method has been developed which, with certain restrictions, permits to determine the average values of the potential functions occurring in heat and mass transfer processes by an approximate analytical procedure.

The method is based on the introduction of an auxiliary function, based essentially on a simplifying assumption. The approximate form of the auxiliary function can be directly determined by Laplace transformation from the differential equation of the system of these equations for the given problem, without applying the inverse transformation.

By numerical calculations it can be shown that the approximate method is of satisfactory reliability in the interval of the independent variable which is of interest in practice.

(A) General

Introduction

Some transport phenomena occurring in chemical unit operations may be described by systems of partial differential equations. The approximate method developed can be applied under the following conditions.

1. The process is stationary and the corresponding system of differential equations contains two independent variables.

2. The partial differential equation in the system of equations is a Fourier function whose boundary condition is Newton's general linear boundary condition.

3. The system of differential equations is linear.

4. Both potential functions converge to the saturation value.

5. The parameters of the differential equations are constant.

The above conditions are fulfilled in many transport phenomena occurring in chemical unit operations.

In problems of *heat transfer* our method may be applied to flowing stationary systems. The problems of heat transfer between flowing, dispersed or continuous solid phases and a flowing gas belong to this category if the source of heat in the dispersed or continuous phase is a linear function of the temperature. As examples we refer to the problem of heat transfer between flowing

dispersed masses and a flowing gas, as well as to the description of tunnel furnaces.

The method may also be applied to *diffusion* problems. In the case when diffusion is not followed by another process (*e.g.* adsorption), the method can be applied, similarly to heat transfer problems for stationary systems.

The method can also be applied to processes where *diffusion and adsorption* (or desorption) take place simultaneously and if the isotherm of adsorption is assumed to be linear. Otherwise condition 3 is not fulfilled, which means that the system of differential equations is not linear.

The method is also applicable to *absorption* processes between a liquid and a gas or between two liquids, because in this case the relation between the two phases — considering Henry's constant — can be given similarly to Newton's boundary condition. If a chemical reaction takes place in the liquid phase, the method can be applied only if it is of the first order.

In the case of processes where *heat and mass transfer* occur *at the same time*, the method is only applicable if the functions representing the source of heat or mass do not affect the linearity of the system of differential equations. Algorithms qualified as practically 'treatable', serving for the mathematical solution of systems of the type mentioned above partly consist of partial, partly of ordinary differential equations, and are available only for some systems of special structure.

These algorithms require an extensive mathematical apparatus. The results obtained with their help are of complicated structure, difficult to survey and can be applied to numerical calculations only by employing a digital computer.

Therefore, it was necessary to find an approximate analytical solution, which does not need an overly complicated mathematical apparatus, is simple to derive and in which the results obtained are easy to survey and suitable for numerical calculations, too.

This idea of an approximate analytical solution and its construction for some cases have already been proposed by KONDRATJEV [1] and HEILIGENSTÄDT [2]. HEILIGENSTÄDT has derived his approximate relations from the exact solution of the differential equation he examined, thus, he could only achieve the aim of obtaining the solutions in a simple form for easy survey. KONDRATJEV elaborated a method rendering possible the approximate solution in a direct way, too, but only in cases when the potential function of the environment is constant. In these cases there is no system of differential equations but only the Fourier partial differential equation. For this function the exact solution is also available, KONDRATJEV's method cannot be generalized according to a previously given algorithm in cases when the potential of the environment (*e.g.* the temperature of gas) is not constant, that is when one has a system of differential equations.

General description of the approximate method

Let the two potential functions figuring in condition (1) be u and u'; and the two independent variables x and y. Let a function of two variables $u(x, y)$ satisfy *e.g.* the Fourier partial differential equation in Cartesian co-ordinates:

$$v_x \frac{\partial u}{\partial x} = a \frac{\partial^2 u}{\partial y^2} \tag{1}$$

in the region

$$-L \leqq y \leqq +L$$

and

$$0 \leqq x < \infty$$

This function describes a stationary process where the medium, defined by potential function u, is moving forward in direction x with velocity v_x.

The other equation of the system of differential equations with two unknowns is of the following form:

$$L(u, u') = 0 \tag{2}$$

where we have only to assume that it is a linear differential equation.

The Newton boundary condition of Eq. (1) is generally of the form

$$\left(\frac{\partial u}{\partial y}\right)_{y-L} = h\,[u' - u(x, L)] \tag{3}$$

and

$$\left(\frac{\partial u}{\partial y}\right)_{y=-L} = -\,h\,[u' - u\,(x, L)]\,. \tag{4}$$

Let the potential function $u(x, y)$ denote the average value in direction y:

$$\bar{u}(x) = \frac{1}{2L} \int_{-L}^{+L} u(x, y)\, dy\,. \tag{5}$$

Let us integrate both sides of equation (1) with respect to y from $-L$ to $+L$. Then we obtain the following general differential equation:

$$v_x \frac{d\bar{u}}{dx} = \frac{ah}{2L} \left[\left(\frac{\partial u}{\partial y}\right)_{y=L} - \left(\frac{\partial u}{\partial y}\right)_{y=-L} \right]. \tag{6}$$

Substituting boundary conditions (3) and (4) into Eq. (6) one obtains

$$v_x \frac{d\bar{u}}{dx} = \frac{ah}{L} [u' - u(x, L)]\,. \tag{7}$$

It is necessary to stress that x is the only independent variable in differential equation (7). If u' is a function of only x, the above statement is trivially true; if, however, $u' = u'(x, y)$, the boundary value $u'(x, L)$ is figuring in Eq. (7). — Without restricting the generalization, we shall assume that $u' = u'(x)$ is a function of one variable only. From the viewpoint of physical considerations this assumption is reasonable because u' generally represents the potential function of the gas or liquid flowing around the solid phase and in this direction, *i.e.* perpendicular to the direction of flow x, the value of the potential function remains unchanged.

Since differential equation (2) is linear, after integrating with respect to y we obtain a linear differential equation of the form:

$$L'(\bar{u}, u') = 0\,. \tag{8}$$

In Eq. (8), too, x is the only independent variable. The solution of the system consisitng of the general differential equations (7) and (8), too, is ambiguous in view of the three unknown functions:

$$\bar{u}(x),\ u'(x) \text{ and } u(x, L)\,.$$

Let us introduce the following function of one variable:

$$z(x) = \frac{u'(x) - u(x, L)}{u'(x) - \bar{u}(x)}\,. \tag{9}$$

For all stationary transport phenomena where there exists $\lim x$, y and $\lim x'$, function zx will obviously have the following properties:

a) $z(0) = 1$
b) $\lim\limits_{x=\infty} z(x) = z_\infty$ where $0 < z_\infty < 1$
c) $z(x)$ decreases monotonously in the interval $x > 0$

The main point of our approximation is:

$$z(x) \cong z_\infty \tag{10}$$

in the case of every $x > 0$. With the application of Eqs (9) and (10), the system of differential equations (7) and (8) can be solved with respect to $\bar{u}(x)$ and $u'(x)$ as a function of z_∞, as the number of the unknown functions has been reduced by one.

Our aim now is to determine the boundary value z_∞. In the course of the determination we shall not use the exact mathematical solution of the system of partial differential equations we started from.

Determination of the limit z_∞

It can be proved that there exists a solution of the starting system of partial differential equations in the following form:

$$u(x, y) = \sum_{k=1}^{\infty} A_k(y)\, e^{-\lambda_k^2 x} \tag{11}$$

and

$$u'(x) = \sum_{k=1}^{\infty} B_k\, e^{-y_k^2 x}\,. \tag{12}$$

The eigenvalue equation of the system of partial differential equations generates the values λ_k. Between the eigenvalues λ_k there exists the following well-known relation [3]:

$$\lambda_2 < \lambda_1 < \lambda_3 \ldots < \lambda_k < \lambda_{k+1} < \ldots$$

The form of $\bar{u}(x)$ obtained upon integrating $u(x, y)$ is

$$\bar{u}(x) = \sum_{k=1}^{\infty} \bar{A}_k\, e^{-\lambda_k^2 x}\,. \tag{13}$$

By comparison of and finding the limit of Eqs (9), (11) and (12), (13) and considering the relation $\lambda_k < \lambda_{k+1}$, we obtain

$$z_\infty = \frac{B_1 - A_{1f}}{B_1 - \bar{A}_1} \tag{14}$$

where A_{1f} denotes the value of the function $A_1(y)$ on the surface $y = L$. The values of B_1, A_{1f} and A_1 can be determined with the application of the Laplace transformation without knowledge of the solutions of the system of partial differential equations $u(x, y)$ and $u'(x)$.

Let us find the Laplace transforms with respect to x of Eqs (11) (12) and (13):

$$\int_0^{\infty} u(x, y)\, e^{-px}\, dx = V(p, y) = \sum_{k=1}^{\infty} \frac{A_k(y)}{\lambda_k^2 + p} \tag{15}$$

$$\int_0^{\infty} u'(x)\, e^{-px}\, dx = V'(p) = \sum_{k=1}^{\infty} \frac{B_k}{\lambda_k^2 + p} \tag{16}$$

$$\int_0^{\infty} \bar{u}(x)\, e^{-px}\, dx = V^*(p) = \sum_{k=1}^{\infty} \frac{\bar{A}_k}{\lambda_k^2 + p} = \frac{1}{2L} \int_{-L}^{+L} V(p, y)\, dy\,. \tag{17}$$

In Eqs (15) and (16) $V(p, y)$ and $V'(p)$ are the solutions of the Laplace-transformed equation system of the starting system of differential equations. In a given case these functions can be determined after performing the Laplace transformation of the starting system of differential equations.

By multiplying both sides of Eqs (15), (16) and (17) by $(\lambda_1^2 + p)$ and passing to the limit for $p \to -\lambda_1^2$, we get:

$$A_{1f} = A_1(L) = \lim_{p=-\lambda_1^2} V(p, L)(\lambda_1^2 + p) \tag{18}$$

$$B_1 = \lim_{p=-\lambda_1^2} V'(p)(\lambda_1^2 + p) \tag{19}$$

$$\bar{A}_1 = \lim_{p=-\lambda_1^2} V^*(p)(\lambda_1^2 + p) \,. \tag{20}$$

Upon substituting expressions (18), (19) and (20) into function (14) and rearranging, we get

$$z_\infty = \lim_{p=-\lambda_1^2} \frac{V'(p) - V(p, L)}{V'(p) - V^*(p)} \,. \tag{21}$$

In summary, the following can be established:

(1) By applying the approximation given by expression (10) for the determination of functions $\bar{u}(x)$ and $u'(x)$, we obtain the system consisting of the general differential equations (7) and (8). In differential equation (7), after applying approximation (10), the limit of $z\infty$ appears.

(2) The limit z_∞ can be solved *without exact solution* of the starting system of differential equations on the basis of Eq. (21), using solely the Laplace transforms $V(p, y)$ and $V'(p)$.

(3) In the knowledge of the necessary initial conditions, the system of differential consisting of (7) and (8) can be solved for functions $\bar{u}(x)$ and $u'(x)$ with the application of Eqs (9) and (10) and using the value z_∞ obtained from function (21). In the following it will be shown that the functions $\bar{u}(x)$ and $u'(x)$ obtained from Eqs (7) and (8) give a very good approximation of the functions $\bar{u}(x)$ and $u'(x)$ derived from the exact solution of the starting system of differential equations in the whole interval of $x > 0$.

(B) Adsorption process on a single grain*

(I) Description of the physical-mathematical model

In the experimental arrangement as shown in Fig. 1, up to moment $t = 0$, the spherical adsorbent grain of radius R is completely isolated from the gas medium containing the adsorbate in volume concentration C_0. Adsorption, thus, has to be followed within the time interval of $0 < t < +\infty$.

* *cf.* [4].

In this model the adsorption process is divided into three main parts.

(1) Mass transfer takes place at the surface of the grain through a boundary layer formed in consequence of incomplete mass transfer. The mass flux density is considered proportional to the difference of concentrations at the two sides of the boundary layer. This flux density evidently agrees with the flux density determined at point $r = R$ in te grain. From the above we obtain Newton's boundary condition:

$$D\left(\frac{\partial C}{\partial r}\right)_{r=R} = \beta[C_0 - C(R;t)], \tag{22}$$

where D is the diffusion coefficient, β the coefficient of mass transfer, and C is the volume concentration of the adsorbate in the grain.

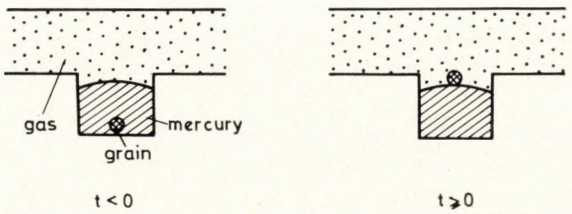

Fig. 1

(2) The concentration in the interior of the grain is determined by Fick's equation expressed in spherical co-ordinates. In consequence of the symmetry of the problem, only the component r of the flux density vector differs from zero, therefore:

$$D\left[\frac{\partial^2 C}{\partial r^2} + \frac{2}{r}\frac{\partial C}{\partial r}\right] = \frac{\partial C}{\partial t} + q, \tag{23}$$

where

q is the volume of material adsorbed in unit time in unit volume of the adsorbate.

(3) The actual adsorption takes place at the pore surface of the grain. The rate of adsorption is considered proportional to the difference between the mass concentration in the pore and at the surface of the pore:

$$q = K(C - C^*). \tag{24}$$

Evidently, this last concentration C^* can be interpreted only in a formal way. In reality, this quantity is proportional to the surface density w of the material already adsorbed and considering a linear isotherm, can be expressed in the following form:

$$C^* = \delta w \tag{25}$$

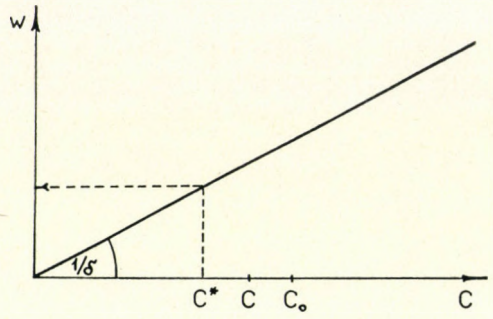

Fig. 2

(Fig. 2). On the other hand, it is also clear that the variation of surface density with time is proportional to the rate of adsorption:

$$\frac{\partial w}{\partial t} = \varkappa q \,. \tag{26}$$

On comparing Eqs (24), (25) and (26) we obtain

$$\frac{\partial w}{\partial t} = \varkappa K C - \varkappa K \delta w \,. \tag{27}$$

In summary, when setting up the physical model, the following conditions have been accepted:

(a) in view of the isotropy of the adsorbent grain and its environment, the problem can be considered as spherosymmetrical;

(b) as shown in Fig. 2, we assume a linear isotherm between the material to be adsorbed and the material after the reaction. It is known, however, that in any other case the problem would be impossible to handle mathematically;

(c) temperature changes in course of the adsorption have been neglected;

(d) eventual changes in the concentration C_0 of the gas due to insufficient supply of material have been neglected;

(e) all the parameters of the process are considered to be constant.

Starting from the above physical model, we arrive at the following mathematical problem; on applying Eqs (22), (23) and (27), and substituting Eq. (26) we obtain:

$$D\left[\frac{\partial^2 C}{\partial r^2} + \frac{2}{r}\frac{\partial C}{\partial r}\right] = \frac{\partial C}{\partial t} + \frac{1}{\varkappa}\frac{\partial w}{\partial t} \,,$$

$$\frac{\partial w}{\partial t} = \varkappa K C - \varkappa K \delta w \,;$$

$$D\left(\frac{\partial C}{\partial r}\right)_{r=R} = \beta[C_0 - C(R,t)]\,, \tag{28}$$

$$C(r,0) \equiv w(r,0) = 0\,,$$

$$0 \leq r \leq R,\quad 0 < t < +\infty\,.$$

This is a system of partial differential equations with two unknowns with respect to the quantities C and w as functions of position and time. We also know the boundary and the initial conditions necesssary for their calculation.

Let us perform the following variable transformation in system (28):

$$w^* = \frac{1}{x}w, \qquad r^* = \frac{r}{R}, \qquad t^* = \frac{tD}{R^2}\,.$$

Then we obtain

$$\frac{\partial^2 C}{\partial r^{*2}} + \frac{2}{r^*}\frac{\partial C}{\partial r^*} = \frac{\partial C}{\partial t^*} + \frac{\partial w^*}{\partial t^*}$$

$$\frac{\partial w^*}{\partial t^*} = gC - sw^*\,; \tag{29}$$

$$\left(\frac{\partial C}{\partial r^*}\right)_{r^*=1} = B[C_0 = C(1,t^*)]\,,$$

$$C(r^*,0) \equiv w^*(r^*,0) = 0,$$

$$0 \leq r^* \leq 1,\ 0 < t^* < +\infty,$$

where the new parameters

$$g = \frac{KR^2}{D}, \qquad s = \frac{\varkappa K \delta R^2}{D}, \qquad B = \frac{\beta R}{D}$$

have been introduced. From (29) it is apparent that the model contains only these three independent parameters.

(II) Determination of the approximate solution of the system of differential equations

Let us integrate both sides of the first equations of (29) with respect to the variable r^* between the limits 0 and 1:

$$\int_0^1 \frac{\partial}{\partial r^*}\left(r^{*2}\frac{\partial C}{\partial r^*}\right) dr^* = \int_0^1 r^{*2}\frac{\partial C}{\partial t^*}\,dr^* + \int_0^1 r^{*2}\frac{\partial w^*}{\partial t^*}\,dr^*\,. \tag{30}$$

First, the usual transformation of the left-hand-side of (29) has been performed:

$$\frac{\partial^2 C}{\partial r^{*2}} + \frac{2}{r^*}\frac{\partial C}{\partial r^*} \equiv \frac{1}{r^{*2}}\frac{\partial}{\partial r^*}\left(r^{*2}\frac{\partial C}{\partial r^*}\right),$$

then both sides were multiplied by r^{*2}. Introducing the averages, over r^*, of variables C and w^*.

$$\bar{C} = 3\int_0^1 r^{*2} C dr^*, \qquad \bar{w}^* = 3\int_0^1 r^{*2} w^* dr^*,$$

and integrating the left-hand-side of (30) we obtain:

$$\left[r^{*2}\frac{\partial C}{\partial r^*}\right]_0^1 = \frac{1}{3}\frac{d\bar{C}}{dt^*} + \frac{1}{3}\frac{d\bar{w}^*}{dt^*} \tag{31}$$

where on the right-hand-side of (31) we made us of the interchangeability of the integration and differentiation procedures. On the basis of physical reasoning, it follows that the left-hand-side of (31) at $r^* = 0$ is zero so that (31) assumes the following form:

$$\left(\frac{\partial C}{\partial r^*}\right)_{r^*=1} = \frac{1}{3}\left(\frac{d\bar{C}}{dt^*} + \frac{d\bar{w}^*}{dt^*}\right) \tag{32}$$

Applying the third equation of (29), the left-hand-side of (32) can be transformed as follows:

$$B[C_0 - C(1, t^*)] = \frac{1}{3}\left(\frac{d\bar{C}}{dt^*} + \frac{d\bar{w}^*}{dt^*}\right). \tag{33}$$

The left-hand-side of (33) can further be rearranged by introducing equation $z(t^*)$ as defined in Eq. (9). In this case:

$$z(t^*) = \frac{C_0 - C(1, t^*)}{C_0 - \bar{C}(t^*)}$$

and with $z(t^*)$ the final form of (33) is the following:

$$3Bz(t^*)[C_0 - \bar{C}(t^*)] = \frac{d\bar{C}}{dt^*} + \frac{d\bar{w}^*}{dt^*}. \tag{34}$$

When integrating the second equation of (29) with respect to r^*, we simply obtain:

$$\frac{d\bar{w}^*}{dt^*} = g\bar{C} - s\bar{w}^*. \tag{35}$$

(34) and (35) are the system of differential equations derived from (29). The initial conditions belonging to it are evidently:

$$\bar{C}(0) = \bar{w}^*(0) = 0. \tag{36}$$

However, the above system of equations cannot be solved unambiguously as it includes three unknown equations:

$$\bar{C}(t^*),\ \bar{w}^*(t^*) \text{ and } z(t^*).$$

Therefore, the approximation described in (10) is applied

$$z(t^*) \approx z_\infty$$

over the whole interval

$$0 < t^* < \infty$$

Physically, the approximation means the following: The mass flow at the surface of the grain towards the pores is considered to be connected not with the surface concentration but with the average concentration of the pore volume of the grain. The deviation resulting from this assumption could be compensated completely if equation $z(t^*)$ were known but we do not have enough equations to determine $z(t^*)$. Thus we try to correct the error at least partly by means of z_∞, which can be determined in another way. This method obviously does not provide the exact solutions of $\bar{C}$ an $\bar{w}^*$.

According to the above, in order to determine the approximate solution, z_∞ has to be calculated first. This will be performed by the method described in the general part of this paper.

Let us find the Laplace transforms of the system of equation (29) and of the boundary condition with respect to t^*. With the aid of the initial conditions concerning C and w^*, we obtain the following form:

$$\frac{d^2 Z}{dr^{*2}} + \frac{2}{r^*}\frac{dZ}{dr^*} = pZ + pV$$

$$pV = gZ - sV$$

$$\left(\frac{dZ}{dr^*}\right)_{r^*=1} = B\left[\frac{C_0}{p} - Z(1, p)\right],$$

where p is the independent variable of the Laplace transforms, and the transforms of C and w^* are introduced as follows:

$$Z(r^*, p) = \int_0^\infty C(r^*, t^*)\, e^{-pt^*}\, dt^*,$$

$$V(r^*, p) = \int_0^\infty w^*(r^*, t^*)\, e^{-pt^*}\, dt^*.$$

Our aim is to determine from the ordinary system of differntial equations the Laplace transform $z(r^*, p)$; with the help of which the value of z_∞ can be determined by finding the limit. Let us substitute the second equation of (37) into the first:

$$\frac{d^2Z}{dr^{*2}} + \frac{2}{r^*}\frac{dZ}{dr^*} - p\left(1 + \frac{g}{p+s}\right)Z = 0$$

and let us introduce the new variable $Z^* = r^*Z$; then the equation will take the following form;

$$\frac{d^2 Z^*}{dr^{*2}} = p\left(1 + \frac{g}{p+z}\right)z^* = 0. \tag{38}$$

One can immediately write the solution of differential equation (38):

$$Z^* = A_1 sh\ \omega\ r^* + A_2 ch\ \omega\ r^*,$$

where:

$$\omega = \sqrt{p\left(1 + \frac{g}{p+s}\right)}.$$

On the basis of this, the solution of Z is

$$Z(r^*, p) = A_1\frac{sh\ \omega\ r^*}{r^*} + A_2\frac{ch\ \omega\ r^*}{r^*}. \tag{39}$$

In consequence of the limited character of the concentration C and, thus, of Laplace transform at the point $r^* = 0$, it evidently follows that $A_2 = 0$. A_1 can be determined by the third equation of (37):

$$A_1 = \frac{B\dfrac{C_0}{p}}{\omega\ ch\ \omega + (B-1)\ sh\ \omega}. \tag{40}$$

Substituting, at last (40) into (39) we obtain:

$$Z(r^*, p) = \frac{B\dfrac{C_0}{p}}{\omega\ ch\ \omega + (B-1)\ sh\ \omega} \cdot \frac{sh\ \omega\ r^*}{r^*}. \tag{41}$$

In order to calculate z_∞, the average value of $z(z^*, p)$ with respect to r^* is also needed. Starting from (41), we obtain:

$$\bar{Z}(p) = 3\int_0^1 r^{*2}\ Z(r^*, p)\ dr^* = \frac{3B\dfrac{C_0}{p}}{\omega\ ch\ \omega + (B-1)\ sh\ \omega}\left[\frac{ch\ \omega}{\omega} - \frac{sh\ \omega}{\omega^2}\right].$$

Now we can write the expression for z_∞ on the basis of Eq. (21). In our case we also need the Laplace transform of C_0, which simply C_0/p.
Hence

$$z_\infty = \lim_{p=p_1} \frac{\dfrac{C_0}{p} - Z(1,p)}{\dfrac{C_0}{p} - \bar{Z}(p)} =$$

$$= \lim_{\omega=\omega_1} \frac{\dfrac{C_0}{p} - \dfrac{B\,C_0/p}{\omega\,ch\,\omega + (B-1)\,sh\,\omega}\,sh\,\omega}{\dfrac{C_0}{p} - \dfrac{3B\,C_0/p}{\omega\,ch\,\omega + (B-1)\,sh\,\omega}\left[\dfrac{ch\,\omega}{\omega} - \dfrac{sh\,\omega}{\omega^2}\right]}. \tag{43}$$

Here p_1 and the equivalent ω_1 are the poles with the smallest absolute values of the Laplace transforms. The poles of both Laplace transforms can be calculated from the solution of the eigenvalue equation

$$\omega ch\omega + (1 - B) sh\,\omega = 0.$$

On passing to the limit, it can be seen that the first terms of both the numerator and denominator vanish, thus (43) will take the following form:

$$z_\infty = \frac{sh\,\omega_1}{3\left[\dfrac{ch\,\omega_1}{\omega_1} - \dfrac{sh\,\omega_1}{\omega_1^2}\right]}. \tag{44}$$

We have to notice that the denominator of the first form in the Laplace transform is obviously zero at every pole. Let us express $ch\,\omega_1$ and substitute it into Eq. (44), then

$$z_\infty = \frac{sh\,\omega_1}{3\left[\dfrac{sh\,\omega_1}{\omega_1^2}(1-B) - \dfrac{sh\,\omega_1}{\omega_1^2}\right]} = -\frac{\omega_1^2}{3B},$$

and considering that $Z(r^*, p)$ has only imaginary poles,

$$z_\infty = \frac{|\omega_1|^2}{3B}. \tag{45}$$

After having determined z_∞ let us return to the approximate solution of the system of differential equations (34)—(35)—(36). Let us substitute, therefore, in (34) $z(t^*)$ by z_∞, and let us introduce $\bar{C}$ and $d\bar{C}/dt^*$ from Eq. (35) and from the derivative of Eq. (35) with respect to t^* into Eq. (34). We obtain the following equation for $\bar{w}^*$:

$$|\omega_1|^2\left[C_0 - \frac{1}{g}\left(\frac{d\bar{w}^*}{dt^*} + s\bar{w}^*\right)\right] = \frac{1}{g}\left(\frac{d^2\bar{w}^*}{dt^{*2}} + s\frac{d\bar{w}^*}{dt^*}\right) + \frac{d\bar{w}^*}{dt^*},$$

or, when arranged in the usual form:

$$\frac{d^2\overline{w}^*}{dt^{*2}} + (s + g + |\omega_1|^2)\frac{d\overline{w}^*}{dt^*} + s|\omega_1|^2\overline{w}^* = C_0 g |\omega_1|^2 . \tag{46}$$

The solution of Eq. (46) can be given immediately:

$$\overline{w}^* = Xe^{\lambda_1 t^*} + Ye^{\lambda_2 t^*} + C_0\frac{g}{s}, \tag{47}$$

where

$$\lambda_{1,2} = \frac{-(s + g + |\omega_1|^2) \pm \sqrt{(s+g + |\omega_1|^2)^2 - 4|\omega_1|^2 s}}{2}$$

X and Y are coefficients.

From Eqs (35) and (47):

$$\bar{C} = \frac{1}{g}\left[X(\lambda_1 + s)e^{\lambda_1 t^*} + Y(\lambda_2 + s)e^{\lambda_2 t^*}\right] + C_0 . \tag{48}$$

Applying the initial conditions (36), we obtain a common system of equations for coefficients X and Y from which they can be determined; thus, the final form of (47) and (48) is:

$$C = C_0\left[1 + \frac{\lambda^2}{\lambda_1 - \lambda_2}\cdot\frac{\lambda_1 + s}{s}e^{\lambda_1 t^*} - \frac{\lambda_1}{\lambda_1 - \lambda_2}\cdot\frac{\lambda_2 + s}{s}e^{\lambda_2 t^*}\right]$$

$$\overline{w}^* = \frac{g}{s}C_0\left[1 + \frac{\lambda_2}{\lambda_1 - \lambda_2}e^{\lambda_2 t^*} - \frac{\lambda_1}{\lambda_1 - \lambda_2}e^{\lambda_2 t^*}\right]. \tag{49}$$

Equation (49) is an approximate analytical system of solutions of the system of ordinary differential equations with respect to averages from the system of partial differential equations (29).

(III) Calculation of the error of the approximate solution

From Ref. [4] the exact solutions for C and w^* in the system of equations (29) are known. From these, the averages of the exact $\bar{C}_e$ and $\overline{w}_e$ values can be easily obtained:

$$\bar{C}_e = 6BC_0 \sum_{\substack{k=1\\ i=1,2}}^{\infty} \frac{B}{B(1-B) - |\omega_k|^2}\varphi_{ik}(1 - e^{p_{ik}t^*}),$$

$$\overline{w}_e^* = 6BC_0 \sum_{\substack{k=1\\ i=1,2}}^{\infty} \frac{B}{B(1-B) - |\omega_k|^2}\varphi_{ik}\left[\frac{g}{s}(1 - e^{-st^*}) - \right. \tag{50}$$

$$\left. - \frac{g}{P_{ik} + s}(e^{p_{ik}t^*} - e^{-st^*})\right]$$

where

$$\varphi_{ik} = \frac{1}{p_{ik}} \frac{(p_{ik} + s)^2}{(p_{ik} + s)^2 + sg}$$

and

$$p_{1k,2k} = \frac{-(s + g + |\omega_k|^2) \pm \sqrt{(s + g + |\omega_k|^2)^2 - 4|\omega_k|^2 s}}{2} .$$

The sequence of ω can be calculated from the following eigenvalue equation:

$$th\, \omega_k = \frac{\omega_k}{1 - B} .$$

As can be seen, the exact averages are much more complicated expressions than the approximations in (49).

In order to obtain a numerical value for the deviation of the approximate solutions from the corresponding exact solution, let us define the following per cent error:

$$\eta_c = \frac{|\bar{C}_e - \bar{C}|}{C_0} \cdot 100, \qquad \eta_{w^*} = \frac{|\overline{w}_e^* - \overline{w}^*|}{\frac{g}{s} C_0} \cdot 100 . \tag{51}$$

Approximation (10) would cause the greatest error evidently at $t^* = 0$ as $z(t^*)$ at this moment differs from z_∞ the most strongly. This, however, is yet not the case, because at $t^* = 0$ the initial conditions $\bar{C}(0) = \overline{W}^*(0) = 0$ have to be fulfilled. Thus, the error will have its maximum somewhere in the interval $0 < t^* < +\infty$.

The values in (51) have been calculated with the following system of parameters:

$$B = 20,\ 40;\ g = 0.2,\ 1;\ s = 0.5;\ 0 \leq t^* \leq 2 .$$

The summation of $\bar{C}_e^*$ and $\overline{W}_e^*$ has been continued up to $k = 30$.

The results are shown in Figs 3, 4, 5 and 6.

According to the expectations, the curves show that the error approaches zero when $t^* \to 0$ and $t^* \to +\infty$.

In the interval the error assumes different values depending on the actual parameters. Apparently, with the increase of B and q the error also increases, but in the t^* range of practical importance the error will never exceed a few per cent. Therefore, the approximation can be considered to be of satisfactory accuracy.

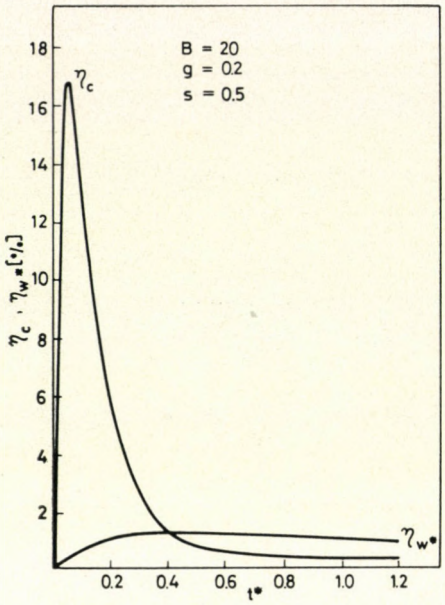

Fig. 3

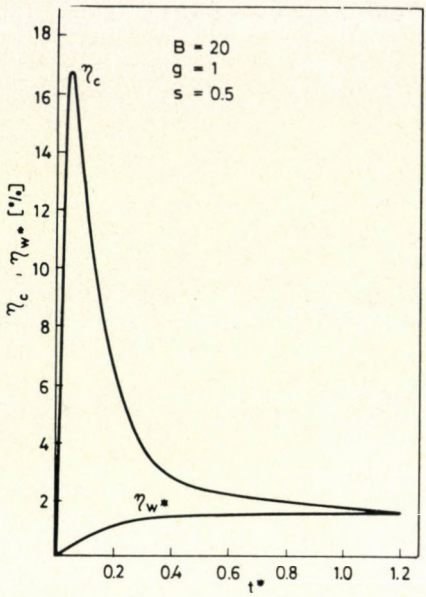

Fig. 4

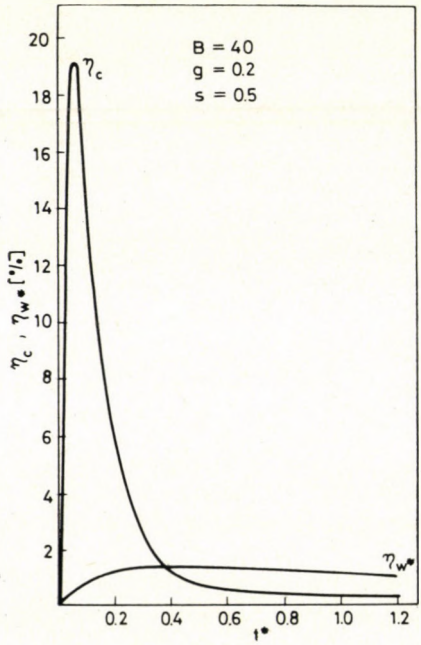

Fig. 5

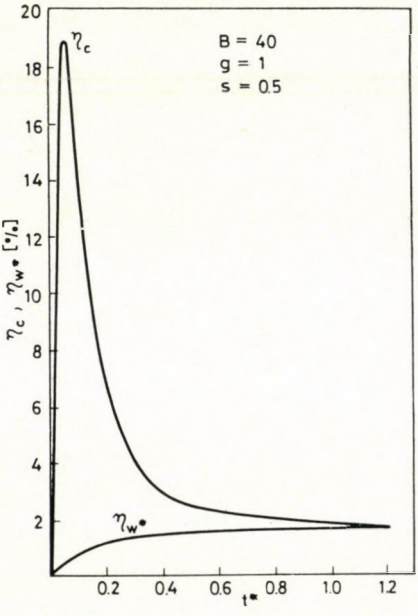

Fig. 6

Symbols

a	specific thermal conductivity,	m
	mass transfer coefficient,	m/h
C	volume concentration of the absorbate in the grain,	m^3/m^3
D	diffusion constant,	m^2/h
h	heat transfer coefficient,	m^{-1}
L	thickness of the charge,	m
q	source intensity,	m^3/h
r	spherical co-ordinate,	m
R	radius of the grain,	m
t	time,	h
v_x	velocity of the medium,	m/h
w	surface density of the adsorbed material,	m^3/m^2
x, y	rectangular co-ordinates,	m

REFERENCES

[1] KONDRATJEV, G. M.: Regularny Teplovy Rezhim. Moskow, 1954
[2] HEILIGENSTÄDT, W.: Wärmetechnische Rechnungen für Industrieöfen. Stahleisen, Düsseldorf 1951
[3] CARSLAW, H. S., JAEGER, I. C.: Conduction of Heat in Solids, Clarendon Press, Oxford 1959
[4] VARGA, K., FEJES, P.: Acta Chimica (Budapest), **71**, 387 1972

Károly POLINSZKY
János FÜLÖP
Károly SEITZ
Tádé VAJDA

1056 — Budapest, Szerb u. 23, Hungary.

Acta Chimica Academiae Scientiarum Hungaricae, 85 (2), pp. 179—190 (1975)

CLEAVAGE OF THE HETEROCYCLIC RING OF ISOFLAVONOIDS BY NUCLEOPHILIC REAGENTS, I

KINETICS EQUILIBRIUM CONDITIONS OF THE CLEAVAGE OF THE PYRONE RING OF ISOFLAVONE (3-PHENYLCHROMONE) IN AQUEOUS ALKALINE MEDIUM

V. SZABÓ and M. ZSUGA*

(Institute of Applied Chemistry, Kossuth Lajos University, Debrecen)

Received October 25, 1973

The γ-pyrone ring of isoflavone **(I)** is opened under quite mild conditions (10^{-2} *M* aqueous NaOH at room temperature), and an equilibrium depending on the concentration of the hydroxide ions will be produced involving isoflavone, the carbanion **VI**, 2-hydroxy-α-hydroxymethylenedeoxybenzoin **(II)**, and 2-hydroxyisoflavanone **(VIII)**.

The activation energy of the rate-determining step of the ring fission process **(I → VI)** is $E^* = (12.9 \pm 0.9)$ kcal.mol^{-1}; its activation entropy is $\Delta S^* = (-13.6 \pm +3.1)$ cal mol^{-1} degree^{-1}. It is supposed that ring opening begins with a reversible bimolecular A_N 2 addition reaction.

The degradation of compound **II** to 2-hydroxydeoxybenzoin proceeds at a much lower rate than the ring opening reaction.

Alkaline hydrolytic decomposition is one of the most useful methods of elucidating the structures of natural isoflavones, as the intermediates **(III)** as well as the final products **(IV, V)** of the hydrolysis can be readily identified. According to our present knowledge, alkaline hydrolysis proceeds in three principal steps [1, 2].

Ring opening and degradation have been effected under various conditions [2, 4, 5, 6, 7], obviously because there is a relation — though not very thoroughly studied — between the direction and rate of the decomposition and the structures involved. This has been pointed out so far by a few authors only [1, 2, 7].

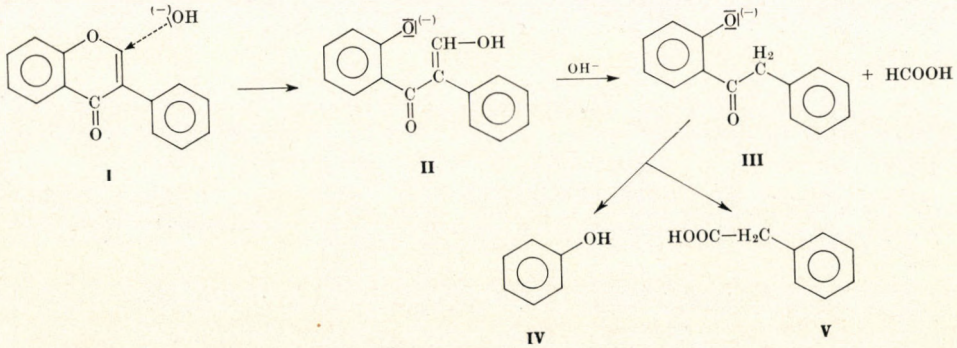

I II III IV V

* This paper is based on the Doctoral Thesis of M. ZSUGA.

Studies by preparative methods have only revealed qualitative connections; therefore, in order to throw some light upon the reactivity and stability of isoflavonoids in nucleophilic reactions we decided to start a kinetic investigation.

Our experiments have shown that — in contradistinction to data given in the literature [7] – isoflavone undergoes a change when exposed even to very mild reaction conditions (such as 10^{-2} *M* aqueous solution of sodium hydroxide at room temperature); the γ-pyrone ring is opened and very slow hydrolytic decomposition occurs to give 2-hydroxydeoxybenzoin; thus the isoflavone molecule is extremely sensitive to nucleophilic attack.

Our former and recent observations have shown that the heterocyclic ring of isoflavone and several monosubstituted isoflavones can be opened also with other nucleophilic agents (hydroxylamine, β-hydroxyethylamine, hydrazine hydrate) to yield the corresponding N-derivatives of deoxybenzoin, or N-heterocyclic derivatives [9].

In this communication we report an investigation of the kinetics and equilibrium conditions of the cleavage of the γ-pyrone ring of isoflavone (3-phenylchromone).

Experimental

The kinetic and equilibrium measurements were carried out by UV spectrophotometry, using a Unicam SP 800 B and Spectromom 202 type apparatus. The cuvette chamber was thermostated to ± 0.1 °C accuracy. Quartz cuvettes with 1.00 cm long light-path, and Reanal reagents of highest analytical purity were used. The isoflavone sample was recrystallized four times, from ethanol and from petroleum ether.

1. Kinetic measurements

The kinetic measurements were carried out in aqueous sodium hydroxide at various concentrations (0.01—0.09 *M*), or in glycine—NaOH or glycine—HCl buffers. The ion strength of the solutions was adjusted always to 0.1, with potassium chloride. Dilution and the triggering of the reaction were carried out in the cuvette which held the aqueous alkaline solution of a given concentration. The stop-watch was started at the moment of injection. Mixing was achieved by rotating the cuvette for a few times. The spectrophotometer was started 15 seconds after injection.

2. Equilibrium measurements

The solutions described above in connection with the kinetical experiments were used. Ten ml of the acid buffer component was mixed with the calculated amount of the isoflavone stock solution; the mixture was then titrated to the required pH value using a burette with 0.05 ml divisions. A 2 ml sample was taken out of this mixture with a pipette and transferred into a cuvette where the extinction of the solution was recorded until the state of equilibrium was reached.

3. Buffering

The acid component of the buffer used contained 0.1 *M* glycine and 0.1 *M* potassium chloride; its alkaline component contained 0.1 *M* sodium hydroxide. Ring cleavage was effected

in the alkaline component of the buffer solution. After completion of the ring cleavage (15 to 20 min), the corresponding amount of the acid component of the buffer was pipetted rapidly into the reaction mixture.

4. Calculations

The best fit of a straight line to the experimental points was calculated by the method of least-squares. If data with inherent deviations were used in further calculations, the deviation of the final result was found on the basis of the Gauss distribution of errors.

Computer programmes in ALGOL-60 were composed and executed with an ODRA-1204 type electronic computer.

Results and discussion

The ultraviolet spectrum of isoflavone in dilute (10^{-2} *M*) aqueous sodium hydroxide solution at room temperature changes rather quickly, then tends towards a relatively stable spectrum; this, for the sake of brevity, we call the limit spectrum (Fig. 1). This limit spectrum differs significantly from the spectrum (Fig. 2) of 2-hydroxydeoxybenzoin recorded in alkaline medium, which compound would be the hydrolysis product to be expected. Thus, the change in the spectrum is not caused by hydrolytic decomposition.

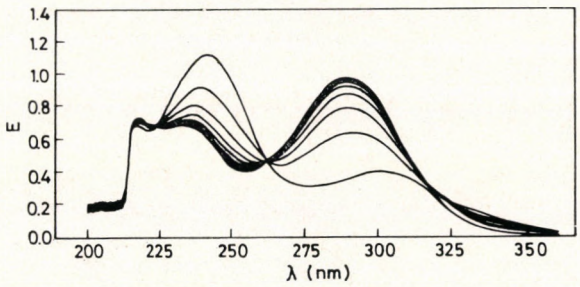

Fig. 1. Change as a function of time of the spectrum of isoflavone in alkaline medium. $c_{OH^-} = 5 \cdot 10^{-2}$ *M*; $c_{iF} = 5 \cdot 10^{-5}$ *M*; $\Delta t = 3'$

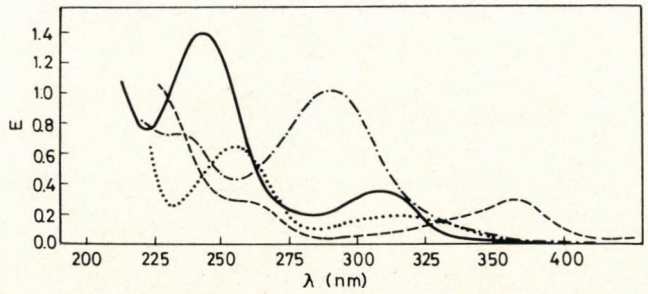

Fig. 2. Spectra of isoflavone, 2-hydroxydeoxybenzoin, and 2-hydroxyisoflavanone. $c = 5 \cdot 10^{-5}$ *M*: - - - - - - - 2-hydroxydeoxybenzoin (0.1 *M* NaOH); — . — . — . — 2-hydroxyisoflavanone (0.1 *M* NaOH); ..... 0.1 *M* HCl; ——— isoflavone (H_2O)

Since in the alkaline aqueous solution mentioned, also the spectrum of 2-hydroxyisoflavanone (**VIII**) tends very rapidly towards the same limit spectrum as obtained from isoflavone, we assigned this spectrum to such an intermediary product which can result, though by different routes (**VIII** → → **VI** → **II** → **XI** and **I** → **VI** → **II** → **XI**), from both compounds. This supposition is illustrated below.

Though the limit spectrum is similar to that of stilbene, we exclude any significant participation of the enolate form **VII**, on the grounds of some experimental facts to be discussed presently.

Catalytic hydrogenation of isoflavone in alkaline medium above pH 11.5 — where its spectrum is identical with the limit spectrum irrespective of the hydroxyide ion concentration — gives 2-hydroxy-α-methyldeoxybenzoin (**IX**) and 1-[2-hydroxyphenyl]-1-hydroxy-2-phenylpropane (**X**). If the concentration of the alkali is increased (0.2—0.5 *M* aqueous ethanolic sodium hydroxide), hydrogenation will become gradually and substantially slower (the production of **X** will cease) and 2-hydroxydeoxybenzoin (**III**) will also appear in the mixture. After the termination of hydrogenation (after the lapse of a constant time of hydrogenation) unchanged isoflavone can be recovered in amounts proportional to the concentration of the alkali.

Since increase of the alkali concentration produces no change in the limit spectrum, the π-electron structure of the compound responsible for the limit spectrum did not suffer such an alteration which would account for the significant change in the reactivity of the molecule. The dependence of reactivity on the pH and the parallel formation of **IX** and **III** (with the spectrum remaining unchanged) cannot be explained by the enolate structure **VII**. The formation of both **IX** and **III** can be rationalized through structure **II**; further, dissociation of the enolic hydroxyl group of **II** to give the di-anion **XI** accounts for the dependence of the reactivity on the pH (**XI** will not be hydrogenated). For this reason, structures **II** and **XI** are assigned to the limit spectrum.

Thus, the change with time of the spectrum of isoflavone in alkaline solution, up to the evolution of the limit spectrum, traces the process of ring fission. At the same time, the hydrogenation experiments offer new preparative evidence for the ring fission of isoflavone in alkaline medium.

Spectrophotometric measurements have shown that when the hydroxido ion concentration is high, equilibria **I** → **VI** → **II** → **XI** → are shifted in the direction of the upper arrows (*cf.* the second row of formulas). According to our results, under similar conditions, transformation **VIII** → **VI** → **II** → **XI** (*cf.* Fig. 3) is much more rapid than **I** → **VI** → **II** → **XI** (compare Figs 1 and 3), thus the rate-determining step of the ring fission is the conversion **I** → **VI**, wherefrom the correlation $k_1 \ll k_2$ follows.

In the course of the dehydration of 2-hydroxyisoflavanone (**VIII**) to isoflavone in the pH range between 8.5 and 9.5, the solution very rapidly gives

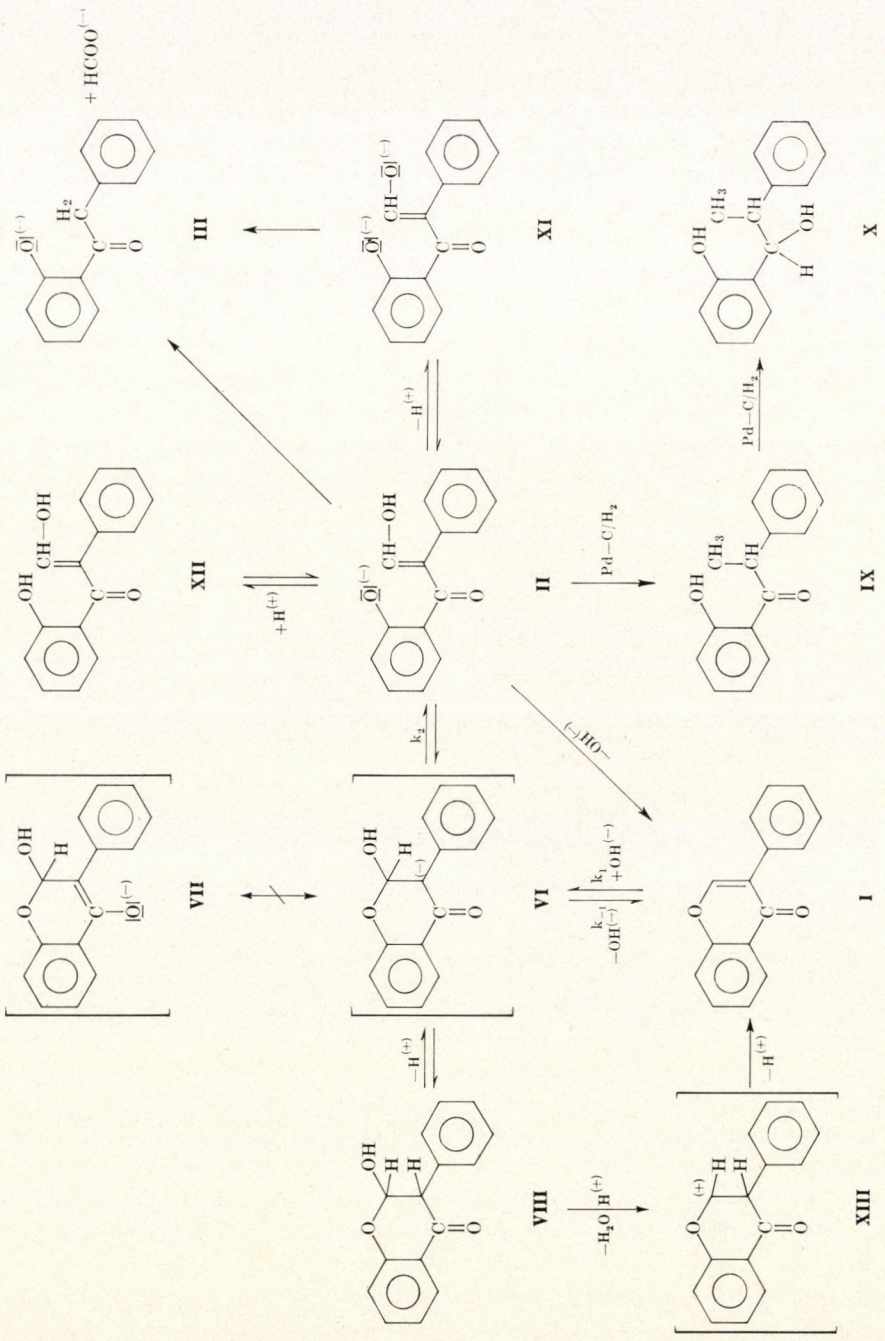

the spectrum corresponding to **II** (no difference between the spectra of **II** and **XI** was detected) and only then, and much more slowly, will the spectrum of isoflavone (**I**) emerge. This experimental finding suggests that ring fission of the carbanion **VI** to **II** is a much more rapid process than elimination of OH^- from **VI** (transformation $\mathbf{VI}^m \rightarrow \mathbf{I}$), even under conditions when only isoflavone is stable, therefore $k_{-1} \ll k_2$. Based on the foregoing, a simplified exposition of this ring fission reaction is:

$$\mathbf{I} + OH^- \underset{k_{-1}}{\overset{k_1}{\rightleftharpoons}} \mathbf{VI}\,(\text{carbanion}) \xrightarrow{k_2} \mathbf{II} \tag{1}$$

In consideration of the structures of **I**, **VIII** and **II**, carbanion **VI** must be postulated as an unstable, reactive intermediary product.

Since $k_2 \ll k_1$, the BODENSTEIN principle [14] is applicable to the formation of the carbanion:

$$\frac{d\,[\mathbf{VI}]}{dt} = k_1\,[\mathbf{I}]\,[OH^-] - k_{-1}\,[\mathbf{VI}] - k_2\,[\mathbf{VI}] = 0 \tag{2}$$

$$[\mathbf{VI}] = \frac{k_1\,[\mathbf{I}]\,[OH^-]}{k_{-1} + k_2} \tag{3}$$

The rate of ring opening will then be:

$$\frac{d[\mathbf{II}]}{dt} = k_2\,[\mathbf{VI}] = \frac{k_2 \cdot k_1}{k_{-1} + k_2}\,[\mathbf{I}]\,[OH^-] \tag{4}$$

Since we have shown above that $k_{-1} \ll k_2$, therefore

$$\frac{d[\mathbf{II}]}{dt} = k_1\,[\mathbf{I}] \cdot [OH^-] \tag{5}$$

$[OH^-]$ being very high, it will remain practically unchanged during the reaction, thus

$$\frac{d[\mathbf{II}]}{dt} = k_b\,[\mathbf{I}] \tag{6}$$

where $k_1[OH^-] = k_b$.

It follows that the differential equation which describes the rate of the ring fission reaction can be traced back to a homogeneous differential equation of first order.

The kinetical study of the ring cleavage reaction was made by following the change in time of the light absorption at 290 nm. The extinction values are shown as a function of time in Figs 3 and 4.

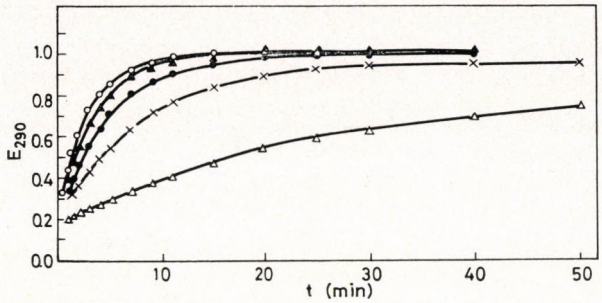

Fig. 3. Change in the light absorption of the reaction mixtures as a function of time and alkali concentration, in the ring cleavage reaction of isoflavone. $t' = 20$ °C; $\lambda = 290$ nm; $c_{iF} = 5 \cdot 10^{-5}\ M = \text{const.}$ — △ — △ — △ — $1 \cdot 10^{-2}\ M$; — × — × — × — × — × $3 \cdot 10^{-2}\ M$; — . — . — . — . — . — $5 \cdot 10^{-2}\ M$; — ▲ — ▲ — ▲ — ▲ — $7 \cdot 10^{-2}\ M$; ○ — ○ — ○ — ○ $9 \cdot 10^{-2}\ M$ NaOH

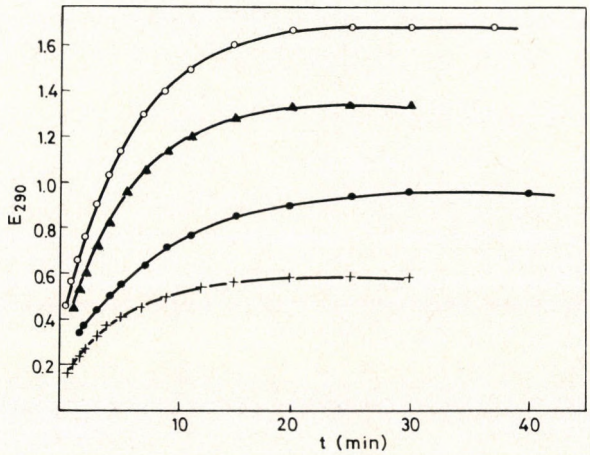

Fig. 4. Change in the light absorption of the reaction mixtures as a function of time and isoflavone concentration, in the ring fission of this compound. $t' = 20$ °C, $\lambda = 290$ nm; [NaOH] $= 5 \cdot 10^{-2}\ M$ const. — × — × — × — $3 \cdot 10^{-5}\ M$; — . — . — . — $5 \cdot 10^{-5}\ M$; — ▲ — ▲ — $7 \cdot 10^{-5}\ M$; — ○ — ○ — ○ — $9 \cdot 10^{-5}\ M$ isoflavone

From the data measured at various temperatures and with various initial concentrations, the apparent rate constant (k_b) was calculated using Eq. (7) [12].

$$\ln(E_{290}^{\infty} - E_{290}) = -k_b\, t + \ln(E_{290}^{\infty} - E_{290}^{0}) \tag{7}$$

where E_{190} is the absorption of light by the reaction mixture at an arbitrary time t.

$$E_{290}^{\infty} = \lim_{t \to \infty} E_{290}; \qquad E_{290}^{0} = \lim_{t \to 0} E_{290}$$

The results of calculations are summarized in Table I.

Table I

Constants (k_b) of the ring fission reaction of isoflavone in aqueous media

$[C_{IF}] \cdot 10^5$	$[NaOH] \cdot 10^2$	t, °C	$k_b \cdot 10^1 . min^{-1}$	$k_1(min^{-1}mol^{-1})$
5	1	20	0.486±0.007	
5	3	20	1.385±0.043	
5	5	20	1.903±0.036	3.80±0.18
5	7	20	2.717±0.011	
5	9	20	3.620±0.012	
3	5	20	2.083±0.017	
7	5	20	2.144±0.072	
9	5	20	1.859±0.035	
5	1	25	0.812±0.014	
5	3	25	1.705±0.008	
5	5	25	3.053±0.090	5.21±0.23
5	7	25	3.802±0.036	
5	9	25	4.974±0.064	
5	1	30	1.298±0.026	
5	3	30	2.622±0.048	
5	5	30	4.499±0.074	8.67±0.33
5	7	30	6.516±0.160	
5	9	30	8.017±0.110	
5	1	35	2.133±0.053	
5	3	35	4.124±0.122	
5	5	35	6.651±0.102	10.99±0.39
5	7	35	8.614±0.268	
5	9	35	12.230±0.276	

With the help of the rate constants thus calculated and using Eq. 8, we reproduced the extinction values corresponding to the various points of time, in order to substantiate the correctness of our suppositions.

$$E_{290} = E_{290}^{\infty}(1 - e^{-k_b t}) + E_{290}^{0} e^{-k_b t} \tag{8}$$

The extinction values measured (E_m) and calculated (E_c) are shown in Table II.

The satisfactory agreement of the measured and calculated values proves that Eq. (7) is a correct description of the kinetics of the reaction. Thus the ring cleavage of isoflavone under the experimental conditions applied can be regarded as a reaction of pseudo-first order.

Table II

Comparison of the calculated and measured light-absorption values
(Reaction conditions: $c_{iF} = 3 \cdot 10^{-5}$, $c_{OH^-} = 5 \cdot 10^{-2}$, and $t' = 20$ °C)

t (min)	$E_{calc.}$	E_{found}	$[\Delta E]$
0.50	$1.54 \cdot 10^{-1}$	$1.56 \cdot 10^{-1}$	$1.81 \cdot 10^{-3}$
1.00	$1.96 \cdot 10^{-1}$	$1.95 \cdot 10^{-1}$	$8.05 \cdot 10^{-4}$
2.00	$2.67 \cdot 10^{-1}$	$2.64 \cdot 10^{-1}$	$3.10 \cdot 10^{-3}$
3.00	$3.25 \cdot 10^{-1}$	$3.18 \cdot 10^{-1}$	$6.99 \cdot 10^{-3}$
5.00	$4.10 \cdot 10^{-1}$	$4.04 \cdot 10^{-1}$	$6.17 \cdot 10^{-3}$
12.00	$5.37 \cdot 10^{-1}$	$5.35 \cdot 10^{-1}$	$1.64 \cdot 10^{-3}$
15.00	$5.54 \cdot 10^{-1}$	$5.55 \cdot 10^{-1}$	$5.35 \cdot 10^{-4}$
20.00	$5.75 \cdot 10^{-1}$	$5.72 \cdot 10^{-1}$	$3.08 \cdot 10^{-3}$

Based upon the data in Table I and upon Fig. 5, it can be stated that the constant k_b is not affected by the initial concentration of isoflavone, and is a linear function of the initial concentration of the hydroxide ions. In view of the kinetic method applied (Ostwald method), this means that the rate-determining step of the ring fission follows first-order kinetics for both isoflavone and hydroxide ion; thus the rate-determining step is kinetically of the second order.

The slopes of the straight lines plotted in Fig. 5 give the rate constants k_1, at various temperatures, of the rate-determining step of the ring fission reaction, on the basis of Eq. (6). (Numerical values are given in the last column of Table I).

From the values of k_1 thus obtained, we calculated the activation energy, $E^* = (12.9 \pm 0.9)$ kcal mol^{-1}, and the activation entropy $\Delta S = (-13.6 \pm 3.1)$ cal mol^{-1} degree^{-1}.

The numerical value of the activation energy and the sign of the activation entropy suggest a bimolecular reaction [13], therefore there is good reason to suppose that the ring fission of isoflavone begins with a bimolecular addition (A_N2) reaction as the rate-determining step (**I** → **VI**), and is stabilized in the form **II** or **XI** (by the rapid transformation **VI** → **II**).

Fig. 3 shows that the ring fission of isoflavone leads to an equilibrium. When the molar absorption, measured after the equilibrium state, has been reached in the reaction mixture, and is plotted as a function of pOH, the equilibrium curve (Fig. 6) of the system isoflavone —NaOH (water) is obtained.

The equilibrium constant of this system, calculated [15] from Eq. (9), is $K = 837 \pm 12$.

$$\frac{\bar{\varepsilon} - \varepsilon_0}{\varepsilon_\infty - \bar{\varepsilon}} = K\,[OH^-] \qquad (9)$$

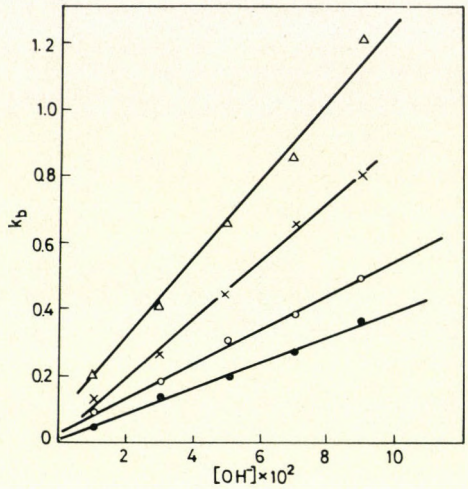

Fig. 5. The apparent reaction rate constants of ring fission as functions of the hydroxide ion and temperature. — . — . — . — 20 °C; — ○ — ○ — ○ — 25 °C; — × — × — × — 30 °C; — △ — △ — 35 °C

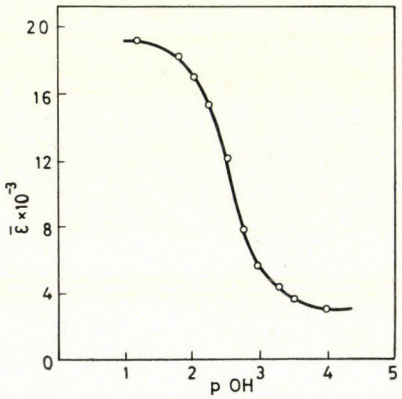

Fig. 6. The mean molar absorption of light as a function of *p*OH at 20 °C, of equilibrium reaction mixtures, the ring opening reaction of isoflavone

where

$$\bar{\varepsilon} = \frac{E_{290}}{d\, c_0}; \qquad \varepsilon_\infty = \lim_{[OH^-]\to\infty} \bar{\varepsilon}; \quad \varepsilon_0 = \lim_{[OH^-]\to 0} \bar{\varepsilon}$$

d = thickness of the layer; c_0 = total concentration.

The equilibrium curve indicates that in a 0.1 *M* aqueous solution of sodium hydroxide practically all isoflavone is present in the open form; Fig. 3 shows that the equilibrium state is reached quite rapidly.

When the alkaline solution, wherein, according to the foregoing discussion, 2-hydroxy-α-hydroxymethylene-deoxybenzoin (**II**) and its enolate (**XI**) are

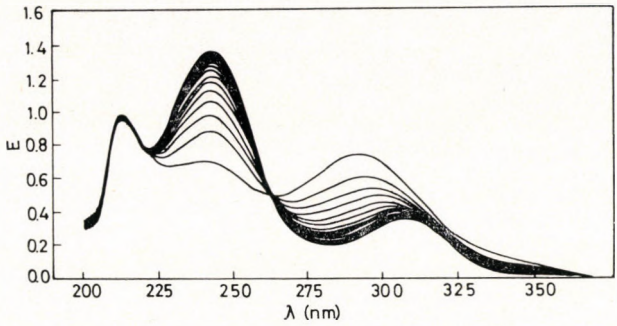

Fig. 7. Experiments with buffering. pH = 9.67; $c = 5 \cdot 10^{-5}$ M; $\Delta t = 2' 15''$

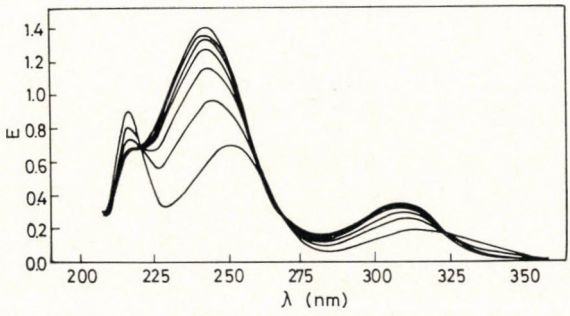

Fig. 8. Experiments with buffering. pH = 6.59; $c = 5 \cdot 10^{-5}$ M; $\Delta t = 60'$

present, is acidified, or when its alkalinity is buffered, isoflavone is again obtained, but along two pathways depending on the degree of acidification or buffering.

If the pH of the buffered solution is higher than 8.5, then (as shown the change of the spectrum) isoflavone (**I**) is formed directly, by **II** → **I** conversion (Fig. 7).

If the pH of the buffered solution is lower than 7.5, 2-hydroxyisoflavanone (**VIII**) is formed [3] at a rate higher than measurable under our experimental conditions, and **VIII** is converted, very slowly, into isoflavone (Fig. 8).

The results of the experiments with buffering suggest that the ring fission of isoflavone should not be regarded as a simple equilibrium process, and this is in support of our idea concerning the mechanism of this reaction. The results of kinetical measurements are also confirmed by preparative experiments [10].

Under our experimental conditions **II** is very slowly degreaded to 2-hydroxydeoxybenzoin (**III**).

Accordingly, in the degradation of isoflavone in alkaline media under the experimental conditions used, two kinetically separable reactions can be distinguished: the first is a ring fission which begins with a reversible bimolec-

ular addition of the type A_N2, and the other is a hydrolysis that proceeds at a rate lower by several orders of magnitude.

The important role ascribed to the carbanion **VI** in the ring fission process will be discussed in a following communication.

REFERENCES

[1] GEISSMANN, T. A.: The Chemistry of Flavonoid Compounds, Pergamon Press, London, 1962, p. 94; SZABÓ, V.: Candidate's Thesis, Debrecen, 1958
[2] WALZ, E.: Ann. **489,** 118 (1931)
[3] FARKAS, L., VÁRADY, L., GOTTSEGEN, Á.: Magyar Kém. Foly. **69,** 460 (1963)
[4] GOTTLIEB, O. R., MAGALHAES, M. T.: J. Org. Chem. **26,** 2449 (1961); BAKER, W.: J. Chem. Soc. **1928,** 1022; CRABBE, P., LEEMING, P. R., DJERASSI, C.: J. Am. Chem. Soc. **80,** 5259 (1958); ROBERTSON, A., SUCKLING, C. W., WHALLEY, W. B.: J. Chem. Soc. **1949,** 1571; KING, F. E., KING, T. J., WARWICK, A. J.: J. Chem. Soc. **1952,** 97; MCMURRY, T. B. H., THENG, C. Y.: J. Chem. Soc. **1960,** 1491; SPÄTH, E., SCHMIDT, O.: Monatsh. **53—54,** 454 (1929); STAMM, O. A., SCHMIDT, H., BÜCHI, J.: Helv. Chim. Acta **41,** 2006 (1958)
[5] BRADBURY, R. B., WHITE, D. E.: J. Chem. Soc. **1951,** 3447
[6] WARBURTON, W. K.: Quart. Revs. **8,** 67 (1954)
[7] INOUE, N.: Sci. Repts. Tohoku Univ., First Ser. **45** (No. 2), 73 (1961)
[8] SZABÓ, V., ANTAL, E.: Tetrahedron Letters **1973,** 1659
[9] SZABÓ, V., BORDA, J.: In press
[10] SZABÓ, V., BORBÉLY, SZ.: In press
[11] ZSUGA, M.: Doctoral Thesis, Debrecen, 1972
[12] WILSON, J. M.: Experiments in Physical Chemistry, Pergamon Press, London, 1962, p. 193; SCHWETLICK, K.: Kinetische Methoden zur Untersuchung von Reaktionsmechanismen, VEB Deutscher Verlag der Wissenschaften, Berlin 1971, p. 57.
[13] LEFFLER, J. E.: J. Org. Chem. **1955,** 1202
[14] BODENSTEIN, N.: Z. Phys. Chem. **85,** 329 (1913)
[15] BECK, M. T.: Chemistry of Complex Equilibria, Akadémiai Kiadó, Budapest 1970, p. 91.

Vince SZABÓ
Miklós ZSUGA } 4010 — Debrecen P. O. B. 10. Hungary.

Acta Chimica Academiae Scientiarum Hungaricae, 85 (2), pp. 191—199 (1975)

CLEAVAGE OF THE HETEROCYCLIC RING OF ISOFLAVONOIDS BY NUCLEOPHILIC REAGENTS, II*

TRANSFORMATIONS OF 2-HYDROXYISOFLAVANONE

V. SZABÓ and M. ZSUGA**

(Institute of Applied Chemistry, Kossuth Lajos University, Debrecen)

Received December 20, 1973

The kinetics of the conversions of 2-hydroxyisoflavanone (**VIII**) have been studied in acid and alkaline solutions. The γ-pyranone ring of **VIII** undergoes cleavage in dilute aqueous alkaline solutions and a phenolate ion (**III**) is produced, like from isoflavone, but at a much higher rate.

The results suggest that the formation of isoflavone from **VIII** is introduced by an instantaneous pre-equilibrium that depends on the pH. Study of this pre-equilibrium has shown that isoflavone can be formed directly as well as indirectly, depending on H_0 and on the pH, either by acid-catalyzed E_1 mechanism, or alkali-catalyzed E_1cB mechanism.

2-Hydroxyisoflavanone is very sensitive to acid, alkali, and heat; it is more stable in acid than in alkali. Its C_3 proton and its C_2 hydroxyl group are easily detached, thus it is a metastable compound which can be regarded as a C-proton acid.

The dehydration of 2-hydroxyisoflavanone (**VIII**) and its derivatives has been studied by several authors [2—10], but no relevant kinetic work seems to have been done. In consequence of this, contradictory conclusions based on preparative evidence have been put forward about the dehydration and about the mechanism of the formation of isoflavone (**I**) through Claisen condensation.

E_2 [3b] as well as E_1cB mechanism [3a] has been suggested for this dehydration reaction, depending on the actual experimental conditons.

On this basis of a supposedly reversible 2-hydroxyisoflavanone—isoflavone conversion [10], some preparative experiences [8, 9] cannot be explained: namely, that buffering (pH $\sim$ 9—10) of the alkaline solution of α-hydroxymethylene-2-hydroxydeoxybenzoin (**XII**) formed by the Claison condensation gives isoflavone, while its acidification (pH 1—4) produces 2-hydroxyisoflavanone; further, that 2-hydroxyisoflavanone is more stable in acid than in neutral medium.

In a former communication [1] we have shown that the equilibrium between isoflavone (**I**), 2-hydroxyisoflavanone (**VIII**) and the α-formyl-2-hydroxydeoxybenzoin phenolate anion (**II**) (this is identical with α-hydroxymethylene-2-hydroxydeoxybenzoin phenolate, called 'phenolate' in the following) is

* For Part I, see Ref. [1].

** This paper is based on the Doctoral Thesis of M. ZSUGA.

in direct connection with the ring fission; therefore, the equilibrium of ring opening and ring closure can also be studied through the kinetics and equilibria of the transformations into 2-hydroxyisoflavanone (**VIII**).

In this paper we wish to support our suggestions about the conversion of 2-hydroxyisoflavanone (**VIII**) into isoflavone (**I**) and, through this, the mechanism of ring opening and ring closure of isoflavone (**I**).

Experimental

The spectra and kinetic data were obtained with a Unicam SP 800-B spectrophotometer, using 1 cm quartz cuvettes. The cuvette chamber was kept at the chosen temperature by means of an ultrathermostat, the accuracy being ± 0.1 °C.

2-Hydroxyisoflavanone was prepared as described in the literature [4]; the compound had m. p. 110—111 °C. For the preparation of the buffer solutions substances of the highest grade of purity (from 'Reanal' Fine Chemicals Co., Budapest) were used. The measurements were made in Sörensen buffers and repeated in Britton—Robinson, as well as in McIlvaine buffers, but no significant deviation ensued. The ion strength was adjusted to the constant value of 0.1 with potassium chloride. The buffer solutions of required pH were prepared in thermostated vessels by potentiometric titration under a constant stream of nitrogen.

The kinetic experiments and calculations were carried out as described in the previous communication [1].

Results and discussion

In aqueous solution above pH 12.4, similarly to isoflavone, but much more rapidly, gives 2-hydroxyisoflavanone (**VIII**) the spectrum shown in Fig. 1; this spectrum remains unchanged for a long time. As discussed in our preceding paper [1], the spectrum can be assigned to the phenolate anion (**II**) or to the α-formyl-2-hydroxydeoxybenzoin phenolate enolate di-anion (**XI**) ('enolate' in what follows). In buffers of lower pH, the spectrum of 2-hydroxyisoflavanone (**VIII**) undergoes changes (Figs 2, 3, 4) which suggest conversion into isoflavone (**I**), the rate and routes being dependent on the pH.

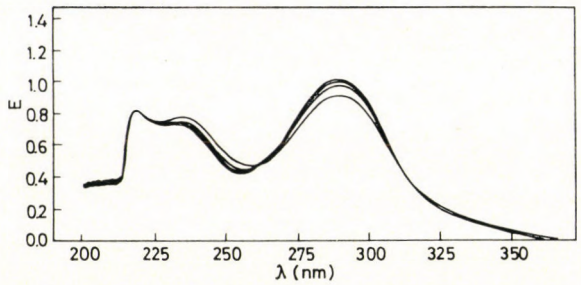

Fig. 1. Change as a function of time of the spectrum of 2-hydroxyisoflavanone at 20 °C. pH 12.47; $c_{IFON} = 5 \cdot 10^{-5}\,M$; $\Delta t = 2'\,15''$

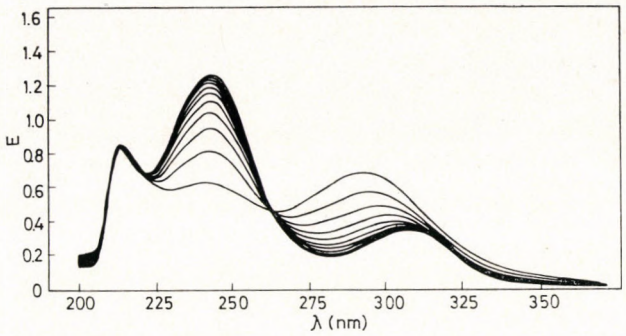

Fig. 2. Change as a function of time of the spectrum of 2-hydroxyisoflavanone at 20 °C. pH 9.44; $c_{IFON} = 5 \cdot 10^{-5}\ M$; $\Delta t = 3'$

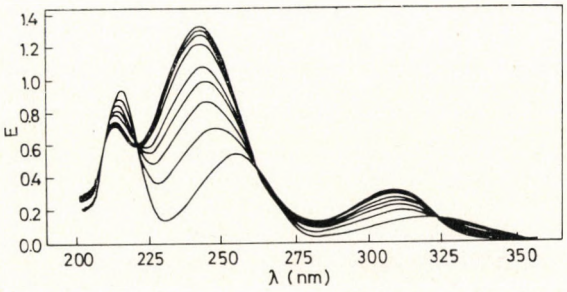

Fig. 3. Change as a function of time of the spectrum of 2-hydroxyisoflavanone at 20 °C. pH 6.95; $c_{IFON} = 5 \cdot 10^{-5}\ M$; $\Delta t = 30'$

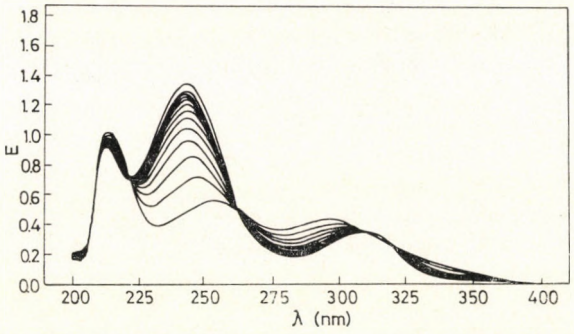

Fig. 4. Change as a function of time of the spectrum of 2-hydroxyisoflavanone at 20 °C. pH 8.12; $c_{IFON} = 5 \cdot 10^{-5}\ M$; $\Delta t = 5'$

From the spectra recorded at given points of time within the spectrum families shown in Figs 2, 3 and 4, we calculated [14] the concentrations of the light-absorbing components responsible for the spectrum. (In these calculations we could not distinguish component **VIII** from component **VI**, and component **II** from component **XI**, because no characteristic deviations were seen.) The results of calculations are shown in Table I.

Table I

Analysis of the families of spectra shown in Figs 2, 3 and 4, at given moments of time

pH	t (min)	$[I] \cdot 10^5 M$	$[VIII] \cdot 10^5 M$	$[II] \cdot 10^5 M$
6.95	30.78	1.14	4.0	0.0
8.12	5.77	1.6	2.4	0.52
9.44	3.77	1.28	1.12	2.17

Table I and the nature of the changes in the spectra show that the spectrum family in Fig. 3 reveals the reaction route 2-hydroxyisoflavanone (**VIII**) → isoflavone (**I**), while the spectra in Figs 2 and 4 suggest the conversions 2-hydroxyisoflavanone (**VIII**) → phenolate (**II**) → isoflavone; deviations in Figs 2 and 4 are due only to variations in the quantitative proportions of the components present.

When the alkaline solution of the enolate (**XI**)—obtainable also by the ring fission of isoflavone — [1] is buffered to pH 9.44 and to 6.95, the conversions occur exactly according to the changes shown by the spectra in Figs 2 and 3, respectively [1]; of course, also the kinetic constants calculated from these changes are in complete agreement [11]. Consequently, for the dehydration of 2-hydroxyisoflavanone (**VIII**) only such a mechanism can be suggested which is in agreement with the findings about the ring fission reaction, since at the same pH values the same components are present in the reaction mixtures in both cases.

Based on these results, we supposed that the formation of isoflavone (**I**) is introduced in both cases by an equilibrium that is very rapidly established (a preliminary equilibrium between components **VIII** → **VI** → **II** → **XI**), which equilibrium is very sensitive to pH and determines the routes of the conversion into isoflavone (Table I).

For a study of this pre-equilibrium 2-hydroxyisoflavanone (**VIII**) was used, for practical reasons (starting of the reaction).

In order to elucidate the mechanism of this conversion, we measured its rate as a function of the pH and of H_0 [13]. The apparent rate constants, k_a, of the dehydration reaction were calculated from the change in time of the light absorption of the reaction mixtures (if pH < 7.5, at $\lambda = 245$ nm; if pH > 7.5 at $\lambda = 290$ nm). In these calculations Eq. (1) was used [17].

$$\ln (E_\lambda^\infty - E_\lambda) = -k_a t + \ln(E_\lambda^\infty - E_\lambda^0) \tag{1}$$

where E_λ is the absorption at wavelength λ,

$E_\lambda^\infty = \lim_{t \to \infty} E_\lambda$; $E_\lambda^0 = \lim_{t \to 0} E_\lambda$; k_a = apparent rate constant. From the values of the constant k_a were the E_λ functions re-calculated (Table II).

Table II

Comparsion of the measured (E_{found}) *and re-calculated* (E_{calcd}) *light absorptions in the dehydration reaction of 2-hydroxyisoflavanone* (VIII)
($c = 5 \cdot 10^{-5} M$; pH = 7.5; $\lambda = 245$ nm)

t (min)	E_{found}	E^*_{calcd}	$\lvert E_{found} - E_{calcd} \rvert$
1.83	0.23	0.236	0.0059
4.83	0.285	0.291	0.0063
7.83	0.335	0.340	0.0051
10.83	0.38	0.383	0.0031
13.83	0.42	0.421	0.0009
16.83	0.46	0.454	0.0058
19.83	0.49	0.484	0.0064
22.83	0.515	0.509	0.0056
25.83	0.535	0.532	0.0028
28.83	0.55	0.552	0.0021
31.83	0.57	0.569	0.0001
34.83	0.585	0.585	0.0003
37.83	0.60	0.599	0.0009
40.83	0.61	0.611	0.0011
43.83	0.62	0.622	0.0017
46.83	0.63	0.631	0.0011
49.83	0.64	0.639	0.0007

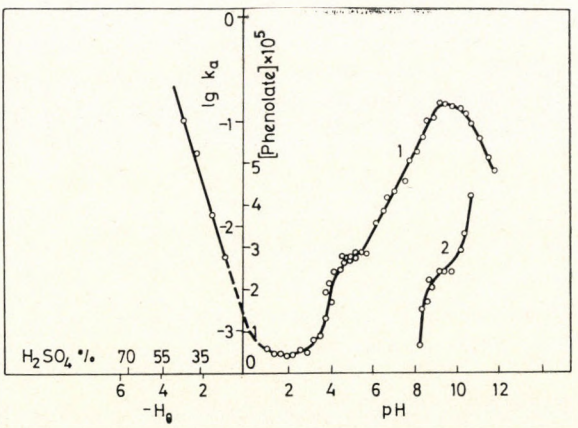

Fig. 5. Logarithm (lg k_a) of the apparent rate constant (1) of the dehydration of 2-hydroxyisoflavanone and change of the concentration (2) of the phenolate (II) as a function of the pH at 20 °C

There is a good agreement between the calculated (E_{calcd}) and measured (E_{found}) extinction figures, thus Eq. (1) is a correct description of the kinetics of this reaction; therefore, under the conditions studied, the dehydration reaction follows pseudo-first-order kinetics. The results of the kinetical tests are shown in Fig. 5.

In the lg k_a *vs.* pH and the lg k_a *vs.* H_0 curves four different sections can be distinguished, which suggest the possibility of various mechanisms of this dehydration.

In sulfuric acid solutions of concentrations higher than normal, the function lg k_a *vs.* H_0 is linear, thus in such solutions the dehydration is catalyzed by the acid and proceeds most probably according to E_1 mechanism, and not as suggested by WHALLEY [3b].

The course of function lg k_a *vs.* pH in the domain between 0 and 9.5 suggests a dehydration catalyzed by a base. In this pH range the function lg k_a *vs.* pH is non-linear, but reveals two steps ($3 \leq$ pH ≤ 5.4 and $6 \leq$ pH $\leq$ ≤ 9.4). The spectrum families (Figs 2 and 3) representing the formation of isoflavone are different in the pH ranges corresponding to the two steps, and the initial spectra of the spectrum families are formed instantaneously. These facts led us to suppose that in the equilibrium state preceding the formation of isoflavone (**I**), two different intermediates may be present, depending on the pH, both of them being capable to give isoflavone (**I**) directly.

The step in the acid pH range 3—5.4 suggests proton dissociation. In this pH range the spectra show unequivocally the conversion: 2-hydroxyisoflavanone → isoflavone (**VIII** → **I**) (Fig. 3; Table I, first line), thus, under these conditions dehydration does not imply ring fission; thus the proton dissociation cannot consist but of the elimination of the highly labile proton at position C_3 [2, 12]. Since the results of measurements were the same, within the limits of error, in various buffers, it is improbable that the increase of the constant k_a is due to the catalytic effect of the anions in the buffers. As the dissociation of the proton proceeds much more rapidly than the elimination of the hydroxyl group (this follows from the preliminary equilibrium) the dehydration occurs in this pH range by E_1cB mechanism. Functions (lg k_a *vs.* pH) of similar pattern have also been described [16] to characterize hydrolyses of various esters following E_1cB mechanism, therefore we consider Function 1 in Fig. 5 as a further piece of evidence for the E_1cB mechanism.

At pH values higher than 6 there is a further increase of lg k_a with the pH, and the caracter of the spectrum change is altered (Figs 2 and 4; 2nd and 3rd lines in Table I). The change in the spectrum suggests that the carbanion (**VI**) is stabilized by ring fission and the phenolate (**II**) is produced [1]; this will then yield isoflavone (**I**) by cyclization due to intramolecular effects.

The significant increase of the apparent reaction rate shows that in the formation of isoflavone (**I**) the phenolate **II** is more reactive than carbanion **VI**.

We suppose that in the cyclization reaction the intramolecular attack by the phenolate group reduces the strength of the C_2–OH bond; thereby the elimination of the hydroxyl group is facilitated, thus the rate of ring formation from **II** is higher than that of the production of isoflavone by the E_1cB mechanism.

By analysis of the components [14] in solutions of different alkalinity, we determined at a given time (5 min) the concentration of the phenolate (**II**), as a function of the pH; a stepwise change was found as shown in Fig. 5 (Curve 2), resulting from the protonation equilibrium **II** → **VI** → **VIII** and the dissociation equilibrium **II** → **XI**.

Comparison of the curves in Fig. 5 shows that it is only up to pH 9.3 that the reaction rate increases in proportion with the concentration of the phenolate (**II**). At this pH the apparent reaction rate has a maximum and begins to decrease. This means that at pH values higher than this the dissociation of phenolate to enolate (**II** → **XI**) becomes more significant. From the point of view of ring closure, the formation of the enolate (**XI**) is an inhibitory factor [15].

Further decomposition of the phenolate (**II** → **III**) need not be considered as a kinetic interference, since the rate of this process is lower by several orders of magnitude than the rate of the reaction studied.

The preceding considerations about the reaction mechanism are summarized in Scheme I.

As reported in the preceding communication [1], the ring fission of isoflavone (**I**) begins with an A_N2 addition reaction of hydroxide ion to yield the carbanion **VI** which, depending on the hydroxide ion concentration, will be stabilized, *via* the phenolate (**II**), in the form of the enolate (**XI**). By gradual and small changes of the pH this enolate (**XI**) can be converted into isoflavone by the route **XI** → **II** → **I**, and the equilibrium conditions are the same as during ring opening. If the pH is greatly and suddenly lowered ($pH \leq 7$), the product is not isoflavone (**I**) but 2-hydroxyisoflavanone (**VIII**), which can be detected in, or isolated from, the mixture, though in this pH range only isoflavone (**I**) is stable [1].

The formation of 2-hydroxyisoflavanone (**VIII**) is easily explicable if we consider that, owing to the preliminary equilibrium, the route **XI** → **II** → **VI** → → **VIII** can yield **VIII** instantaneously according to the pH of the solution ($pH < 7$); therefore, in acid solution, the formation of 2-hydroxyisoflavanone (**VIII**) from the enolate (**XI**) has higher kinetic possibility than the formation of isoflavone (**I**).

The views held concerning 2-hydroxyisoflavanone (**VIII**) must be fundamentally revised. It is a metastable compound very sensitive to heat, acid, and alkalies; its C_2—OH group and its C_3 proton are easily detached. Since the dissociation of the C_3 proton occurs under less vigorous chemical conditions

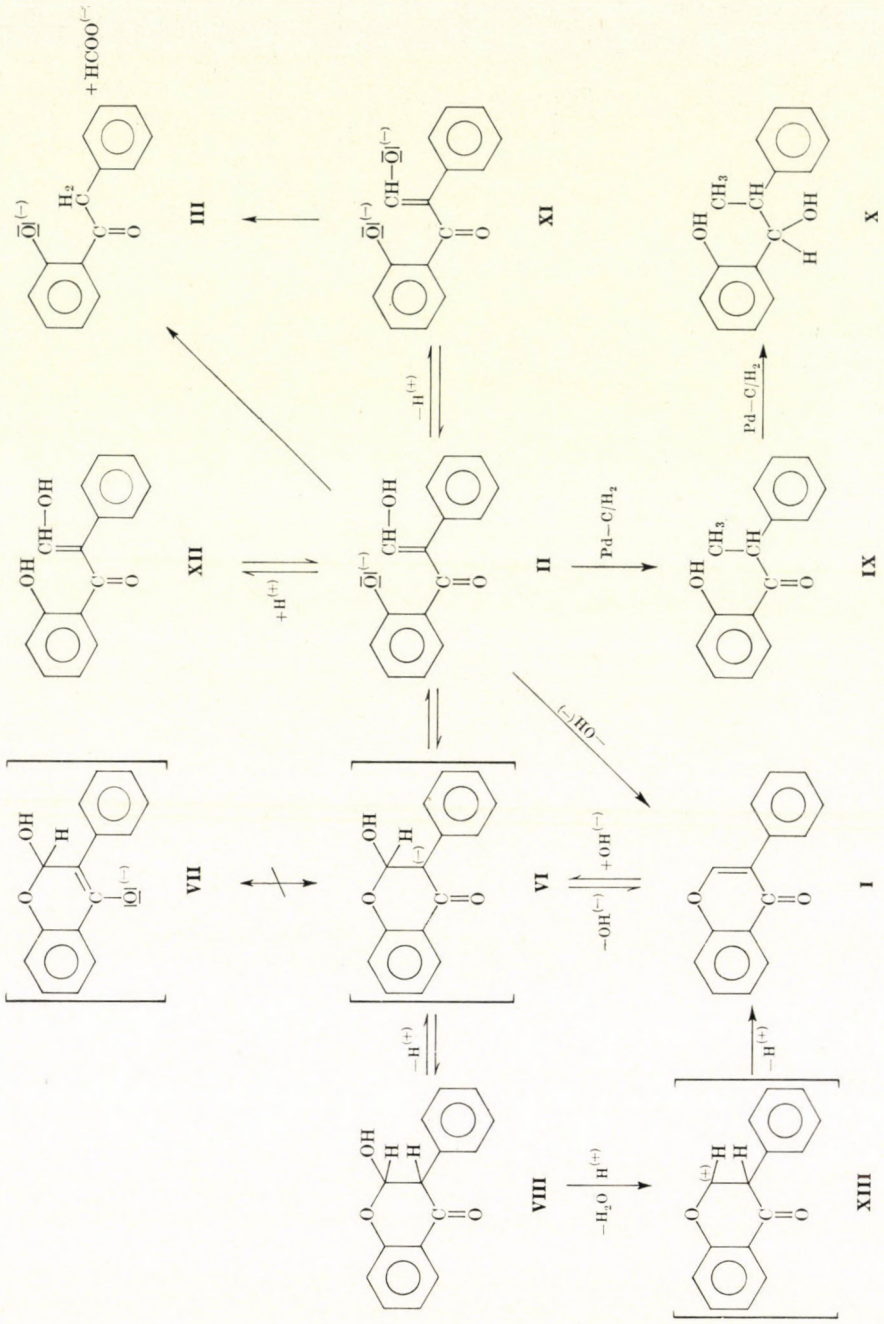

than needed for the elimination of the PH group, the compound should be regarded as predominantly a C-proton acid. Its ring is opened in very dilute alkaline solutions (pH $\sim$ 8). Under the conditions mentioned it will be converted into isoflavone, but the same conditions will not produce 2-hydroxyisoflavanone from isoflavone; thus the **VIII** $\rightarrow$ **I** conversion cannot be considered reversible [10]. In consequence, 2-hydroxyisoflavanone (**VIII**) must be regarded as a kinetically possible by-product of the formation of isoflavone.

REFERENCES

[1] Szabó, V., Zsuga, M.: Acta Chim. (Budapest) (In press)
[2] Baker, W., Chadderton, J., Harborne, J. B., Ollis, W. D.: J. Chem. Soc. **1953,** 1852 and 1855
[3] Geissman, T. A. (Ed.): The Chemistry of Flavanoid Compounds. Pergamon Press, Oxford 1962
[3]a Ollis, W. D.: The Isoflavanoids, p. 353 in Ref. [3]
[3]b Whalley, W. B.: The Stereochemistry of Flavanoid Compounds, p. 462 in Ref. [3]
[4] Kukla, A., S., Seshadri, T. R.: Tetrahedron **18,** 1443 (1962). Mehta, A. C., Seshadri, T. R.: Proc. Ind. Acad. Sci. **38A,** 381 (1953); C. A. **49,** 2431b. Narasimhachari, N., Rajogopalan, D., Seshadri, T. R.: J. Sci. Ind. Research **12,** 287 (1953); C. A. **49,** 13981. Robertson, A., Whalley, W. B.: J. Chem. Soc. **1954,** 1440 Suginome, H., Iwadare, T.: Bull. Chem. Soc. Japan **39,** 1535 (1966) Whalley, W. B.: J. Chem. Soc. **1955** 105
[5] Yamaguchi, S., Ito, S., Nakamura, A., Inoue, N.: Bull. Chem. Soc. Japan **39,** 622 (1966)
[6] Narasimachari, N., Rajogapalan, D., Seshadri, T. R.: J. Sci. Ind. Research **11B,** 347 (1952); C. A. **47,** 10527 g
[7] Whalley, W. B.: J. Chem. Soc. **1953** 3366
[8] Szabó, V.: Thesis, Debrecen, 1958
[9] Szabó, V., Borbély, Sz.: Unpublished results
[10] Farkas, L., Várady, J., Gottsegen, Á.: Tetrahedron Letters **1966,** 351
[11] Zsuga, M.: Thesis, Debrecen, 1972
[12] Rama Rao A. V., Telang, S. A., Madhavan Nair P.: Indian J. Chem. **2,** 431 (1964)
[13] Paul, M. A., Long, F. A.: Chem. Rev. **1957,** 1
[14] Katakis, D.: Anal. Chem. **37** (7), 876 (1965)
[15] Bazsa, Gy., Beck, M.: Kémiai Közlemények **36,** 167 (1971)
[16] Pratt, R. F., Bruice, T. C.: J. Am. Chem. Soc. **92** (20), 5956 (1970)
[17] Schwetlick, K.: Kinetische Methoden zur Untersuchung von Reaktionsmechanismen, VEB Deutscher Verlag der Wissenschaften, Berlin 1971, p. 57

Vince Szabó
Miklós Zsuga } 4010 Debrecen 10, Hungary.

Acta Chimica Academiae Scientiarum Hungaricae, 85 (2), pp. 201—213 (1975)

LABELLED AMINO ACIDS AND THEIR DERIVATIVES, VI*

PREPARATION OF L-ORNITHINE-[5-^{3}H] AND L-LYSINE-[6-^{3}H]

I. MEZŐ**, M. HAVRÁNEK***, I. TEPLÁN**, J. BENEŠ***, B. TANÁCS****

*(** 1st Institute of Biochemistry of the Semmelweis University Medical School, Budapest, ***Isotope Laboratory of the Institutes for Biological Research of the Czechoslovak Academy of Sciences, Prague, and ****Institute of Isotopes of the Hungarian Academy of Sciences, Budapest)*

Received February 14, 1974

γ-Cyano-L-α-aminobutyric acid and δ-cyano-L-norvaline were prepared from the appropriate α-tosyl derivatives by means of electrolytic detosylation. Catalytic hydrogenation of γ-cyano-L-α-aminobutyric acid and δ-cyano-L-norvaline yielded L-ornithine and L-lysine, respectively. The reduction was also effected, with sodium borohydride in the presence of Raney nickel. L-ornithine-[5-^{3}H] and L-lysine-[6-^{3}H] were prepared in both ways. Reduction with sodium borotritide was found to be particularly advantageous since it made possible the preparation of compounds with high specific activity.

Several literature data are available for the preparation of the biologically important α,ω-diamino acids labelled with tritium.

BIRKOFER and HEMPEL [1] reported the synthesis of DL-lysine-[4,5-^{3}H] through catalytic tritiation of acetylamino-(4-amino-2-butenyl)malonic acid diethyl ester hydrochloride (**I**) followed by a hydrolysis step. Recently, Soviet authors [2] published further data in connection with the synthesis of **I**. FRIDKIN *et al.* [3] converted DL-lysine-[4,5-^{3}H], prepared by the catalytic tritiation of **I**, into N^{ε}-trifluoroacetyl-L-lysine-[4,5-^{3}H] in a synthesis path involving several steps and subsequent enzymic hydrolysis. This procedure may also be suitable for the preparation of L-lysine-[4,5-^{3}H] with high specific activity. The method suggested for the preparation of DL-ornithine-[2,3-^{3}H] was elaborated by BIRKOFER *et al.* [4], applying catalytic tritiation of 2-acetylamino-5-(2-chloroacetylamino)-2-pentenic acid followed by the hydrolysis of the product. These methods are suitable primarily for the preparation of DL-lysine and DL-ornithine with high specific activity. PLENTL *et al.* [5], as well as BRUNDISH *et al.* [6] started from the appropriate DL-amino acid and, under racemization conditions — in acetic anhydride containing also CH_3COOT formed from the HTO added — the acyl derivatives of amino acids labelled with tritium in the α-position were obtained; these were then subjected to enzymic hydrolysis to yield L-lysine-[2-^{3}H] and L-ornithine-[2-^{3}H]. However, only amino acids with low specific activity can be prepared by this method.

JANSEN *et al.* [7] synthesized L- and D-2,6-diamino-4-hexynic acid; these

* Part V: Acta Chim. (Budapest) **84**, 109 (1975)

compounds can be applied in the preparation of L- and D-lysine-[4,5-^{3}H], but experimental details regarding neither the catalytic hydrogenation nor the catalytic tritiation procedure were published.

In our earlier papers [8—10] the utilization of ω-cyano-L-α-amino acids and their derivatives in the preparation of α,ω-L-diamino acids labelled with tritium in the ω-position was discussed.

In the present paper we describe details of our previous work [10] and a reduction procedure which has not been applied heretofore in the preparation of α,ω-L-diamino acids; this method is suitable for the synthesis of α,ω-L-diamino acids labelled with tritium and having high specific activity. The advantage of the present technique is that L-ornithine-[5-^{3}H] and L-lysine-[6-^{3}H] can be obtained in a one-step reaction from the optically active amino acid derivatives. The method can naturally be extended to the synthesis of amino acids labelled with deuterium, too.

In the synthesis of L-ornithine-[5-^{3}H] and L-lysine-[6-^{3}H], the starting materials are tosyl-L-glutamine (**II**), which can easily be obtained [11], and tosyl-L-homoglutamine (**IV**), respectively. Compound **IV** was prepared from tosyl-L-α-aminoadipic acid [13] according to the method suggested by GUT and RUDINGER [12]. We amied at the elaboration of a reaction series yielding ω-cyano derivatives suitable for tritium incorporation, starting from the available ω-carboxamide derivatives and applying a reduction process. The methods generally used [9, 14—17] are unsuitable for the dehydration of **II** and **IV**, owing to the simultaneous presence of the tosylamino and the adjacent free carboxyl groups. This difficulty has been overcome by the utilization of the method proposed by ZAORAL and RUDINGER [18] (Method A, Fig. 1) developed originally for the synthesis of γ-cyano-tosyl-L-α-aminobutyric acid (**III**).

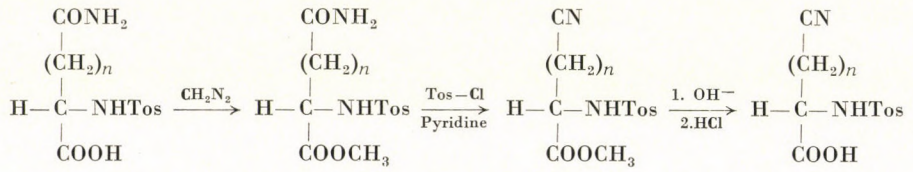

II $n = 2$
IV $n = 3$

V $n = 3$

VI $n = 3$

III $n = 2$
VII $n = 3$

Fig. 1

An alternative possibility was the use of N,N-dimethylchloroformimidium chloride (**VIII**) reagent as a dehydrating agent in the preparation of ω-cyano-tosyl-L-α-amino acids (Method B, Fig. 2).

In the earlier experiments, reagent **VIII** was prepared from dimethylformamide and phosgene in chloroform solution by the method of ARNOLD and SORM [19—21]. The reagent is stable only for a few weeks, even in cold

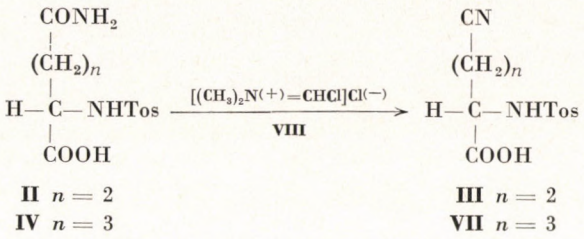

II $n = 2$ **III** $n = 2$
IV $n = 3$ **VII** $n = 3$

Fig. 2

storage. In the recent experiments, reagent **VIII** was prepared immediately before the dehydration, by the reaction of dimethylformamide with thionyl chloride [22—25].

Compound **VII** was obtained according to the method proposed by ZAORAL and RUDINGER [18] (Method A). Methods A and B yielded **III** and δ-cyano-tosyl-L-norvaline (**VII**) with perfectly identical physical and chemical properties. The application of the modified Method B is particularly advantageous, since the dehydration step can be accomplished rapidly, in a well-reproducible way and in high yield.

The methods widely applied to the elimination of the tosyl group [26] could not be utilized here, since in each of them the nitrile group would be attacked, thus α,ω-diamino acids could not be obtained by catalytic hydrogenation or titration of the compounds formed. Therefore, the tosyl group was eliminated in an electrolytic reduction process, according to HORNER and NEUMANN [27, 28], since KASAFÍREK [29, 39] pointed out in the case of β-cyano-tosyl-L-α-alanine that the procedure is suitable for selective removal of the tosyl group, with no adverse effect on the nitrilo group. The reduction was carried out in methanol in the presence of tetramethylammonium chloride which, as established by the authors mentioned [28], acts not only as a mediator in electron transfer, but the amalgam (TMA) formed from the tetramethylammonium ion also ensures the high negative deposition potential required for the reduction*.

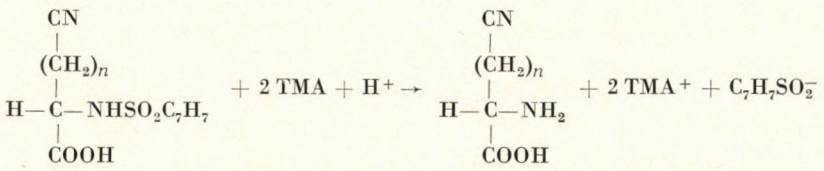

III $n = 2$ **IX** $n = 2$
VII $n = 3$ **X** $n = 3$

Fig. 3

* After having completed our experimental work, we were informed about the electrolytic detosylation procedure elaborated by IVASAKI, MATSUMOTO *et al.* [38].

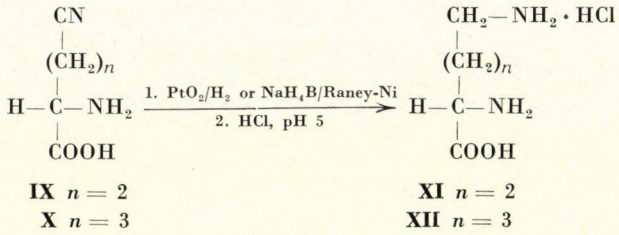

IX $n = 2$
X $n = 3$

XI $n = 2$
XII $n = 3$

Fig. 4

The ω-cyano-L-α-amino acids [39] prepared in the above manner were hydrogenated in acetic acid in the presence of Adam's platinum(IV)-oxide catalyst.

L-Ornithine and L-lysine were obtained in optically and chemically pure state; in both cases the amino acids were isolated in the form of their monohydrochlorides [30]. Since the diamino acids were optically pure, no racemization had taken place in the previous steps of the synthesis, either.

It was already observed in the earlier experiments [9] that isotope exchange takes place to a higher extent in acetic acid and thus the specific activity of the product is lower, than in the experiments carried out in acetic anhydride medium. The hydrogenation of ω-cyano-L-α-amino acid was also tried in acetic anhydride suspension in the presence of platinum(IV)-oxide catalyst, but it failed to proceed.

L-Ornithine-[5-^{3}H] monohydrochloride was prepared in 0.1 mmol amount by catalytic tritiation with carrier-free tritium gas. After dilution with a 13.4-fold amount of L-ornithine monohydrochloride, L-ornithine-[5-^{3}H] monohydrochloride of an activity of 19.5 mCi/mmol was obtained.

L-Lysine-[6-^{3}H] monohydrochloride of 26.6 mCi/mmol activity was obtained under similar conditions (using a 14.3-fold amount of L-lysine monohydrochloride for dilution). Supposing that the yield is nearly 100% in the course of the reduction, on the basis of the above data, L-ornithine-[5-^{3}H] monohydrochloride and L-lysine-[6-^{3}H] monohydrochloride of 280 mCi/mmol and 410 mCi/mmol specific activity, respectively, could be prepared without dilution. In order to make the expriments more accurate, the reactions were repeated using 0.31 mmol of δ-cyano-L-norvaline (**X**) in the catalytic tritiation. An 11 h reaction period was required in this case. The purification of L-lysine dihydrochloride and its isolation as a pure substance on small scale could only be achieved by means of gradient ion-exchange chromatography. In the ion-exchange chromatography, Dowex 50W-X8 resin (100—200 mesh) (H^+-form) was used, which is usually applied in the separation and purification of basic amino acids [31—33], elution was effected with hydrochloric acid solutions of gradually increasing concentration. The hydrochloric acid fractions of lower concentration contained the starting δ-cyano-L-norvaline

and L-homoglutamine formed by its hydrolysis. This mixture exhibited a slight radioactivity, indicating that during the prolonged reaction period the occurrence of hydrogen–tritium exchange reactions at other points of the molecule must also be taken into consideration. L-Lysine-[6-^{3}H] appeared in the fractions of higher hydrochloric acid concentration; this substance could be obtained in radiochemically pure state in the form of its hydrochloride. Its specific radioactivity was in good agreement with the results of earlier experiments. This value was in the same order of magnitude as the specific activity values measured with labelled α,ω-diamino acids prepared by means of catalytic tritiation in acetic acid medium, as described in our previous paper [9]. Since the highest specific activity value obtained was 410 mCi/mmol in the repeated experiments, we assume that this is the highest specific activity attainable under the given experimental conditions [34].

The preparation of amino acids of higher specific activity required by biological research seemed only to be possible in another way.

Our earlier favourable experiences with the use of sodium tetrahydridoborate(III) labelled with tritium (in the following: sodium borotritide) [35, 36] directed our attention to reduction procedures effected with this reagent. The application of other complex metal hydrides could not be considered, owing to the possible reduction of the α-carboxyl group. Researches by EGLI [37] elucidated the mechanism of the reduction of nitriles with sodium borohydride and the difficulties encountered during the reaction, which earlier hindered the utilization of sodium borohydride in the reduction of nitriles to primary amines. These results were extended to the reduction of optically active ω-cyano-L-α-amino acids, in the course of which γ-cyano-L-α-aminobutyric acid (**IX**) was reduced into optically pure L-ornithine with sodium borohydride in alkaline methanolic medium in the presence of Raney nickel, in satisfactory yield. δ-Cyano-L-norvaline (**X**) was converted into optically pure L-lysine in a similar manner in an acceptable yield (Fig. 4).

In the case of δ-cyano-L-norvaline the reduction was accomplished with sodium borotritide of 3.3 Ci/mmol specific activity under the reaction conditions given above. The total reaction period was 30 min. Inorganic ions were removed by means of Dowex 50W-X4 resin (H^+-form). The starting material present in minute amounts in the reaction mixture and the decomposition products formed by its hydrolysis which were detectable by the ninhydrin reaction on the thin-layer chromatogram, but not on the basis of their radioactivities, were removed by means of ion-exchange chromatography.

After purification, L-lysine-[6-^{3}H] dihydrochloride of 755 mCi/mmole specific activity was obtained (chemical yield: 75%); this was then converted into L-lysine-[6-^{3}H] monohydrochloride in the usual manner [30]; the specific activity of the product was 847.5 mCi/mmol. Similarly to the above procedure, an aliquot of sodium borotritide of 3.3 Ci/mmol specific activity was used to

reduce γ-cyano-L-α-aminobutyric acid into L-ornithine-[5-^{3}H]. After proper purification, the specific activity of the product isolated as the dihydrochloride was 655 mCi/mmol, while that of L-ornithine-[5-^{3}H] monohydrochloride obtained from it was found to be 706.6 mCi/mmol.

The results obtained in repeated experiments agree within the experimental error. They indicate that isotope exchange reaction takes place only to a limited extent during the reaction, thus the preparation of L-ornithine-[5-^{3}H] and L-lysine-[6-^{3}H] of high specific activity is possible economically, in satisfactory yields.

Experimental

The experimental work was carried out in the Institute of Isotopes of the Hungarian Academy of Sciences and in the Isotope Laboratory of the Institutes for Biological Research of the Czechoslovak Academy of Sciences.

M. p.'s are uncorrected; they were determined on a Kofler apparatus. The optical rotation measurements were made with a photoelectric polarimeter in the Institute of Organic Chemistry and Biochemistry of the Czechoslovak Academy of Sciences *(a)* and with a Schmidt–Haensch polarimeter in the Chemical Technology Department of the L. Eötvös University, Budapest *(b)*. In the thin-layer chromatographic tests, Silufol® layers (S) (Made in Czechoslovakia) and Merck DC-Alufolien Kieselgel layers (M) were used. The solvent systems used in the thin-layer chromatographic work were the following:

(1) Ethyl acetate : pyridine : glacial acetic acid : water 240 : 20 : 6 : 11
(2) Ethyl acetate : pyridine : glacial acetic acid : water 120 : 20 : 6 : 11
(3) Chloroform : methanol : conc. ammonium hydroxide 20 : 20 : 9

The radiochromatograms were evaluated with a Bertold Dünnschicht-Scanner LB 2721 apparatus.

The radioactivity of the labelled compounds was measured with a Packard 3375 liquid scintillation spectrometer.

The substances prepared were dried at room temperature over phosphorus(V)-oxide in vacuum. Analytical samples were recrystallized repeatedly only in the cases where specially stated. Here the samples were dried at 60—70 °C over phosphorus(V)-oxide in vacuum.

Tosyl-L-homoglutamine methyl ester (V) (Method A)

Tosyl-L-homoglutamine (2.48 g; 7.55 mmol) was suspended in methanol (150 ml), and an ethereal solution of diazomethane was slowly added to the suspension with stirring. The solid dissolved. The addition of the ethereal solution of diazomethane was continued until the reaction mixture turned pale yellow. It was allowed to stand for 1 h then a mixture of glacial acetic acid (0.5 ml) and ether (5 ml) was added to the suspension, and it was filtered after standing for 1 h. The filtrate was evaporated to dryness in vacuum, and the semicrystalline residue was mixed with petroleum ether. The mixture was allowed to stand in a refrigerator, filtered, and washed with petroleum ether. The weight of the colourless crystalline product was 2.41 g (93%) m. p. 115—120 °C.

For analysis the sample was recrystallized from ethanol with petroleum ether; m. p. 120—122 °C.

$C_{14}H_{20}N_2O_5S$ (328.4). Calcd. C 51.20; H 6.14; N 8.53. Found C 51.43; H 6.27; N 8.35.

δ-Cyano-tosyl-L-norvaline methyl ester (VI)

Compound **V** (500 mg; 1.52 mmol) was dissolved in absolute pyridine (1.2 ml). Tosyl chloride (600 mg; 2.62 mmol) was added to the solution. In the course of the slightly exothermal reaction the colour of the reaction mixture became reddish. The mixture was allowed to stand for 10 min then heated slowly to 80 °C in an oil bath. After cooling, 20 ml ice-water

was added to the reaction mixture. The crystalline material which separated was filtered off and washed with some ice-water. After drying, 329 mg (70%) of a pale brown product was obtained; m. p. 93—98 °C.

For analysis the sample was recrystallized from methanol using charcoal and addition of water; m. p. 93—98 °C.

$C_{14}H_{18}N_2O_4S$ (310.4). Calcd. C 54.17; H 5.85; N 9.03. Found C 54.15; H 5.68; N 8.83.

δ-Cyano-tosyl-L-norvaline (VII) (Method A)

Compound **VI** (310 mg; 1 mmol) was dissolved in 1 *N* sodium hydroxide (2 ml). After standing for 1.5 h, the solution was filtered and acidified with 2 *N* hydrochloric acid, with cooling. The solution was refrigerated for a few hours, the crystalline material **VII** which separated was filtered off and washed with some cold water. After drying, the weight of the colourless crystalline product was 234 mg (79%); m. p. 125—130 °C. For analysis the sample was recrystallized twice from ethyl acetate with petroleum ether; m. p. 131—132 °C.

$C_{13}H_{16}N_2O_4S$ (296.3). Calcd C 52.69; H 5.44; N 9.45. Found C 52.70; H 5.65; N 9.10.

γ-Cyano-tosyl-L-α-aminobutyric acid (III) (Method B)

Absolute dimethylformamide (30 ml) was cooled to −10 °C, then a solution of freshly distilled thionyl chloride (6.65 ml ~ 10.83 g; 91.3 mmol) dissolved in absolute chloroform (15 ml) was poured into the cooled dimethylformamide under stirring. After 20 min, further cold absolute chloroform (105 ml) was added to the chilled reaction mixture. Then tosyl-L-glutamine (9.0 g; 30 mmol) was suspended in the above solution, it was stirred for 50 min and the temperature of the reaction mixture was allowed to rise to room temperature. It was then cooled and stirred for 20 min at 0 °C. A red-coloured reaction mixture was obtained, from which gaseous components were removed by suction with a pump. The residue was mixed with 15% sodium carbonate solution and the aqueous phase was adjusted to pH 8 by the addition of sodium carbonate solution. This phase was separated, and the chloroform layer was extracted three times with saturated sodium hydrogen carbonate solution (50 ml). The combined aqueous solutions were washed with chloroform. The traces of chloroform were removed from the aqueous solution in vacuum.

The solution was filtered and acidified; compound **III** began to crystallize on seeding. The reaction mixture was refrigerated for a few hours, the crystals which separated were filtered off and washed with cold water. Pale yellow crystalline **III** was obtained. The weight of the product after drying was 5.70 g (65%); m. p. 141—144 °C.

Crude **III** (5.5 g) was dissolved in hot water (33 ml), treated with charcoal and refrigerated; the crystalline product was filtered off, washed with cold water and dried. Colourless crystals (4.66 g) were obtained, m. p. 143—145 °C. Yield of recrystallization: 84.7%. R_f 0.26 (S; 1). $[\alpha]_D^{25}$ +21.7° (c = 2.7; MeOH) (*a*); $[\alpha]_D^{22}$ +21.1° (c = 2.7; MeOH) (*b*).

$C_{12}H_{14}N_2O_4S$ (282.3). Calcd. C 51.05; H $4_6$99; N 9.92 Found C 50.91; H 4.93; N 9.86.

δ-Cyano-tosyl-L-norvaline (VII) (Method B)

Absolute dimethylformamide (40 ml) was cooled to −10 °C and a solution of thionyl chloride (8.9 ml ~ 14.5 g; 108 mmol) in absolute chloroform (20 ml) was added with cooling and stirring. After 20 min a further amount of cold absolute chloroform (140 ml) was added to the chilled reaction mixture; this was followed by the addition of tosyl-L-homoglutamine (11 g; 35 mmol). For the rest, the procedure described in Method B for the preparation of compound **III** was followed.

The oily material which separated after acidifying the solution solidified on seeding; it was let to stand in a refrigerator, filtered off, washed with cold water and dried, to obtain 6.26 g (59.5%) of yellow-coloured **VII**; m. p. 128—130 °C.

Crude **VII** (6.1 g) was dissolved in hot ethyl acetate (40 ml), decolorized with charoal and washed twice with hot ethyl acetate (5 ml). After allowing to cool a little, petroleum ether (50 ml) was added slowly to the solution. On the addition of 35 ml of petroleum ether, the solution became slightly opalescent; it was then seeded with a crystal and refrigerated for a few hours. The product was washed with a 1 : 1 mixture of ethyl acetate and petroleum ether (2×10 ml), then with petroleum ether, and dried. Colourless crystalline **VII** was obtained (5.3 g), m. p. 130—132 °C. Yield of recrystallization: 86.8%. R_f 0.57 (S; 2).
$[\alpha]_D^{25}$ +16.8° (c = 2.7; MeOH) (*a*); $[\alpha]_D^{22}$ +16.7° (c = 2.7; MeOH) (*b*).

$C_{13}H_{16}N_2O_4S$ (296.35). Calcd. C 52.69; H 5.44; N 9.45. Found C 52.45; H 5.50; N 9.38.

γ-Cyano-L-α-aminobutyric acid (IX)

γ-Cyano-tosyl-L-aminobutyric acid (7.0 g; 24.8 mmol) was dissolved in methanol (150 ml), and tetramethylammonium chloride (8.0 g; 73 mmol) was added to the solution. The methanolic solution was poured into a beaker which contained mercury (60 ml) in a layer thickness of about 5 mm. A porcellain diaphragm was immersed into the solution, and a solution of tetramethylammonium chloride (4 g) in water (50 ml) was poured into the diaphragm. A graphite electrode (anode) was placed into the aqueous solution in side the diaphragm, and a platinum wire was put into the mercury (cathode). The reaction mixture was cooled to +10 °C and cooling by circulating water was also provided within the diaphragm. The electrolysis was started at a voltage of 24 V and a current of 0.5 Amp. The electrolysis was then continued for 5 h at 18—24 V and 0.5—1.3 Amp. An increase in the voltage and decrease in the current indicated the completion of the electrolysis. The diaphragm was removed from the beaker; its surface was rinsed into the reaction mixture with methanol, water and again with methanol. The composition of the reaction mixture was adjusted to a methanol–water ratio of about 1 : 1 by the addition of water. The solution was decanted from the mercury, and the mercury was washed with an 1 : 1 mixture of methanol and water. The aqueous methanolic solution was filtered and applied to a column of Dowex 50W-4X (H^+) resin (150—160 ml) and washed until neutral reaction. The amino acid was eluted first with 3% then with 5—6% ammonium hydroxide solution. The eluate giving positive ninhydrin reaction (about 500 ml) was concentrated in vacuum to 50—70 ml. The residue was treated with charcoal and concentrated to 10 ml. The solution containing some crystalline material was brought to boiling and ethanol (40 ml) was slowly added to the clear solution; crystalline **IX** separated. The suspension was allowed to stand in a refrigerator, filtered, washed three times with ethanol (4 ml each) and dried. Colourless crystalline **IX** was obtained (2.27 g; 71.45%), m. p. 220—235 °C (*d*). R_f 0.56 (S; 3).

$[\alpha]_D^{22}$ +27.4° (*c* = 0.5; H_2O) (*a*); $[\alpha]_D^{22}$ +28.0° (*c* = 0.5; H_2O) (*b*);
$[\alpha]_D^{22}$ +46.0° (*c* = 1.0; 0.5 *N* HCl) (*b*).

$C_5H_8N_2O_2$ (128.13). Calcd. C 46.87; H 6.29; N 21.86. Found C 46.87; H 6.26; N 21.68.

δ-Cyano-L-norvaline (X)

δ-Cyano-tosyl-L-norvaline (4.0 g; 10.12 mmol) and tetramethylammonium chloride (3.5 g; 31.9 mmol) were dissolved in methanol (100 ml). The solution was poured into a beaker containing mercury (60 ml) in a layer thickness of about 5 mm. A porcellain diaphragm was placed into the methanolic solution and a solution of tetramethylammonium chloride (2 g) in water (40 ml) was poured into it. The reaction mixture was cooled to +10 °C and, after arranging the electrodes (see **IX**). the electrolysis was effected at this temperature for 2 h at a voltage of 24—19.5 V and with a current of 0.4—1.25 Amp. The surface of the diaphragm was then rinsed into the reaction mixture with methanol and water. After filtration, the reaction mixture with a composition of about 1 : 1 methanol–water was transferred onto a Dowex 50W-4X (H^+) resin column of about 80 ml volume, washed to neutral reaction in the usual manner, and eluted. The eluate giving positive ninhydrin reaction was concentrated to about 30 ml in vacuum, treated with charcoal and washed with hot water. The solution was concentrated to 20 ml in vacuum. 60 ml of ethanol was added to the solution. The crystal suspension was refrigerated for a few hours, then the product was filtered off, washed with ethanol and dried to give colourless crystalline **X**. (1.02 g; 70.8%), m. p. 230—237 °C (*d*). R_f 0.6 (S; 3).

$[\alpha]_D^{25}$ +10.0° (*c* = 0.50, H_2O) (*a*); $[\alpha]_D^{22}$ +10.0° (*c* = 0.50, H_2O) (*b*);
$[\alpha]_D^{22}$ +30.0° (*c*) = 1.0, 0.5 *N* HCl) (*b*).

$C_6H_{10}N_2O_2$ (142.16). Calcd. C 50.69; H 7.009; N 19.71. Found C 50.75; H 7.06; N 19.08.

L-Ornithine hydrochloride (XI) (Catalytic hydrogenation)

Platinum(IV)-oxide (70 mg) was suspended in glacial acetic acid (3 ml) and hydrogenated as long as absorption of hydrogen could be observed. Then **IX** (256.6 mg; 2 mmol) was suspended in glacial acetic acid (12 ml) and added to the catalyst. Hydrogenation was continued for 3 h at 24 °C at a pressure of 740 torr. The volume of hydrogen absorbed was 96 ml. The solid dissolved gradually in the course of hydrogenation. The catalyst was removed by filtration, the filter was washed with glacial acetic acid, and the acetic acid solution was concentrated in vacuum. The residue was mixed with 2 *N* hydrochloric acid (15 ml). The solution was boiled for 15 min and concentrated in vacuum. The residue was dissolved in water and the water evaporated in vacuum; hot water (1.5 ml) was added to the dry residue, the mixture was fil-

tered and the filter washed twice with hot water (0.5 ml). Absolute ethanol (7.5 ml) was added to the aqueous solution and the pH was adjusted to 5 with an ethanol–pyridine mixture (1:1). A crystalline substance separated; more ethanol (4 ml) was then added to the suspension, and it was refrigerated for 4 hrs; the crystals were filtered off, washed with ethanol and dried. Compound **XI** was obtained as colourless crystals (193 mg; 57.26%), m. p. 233–237 °C(d.).
R_f = 0.17 (S; 3).

$[\alpha]_D^{22}$ +22.5° (c = 1.8, 5 N HCl) (*b*).

$C_5H_{13}N_2O_2Cl$ (168.2). Calcd. C 35.62; H 7.77; N 16.61; Cl^- 21.02. Found C 35.55; H 7.80; N 16.56; Cl^- 20.75.

L-Lysine hydrochloride (XII) (Catalytic hydrogenation)

Platinum(IV)-oxide (48.5 mg) was suspended in glacial acetic acid (3 ml) and hydrogenated as long as hydrogen absorption was observed. Then a suspension of δ-cyano-L-norvaline (145 mg; 1.02 mmol) in glacial acetic acid (14 ml) was added to the catalyst and hydrogenated for 3 h at 23 °C under a pressure of 735 torr. The volume of hydrogen consumed was 61 ml. The crystalline substance dissolved during hydrogenation. The catalyst was filtered off, the filter was washed with glacial acetic acid and the filtrate evaporated to dryness in vacuum. The residue was boiled with 2 N HCl (10 ml) for 15 min. The acid solution was evaporated to dryness in vacuum, and water was distilled from the residue. The solid residue was dissolved in water (0.5 ml); absolute ethanol (4.5 ml) was added to the solution and **XII** was precipitated with a mixture of ethanol and pyridine (1 : 1) at pH 5. In the course of crystallization, additional ethanol was added to the solution (5 ml), it was refrigerated, then filtered and the precipitate was washed with ethanol and dried to give colourless crystalline **XII** (113.6 mg; 61.0%). R_f 0.15 (S; 3).

$[\alpha]_D^{22}$ +19.7° (c = 1.5, 5 N HCl) (*b*).

$C_6H_{15}N_2O_2Cl$ (182.6). Calcd. C 39.46; H 8.28; N 15.35; Cl^- 19.45. Found C 39.39; H 8.25; N 15.34; Cl^- 19.05.

L-Ornithine hydrochloride (XI) (Reduction with sodium borohydride)

γ-Cyano-L-α-aminobutyric acid (1.281 g; 10 mmol) was dissolved in a mixture of methanol (10 ml), water (5 ml) and 4 N sodium hydroxide solution (2.5 ml). Five spatula portions of Raney nickel were added to the stirred solution which was then placed into a water bath of 36–38 °C. A solution of sodium borohydride (590 mg; 15.6 mmol) in 0.5 N NaOH (2.5 ml) was added slowly to the reaction mixture during about 10 min. The temperature of the reaction mixture rose to +42 °C. It was stirred further for 20 min, filtered, then divided into 3 equal parts.

(*a*) One-third volume of the reaction mixture was acidified with conc. hydrochloric acid with cooling and stirring, then evaporated to dryness in vacuum. Water was distilled from the residue. The residue was dissolved in ethanol (10 ml), the inorganic salt which separated was filtered off and washed with three 2 ml portions of ethanol. The solution was stored in a refrigerator overnight. The small amount of inorganic salt was filtered off and washed twice with ethanol (1.5 ml each). The ethanolic solution was adjusted to pH 5 with a mixture of ethanol and pyridine (1 : 1), whereupon a crystalline material separated. The suspension was refrigerated for a few hours, then the precipitate was filtered off and washed with ethanol to obtain colourless crystalline **XI** (337.4 mg; 60.0%). R_f 0.18 (S; 3).

$[\alpha]_D^{25}$ +21.0° (c = 1, H_2O) (*a*).

$C_5H_{13}N_2O_2Cl$ (168.62). Calcd. N 16.61; Cl^- 21.02. Found N 15.98; Cl^- 20.13.

A portion of the above material (260 mg) was recrystallized from a mixture of water (2 ml) and ethanol (10 ml). It was refrigerated for 3 h. The product was filtered off, washed with ethanol and dried to give colourless crystalline **XI** (158.5 mg), the yield of recrystallization: 61.0%. R_f 0.15 (M; 3).

$[\alpha]_D^{22}$ +21.5° (c = 2.0, 5 N HCl) (*b*).

$C_5H_{13}N_2O_2Cl$ (168.6). Calcd. C 35.62; H 7.77; N 16.61; Cl^- 21.02. Found C 35.41; H 7.54; N 16.36; Cl^- 20.94.

(*b*) One-third volume of the reaction mixture was transferred to Dowex 50W-4X (H^+) resin (30 ml). The column was washed until neutral reaction was obtained, then eluted with 3% ammonium hydroxide solution. The eluate giving positive ninhydrin reaction was collected. This eluate was concentrated in vacuum to leave a syrupy residue which was mixed with

1 *N* HCl (10 ml). The solution was filtered, and the filter was washed with 1 *N* HCl (10 ml). The filtrate was evaporated in vacuum, and water (10 ml) was distilled from the residue. The residue was dissolved in ethanol (7 ml), the solution was filtered and the residue washed twice with ethanol (1.5 ml each). The solution was adjusted to pH 5 with a 1 : 1 mixture of ethanol and pyridine, whereupon colourless crystals began to separate. The suspension was refrigerated, then the product was filtered off and washed with ethanol to obtain **XI** as a colourless crystalline product (348.0 mg; 61.9%). R_f 0.18 (S; 3).

$[\alpha]_D$ +21.0° (c = 1, H_2O) (*a*).

$C_5H_{13}N_2O_2Cl$ (168.6). Calcd. N 16.61; Cl⁻ 21.02. Found N 15.92; Cl⁻ 20.26.

L-Lysine hydrochloride (XII) (Reduction with sodium borohydride)

δ-Cyano-L-norvaline (567.6 mg; 4.0 mmol) was dissolved in a mixture of methanol (5 ml), water (2.5 ml) and 4 *N* sodium hydroxide (1 ml). Three portions of Raney nickel were added to the solution by means of a spatula. The reaction mixture was immersed into a water bath of 36—38 °C, then a solution of sodium borohydride (242.0 mg; 6.4 mmol) in 0.5 *N* NaOH (1.2 ml) was added dropwise to the reaction mixture during 10 min, with stirring. The reaction mixture was stirred further for 30 min, then filtered and the filtrate was transferred to Dowex 50X-X4 (H^+) resin (about 20 ml). The column was washed until neutral and eluted with 3% ammonium hydroxide solution. The eluates giving positive ninhydrin reaction were collected and evaporated in vacuum. The viscous residue was dissolved in 2 *N* HCl (2 ml). Absolute ethanol (4 ml) was added to the solution, then the pH was adjusted to 5 with a mixture of ethanol and pyridine. Precipitation of crystalline material was effected by the addition of ethanol (14 ml); the mixture was refrigerated for 4 h, then the product was filtered off, washed with ethanol and dried, to obtain **XII** as colourless crystals (461.8 mg, 63.3%). R_f 0.15 (S; 3).

$[\alpha]_D^{22}$ +19.0 (c = 2.0, 5 *N* HCl) (*b*).

$C_6H_{15}N_2O_2Cl$ (182.6). Calcd. N 15.35; Cl⁻ 19.45. Found N 14.85; Cl⁻ 19.01.

Crude L-lysine hydrochloride (390 mg) was dissolved in hot water (2 ml) and treated with charcoal. The solution was filtered and the filter washed with two 0.5 ml portions of water. Absolute ethanol (21 ml) was added to the filtrate. The crystal suspension was refrigerated, the product was filtered off, washed with ethanol and dried to give colourless crystalline **XII** (320.0 mg) the yield of recrystallization: 82.1%. R_f 0.17 (M; 3).

$[\alpha]_D^{22}$ +19.5° (c = 2.0, 5 *N* HCl) (*b*).

$C_6H_{15}N_2O_2Cl$ (182.6). Calcd. C 39.46; H 8.28; N 15.35; Cl⁻ 19.45. Found C 39.35; H 8.37; N 14.98; Cl⁻ 19.10.

Radioactive experiments

L-Ornithine-[5-^{3}H] hydrochloride (XII-[^{3}H]) (Catalytic tritiation)

γ-Cyano-L-α-aminobutyric acid (15 mg; 0.117 mmol) was catalytically tritiated in glacial acetic acid (1 ml) in the presence of platinum(IV)-oxide under a pressure of 690 torr. The reaction period was 5 h. The amount of carrier-free tritium gas absorbed was 6.18 ml (N. T. P.) = 16.07 Ci. After the accomplishment of the reaction, the solution was filtered, washed, and the acetic acid was removed in vacuum. The residue was refluxed in 2 *N* HCl (2 ml) for 15 min, the hydrochloric acid was then removed in vacuum. Water (5 ml) was distilled from the residue. The remaining solid was dissolved in water (1.5 ml) and L-ornithine hydrochloride (Calbiochem) (263.7 mg) was added to the solution. It was filtered, the filter was washed with water (0.5 ml) and 50% ethanol (1 ml). The solution was adjusted to pH 5 with a 1 : 1 mixture of ethanol and pyridine (2 drops). Ethanol (14 ml) was then added, the solution was refrigerated overnight the product was filtered off, washed with ethanol and dried to obtain colourless **XI**-[^{3}H] 183.7 mg. R_f 0.18 (S; 3). The radiochemical purity was higher than 98%. Specific activity: 116.0 μCi/mg molar activity: 19.56 mCi/mmol. As calculated from the dilution with the 13.359-fold amount of L-ornithine hydrochloride, without dilution a product having a specific activity of 280.85 mCi/mmol could be obtained.

L-Lysine-[6-^{3}H] hydrochloride (XII-[^{3}H]) (Catalytic tritiation)

δ-Cyano-L-norvaline (15 mg; 0.1055 mmol) was tritiated in glacial acetic acid (1 ml) in the presence of platinum(IV)-oxide (7.5 mg) at a pressure of 685 torr. The amount of the carrier-free tritium gas absorbed during the 6.5 h reaction period was 5.198 ml (N. T. P.) =

= 13.51 Ci. The solution was filtered and the acetic acid removed in vacuum. The residue was refluxed with 2 *N* hydrochloric acid (3 ml) for 15 min, then the hydrochloric acid was distilled in vacuum. Water (5 ml) was distilled from the residue. The residue was dissolved in water (1.5 ml) and L-lysine hydrochloride (Calbiochem) (277.2 mg) was added to the solution. The solution was filtered and the filter washed with water (0.5 ml) and 50% ethanol (1.0 ml). The solution was adjusted to pH 5 with a mixture of ethanol and pyridine. Compound **XII**-^{3}H was precipitated by the addition of ethanol (16 ml); the suspension was refrigerated overnight, then the product was filtered off, washed with ethanol and dried to obtain colourless **XII**-[^{3}H] (181.3 mg). R_f 0.16 (S; 3). The radiochemical purity was higher than 98%. Specific activity: 145.89 μCi/mg; molar activity: 26.65 mCi/mmol. On the basis of the dilution with a 14.383-fold amount of L-lysine hydrochloride, the calculated value of specific activity without dilution would be 410 mCi/mmol.

L-Lysine-[6-^{3}H]dihydrochloride (XII-[^{3}H]) (Catalytic tritiation without dilution)

δ-Cyano-L-norvaline (44 mg; 0.31 mmol) was tritiated in glacial acetic acid medium (2 ml) in the presence of platinum(IV)-oxide (19 mg) at 695 torr pressure. The reaction mixture absorbed 17.907 ml (N. T. P.) = 46.55 Ci of carrier-free tritium gas during the 11 h reaction period. The solution was filtered, washed, and the acetic acid removed in vacuum. The residue was refluxed with 2 *N* HCl (10 ml) for 10 min, then the hydrochloric acid was removed in vacuum. The residue was dissolved in water and applied to a Dowex 50W-X8 (100—200 mesh) (H^+) resin column (about 10—15 ml of resin). The resin column was washed until neutral reaction was obtained, and eluted first with 0.5 *N* HCl, then the concentration of hydrochloric acid was gradually increased. The elution was finished with 3 *N* HCl. Thin-layer chromatograms were prepared from the eluates (S; 3). Eluates of lower hydrochloric acid concentration contained the non-reduced **X** and the L-homoglutamine formed from it by hydrolysis during the work-up. These fractions were evaporated together in vacuum. After drying over phosphorus pentoxide and sodium hydroxide pellets, a glasslike solid (10.8 mg) was obtained. The specific activity of this mixture was 0.452 mCi/mg. The eluates containing **XII**-^{3}H were evaporated in vacuum and water (5 ml) was distilled from the residue. It was then dissolved in ethanol (2 ml) and a solid was precipitated from the solution by adding absolute ether (20 ml). The mother liquor was decanted and the solid was twice suspended in acetone (10 ml each) and decanted. The solid residue was dried to constant weight over phosphorus pentoxide and sodium hydroxide pellets in vacuum to give, L-lysine-[6-^{3}H] dihydrochloride (33.8 mg). R_f 0.15 (S; 3). The radiochemical purity was higher than 98%. Specific activity: 1.884 mCi/mg; molar activity: 378.67 mCi/mmol.

L-Lysine-[6-^{3}H] hydrochloride (XII-[^{3}H]) (Reduction with sodium borotritide)

δ-Cyano-L-norvaline (128 mg; 0.9 mmol) was dissolved in a mixture of methanol (2 ml), water (0.5 ml) and 4 *N* sodium hydroxide (0.225 ml). Two portions of Raney nickel were added to the solution by means of a spatula, and it was heated on a water bath of 36—38 °C. Sodium borohydride (32 mg; 0.846 mmol) was dissolved in 0.5 *N* NaOH (1 ml). Sodium borotritide (48 mg; 1.8 mol) with a specific activity of 87.5 mCi/mg and a molar activity of 3.31 Ci/mmol) was dissolved in 0.5 *N* NaOH (2 ml).

Of the sodium borohydride solutions specified above, an aliquot (1 ml; 0.9 mol) of the sodium borotritide solution was added first to the vigorously stirred reaction mixture during 7 min. Ten minutes later, an aliquot (0.5 ml) of the sodium borohydride solution was added to the reaction mixture, thus ensuring an excess of the reducing agent. The reaction mixture was stirred at 36—38 °C for 20 min, then filtered, washed with water and applied to a Dowex-50W-X4 resin column (50 ml). The column was washed until neutral, then eluted with 3% ammonium hydroxide solution. The eluate giving positive ninhydrin reaction was evaporated to dryness in vacuum. The residue was dissolved in 0.2 *N* HCl (10 ml) and applied to a Dowex 50W-X8 (100—200 mesh) (H^+) resin column (10 ml), and washed to get neutral reaction. Elution was started with 0.5 *N* HCl, then the concentration of hydrochloric acid was gradually increased to 4 *N*. Fractions of 10 ml were collected. The amino acid content of the fractions was examined by means of thin-layer chromatography. L-Lysine hydrochloride (Calbiochem) was used as standard. The fractions containing lysine were collected and evaporated to dryness in vacuum. Water was distilled from the residue, then the solid was dried over phosphorus pentoxide and sodium hydroxide pellets in vacuum. A pale yellow foamlike substance was obtained (190.5 mg), which was rubbed with absolute acetone (5 ml), decanted, and the treatment with acetone was repeated. The solid residue was dried again, as described above, to

obtain pale yellow, powderlike L-lysine-[6-^{3}H] dihydrochloride (146.3 mg; chemical yield: 74%). R_f 0.17 (M; 3). The radiochemical purity was 95%. Specific activity: 3.446 mCi/mg; molar activity: 755.46 mCi/mmol.

The above-described crude **XII**-[^{3}H] (145 mg) was dissolved in water (0.5 ml), and ethanol (0.5 ml) was added to the solution. It was neutralized with a mixture of ethanol and pyridine, then a crystalline substance was precipitated by the addition of ethanol (9.5 ml). The suspension was allowed to stand, the product was then filtered off and washed with ethanol to obtain L-lysine-[6-^{3}H] monohydrochloride (78.5 mg). Yield: 65%. R_f 0.17 (M; 3). The radiochemical purity was higher than 99%. Specific activity: 4.64 mCi/mg; molar activity: 847.53 mCi/mmole.

L-Ornithine-[5-^{3}H] hydrochloride (XI-[^{3}H]) (Reduction with sodium borotritide)

γ-Cyano-L-α-aminobutyric acid (115 mg; 0.9 mmol) was dissolved in a mixture of methanol (2 ml), water (0.5 ml) and 4 *N* sodium hydroxide (0.225 ml). Two portions of Raney nickel were added to the solution by means of a spatula, then the mixture was placed into a water bath of 36—38 °C. An aliquot (1 ml) of the sodium borotritide solution specified in the synthesis of **XII**-^{3}H was added to the reaction mixture in 6—8 min. (The sodium borotritide solution had been stored for about 20 min before use.) Ten minutes later, an aliquot (0.5 ml) of the inactive sodium borohydride was added to the reaction mixture. The processing of the reaction mixture was the same as described for the reduction of **XII**-[^{3}H] with sodium borohydride. The hydrochloric acid fractions containing L-ornithine-[5-^{3}H] were evaporated to dryness in vacuum, water was distilled from the residue, and the product was dried as described above. The slightly tacky residue was dissolved in ethanol (2 ml), and ether (20 ml) was slowly added to the solution. A solid substance precipitated. The mother liquor was decanted, the residue was treated with absolute ether and after decanting it was dried as was mentioned above to obtain colourless crystalline L-ornithine-[5-^{3}H] dihydrochloride (120.9 mg; chemical yield: 66.2%). R_f 0.15 (M; 3). Radiochemical purity: 93%. Specific activity: 3.191 mCi/mg; molar activity: 655.0 mCi/mmol.

The crude **XI**^{2}[^{3}H] (118 mg) was dissolved in water (0.5 ml), and ethanol (2 ml) was added to the solution. It was neutralized with a mixture of ethanol and pyridine. On the addition of ethanol (8.5 ml), a crystalline substance precipitated which was L-ornithine-[5-^{3}H] monohydrochloride (67.2 mg; 69.2%). R_f 0.15 (M; 3). The radiochemical purity was higher than 99%. Specific activity: 4.194 mCi/mg; molar activity: 706.7 mCi/mmol.

*

One of the authors (I. M.) is grateful to the Czechoslovak Academy of Sciences and the Hungarian Academy of Sciences for providing the possibility of working for two longer periods in the Isotope Laboratory of the Institutes for Biological Research of the Czechoslovak Academy of Sciences. The authors' thanks are due to dr. Cs. ÖMBÖLY for the radioactivity measurements, to dr. I. FRIČ, to Mrs. H. PILAŘOVÁ (*a*) and Mrs. M. BARTHA (*b*) for the optical rotation measurements, and to Mrs. M. BALOGH (*b*) and Mr. J. VLNA for the microanalyses. Mr. A. SZABÓ's valuable help in the radioactive experiments is acknowledged with thanks.

REFERENCES

[1] BIRKOFER, L., HEMPEL, K.: Chem. Ber. **93,** 2282 (1960)
[2] MIHAILOVA, V. N., BULAT, A. D., USAEVICH, YU. YA.: Zhur. Obshch. Khim. **43,** 1412 (1973)
[3] FRIDKIN, M., SOKOLOVSKY, M., KATCHALSKI, E.: Biopolymers **2,** 123 (1964)
[4] BIRKOFER, L., HEMPEL, K., NOUVERT, W.: Chem. Ber. **98,** 3200 (1965)
[5] PLENTL, A. A., KELLY, W. K.: Anal. Biochem. **17,** 397 (1966)
[6] BRUNDISH, D. E., ELLIOT, D. F., WADE, R.: J. Lab. Comp. **7,** 473 (1971)
[7] JANSEN, A. C. A., KERLING, K. E. T., HAVINGA, E.: Rec. Trav. Chim. **89,** 861 (1970)
[8a] HAVRÁNEK, M., KOPECKÁ-SCHADTOVÁ, H., VEREŠ, K.: J. Lab. Comp. **6,** 345 (1970)
[8b] HAVRÁNEK, M.: Candidate Thesis, Prague, (1968)
[9] THYAGARAJAN, S., MEZŐ, I., TEPLÁN, I., MÁRTON, J.: Acta Chim. (Budapest) **73,** 23 (1972)
[10] HAVRÁNEK, M., MEZŐ, I.: Acta Chim. (Budapest) **77,** 341 (1973)
[11] RUDINGER, J.: Coll. Czech. Comm. **19,** 365 (1954)
[12] GUT, V., RUDINGER, J.: Coll. Czech. Chem. Comm. **28,** 2953 (1963)

[13] RUDINGER, J., FARKAŠOVÁ, H.: Coll. Czech. Chem. Comm. **28,** 2941 (1963)
[14] RESSLER, C., RATZKIN, H.: J. Org. Chem. **26,** 3356 (1961)
[15] KASHELIKAR, D. V., RESSLER, C.: J. Am. Chem. Soc. **86,** 2467 (1964)
[16] LIBEREK, B.: Bull. Acad. Polon. Sci. **10,** 227 (1962)
[17] LIBEREK, B., BUCZEL, CZ., GRZONKA, Z.: Tetrahedron **22,** 2303 (1966)
[18] ZAORAL, M., RUDINGER, J.: Coll. Czech. Chem. Comm. **24,** 1993 (1959)
[19] ARNOLD, Z., ŠORM, F.: Coll. Czech. Chem. Comm. **23,** 452 (1958)
[20] ARNOLD, Z.: Coll. Czech. Chem. Comm. **24,** 4048 (1959(
[21] EISLER, K.: Dissertation. Technical University, Prague, (1964)
[22] RESSLER, C., NAGARAJAN, G. R., KIRISAWA, M., KASHELIKAR, D. V.: J. Org. Chem. **36,** 3960 (1971)
[23] RESSLER, C., KASHELIKAR, D. V.: J. Am. Chem. Soc. **88,** 2025 (1966)
[24] EILINGSFELD, H., SEEFELDER, M., WEIDINGER, H.: Angew. Chem. **72,** 836 (1960)
[25] BOSSHARD, H., MORY, R., SCHMID, M., ZOLLINGER, H.: Helv. Chim. Acta **42,** 1653 (1959)
[26] SCHÖRDER, E., LÜBKE, K.: The Peptides, Academic Press, New York 1965, Vol. I, pp. 15
[27] HORNER, H., NEUMANN, H.: Chem. Ber. **98,** 3462 (1965)
[28] HORNER, L., NEUMANN, H.: Chem. Ber. **98,** 1715 (1965)
[29] KASAFÍREK, E. (Pharmaceutical and Biochemical Research Institute, Prague): Unpublished results
[30] GREENSTEIN, J., WINITZ, M.: The Chemistry of the Amino Acids, John Wiley and Sons, New York 1961, pp. 2101, 2478.
[31] HAUSMANN, W. K., BORDERS, D. B., LANCASTER, J. E.: J. Antibiotics **22,** 207 (1969)
[32] BODÁNSZKY, A. A., BODÁNSZKY, M.: J. Antibiotics **23,** 149 (1970)
[33] TÓTH-SARUDY, É.: Doctoral Thesis, Budapest, (1971)
[34] MÁRTON, J., KOVÁCS, Á.: Acta Chim. (Budapest) **73,** 11 (1972)
[35] MEZŐ, I., TANÁCS, B., TEPLÁN, I., BURSICS, L., MÁRTON, J.: Acta Chim. Budapest **70,** 83 (1971)
[36] TANÁCS, B., SZARVAS, T.: Radioisotopy, Prague **12,** 627 (1971)
[37] EGLI, R. A.: Helv, Chim. Acta **53,** 47 (1970)
[38] IWASAKI, T., MATSUMOTO, K., MATSUOKA, M.: Bull. Chem. Soc. Japan **46,** 852 (1973)
[39] a. KASAFÍREK, E., HAVRÁNEK, M., RUDINGER, J.: Unpublished results
b) EISLER, K., RUDINGER, J.: Unpublished results see: KATSOYANNIS, P. G.: The Chemistry of Polypeptides, Plenum Press, New York, London 1973, pp. 103

Imre Mező; 1088 Budapest, Puskin u. 9, Hungary
István Teplán; 1051 Budapest, Münnich F. u. 7. Hungary
Miloš HAVRÁNEK, Josef BENEŠ } 142 20 Praha 4-Krč, K výzkumným ústavům 1083 Czechoslovakia.

Acta Chimica Academiae Scientiarum Hungaricae, 85 (2), pp. 215–219 (1975)

THE STRUCTURE OF COGOMYCIN, A POLYENE ANTIBIOTIC

(SHORT COMMUNICATION)

V. Pozsgay*, J. Tamás** and G. Czira**

*(*Chemical Research Laboratories, BIOGAL Pharmaceutical Works, Debrecen, **Central Research Institute for Chemistry of the Hungarian Academy of Sciences, Budapest)*

Received June 3, 1974

Polyene antibiotics continue to attract a great deal of attention due to both theoretical and practical aspects [1–3]. A polyene antibiotic (S-232) was isolated [4] in the BIOGAL Pharmaceutical Works from *Streptomyces fradiae* [5] found in a soil of Eastern Hungary. The fermentation fluid [4] was acidified with oxalic acid, the mycelium was filtered off and then repeatedly extracted with acetone. After evaporating the solvent, the remaining solid was extracted with methanol. The crude material obtained after evaporating the methanol was purified by repeated crystallizations from methanol. The pure product was paper-chromatographically homogeneous in at least 90% [Whatman 1 paper; solvent systems: (1) methyl isopropyl ketone : : methanol : water (50 : 1 : 0.4) and (2) methyl isobutyl ketone : 1-butanol : : water (50 : 15 : 3) visualization: UV light].

We report herewith our structural studies on this antibiotic, named cogomycin (**I**), which is now shown to have gross structure A identical with that of fungichromin [6] and lagosin [7, 8].

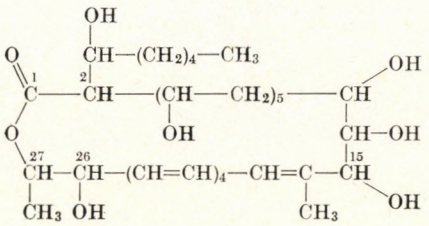

A

The UV spectrum of cogomycin [m. p. 190–210 °C (dec.); $[\alpha]_D^{25}$ – 157° (in methanol, $c = 0.25$); λ_{max}^{EtOH} (nm) (log ε): 357 (4.93), 339 (4.94), 322 (4.69), 309 (4.34), 295 (3.90)] shows that **I** contains a methylpentaene chromophore [9] which is not conjugated to a C=O group [10]. The IR spectrum (KBr) indicates a conjugated polyene chain (1005 cm^{-1}), and unconjugated C=O group (1730 cm^{-1}) and a large number of OH groups, in addition to aliphatic

groups. Its 100 MHz ^{1}H-FT-NMR spectrum (δ C_5D_5N) contains methyl peaks at 0.82 (m), 1.62 (d, **J** = 6.5 Hz) and 2.06 (s), a methylene peak (1.32, m), as well as peaks of olefinic protons (6—7.2, m). A tripletlike multiplet at 3.2 of approximately one proton corresponds to the C-2 proton. A strongly distorted quartet occurs at 5.4 ppm which was demonstrated by the spin decoupling method to be coupled with the resonance centered at 1.62 ppm. Thus this quartet corresponds to the C-27 proton.

The mass spectrum of cogomycin-polyacetate [m. p. 75—80 °C; $[\alpha]_D^{25}$ + 33° (in methanol, c = 0.45)] showed a molecular ion at m/e 1090.498 ($C_{55}H_{78}O_{22}$). Additionally, the mass spectrum showed ions for losses of one to ten acetic acid units. These correspond to ten hydroxyl groups in **I**, to a molecular weight of 670, the molecular formula being $C_{35}H_{58}O_{12}$.

For the identification of the part between the C-15 and C-26 carbon atoms, **I** was successively treated with K_2CO_3 and $NaIO_4$. 2-Methyl-2,4,6,8,10-dodecapentaenedial (**II**) was obtained (m. p. 135—143 °C, lit. [7] m. p. 145—147 °C), identified by its spectral characteristics: UV λ_{max}^{EtOH} (nm) (log ε): 398 (4.857), 381 (4.861), 280 (3.71); IR (KBr): 3030, 2990, 2721, 1670, 1610, 1569, 1015, 1005 cm^{-1}; ^{1}H-NMR (δ $CDCl_3$): 1.91 (3H s $\underline{CH}_3-\underset{\underset{CHO}{|}}{C}=C$), 6.08—7.1 (9H m $\underline{CH}=$), 9.42 (1H s $O\underline{HC}-\underset{\underset{CH_3}{|}}{C}=$), 9.55 (1H d $O\underline{HC}-CH=$). The mass spectrum exhibits a molecular ion at m/e 202.0981 ($C_{13}H_{14}O_2$) which can lose a CHO group. Addition of $NaBH_4$ to the EtOH solution of **II** resulted in a radical change in the UV spectrum: λ_{max}^{EtOH} (nm) (log ε): 350 (4.94), 333.5 (4.95), 317.5 (4.73), 305 (4.40) and 290 (3.98), indicating a pentaene chain not conjugated to a C=O group.

When the above reaction sequence was carried out in the reverse order, *i.e.* the vicinal glycol cleavage preceded the ester hydrolysis, 12,13-dihydroxy-2-methyl-2,4,6,8,10-tetradecapentaenal (**III**) was obtained (m. p. 112—117 °C, lit. [7] m. p. 117—121 °C). **III** had the following spectral properties: UV λ_{max}^{EtOH} (nm) (log ε): 375 (4.71), 265 (3.98); IR (KBr): 3410, 3018, 2720, 1660, 1615 1004 cm^{-1}; ^{1}H-NMR (δ $CDCl_3$): 1.13 (3H d $\underline{CH}_3-CH<$), 1.86 (3H s $\underline{CH}_3-C=$), 3.02 (2H s $O\underline{H}$), 3.90 (1H m H-12), 4.16 (1H m H-13). The mass spectrum showed a molecular ion at m/e 248.1411 ($C_{15}H_{20}O_3$). On treatment of the EtOH solution of **III** with $NaBH_4$ an UV spectrum characteristic of pentaenes not conjugated to a C=O group was obtained which was almost identical with the corresponding spectrum of **II**.

Upon hydrogenation (Pd-C, MeOH; hydrogen uptake 4.8—5.2 moles) **I** gave a white compound [m. p. 157—167 °C; $[\alpha]_D^{25}$ + 1.76 (in methanol, c = 2.0); IR (KBr): 1719 (C=O), 841, no bands at 1005 and between 3000 and 3100 cm^{-1}], from which upon successive $NaIO_4$ and KOH treatment a

paraffinlike compound was isolated [m. p. 25—30 °C; IR (liquid film) 3400, 2713, 1728 cm^{-1}; ^{1}H-NMR (δ $CDCl_3$): 1.10 (3H d CH_3—CH<), 1.14 (3H d CH_3—CH<), 2.36 (1H m CH—CHO), 9.56 (1H d CHO)]. On the basis of spectroscopic evidence, we assign structure **IV** to this compound. In the mass spectrum the detectable ion of highest mass occurs at m/e 213.1071 ($C_{13}H_{25}O_2$). This ion and the abundant ions at m/e 45 and 57 can be rationalized by the following fragmentation cleavages:

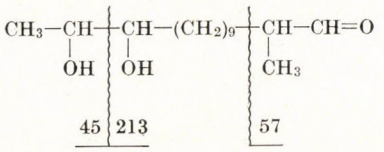

IV

The structures of **II**, **III** and **IV** and their methods of preparation indicate that the ester (lactone) is closed at C-26 or C-27, *i.e.* one of the two OH groups is masked.

In order to identify the side chain on C-2, **I** was subjected to a base-catalyzed retro-aldol cleavage. Capronaldehyde and also a small amount of acetaldehyde were isolated as their 2,4-dinitrophenylhydrazones.

Hydrogenation of **I** (Pd-C, MeOH) followed by reduction of the C-1 carbonyl group with $LiAlH_4$ gave a solid (neither C=C nor C=O bands in the IR spectrum) which, upon pertrimethylsilylation yielded a colourless gum (**V**) whose mass spectrum showed no molecular ion. The ions observed in the mass spectrum can be derived from the molecular ion of the proposed structure (see below) by assuming elimination of the trimethylsilanol (TMSOH) units, cleavage of the skeleton at β position to the TMSO groups, or by combination of these processes. The mass spectrum of **V** and the interpretation of the important peaks are as follows: m/e (%): 1431 (0.5); 1368 (0.2) M—2TMSOH; 1341 (0.1) 1431—TMSOH; 1278 (0.7) M—3TMSOH; 1251 (0.1) 1431—2TMSOH; 1188.773 (0.7) $C_{59}H_{128}O_8Si_8$, M—4TMSOH; 1175 (0.3); 1085 (0.6) 1175—TMSOH; 989 (0.3); 899 (0.3) 989—TMSOH; 803 (0.8); 713 (1.1) 803—TMSOH; 701 (2.4); 611.3784 (2.7) $C_{31}H_{63}O_4Si_4$, 701—TMSOH; 577.8868 (13) $C_{28}H_{65}O_4Si_4$; 521 (11) 701—2TMSOH; 475.8516 (23) $C_{24}H_{55}O_3Si_3$; 385 (18) 475— TMSOH; 357.2639 (17) $C_{19}H_{41}O_2Si_2$, 475—118; 217.1070 (29) $C_9H_{21}O_2Si_2$; 191 (39); 173.1360 (100) $C_9H_{21}OSi$; 117 (12); 73 (33). Moreover, from the chemical formula of **V** (see M—4TMSOH fragment) it also follows that in cogomycin the ester function must be a lactone, since **V** contains the same number of carbon atoms as A, in addition to that of the TMS groups.

The mass spectra of pertrimethylsilyl-cogomycin (**VI**) and pertrimethylsilyl-decahydrocogomycin (**VII**) were also recorded. The upper parts of these spectra are practically identical with the published partial mass spectra of the

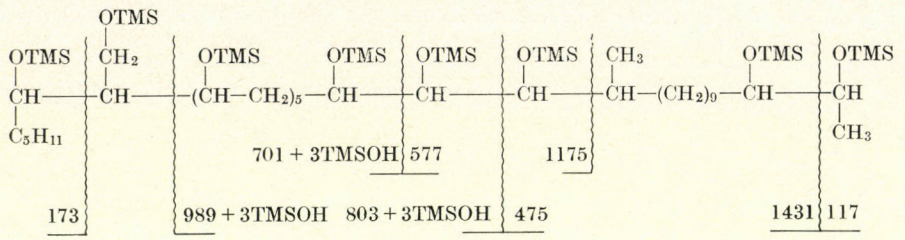

V

trimethylsilyl derivatives of lagosin and decahydrolagosin, respectively [8]. The lower mass regions of the spectra of **VI**, **VII** and pertrimethylsilyl-lagosin exhibit ions corresponding to fragmentation of the skeleton. Localization of the pentaene unit and the position of lactonization can be confirmed by means of these ions.

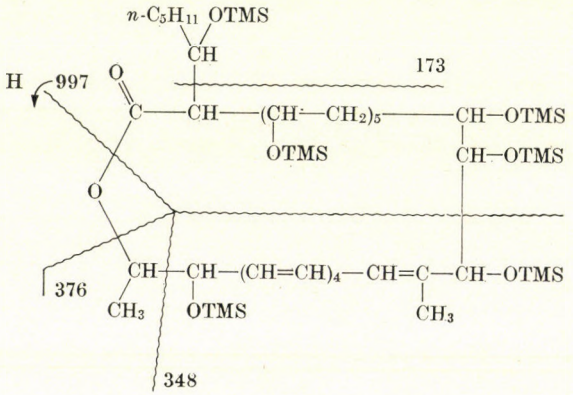

VI

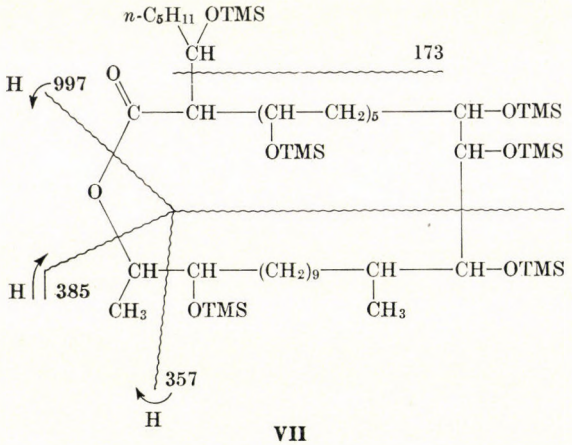

VII

Concerning the relationship between cogomycin and lagosin which, in turn, could not be differentiated from fungichromin [7], it should be noted that there are some differences between the $[\alpha]_D$ values and also in the relative intensities of the CD maxima [CD cogomycin λ_{max}^{EtOH} (nm) ($\Delta\varepsilon$): 357 (−5.16), 338 (−5.65), 323 (−4.56), 309 (−2.48), 246 (+6.85); CD lagosin: 357 (−4.24), 338 (−4.67), 323 (−3.11), 309 (−1.84), 246 (+4.38)]. These small differences can be interpreted by differences in the absolute configuration at one or more chiral centres, or simply by the possible presence of closely related substances having different spectral properties.

Accordingly, this is the third case of isolating a polyene antibiotic of the same gross structure as a metabolite produced by microorganisms found in different soil samples.

*

This work was supported by the BIOGAL Pharmaceutical Works, Debrecen. Thanks are due to Dr. A. LÉVAI, Debrecen (CD spectra), Dr. R. W. RICKARDS, Canberra (mass spectrum of pertrimethylsilyl-lagosin), Dr. S. SZABÓ, Debrecen (IR spectra), Dr. L. SZILÁGYI, Debrecen (100 MHz ^{1}H-NMR spectra), Dr. V. THALLER, Oxford (samples of lagosin) and to Dr. T. WIRTHLIN, VARIAN AG, Zug (^{1}H-FT-NMR spectrum of cogomycin and spin decoupling experiments).

REFERENCES

[1] RINEHART, K. L., JR., LEAR, G. E.: Antibiotics. In "Biochemical Applications of Mass Spectrometry", Ed. WALLER, G. R., John Wiley and Sons, New York 1972
[2] KELLER-SCHIERLEIN, W.: Fortschr. Chem. org. Naturst. **30,** 313 (1973)
[3] HAMILTON-MILLER, J. M. T.: Bacteriol. Rev. **37,** 166 (1973)
[4] HARCSA, J., HORVÁTH, F., KASZAB, I., PINTÉR, L., TÓTH, O., TÓTH, N., VÉGH, J.: Hungarian Pat. 164, 195 (1972)
[5] Determined by SZABÓ, J. of the Institute for Soil Sciences and Agrochemistry of the Hungarian Academy of Sciences
[6] COPE, A. C., BLY, R. K., BURROWS, E. P., CEDER, O. J., CIGANEK, E., GILES, B. I., PORTER, R. F., JOHNSON, H. E.: J. Am. Chem. Soc. **84,** 2170 (1962)
[7] DHAR, M. L., THALLER, V., WHITING, M. C.: J. Chem. Soc. **1964,** 842
[8] GOLDING, B. T., RICKARDS, R. W., BARBER, M.: Tetrahedron Letters **1964,** 2615
[9] OROSHNIK, W., MEBANE, A. D.: Fortschr. Chem. org. Naturst. **21,** 17 (1963)
[10] SCHLEGEL, R., THRUM, M.: Experientia **24,** 11 (1968)

Vince POZSGAY; 4042 Debrecen, Hungary
József TAMÁS, Gábor CZIRA } 1088 Budapest, Puskin u. 11—13. Hungary.

Acta Chimica Academiae Scientiarum Hungaricae, 85 (2), pp. 221—232 (1975)

COPOLYMERIZATION OF 3-METHYL-1-PENTYN-3-OL WITH *p*-DIETHYNYLBENZENE

V. BULACOVSCHI and CR. SIMIONESCU

(Macromolecular Chemistry Department, Polytechnical Institute of Jassy, Romania)

Received December 18, 1973

The copolymerization of 3-methyl-1-pentyn-3-ol (MP) with *p*-diethynylbenzene (*p*-DEB) was investigated, using palladium triphenylphosphine as catalyst. A mechanism is suggested for the copolymerization reaction.

Structural investigations on the obtained copolymers show the insertion of the *p*-DEB units into the poly (MP) chains. This gives rise to changes in the electrical and thermal properties of the products. Both the copolymers and the homopolymers had low crystallinity indices.

Investigations on the synthesis of polymers and copolymers from acetylene and its derivatives [1—7] are more and more numerous, although the polymerization presents some difficulties. Acetylenic monomers are less reactive than vinyl monomers, and the polymeric products have lower molecular weights.

Attempts have been made to prepare polymers with conjugated structure for utilization as semiconductors. In these experiments some new monomer systems and the catalytic efficiency of new catalysts were investigated. Transition metal complexes or transition metal salts were found effective for the polymerization of acetylenic monomers [8, 9].

In the present work, palladium triphenylphosphine (TFF-Pd) was used in the copolymerization of 3-methyl-1-pentyn-3-ol (MP) with *p*-diethynylbenzene (*p*-DEB), and the micro- and macrostructure of the obtained copolymers and some of their electrophysical properties were investigated.

Using *p*-DEB as a second component in the reaction mixture, we tried to accomplish the improvement of the electrical and mechanical properties of poly(methylpentynol) as a consequence of chain cross-linking which occurs during the copolymerization process.

Experimental

Materials

p-Diethynylbenzene was prepared and purified by sublimation as described by HAY [10]. 3-Methyl-1-pentyn-3-ol (Air Reduction Chemical Co.) was distilled at normal pressure before utilization. The catalyst TFF-Pd was prepared and purified as described in the literature [11]. All solvents used for the solution polymerization were chemically pure; they were distilled before utilization.

Copolymerization

The mixture made of MP (0.045 mol) and different quantities of *p*-DEB, were placed in a round-bottom flask fitted with a condenser and containing the catalyst (molar ratio MP: TFF-Pd = $3.1 \cdot 10^2$). The reaction was carried out in a silicone oil bath at 130 ± 0.5 °C. The copolymer was dissolved in acetone and precipitated by pouring the solution into a large amount of acid-containing (HCl) water. After filtration and washing with water, the copolymer was dried in vacuum over P_2O_5, then extracted with ether at room temperature. The poly (MP) homopolymer and unreacted monomers are soluble in this solvent. For comparative studies polymers of MP were synthesized by the bulk polymerization method, using the same catalyst. In this case the reaction was run at the boiling point of the monomer. With the same purpose, MP was polymerized in DMF solution, using $PdCl_2$ catalyst.

Characterization of the copolymers

The UV spectra of the copolymers were recorded in MeOH solution with a "CF_4— Optica Milano" spectrometer. Vibration spectra were obtained in KBr pellets with a "UR-20 Karl Zeiss-Jena" apparatus. For the NMR spectra $CDCl_3$ solvent and tetramethylsilane internal standard were used. The measurements were made at 25 °C with a 60 MHz JEOL spectrometer. Electron microscopic studies were run on a JEM-120 equipment; for better visualization, the samples were metallized in vacuum. Diffraction spectra of the obtained products were performed on a "Kristalloflex-4-SIEMENS" apparatus with Cu cathode, Ni filter and registering goniometer.

Results and discussion

Table I summarizes the conditions of preparation and some of the characteristics of the obtained copolymers. One can see the influence of the temperature and reaction time on the conversion of the monomers. As shown, an increase of the *p*-DEB quantity in the starting monomer mixture lowers the

Table I

The bulk copolymerization of MP with p-DEB
(molar ratio MP : TFF-Pd = $3.1 \cdot 10^2$)

Exp. No.	Molar ratio MP/*p*-DEB	Temp., °C	Time, hr	Conversion, %	Ether solubility, %	Mn[b]	Softening range, °C
1	20	130	12	92.80	100	—	130—135[a]
2	20	130	8	80.1	100	430	130—135[a]
3	10	130	8	84.37	90.1	619	155—180[a]
4	5	130	8	85.32	31.28	—	>260 >260
5	2.5	130	8	87.32	8.0	—	>260
6	10	100	6	65.5	90.75	—	—
7	10	100	10	76.6	55.5	—	—

[a] The softening range refers to the soluble fraction
[b] The molecular weight was determined by the cryoscopic method in dioxan

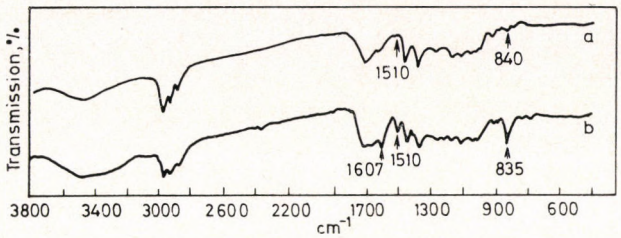

Fig. 1. IR spectra of the MP-*p*-DEB copolymers (Table I). (a) Copolymer soluble in ether (No. 3). (b) The insoluble copolymer (No. 5)

ether solubility of the copolymer. From the structural point of view, the soluble fraction should be regarded as poly(MP) which has randomly inserted *p*-DEB units in the molecular chain. Even the softening temperature (155—180 °C) of the soluble copolymer is shifted to higher values compared with bulk-polymerized poly(MP), prepared with the same complex as catalyst (125—135 °C) [12]. The ether-insoluble copolymer is slightly soluble in methanol, acetone or dioxan; depending on the rate of feeding of the monomer and on the reaction temperature, the solubility varies between 5 and 25%.

The presence of *p*-DEB in the copolymers was proved by the electronic and vibration spectra. In the IR spectra shown in Fig. 1, besides the absorption bands due to MP, one can see the characteristic peaks of the *p*-substituted phenyl ring. More pronounced are the absorption maxima at 835 cm^{-1}, 1510 cm^{-1} and 1607 cm^{-1}; their intensity is much lower in the soluble fraction (a) than in the spectra of the copolymer which is insoluble in ether (b). The weak

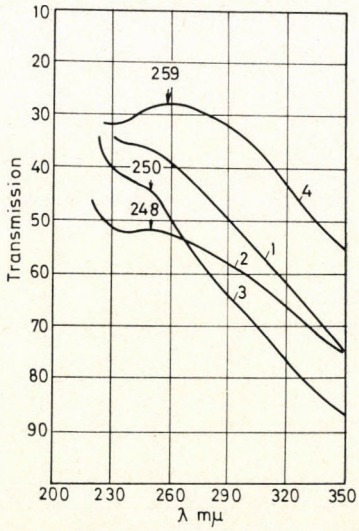

Fig. 2. UV spectra of the MP-*p*-DEB copolymers (solvent : methanol). [The notations refer to the copolymers in the order: No. 2, 3, 5, 7 (Table I)]

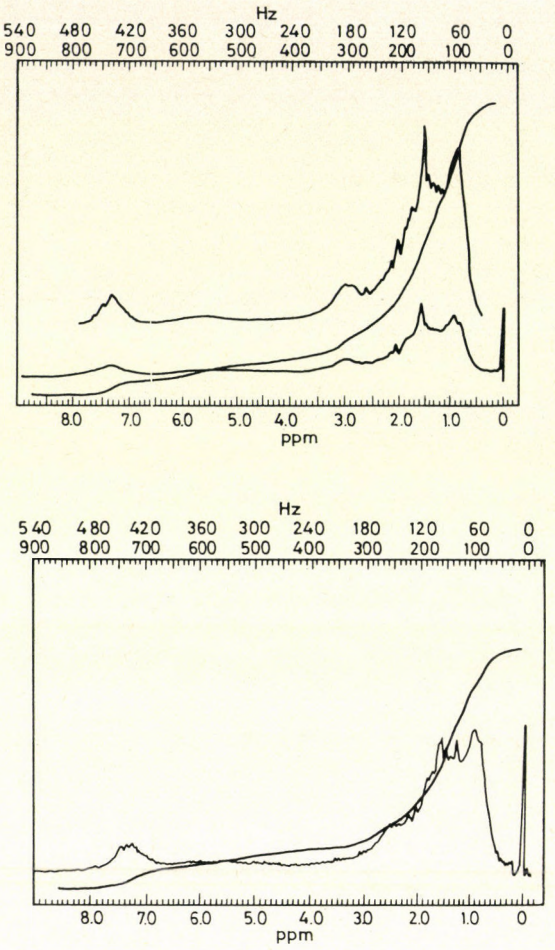

Fig. 3. NMR spectra of the copolymers: (a) No. 2; (b) No. 3 (Table I)

band at 1000 cm^{-1}, which in the MP homopolymer was assigned to *trans*-transoidal conjugated systems [12], is less marked in the copolymers. For both products a broad absorption is present in the region 1650—1730 cm^{-1}. Literature data [13] assign this maximum to the coupling of the C=C stretching vibrations of double bonds and the OH bending vibrations of the alcoholic groups from the MP monomer units.

The UV spectra have, in general, very broad bands in the 240—260 mμ region (Fig. 2), characteristic of the benzene ring. However, for the products from experiments Nos 2 and 3, a small shoulder appears at 240—248 mμ, which finally becomes a distinct maximum at 248 mμ (Curve 2). A similar spectrum was found for the copolymer from experiment No. 7 (Table I) where there is a marked maximum at 260 mμ. The shift to longer wavelengths of the

absorption maxima reveals an extension of the conjugated system as the benzene ring is built into the poly(MP) chains.

The NMR spectra also prove the presence of *p*-DEB in the copolymer chains. Starting from the higher fields, one can see a broad maximum at $\delta =$ $= 0.5-2.6$ ppm (Fig. 3a) and $\delta = 0.3-2.2$ ppm (Fig. 3b) assigned to the aliphatic protons from the radical attached to the acetylenic carbon of the MP units. A strong maximum appears at different fields which should be assigned to the OH resonance. For the MP : *p*-DEB = 20 molar ratio this maximum is well outlined at $\delta = 2.35$ ppm, but it is slightly shifted to higher fields ($\delta = 2.5$ ppm) in the MP : *p*-DEB = 10 copolymer. In the latter case, practically it merges with the aliphatic proton absorption.

The spectra in the $\delta = 6.8-7.7$ ppm range are similar for both analyzed products, showing the absorption of aromatic unsubstituted protons. There is a good correlation between the intensity increase of the signal (product from experiment No. 3) and the modifications in the ratio of the starting monomer mixture.

Table II

Exp. No.	Molar ratio MP/*p*-DEB	Solubility in ether	Elemental analysis [a] %	
			C	H
2	20	soluble	71.07	6.20
3	10	soluble	72.50	6.78
3	10	insoluble	70.24	5.91

[a] After burning, a small amount of ash is left

The elemental analyses summarized in Table II show practically the same composition for both products. A slightly higher carbon content can be seen for the soluble fraction from the copolymer No. 3. On the basis of the elemental analyses, the copolymer composition should correspond to the MP : : *p*-DEB = 10 molar ratio.

Regarding the polymerization of acetylene derivatives with complex catalysts, some reaction mechanisms are proposed in the literature [8, 13—15], which essentially start from the idea that the polymerization promoter takes part in the acetylide formation. In the studied system the quantity of the starting monomers is much higher than that of the catalyst. Thus diacetylide formation appears to be certain, where obviously there is a competition between the two monomers. According to its structure and reactivity, *p*-DEB will co-ordinate two molecules of TFF-Pd, and the binding of MP is possible at the two acetylide groups:

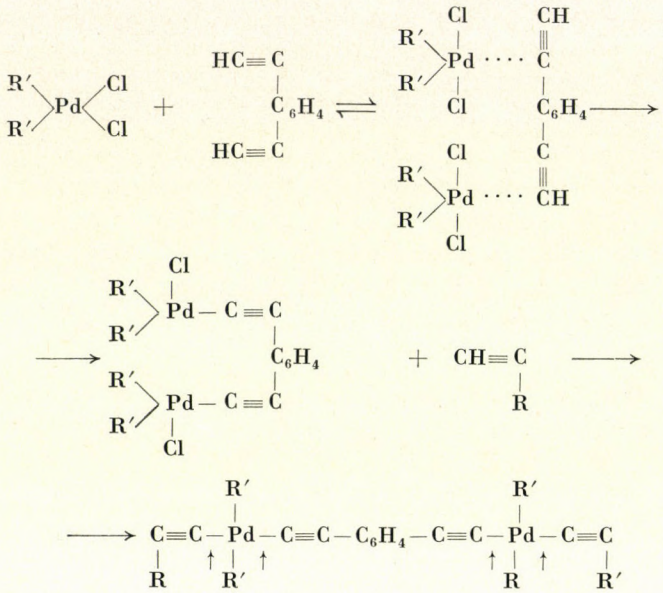

The chain growth consists in coordination followed by the binding of the monomer units (MP or *p*-DEB) in both directions (in the places indicated by arrows). Because of the reaction conditions and the big excess of the MP monomer, the MP diacetylides will be encountered more often:

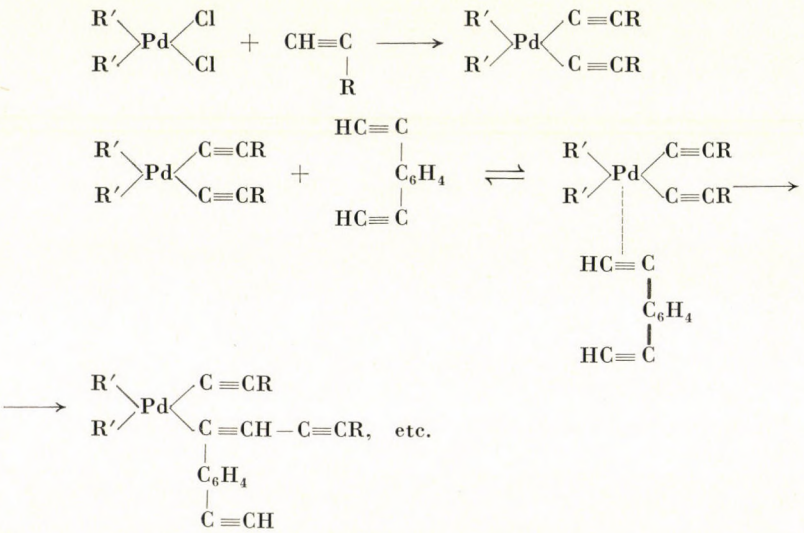

In these schemes R' represents $(C_6H_5)_3P$, and R is $HO-\overset{|}{C}(CH_3)-CH_2-CH_3$

The TFF-Pd bound to the free acetylenic group will give a new reaction center and, at the same time, the possibility of cross-linking in the product.

Diffraction studies on the copolymers, as well as on the poly(methylpentynol) homopolymers taken for comparison, showed rather low crystallinity indices (Table III). The structure of the poly(MP) chains is, as a result of hy-

Table III

Structural properties of polymers and copolymers from MP and p-DEB

No.	Sample	Type of polymerization	Catalyst	Molar ratio MP/TFF-Pd (concentration)	Reaction temperature, °C	Crystallinity index, %
8	Poly (MP)	bulk	TFF-Pd	$6.2 \cdot 10^2$	reflux	23.70
9	Poly (MP)	bulk	TFF-Pd	$3.73 \cdot 10^2$	reflux	22.21
10	Poly (MP)	bulk	TFF-Pd	$2.5 \cdot 10^2$	reflux	19.14
11	Poly (MP)	DMF solution	$PdCl_2$	$3.67 \cdot 10^{-2}$mol/l	100	16.03
12	Poly (MP	DMF solution	$PdCl_2$	$3.67 \cdot 10^{-2}$mol/l	85	15.00
13	Poly (MP)	DMF solution	$PdCl_2$	$3.67 \cdot 10^{-2}$mol/l	25	19.08
2[a]	Copolymer MP : *p*-DEB = 20	bulk	TFF-Pd	$3.1 \cdot 10^2$	130	26.76
3[b]	Copolymer MP : *p*-DEB = 10	bulk	TFF-Pd	$3.1 \cdot 10^2$	130	23.69
4[b]	Copolymer MPa : *p*-DEB = 5	bulk	TFF-Pd	$3.1 \cdot 10^2$	130	20.61

[a] Copolymer soluble in ether
[b] Copolymer insoluble in ether

drogen bonding, slightly modified by copolymerization with *p*-DEB. The crystallinity is a little higher in spite of its decrease with molar ratio modification. Lower crystallinity indices were found when solution polymerization of the MP was made; at the same time, an opposite dependence was observed between the reaction temperature and crystallinity. The highest molecular weight ($\overline{M}n = 1020$) was measured for the product made at 25 °C. The diffractograms of the polymers and copolymers (Fig. 4) are similar, showing two distinct maxima at $2\Theta = 17°$ and $2\Theta = 9.5°$. This must be so because of the similar structures of both products, the polymers and copolymers.

There is little information in the literature on the morphological structure of the polymers from acetylene and its derivatives [16, 17], as these investigations are in the stage of beginning. The electron microscopic pictures for the above copolymers and polymers (Fig. 5) are characterized by a complex globular structure. Often their concatenation into linear formations can be seen. A more ordered and looser structure appears in the case of the copolymer; this should be due to the influence of the *p*-DEB monomer units taking part

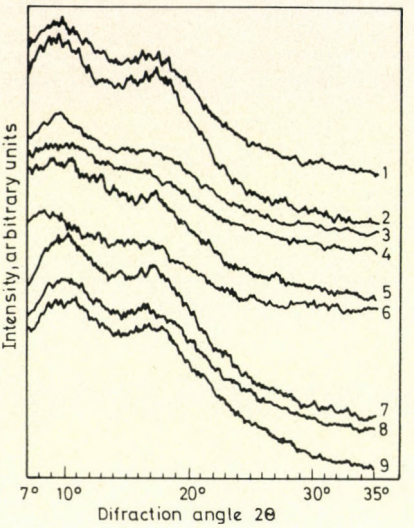

Fig. 4. Diffraction spectra of the polymers and copolymers from MP and MP + *p*-DEB. (Notations according to Table III)

in the structure. The same conclusions can be drawn from a comparison of the crystallinity indices calculated for the two products (26.76% and 22.21%, respectively).

The electrical properties of the homopolymers and copolymers were also investigated (Table IV). Measurements on a d. c. bridge between 25 and 90 °C

Table IV

Electrical characteristics of the polymers and copolymers from MP and MP- p-DEB (catalyst: TFF-Pd)

No.	Sample	Reaction time, hr	Molar ratio MP/TFF-Pd	$\sigma_{50}°$ ohm^{-1}cm^{-1}	$E_{a_{1/2}}$ eV	ΔH gauss	Spin/g
10	Poly (MP) (bulk)	24	$2.5 \cdot 10^2$	$<10^{-16}$	2.12	—	—
9	Poly (MP) (bulk)	24	$3.73 \cdot 10^2$	$7.58 \cdot 10^{-15}$	1.49	8.0	$1.02 \cdot 10^{19}$
2[a]	Copolymer (MP: *p*-DEB = = 20)	8	$3.1 \cdot 10^2$	$3.16 \cdot 10^{-14}$	1.65	7.2	$1.42 \cdot 10^{19}$
5	Copolymer (MP: *p*-DEB = = 2.5)	8	$3.1 \cdot 10^2$	$\sigma_{25°} = 5.4 \cdot 10^{-15}$	—	7.6	$1.64 \cdot 10^{19}$

[a] soluble fraction

showed poor conductivities, close to the upper limit of insulators. Better semiconducting properties are obtained for the copolymers in the case of double

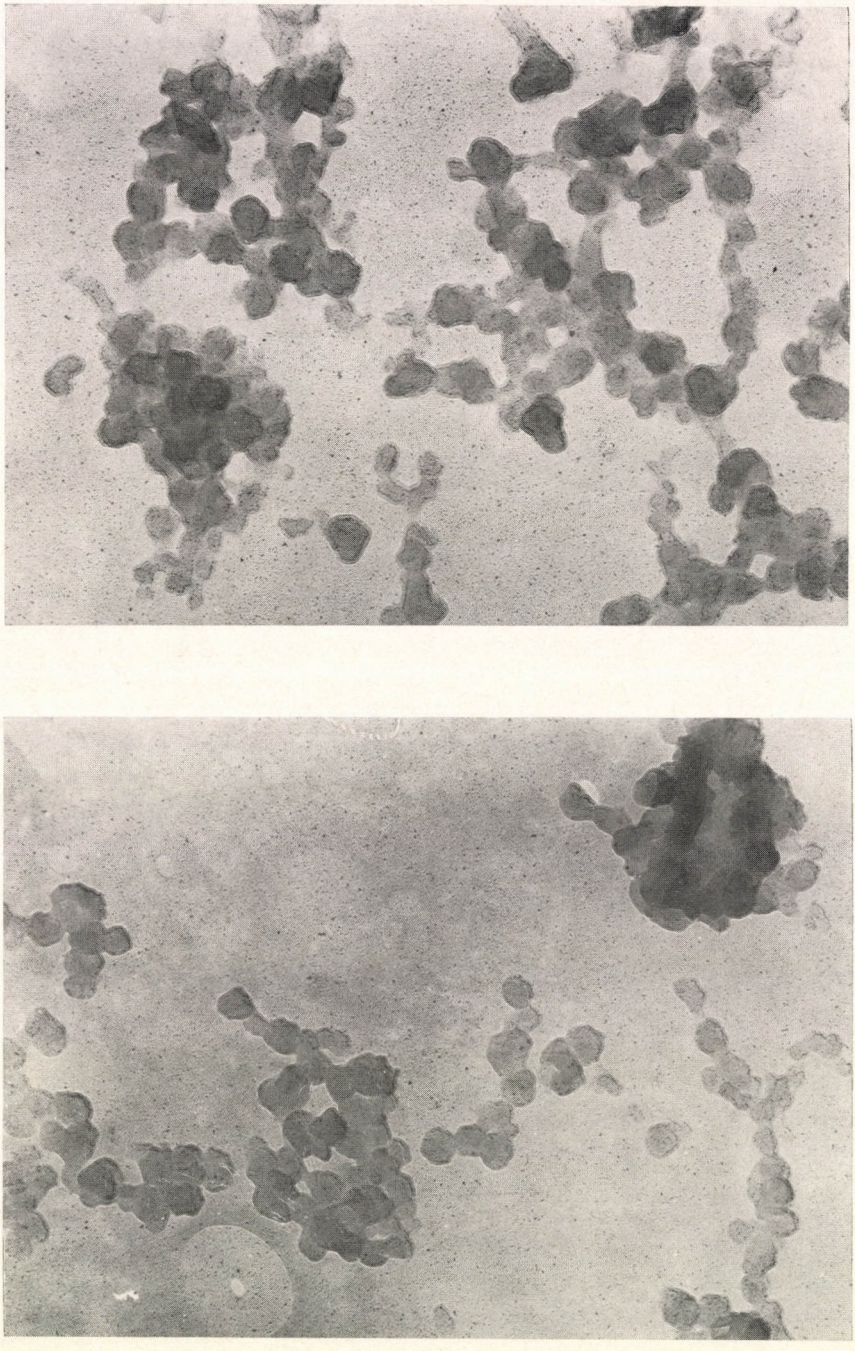

Fig. 5. Electron microscopic structures (a) the copolymer (No. 2), (b) Poly (MP), bulk-polymerized (No. 9) (magnification: $\times 51{,}000$)

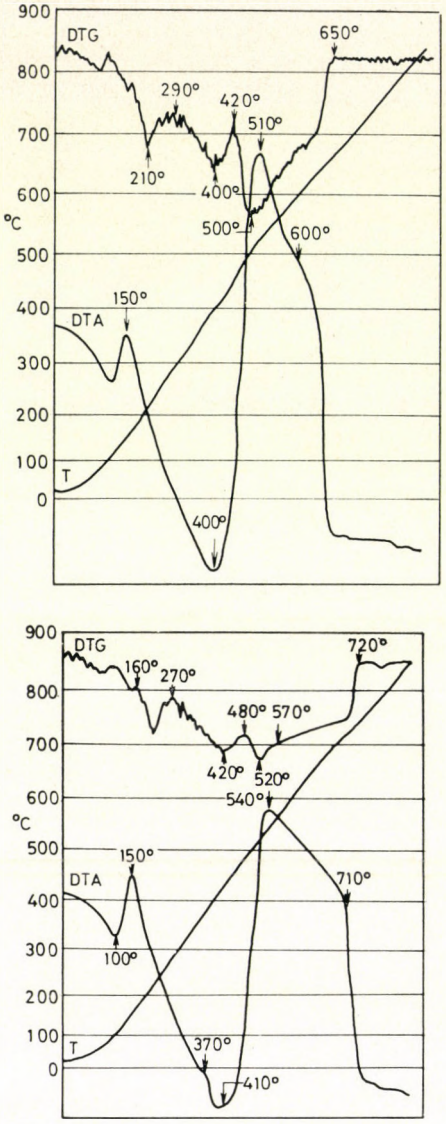

Fig. 6. Decomposition thermograms of the polymers and copolymers. (a) Poly (MP), bulk-polymerized (No. 10). (b) The copolymer MP-*p*-DEB = 2.5 (No. 5) (TG = 50 mg)

bond extension. The copolymer made from a monomer mixture of MP : *p*-DEB = 2.5 ratio, was a powderlike material which could not be compressed into pellets. Nevertheless, the measured conductivity at 25 °C (in powder) suggested better properties at higher temperatures. For all analyzed samples a linear dependence could be established between lg σ and 1/T, which is characteristic of semiconductors. The activation energies are, in general, close

for the two kinds of products and similar to the literature data. For the copolymer No. 2 (Table IV) the temperature dependence of the conductivity shows two values of the activation energy. The difference between the two values can be explained in terms of conductivity-type modification with temperature.

The polymers give narrow symmetrical ESR signals ($\Delta H_{max} = 7-8$ gauss) which lack hyperfine structure. They show high concentrations of unpaired spins, without significant difference between the analyzed samples. Very likely, there is little relationship between the tape of the polymer and the ESR intensity. For the insoluble polymer a higher spin concentration was expected owing to a more extensive conjugation resulting from the interposition of benzene rings between the poly(MP) chains (compare Nos 9 and 5). It seems that even the nature of the ESR signal cannot be closely correlated with the π-electron delocalization in a conjugated system.

There are some differences between the types of the synthesized products regarding their behaviour on heating. The thermograms show very complex processes, accompanied by great caloric effects, which are difficult to disentangle (Fig. 6). Such effects indicate some internal structural modifications involving hydroxylic functional groups. Both products have similar weight losses and, naturally, the homopolymer shows greater destruction as a reflection of its particular structure.

All polymers and copolymers based on MP and *p*-DEB are characterized by good thermal stability up to 250 °C. Above this temperature weight losses are more pronounced. Somewhat different behaviour is shown by the copolymer with MP : *p*-DEB = 2.5 molar ratio. This product with a cross-linked structure had the best thermal stability; weight losses exceeding 50% were observed only above 600 °C.

Conclusions

The copolymerization of MP with *p*-DEB gives more or less cross-linked products depending on the molar ratio in the starting monomer mixture. Double-bond conjugation is more extended in the copolymers as reflected by their thermal behaviour and electrical properties.

Spectral studies on the copolymers have shown that *p*-DEB is built into the macromolecular chain. Comparing the aromatic proton signal intensities, it seems that the copolymer structure depends on the initial monomer composition, even if the elemental analyses do not bring out the difference.

It is somewhat puzzling why the polymers and copolymers made with this catalyst have so low crystallinity indices.

REFERENCES

[1] PRICE, C. C., GREEN, C. E.: J. Polymer Sci. **6,** 111 (1951)
[2] DOAK, K. W.: J. Am. Chem. Soc. **72,** 4681 (1950)
[3] HAY, S. A., BOLON, D. A., LEIMAR, K. R.: J. Polymer Sci. A-**1, 8,** (4), 1022 (1970)
[4] PRICE, C. C., MCKEEN, T. F.: J. Polymer Sci. **41,** 445 (1959)
[5] KRYAZEV, I. G., SEMENOVA, E. F., CERKASHIN, M. I.: Izv. AN SSSR, **1967,** 713
[6] HIGASHIMURA, H.: Kogyo Kagaku Zasshi **69,** 1243 (1966)
[7] WALACH, J., MANASEN, J.: Polymer Sci. A-**1,** 7, 1983 (1969)
[8] FURLANI, A., COLLAMATI, I., SARTORI, G.: J. Organometallic Chem. **17,** 463 (1969)
[9] BRAILOVSKII, S. M., KALIYA, O. L., TEMKIN, O. N., FLID, R. M.: Kinet. i Kataliz **9,** 177 (1968)
[10] HAY, A. S.: J. Org. Chem. **25,** 4, 637 (1960)
[11] ITATANI, H., BAILAR, JR., J. C.: J. Am. Oil Chemists' Soc. **44,** 147 (1967)
[12] BULACOVSCHI, V.: Doctoral Thesis, Polytechnical Institute of Jassy, 1973
[13] FURLANI, A., BICEV, P., CARUSI, P., RUSSO, M. V.: J. Polymer Sci. B-**9,** 19 (1971)
[14] MERIWETHER, L. S., COLTHUP, E. C., KENERLY, G. W.: J. Org. Chem. **26,** 5155 (1961); *ibid.* **26,** 5163 (1961)
[15] SIMIONESCU, CR., DUMITRESCU, SV., PERCEC, V., NEGULESCU, I., DIACONU, I.: J. Polymer Sci. Pt. C, **42,** 201 (1973)
[16] BERLIN, A. A.: J. Macromol. Sci. Chem. A-**5, 7,** 1187 (1971)
[17] SIMIONESCU, CR., DUMITRESCU, SV., LEANČA, M., DĂRÎNGĂ, M., GROVU, M.: Rev. Roum. Chim. **17,** 304 (1972)

V. BULACOVSCHI
CR. SIMIONESCU
Macromolecular Chemistry Department,
Polytechnical Institute of Jassy, 23 August 11 A. Jassy,
Romania.

INDEX

PHYSICAL AND INORGANIC CHEMISTRY — PHYSIKALISCHE UND ANORGANISCHE CHEMIE — ФИЗИЧЕСКАЯ И НЕОРАНИЧЕСКАЯ ХИМИЯ

LENGYEL, T.: Investigations on Ion-exchange Equilibria with Radioactive Tracer Method, XVIII. Determination of the Stability Constant of $Cd_2(OH)_2^{2+}$ with the Aid of Ion-exchange Technique 125

KHADIKAR P. V. and AMERIA R. L. Studies on Some 5-Nitrosalicylate Complexes .. 131

PAÁL, T. and BARCZA, L.: The Formation of Ethylene Glycol–Borates in Aqueous Medium, I. 139

RYTTER, E.: On the Classification of Normal Modes of Vibration, II. The Interaction Terms in Energy Distributions 147

SÓVÁGÓ, I., GERGELY, A. and POSTA, J.: Equilibria of Alfa-amino Acid Complexes of Transition Metal Ions, VII. Effect of the Aliphatic Carbon Chain on the Thermodynamics and Structure of Ni(II)-amino acid Complexes 153

POLINSZKY, K., FÜLÖP, J., SEITZ, K. and VAJDA, T.: Approximate Analytical Determination of the Average Values of Potential Functions Occurring in Chemical Transport Phenomena 161

ORGANIC CHEMISTRY — ORGANISCHE CHEMIE — ОРГАНИЧЕСКАЯ ХИМИЯ

SZABÓ, V. and ZSUGA, M.: Cleavage of the Heterocyclic Ring of Isoflavonoids by Nucleophilic Reagents, I. Kinetics Equilibrium Conditions of the Cleavage of the Pyrone Ring of Isoflavone (3-Phenylchromone) in Aqueous Alkaline Medium 179

SZABÓ, V. and ZSUGA, M.: Cleavage of the Heterocyclic Ring of Isoflavonoids by Nucleophilic Reagents, II. Transformations of 2-Hydroxyisoflavanone 191

MEZŐ, I., HAVRÁNEK, M., TEPLÁN, I., BENES, J. and TANÁCS, B.: Labelled Amino Acids and their Derivatives, VI. Preparation of L-Ornithine-[5-^{3}H] and L-Lysine-[6-^{3}H] 201

POZSGAY, V., TAMÁS, J. and CZIRA, G.: The Structure of Cogomycin, a Polyene Antibiotic (Short Communication) 215

BULACOVSCHI, V. and SIMIONESCU, CR.: Co-polymerization of 3-Methyl-1-pentyn-3-ol with *p*-Diethynylbenzene 221

Printed in Hungary

A kiadásért felel az Akadémiai Kiadó igazgatója — Műszaki szerkesztő: Zacsik Annamária

A kézirat nyomdába érkezett: 1975. I. 24. — Terjedelem: 9,8, (A/5) ív, 46 ábra

75.1376 Akadémiai Nyomda, Budapest — Felelős vezető: Bernát György

ACTA CHIMICA
ТОМ 85 — ВЫП 2

РЕЗЮМЕ

Исследование ионообменных равновесий с помощью метода рациоактивных изотопов, XVIII

Определение константы устойчивости $Cd_2(OH)_2^{+2}$ с помощью техники ионного обмена

Т. ЛЕНДЬЕЛ

Используя в качестве жидкого ионообменника ди-2-этилгексил фосфорную кислоту, был изучен двухядерный гидроксо комплекс кадмия.

Было найдено, что при повышенных концентрациях кадмия в области pH = 3 ÷ 4 доминируют частицы свободного металла и общая константа устойчивости $Cd_2(OH)_2^{+2}$ может быть рассчитана за счет некоторых упрощений и оказалось $\lg \beta_{22} = 23{,}9$.

Исследование некоторых комплексов 5-нитросалицилата

П. В. ХАДИКАР и Р. Л. АМЕРИА

Константы образования комплексов 5-нитросалициловой кислоты с Cu(II), Ni(II), Co(II), Mn(II) и Fe(II) были определены методом Кальвина—Бьеррума. Приближенные величины констант образования были определены, исходя из произведено с помощью метода наименьших квадратов. По стабильности комплексы располагаются в следующем порядке: Cu(II) > Zn(II) > Ni(II) > Co(II) > Fe(II) > Mn(II). Связь в комплексах обсуждается на основе иК спектров изолированных комплексов, а их стереохимия на основе магнетохимических исследований.

Образование боратов этиленгликоля в водной среде, I

Т. ПААЛ и Л. БАРЦА

Равновесие, утсанавливающееся в растворе, содержащем 0,01 ÷ 0,02 М борной кислоты, 0,1 ÷ 2,0 М этилен-гликоля и 1,0 М $Na(ClO_4)$ в качестве инертной соли, было исследовано при 25°C pH-метрическим методом. Образуются комплексы боратгликоля с составом 1 : 1 и 1 : 2 с константами устойчивости $\beta_{011} = 1{,}78 \pm 0{,}03$ и $\beta_{012} = 0{,}12 \pm 0{,}03$, соотвественно. Кислоты, соответствующие двум анионам, по крайней мере, в 100 раз сильнее борной кислоты; их образованием можно пренебречь.

Классификация нормальных видов колебаний, II

Выражения взаимодействий в распределениях энергии

Э. РИТТЕР

Сравнивались распределения потенциальной, кинетической и общей энергий в случае 12 молекул, для которых были известны «точные силовые поля». Все эти распределения становятся равными, если выражения взаимодействия равно распределены между соотвествующими координатами симметрии, как полагали Пулай и Тёрёк. Однако, как было показано в данном сообщении, эта процедура не пригодна для некоторых молекул. Предлагалось, чтобы метод распределения общей энергии с отдельным расчетом выражений взаимодействий был использован в классификации нормальных типов колебаний.

Равновесие комплексов α-аминокислот с ионами переходных металлов, VII

Эффект алифатической углеродной цепочки на термодинамические и структурные факторы комплексов Ni(II) с ажинокислотами

И. ШОВАГО, А. ГЕРГЕЙ и Й. ПОШТА

Были произведены p*H*-метрические измерения равновесий с целью определения констант стабильности комплексов Ni(II) с глицином, α-аланином, α-аминобутировой кислотой, норвалином и норлеуцином. Соответствующие им величины энтальпий и энтроний были получены за счет калориметрических исследований. Комплексы глицина обладают чрезвычайной стабильностью, что связано с их более высоким изменением энтальпии. Периодическое изменение, зависящее от парного-непарного числа углеродных атомов, наблюдалось в соотвествующих термодинамических данных в серии от аланина до норлеуцина. На основе спектров комплексов Ni(α-аминокислова)$_2$. $2H_2O$ было установлено, что структура соединений, находящихся в твердом состоянии и в жидком растворе, может значительно различаться. В твердом состоянии удлинение углеродной цепочки вызывает повышенное искажение структуры; подобным образом это выражается в периодическом изменении, зависящем от числа углеродных атомов.

Приближенно аналитическое определение средних величин потенциальных функций в явлениях химического транспорта

К. ПОЛИНСКИ, Й. ФЮЛЁП, К. СЕЙТЦ и Т. ВАЙДА

Был разработан относительно простой метод, позволяющий приближенно аналитическим путем, с некоторыми ограничениями, определить средние величины потенциальных функций в процессах теплового и массового транспорта.

Метод основан на введении вспомогательных функций и сущность приближения сформулирована в смысле вводимых приближений. Приближенная форма вспомогательных функций может быть непосредственно определена с помощью трансформации Лапласа из дифференциального уравнения или системы таких уравнений, описывающих проблему без использования инверсной трансформации.

С помощью числовых расчетов может быть показано, что приближенный метод обладает удовлетворительной надежностью в интервале независимых переменных, представляющий интерес с практической точки зрения.

Разрыв гетерокольца изофлавоноидов с помощью нуклеофильных реактантов, I

Кинетика и условия равновесия раскрытия и отрыва пиронового кольца изофлавона (3-фанилхромона) в водной

В. САБО и М. ЖУГА

γ-Пироновое кольцо изофлавона (I) легко раскрывается уже в мягких условиях (10^{-2} М водная NaOH, комнатная температура) и в зависимости от концентрации гидроксильного иона устанавливается равновесие между изофлавоном, карбанионом VI, 2-гидрокси-α-гидроксиметилендезоксибензоином (II) и 2-гидроксиизофлавоном (VIII).

Энергия и энтропия активации ступени (I – VI), лимитирующей скорость реакции раскрытия кольца, равны $E^* = 12{,}9(\pm 0{,}9)$ ккал/моль и $\Delta S^* = (-13{,}6 \pm 3{,}1)$ кал. моль$^{-1}$. град$^{-1}$, соответственно. Полагается, что раскрытие кольца начитается обратимой, бимолекулярной реакцией присоединения типа An2.

Разложение соединения II до 2-гидроксидезоксибензоина протекает независимо от концентрации гидроксильного иона и намного медленнее, чем раскрытие кольца.

Расщепление гетерокольца изофлавоноидов с помощью нуклеофильных реактантов, II

Превращения 2-гидроксиизофлаванона

В. САБО и М. ЖУГА

Была исследована кинетика превращения 2-гидроксиизофлаванона (VIII) в кислых и щелочных средах. Было установлено, что γ-пиранонное кольцо соединения VIII раскрывается в уже разбавленных водно-щелочных растворах с образованием фанолятного иона (II), как и в случае изофлавона, но лишь с гораздо большей скоростью.

Исходя из результатов можно заключить, что образованию изофлавона из VIII предшествует предварительное мгновенное равновесие, зависящее от pH. Исследование этого предварительного равновесия указывает на то, что изофлавон (I) образуется как прямым, так и косвенным путем из VIII как по механизму кислотного катализа E_1, так и по механизму основного катализа E_1cB в зависимости от H_0 и pH.

Соединение VIII является очень чувствительным к кислоте, щелочи и теплу; в кислоте оно оказалось более стабильным, чем в щелочи. Оно легко теряет как протон при C_3, так и гидроксильную группу при C_2. Поэтому его можно считать метастабильным соединением и относить к С—Н кислотам.

Меченые аминокислоты и их производные, VI

Получение L-орнитина-5-H^3 и L-лизина-6-H^3

И. МЕЗЁ, М. ХАВРАНЕК, И. ТЕПЛАН и Б. ТАНАЧ

γ-Циано-L-α-аминомасляная кислота и δ-циано-L-норвалин были получены из соотвествующих α-тозиловых производных с помощью злектролитического детозилирования. С помощью каталитического гидрирования из γ-циано-L-α-аминомасляной кислоты был получен L-орнитин, а из δ-циано-L-новалина — L-лизин. Восстановление проводили с помощью натрийборгидрида в присутствии никеля Ренея. L-Орнитин-[5 – H^3] и L-лизин-[6 – H^3] были получены с помощью обоих методов. Особенно важным оказалось восстановление с помощью натрийборотритида, чтопозволяет получение соединений с болшой удельной активностью.

Сополимеризация 3-метил-1-пентин-3-ола с п-диэтинилбензолом

В. БУЛАКОВСКИ и К. СИМЬОНЕСКУ

Сополимеризация 3-метил-1-пентин-3-ола (МП) с п-диэтинилбензолом (п–ДЭБ) была исследована, используя в качестве катализатора палладий трифенилосфин. Был предложен механизм процесса сополимеризации.

Структурные исследования полученного сополимера указывают на включение единиц п-ДЭБ в полимерную цепочку поли-(МП). Это отражается на электрических и термических свойствах полученных продуктов. Как сополичеры так и гомополимеры обладают низкими индексами кристалличности.

Säurehydrolyse glykosidischer Bindungen

von J. Szejtli

Die Säurehydrolyse der Glykosidbindungen ist in zusammenfassender Bearbeitung dargestellt. Kapitel 1 behandelt die Kinetik und den Mechanismus der Reaktion. Die bei der Hydrolyse wahrnehmbaren Erscheinungen werden je nach ihrer Zuordnung zu den sog. äußeren oder inneren Faktoren in Artikeln dergelegt (Kapitel 2: Reaktionsbindungen, Kapitel 3, 4 und 5: Einfluß der Glykosyl- und Aglykonteile, sowie des Brückenatoms). Kapitel 6 hat zum Gegenstand die Hydrolyse der Oligo- und Polysaccharide, und Kapitel 7 ist den Nebenreaktionen gewidmet. Das letzte Kapitel bildet eine Sammlung der Reaktionsgeschwindigkeitskonstanten und Aktivierungsparameter.

In deutscher Sprache · Etwa 350 Seiten · Ganzleinen

Eine Gemeinschaftsausgabe — vertrieben in der DDR, in der BRD, in Österreich und in der Schweiz von Fachbuch Verlag, Leipzig, in allen anderen Ländern von Kultura, Budapest, ISBN 963 05 0520 7

Akadémiai Kiadó
Budapest

Fachbuch Verlag
Leipzig

ACTA IMEKO 1973

6th International Measurement Congress
Measurement and Instrumentation

Edited by J. SOLT, E. NIKA and TH. KEMÉNY
Editor in chief: GY. STRIKER

ACTA IMEKO 1973 presents to the readers the collection of all papers delivered at the 6th Congress of the International Measurement Confederation held in Dresden, June 1973. It contains 165 original, heretofore unpublished contributions by authors coming from 23 different countries. The full text of the contributions – which were presented at the Congress only in their shortened version – are in many cases followed by discussion remarks.

Papers published in the original languages, mostly in English and in German · In three volumes · Together approx. 2000 pages · Rotaprinted

A co-edition – distributed in the socialist countries by Kultura, Budapest, ISBN 963 05 0299 2; in all other countries by North Holland Publishing Co., Amsterdam

---

AKADÉMIAI KIADÓ
Budapest

NORTH HOLLAND PUBLISHING Co.,
Amsterdam

The Acta Chimica publish papers on chemistry, in English, German, French and Russian.

The Acta Chimica appear in volumes consisting of four parts of varying size, 4 volumes being published a year.

Manuscripts should be addressed to

Acta Chimica
Budapest 112/91 Műegyetem

Correspondence with the editors should be sent to the same address.

The rate of subscription is $ 32.00 a volume.

Orders may be placed with "*Kultúra*" Foreign Trade Company for Books and Newspapers (1389 Budapest 62, P. O. B. 149. Account No. 218 10990) or with representatives abroad.

Les Acta Chimica paraissent en français, allemand, anglais et russe et publient des mémoires du domaine des sciences chimiques.

Les Acta Chimica sont publiés sous forme de fascicules. Quatre fascicules seront réunis en un volume (4 volumes par an).

On est prié d'envoyer les manuscrits destinés à la rédaction à l'adresse suivante:

Acta Chimica
Budapest 112/91 Műegyetem

Toute correspondance doit être envoyée à cette même adresse.

Le prix de l'abonnement est de $ 32,00 par volume.

On peut s'abonner à l'Entreprise pour le Commerce Extérieur de Livres et Journaux «*Kultúra*» (1389 Budapest 62, P.O.B. 149 Compte-courant No. 218 10990) ou à l'étranger chez tous les représentants ou dépositaires.

«*Acta Chimica*» издают трактаты из области химической науки на русском, французском, английском и немецком языках.

«*Acta Chimica*» выходят отдельными выпусками разного объема. 4 выпуска составляют один том. 4 тома публикуются в год.

Предназначенные для публикации рукописи следует направлять по адресу:

Acta Chimica
Budapest 112/91 Műegyetem

По этому же адресу направлять всякую корреспонденцию для редакции.

Подписная цена — $ 32,00 за том.

Заказы принимает предприятие по внешней торговле книг и газет «*Kultúra*» (1389 Budapest 62, P. O. B. 149. Текущий счет № 218 10990) или его заграничные представительства и уполномоченные.

Reviews of the Hungarian Academy of Sciences are obtainable at the following addresses:

AUSTRALIA

C. B. D. Library and Subscription Service
Box 4886, G. P. O.
Sydney N. S. W. 2001

Cosmos Bookshop
145 Acland St.
St. Kilda 3182

AUSTRIA

Globus
Höchstädtplatz 3
A–1200 Wien XX

BELGIUM

Office International de Librairie
30 Avenue Marnix
1050-Bruxelles

Du Monde Entier
162 Rue du Midi
1000-Bruxelles

BULGARIA

Hemus
Bulvar Ruszki 6
Sofia

CANADA

Pannonia Books
P. O. Box 1017
Postal Station "B"
Toronto, Ont. M5T 2T8

CHINA

C N P I C O R
Periodical Department
P. O. Box 50
Peking

CZECHOSLOVAKIA

Mad'arská Kultura
Národní třida 22
115 66 Praha

PNS Dovoz tisku
Vinohradská 46
Praha 2

PNS Dovoz tlače
Bratislava 2

DENMARK

Ejnar Munksgaard
Nörregade 6
DK–1165 Copenhagen K

FINLAND

Akateeminen Kirjakauppa
P. O. Box 128
SF–00101 Helsinki 10

FRANCE

Office International de Documentation et Librairie
48 Rue Gay Lussac
Paris 5

Librairie Lavoisier
11 Rue Lavoisier
Paris 8

Europeriodiques S. A.
31 Avenue de Versailles
78170 La Celle St. Cloud

GERMAN DEMOCRATIC REPUBLIC

Haus der Ungarischen Kultur
Karl-Liebknecht-Strasse 9
DDR–102 Berlin

Deutsche Post
Zeitungsvertriebsamt
Strasse der Pariser Kommüne 3–4
DDR–104 Berlin

GERMAN FEDERAL REPUBLIC

Kunst und Wissen
Erich Bieber
Postfach 46
7 Stuttgart S

GREAT BRITAIN

Blackwell's Periodicals
P. O. Box 40
Hythe Bridge Street
Oxford OX1 2EU

Collet's Holdings Ltd.
Denington Estate
London Road
Wellingborough Northants NN8 2QT

Bumpus Haldane and Maxwell Ltd.
5 Fitzroy Square
London W1P 5AH

Dawson and Sons Ltd.
Cannon House
Park Farm Road
Folkestone, Kent

HOLLAND

Swets and Zeitlinger
Heereweg 347b
Lisse

Martinus Nijhoff
Lange Voorhout 9
The Hague

INDIA

Hind Book House
66 Babar Road
New Delhi 1

India Book House
Subscription Agency
249 Dr. D. N. Road
Bombay 1

ITALY

Santo Vanasia
Via M. Macchi 71
20124 Milano

Libreria Commissionaria Sansoni
Via Lamarmora 45
50121 Firenze

JAPAN

Kinokuniya Book-Store Co. Ltd.
826 Tsunohazu 1-chome
Shinjuku-ku
Tokyo 160–91

Maruzen and Co. Ltd.
P. O. Box 5050
Tokyo International 100–31

Nauka Ltd.–Export Department
2–2 Kanda
Jinbocho
Chiyoda-ku
Tokyo 101

KOREA

Chulpanmul
Phenjan

NORWAY

Tanum-Cammermeyer
Karl Johansgatan 41–43
Oslo 1

POLAND

Węgierski Instytut Kultury
Marszalkowska 80
Warszawa

BKWZ Ruch
ul. Wronia 23
00–840 Warszawa

ROUMANIA

D. E. P.
Bucureşti

Romlibri
Str. Biserica Amzei 7
Bucureşti

SOVIET UNION

Sojuzpechatj – Import
Moscow
and the post offices in each town

Mezhdunarodnaya Kniga
Moscow G–200

SWEDEN

Almqvist and Wiksell
Gamla Brogatan 26
S–101 20 Stockholm

A. B. Nordiska Bokhandeln
Kunstgatan 4
101 10 Stockholm 1 Fack

SWITZERLAND

Karger Libri AG.
Arnold-Böcklin-Str. 25
4000 Basel 11

USA

F. W. Faxon Co. Inc.
15 Southwest Park
Westwood, Mass. 02090

Stechert-Hafner Inc.
Serials Fulfillment
P. O. Box 900
Riverside N. J. 08075

Fam Book Service
69 Fifth Avenue
New York N. Y. 10003

Maxwell Scientific International Inc.
Fairview Park
Elmsford N. Y. 10523

Read More Publications Inc.
140 Cedar Street
New York N. Y. 10006

VIETNAM

Xunhasaba
32, Hai Ba Trung
Hanoi

YUGOSLAVIA

Jugoslovenska Knjiga
Terazije 27

Beograd
Forum
Vojvode Mišića 1
21000 Novi Sad

ACTA CHIMICA

ACADEMIAE SCIENTIARUM HUNGARICAE

ADIUVANTIBUS

V. BRUCKNER, GY. DEÁK, K. POLINSZKY,
E. PUNGOR, G. SCHAY, Z. G. SZABÓ

REDIGIT

B. LENGYEL

TOMUS 85 FASCICULUS 3

AKADÉMIAI KIADÓ, BUDAPEST

1975

ACTA CHIM. (BUDAPEST) ACASA 2 85 (3) 233–346 (1975)

ACTA CHIMICA

A MAGYAR TUDOMÁNYOS AKADÉMIA KÉMIAI TUDOMÁNYOK OSZTÁLYÁNAK IDEGEN NYELVŰ KÖZLEMÉNYEI

SZERKESZTI

LENGYEL BÉLA

TECHNIKAI SZERKESZTŐK

DEÁK GYULA és HARASZTHY-PAPP MELINDA

Az Acta Chimica német, angol, francia és orosz nyelven közöl értekezéseket a kémiai tudományok köréből.

Az Acta Chimica változó terjedelmű füzetekben jelenik meg, egy-egy kötet négy füzetből áll. Évente átlag négy kötet jelenik meg.

A közlésre szánt kéziratok a szerkesztőség címére (Budapest 112/91 Műegyetem) küldendők.

Ugyanerre a címre küldendő minden szerkesztőségi levelezés. A szerkesztőség kéziratokat nem ad vissza.

Megrendelhető a belföld számára az „Akadémiai Kiadó"-nál (1363 Budapest Pf 24. Bankszámla 215 11488), a külföld számára pedig a „Kultúra" Könyv- és Hírlap Külkereskedelmi Vállalatnál (1389 Budapest 62, P.O.B. 149 Bankszámla: 218 10990) vagy annak külföldi képviseleteinél és bizományosainál.

Die Acta Chimica veröffentlichen Abhandlungen aus dem Bereiche der chemischen Wissenschaften in deutscher, englischer, französischer und russischer Sprache.

Die Acta Chimica erscheinen in Heften wechselnden Umfanges. Vier Hefte bilden einen Band. Jährlich erscheinen 4 Bände.

Die zur Veröffentlichung bestimmten Manuskripte sind an folgende Adresse zu senden:

Acta Chimica
Budapest 112/91 Műegyetem

An die gleiche Anschrift ist auch jede für die Redaktion bestimmte Korrespondenz zu richten. Abonnementspreis pro Band: $ 32,00.

Bestellbar bei dem Buch- und Zeitungs-Außenhandels-Unternehmen »*Kultúra*« (1389 Budapest 62, P.O.B. 149 Bankkonto Nr. 218 10990) oder bei seinen Auslandsvertretungen und Kommissionären.

Acta Chimica Academiae Scientiarum Hungaricae, Tomus 85 (3), pp. 233—247 (1975)

EFFECT OF THE AXIAL INJECTION OF ARGON ON AN ANALYTICAL LIGHT SOURCE, II

COMPARATIVE STUDY OF SELF-ABSORPTION

L. PAKSY[1] and I. LAKATOS[2]

([1]Lenin Metallurgical Works, Miskolc,
[2]Petroleum Engineering Research Laboratory of the
Hungarian Academy of Sciences, 3515 Miskolc—Egyetemváros)

Received July 13, 1974

As a starting point in the detailed study of the decrease of self-absorption observed on the axial injection of argon, fundamental investigation of a comparative nature were carried out. It was shown in these that, when using argon, the air is expelled from the plasma, the decrease of the self-absorption always occurs independently of the excitation conditions and the nature of the spectral line, and the change in the self-absorption is not accompanied unambiguously by a variation in the character of the spectrum.

In the course of the experiments Mg and Al electrodes were used, and the argon was injected into the spark or the arc burning in the air atmosphere without the application of a gas-cell. The change in the self-absorption was studied with regard to both atomic and ionic lines of these elements.

Introduction

It is generally known that the radiation emitted in the inner space of the plasma is absorbed in the outer, cold shell of the analytical light source, i. e. self-absorption occurs. As a consequence of this process the profile of the spectral lines changes characteristically: their peaks become flatter, and their width at one-half height increases [1]. In the case of many spectral lines or those with high radiation intensities, certain lines apparently split as a result of self-absorption, for the absorption takes place at the center of the line broadened by the various effects [1, 2]. This latter case is referred to as "reversal".

It has been briefly reported [3, 4] that the self-absorption decreases considerably when argon is injected axially into the open electrode space. The detailed investigation of this phenomenon is of importance from both theoretical and practical aspects, for on the basis of the experimental results

a) conclusions can be drawn on the processes occurring in the plasma or on the electrode surface upon axial injection of argon, and hence on certain properties of the plasma; and

b) it would undoubtedly be of value from an analytical point of view if the self-absorption were decreased in the analytical or reference lines, for given line-pairs could be used in a wider concentration range.

It can further be assumed that the decrease of the self-absorption will lead to an improvement in the reproducibility of the analytical results. Together with favourable changes in the upper sections of the analytical curves the lower sections may also develop favourably for lines lying in a certain excitation-potential interval, *i. e.* both the detection limit and the reproducibility improve compared to those in an atmosphere of air. From an analytical aspect, this is a very desirable, but in most cases a rarely-attainable end.

The present paper discusses some of our experiments and results relating to self-absorption, and which are of a comparative nature. The comparison extends to the following:

a) the presence and effect of argon in the case of injection into the open electrode space and with the Schöntag gas-cell;

b) the effect of argon under various excitation conditions; and

c) a comparison of the variation of self-absorption in the case of spectral lines relating to different term series.

Experimental

Mainly solid metal electrodes were used in the experimental work. In the interest of the clarification of the effects and their interpretation over as wide a range as possible, both spark- and arc excitation were employed, and the excitation parameters were varied between wide limits. Accordingly, the characteristic experimental conditions in the individual experiments are always indicated. (In general the data in Table I of Ref. [5] are valid.)

The variation of self-absorption was established *via* the line-profile change, with a GB-1 recorder connected to a Zeiss G II microphotometer. Depending on the task, *e. g.* the observability of the peak, the conditions of the recording varied somewhat, and these were also influenced by the photographic blackening of the spectral line to be recorded. In the recordings the slit-width of the microphotometer was 5 μ, the chart speed was 30 mm/min, and the speed of movement of the plate was varied in the range of 0.1—30 mm/min. The majority of the recordings were made on logarithmic paper. It follows from this that the relative changes of the line intensities can be estimated, though the recordings are not suitable for the establishment of the actual intensity values.

In the text and the individual Figures the electrode-pair combinations are denoted as follows: Mg°/Mg, where the first is always the upper electrode, and the second the lower electrode. The sign ° indicates the electrode having a bored hole.

Results and discussion

1. The presence of argon in the open electrode space

An essential change, as compared to the previous arrangements (which are outlined in Ref. [5]), is that the argon atmosphere is produced by injection of the gas into the open electrode space through the bored hole of the upper electrode. Accordingly, before the effect of this injection can be compared with the effects of other factors, it must be proved that

a) argon does actually enter the plasma as a consequence of this new arrangement; and

b) this means of producing the gas atmosphere is at least as effective as *e. g.* the use of the Schöntag gas-cell.

In the comparative examination mentioned above the plasma produced by the axial injection into the open electrode space is compared with the plasma in the gas-cell and the open air, respectively.

In the course of our experiments the spectrum of the Mg°/Mg electrode pair was studied with strongly spark-like excitation (C = 12 nF, L=O mH) in the wavelength interval of 345—490 nm. Under such excitation conditions many lines of monoionized argon appear in the spectrum, while at the same time the lines of monoionized nitrogen can also be well detected (Table I). The spectra obtained in the above spectral range are given in Figs 1—3.

It can be quite clearly established from Figs 1—3 that the nitrogen lines (denoted by the letters a—g) disappear only on the axial injection of argon

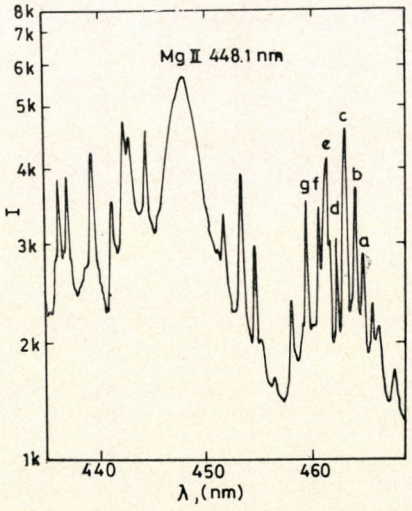

Fig. 1. Detail of a spectrum made by the Mg°/Mg electrode pair in a stationary air atmosphere. The data on lines *a* — *g* are given in Table I

Table I

Spectral data on nitrogen and argon lines to be seen in Figs 1—3 [7]

Lines II and I of N

Designation of spectral line	Wavelength nm	E_1(eV)	E_2(eV)	T_1	T_2	J
a	464.309	18.47	21.15	3s	$^3P^\circ$ — 3p	^3P 2—1
b	464.000	18.47	21.15	3s	$^3P^\circ$ — 3p	^3P 2—1
c	463.054	18.47	21.15	2s	$^3P^\circ$ — 3p	^3P 2—2
d	462.139	18.46	21.15	3s	$^3P^\circ$ — 3p	^3P 1—0
e	461.387	18.46	21.15	3s	$^3P^\circ$ — 3p	^3P 1—1
f	460.716	18.46	21.15	3s	$^3P^\circ$ — 3p	^3P 0—1
g	460.148	18.46	21.16	3s	$^3P^\circ$ — 3p	^3P 1—2

Lines II of Ar

Designation of spectral line	Wavelength nm	E_1(eV)	E_2(eV)	T_1	T_2	J
1	484.782	16.75	19.30	4s	^4P — 4p	$^4P^\circ$ 3/2—1/2
2	480.602	16.64	19.22	4s	^4P — 4p	$^4P^\circ$ 5/2—5/2
3	476.486	17.26	19.87	4s	^2P — 4p	$^2P^\circ$ 1/2—3/2
4	473.590	16.64	19.26	4s	^4P — 4p	$^4P^\circ$ 3/2—3/2
5	472.686	17.14	19.76	4s	^2P — 4p	$^2D^\circ$ 3/2—3/2
6	465.789	17.14	19.80	4s	^2P — 4p	$^2P^\circ$ 3/2—1/2
7	460.956	18.45	21.13	4s	^2D — 4p	$^2F^\circ$ 5/2—7/2
8	458.996	18.43	21.13	4s	^2D — 4p	$^2F^\circ$ 3/2—5/2
9	457.935	17.26	19.27	4s	^2P — 4p	$^2S^\circ$ 1/2—1/2
10	454.505	17.14	19.87	4s	^2P — 4p	$^2P^\circ$ 3/2—3/2
11	443.019	16.81	19.61	4s	^4P — 4p	$^4D^\circ$ 1/2—3/2
12	442.601	16.75	19.55	4s	^4P — 4p	$^4D^\circ$ 3/2—5/2
13	437.966	16.81	19.64	4s	^4P — 4p	$^4D^\circ$ 1/2—1/2
14	437.133	16.42	19.26	3d	^4D — 4p	$^4P^\circ$ 5/2—3/2

E_1 and E_2: lower and upper electron energy levels, in eV.
T_1 and T_2: corresponding energy level symbols without the inner quantum number
J: the inner quantum numbers

(Fig. 2), and only in this case do the lines of argon appear. The photos were made on the complete electrode space, and thus, in spite of the fact that the plasma is surrounded by air on the axial injection, there is still more argon in it than in the case of the gas-cell. As regards the expulsion of nitrogen or air, therefore, the former arrangement is not only simpler, but more effective

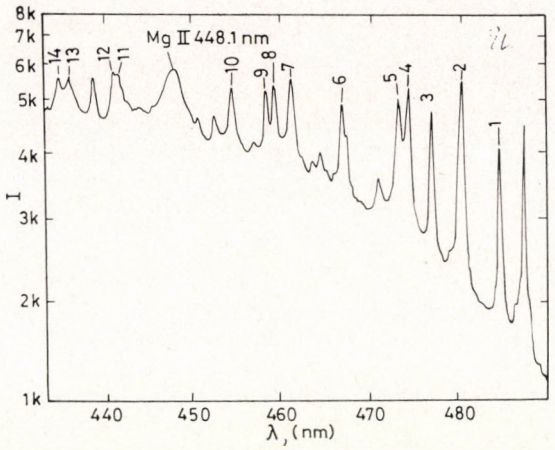

Fig. 2. Detail of a spectrum made by the Mg°/Mg electrode pair with axial injection of argon. Flow rate: 2 dm³/min. The data on lines 1—14 are given in Table I

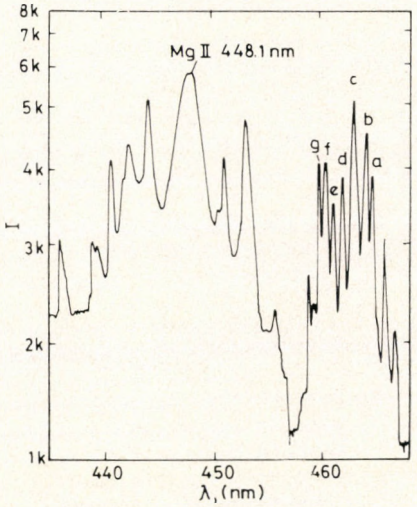

Fig. 3. Detail of a spectrum made by the Mg°/Mg electrode pair in a Schöntag gas-cell. Argon flow rate: 2 dm³/min. The data on lines *a*—*g* are given in Table I

too (The volume of the gas-cell is about 50 ml, and the flow rate of 2000 ml/min unquestionably ensure good flushing).

However, the above experiment may be objected to on the grounds that the excitation conditions vary and this is why the ionic lines of nitrogen disappear from the spectrum. It can be established from Table I, on the other hand, that the argon lines appearing in place of the nitrogen are also ionic lines, and indeed, their excitation potential almost coincides with that of the ionic nitrogen lines. A study was additionally made of the behaviour of the atomic lines of nitrogen which cannot be seen in Figs 1—3. It was

found that, in agreement with the foregoing, the N I 410.9 nm and N I 415.1 nm lines, for instance, can similarly be detected only in the gas-cell and in a stationary air atmosphere. From these experimental results it is obvious that the air is actually expelled from the plasma on the axial injection of argon, although the electrode space is completely open.

2. Comparison of the atomosphere effect with the effect of varying the character of excitation

The change of the gas atmosphere surrounding the plasma can affect the excitation processes to the same large extent as, for example, changes in the character of excitation (spark-like or arc-like) [6]. In the former case the excitation is influenced directly from within, *via* the effect on the light excitation processes, while in the latter case it is influenced from outside by the variation of the circuit characteristics. In the interest of the clarification of the processes occurring, therefore, the self-absorption decrease observed on the axial injection of argon was compared with the change of self-absorption observed under the various excitation conditions.

Mention will be made here of the findings in the case the Mg°/Mg electrode pair, as a typical example of our experimental results. The details of the spectrum of magnesium in the wavelength interval 277—295 nm under spark-like (C=6 nF; L=O mH) and arc-like (C=6 nF; L=5 mH) excitation conditions can be seen in Figs 4 and 5.

Certain marked differences can be observed between the two Figures:

a) In magnesium line 12 the self-absorption (reversal) can be observed to increase with increasing self-induction, while simultaneously the asymmetry to be seen in Fig. 4 disappears;

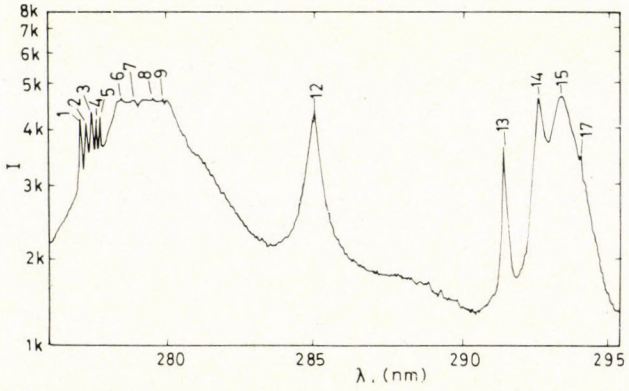

Fig. 4 Detail of a spectrum made by the Mg°/Mg electrode pair in a stationary air atmosphere. Excitation conditions: $C = 6$ nF, $L = 0$ mH. The data on the magnesium atomic and ionic lines 1—17 are given in Table II

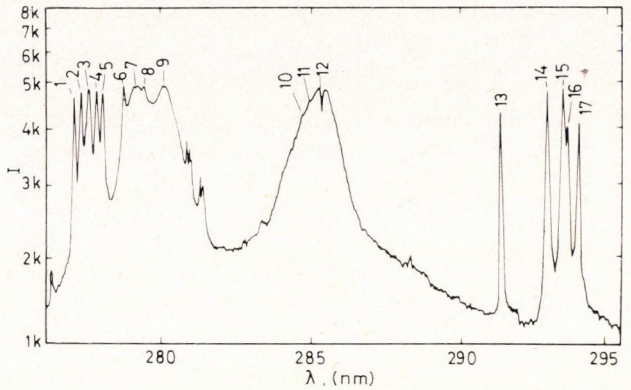

Fig. 5. Detail of a spectrum made by the Mg°/Mg electrode pair in a stationary air atmosphere Excitation conditions: C = 6 nF, L = 5.0 mH

Table II

Spectral data on magnesium lines to be seen in Figs 4—6

Designation of spectral line	Wavelength	Ionization state	E_1(eV)	E_2(eV)	T_1	T_2	J
1	277.669	I	2.71	7.18	$3p\ ^3P°$	$3p^2\ ^3P$	1—2
	277.669	I	2.71	7.17	$3p\ ^3P°$	$7s\ ^3S$	0—1
2	277.827	I	2.71	7.17	$3p\ ^3P°$	$3p^2\ ^3P$	0—1
	277.827	I	2.71	7.17	$3p\ ^3P°$	$7s\ ^3S$	
3	277.983	I	2.72	7.18	$3p\ ^3P°$	$3p^2\ ^3P$	2—2
	277.983	I	2.71	7.17	$3p\ ^3P°$	$3p^2\ ^3P$	1—1
4	278.123	I	2.72	7.17	$3p\ ^3P°$	$7s\ ^3S$	2—1
	278.142	I	2.71	7.17	$3p\ ^3P°$	$3p^2\ ^3P$	1—0
5	278.297	I	2.72	7.17	$3p\ ^3P°$	$3p^2\ ^3P$	2—1
6	279.087	II	4.42	8.86	$3p\ ^2P°$	$3d\ ^2D$	1/2—3/2
7	279.553	II	0.00	4.43	$3s\ ^2S$	$3p\ ^2P°$	1/2—3/2
8	279.700	II	4.43	8.86	$3p\ ^2P°$	$3d\ ^2D$	3/2—5/2
9	280.027	II	0.00	4.43	$3s\ ^2S$	$3p^2\ P°$	1/2—1/2
10	284.834	I	2.71	7.06	$3p\ ^3P°$	$5d\ ^3D$	1—2
11	285.166	I	2.72	7.06	$3p\ ^3P°$	$5d\ ^3D$	
12	285.213	I	0.00	4.35	$3s^2\ ^1S$	$3p\ ^1P°$	0—1
13	291.545	I	5.75	10.00	$3d\ ^1D$	$3d\ ^1D°$	2—2
14	292.863	II	4.42	8.65	$3p\ ^2P°$	$4s\ ^2S$	1/2—1/2
15	293.651	II	4.43	8.65	$3p\ ^2P°$	$4s\ ^2S$	3/2—1/2
	293.674	I	2.71	6.93	$3p\ ^3P°$	$6s\ ^3S$	0—1
16	293.847	I	2.71	6.93	$3p\ ^3P°$	$6s\ ^3S$	1—1
17	294.199	I	2.72	6.93	$3p\ ^3P°$	$6s\ ^3S$	2—1

b) the ionic magnesium lines 14 and 15 become narrower on the increase of self-induction;

c) new atomic magnesium lines (10 and 11) appear in Fig. 5; and

d) in contrast with expectations, the self-absorption of the ionic magnesium lines 7 and 9 changes to only a small extent on the increase of self-induction.

(The data on the individual spectral lines are listed in Table II).

As the next step in our experiments, argon was injected axially under the (arc-like) 'external' parameters corresponding to Fig. 5. The spectrum thus obtained can be seen in Fig. 6.

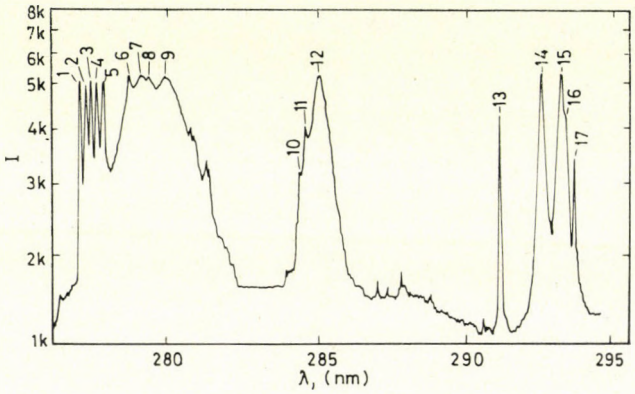

Fig. 6. Detail of a spectrum made by the Mg°/Mg electrode pair with axial injection of argon. Excitation conditions: C = 6 nF, L = 5.0 mH. Argon flow rate: 1 dm^3/min

Figure 6 shows that the greatest change is to be observed in the Mg I 285.2 nm line: the reversal is eliminated and the width at one-half height of the line decreases. From this phenomenon it might be said that the effect of argon corresponds to the very large variation in the self-induction (L=O→5), for the line in Fig. 6 is more similar to that in Fig. 4 than to that in Fig. 5. This argument, however, is contradicted by the following facts:

a) The 'excess' line (10 and 11) observed on the increase of the self-induction remain unchanged;

b) the profiles (peaks) of the ionic magnesium lines 14 and 15 are not changed either; and

c) the profiles of the ionic magnesium lines 7 and 9 are similarly unchanged.

The above findings indicate, therefore, that it is not a question of the nature of the spectrum becoming more 'spark-like', for the effect corresponding to the variation of the external parameters can be observed only on a single atomic line.

The change in the excitation character is also strikingly revealed by the behaviour of the atomic magnesium line 13. It is clear from Table II that this is an autoionization line, *i.e.* the energy of the excited level is higher than the ionization energy. The intensity of this line compared to the adjacent ionic lines 14 and 15 in Fig. 4 is lower than in Fig. 5, in accordance with the fact that in the more spark-like discharge the equilibrium is displaced towards the ionization, and in the more arc-like discharge towards the recombination. It can be seen, however, that the blackening ratio of these lines does not change upon argon injection, nor does the nature of the excitation, corresponding to the fact that the photos shown in Figs 5 and 6 have been taken under identical circuit conditions. If the blackening ratio of the lines is measured, then we obtain the following values:

Atmosphere	Excitation conditions	Mg II 292.8/Mg I 291.5
Stationary air	C = 6.0 nF L = 0 mH	1.00
Stationary air	C = 6.0 nF L = 5 mH	0.75
Axial argon injection	C = 6.0 nF L = 5 mH	0.85

The situation is similar in the case of an a.c. arc:

Atmosphere	Excitation conditions	Mg II 292.8/Mg I 291.5
Stationary air	I = 4 A	0.18
Axial argon injection	I = 4 A	0.28
Stationary air	I = 8 A	0.23
Axial argon injection	I = 8 A	0.26

The experimental data reported show that no matter whether the effect of argon injected axially is examined in a spark-discharge or in an arc-discharge, this does not exert such a decisive influence on the nature of the spectrum as do the circuit ('external') conditions. The fact that in addition the self-absorption observed in the atomic and ionic lines of magnesium changes considerably, indicates that the primary cause of the decrease in the self-absorption should not be sought in the variation of the nature of the excitation.

3. *Comparison of the variation of self-absorption in the case of spectral lines relating to different term series*

Although it appeared from the above that the self-absorption decreased in both the atomic and the ionic lines, it was also necessary to examine whether there is a difference between the behaviours of spectral lines belonging to

Table III

Spectral data on atomic aluminium lines to be seen in Figs. 7—12

Wavelength nm	E_1 (eV)	E_2 (eV)	T_1	T_2	J	No. of Figure
396.152	0.01	3.14	$3p\ ^2P^\circ$	$4s\ ^2S$	3/2—1/2	7
394.401	0.01	3.14	$3p\ ^2P^\circ$	$4s\ ^2S$	1/2—1/2	7
266.039	0.01	4.67	$3p\ ^2P^\circ$	$5s\ ^2S$	3/2—1/2	8
265.248	0.01	4.67	$3p\ ^2P^\circ$	$5s\ ^2S$	1/2—1/2	8
237.834	0.01	5.22	$3p\ ^2P^\circ$	$6s\ ^2S$	3/2—1/2	9
237.207	0.00	5.22	$3p\ ^2P^\circ$	$6s\ ^2S$	1/2—1/2	9
237.207	3.61	8.84	$3p^2\ ^4P$	$3d\ ^4D$	5/2—7/2	9
309/271	0.01	4.02	$3p\ ^2P^\circ$	$3d\ ^2D$	3/2—5/2	10
309.284	0.01	4.02	$3p\ ^2P^\circ$	$3d\ ^2D$	3/2—5/2	10
308.215	0.00	4.02	$3p\ ^2P^\circ$	$3d\ ^2D$	1/2—3/2	10
257.540	0.01	4.83	$3p\ ^2P^\circ$	$4d\ ^2D$	3/2—3/2	11
257.510	0.01	4.83	$3p\ ^2P^\circ$	$4d\ ^2D$	3/2—5/2	11
256.798	0.00	4.83	$3p\ ^2P^\circ$	$4d\ ^2D$	1/2—3/2	11
237.335	0.01	5.24	$3p\ ^2P^\circ$	$5d\ ^2D$	3/2—3/2	9
237.356	3.61	8.83	$3p^2\ ^4P$	$3d\ ^4D$	5/2—5/2	9
237.312	0.01	5.24	$3p\ ^2P^\circ$	$5d\ ^2D$	3/2—5/2	9
236.930	3.60	8.83	$3p^2\ ^4P$	$3d\ ^4D^\circ$	3/2—5/2	9
236.761	3.60	8.83	$3p^2\ ^4P$	$3d\ ^4D^\circ$	1/2—3/2	9
236.705	0.00	5.24	$3p\ ^2P^\circ$	$5d\ ^2D$	1/2—3/2	9
226.922	0.01	5.48	$3p\ ^2P^\circ$	$6d\ ^2D$	3/2—3/2	12
226.910	0.01	5.48	$3p\ ^2P^\circ$	$6d\ ^2D$	3/2—5/2	12
226.374	0.01	5.49	$3p\ ^2P^\circ$	$7s\ ^2S$	3/2—1/2	12
226.346	0.00	5.48	$3p\ ^2P^\circ$	$6d\ ^2D$	1/2—3/2	12

different term series of a given element. To this end, let us consider the atomic lines of aluminium belonging to the 3p-ns and 3p-nd term series, in a stationary air atmosphere and with the axial injection of argon. The phenomena observed in these lines can be seen in the spectra of Figs 7—12. The spectral data on the relevant lines are given in Table III.

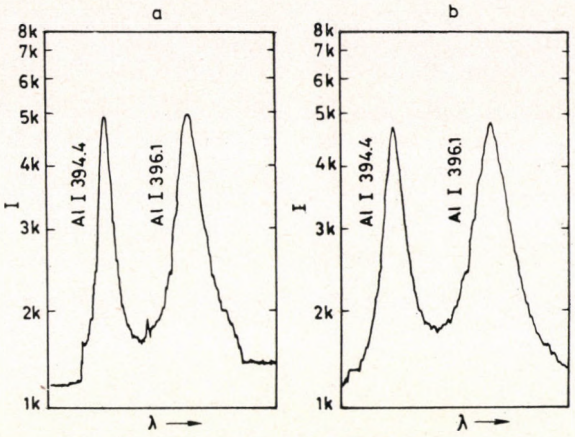

Fig. 7. Profile of Al I 394.4 nm and Al I 396.1 nm lines (a) in a stationary air atmosphere, and (b) in the case of the axial injection of argon

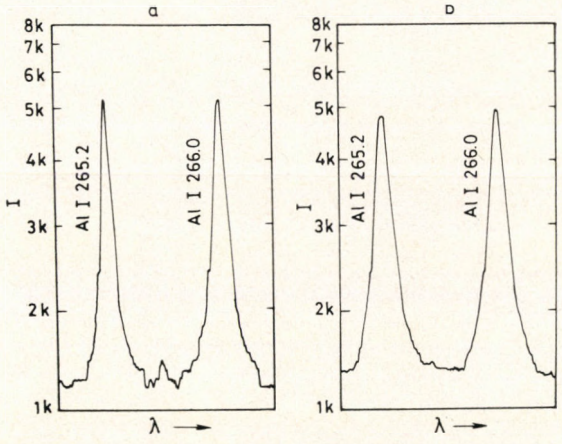

Fig. 8. Profile of the Al I 266.0 nm and the Al I 265.2 nm lines (a) in a stationary air atmosphere, and (b) in the case of the axial injection of argon

The behaviour of the spectral lines belonging to the 3p-ns term series can be seen in Figs 7—9. The profile of these lines in argon does not show a change compared to that exhibited in an air atmosphere; indeed, in some cases the width at one-half height is larger on the axial injection of argon. The reason for this is probably that

a) because of the stronger blackening, the Al I 394.401 nm line in Fig. 7 exhibits line-broadening in the photographic profile; and

b) the Al I 237.207 nm line in Fig. 9 coincides with an atomic aluminium line belonging to another energy-level series, and the increase of the intensities

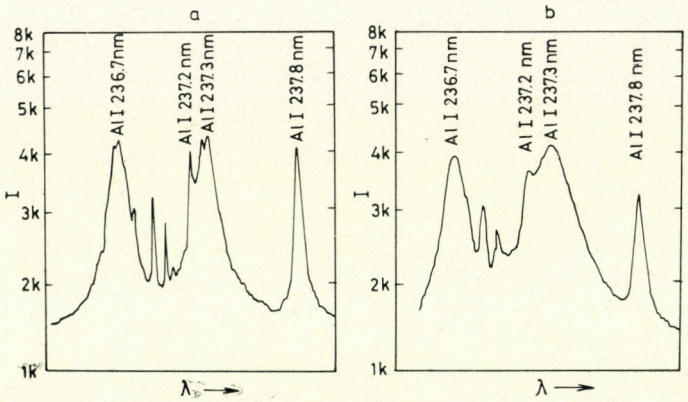

Fig. 9. Profile of the Al I 236.7 nm, Al I 237.2 nm, Al I 237.31 nm, Al 237.33 and Al I 237.8 nm lines (a) in a stationary air atmosphere, and (b) in the case of the axial injection of argon. The data on the spectral lines in the Figure are given in Table II

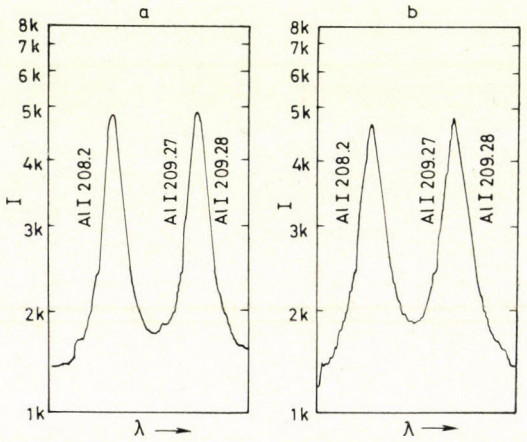

Fig. 10. Profile of the Al I 308.2 nm, Al I 309.27 nm and Al I 309.28 nm lines (the latter two unresolved) (a) in a stationary air atmosphere, and (b) in the case of the axial injection of argon

of the spectral lines together with the coincidence similarly lead to the broadening of the photographic line profile.

The profiles of the spectral lines belonging to the 3p-nd term series can be seen in Figs 10—12 and Fig. 9 (in this latter together with lines belonging to the 3p-ns series). It is characteristic of this series, however, that in air its members exhibit self-absorption, which ceases on the axial injection of argon. Although no reversal can be observed in air in the case of the Al I 308.2 nm and Al I 309.2 nm lines to be seen in Fig. 10, with argon, the flattening of the peaks was eliminated. The different behaviour of the spectral lines

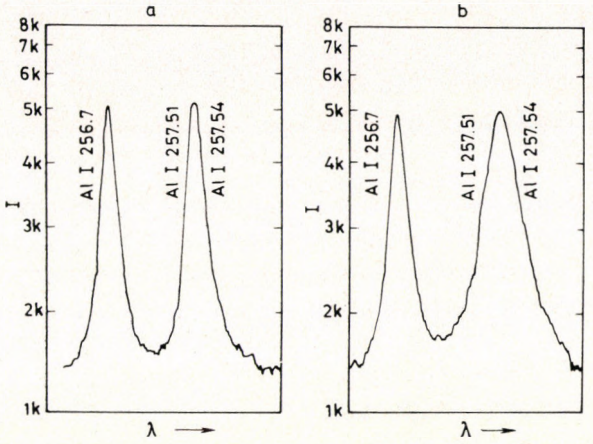

Fig. 11. Profile of the Al I 257.54 nm, Al I 257.51 nm and Al I 256.7 nm lines (the former two unresolved) (a) in a stationary air atmosphere, and (b) in the case of the axial injection of argon

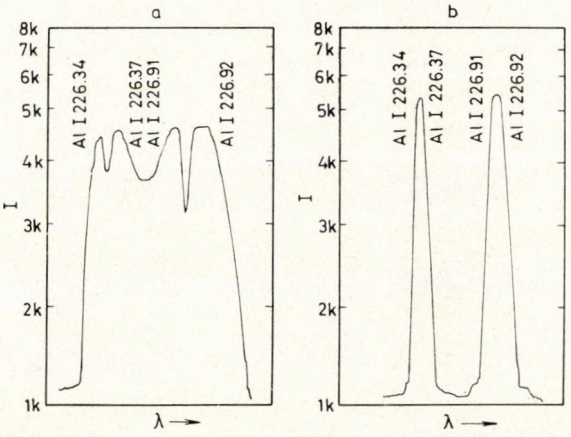

Fig 12. Profile of the Al I 226.92 nm, and Al I 226.91 nm (unresolved), and the Al I 226.37 nm and Al I 226.34 nm (unresolved) lines (a) in a stationary air atmosphere, and (b) in the case of the axial injection of argon

of the series can be well seen in Fig. 9, where they appear together with the 3p-ns series.

In the line of the 3p-nd exhibiting strong self-absorption, not only does the self-absorption decrease on the axial injection of argon, but the line-shift observed in air (not occurring because of self-absorption) is eliminated too. This latter phenomenon, however, will not be dealt with here.

In connection with the different behaviours of the two term series it should be noted that in each case parts *a* and *b* of the Figures were obtained

under identical recording conditions. A grade 3 filter was used in the recording, and the line scale to be measured was always chosen so that its blackening lay on the linear section for the blackening curve. Overall, therefore, this possibility of error can be discounted.

Conclusions

From the comparative experiments it can be established that

1. even with an open electrode space, on the axial injection of argon the plasma primarily contains argon and the air is expelled;

2. compared to the stationary air atmosphere, under the same excitation conditions, the self-absorption in the spectra decreases considerably. This decrease occurs in both arc and spark discharges, and for both atomic and ionic lines, and is not implicitly accompanied by an unambiguous change in the excitation character (spectral character); and

3. the change in the self-absorption can be observed in all those lines which also exhibit self-absorption or reversal in an air atmosphere.

In connection with the final point it must be noted that from this respect the spectral lines belonging to different term series may behave differently in an air atmosphere, even if they belong to the same ground level. It follows from this that the spectral lines belonging to the different term series do not behave uniformly on the injection of argon either.

For the moment the conclusion may be drawn from the observed phenomena that the nature of the spectra, the line profiles, the self-absorption, etc. can also be changed significantly by the axial injection of argon. The change cannot be attributed simply to the variation of the excitation character, nor can it be explained by the change in the populations of the levels.

The decrease of self-absorption is only part of the complex effects occurring as a consequence of the axial injection of argon. Thus, the explanation of the phenomenon can only be given together with other phenomena, and in agreement with them.

Other phenomena connected with self-absorption will be discussed in a subsequent publication.

REFERENCES

[1] Mika, J., Török, T.: Emission spectral analysis, vol. I. p. 87—88 (in Hungarian). Akadémiai Kiadó, Budapest, 1970
[2] Boumans, P. W. J.: Theory of Spectrochemical Excitation, p. 88. London, 1968
[3] Paksy, L.: Kémiai Közlemények, **27**, 23 (1967)

[4] LAKATOS, I., PAKSY, L.: Seventh Metallurgical Materials Testing Conference, Balatonszéplak, II, 53 (1973); Magy. Kém. Foly. **79**, 392 (1973)
[5] LAKATOS, I., PAKSY, L.: Acta Chim. (Budapest) **81**, 31 (1974)
[6] LAQUA, K.: Spectr. Acta, **4**, 237 (1950)
[7] STRIGANOV, A. R., SVENTITSKII, N. S.: Tablitsy spektralnykh linii neytralnykh i ionizovanykh atomov, Atomizdat, Moscow, 1966

István LAKATOS; 3515 Miskolc—Egyetemváros, Pf. 2. Hungary
László PAKSY; 3540 Miskolc, Lenin Kohászati Művek, Vegyészeti Osztály, Hungary.

Acta Chimica Academiae Scientiarum Hungaricae, Tomus 85 (3), pp. 249—260 (1975)

EFFECT OF THE AXIAL INJECTION OF ARGON ON AN ANALYTICAL LIGHT-SOURCE, III

VARIATION OF SELF-ABSORPTION IN THE ELECTRODE SPACE AND WITH THE GAS RATE AND CONCENTRATION

L. PAKSY[1] and I. LAKATOS[2]

([1]Lenin Metallurgical Works, Miskolc
[2]Petroleum Engineering Research Laboratory of the Hungarian Academy of Sciences, 3515 Miskolc—Egyetemváros)

Received July 13, 1974

As a result of the axial injection of argon, the self-absorption of the atomic lines decreases considerably in every layer between the electrodes in both common and foreign auxiliary electrode systems. The experimental results indicate that the decrease in self-absorption depends on the rate of gas injection used, but is independent of the nature of the excitation (spark or arc excitation). The behaviour of the ionic lines is similar to that of the atomic lines, but the extent of self-absorption decrease is smaller in the case of the ionic lines than for the atomic lines. From a practical aspect the self-absorption decrease resulting from the axial injection of argon permits spectral lines tending strongly to self-absorption to be used in a. c. arc-excitation up to concentrations of 10%.

Introduction

In our earlier investigations [1—3] it has been found that as a result of the axial injection of argon the self-absorption of the spectral lines decreases to a considerable extent. It has also been established that this decrease is independent of the excitation conditions and the nature of the spectral line, and further, that the change in self-absorption is not accompanied unambiguously by the variation of the spectral character [4]. On the basis of the experimental results the majority of the phenomena was attributed to the fact that in the case of the axial injection of argon no appreciable cold zone can develop around the plasma.

In order to obtain more experimental data and support the earlier findings, the change in self-absorption has been further studied in the present work. An examination has been made of whether self-absorption varies uniformly in the various layers of the plasma (along the electrode space), and of what factors affect this. This is closely connected with the study of the dependence on the rate of gas injection, a factor presumably playing one of the most important roles. In addition, a study is made from a practical aspect with regard to the upper concentration limit at which the axial injection of argon exerts an effect on the self-absorption line.

Experimental

Data on apparatus, materials, electrodes and processing of the spectral plates can be found in earlier publications [3,4]. Similarly, the magnification of the spectra with a recording photometer has also been reported in detail [4]. In the study of the effect of concentration the electrodes consisted of the B.A.M. (Bundesanstalt für Materialprüfung, Berlin-Dahlem) comparative sample series. The designation of the electrode system too is unchanged, *e.g.* Mg°/Mg, where the first is always the upper electrode and the second the lower electrode. The symbol ° indicates the electrode having a bored hole. Attention is always drawn to experimental conditions different from the usual ones.

Results and discussion

1. Variation of self-absorption along the longitudinal axis of the electrode space

The change in self-absorption along the longitudinal axis of the analytical light source was studied in both common and foreign auxiliary electrode systems, since the material distributions are presumably different in the two electrode systems. Consequently, it may be assumed that the effect of injection of argon on the self-absorption also differs in the two systems, considering that the self-absorption is always a function of the concentration of the element in question in a given vapour space.

Study of a common auxiliary electrode system

As in previous investigations, the phenomena observed in the common auxiliary electrode system were studied with Mg°/Mg and Al°/Al electrodes. The gap between the electrodes used was 3 or 6 mm, and the electrode space was always investigated as four equal spatial layers 0.75 or 1.5 mm wide. Since the Mg electrode is strongly oxidized in an atmosphere of air when an arc discharge is applied, the recordings were made with arc-like spark excitation ($C = 12$ nF, $L = 1.5$ mH).

Figures 1—4 show the change in the profile of the Mg I 285.2 nm line for the spaces between the electrodes when the Mg°/Mg electrode system is employed. The spatial resolving was carried out with an intermediate focussing.

To illustrate the difference in the Figures, the line profiles obtained from a given spatial part (a) in a stationary air atmosphere, and (b) on the axial injection of argon (rate = 0.5 dm^3/min) were plotted side by side. The electrode gap was 3 mm, and the height of the intermediate diaphragm was 0.75 mm.

It can be established from the Figures that:

(a) In agreement with previous findings, in an atmosphere of air significant self-absorption and reversal can be detected in the Mg I 285.2 nm

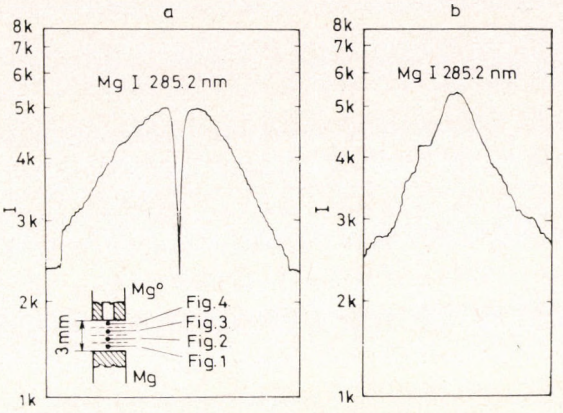

Fig. 1. Change of the profile of the Mg I 285.2 nm line in the Mg°/Mg electrode system in the 0—0.75-mm layer above the Mg electrode (a) in a stationary air atmosphere, and (b) with axial injection of argon

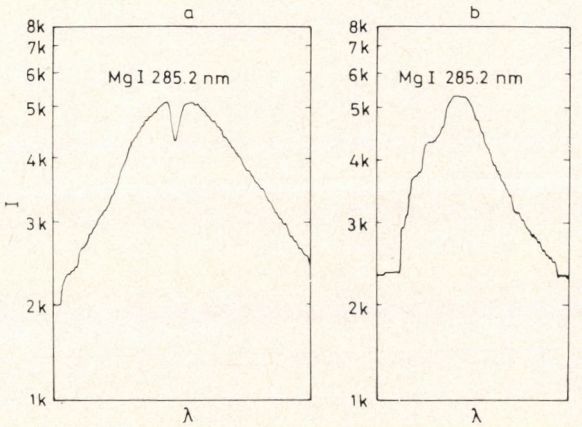

Fig. 2. Change of the profile of the Mg I 285.2 nm line in the Mg°/Mg electrode system in the 0.75—1.50-mm layer above the Mg electrode (a) in a stationary air atmosphere, and (b) with axial injection of argon

line in all four quadrants. In the two central quadrants the reversal is of lower extent, and the width at one-half height of the line profile is smaller before the drilled Mg electrode. This is presumably a consequence of the fact that there is a 3-mm drilling in the upper electrode (Mg°), and thus the evaporation proceeds on a smaller surface compared to the lower electrode; the upper electrode therefore discharges less matter into the analytical light source. It is also clear that there is not always a linear proportionality between the flattening of the peaks of the line and the width of reversal. Thus, in spite of the wider profile, the Mg I 285.2 nm line in Fig. 2a exhibits a smaller re-

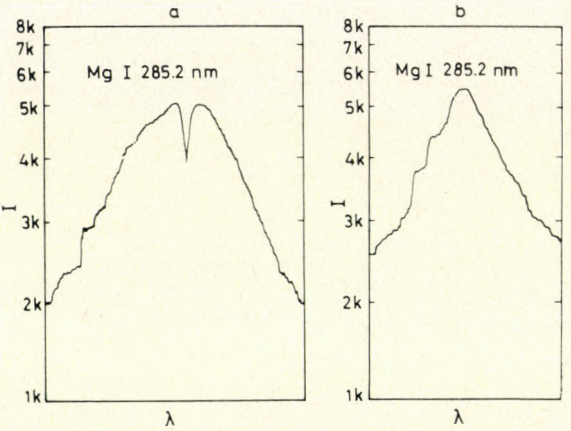

Fig. 3. Change of the profile of the Mg I 285.2 nm line in the Mg°/Mg electrode system in the 0.75—1.50-mm layer below the Mg° electrode (a) in a stationary air atmosphere, and (b) with axial injection of argon

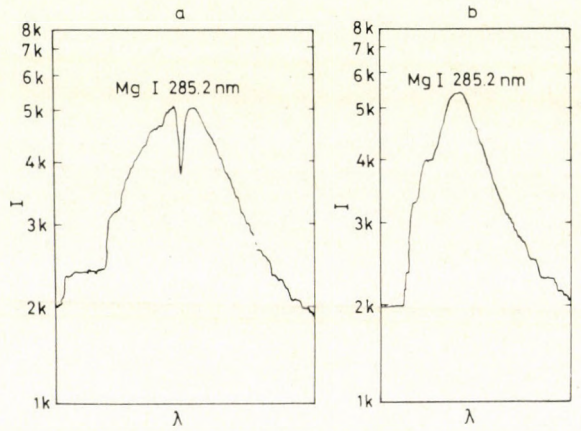

Fig. 4. Change of the profile of the Mg I 285.2 nm line in the Mg°/Mg electrode system in the 0—0.75-mm layer below the Mg° electrode (a) in a stationary air atmosphere, and (b) with axial injection of argon

versal compared to that in Fig. 1a. (In $P_{1/2}$ transformed units, the line blackening values measured by microphotometer were —0.65 and —0.49 respectively. These values are the averages of the maxima observed at the edges of the line.)

(b) In an argon atmosphere (Figs 1b—4b) self-absorption is eliminated in all cases, and the line profiles too become more similar to one another. Here again, however, a slight difference can be observed. In contrast with the other layers, for example, width at one-half height of the line is smaller below the Mg° electrode.

Besides the Mg I 285.2 nm line, the Mg II 280.2 nm, Mg II 279. 8 nm, Mg II 279.6 nm and Mg II 279.1 nm ionic lines were also studied, under the same experimental conditions as before. The behaviour of this line group in the 0—0.75-mm layer above the Mg electrode is presented in Fig. 5 (a) in a stationary air atmosphere, and (b) with the axial injection of argon.

As observed previously, the lines belonging to the lower excitation level (280.2 nm and 279.6 nm) show reversal in air, but this is eliminated as a result of argon injection. It is clear too from a comparison of Figs 1b and 5b that the Mg I 285.2 nm line undergoes a more extensive change upon the injection of argon than do the Mg II 280.2 nm and 279.6 nm ionic lines.

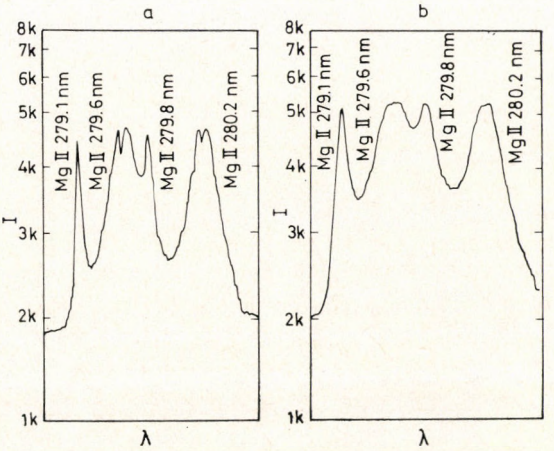

Fig. 5. Behaviour of the Mg II 280.2 nm, Mg II 279.8 nm, Mg II 279.6 nm and Mg II 279.1. nm ionic lines in the Mg°/Mg electrode system in the 0—0.75-mm layer above the Mg electrode (a) in a stationary air atmosphere, and (b) with axial injection of argon

As regards the explanation of the phenomenon it should be noted here that in the earlier-used semiclosed atmosphere (Schöntag gas-cell) no decrease of the reversal of either the atomic or the ionic lines can be observed even with a tangential argon inflow rate of 3 dm^3/min.

Foreign auxiliary electrode system

The behaviour of the same lines was also studied under the same experimental conditions as before, but in a foreign auxiliary electrode system. The change in the absorption of the Mg I 285.2 nm line in the different quadrants between the electrodes can be seen in Figs 6—9 for the case of the Al°/Mg electrode system.

The Figures lead to the following conclusions:

Because of the natural mass-transfer process the blackening of the line decreases towards the foreign auxiliary electrode, and indeed, even when this

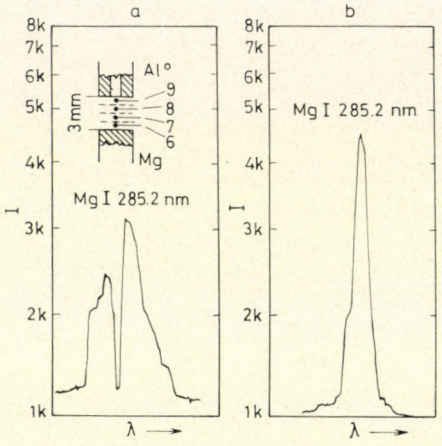

Fig. 6. Change of the profile of the Mg I 285.2 nm line in the Al°/Mg electrode system in the 0—0.75-mm layer above the Mg electrode (a) in a stationary air atmosphere, and (b) with axial injection of argon

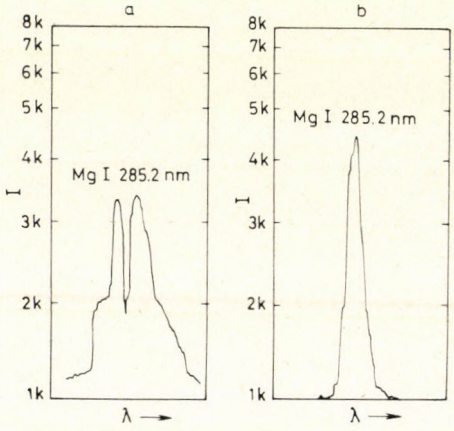

Fig. 7. Change of the profile of the Mg I 285.2 nm line in the Al°/Mg electrode system in the 0.75—1.50-mm layer above the Mg electrode (a) in a stationary air atmosphere, and (b) with axial injection of argon

is taken into account, it is surprisingly low under the Al° electrode. Even in spite of the obvious decrease of the amount of material, however, the reversal can be detected in all layers in an atmosphere of air. The asymmetry in layer I is striking (Fig. 6a). As a consequence of argon injection, the reversal in the Mg I 285.2 nm line is lost and the line profiles become narrower.

Figure 10 shows the behaviour of the Mg II 280.2 nm, Mg II 279.8 nm, Mg II 279.6 nm and Mg II 279.1 nm ionic lines in the Al°/Mg electrode system, in the 0—0.75-mm layer above the Mg electrode, (a) in a stationary air atmosphere, and (b) with the axial injection of argon.

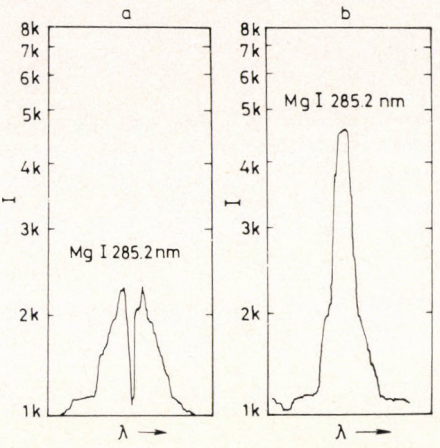

Fig. 8. Change of the profile of the Mg I 285.2 nm line in the Al°/Mg electrode system in the 0.75—1.50-mm layers below the Al° electrode (a) in a stationary air atmosphere, and (b) with axial injection of argon

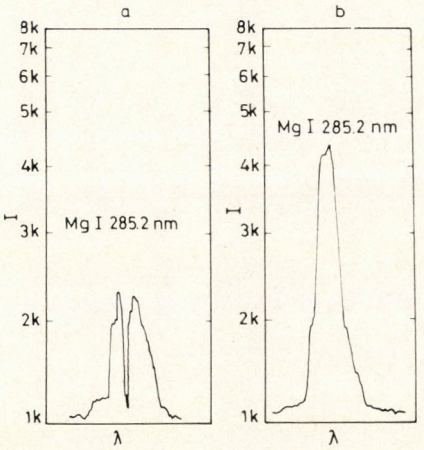

Fig. 9. Change of the profile of the Mg I 285.2 nm line in the Al°/Mg electrode system in the 0—0.75-mm layer below the Al° electrode (a) in a stationary air atmosphere, and (b) with axial injection of argon

It emerges from a comparison of Figs 10a and 10b that the self-absorption in the Mg II ion lines does not appear in the foreign auxiliary electrode system either.

2. Effect of the rate of injection of argon on self-absorption

In previous experiments the rate of injection of argon was 0.5 dm^3/min. It was seen before that even at such a low injection rate, self-absorption decreases very considerably. In some cases, however, (and strikingly for just

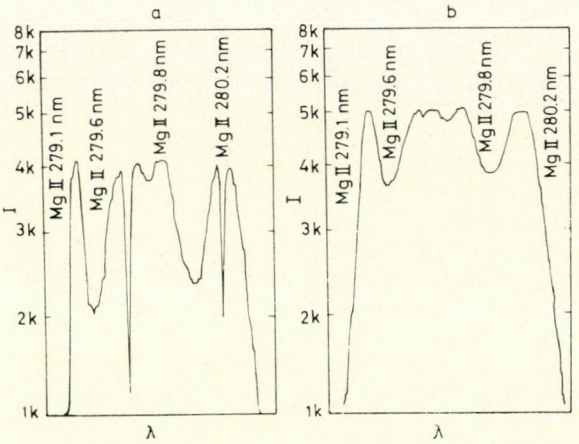

Fig. 10. Behaviour of the Mg II 280.2 nm, Mg II 279.8 nm, Mg II 279.6 nm and Mg II 279.1 nm ionic lines in the Al°/Mg electrode system in the 0—0.75-mm layer above the Mg electrode (a) in a stationary air atmosphere, and (b) with axial injection of argon

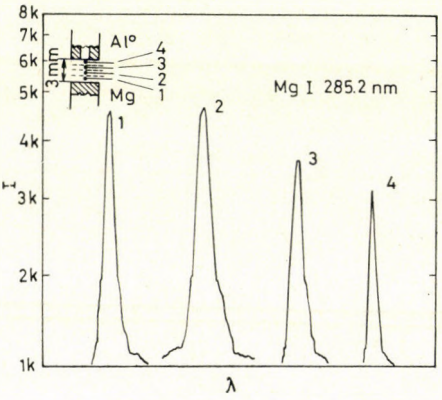

Fig. 11. Change of the profile of the Mg I 285.2 nm line in the Al°/Mg electrode system in the layers between the electrodes, with the axial injection of 4.0 dm^3 argon per min

the ionic lines at higher excitation energies) at such a rate the reversal was not completely eliminated (Fig. 5b). It is therefore essential to examine how the self-absorption varies as a function of the rate of injection of argon.

Figure 11 shows the profile of the Mg I 285.2 nm line in the layers between the two electrodes for the Al°/Mg electrode system, at an axial argon injection rate of 4.0 dm^3/min.

Figure 12 shows the profiles of the Mg II 280.2 nm, Mg II 279.8 nm, Mg II 279.6 nm and Mg II 279.1 nm ionic lines in the Al°/Mg electrode system with axial injection of argon at the rate of 4.0 dm^3/min.

By comparison of these Figures with Figs 1—4 it can be established that the reversal in the Mg I 285.2 nm line is eliminated at an argon injection

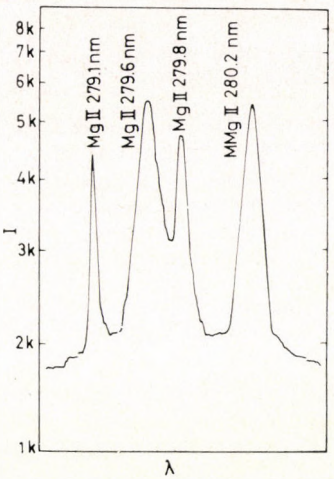

Fig. 12. Change of the profile of the Mg II 280.2 nm, Mg II 279.8 nm, Mg II 279.6 nm and Mg II 279.1 nm ionic lines in the Al°/Mg electrode system in the 0—0.75-mm layer above the Mg electrode, with the axial injection of 4.0 dm^3 argon per min

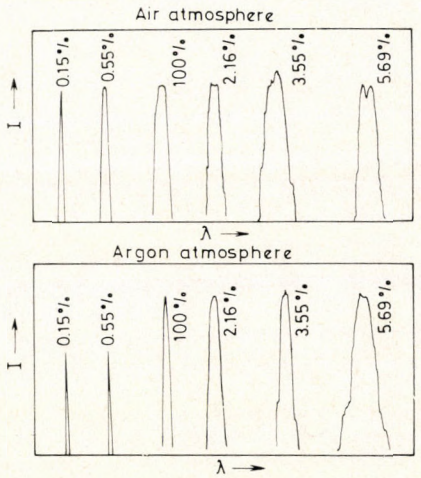

Fig. 13. Change of the profile of the Mg I 285.2 nm line in aluminium alloys with various magnesium contents in the 0—1.5-mm layer above the Al electrode (a) in a stationary air atmosphere, and (b) with the axial injection of argon

rate of 0.5 dm^3/min, while on the increase of the rate of injection to 4 dm^3/min, the width at one-half height of the line decreases. For the ionic Mg lines, on the other hand, at an argon injection rate of 4 dm^3/min it can be observed that while there is hardly any variation in the Mg II 279.8 nm and Mg II 279.1 nm lines (since these are anyway not self-absorption lines), the profiles of the other two ionic Mg lines change strongly; more exactly, on the increase of the rate of injection the widths at one-half height become increasingly smaller.

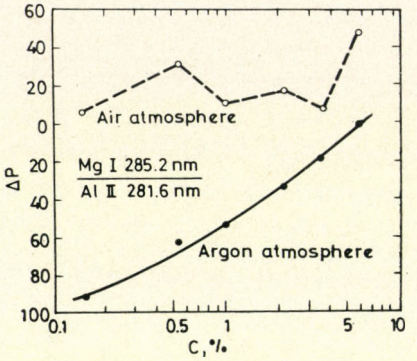

Fig. 14. Concentration dependence of the Mg I 285.2 nm/Al II 281.6 nm pair ratio in a stationary air atmosphere and with the axial injection of argon in an a. c. arc

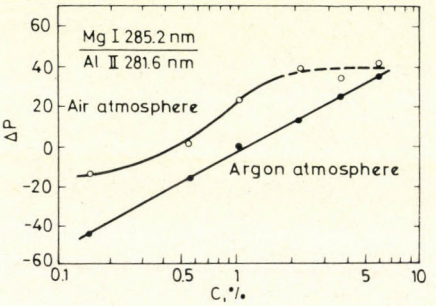

Fig. 15. Concentration dependence of the Mg I 285.2 nm/Al II 281.6-nm line-pair ratio in a stationary air atmosphere and with the axial injection of argon, using arc-like spark excitation

Experiments were also made with Al, Sn and Zn electrodes in both common and foreign auxiliary electrode systems (a C electrode was employed as counter-electrode), and it was found that in all cases examined the reversal in the lines was lost at argon injection rates of 0.5—5.0 dm^3/min. For other reasons, which will be discussed later, the blackening of certain lines simultaneously decreased above a critical value of the argon injection rate. It must be noted that, similarly to Mg, several ionic lines of Sn also exhibit reversal in spite of the state of ionization, and that this is eliminated on the injection of argon. For the electrodes mentioned the use of a semiclosed, tangential-inflow argon cell was also ineffective as regards the decrease of self-absorption.

3. Dependence of the change in the self-absorption on the concentration

From the aspect of practical application it is important to know to what weight percent the given self-absorption line can be used for analytical purposes if argon injection is employed.

To clarify this question, a study was made among others of the behaviour of the Mg I 285.2 nm line in Al alloys in an a.c. arc and in an arc-like spark in the range of 0.15—5.7%. Comparative samples B–1, B–3, B–5, C–1, C–4 and C–6 of B.A.M. type were used in the experiments.

Figure 13 shows the variation of the profile of the Mg I 285.2 nm line in aluminium alloys with various Mg contents. The recording was made in an a.c. arc (6A) in a stationary air atmosphere and at an axial argon-injection rate of 1.0 dm^3/min. The electrode gap was 6 mm, the electrode pair used was Al°/Al_{st}, where Al° is the spectrally pure electrode and Al_{st} is the alloy electrode of known composition, and the focussing was carried out in the 0—0.5-mm layer above the Al_{st} electrode.

It is clear from Fig. 13 that as a result of the injection of 1.0 dm^3 argon per min, the self-absorption of the line decreases considerably throughout the entire concentration range examined. From an analytical aspect, however, it is necessary to investigate the course of the straight calibration lines, in spite of the change in the line profiles, since even a slight self-absorption may be detrimental for quantitative analysis.

Figure 14 shows the analytical curves obtained from the Mg I 285.2 nm/Al II 281.6 nm line-pair ratio in a stationary air atmosphere and with the axial injection of argon in an a.c. arc (6 A), while Fig. 15 gives the same plots for arc-like spark excitation (C = 12 nF, L = mH). The data on the compositions of the samples are given in Fig. 13.

From the Figures it can be established that in an a.c. arc with a current of 6 A the analytical curve and thus the otherwise self-absorption line of Mg can be used if argon is injected. A similar result is obtained for arc-like spark excitation. A further advantage is that the number of lines of the basic material and the alloy which are suitable for analytical purposes, increases as a consequence of the decrease in self-absorption.

Conclusion

From the experimental results reported it can be established that as a consequence of the axial injection of argon

(a) in the common and foreign auxiliary electrode systems the self-absorption of the atomic lines decreases and the reversal of the lines is eliminated in every layer between the electrodes;

(b) the decrease of self-absorption and the elimination of the reversal of the line are functions of the flow rate of the gas;

(c) in addition to the changes connected with self-absorption, other line-profile changes too appear above the critical gas-flow rates;

(d) the behaviour of the ionic lines is similar to that of the atomic lines, but the change is generally smaller; and

(e) the self-absorption decrease attained permits the use of spectral lines tending strongly to self-absorption for analytical purposes in a.c. arc excitation, even in the case of high concentration ($\sim$10%).

The phenomena reported are further evidence in support of our earlier assumption that the decrease in self-absorption can be attributed in part to the decrease in thickness of the cold vapour space surrounding the plasma. The exclusively physical (flow kinetics) interpretation of the phenomenon, however, must in all probability be rejected in the light of the newer results, for on the axial injection of air, nitrogen and oxygen, a decrease can hardly be observed in the self-absorption. The favourable effect in question appears only on the axial injection of argon or krypton.

REFERENCES

[1] LAKATOS, L., PAKSY, L.: Seventh Metallurgical Materials Testing Conference, Balatonszéplak, II, 53 (1973)
[2] PAKSY, L., LAKATOS, I.: Magy. Kém. Foly. **80,** 67 (1974)
[3] LAKATOS, I., PAKSY, L.: Acta Chim. (Budapest) **81,** 31 (1974)
[4] PAKSY, L., LAKATOS, I.: Acta Chim. (Budapest) **85,** 233 (1975)

István LAKATOS; 3515 Miskolc—Egyetemváros, Pf. 2. Hungary
László PAKSY; 3540 Miskolc, Lenin Kohászati Művek, Vegyészeti Osztály, Hungary.

Acta Chimica Academiae Scientiarum Hungaricae, Tomus 85 (3), pp. 261–267 (1975)

INVESTIGATIONS ON METAL COMPLEXES CONTAINING OPTICALLY ACTIVE LIGANDS, I

COMPLEXES OF D- AND L-*THREO*-1-(*P*-NITROPHENYL) 2-AMINO-PROPANEDIOL-1,3 FORMED WITH PALLADIUM(II) IONS

J. GAÁL and J. INCZÉDY

(Institute of Analytical Chemistry, University for Chemical Engineering, Veszprém)

Received September 6, 1974

The stability constants of D- and L-*threo* 1-(*p*-nitrophenyl)-2-amino-propanediol-1,3 complexes formed with palladium(II) ions were determined by pH-metric titration. Solid $Na_2[Pd_2L_3Cl_6]$ was prepared, using racemic-*threo*-1-(*p*-nitrophenyl)2-amino-propanediol-1,3; and $[PdL_2]Cl_2 \cdot 2{,}5\ H_2O$ was prepared using D- and L-*threo*-1-(*p*-nitrophenyl)-2-amino-propanediol-1,3.

It has been found at the determination of stability constants of complexes formed with different pure optical isomers but with the same metal ion, that between the stability of the complexes of the enantiomers there are differences only in few cases. In the examination of reactions of pure optically active and racemic compounds, DWYER and MELLOR [1] observed that if the racem compound was used, the formed complexes contain preferentially those ligands, which are of identical optical rotatory. So the composition of the formed complexes are in most cases $[M(l\text{-}L)_n]$ and $[M(d\text{-}L)_n]$, where M denotes the metal ion and L the ligand. Since the complexes formed in 1 : 1 ratio, they behave as a racemic compound.

In other cases the optically active bi- and tridentate ligands form complexes with Cu(II), Ni(II), Zn (II), Mn (II), Co(II), Co(III), Cr(III) and Al(III)-ions of the following compositions:

$$[M(l\text{-}L)_n], \quad [M(d\text{-}L)_n] \quad \text{and} \quad [M(l\text{-}L)_m(d\text{-}L)_{n-m}].$$

If the metal ion became an assymmetric center in the complex formed, there were differences between the stability constants and other physical properties of the complexes containing mixed and pure optical isomers [2]–[5].

In our experiments the complex formation reactions of the D-, L- and racemic *threo*-1-(*p*-nitrophenyl)-2-amino-1,3 propanediol (aminodiol: AD) with palladium (II) ions were investigated. Namely, it has been found earlier [6] that there are slight differences in the stability of the complexes of the enantiomers formed with copper(II) ions.

The protonation constants of D-, L- and racemic aminodiol have been determined earlier. For the determination of the stability constants, pH-metric

titrations [7] of the acid salt of the complex forming ligand in the absence and presence of the metal ion were carried out. From the data of the titration curves the free ligand concentration of the solution, L and the average ligand number, $\bar{n}$ were calculated (in which the ratio of the concentration of the bound ligand to the concentration of the total metal ions was considered) using the following equations:

$$[\mathrm{L}] = \frac{C_{\mathrm{HL}} - \Delta a C_{\mathrm{HL}}}{[\mathrm{H}^+]K + 1} \tag{1}$$

$$\bar{n} = \frac{C_{\mathrm{HL}} - [L]([\mathrm{H}^+]K + 1)}{C_{\mathrm{M}}} \tag{2}$$

where K is the protonation constant of the base, C_{HL} is the total concentration of the base, C_{M} is the total concentration of the metal ion, and Δa is the difference between the points of the titration curves obtained in the absence and presence of metal ions with the same pH value. From the conditional stability constants K' determined by the graphic method of BJERRUM, the stability constants K were calculated using the following equation:

$$K = \frac{{}^{!}K'}{\alpha_{\mathrm{Pd(Cl)}} + \alpha_{\mathrm{Pd(OH)}}} - 1 \tag{3}$$

In the calculation as side reactions of the palladium ions, the chloro- and hydroxo-complex formations were considered.

$$\alpha_{\mathrm{Pd(Cl)}} = 1 + [\mathrm{Cl}]\beta_1 + [\mathrm{Cl}]^2\beta_2 + \ldots + [\mathrm{Cl}]^4\beta_4 \tag{4}$$

$$\alpha_{\mathrm{Pd(OH)}} = 1 + [\mathrm{OH}]\beta_1 + [\mathrm{OH}]^2\beta_2 \tag{5}$$

where $-\beta^{-s}$ are the corresponding overall stability constants of the chloro ($\lg \beta_1 = 3.88$ $\lg \beta_2 = 6.94$ $\lg \beta_3 = 9.08$ $\lg \beta_4 = 10.42$) [8] and hydroxo ($\lg \beta_1 = 13.0$ $\lg \beta_2 = 26.5$) complexes [9] resp.

It has been found that D- and L-aminodiol form regular complexes of 1 : 1 and 2 : 1 compositions with palladium(II) ions and the stability constants are practically identical. According to the calculations it has been considered that if the concentration of the chloride is higher than 0.1 M and the pH < 5.0, only the following reactions take place:

$$[\mathrm{PdCl_4}]^{2-} + \mathrm{HL}^+ \rightleftharpoons [\mathrm{PdCl_2L}] + \mathrm{H}^+ + 2\mathrm{Cl}^- \tag{6}$$

$$[\mathrm{PdCl_2L}] + \mathrm{HL}^+ \rightleftharpoons [\mathrm{PdL_2}]^{2+} + \mathrm{H}^+ + 2\mathrm{Cl}^- \tag{7}$$

So in Eq. (3) only the value of $\alpha_{\mathrm{Pd(Cl)}}$ is dominating, *i.e.* $\alpha_{\mathrm{Pd(OH)}}$ can be neglected (see the titration curves in Fig.1). If the solution contains chloride ions in low concentration a hydrolytic side reaction takes place.

It has been found that if the pH > 5.0 regular complexes do not form, the following reactions may be assumed (see titration curves in Fig. 2):

a) Formation of mixed hydroxo-complexes

$$[PdL_2]^{2+} + H_2O \rightleftharpoons [PdL_2(OH)]^+ + H^+$$

b) The proton loss of the hydroxyl-group of the ligands

$$[PdL_2]^{2+} \rightleftharpoons [PdL(H^{-1}L)]^+ + H^+ \qquad (8)$$

From the titration curve in Fig. 3 the stability constants of regular complexes were calculated by the modified method of BJERRUM [10]. The calculated logarithmic values of the overall stability constants of the corresponding complexes found in the experiments of different conditions are summarized in Table I.

Table I

lg β_1	lg β_2	Concentration of chloride ions 1 *M*	The corresponding titration curves (number of figure)
16.11	31.30	0.73	1
16.10	31.70	0.01	2
15.85	30.89	0	3

From the data of Table I, it can be seen that the values calculated from experimental data found at different conditions, are quite identical. The observed little deviations can be explained as following:

a) The side reactions of palladium ion (formation of chloro- and hydroxo-complexes) were taken into consideration with constants obtained by different methods.

b) The ionic strenght of the solution investigated was different.

Experimentals

Materials and instruments:

A.g. D-, L- and racemic-aminodiol ($[\alpha]_D = +25.3°$ and $[\alpha]_D = -26.2°$) and palladium(II) chloride were used.

For the pH-metric titrations an Universal pH meter (Radelkis, Hungary) with glass and calomel electrodes, and for the thermoanalytical measurements a derivatograph (MOM, Hungary) were used.

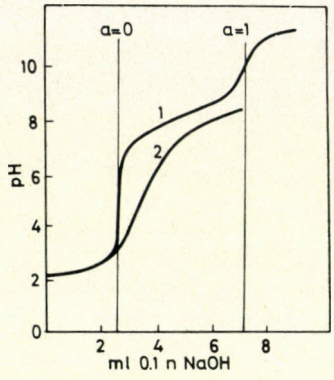

Fig. 1. Titration of $9 \cdot 10^{-3}$ *M* D- or L-aminodiol in the absence (1) and in the presence of $1 \cdot 10^{-3}$ *M* palladium(II) ion (2) (0.73 *M* sodium chloride, $1.5 \cdot 10^{-2}$ *M* hydrochloric acid, 40% methanol)

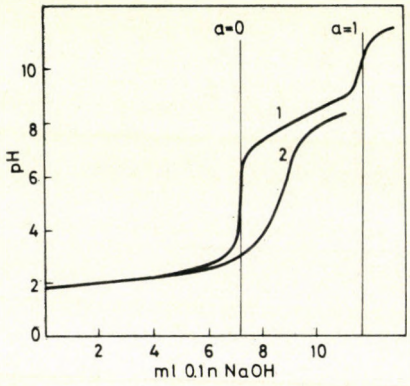

Fig. 2. Titration of $9 \cdot 10^{-3}$ *M* D- or L-aminodiol in the absence (1) and in the presence of $1 \cdot 10^{-3}$ *M* palladium(II) ion (2) ($1.5 \cdot 10^{-2}$ *M* perchloric acid, 40% methanol)

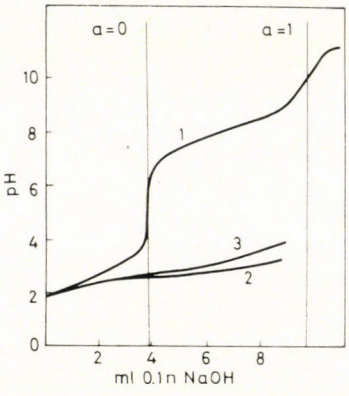

Fig. 3. Titration of $5.2 \cdot 10^{-3}$ *M* D- or L-aminodiol in the absence (1) and in the presence of $5.20 \cdot 10^{-3}$ *M* (2) $2.60 \cdot 10^{-3}$ *M* (3) palladium(II) ion ($7.8 \cdot 10^{-3}$ *M* and after than $3.9 \cdot 10^{-3}$ perchloric acid, 40% methanol)

pH-metric titrations:

The titrations were carried out in three ways. In the experiments the following solutions were used:

1. $9 \cdot 10^{-3}$ *M* D- or L-aminodiol, $1 \cdot 10^{-3}$ *M* palladium(II) chloride, 0.73 *M* sodium chloride, $1.5 \cdot 10^{-2}$ *M* hydrochloric acid, 40% methanol. The obtained titration curve is given in Fig. 1.

2. $9 \cdot 10^{-3}$ *M* D- or L-aminodiol, $1 \cdot 10^{-3}$ *M* palladium(II) chloride, $1.5 \cdot 10^{-2}$ *M* perchloric acid, 40% methanol. The titration curve is given in Fig. 2.

3. $5.2 \cdot 10^{-3}$ *M* D- or L-aminodiol, $5.2 \cdot 10^{-3}$ *M* palladium(II) chloride, $7.8 \cdot 10^{-3}$ *M* perchloric acid, 40% methanol, $5.2 \cdot 10^{-3}$ *M* D- or L-aminodiol, $2.6 \cdot 10^{-3}$ *M* palladium(II) chloride, $3.9 \cdot 10^{-3}$ *M* perchloric acid. 40% methanol. The titration curve is given in Fig. 3.

(For the titrations 0.1 *N* standard sodium hydroxyde solution was used.)

The protonation constant of the bases were determined from the data of titration curves obtained in the titration of the solutions of similar composition but in the absence of palladium(II) ions (See curves 1 in Figs 1, 2, 3). It was found that the protonation constants of D- and L-aminodiol are very close to each other, $\lg K = 7.94 \pm 0.02$ and $\lg K = 7.97 \pm 0.02$, resp.

Solution of racemic-aminodiol of very similar composition was also titrated, and the titration curve obtained and also the calculated protonation constant were found to be the same as that of the pure optical isomers ($\lg K = 7.98 \pm 0.02$).

In the presence of palladium(II) ions a precipitate was formed during the titration in the solution at pH 4.5. The precipitate was filtered, washed and dried at room temperature and its composition was $Na_2[Pd_2L_3Cl_6]$.

The chloride ion content of the precipitate was determined by the argentometric titration method of Volhard. The amount of the palladium(II) ions was determined after mineralization of the organic material, using a 3 : 1 : 1 H_2SO_4–HNO_3–$HClO_4$ mixture, by a spectrophotometric method [11]. For the determination of the organic substance and water content of the complex thermoanalytical measurements were carried out in air atmosphere. According to the TG, DTA and DTG curves the solid complex did not contain water of crystallization. The decomposition of the complex started at 150 °C, presumably according to the following equation:

$$Na_2[Pd_2L_3Cl_6] \longrightarrow 2PdCl_2 + 2NaCl + 3L \qquad (9)$$

The oxidative decomposition of the organic ligands terminated at 650 °C. Sodium chloride formed by the decomposition melted at 820 °C [12].

If the solution of racemic-aminodiol in presence of palladium(II) ions was titrated with potassium or barium hydroxide instead of sodium hydroxide solution, the composition of the obtained precipitates was found to be similar. However, if ammonium hydroxide was used as titrant precipitate did not form in the solution. The solubilities of the three different precipitates were determined in different solvents. The results are summarized in Table II.

Table II

Solvent	$Na_2[Pd_2L_3Cl_6]$	$K_2[Pd_2L_3Cl_6]$	$Ba[Pd_2L_3Cl_6]$
	g/100 ml		
Chloroform	0	0	0
Carbon tetrachloride	0	0	0
Methyl-ethyl-ketone	0.83	0.53	0.40
Methyl-iso-butyl-ketone	0.35	0.47	0.38
Acetone	1.33	1.20	0.45
1,4-Dioxan	0.02	0.04	0.01
Ethyl acetate	0.14	0.60	0.04
Diethyl ether	0	0	0
Di-iso-propyl ether	0	0	0

Using D- or L-aminodiol, we tried to prepare complexes of similar composition by the following way: The pH of the solution containing D- or L-aminodiol and palladium(II) ions was adjusted to 4.5 by the addition of sodium hydroxide. 50 ml of this solution was extracted five times with 20 ml methyl-iso-butyl-ketone. The extracts were collected and reduced to about two thirds in volume by evaporation in vacuum (at 22 °C) and the residue of the solvent was removed by vigorous stream of air at room temperature. The examination of the solid complex obtained was carried out as described above. The composition of the complex was: $[PdL_2]Cl_2 \cdot 2.5\ H_2O$.

For the explanation of the different behaviour of the complexes prepared, using optically active and racemic-aminodiol, it can be assumed that the reason of the high solubility of the complexes formed from the pure enantiomers is that two L- or two D-aminodiols are bound to the palladium(II) ions. The complex formed from the racemic-aminodiol, however, contains three ligand, from which one is of the opposite form, and the solubility of the complex formed is low. Since the filtrate of the precipitate does not show optical rotation, it must be assumed that complexes of composition ML_2D and MDL_2 formed with the same probability.

REFERENCES

[1] DWYER, F. P., MELLOR, D. P.: Chelating Agents and Metal Chelates, Academic Press, New York, London, 1964
[2] DAVAVNKOV, V. A., KURGANOV, A. A., ROGOZSIN, S. V.: Uspekhi Khim. (in print)
[3] KARCZYNSKI, F., PUSCAZSNI, M.: Rocz. Chem. **46,** 1489 (1972)
[4] MORRIS, P. J., MARTIN, R. R.: J. Inorg. Nucl. Chem. **32,** 2891 (1970)
[5] RITSMA, J. H., VAN DE GRAMPEL, J. C., JELLINEK, F.: Rec. Trav, Chim. **88,** 411 (1969)
[6] GAÁL, J., INCZÉDY, J.: J. Chrom. (in print)
[7] INCZÉDY, J.: Analytical Applications of Complex Equilibria, Műszaki Könyvkiadó, Budapest, 1971
[8] BURGER, K.: Acta Chim. Acad. Sci. Hung. **40,** 261 (1964)
[9] IZATT, R. M., EATOUGH, D., CHRISTENSEN, J.: J. Chem. Soc. A. **1967** 915
[10] CHABEREK, S., MARTELL, A. E.: J. Am. Chem. Soc. **74,** 5052 (1952)
[11] BEAMISH, F. E.: Talanta **12,** 743 (1965)
[12] LIPTAY, G.: Atlas of Thermoanalytical Curves, Vol. 1. Akadémiai Kiadó, Budapest, 1971

Judit GAÁL
János INCZÉDY } 8201 Veszprém, Schönherz Z. u 10. Hungary.

Acta Chimica Academiae Scientiarum Hungaricae, Tomus 85 (3) pp. 269—272 (1975)

PARAMETRIC APPROACH TO THE ANALYSIS OF INFRARED INTENSITIES

T. R. ANANTHAKRISHNAN and G. ARULDHAS

(Department of Physics, University of Kerala, Kariavattom, Trivandrum, India)

Received October 17, 1973

In revised form, November 20, 1974

Absolute infrared intensities of polyatomic molecules are related to an orthogonal matrix A consisting of parameters, through an equation of the form $\vec{\mu}_Q \cdot \tilde{\vec{\mu}}_Q = \tilde{A} k A$ where $\vec{\mu}_Q$ is a column matrix consisting of dipole moment derivatives with respect to the normal coordinates and k is a symmetric matrix involving the molecular geometry and the dipole moment derivatives with respect to the internal symmetry coordinates. Analysis of the above equation with special reference to the second order vibrational species leads to the interesting result that there can be two sets of force fields fitting the intensity data.

Recent techniques [1—11] in the parameter representation of molecular constants have opened a new approach to the analysis of molecular vibrations. The extension of parameter techniques to Coriolis coupling constants [10] and isotopic frequencies [11] in the second order vibrational problems has led to methods for calculating two sets of force constants that fit these experimental data and the vibrational frequencies exactly. Here we present a similar parametric approach to the analysis of infrared intensities.

The observed band intensities Γ_i are related to the derivative $\partial\vec{\mu}/\partial Q_i$ of dipole moment $\vec{\mu}$ with respect to a given normal coordinate Q_i by the expression

$$\Gamma_i = \frac{N\pi d_i}{3c^2\omega_i}(\partial\vec{\mu}/\partial Q_i)^2 \tag{1}$$

Here N is the Avogadro number and d_i is the degeneracy of the band 'i' with harmonic frequency ω_i. The $\partial\vec{\mu}/\partial Q_i$ is further related to the dipole moment gradients with respect to the prescribed symmetry coordinates S_j by the expression

$$\partial\vec{\mu}/\partial Q_i = \sum_j L_{ji}(\partial\vec{\mu}/\partial S_j) \tag{2}$$

Here the transformation elements L_{ji} relate the symmetry coordinates to the normal coordinates. Arranging Eq. (2) in matrix form

$$\vec{\mu}_Q = \tilde{L}\vec{\mu}_S \tag{3}$$

μ_Q and $\vec{\mu}_S$ are n$\times$1 column matrices consisting of $\partial\vec{\mu}/\partial Q_i$ and $\partial\vec{\mu}/\partial S_j$ elements, respectively. L is an n$\times$n transformation matrix defined through the relation $S = LQ$ where S and Q are column matrices consisting of elements Q_i and S_j respectively. 'n' refers to the order of the vibrational species. Multiplying Eq. (3) by its transpose

$$\vec{\mu}_Q \cdot \tilde{\vec{\mu}}_Q = \tilde{L}\vec{\mu}_S \cdot \tilde{\vec{\mu}}_S L \tag{4}$$

In the parametric approach we put

$$L = TA \tag{5}$$

Here T is a triangular matrix with $T_{ij} = 0$, $i < j$ satisfying the condition $T\tilde{T} = G$ (G being the usual G matrix of WILSON [12]) and A is an orthogonal matrix [5] consisting of parameters. Thus Eq. (4) becomes

$$\vec{\mu}_Q \cdot \tilde{\vec{\mu}}_Q = \tilde{A}\tilde{T}\vec{\mu}_S \cdot \tilde{\vec{\mu}}_S TA \tag{6}$$

Putting $\tilde{T}\vec{\mu}_S \cdot \tilde{\vec{\mu}}_S T = k$, Eq. (6) becomes

$$\vec{\mu}_Q \cdot \tilde{\vec{\mu}}_Q = \tilde{A}k\mathrm{A} \tag{7}$$

Since A is an orthogonal matrix, it follows that the trace of k is invariant even after the operation $\tilde{A}kA$. This leads to the interesting G sum rule [13]

$$\sum_i (\partial\vec{\mu}/\partial Q_i)^2 = \sum_{ij} (\partial\vec{\mu}/\partial S_i \cdot \partial\vec{\mu}/\partial S_j)G_{ij} \tag{8}$$

For $n = 2$, the elements of matrix k are

$$k_{11} = [T_{11}\partial\vec{\mu}/\partial S_1 + T_{21}\partial\vec{\mu}/\partial S_2]^2 \tag{9}$$

$$k_{22} = [T_{22}\,\partial\vec{\mu}/\partial S_2]^2 \tag{10}$$

$$k_{12} = [T_{11}\partial\vec{\mu}/\partial S_1 + T_{21}\,\partial\vec{\mu}/\partial S_2] \cdot [T_{22}\partial\vec{\mu}/\partial S_2] \tag{11}$$

The A matrix, in this case, has been put in the simple form

$$A = \begin{bmatrix} \cos\varphi & \sin\varphi \\ \sin\varphi & -\cos\varphi \end{bmatrix} \tag{12}$$

Substitution of Eqs (9) to (12) into (7) yields three relations

$$(\partial\vec{\mu}/\partial Q_1)^2 = k_{11}\cos^2\varphi + k_{22}\sin^2\varphi + 2k_{12}\cos\varphi\ \sin\varphi \tag{13}$$

$$(\partial\vec{\mu}/\partial Q_2)^2 = k_{11}\ \sin^2\varphi + k_{22}\ \cos^2\varphi - 2k_{12}\ \cos\varphi\ \sin\varphi \tag{14}$$

$$\pm\partial\vec{\mu}/\partial Q_1 \cdot \partial\vec{\mu}/\partial Q_2 = (k_{11} - k_{22})\ \cos\varphi\ \sin\varphi - k_{12}\ \cos 2\varphi \tag{15}$$

Since $(\partial\vec{\mu}/\partial Q_1)^2 + (\partial\vec{\mu}/\partial Q_2)^2 = k_{11} + k_{22}$ is a constant, by virtue of Eq. (8), the value of φ calculated from Eq. (13) or (14) should lead to the same result. Further, the quadratic nature of these equations suggests the existence of two possible values of φ fitting the equations. Solution of Eq. (13) gives

$$\tan\varphi = \frac{-k_{12} \pm \sqrt{k_{12}^2 - [k_{11} - (\partial\vec{\mu}/\partial Q_1)^2][k_{22} - (\partial\vec{\mu}/\partial Q_1)^2]}}{[k_{22} - (\partial\vec{\mu}/\partial Q_1)^2]} \tag{16}$$

Solution of Eq. (14) gives

$$\tan\varphi = \frac{+k_{12} \pm \sqrt{k_{12}^2 - [k_{11} - (\partial\vec{\mu}/\partial Q_2)^2][k_{22} - (\partial\vec{\mu}/\partial Q_2)^2]}}{[k_{11} - (\partial\vec{\mu}/\partial Q_2)^2]} \tag{17}$$

The plus and minus signs in the numerator of these equations yield the two possible values of φ in the range 0 to π. Upon substituting these two values of φ in Eqs (12) and (5) in turn, we get two sets of L matrices. Since the force constant elements F_{ij} can be generated [14] from the observed wavelengths λ_i through the relation $\tilde{L}^{-1}\Lambda L^{-1} = F$, along with the two sets of L matrices obtained above, one arrives at the interesting conclusion that there are two sets of force constants that exactly fit the $\partial\vec{\mu}/\partial S$ values and the intensity data.

It may be noted that Eq. (15) is also quadratic in φ, but will lead to four values of φ (two of which must coincide with those obtained from Eqs (16) and (17)), owing to the difficulty associated with the sign ambiguity of $\partial\vec{\mu}/\partial Q$ values.

The use of Eqs (16) and (17) for the evaluation of φ and hence the two sets of force constants demands very accurate values of $(\partial\vec{\mu}/\partial Q)^2$ and k. The former can be obtained with reasonable accuracy from the intensity data through Eq. (1). Moreover, Eq. (16) or (17) can be conveniently selected according to whichever Γ_i value is available with the least dispersion (that arises from the least squares analysis of the data for Beer's law). The k elements involve $\partial\vec{\mu}/\partial S_i \cdot \partial\vec{\mu}/\partial S_j$ terms and the recent CNDO/2 and INDO molecular orbital techniques [15—17] have opened routes for calculating the $\partial\vec{\mu}/\partial S$ values with specified directions, to a good approximation. However, we note that the accuracy of these semiempirical methods is not high enough to enable direct substitution of k into Eqs (16) or (17). At present, the identity of the $\tan\varphi$ values given by Eqs (16) and (17) can be used as a delicate check for the accuracy of $\partial\vec{\mu}/\partial S$ values obtained by orbital techniques in the second order cases. This condition can, however, be traced back to the validity of the G sum rule obtainable from the sum of Eqs (13) and (14).

The existence of two sets of force constants fitting the two frequencies as well as a third additional data, such as Coriolis coupling constants [10, 18,

19], isotopic frequencies [11], rotation distortion constants [18, 19] or one of the vibrational amplitudes [20], in the case of second order vibration species have already been noted. The results obtained from this work include absolute intensities in the list. In such cases a fourth additional data has to be used to eliminate the anomalous φ values.

REFERENCES

[1] PERSON, W. B., CRAWFORD, Jr. B.: J. Chem. Phys., **26,** 1295 (1957)
[2] TÖRÖK, F., PULAY, P.: Acta Chim. Acad. Sci. Hung., **44,** 287 (1965); **47,** 273 (1966); **56,** 285 (1968)
[3] PULAY, P.: Acta Chim. Acad. Sci. Hung., **52,** 49 (1967); **57,** 373 (1968)
[4] TÖRÖK, F.: Acta Chim. Acad. Sci. Hung., **52,** 205 (1967); **57,** 141 (1968); **60,** 97 (1969)
[5] TÖRÖK, F., PULAY, P.: J. Mol. Struct., **3,** 1 (1969); **3,** 283 (1969)
[6] ALIX, A. BERNARD, L.: Z. Naturforsch., **25a,** 217 (1970),
[7] ALIX, A., BERNARD, L.: C. R. Acad. Sci. Paris, **272b,** 528 (1971)
[8] ALIX, A., BERNARD, L.: J. Chim. Phys., **68,** 1161 (1971)
[9] REDINGTON, R. L., KHIDIR ALJIBURY, A. L.: J. Mol. Spectr., **37,** 494 (1972)
[10] ANANTHAKRISHNAN, T. R., ARULDHAS, G.: J. Mol. Struct., **13,** 163 (1972)
[11] ANANTHAKRISHNAN, T. R., GIRIJAVALLABHAN, C. P., ARULDHAS, G.: J. Mol. Struct., **16,** 149 (1973)
[12] WILSON, Jr. E. B.: J. Chem. Phys., **9,** 76 (1941)
[13] CRAWFORD, Jr. B.: J. Chem. Phys., **20,** 977 (1952)
[14] WILSON, E. B., DECIUS, J. C. and CROSS, P. C.: Molecular Vibrations. McGraw-Hill, New York 1955
[15] POPLE, J. A., SEGAL, G. A.: J. Chem. Phys., **44,** 3289 (1966)
[16] SEGAL, G. A., KLEIN, M. L.: J. Chem. Phys., **47,** 4236 (1967)
[17] POPLE, J. A., BEVERIDGE, D. L., DOBOSH, P. A.: J. Chem. Phys., **47,** 2026 (1967)
[18] HOY, A. R., STONE, J. M. R., WATSON, J. K. G.: J. Mol. Spectr., **42,** 393 (1972)
[19] ALLAN, A., DUNCAN, J. L., HOLLOWAY, J. H., MCKEAN, D. C.: J. Mol. Spectr., **31,** 368 (1969)
[20] ANANTHAKRISHNAN, T. R., GIRIJAVALLABHAN, C. P., ARULDHAS, G.: Indian J. Pure Appl. Phys., **11,** 648 (1973)

T. R. ANANTHAKRISHNAN
G. ARULDHAS
Department of Physics, University of Kerala, Kariavattom — 695581 Trivandrum, India.

Acta Chimica Academiae Scientiarum Hungaricae, Tomus 85 (3), pp. 273–288 (1975)

INVESTIGATIONS ON THE CORRELATION BETWEEN THE OPTIMUM THICKNESS OF MÖSSBAUER ABSORBENTS AND CERTAIN EXPERIMENTAL PARAMETERS

S. NAGY, B. LÉVAY and A. VÉRTES

(Department of Physical Chemistry and Radiology, Eötvös Loránd University, Budapest)

Received June 3, 1974

Optimization of the thickness of Mössbauer absorbent was investigated. It was considered to be optimal the absorbent thickness at which the shortest measuring time is necessary to obtatin an effect of k times greater than the statistical deviation of the base line.

It was shown that if the concentration of the Mössbauer atoms is unknown $2/\mu$ is the best estimation for the optimal absorbent thickness, where μ is the mass absorption coefficient of the absorbent.

Introduction

The optimum choice of the experimental parameters (thickness of absorbent, concentration of Mössbauer nuclei, time of measurement, etc.) is an important problem in Mössbauer spectroscopy when a particular sample or a sample series with varying composition is analysed. The optimization of experimental parameters is particularly essential when the intensity of the source, the concentration of Mössbauer nuclei or the Debye–Waller factor, determining the magnitude of effect, are low. For a sample with a particular composition it is most important to find the appropriate layer thickness of the absorbent, because an increase in thickness increases the nuclear resonance absorption, but it also promotes the absorption due to electrons (photo-effect).

Until recently only a few papers have dealt with experiments on the optimization of experimental parameters, and no uniform standpoint has been reached, either, as to when experimental conditions can be regarded optimal [1–3].

The problem has been treated most generally by PROTOP and NISTOR [2]. According to their definition, the optimum thickness of Mössbauer absorbent is the one at which a Mössbauer parameter can be determined within the shortest time with a given accuracy. The above authors were actually concerned with the isomeric shift, but they also reported the basic relationships for the general treatment. The magnitude of Mössbauer effect is characterized in their

paper by the formula of MARGULIES *et al.* [4], which holds for band shapes of Breit–Wigner type:

$$\eta(0) = f\left[1 - e^{-\frac{t}{2}} I_0\left(\frac{t}{2}\right)\right] \tag{1}$$

where f is the Debye–Waller factor of the source, t is the 'effective thickness' of the absorbent, and I_0 is the zero order modified primary Bessel function.

The effective thickness can be given as

$$t = f' n a \sigma_0 x$$

where f' is the probability of recoil-free nuclear resonance absorption in the absorbent,

n is the number of atoms per cubic centimetres,

a is the atomic fraction of Mössbauer atoms in the absorbent,

σ_0 is the maximum cross-section of resonance absorption, and

x is the thickness of absorbent in cm.

In one of our previous papers [3], where the optimum thickness was defined in a manner essentially similar to the definition of PROTOP and NISTOR, the magnitude of the Mössbauer effect was investigated in cases when the concentration of Mössbauer nuclei in the sample is low. The effect was calculated, however, by Eq. (2), which can be derived from the simple law of absorption:

$$S_M = [1 - e^{-\mu_M x_M d}] f \tag{2}$$

where μ_M is the coefficient of nuclear resonance absorption, in cm^2/g, x_M is the weight fraction of Mössbauer atoms, and d is the thickness of absorbent in g/cm^2.

The correlations found by PROTOP and NISTOR are sophisticated, mathematically untractable, and they contain the optimum thickness or time of measurement only implicitly. Hence, the effect of various experimental parameters on the optimum conditions have been studied only for certain limiting cases.

In contrast, our approximation is easy to treat mathematically, and yields equations that can readily be solved for the optimum thickness. The two approaches lead to the same results at low concentrations or low effective thicknesses.

The object of this paper is to investigate in detail the general conclusions that can be derived for the various experimental parameters from the formulas of PROTOP and NISTOR, and to study the performance of our more tractable formulas for thicker layers and higher concentrations.

Discussion

As follows from the above, the layer thickness is regarded optimum if an effect that is k times higher than the statistical error, δ, of the base line of the spectrum can be measured under the possible shortest time. (k is here a positive number, chosen arbitrarily according to the demands of a particular measurement.) This condition can be given by the equation

$$\eta(0) \simeq S_M \geq k\delta \tag{3}$$

where $\eta(0)$ and S_M, respectively, represent the magnitude of the effect, *i.e.* the ratio of the depth of the peak and the height of the base line, both expressed in count numbers. The expected relative value of the statistical error of N_∞ is given by the well-known expression

$$\delta^2 = \frac{1}{N_\infty} \tag{4}$$

The subscript of N_∞ refers to the condition that one must consider the average of the pulses stored in channels well away from the maximum absorption.

If, in the absence of absorbent, the channels each detect A_0 particles per unit time, in the presence of absorbent causing general absorption (due primarily to the photo effect) the number of pulses collected in the channels under a period τ can be given as

$$N_\infty = A_0 \tau e^{-\mu d} \tag{5}$$

where μ is the mass absorption coefficient.

In order to make the equations more comparable, the uniform notation

$$\frac{t}{2} = \mu_M x_M d = \beta d \tag{6}$$

will be used throughout.

Thus, on the basis of Eqs (1)—(5), the minimum measuring time corresponding to a given accuracy can be given by the expression

$$\tau = \frac{k^2}{A_0 f^2} \frac{e^{\mu d}}{[1 - e^{-\beta d} I_0(\beta d)]^2} \tag{7}$$

or, on the basis of the approximate formula

$$\tau = \frac{k^2}{A_0 f^2} \frac{e^{\mu d}}{[1 - e^{-\beta d}]^2} \tag{8}$$

Consequently, β is a quantity proportional to the concentration of Mössbauer atoms and to the coefficient of resonance absorption.

The only difference between the exact (7) and the approximate (8) relationships is the presence of the Bessel function in the former, but it is just this difference that makes the mathematical treatment less tractable.

If all parameters are fixed, and the effects of only the layer thickness and the concentration (d and β) are studied, instead of investigating the time of measurement τ, it is sufficient to investigate the function*

$$T(d) = \frac{e^{\mu d}}{[1 - e^{-\beta d} I_0(\beta d)]^2} \tag{9}$$

or in the simplified case

$$T'(d) = \frac{e^{\mu d}}{[1 - e^{-\beta d}]^2} \tag{10}$$

This function has a minimum at the same layer thickness as function $\tau(d)$.

If in a series of experiments the concentration of the Mössbauer nuclei changes so that μ remains approximately constant (this is a frequent case in practice), it is worth using the notations

$$Z = \mu d \tag{11}$$

and

$$\gamma = \frac{\beta}{\mu} \tag{12}$$

In the subsequent treatment Z and γ denote quantities which are proportional to the layer thickness and the concentration of Mössbauer atoms, respectively.

With this notation Eqs (9) and (10) can be written as

$$T(Z) = \frac{e}{[1 - e^{-\gamma Z} I_0(\gamma Z)]^2} \tag{13}$$

and

$$T'(Z) = \frac{e^Z}{[1 - e^{-\gamma Z}]^2} \tag{14}$$

* When, for instance, from the radiation of an iron source of medium activity $A_0 = 400$ cpm is detected in one channel without absorbent, the Debye–Waller factor of the source is $f = 0.5$, and it is required in the measurement that $\eta(0)$ must be at least $k = 10$ times higher than the relative scattering of the baseline, the numerical value of the measurement time τ in minutes will be equal to the measurement time factor T:

$$\tau = T \text{ (min)}$$

Fig. 1 shows a plot of $T(Z)$, *i.e.* the measurement time factor proportional to the required time, against the layer thickness, for various values of γ, *i.e.* concentration.

It can be seen that for a given concentration the time of measurement passes a minimum at a certain layer thickness. The minimum, *i.e.* optimal T is denoted by T_{opt}, and the corresponding value of Z by Z_{opt}. (When the approximate formula is used, the notation is T'_{opt} and Z'_{opt}, respectively.)

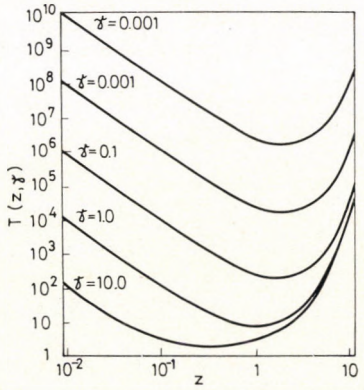

Fig. 1. The measurement time factor $T(Z)$ around the optimum as a function of the transformed layer thickness, Z

It can also be seen that for low γ the minimum is quite sharp. It is therefore not irrelevant from the aspect of measurement time how far the actual Z is from Z_{opt}. According to Eq (11), there is a simple correlation between Z_{opt} and the optimum layer thickness:

$$d_{opt} = \frac{Z_{opt}}{\mu} \tag{15}$$

The equation yielding Z_{opt} can be derived from Eq. (13) by applying the condition $dT(Z)/dZ = 0$:

$$1 - e^{-\gamma Z_{opt}}[(1 + 2\gamma)I_0(\gamma Z_{opt}) - 2\gamma I_1(\gamma Z_{opt})] = 0 \tag{16}$$

In this equation I_1 is the first order primary modified Bessel function.

According to SHIMONY [1] the thickness of absorbent is optimum when under unit time the possible greatest effect can be obtained. On the basis of this definition the optimum $Z(Z_S)$ can be determined from the equation

$$1 - e^{-\gamma Z_S}[(1 + \gamma)I_0(\gamma Z_S) - \gamma I_1(\gamma Z_S)] = 0 \tag{17}$$

The application of the approximate Eq. (14) leads to the simple result

$$Z'_{\text{opt}} = \frac{ln(1 + 2\gamma)}{\gamma} \tag{18}$$

It can be seen from Fig. 1 and Eqs (16) and (18) that Z_{opt}, proportional to the optimum layer thickness, is a function of γ, proportional to the concentration.

The functions $Z_{\text{opt}}(\gamma)$ determined from Eq. (16) by computer iteration, and $Z'_{\text{opt}}(\gamma)$, determined simply from Eq. (18), are shown in Fig. 2. The two functions are in surprisingly good agreement over the range under study.

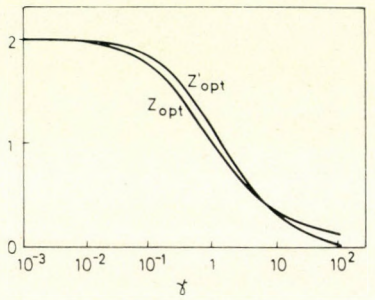

Fig. 2. The transformed optimum layer thickness as a function of γ, a variable proportional to concentration. It can be seen that at low γ the value of Z_{opt} calculated from the Lambert–Beer law is a good approximation to the exact Z_{opt}.

Fig. 2 indicates that $Z_{\text{opt}}(\gamma)$ and $Z'_{\text{opt}}(\gamma)$ approach finite limits, denoted by ζ and ζ', when $\gamma \to 0$. It can be found readily from Eq. (18), and after a little calculation from Eq. (16) (see Appendix I) that

$$\zeta = \zeta' = \lim_{\gamma \to 0} Z_{\text{opt}} = \lim_{\gamma \to 0} Z'_{\text{opt}} = 2 \tag{19}$$

Eq. (17) leads in a similar manner to the limit of SHIMONY's optimum, Z_S:

$$\lim_{\gamma \to 0} Z_S = 1 \tag{20}$$

Consequently, the limit of optimum layer thickness, extrapolated to zero concentration is

$$\lim_{\gamma \to 0} d_{\text{opt}} = \lim_{\gamma \to 0} d'_{\text{opt}} = \frac{\zeta}{\mu} = \frac{2}{\mu}$$

according to both the exact and the approximate formulas.

Consequently, the optimum layer thickness at low concentrations can be determined alone from the general absorption coefficient of the absorbent, which is easy to determine experimentally.

Fig. 1 also indicates that the change in concentration (γ) affects not only the location of the minimum (Z_{opt}) of the function $T(Z,\gamma)$, but the optimum measurement time factor, T_{opt}, as well.

Fig. 3 shows the function $T_{opt}(\gamma)$, calculated with computer, and the function

$$T'_{opt} = \frac{(1+2\gamma)^{\frac{1+2\gamma}{\gamma}}}{(2\gamma)^2} \tag{21}$$

obtained from Eqs (14) and (18). There is a very good agreement between these curves, too.

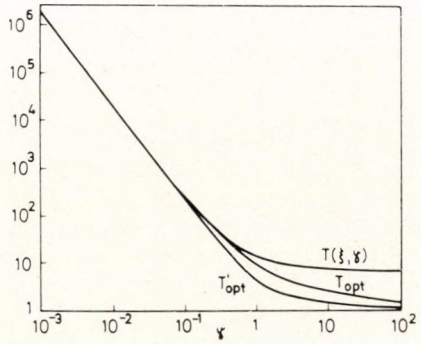

Fig. 3. The optimum measurement time factor as a function of γ. T'_{opt} is the approximate function calculated from the Lambert—Beer law

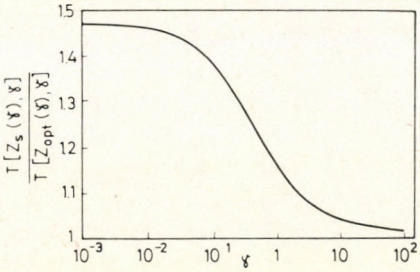

Fig. 4. The ratio of measurement time factors corresponding to the optimum layer thickness according to SHIMONY and this work, respectively. It can be seen that at low γ SHIMONY's layer thickness, Z_S, is not optimum with respect to the time of measurement

The functions are apparently decreasing monotonically. In the case $\gamma \to 0$ they become infinite. When $\gamma \to \infty$, the limit of T_{opt}, as will be shown later, is 1, and a same value is obtained for T'_{opt} from Eq. (21). These limits imply that the time of measurement increases beyond limits with the decreasing concentration of Mössbauer atoms, but it cannot be decreased to an arbitrary value by increasing the concentration.

It is surprising that the approximate formula gives the same result as the exact one, not only for the case $\gamma \to 0$, but also when $\gamma \to \infty$.

Fig. 4 shows a plot of the ratio of SHIMONY's optimum, T_S and our T_{opt} against γ.

It can be seen that at low γ SHIMONY's optimum thickness and measurement time deviate substantially from those derived from the criteria of optimum recommended by PROTOP and NISTOR, or the authors of this work.

At low values of γ (if $\gamma Z \to 0$, together with γ) Eq. (13) can be simplified by expanding the denominator into power series, and neglecting the terms higher than first power:

$$T(Z) \approx \frac{e^Z}{(\gamma Z)^2} \tag{22}$$

wherefrom

$$T_{opt}(\gamma) = \frac{e^{Z_{opt}}}{(\gamma Z_{opt})^2} \tag{23}$$

By substituting $\zeta = 2$ for Z_{opt}, which proved to be permissible for low γ, we obtain

$$T_{opt}(\gamma) \approx \frac{e^\zeta}{(\gamma\zeta)^2} = \left(\frac{e}{2\gamma}\right)^2 \tag{24}$$

For low values of γ the same result can be obtained from the approximate Eq. (14).

The increase in minimum time of measurement upon changing the value of Z_{opt} corresponding to γ by a factor of λ has also been investigated. For this goal the ratio of $T_\lambda(\gamma)$, belonging to λZ_{opt} and $T_{opt}(\gamma)$, belonging to Z_{opt}, is to be studied in the limiting case $\gamma \to 0$. The ratio decreases monotonically with increasing γ, therefore its limit, $\vartheta(\lambda)$ may also be regarded as an upper bound of the expected increase in the required time of measurement.

On the basis of Eqs (22), (23) and (19) the limit of the increase in time is

$$\vartheta(\lambda) = \lim_{\gamma \to 0} \frac{T_\lambda(\gamma)}{T_{opt}(\gamma)} = \lim_{\gamma \to 0} \frac{e^{(\lambda-1)Z_{opt}}}{\lambda^2} = \frac{e^{(\lambda-1)\zeta}}{\lambda^2} \tag{25}$$

By substituting $\zeta = 2$, we obtain

$$\vartheta(\lambda) = \frac{e^{2(\lambda-1)}}{\lambda^2} \tag{25a}$$

The function $\vartheta(\lambda)$ is shown over the range of $10^{-1} \leq \lambda \leq 4$ in Fig. 5. When λ is between 0.7 and.1.4, ϑ assumes a value between 1 and 1.1, *i.e.* the time is

at most 10% higher than optimum. When λ is between 0.5 and 1.8, $1 \leq \vartheta \leq$ ≤ 1.5, and the increase of time is still below 50%. Outside the range of $0.5 \leq$ $\leq \lambda \leq 1.8$, however, ϑ increases rapidly.

When Mössbauer spectroscopy is applied in analysis, the concentration of Mössbauer nuclei is unknown, and perhaps not even the factor f' of the absorbent is known. Consequently, γ is unknown. What layer thickness should

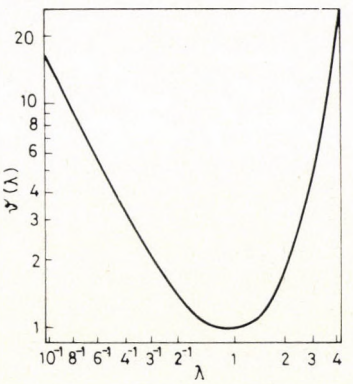

Fig. 5. The function $\vartheta(\lambda)$ for determining an upper estimate of the increase in the time of measurement:

$$\vartheta(\lambda) \geq \frac{T(\lambda Z_{\mathrm{opt}})}{T(Z_{\mathrm{opt}})}$$

then be used? It follows from the above that it is not worth using a thickness greater than that corresponding to ζ, since Z_{opt} is always lower than ζ. (Of course, it may occur in practice that ζ is so small that such a thin sample cannot be prepared. In these cases the possible thinnest layer is to be used.)

Fig. 3 also shows the measurement time factor $T(\zeta,\gamma)$ belonging to the layer thickness ζ as a function of γ. As can be seen, $T(\zeta,\gamma)$ will deviate from T_{opt} by more than 10% only above $\gamma = 0.3$, but in this region T is already very small, and thus the absolute increase of time is not too great.

Moreover, it can be shown (see Appendix II) that if a layer thickness of $\lambda\zeta$ is chosen, the corresponding measuring time factor, $T(\lambda\zeta,\gamma)$ has a finite limit value, even when $\gamma \to \infty$.

In the special case of $\lambda = 1$:

$$\lim_{\gamma\to\infty} T(\zeta,\gamma) = e^{\zeta} = e^2 \approx 7.4 \tag{26}$$

It can also be shown that, as already mentioned, T_{opt}, belonging to the optimum layer thickness, also has a finite limit value when $\gamma \to \infty$ (see Appendix III:)

$$\lim_{\gamma\to\infty} T_{\mathrm{opt}} = 1 \tag{27}$$

Consequently, the required or optimum time of measurement can be decreased to only a given limit by increasing the concentration.*

Conclusions

The analysis of the correlations between the required time of measurement and the layer thickness of the absorbent or the concentration of Mössbauer atoms has led to the following important conclusions:

For a particular concentration the required time of measurement is minimum if a sample with optimum layer thickness is chosen.

At low concentrations the optimum layer thickness is, to a good approximation, $2/\mu$. Even for high concentrations, the minimum required time corresponding to this layer thickness will not exceed 7.4 T_{opt}. In the high concentration range, however, the optimum measurement time strongly decreases.

It is unnecessary to choose too high concentrations, because the required time of measurement can be reduced to only a certain limit by increasing the concentration.

For low concentrations, however, when the required time of measurement is long anyway, it is recommended to choose a layer thickness as close as possible to the optimum, since if the deviation from the optimum exceeds 30—50%, the time of measurement abruptly increases.

Thus, if γ is unknown, a convenient choice of thickness is $2/\mu$, corresponding to ζ. In this case, according to Fig. 6, the increase in time factor is less than about 7 for any γ.

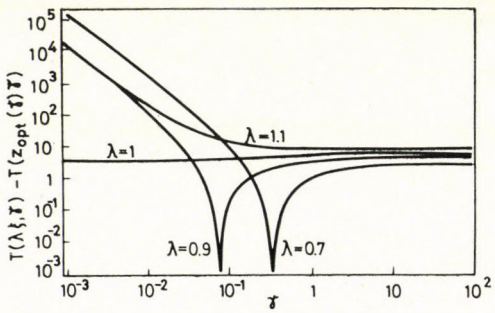

Fig. 6. The expected increase in measurement time factor as a function of γ for fixed layer thickness (*i. e.* independent of γ). It can be seen that for the layer thickness of $Z = \zeta$ the calculated measurement time factor approaches evenly the optimum

* In practice, the measurement time factor cannot even be decreased to the limit $T = 1$, since the increase of concentration is limited by the fact that only a finite number of atoms may be present in a given volume. Nevertheless, the behaviour of the functions had to be also investigated at the limit $\gamma \to \infty$, because the attainable maximum of γ depends on the nature of the various Mössbauer atoms.

The mathematically tractable formulas, derived on the basis of the simple absorption law, can be used to advantage in the calculation of optimum layer thickness, since they give a very good approximation to the exact, but more sophisticated equations.

When the absorption spectrum splits into several lines (with the same half-intensity widths), a particular layer thickness will not be optimum for all lines. If the object is to optimize with respect to line i, all the above considerations hold, just γ should be replaced by $\gamma_i = W_i\gamma$, where W_i is the relative intensity of the ith line.

In the case of several lines, the most convenient layer thickness is still $d = \frac{2}{\mu}$ if γ is unknown. This follows directly from Eq.(22), since $\gamma = \gamma_i/W_i$ approaches zero together with γ_i. The optimum layer thickness in this respect is, therefore, independent of splitting.

It must be noted that the above considerations pertain to the case when the intensity of the background radiation, $h(Z)$ is negligible. In the case of non-negligible background the equations become slightly more complicated, for instance Eq.(13) of the measurement time factor must be multiplied by the expression $[1 + g(Z)\, e^Z]$, where $g(Z) = h(Z)/A_0$. Although the run of the functions under study remains essentially unchanged, their limits at $\gamma \to 0$ and $\gamma \to \infty$ will be different. The limit $\zeta = \lim_{\gamma \to 0} Z_{\text{opt}}$, which is the most important in our treatment, can be calculated from the equation

$$\zeta = \frac{2}{1 + \dfrac{g(\zeta) + g'(\zeta)}{g(\zeta) + e^{\zeta}}}$$

where $g'(\zeta)$ is the first derivative of g with respect to Z at the place ζ.

When the background is independent of the layer thickness, *i.e.* $g(\zeta) = g_0$ and $g'(\zeta) = 0$, ζ decreases asymptotically from 2, belonging to $g_0 = 0$, to 1 with increasing background ratio, g_0.

As to the case when the background depends on the layer thickness, *i.e.* $g'(\zeta) \neq 0$, it is only noted that one can conceive such experimental conditions under which ζ becomes greater than 2.

Thus, when the concentration of the Mössbauer atoms, γ, is low or unknown, a layer thickness of $d = \zeta/\mu$ is again the most convenient. Of course, now ζ is generally not 2, but a value determined by the above equation.

Appendix I

If $\gamma Z_{opt} \to 0$ together with γ, no great error will be introduced if in Eq. (16) only the zero- and first-order terms of the Maclaurin series of the exponential and Bessel functions are taken into account:

$$e^{-\gamma Z_{opt}} \approx 1 - \gamma Z_{opt}$$

$$I_0(\gamma Z_{opt}) \approx 1$$

$$I_1(\gamma Z_{opt}) \approx \frac{\gamma Z_{opt}}{2}$$

Substituting these expansions into Eq. (16), and dividing both sides by $\gamma \neq 0$, we obtain

$$-\gamma^2 Z_{opt}^2 + (3\gamma + 1) Z_{opt} = 2$$

wherefrom

$$\zeta = \lim_{\gamma \to 0} Z_{opt} = 2$$

Appendix II

Calculation of $\lim_{\gamma \to \infty} T(\lambda\zeta,\gamma)$.

If the layer thickness corresponds to $Z = \lambda\zeta$, we may write, on the basis of Eq. (13), $T(Z,\gamma)$ in the form

$$T(\lambda\zeta, \gamma) = \frac{e^{\lambda\zeta}}{\left[1 - \frac{I_0(r)}{e^r}\right]^2}$$

where: $r = \gamma\lambda\zeta$.

If $\gamma \to \infty$, then $r \to \infty$, and therefore

$$\lim_{\gamma \to \infty} T(\lambda\zeta, \gamma) = \frac{e^{\lambda\zeta}}{\left[1 - \lim_{r \to \infty} \frac{I_0(r)}{e^r}\right]^2} \tag{28}$$

It will be shown that

$$\lim_{r \to \infty} \frac{I_0(r)}{e^r} = 0 \tag{29}$$

Let y denote a complex number. Then the convergence radius of the complex-variable function

$$I_0(y) = 1 + \frac{1}{(1\,!)^2}\left(\frac{y}{2}\right)^2 + \ldots + \frac{1}{(n\,!)^2}\left(\frac{y}{2}\right)^{2n} + \ldots \tag{30}$$

is infinite [5]. For such functions the estimate

$$M(r) < \mu(r)[\ln \mu(r)]^{1/2+\varepsilon} \tag{31}$$

must hold [6], where

$\varepsilon > 0$ is a pre-fixed (arbitrarily small) number,
$r > 0$ is an arbitrarily large real number,
$\mu(r)$ is the maximum term of the power series of $I_0(r)$, and
$M(r)$ is the maximum of $|I_0(y)|$ on the closed circular plate $|y| \leq r$.

Estimation of $\mu(r)$

Since the terms in the expansion of $I_0(r)$ increase until a certain index and then decrease, one should find the highest index at which the term is not less than the preceding one. Let this index be m. Then we have

$$\frac{1}{(m-1)!^2}\left(\frac{r}{2}\right)^{2m-} \leq \frac{1}{m!^2}\left(\frac{r}{2}\right)^{2m} = \mu(r)$$

Upon simplification and rearrangement we obtain

$$m^2 \leq \left(\frac{r}{2}\right)^2$$

Since $r > 0$,

$$m \leq \frac{r}{2}$$

must hold. The highest integer which satisfies this condition is the integral fraction of $r/2$, *i.e.*

$$m = \left[\frac{r}{2}\right] \tag{32}$$

Using this value of m, we obtain the maximum term:

$$\mu(r) = \frac{1}{\left[\frac{r}{2}\right]!^2}\left(\frac{r}{2}\right)^{2\left[\frac{r}{2}\right]} \tag{33}$$

Using the evident inequality

$$\frac{r}{2} < \left[\frac{r}{2}\right] + 1$$

and returning to the notation of Eq. (32), an upper estimate of Eq. (33) can be given:

$$\mu(r) < \frac{1}{m!^2}(m+1)^{2m} \tag{34}$$

Taking into account that STRILING's formula

$$m! \approx \left(\frac{m}{e}\right)^m \sqrt{2\pi m}$$

provides a lower estimate for $m!$, the right-hand side of Eq. (34) can be further increased:

$$\mu(r) < \frac{e^{2m}}{2\pi m}\left(1 + \frac{1}{m}\right)^{2m} \tag{35}$$

As $(1 + 1/m)^m$ approaches e in a monotonic increasing series when m approaches infinite, the right-hand side of Eq. (35) can be increased by replacing $(1 + 1/m)^m$ with e:

$$\mu(r) < \frac{e^{2(m+1)}}{2\pi m} \tag{36}$$

Since

$$m = \left[\frac{r}{2}\right] > \frac{r}{2} - 1$$

and

$$m = \left[\frac{r}{2}\right] \leq \frac{r}{2}$$

the right-hand side of Eq. (36) can be increased by replacing m in the exponent with $r/2$ and in the denominator with $(r/2 - 1)$:

$$\mu(r) < \frac{e^{r+2}}{\pi(r-2)} \tag{37}$$

On the basis of Eq. (37):

$$\ln \mu(r) < r + 2 - \ln[\pi(r-2)]$$

It may be assumed that $\pi(r - 2) > e^4$ (since $r \to \infty$), hence

$$\ln \mu(r) < r - 2 \tag{38}$$

Substituting Eqs (37) and (38) into Eq. (31), and choosing $\varepsilon = 1/6$, we obtain

$$M(r) < \frac{e^{r+2}}{\pi}(r-2)^{-\frac{1}{3}} \tag{39}$$

With the use of Eq. (39) we can calculate the limit in question:

$$0 \leq \lim_{r\to\infty} \frac{I_0(r)}{e^r} \leq \lim_{r\to\infty} \frac{M(r)}{e^r} \leq \frac{e^2}{\pi} \lim_{r\to\infty} (r-2)^{-\frac{1}{3}} = 0$$

or

$$0 \leq \lim_{r\to\infty} \frac{I_0(r)}{e^r} \leq 0$$

Consequently, as stated by Eq. (29), the limit is zero:

$$\lim_{r\to\infty} \frac{I_0(r)}{e^r} = 0$$

Substituting this result into Eq. (28), we obtain

$$\lim_{\gamma\to\infty} T(\lambda\zeta, \gamma) = e^{\lambda\zeta}$$

The function $T(\lambda\zeta, \gamma)$ is monotonically decreasing, because the function $I_0(r)/e^r$ behaves similarly. This can be seen from the derivative

$$\frac{d}{dr}\frac{I_0(r)}{e^r} = \frac{I_1(r) - I_0(r)}{e^r} < 0$$

since

$$I_1(r) < I_0(r)$$

holds for any value of r.

Appendix III

We have shown in Appendix II that

$$\lim_{\gamma\to\infty} T(\lambda\zeta, \gamma) = e^{\lambda\zeta} \tag{40}$$

This relationship can be utilized in the calculation of $\lim_{\gamma\to\infty} T_{\text{opt}}(\gamma)$.

It is obvious that for a given value of λ between 0 and 1

$$T_{\text{opt}}(\gamma) = T(Z_{\text{opt}}, \gamma) \leq T(\lambda\zeta, \gamma)$$

According to the definition of Z_{opt}, this relationship holds for any γ, including the limit $\gamma \to \infty$. Taking into account Eq. (40), we obtain

$$\lim_{\gamma\to\infty} T_{\text{opt}}(\gamma) \leq \lim_{\gamma\to\infty} T(\lambda\zeta, \gamma) = e^{\lambda\zeta}$$

This relationship holds for all $\lambda > 0$, hence for the limit $\lambda \to 0$, as well:

$$\lim_{\lambda\to 0} \lim_{\gamma\to\infty} T_{\text{opt}}(\gamma) = \lim_{\gamma\to\infty} T_{\text{opt}}(\gamma) \leq \lim_{\lambda\to 0} e^{\lambda\zeta} = 1$$

Consequently, we have

$$\lim_{\gamma \to \infty} T_{\text{opt}}(\gamma) \leq 1 \tag{41}$$

Now, for any Z_{opt} a γ-dependent value of $\lambda_0 > 0$ can be found such that Z_{opt} can be written in the form

$$Z_{\text{opt}} = \lambda_0 \zeta$$

Then, we can write

$$1 < e^{\lambda_0 \zeta} < T(\lambda_0 \zeta, \gamma) = T_{\text{opt}}(\gamma)$$

since the function $T(\lambda_0 \zeta, \gamma)$ decreases monotonically with increasing γ (see Appendix II), and therefore its value is always greater than its limit at infinite γ (which is, according to Eq. (40), just $e^{\lambda_0 \zeta}$).
Consequently, the inequality

$$1 < T_{\text{opt}}(\gamma)$$

holds for any γ, including the limit at $\gamma \to \infty$:

$$1 \leq \lim_{\gamma \to \infty} T_{\text{opt}}(\gamma) \tag{42}$$

From a comparison of Eqs (41) and (42) we obtain

$$\lim_{\gamma \to \infty} T_{\text{opt}}(\gamma) = 1$$

*

Acknowledgements: We would like to thank Dr. L. KORECZ and Dr. M. SIMONOVITS for helpful discussions.

REFERENCES

[1] SHIMONY, U.: Nucl. Instr. Methods, **37,** 348 (1965)
[2] PROTOP, C., NISTOR, C.: Rev. Roum. Phys. **12,** 653 (1967)
[3] VÉRTES, A., FRAKNÓY-KŐRÖS, V., LÉVAY, B., GELENCSÉR, P. A., RANONGAJEC-KOMOR, M.: Acta Chim. (Budapest), **74,** 151 (1972)
[4] MARGULIES, S., EHRMANN, F. R.: Nucl. Instr. Methods, **12,** 131, (1961); MARGULIES, S., DEBRUNNER, P., FRAUENFELDER, H.: Nucl. Instr. Methods, **21,** 217 (1963)
[5] WATSON, G. N.: A Treatise on the Theory of Bessel Functions, Cambridge 1944
[6] PÓLYA, G., SZEGŐ, G.: Aufgaben und Lehrsätze aus der Analysis, Springer-Verlag, Berlin—Göttingen—Heidelberg, 1954

Sándor NAGY
Béla LÉVAY
Attila VÉRTES
1088 Budapest, Puskin utca 11—13. Hungary.

Acta Chimica Academiae Scientiarum Hungaricae, Tomus 85 (3), pp. 289—298 (1975)

LATTICE DYNAMICS STUDY OF CRYSTALLINE TETRAPHENYLSILANE

F. CSER,[1] L. PÁRKÁNYI[2] and P. HENCSEI[2]

([1]Research Institute for Plastics, Budapest, [2]Institute of Inorganic Chemistry, Technical University, Budapest)

Received August 21, 1974

Conformational and lattice energy calculations were performed on the tetraphenylsilane molecule, using data derived from X-ray structure determinations and quantum chemical calculations. The main features of the thermal motion in the lattice were established.

The calculated lattice energy (−177.78 kJ/mol = −42.65 kcal/mol) is in good agreement with the value obtained from experimental data (−182.63 kJ/mol = = −43.65 kcal/mol).

Thermal parameters of the X-ray study were connected with the conformational and lattice energy changes due to the movement of the molecule in the crystal lattice.

Introduction

The force-field principle is widely applied for the determination of the energy functions attributed to the movement of molecular segments. The force-field principle also provides a successful method for the calculation of the energy barriers of the segment rotations. The thermal parameters of an X-ray structure determination are to describe the atomic motion in the crystal lattice, but there is a good deal of errors accumulated in these parameters. The knowledge of the energy function permits to estimate the magnitude of errors in the thermal parameters.

Several crystal structures have been determined by using potential functions of the above type. It is worth pointing out that the calculated energy values have a real meaning.

Our aim was to correlate the changes in conformational and lattice energy (due to the movement of the molecule) with the librational and vibrational data derived from the thermal parameters of a known crystal structure. For the purpose of this study, the relatively simple tetraphenilsilane (TPHSI) molecule studied from various aspects, was chosen. In addition to calorimetric data, two determinations of the TPHSI crystal structure [1, 2] were available.

Methods of calculation

1. *Quantum chemical calculations*

Quantum chemical calculations were performed for the TPHSI molecule, using X-ray structural data [1]. The calculation of the σ-bond system was carried out by DEL RE's method [3]. Apart from the original C–C and C–H parameters, a modified inductive parameter γ_{CH} and parameters determined for the Si–C bond [4] were applied.

The PARISER–PARR–POPLE method [5, 6] was used for the calculations of the π-bond system. The double-center repulsion integrals were approximated by the formula of MATAGA and NISHIMOTO [7]. The resonance integrals were calculated on the basis of the equation of WOLFSBERG and HELMHOLTZ [8]. A value of 0.6426 was ascribed to parameter k. This value was determined from the overlap and resonance integrals of the C–C bond in benzene, using BURNS' effective nuclear charges [9] for the calculation of the overlap integrals. Computations were performed on an ICL 1903/A computer, using the PPP program of PACKER and FORD. Input data are listed in Table I.

Table I

Input data for the PPP calculation of the TPHSI molekule (eV)

$U_{Si} = -1.10$	$\beta_{SiC} = -1.3115$	$\beta_{45} = -2.5016$
$U_C = -11.16$	$\beta_{12} = -2.4030$	$\beta_{56} = -2.3908$
$\gamma_{SiSi} = 3.762$	$\beta_{23} = -2.4767$	$\beta_{16} = -2.3692$
$\gamma_{CC} = 11.13$	$\beta_{34} = -2.4396$	

2. *Conformational analysis*

Conformational analysis calculations were performed, using the program CONFORM [11] based on the WESTHEIMER–HENDRICKSON–WIBERG method [10]. The potential function applied is as follows:

$$E_{tot} = \frac{1}{2}\sum k_{ij}^{l}(l_{ij} - l_{ij}^{\circ})^2 + \frac{1}{2}\sum k_{ijk}^{th}(th_{ijk} - th_{ijk}^{\circ})^2 +$$

$$+ \frac{1}{2}\sum V^0(1 - \cos((\Phi_{jk} - \Phi_{jk}^{\circ})n)) + \sum e_{ij}\left(\left(\frac{R_{ij}^{\circ}}{R_{ij}}\right)^{12} - 2\left(\frac{R_{ij}^{\circ}}{R_{ij}}\right)^{6}\right) +$$

$$+ \sum \frac{1389}{\varepsilon_0}\frac{Q_iQ_j}{R_{ij}} \qquad \text{(kJ/mol)}$$

where l_{ij} is the bond distance between atoms i and j (Å), l_{ij}° is an equilibrium distance between atoms i and j (Å) (dependent on the hybridization), k_{ij}^{l} is the force constant of the valence deformation (mdyn/Å), th_{ijk} is the bond angle between atoms i, j and k (rad), $\mathrm{th}_{ijk}^{\circ}$ is the equilibrium angle at atom j (depending on the hybridization of j), k_{ijk}^{th} is the force constant of the bond angle deformation (mdyn Å/rad^2), V° is the maximum of the bond torsion potential function (kJ/mol), n is the number of the maxima of the torsion potential function, Φ_{jk} is the valence torsion angle between atoms j and k (rad), Φ_{jk}° is the valence torsion angle belonging to the minimum energy, R_{ji}° (or if the atoms are connected to a common atom: $R_{ij}^{\circ\prime} = R_{ij}^{\circ} - 0.9$ Å) is the van der Waals distance, ε_0 is the dielectric constant (3.5), Q_i and Q_j are the partial charges of atoms i and j.

Energy function parameters of the bond lenght and torsional deformation taken from Refs [12—15] are listed in Table II. (Units are given as required by the input of the program.)

Table II

Parameters used in the energy functions

Type of bond	k_{ij}^{l} (mdyn/Å)	l_{ij}^{0} (Å)	V° (kJ/mol)	Φ_{jk}^{0}	n
C_A—Si	2.97	1.87	1.38	0	3
C_A—C_A	8.00	1.397	20.9	0	2
C_A—H	5.03	1.085	—	—	—

Type of angle	k_{ijk}^{th}(mdyn Å/rad^2)	th_{ijk}^{0} (deg)
C_A—Si—C_A	0.57	110.55
Si—C_A—C_A	0.80	120.0
C_A—C_A—C_A	0.86	120.0
C_A—C_A—H	0.86	120.0

3. *Calculation of the lattice energy*

The potential function used for the calculation of the lattice energy was as follows [12]:

$$E_S = \sum_{i=1}^{N} \sum_{j=1}^{N} \sum_{S=1}^{SYM} \left(e_{ij} \left(\left(\frac{R_{ij}^{\circ}}{R_{ij}} \right)^{12} - 2 \left(\frac{R_{ij}^{\circ}}{R_{ij}} \right)^{6} \right) + \frac{1389}{\varepsilon_0} \frac{Q_i Q_j}{R_{ij}} \right)_S$$

where N is the number of atoms in the asymmetric unit (the molecule as a whole was considered as an asymmetric unit, $N = 45$), SYM is the number of symmetry operations (the sum of the translational and rotational operators which generate the whole environment of the arbitrarily chosen molecule). The atomic coordinates of the 14 neighbouring molecules were determined by HIRSCHFELD's method [16]. Other parameters of the energy function are identical with those of the program CONFORM.

4. *Thermal analysis*

Thermal analysis calculations were performed by the method of SHOMAKER and TRUEBLOOD [17], starting data were the b_{ij} values taken from Ref. [1] and transformed to the U_{ij} form.

Results

1. *Quantum chemical calculations*

Calculations were performed for the planar Si-phenyl segment instead of the whole three-dimensional molecule.

The results, π-bond orders, the resultant σ and π partial charges are shown in Table III. The numbering of the atoms is shown in Fig. 1.

Table III

Results of the DEL RE *and PPP calculations on the TPHSI molecule*

π-bond orders	$\sigma + \pi$ partial charges
$P_{SiC} = 0.187$	$\delta_{Si} = +0.1552$
$P_{12} = 0.646$	$\delta_1 = -0.0953$
$P_{23} = 0.680$	$\delta_2 = -0.0174$
$P_{34} = 0.652$	$\delta_3 = -0.0418$
$P_{45} = 0.678$	$\delta_4 = -0.0322$
$P_{56} = 0.658$	$\delta_5 = -0.0417$
$P_{16} = 0.663$	$\delta_6 = -0.0163$
	$\delta_{H2} = +0.0415$
	$\delta_{H3} = +0.0410$
	$\delta_{H4} = +0.0409$
	$\delta_{H5} = +0.0410$
	$\delta_{H6} = +0.0415$

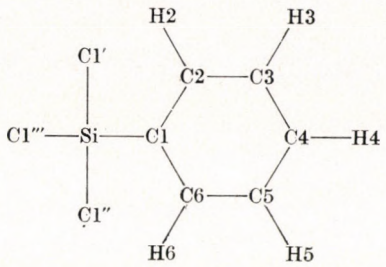

Fig. 1. Reference polar coordinate system

The bond lengths were re-calculated from the π-bond-orders, using JULG's formula [18]:

$$l_{ij} = (2.80/0.5(Z_i + Z_i)^{1/2}(1.52 - 0.19p_{ij}))$$

where Z_i and Z_j are Burn's effective nuclear charges and p_{ij} is the bond-order. The results are shown in Table IV together with the bond lengths and angles provided by the structure determination [1] and the CONFORM program.

2. *Conformation analysis*

Bond lengths and angles belonging to the minimum energy state calculated by conformational analysis together with some torsion angles are listed in Table IV.

Table IV

Bond lengths (Å) *and bond angles* (*deg*) *of the TPHSI molecule*

Bond	Ref. [1]		Ref. [2]		PPP	CONFORM
Si—C1	1.863	(7)	1.872	(7)	—	1.883
C1—C2	1.398	(11)	1.386	(11)	1.397	1.410
C2—C3	1.377	(13)	1.377	(13)	1.391	1.404
C3—C4	1.388	(13)	1.379	(14)	1.396	1.407
C4—C5	1.367	(13)	1.367	(13)	1.391	1.406
C5—C6	1.402	(13)	1.387	(12)	1.395	1.408
C6—C1	1.405	(11)	1.402	(10)	1.394	1.408
C1′—Si—C1	108.2	(3)	107.7	(5)		108.22
C1″—Si—C1	110.1	(5)	110.3	(3)		110.10
Si—C1—C2	121.4	(5)	121.1	(6)		118.95
Si—C1—C6	122.9	(5)	122.8	(5)		121.29
C6—C1—C2	115.7	(7)	116.1	(7)		119.74
C1—C2—C3	123.8	(7)	123.8	(9)		120.13
C2—C3—C4	117.8	(9)	119.7	(9)		120.10
C3—C4—C5	122.0	(9)	119.9	(8)		119.82
C4—C5—C6	118.7	(8)	119.9	(8)		120.23

The calculated strain energy is 102.93 kJ/mol (24.60 kcal/mol). The atomic coordinates of the minimum energy state were transformed to polar coordinates.

The energy function for the rotation of the phenyl group about the Si–C bond axis was also calculated. The potential function of the rotation is shown in Fig. 2.

The minimum energy of the rotation, 102.63 kJ/mol (24.53 kcal/mol), corresponds to a torsion of 8.0°. (The calculated value for the lattice is 14.02°.)

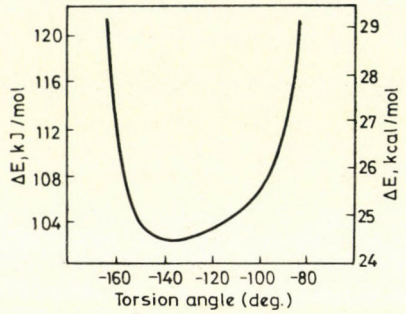

Fig. 2. Energy function of the rotation of the phenyl group about the Si–C bond axis

The curve has a broad minimum, thus only small changes in energy are expected at relatively large torsions of the phenyl group around the Si–C bond. The bond lengths and angles of the molecule (regardless of the C–H bonds, where the repulsion centre is farther by ca. 0.1 Å than the maximum electron density [19]) are in accordance with the X-ray structure determination. (Note that the value of $l^{\circ}(C_A - C_A) = 1.397$ Å is an optimized value, which is relatively high, owing to the nature of the calculation.)

3. *Lattice energy*

The calculated lattice energy is −177.78 kJ/mol (−42.49 kcal/mol), greater than that determined by AKHMED *et al.* [20] −143.51 kJ/mol (−34.30 kcal/mol). The value calculated from experimental data is −182.63 kJ/mol (−43.65 kcal/mol), which was derived from the following terms: $H_1 = \overline{G}_p$ (298 K, $\Delta t = 509-298$) = 86.40 kJ/mol (20.65 kcal/mol) [21, 22, 23], H_2 (heat of melting) = 35.15 kJ/mol (8.4 kcal/mol) measured by DSC, H_3 (heat of evaporation at 652K) = 61.09 kJ/mol (14.6 kcal/mol) [24]. $H_4 = \int_{652\ K}^{298\ K} C_p dt$ in the vapour state and $H_5 = \int_{509\ K}^{652\ K} C_p dt$ in the liquid state were not taken into account.

Energy is required for the differential shifts in the x, y, and z directions (the first derivatives of the energy function are zero and the second ones are positive). The mass center of the molecule is in an energy minimum. As for the rotations, differential rotation about the z axis requires energy but energy is gained by the rotation perpendicular to z (up to 10^{-4} rad). Regarding the rotation around the center of mass, the molecule is not in a minimum energy state according to our calculations, though a rotation of 0.02 rad requires energy.

All the non-bonded intermolecular distances are on the attractive side of the potential curve.

4. *Thermal motion*

Several variations were tried for the analysis of the thermal motion. Successful solutions were obtained in the following three cases:

(a) All non-hydrogen atoms of the molecule were regarded as rigid bodies with the restrictions of the lattice symmetry (mean e.s.d.'s of the U_{ij}'s: 0.0109 Å^2);

(b) same as under (a) but without the restrictions of the lattice symmetry (mean e.s.d.'s of the U_{ij}'s: 0.0090 Å^2);

(c) one phenyl group together with the silicon atom is regarded as a rigid body without lattice symmetry restrictions (mean e.s.d.'s of the U_{ij}'s: 0.0051 Å^2).

The calculated and experimental U_{ij}'s of the latter case are summarized in Table V. The vibrational and librational tensors and main axes of the thermal ellipsoids with their direction cosines with respect to the crystallographic axes are shown in Table VI.

Table V

Experimental and calculated values of U_{ij} 10^4

The data from Ref. [1] are in the first column and the calculated values in the second column. (The thermal parameters are expressed in the following form: $\exp[-2\pi^2(U_{11}h^2a^{*2} + U_{22}k^2b^{*2} + U_{33}l^2c^{*2} + 2U_{12}hka^*b^* + 2U_{13}hla^*c^* + 2U_{23}klb^*c^*)]$)

	U_{11}		U_{22}		U_{33}		U_{12}		U_{13}		U_{23}	
Si	246	237	264	221	279	226	0	−12	0	−45	0	−100
C1	260	273	333	302	381	376	−30	−48	60	96	47	46
C2	413	455	606	627	407	414	50	91	−33	−26	56	110
C3	453	388	726	751	496	533	−167	−208	−45	−59	−51	−32
C4	599	719	486	482	407	342	−170	−143	43	−13	−74	−100
C5	673	648	380	375	564	580	27	45	91	122	−16	5
C6	440	480	406	442	587	651	37	20	37	78	21	55

Table VI

Vibrational (L), librational (ω) tensors and main axes of the librational and vibrational ellipsoids together with their direction cosines relative to the crystallographic axes
E.s.d.'s are given in parentheses

$$L = \begin{matrix} 0{,}428(4) & -0.003(3) & 0\ 003(3) \\ & 0.003(3) & 0.003(3) \\ & & 0.040(3) \end{matrix} \qquad \omega = \begin{matrix} 0.000(1) & 0.000(1) & -0.000(1) \\ & 0.007(3) & 0.005(2) \\ & & 0.010(2) \end{matrix}$$

$L(i)$	$(u_2)^{1/2}$ (Å)	x_u	y_u	z_u
1	0.2065	0.0198	0.6056	0.7956
2	0.1941	0.3993	−0.7343	0.5491
3	0.1621	0.9166	0.3068	−0.2563

$\omega(i)$	$(u^2)^{1/2}$(rad)	x_u	y_u	z_u
1	0.1145	0.0648	−0.5911	−0.8040
2	0.0566	0.2471	0.7901	−0.5610
3	0.000	0.9668	−0.1623	0.1973

The centre of the termal motion is in the neighbourhood of the mass centre of the molecule, *i.e.* in the immediate neighbourhood of the silicon atom ($X = 0.258$; $Y = 0.312$; $Z = 0.589$ Å).

The L_1 and L_2 main librational axes are inclined relative to the Si–C bond axis at angles of 21.7° and 82.7°, respectively. The L_2 axis forms an angle of 16.1° with the normal of the phenyl plane. Thus the axis of greatest libration nearly coincides with the Si–C bond axis, and this may be regarded as the main libration. This is in accordance with the reduced energy barrier to the rotation of the phenyl group about the Si–C bond axis, as deduced from the conformational energy function. Libration, parallel to the phenyl planes is the second order libration axis, while libration normal to the phenyl planes is strongly hindered.

From the viewpoint of vibration, to whole molecule behaves as rigid body (in all cases solutions could be obtained for the vibrational ellipsoid) and this corresponds to the lattice energy changes calculated for the differential shifts in the x, y and z directions. A similar phenomenon was found in a study of the lattice energy of diketopiperazine by GIACOMELLO and GIGLIO [25].

Conclusions

It has been established that the geometric image of the TPHSI molecule is primarily determined by the internal strain energy. The molecular symmetry (distorted tetrahedron) follows from this. The energy of rotation of the phenyl group about the Si–C bond axis is small and this energy is affected only to a small extent by spatial packing in the lattice. This is why libration occurs mainly about this axis. The movement of the phenyl group in the normal directions of its plane is hindered by close packing.

In the librational sense only the phenyl–silicon segment, whereas from the viewpoint of vibration, the whole molecule can be considered as a rigid body. The centre of vibration practically coincides with the position of the silicon atom and the extent of vibration is determined by close packing.

The results of the quantum chemical calculations and conformation analysis are in accordance.

The rigid body motion derived from thermal parameters, completed with energy calculations, permits conclusions on the real molecular motion in the crystal lattice and so thermal parameters may be separated from the errors accumulated in them. Experimental and calculated lattice energies show a good agreement. Similarly good results were obtained for the acenaphthylene molecule [12] so, presumably, the parameters used in the lattice energy calculation and the potential function applied are fairly good approximations.

REFERENCES

[1] Párkányi, L., Sasvári, K.: Periodica Polytechnica, **17,** 271 (1973)
[2] Glidewell, C., Sheldrick, G. M.: J. Chem. Soc. (A) **1971** 3127
[3] Del Re, G.: J. Chem. Soc., 4031
[4] Nagy, J., Hencsei, P., Réffy, J.: Acta Chim. Acad. Sci. Hung., **65,** 41 (1970)
[5] Pariser, R., Parr, R. G.: J. Chem. Phys., **21,** 466 (1953)
[6] Pople, J. A.: Trans. Faraday Soc., **49,** 1375 (1953)
[7] Mataga, N., Nishimoto, K.: Z. Physik. Chem., **13,** 140 (1957)
[8] Wolfsberg, M., Helmholtz, L.: J. Chem. Phys., **20,** 837 (1952)
[9] Burns, G.: J. Chem. Phys., **41,** 1521 (1964)
[10] Wiberg, K. B.: J. Amer. Chem. Soc., **87,** 1070 (1967)
[11] Cser, F.: CONFORM. *Program for computing the strain energy and equlibrium conformation of free molecules.* Res. Inst. Plastic Industry, Budapest (1972)
[12] Cser, F.: Acta Chim. (Budapest) **80,** 317 (1974)
[13] Oulette, R. J.: J. Amer. Chem. Soc. **94,** 7674 (1972)
[14] Allinger, N. L., Hirsch, J. A., Miller, M. A., Thyminski, J. J., Van Catledge, F. A.: J. Amer. Chem. Soc., **90,** 1199 (1968)
Allinger, N. L., Trible, M. T., Miller, M. A., Wertz, D. H.: J. Amer. Chem. Soc., **93,** 1637 (1971)
[15] Altona, C., Sunderalingam, M.: J. Amer. Chem. Soc., **92,** 1955 (1970)
[16] Hirschfeld, F. L.: Acta Cryst., A**24,** 301 (1968)
[17] Shomaker, V., Trueblood, K. N.: Acta Cryst., B **24** 63 (1968)
[18] Julg, A.: Chimie quantique. Dunod, Paris (1967)
[19] Williams, D. E.: Acta Cryst, A **27,** 452 (1971)

[20] AKHMED, N. A., KITAYGORODSZKII, A. I., MIRSKAYA, K. V.: Acta Cryst., B **27,** 867 (1971)
[21] KRESKOV, A. P., MIKHAYLENKO, Y. Y., YAKIMOVICH, G. F.: Zh. Fiz. Khim., **28,** (1954)
[22] TOPICHEV,, A. V., NAMOTKIN, N. S.: Dokl. A., SSSR **80,** 897 (1951)
[23] BILOW, N., BRADY, J. L., SEGAL, C. L.: J. Org. Chem., **26,** 929 (1961)
[24] NURULLAEV, N. G., KOSTRUKOV, V. N., MOSIN, A. M.: Zs. Fiz. Khim., **43,** 2143 (1969)
[25] GIACOMELLO, P., GIGLIO, E.: Acta Cryst., A **26,** 324 (1970)

Ferenc CSER; 1950 Budapest, Hungária krt 114. Hungary.
László PÁRKÁNYI; 1525 Budapest, POB 17. Hungary.
Pál HENCSEI; 1502 Budapest, POB 91. Hungary.

Acta Chimica Academiae Scientiarum Hungaricae, Tomus 85 (3), pp 299—311 (1975)

PREPARATION AND INVESTIGATION OF LEWIS ACID COMPLEXES, X*

INVESTIGATION OF THE TITANIUM TETRACHLORIDE AND ETHOXYTITANIUM TRICHLORIDE COMPLEXES OF TRIACETYLLEVOGLUCOSAN

L. FENICHEL,[1] GY. DEÁK,[2] S. HOLLY,[3] P. BAKÓ,[1] and Z. CSŰRÖS[1]

([1]*Department of Organic Chemical Technology, Technical University, Budapest;* [2]*Institute of Experimental Medicine of the Hungarian Academy of Sciences;* [3]*Central Research Institute for Chemistry of the Hungarian Academy of Sciences, Budapest*)

Received May 9, 1974

The reaction between triacetyllevoglucosan and titanium tetrachloride has been studied by the investigation of their addition complex compounds. It has been shown that the $< 1,6 >$ oxigen bridge of triacetyllevoglucosan is opened during the reaction, and the reaction product is identical with the complex formed from 2,3,4-triacetyl-α-D-gluco-pyranosyl chloride with 2 moles of titanium tetrachloride.

It has been found that the reaction is catalyzed, in addition to compounds containing active hydrogen, also by ethoxytitanium trichloride.

The reaction of 2,3,4-triacetyl $< 1,5 > \beta < 1,6 >$ glucosan, also called triacetylglucosan (in the following: TAL) with titanium tetrachloride has been described by ZEMPLÉN and CSŰRÖS [1] (Fig. 1). Titanium tetrachloride (5.25

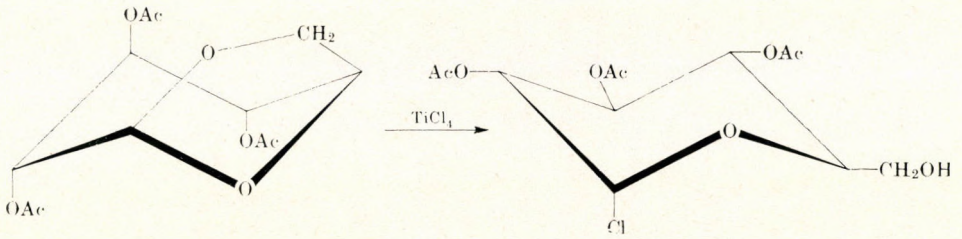

Fig. 1. The reaction of triacetyllevoglucosan with $TiCl_4$

moles) was added to a solution of TAL (1 mole) in chloroform, where upon a yellow precipitate formed. The reaction mixture was boiled for 4 hrs, then poured into ice-water. The chloroform phase was processed to obtain 2,3,4-triacetyl-α-D-glucopyranosyl chloride (in the following: TGC) in a yield of 59%. From TAL of 1C conformation, TGC of C1 conformation was obtained. In the latter compound the substituents are, with the exception of the chlorine atom, in *equatorial* steric position.

* Part IX: CSŰRÖS, Z., DEÁK, G., FENICHEL, L., HOLLY, S., and PÁLINKÁS, J.: Acta Chim. (Budapest) **80,** 193 (1974)

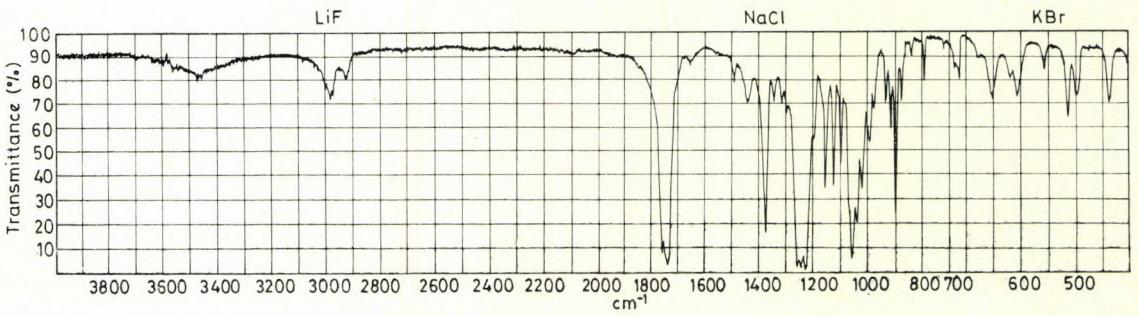

Fig. 2. IR spectrum of triacetyllevoglucosan (in KBr)

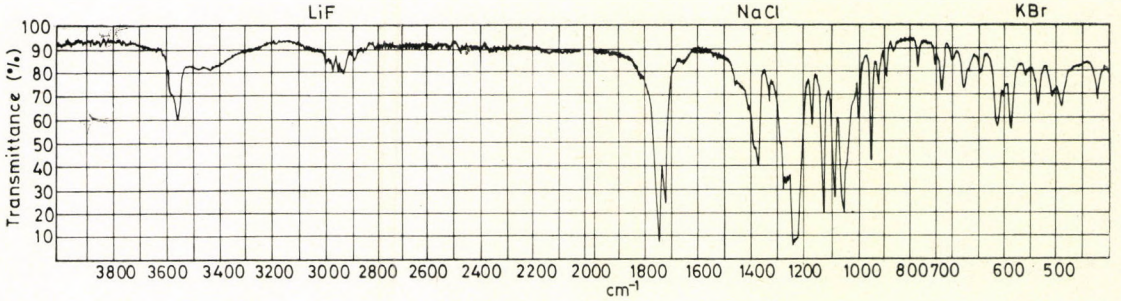

Fig. 3. IR spectrum of 2,3,4-triacetyl-α-D-glucopyranosyl chloride (in KBr)

In the course of later investigations [2, 3] it appeared that the reaction did not take place in pure absolute chloroform, but a co-catalyst was needed; this may be water, alcohol, phenol, or acetic acid, etc. The most favourable effect was found when 0.5 mole of the co-catalyst was taken for each mole of TAL in the presence of at least 2 moles of $TiCl_4$ reagent. The co-catalytic effect of the said compounds was attributed to their proton donor character. The investigations made with chloroform as the reaction medium gave only a qualitative picture.

Recent experiments

In our experiments, the reaction of TAL with $TiCl_4$ was followed by the isolation and investigation of the complexes formed in the reaction mixture. The titanium and chlorine contents of the complexes were determined and their IR spectra recorded. The complexes were then decomposed with water, the sugar part was extracted with chloroform, and the progress of the reaction was estimated from the chlorine content of the evaporation residue.

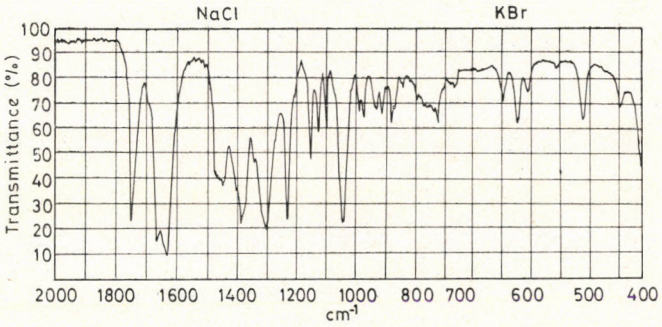

Fig. 4. IR spectrum of the triacetyllevoglucosan–$TiCl_4$ complex (in paraffin oil)

The complexes of TAL have been prepared in abs. chloroform with 1 mole of $TiCl_4$, as well as with an excess of $TiCl_4$ (Table I). The characteristic bands of the IR spectra of the compounds are shown in Table II. Primarily, the $\nu C = O$ and $\nu_{as}CC(= O)O$ bands of the acetyl groups are considered, which are shifted in the $TiCl_4$ complexes, as compared with the bands of the basic compound.

Comparison of the IR spectra of TAL and TGC (Figs 2 and 3) with that of the TAL · $TiCl_4$ complex (Fig. 4) shows that one of the carbonyl bands (that at 1760 cm^{-1}) of the basic compound has been preserved at 1750 cm^{-1}, while the band representing presumably two carbonyl groups at 1735 cm^{-1} has shifted, and new bands appear at 1663 and 1633 cm^{-1}. The assumption

Table I

Conditions of preparation of the complex compounds

No.	Conditions of complex formation	Complex						Conversion, %
		Chlorine content, %		Ti content, %	$[\alpha]_D^{20}$ (aceto-nytrile)	Colour	Solubility	
		measured	calculated (S : L molar ratio)*					
I	TAL : $TiCl_4$ 1 : 1; 20 °C	28.43 28.06	29.7/1 : 1	10.2 10.1	−23.7	white	—	
II	TAL : $TiCl_4$ 1 : 5.25; 20 and 63 °C	36.9—39.0	37.2/2 : 3	11.9/12.10	−17.4	yellow	—	0.025—6.2
III	TAL : $EtOTiCl_3$ 1 : 1; after 1 hr boiling (63 °C) precipitated with petroleum ether	20.9	21.8/1 : 1	9.9/9.83		white	soluble	5.6
IV	TAL : $EtOTiCl_3$ 1 : 2; after 1 hr boiling (63 °C) precipitated with petroleum ether	27.9	30.98/1 : 2	12.2/13.95		white	soluble	1.7
V	TAL : $EtOTiCl_3$ 1 : 3; after 1 hr boiling (63 °C) precipitated with petroleum ether	35.4	36.01/1 : 3	15.9/16.22		white	soluble	8.8
VI	TGL : $TiCl_4$ 1 : 1; 20 °C	27.5	29.7/1 : 3	10.0/10.1	+ 135.9	white	soluble in the the cold	
VII	TGC : $TiCl_4$ 1 : 2; 20 °C	43.2 43.0	42.6/1 : 2	14.5/14.4	+69.0	yellow	—	
VIII	TAL : 1/2 $EtOTiCl_3$: 5.25$TiCl_4$ 1 hr of boiling	39.1	39.7/1 : 1/2 : : 1 1/2	14.1	+53.6	yellowish-white	partly soluble on heating	80.6 79.5
IX	TAL : $EtOTiCl_3$: $TiCl_4$ 1 : 1 : 2; 20 °C	35.2	36.7/1 : 1 : 2	—	−13.7	yellowish-white	sparingly soluble	0.9

* S = substrate
L = Lewis acid

Table II

Characteristic bands of the IR spectra of the complexes and their starting materials

Compound	Fig. No.	$\nu C=O$	$\Delta\nu C=O$**	$\nu_{as}CC(=O)O$	$\nu C-O-Ti$	$\nu C-Cl$	$\nu Ti-Cl$
TAL	2	1760, 1735	—	1255, 1240 1222	—	—	—
TGC	3	1745, 1720	—	1275, 1235 1220	—	606	—
TAL–$TiCl_4$ 1 : 1	4	1750, 1663 1633	72/102	1300, 1230	—	—	448, < 400
TAL–$TiCl_4$ 2 : 3	5	1705, 1640	55/95	1285	—	—	435, 410
$EtOTiCl_3$	7				1105, 1070		480
TAL–$2EtOTiCl_3$	9	1750, 1680	55	1290, 1230	1105		450, 405
TGC · $TiCl_4$	10	1755, 1680	40	1295, 1220	1115	615	405
TGC · $2TiCl_4$	12	1680, 1650	40—95	1285	1105	615	425, 405
*TAL : $1/2EtOTiCl_3$: $5.25TiCl_4$	13	1680, 1660	40—85	1285	1105	615	405
*TAL : $1EtOTiCl$: 1_3TiCl_4	14	1670 (1640 shoulder)		1290	1100		450 (shoulder), 400

* Starting molar ratios

** $\Delta\nu C{=}O = \nu C{=}O_{original} - \nu C{=}O_{shifted}$

may be ventured that $TiCl_4$ forms the complex with the acetyl groups at C–2 and C–4, which are in identical steric positions.

In the spectrum of the complex, one of the $\nu_{as}CC(=O)O$ bands of TAL is present at 1230 cm^{-1}, while the other two are shifted to 1300 cm^{-1}.

When the complex is made in carefully purified and dried chloroform with an excess of $TiCl_4$, the resulting compound contains about 1.5 molecules of $TiCl_4$ per 1 molecule of TAL, as shown by a large number of experiments.

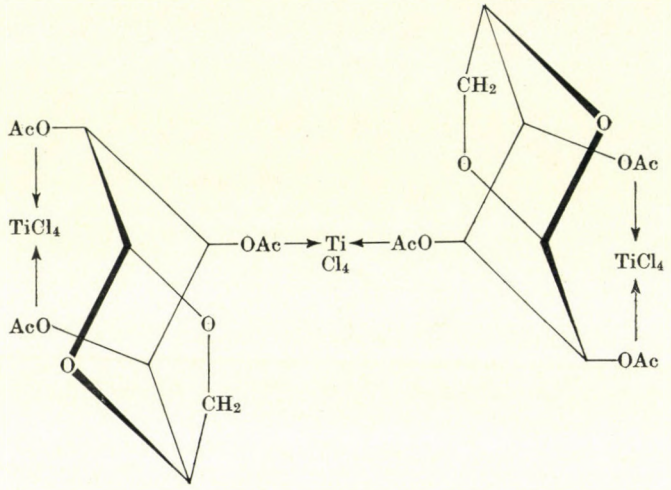

Fig. 5. Steric structure of the triacetyllevoglucosan–$TiCl_4$ complex of 2 : 3 molar ratio

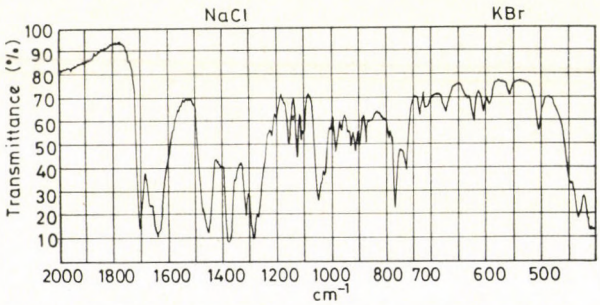

Fig. 6. IR spectrum of the triacetyllevoglucosan–$TiCl_4$ complex of 2 : 3 molar ratio (in paraffin oil)

Therefore, a structure is assumed for the complex, in which the C–3 acetyl groups of two molecules are linked by one $TiCl_4$ molecule, while each pair of the C–2 and C–4 acetyl groups is complexed with one molecule of $TiCl_4$ (Fig. 5). In the IR spectrum of this complex (Fig. 6) the carbonyl band at 1760 cm^{-1} has practically disappeared, indicating that no free carbonyl group is present. A new band is exhibited at 1705 cm^{-1}, which has not been observed earlier in any of the complexes, and an intense carbonyl band is found also

at 1640 cm^{-1} with a shoulder at 1660 cm^{-1}. A similar doubling is exhibited by the band of the νTi–Cl vibration at 445 and 410 cm^{-1}. Ring cleavage does not occur to a considerable extent even on heating; on decomposing these complexes, the initial TAL is recovered. When the 2 : 3 complex is agitated in chloroform with 1 mole of TAL, the 1 : 1 complex is obtained and, *vice versa*, the 1 : 1 complex can be converted into the 2 : 3 complex; thus the two compounds are reversibly interconvertible.

Table III

The reaction of TAL with $TiCl_4$ in the presence of $EtOTiCl_3$. TAL : $TiCl_4$ molar ratio 1 : 5.25
Boiling time: 1 hr

Molar ratio TAL : $EtOTiCl_3$	Conversion, %
1 : 0.1	5.5
1 : 0.25	8.4
1 : 0.5	79.5
1 : 1	86.2
1 : 2	76.6
1 : 3	58.1

In further experiments the effect of co-catalysis was investigated. One mole of TAL was refluxed with 5.25 moles of $TiCl_4$ for 1 hour in the presence of 1 mole ethanol co-catalyst. The average conversion, calculated on the basis of the chlorine content of the sugar part, was 77.8%. When the experiment was carried out by previously boiling the solution of $TiCl_4$ and ethanol in chloroform for 30 minutes and adding TAL to it, only subsequently followed by boiling again for 1 hour, practically the same conversion (78.2%) was obtained. Thus, contrary to earlier considerations [2, 3], it has been concluded that the co-catalytic effect is not due to HCl or to protons formed from ethanol and $TiCl_4$, since the greatest part of gaseous HCl must have departed during the 30 minutes of boiling. In order to prove that the co-catalytic effect is due to ethoxytitanium trichloride ($EtOTiCl_3$) presumably formed, pure $EtOTiCl_3$ has been prepared and added to the TAL—$TiCl_4$ reaction mixture (Table III). The results show that when the TAL : $EtOTiCl_3$ molar ratio reaches the value of 1 : 0.5 conversion, suddenly increases to attain maximum at a molar ratio of 1 : 1. On further increase of the quantity of the co-catalyst, the conversion begins to decrease.

Accordingly, compounds which can not afford protons by dissociation, such as $EtOTiCl_3$, may also play the role of a co-catalyst. Thus the compound $EtOTiCl_3$ was examined in greater detail. Its IR spectrum (Fig. 7) has dominant bands at 1105 and 1070 cm^{-1}; one of them can be assigned presumably to the

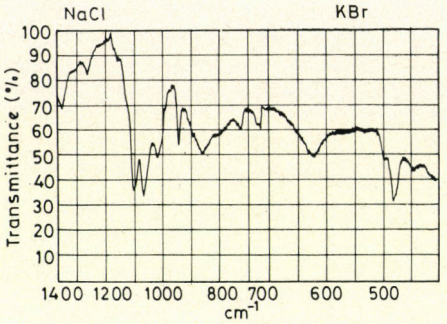

Fig. 7. IR spectrum of $EtOTiCl_3$ (in paraffin oil)

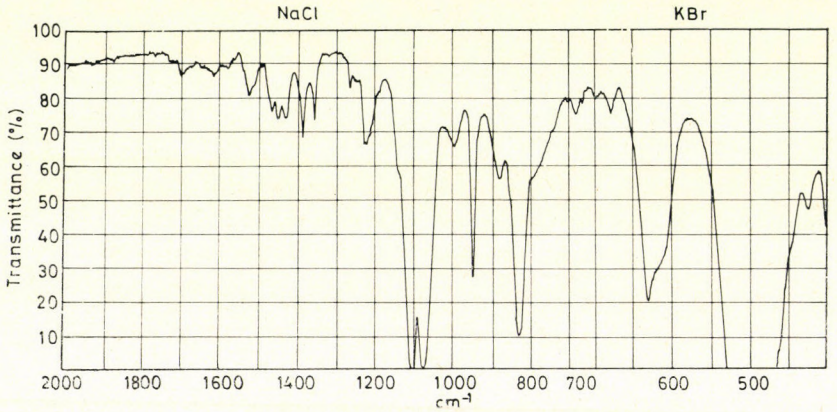

Fig. 8. IR spectrum of the 1 : 10 molar mixture of $EtOTiCl_3$ in chloroform solution

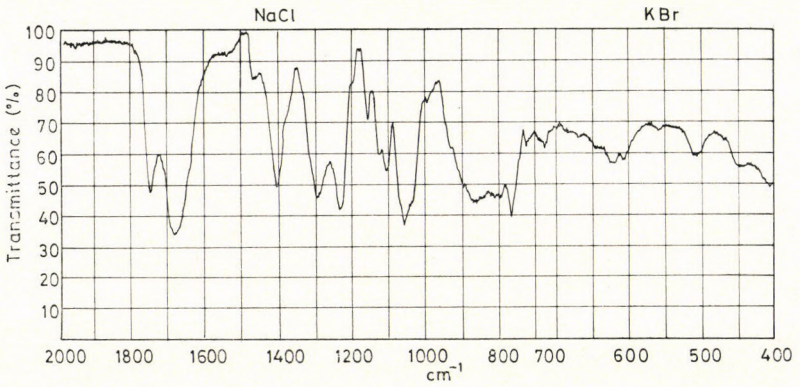

Fig. 9. IR spectrum of the triacetyllevoglucosan–2 $EtOTiCl_3$ complex (in paraffin oil)

vibration of the C–O–Ti bond. A similarly intense band is the vibration of νTi–Cl at 480 cm^{-1}. It could be assumed that though $EtOTiCl_3$ is primarily a Lewis acid, it may also behave as a Lewis base owing to its ether oxygen atom. This is, however, inconsistent with the finding that the IR spectrum of the mixture of 1 : 10.5 molar ratio recorded in $EtOTiCl_3$: $TiCl_4$ solution in chloroform (Fig. 8) is only a superposition of the spectra of $EtOTiCl_3$ and $TiCl_4$, so that no complex has been formed; thus, $EtOTiCl_3$ does not come into consideration as a Lewis base.

Next, the functioning of $EtOTiCl_3$ as a Lewis acid was investigated. The complexes of TAL with 1, 2 and 3 moles of $EtOTiCl_3$ have been prepared.

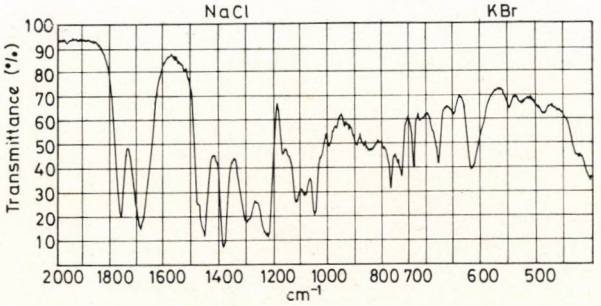

Fig. 10. IR spectrum of the 2,3,4-triacetyl-α-D-glucopyranosyl chloride–$TiCl_4$ complex of 1 : 1 molar ratio (in paraffin oil)

The IR spectrum of the 1 : 2 complex is shown in Fig. 9. The band at 1750 cm^{-1} is due to the ester carbonyl group which remained free; the band at 1680 cm^{-1} is assigned to the two carbonyl groups in covalent bond. Taking into consideration also the spectra of the 1 : 1 and 1 : 3 complexes (not shown here), it may be assumed that one carbonyl group is complexed with 1 molecule of $EtOTiCl_3$, and the corresponding νC=O band is shifted by 45 cm^{-1} towards lower wavenumbers. Two moles of $EtOTiCl_3$ resulted in a decrease of the wavenumber by 55 cm^{-1}. The intensities of the shifted νC=O and ν_{as}CC(=O)O bands increase with increasing $EtOTiCl_3$ ratio in the complex, as compared with the non-shifted bands, and finally, the band characteristic of the free ester group becomes very weak in the spectrum. The incorporation of $EtOTiCl_3$ into the complex is shown by the relative increase in intensity of the band at 1105 cm^{-1}, characteristic of the C—O—Ti bond. An examination of the extent of the shifting of the bands reveals that $EtOTiCl_3$ is a weaker Lewis acid than $TiCl_4$; for the first $\Delta\nu$C=O is 55—70, for the latter 75—100 cm^{-1}. On the other hand, a substantial difference is that $TiCl_4$ is a hexacovalent, bifunctional Lewis acid, whereas it seems that $EtOTiCl_3$ can accept only one donor group.

The complex of the end-product of the TAL–$TiCl_4$ reaction, TGC, formed with 1 mole of $TiCl_4$ has also been prepared. In this case, actually 2,3,4-triacetyl-

-6-O-$TiCl_3$-α-D-glucopyranosyl chloride is formed, which itself can form complexes.

A comparison of the spectra of TAL and TGC (Figs 2 and 3) shows that the positions and the intensity ratio of the carbonyl bands are different in the two spectra. It appears that the band at 1745 cm^{-1} in TGC corresponds to two carbonyl groups, and the band at 1720 cm^{-1} to one carbonyl group. In spite of the fact that all acetyl groups are in *equatorial* position, the C–4 acetyl, owing to its vicinity to the C–6 OH group, has a distinguished position. The investigation of the ratio of the original and shifted $\nu C{=}O$ (1755 and 1680 cm^{-1}) and $\nu_{as}CC(=O)O$ (1220 and 1295 cm^{-1}) bands in the spectrum of the complex (Fig. 10) permits to assume that one acetyl group, probably the one linked to C–4, is in complex bonding, so that the structure is as shown in Fig.11.

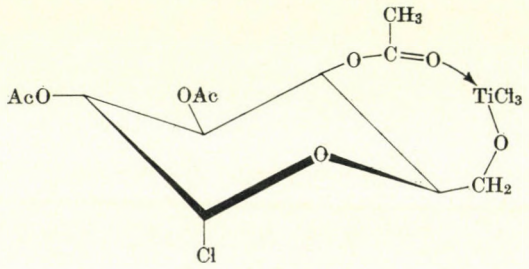

Fig. 11. Structure of the 2,3,4-triacetyl-α-D-glucopyranosyl chloride–$TiCl_4$ complex of 1 : 1 molar ratio

In the IR spectrum of the TGC · $2TiCl_4$ complex (Fig. 12), the intensities of the original (non-shifted) $\nu C{=}O$ and $\nu_{as}CC(=O)O$ bands are low. The increased intensity of the νC–O–Ti band at 1105 cm^{-1}, as compared with the $\nu_{s}CC(=O)O$ band at 1045 cm^{-1}, is remarkable (it must be borne in mind in

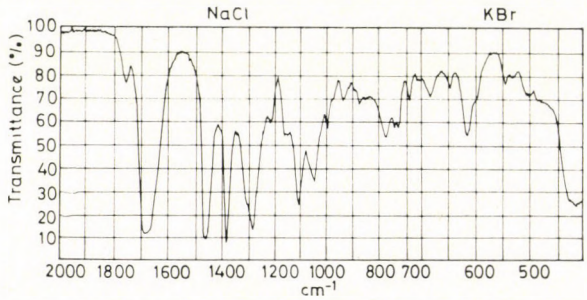

Fig. 12. IR spectrum of the 2,3,4-triacetyl-α-D-glucopyranosyl chloride –$TiCl_4$ complex of 1 : 2 molar ratio (in paraffin oil)

connection with the band appearing in the vicinity of 1110 cm^{-1} that the C–H deformation vibration of the hydrogen atom linked to C–1 of TGC also appears at this position [7]).

The broad carbonyl band between 1680 and 1660 cm^{-1} arises from the complexes formed with $TiCl_4$ and $-CH_2-O-TiCl_3$. It can be assumed that the first is complexed with one, and the latter with two acetyl groups. In spite of the fact that the 1 : 1 complex is soluble also in cold chloroform, while the 2 : 1 complex is insoluble, there is no proof that an intermolecular linkage is formed with $TiCl_4$ as the connecting bridge.

Stoichiometrically, the TGC · $2TiCl_4$ complex corresponds to the composition of that end-product complex, which is formed at the end of the reaction of TAL with an excess of $TiCl_4$.

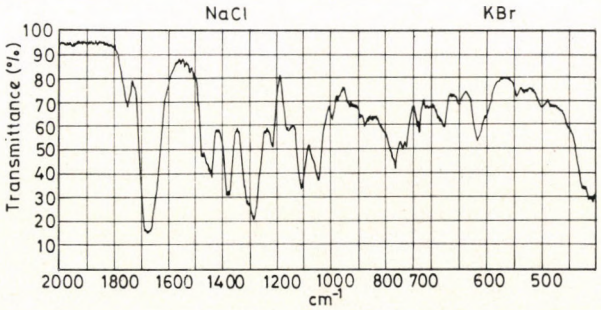

Fig. 13. IR spectrum of the complex obtained from a 1 : 1/2 : 5.25 molar mixture of triacetyl-levoglucosan–$EtOTiCl_3$–$TiCl_4$ after a reaction time of 1 hour (in paraffin oil)

Next, a reaction mixture was investigated which was obtained by refluxing 1 mole of TAL in the presence of 0.5 mole of $EtOTiCl_3$ with an excess of $TiCl_4$ for 1 hour. The extent of ring cleavage was, on the basis of the chlorine content of the sugar part, 79.5%. The IR spectrum of the complex (Fig. 13) is almost completely identical with that of the complex TGC · $2TiCl_4$ (Fig. 12), only the intensity ratio of the 1105 and 1045 cm^{-1} bands is smaller than for the latter. This indicates that the alkoxy-$TiCl_3$ content of the reaction product is lower than in TGC · $2TiCl_4$, as a consequence of the fact that the opening of the TAL $< 1, 6 >$ ring did take place only to 79.5%.

In the further experiments, TAL—TGC mixtures of various composition were treated in chloroform solution with $TiCl_4$, and the IR spectrum of the complex which separated was compared with the IR spectrum of the complex of such TAL-$TiCl_4$ reaction mixtures which had similar ratio of unconverted TAL and TGC formed, as shown by the chlorine content of the sugar component. The IR spectra were closely similar. On the basis of all this, it is reasonable to assume that the complex present at the end of the reaction in the TAL–$TiCl_4$ reaction mixture is identical with the complex obtained from TAL with excess $TiCl_4$, in which the $-CH_2-O-TiCl_3$ group is complexed with one, and one molecule of $TiCl_4$ with two acetyl groups.

The question arises what is the role of $EtOTiCl_3$ in the reaction. It has been said above that this compound can form a complex with TAL in which one molecule of $EtOTiCl_3$ is linked to each acetyl group. The problem is whether it is capable of doing the same in the presence of an identical quantity or even an excess of $TiCl_4$. It can be seen in the IR spectrum of the complex formed at room temperature by the joint action of two moles of $TiCl_4$ and one mole of $EtOTiCl_3$ (Fig. 14) that $EtOTiCl_3$ is present in the complex. This is proved by the relative increase in intensity of the band at 1110 cm^{-1}, as

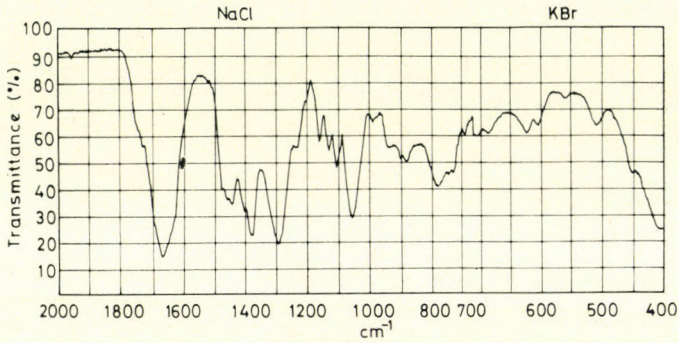

Fig. 14. IR spectrum of the complex obtained from a 1 : 1 : 2 molar mixture of triacetyl-levoglucosan–$EtOTiCl_3$–$TiCl_4$

compared with the band at 1045 cm^{-1} of TAL (the $\nu C-O-Ti$ and the 1100 cm^{-1} band of TAL are superimposed), while the originally sharp carbonyl band at 1670 cm^{-1}, which is characteristic of complex formation with alkoxytitanium trichloride, appears with a broadening to 1640 cm^{-1}, indicative of complex formation with $TiCl_4$. On the other hand, the sharp band at 1705 cm^{-1}, characteristic of intermolecular coordination, is absent.

This result shows that $EtOTiCl_3$ can form a complex with one of the acetyl groups of TAL even in the presence of $TiCl_4$. On the evidence of all this, and taking into consideration that $EtOTiCl_3$ forms a complex with one acetyl group only, further that these complexes (even the mixed complexes formed with $TiCl_4$) are relatively better soluble in chloroform, it may be assumed that the role of the $EtOTiCl_3$ co-catalyst is to form monofunctional complexes, preventing thereby the formation of intermolecular associates, which are, in account of steric or solubility reasons, unfavourable for the ring cleavage reaction. An associate of this kind is, *e.g.*, the 2 : 3 complex (Fig. 6), in the case of which there is practically no ring opening.

Experimental

Triacetyllevoglucosan (TAL) and 2,3,4-triacetyl-α-D-glucosyl chloride (TGC) were prepared and purified as described earlier [4].

Ethoxytitanium trichloride was prepared according to NESMEYANOV *et al* [5].

Calc. Cl 53.36; Ti 24.03

Found Cl 53.07; Ti 24.27%.

The complexes were prepared in a special apparatus, by adding dropwise the chloroform solution of $TiCl_4$ or $EtOTiCl_3$ to the solution of the substrate in chloroform. The mode of preparation and the method of investigation of the complexes have been described in detail [6].

The IR spectra were recorded with a Zeiss UR 10 instrument.

REFERENCES

[1] ZEMPLÉN, G., CSŰRÖS, Z.: Ber. **62,** 993 (1929)
[2] CSŰRÖS, Z., DEÁK, GY., HARASZTHY-PAPP, M.: Acta Chim. Acad. Sci. Hung. **21,** 181 (1959)
[3] CSŰRÖS, Z., DEÁK, GY., HARASZTHY-PAPP, M.: Acta Chim. Acad. Sci. Hung. **21,** 193 (1959)
[4] CSŰRÖS, Z., DEÁK, GY., FENICHEL, L.: Acta Chim. Acad. Sci. Hung. **21,** 169 (1960)
[5] NESMEYANOV, A. N., FREYDLINA, R. H., NOGINA, A. N.: Dokl. Akad. Nauk. USSR Otdel. Khim. Nauk. 1952, 1037
[6] CSŰRÖS, Z., DEÁK, GY., HOLLY, S., TÖRÖK-KALMÁR, A., ZÁRA-KACZIÁN, E.: Acta Chim. Acad. Sci. Hung. **62,** 95 (1959)
[7] CSŰRÖS, Z., DEÁK, GY., FENICHEL, L., HOLLY, S., PÁLINKÁS, J.: Acta Chim. (Budapest) **80,** 193 (1974)

László FENICHEL; 1111 Budapest, Műegyetem rkp. 3. Hungary.
Gyula DEÁK; 1083 Budapest, Szigony u. 43. Hungary.
Sándor HOLLY; 1025 Budapest, Pusztaszeri u. 57—69. Hungary.
Péter BAKÓ, Zoltán CSŰRÖS } 1111 Budapest, Műegyetem rkp. 3. Hungary.

Acta Chimica Academiae Scientiarum Hungaricae, Tomus 85 (3), pp 313—326 (1975)

PREPARATION AND INVESTIGATION OF LEWIS ACID COMPLEXES, XI*

INVESTIGATION OF THE MECHANISM OF THE RING CLEAVAGE REACTION OF TRIACETYLLEVOGLUCOSAN

L. FENICHEL,[1] GY. DEÁK,[2] P. BAKÓ,[1] S. HOLLY[3] and Z. CSŰRÖS[1]

([1]Department of Organic Chemical Technology, Technical Univestity, Budapest; [2]Institute of Experimental Medicine of the Hungarian Academy of Sciences; [3]Central Research Institute for Chemistry of the Hungarican Academy of Sciences, Budapest)

Received May 9, 1974

The reaction of triacetyllevoglucosan and $TiCl_4$ has been studied by examination of their addition complex compounds.

It has been found that propoxy-, butoxy- an phenoxytitanium trichloride are all co-catalysts of the reaction. On the basis of kinetic measurements, a reaction mechanism is suggested.

In the course of the investigation of the reaction of triacetyllevoglucosan with acyl halides catalyzed by ferric chloride, the new compound 2,3,4-triacetyl-6-benzoyl-α-D-glucopyranosyl choride has been prepared.

In our previous communication [1] the co-catalytic effect of ethoxytitanium trichloride ($EtOTiCl_3$) in the reaction of 2,3,4-triacetyllevoglucosan (in the following: TAL) and titanium tetrachloride leading to the end-product 2,3,4-triacetyl-α-D-glucopyranosyl chloride; the minimum amount of about 0.5 mole of $EtOTiCl_3$ per one mole of TAL was found necessary. In the present communication this co-catalytic effect is investigated in greater detail, and co-catalysis by other compounds is also discussed.

The co-catalytic effect of alkoxytitanium chlorides

Table I lists the extent of ring cleavage (the conversion) for different TAL : $TiCl_4$: $EtOTiCl_3$ reaction mixtures. The first three experiments show that in the presence of 0.5 mole of $EtOTiCl_3$, there is practically no reaction with 1 mole of $TiCl_4$; at least 2 moles of $TiCl_4$ are needed, and a further increase of the reagent (5.25 mole $TiCl_4$) accelerates the reaction.

In the next series of experiments the TAL : $EtOTiCl_3$ molar ratio was 1 : 1. The results of experiment No. 4 are very suprising: in a TAL : $TiCl_4$: :$EtOTiCl_3$ mixture of 1 : 1 : 1 molar ratio the progress of the reaction is consider-

* Part X: see Ref. [1]

able. In the IR spectrum of the 1 : 1 : 1 complex (Fig. 1), the appearance of the band at 1105 cm^{-1} and of the $\nu C-Cl$ band at 615 cm^{-1} and their intensities also prove that the ring cleavage has occurred. It is known from our previous communication [1] that $EtOTiCl_3$ alone is unable to split the $< 1, 6 >$ ring

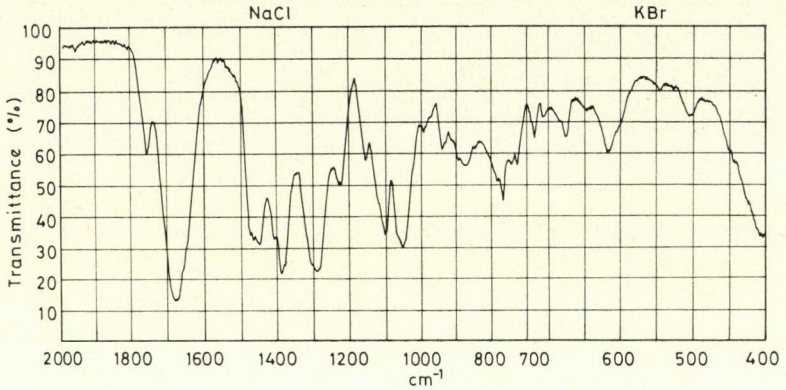

Fig. 1. IR spectrum (in paraffin oil) of the triacetyllevoglucosan–$EtOTiCl_3$–$TiCl_4$ complex of 1 : 1 : 1 molar ratio, obtained after refluxing for 1 hr

of levoglucosan. In the present case probably $EtOTiCl_3$ undergoes disproportionation according to the equilibrium below, and the additional amount of $TiCl_4$ produced in this way can participate in the reaction:

$$2EtOTiCl_3 \rightleftharpoons TiCl_4 + (EtO)_2TiCl_2.$$

If the quantity of $TiCl_4$ is decreased to 0.5 mole (experiments No. 9 and No. 10), ring cleavage proceeds only poorly, indicating that also some of the $TiCl_4$ formed by disproportionation is utilized for complex formation, and this amount does not participate in the actual reaction. As evidenced by the last experiment in Table I, when the co-catalyst is added later than the $TiCl_4$ to the reaction mixture, its effect is less than when added directly to TAL. Titanium tetrachloride present in an excess evidently precedes $EtOTiCl_3$ in complex formation, so that the latter is retarded in excercising its action.

In addition to $EtOTiCl_3$, $(EtO)_2TiCl_2$ $(EtO)_4Ti$ have also been prepared and their co-catalytic action compared in the presence of $TiCl_4$ (Table II).

The results show that this action becomes gradually weaker in the given order, so that $EtOTiCl_3$ is the best co-catalyst among these compounds. We investigated whether $(EtO)_2TiCl_2$ and $(EtO)_4Ti$ can form complexes with TAL. Complex formation could not be verified either by preparative methods or with the aid of IR spectroscopy. Thus, it seems that the complex is unstable and the equilibrium of complex formation is strongly shifted towards the

Table I

Reaction of triacetyllevoglucosan with $TiCl_4$ in chloroform, in the presence of $EtOTiCl_3$ co-catalyst

No.	TAL : $TiCl_4$: CO-catalyst molar ratio	Reflux time, %	Conversion, %	Complex	
				Cl content, %	$[\alpha]_D^{20}$ (CH_3CN)*
1	$1 : 1 : \frac{1}{2}$	1	4.0	25.0	−21.9
2	$1 : 2 : \frac{1}{2}$	1	54.0	—	48.0
3	$1 : 5.25 : \frac{1}{2}$	1	80.6	39.1	53.6
4	1 : 1 : 1	1	41.9	32.1	24.9
			42.8	34.2	
5	1 : 2 : 1	—	0.9	35.2	−13.7
6	1 : 2 : 1	1	55.2	36.5	—
7	1 : 5.25 : 1	—	0.5	40.6	—
8	1 : 5.25 : 1	1	86.2	38.6	59.2
9	$1 : \frac{1}{2} : 2$	1	21.3	20.1	—
10	$1 : \frac{1}{2} : 3$	1	10.1	34.9	—
11	1 : 5.25 : 1	1	68.9	Addition: $EtOTiCl_3$ was added to the TAL + $TiCl_4$ complex	

Calculated chlorine content of the complexes, %

TAL : $TiCl_4$ molar ratio 1 : 1	29.7
TAL : $TiCl_4$ molar ratio 1 : 2	42.6
TAL : $TiCl_4$: $EtOTiCl_3$ 1 : 1 : 1	36.6
TAL : $TiCl_4$: $EtOTiCl_3$ 1 : 1.5 : 0.5	39.5

* Specific rotation of the TGC : $TiCl_4$ complex of 1 : 2 molar ratio: +69.0°

Table II

Reaction of triacetyllevoglucosan with $TiCl_4$ in chloroform in the presence of ethoxytitanium chloride co-catalyst.

TAL : $TiCl_4$: co-catalyst molar ratio 1 : 5.25 : 1. Reflux time: 1 hr

Co-catalyst	Conversion, %	Complex		
		$[\alpha]_D^{20}$ (CH_3C	Cl content, %	Ti content, %
Ethoxytitanium trichloride	86.2	58.2	38.6	—
Diethoxytitanium dichloride	65.5	+51.6	32.05	15.08
			29.80	
Diethoxytitanium dichloride**	78.5	+53.6	35.1	14.1
Tetraethoxytitanium	38.0	—	—	—

** EtO_2TiCl_2 was first allowed to react with $TiCl_4$ for 1 hr, and TAL was added only afterwards.

starting materials, or that no complex is formed at all; in the latter case it has to be assumed that $EtOTiCl_3$ is produced in the system according to the following disproportionation equilibrium:

$$(EtO)_2TiCl_2 + TiCl_4 \rightleftharpoons 2EtOTiCl_3.$$

The existence of this equilibrium seems to be supported by the fact that the extent of TAL ring cleavage increases, when $(EtO)_2TiCl_2$ is previously made to react with $TiCl_4$.

The facts that $EtOTiCl_3$ is only a monofunctional complexing agent [1], further that $(EtO)_2TiCl_2$ does not give rise to complex formation at all, may have a dual explanation. In the first place, the oxygen atom linked to the Ti atom is less electronegative than the chlorine atom, further, it has a distinct $+T$ character; therefore, its unshared electron pairs will move towards the central Ti atom and partly decrease its electron deficiency (back-donation effect). Moreover, the ethoxy groups may also cause steric hindrance.

In addition to the case of $EtOTiCl_3$, the co-catalytic effect of other alkoxytitanium trichlorides has also been investigated (Table III). The results show that ethoxy-, propoxy- and butoxy-$TiCl_3$ have similar co-catalytic effect; this shows the relatively unimportant role of the steric factor as compared with the electron shift.

Similarly to $EtOTiCl_3$, TAL complexes could also be isolated with propoxy- and butoxytitanium trichloride, and the same holds true for phenoxytitanium trichloride ($PhOTiCl_3$).

Table III

Reaction of triacetyllevoglucosan with $TiCl_4$ in chloroform in the presence of co-catalysts

TAL : $TiCl_4$ molar ratio 1 : 5.25

Co-catalyst	Quantity of co-catalyst mole per 1 mole of TAL	time, hr	conversion, %	Complex content		$[\alpha]_D^{20}$ (CH_3CN)
				Cl %	Ti %	
Ethoxytitanium trichloride	1	—	0.47	40.6	15.1	—
Propoxytitanium trichloride	1	—	0.78	40.5	14.4	—
Butoxytitanium trichloride	1	—	7.9	42.2	14.1	−9.8
Ethoxytitanium trichloride	1	1	86.2	38.6	—	+58.1
Propoxytitanium trichloride	1	1	83.7	41.3	—	—
Buthoxytitanium trichloride	1	1	85.5	37.5	14.3	+48.6
Phenoxytitanium trichloride	1/2	1	59.5	39.8	14.9	+43.5

In the IR spectrum of $PhOTiCl_3$ (Fig. 2) the bands at 1580 and 1480 cm^{-1} arise from the skeletal vibration of the phenyl group, the band at 1220 cm^{-1} from the stretching vibration of $C_{Ar}—O$ and the band at 920 cm^{-1} from the O—Ti stretching vibration. The ν Ti—Cl band appears at 475 cm^{-1}.

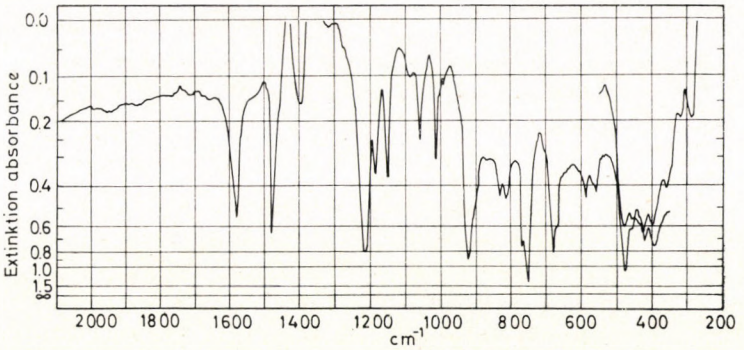

Fig. 2. IR spectrum of phenoxytitanium trichloride (in paraffin oil)

In the IR spectrum of the TAL · $2PhOTiCl_3$ complex (Fig. 3), the shifted carbonyl bands are found at 1665 cm^{-1}, *i.e.* by 15 cm^{-1} lower than in the spectrum of TAL · $2EtOTiCl_3$. At 1750 cm^{-1} a non-shifted carbonyl band is present, which is due to a relatively large quantity of acetyl groups, taking no part in the complex formation. The shifted $\nu_{as}CC(=O)O$ band appears near 1270 cm^{-1}. The non-shifted $\nu_{as}CC(=O)O$ at 1220 cm^{-1} is overlapped by the $C_{Ar}—O$ stretching vibration. The νTi—Cl vibration has been shifted by complex formation from 480 cm^{-1} to 380 cm^{-1}. The Ti content of the complex is close to the calculated value, however, its chlorine content is lower, which is consistent with the experience that alkoxy- and aryloxytitanium trichlorides and their complexes are very unstable, readily losing chlorine.

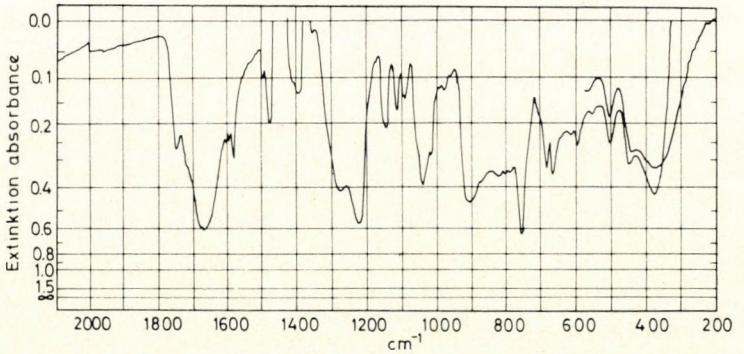

Fig. 3. IR spectrum (in paraffin oil) of the triacetyllevoglucosan–phenoxytitanium trichloride complex of 1 : 2 molar ratio

The co-catalytic effect of protic compounds

In the following, the co-catalytic effect of a few protic compounds has been studied. Such compounds are water, phenol, acetic acid and alcohols with different chain length (Table IV). Owing to its restricted solubility in chloroform, water makes possible only a rather slow reaction, but even so, in 4 hours a conversion of 68.7% is attained. The co-catalytic action of the different alcohols is nearly identical, that of acetic acid is similar, and that of phenol weaker. A comparison with the data in Table III shows that alkoxytitanium trichlorides are somewhat better co-catalysts than alcohols. Naturally, it must be taken into account that alcohols also react with 1 mole of $TiCl_4$, decreasing thereby its excess in the reaction mixture. Presumably, $TiCl_4$ gives orthotitanic acid trichloride with water, alkoxytitanium trichloride with alcohols, phenoxytitanium trichloride with phenol and acetoxytitanium trichloride with acetic acid.

In the IR spectra of the complexes isolated from the reaction mixture, it is relatively the easiest to detect $PhOTiCl_3$. The IR spectrum of the complex isolated after refluxing for 1 hr a reaction mixture of 1 : 1 : 5.25 TAL : phenol : : $TiCl_4$ starting composition (Fig. 4), has the characteristic bands of $PhOTiCl_3$, such as bands at 1585, 1480 and 920 cm^{-1}. The phenol content of both the complex and the mother liquor was determined, using Koppeschaar's method, decomposition with water. It has been established that 1 mole of the complex contains about 0.5 mole of phenol, in the form of $PhOTiCl_3$, and 1.5 mole of $TiCl_4$. Considering also the relatively good solubility of this 'mixed' complex (TAL · 0.5 $PhOTiCl_3$ · 1.5 $TiCl_4$) in warm chloroform, this composition supports our earlier conclusions [1], according to which 1 mole of alkoxy- or aryloxy-$TiCl_3$ per 2 moles of TAL is sufficient to prevent the formation of molecule associates and to make possible ring cleavage.

The IR spectrum (Fig. 5) of the complex prepared by refluxing for 1 hour a reaction mixture of TAL, acetic acid and $TiCl_4$ (1 : 1 : 5.25), shows the presence of the bands of acetoxytitanium trichloride [2] at 1545—1520 cm^{-1}.

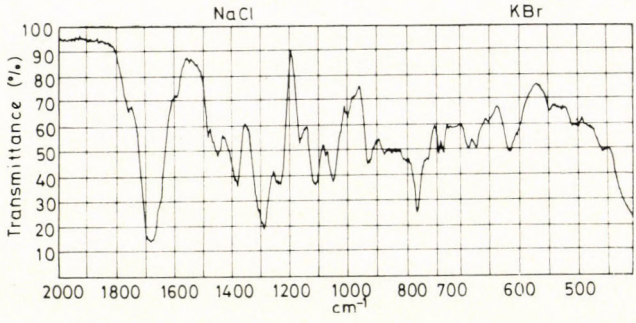

Fig. 4. IR spectrum (in paraffin oil) of the complex obtained from a triacetyllevoglucosan–phenol–$TiCl_4$ mixture of 1 : 1 : 5.25 initial molar ratio after refluxing for 1 hr

Table IV

Reaction of triacetyllevoglucosan with $TiCl_4$ in chloroform, in the presence of various co-catalysts

TAL : $TiCl_4$ molar ratio 1 : 5.25

Co-catalyst	Quantity of co-catalyst mole per 1 mole of TAL	Reflux time hr	Conversion, %	Complex			Note
				Cl content %	Ti content %	$[\alpha]_D^{20}$ (CH_3CN)	
Water	1	0	0.12	41.2 41.6	14.7	—17.0	Decomposition point: 127—130 °C
Water	1	1	2.5	41.9 42.5	14.5	—12.0	Decomposition point: 131—134 °C
Water	1	2	18.8	43.2 43.0	14.4	—5.8	Decomposition point: 126—128 °C
Water	1	3	35.7	43.0 44.1	15.0	13.1	Decomposition point: 126—128 °C
Water	1	4	68.7	41.6 42.6	14.1	34.7	Decomposition point: 125—130 °C
Ethanol	1	1	77.8	40.3	—	54.6	
Ethanol*	1	1	78.2	40.4	—	59.2	
Ethanol	1	4	83.8	—	—	—	
Propanol	1	4	83.3	40.2	15.2	68.0	
Butanol	1	4	84.2	37.5	—	64.1	
Phenol	1	0	2.7	30.4 30.3	14.6	—18.3	$PhOTiCl_3$ content: 0.418 mole per 1 mole of TAL
Phenol	1/2	1	46.9	34.1	—	—	$PhOTiCl_3$ content: 0.470 mole per 1 of TAL
Phenol	1	1	50.8	37.9	—	50.3	$PhOTiCl_3$ content: 0.502 mole per 1 mole of TAL
Phenoxytitanium trichloride	1/2	1	59.5	39.8	14.9	43.5	
Phenoxytitanium trichloride**	1	1	58.5	36.2	—	43.1	$PhOTiCl_3$ content: 0.435 mole per 1 mole of TAL
Acetic acid	1	0	8.5	38.5 38.7	—	6.6	
Acetic acid	1/2	1	73.0	—	—	63.0	
Acetic acid**	1	1	78.1	36.1	—	60.8	
Acetic acid	2	1	90.8	—	—	—	

* The mixture of $TiCl_4$ and alcohol was first refluxed for 30 min and TAL was added only afterwards.

** TAL : $TiCl_4$ molar ratio 1 : 3

Calculated chlorine content of the complexes,	%
TAL : $TiCl_4$ of 1 : 2 molar ratio	42.6%
TAL : $TiCl_4$: $EtOTiCl_3$ of 1 : 1.5 : 0.5 molar ratio	39.5%
TAL : $TiCl_4$: $AcOTiCl_3$ of 1 : 1.5 : 0.5 molar ratio	39.1%
TAL : $TiCl_4$: $PhOTiCl_3$ of 1 : 1.5 : 0.5 molar ratio	33.08%

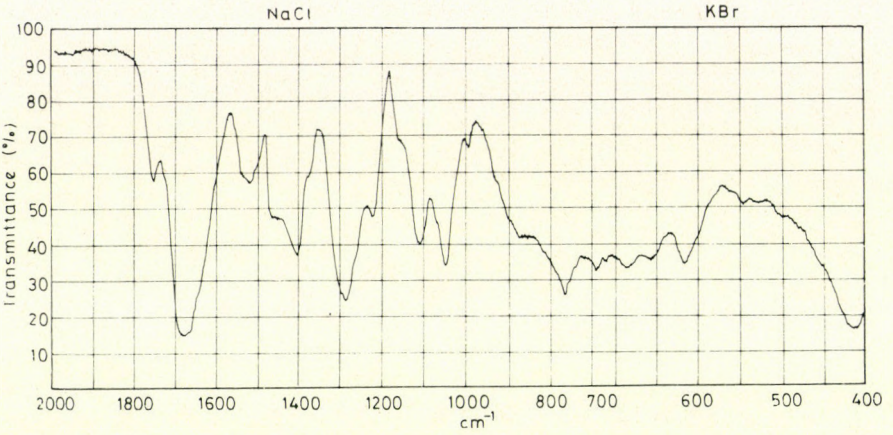

Fig. 5. IR spectrum (in paraffin oil) of the complex obtained from a triacetyllevoglucosan–acetic acid–$TiCl_4$ mixture of 1 : 1 : 5.25 initial molar ratio after refluxing for 1 hr

Kinetic investigations

Co-catalysis by acetic acid also made possible to follow the reaction kinetically. This had been done earlier [3] in nitromethane solution; however, since $TiCl_4$ forms a complex also with nitromethane, the conclusions drawn from these experiments are not unconditionally valid for the reaction in chloroform.

In chloroform containing acetic acid, a clear solution was obtained, thus the reaction could be followed by polarimetry. On substituting the data of optical activity into the polarometric formula of first order

$$kt = \ln \frac{\alpha_\infty - \alpha_0}{\alpha_\infty - \alpha_t}$$

(where α_0 is the optical rotation extrapolated for the 0th minute, α_∞ the value of rotation read after 24 hours, and α_t the optical activity at time t), a straight line was obtained on graphical plotting, proving that the reaction proceeded according to first order kinetics.

The results of kinetic investigations carried out at 57 °C are shown in Table V. The table comprises, in addition to the molar ratios of the components, those molar ratios, which result when CH_3COOH is converted with the $TiCl_4$ present, nearly quantitatively, into $AcOTiCl_3$.

The following conclusions can be drawn from the results:

(1) The reaction proceeds according to first order kinetics, so that the probable mechanism of the ring cleavage is S_N1.

(2) In the TAL : $TiCl_4$: $AcOTiCl_3$ mixture of 1 : 1 : 1 molar ratio, the

reaction rate is very low, which indicates that even if HCl formed from $TiCl_4$ and acetic acid remains in the solution at 57 °C, its role in itself is unimportant.

(3) In the TAL : $AcOTiCl_3$ mixtures of 1 : 2 molar ratio, the rate suddenly increases at 1.5 mole of $TiCl_4$, indicating that there is a limit value between 1 and 1.5 mole, which is decisive from the point of view of the reaction. This is consistent with the results obtained for the isolated complexes, where the TAL : $TiCl_4$: co-catalyst molar ratio was about 1 : 1.5 : 0.5. On further increase of the ratio of $TiCl_4$, the reaction rate increases only moderately.

(4) An investigation of the effect of $AcOTiCl_3$ at 1 : 2 TAL : $TiCl_4$ molar ratio shows that using 1, 2 and 3 moles of co-catalyst, the rate constant of the reaction increases near in proportion to the $AcOTiCl_3$ concentration ($k \cdot 10^4 = 220$, 456 and 615 min^{-1}).

(5) Maintaining a TAL : $TiCl_4$: $AcOTiCl_3$ molar ratio of 1 : 3 : 1, but doubling the concentration of all the components, $k \cdot 10^4$ increases to almost twice of its original value ($269 \rightarrow 461$ min^{-1}).

On the basis of (4) and (5) it appears as if the reaction were of pseudo-first order, with the value of k depending also on the concentration of $AcOTiCl_3$; i.e. $AcOTiCl_3$ seems to have a catalytic effect. However, caution should be excercised in drawning conclusions, because the equilibrium

$$TiCl_4 + CH_3COOH \rightleftharpoons AcOTiCl_3 + HCl$$

may not be completely shifted to the right side in the reaction mixture, further the HCl formed may slightly affect the results. Also the effect of acetic acid differs somewhat from that of the other co-catalysts, because at co-catalyst/TAL molar ratios of < 1 the conversion is further increased (Tables IV and V), while with the other co-catalysts maximal efficiency is found at a molar ratio of about 1 [1].

On the other hand, the results of kinetic measurements agree with the preparative experiments carried out with each of the co-catalysts in the respect that a certain limit value of the TAL : $TiCl_4$ molar ratio is required in order to attain a satisfactory reaction rate and conversion, and this limit value is, according to experience, in the vicinity of 1.5 mole $TiCl_4$/TAL.

This quantity of $TiCl_4$ is bound during complex formation by the donor atoms in the acetyl group of TAL, so that it cannot participate anymore in the reaction. The first $TiCl_4$ molecule can be bound to the *axial* C—2 and C—4 acetyl groups of TAL, and the second $TiCl_4$ to the *axial* C—3 carbonyl. This latter may form a bridge between 2 molecules of TAL, giving rise to a complex which is insoluble in chloroform.

In this complex of $2TAL \cdot 3TiCl_4$ composition [1] the $TiCl_4$ molecules are coordinatively saturated, and can no longer attack the $<1, 6>$ oxygen bridge; on the other hand, the possible attack of another molecule of $TiCl_4$

Table V

Rate constants in the reaction of triacetyllevoglucosan with $TiCl_4$ in chloroform, in the presence of acetic acid at 57 °C

TAL : $TiCl_4$: acetic acid, molar ratio	TAL : $TiCl_4$: $AcOTiCl_3$, molar ratio*	Substrate concentr., mole/l	$TiCl_4$ concentration, mole/l	Acetic acid concentr., mole/l	$k \cdot 10^4$ min^{-1}
1 : 2 : 1	1 : 1 : 1	0.035	0.070	0.035	12
1 : 3 : 2	1 : 1 : 2	0.035	0.105	0.070	94
1 : 3.5 : 2	1 : 1.5 : 2	0.035	0.122	0.070	366
1 : 4 : 2	1 : 2 : 2	0.035	0.140	0.070	456
1 : 5.25 : 2	1 : 3.25 : 2	0.035	0.182	0.070	463
1 : 3 : 1	1 : 2 : 1	0.035	0.105	0.035	220
1 : 4 : 1	1 : 3 : 1	0.035	0.140	0.035	269
1 : 4 : 1**	1 : 3 : 1	0.070	0.280	0.070	461
1 : 5 : 3	1 : 2 : 3	0.035	0.175	0.105	615

* Assuming that the $TiCl_4 + CH_3COOH \rightarrow AcTiCl_3 + HCl$ reaction proceeds to a great extent.

** Double concentration

is sterically hindered. Linked to a C—3 acetyl group, the co-catalyst, as a monofunctional Lewis acid, prevents the formation of molecule associates.

On the basis of what has been said above, the various complexes have the following role in the reaction mechanism: in the absence of co-catalyst, only a complex of $2TAL \cdot 3TiCl_4$ is formed, which is incapable of conversion [1]. Such a complex is formed also in the presence of a co-catalyst, however, under the conditions of the reaction, this complex can be converted into a mixed complex containing also the co-catalyst ($TAL \cdot TiCl_4 \cdot$ co-catalyst). Moreover, from the mixed complex and $TiCl_4$ a complex of the composition $TAL \cdot 2TiCl_4$ may also be formed. According to our assumption, in the latter complex one of the $TiCl_4$ molecules is attached to the C—2 and C—4 acetyl groups, while the other to the C—3 acetyl group. Since under these conditions there is no free, *i.e.* non-coordinated TAL in the system, no complex with cross-linked structure can be formed. In this case, $TiCl_4$ linked to the C—3 acetyl group becomes coordinatively saturated by attachment to the $<1,6>$ oxygen bridge of acetal character, which is in sterically favourable position. This is the complex through which the ring cleavage reaction occurs (Fig. 6). The rate determining step is the dissociation of the $C_1—O_{(anh)}$ bond, which is produced by $TiCl_4$ through the loosening of this linkage by the dative bond formed between oxigen and titanium:

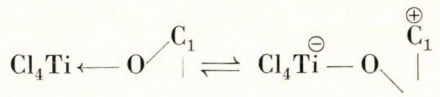

In the transition state, the carbonium ion under formation is conjugated with the oxygen of the semiacetal $<1, 5>$ ring, which stabilizes the cation to a certain degree, and this facilitates the progress of the ring cleavage reaction.

The C—6 methyleneoxytitanium tetrachloride anion transfers chloride ion to the C_1 carbonium ion in a very quick reaction (Fig. 6). Since the levoglucosan molecule is, on account of its three substituents of *axial* steric position, in a rather stressed chair form held together by the $< 1, 6>$ oxygen bridge, on the rupture of this ring the 1C conformation is converted to C 1, thereby the substituents in positions 2, 3 and 4 get into *equatorial* position. This is made likely also by the continuous change in rotation during the reaction. The change in conformation cannot be prevented even by the coordinate bond of $TiCl_4$ holding together the C—2 and C—4 acetyl groups. This bond is ruptured, and the new bond is formed presumably between the C—2 and C—3 acetyl groups. The methyleneoxy-$TiCl_3$ group also forms complexes, probably with the neighbouring C—4 acetyl group. (It is possible that the conformational change occurs already in the transitory carbonium ion, when the initial semichair form is transformed into a more stable modification.)

It can be assumed that, depending on the concentration ratios, the cocatalyst is also involved in the end-product complex and can be incorporated in the same. The presence of 'free' carbonyl group, detectable in the IR spectrum of most of the end-product complexes also supports this assumption;

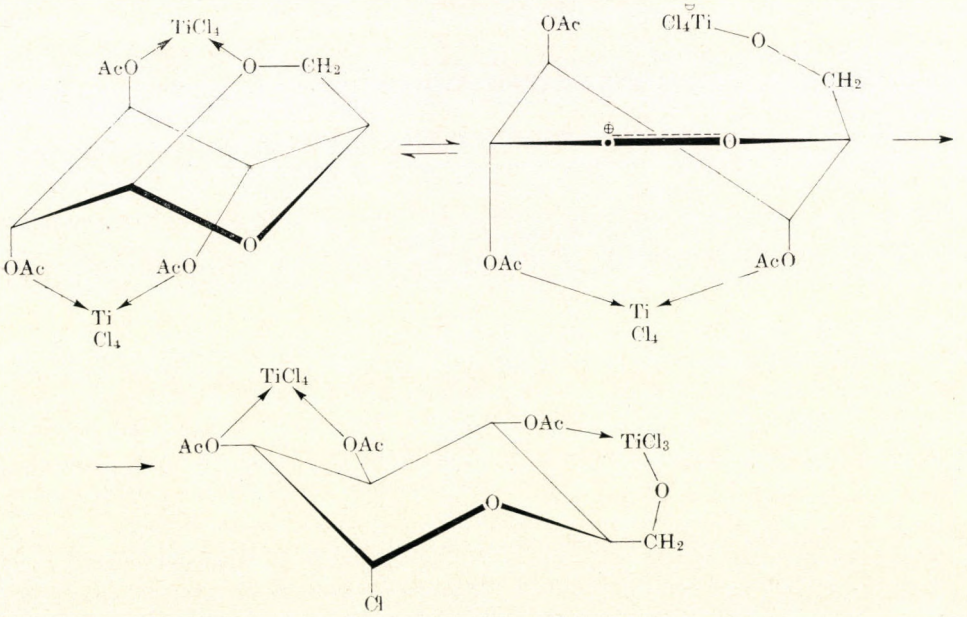

Fig. 6. Mechanism of the ring cleavage reaction of triacetyllevoglucosan

during the complex formation of the monofunctional co-catalyst a free carbonyl group must also be present in addition to bound ones.

The answer to the question, why the α-anomer is formed in the reaction, is that with the halogen derivatives of glucopyranoses this is the thermodynamically more stable anomer [4]. In the chlorination of triacetyllevoglucosan, the bulky $-TiCl_4^{\ominus}$ group in the transitory carbonium ion is protected by steric hindrance against attack from the other direction, so that also for this reason mainly the α-anomer is formed. Even if a small amount of the β-chloro derivative would be formed in the reaction, for which there is no evidence, this would be quickly transformed at the temperature of the reaction and in the presence of the high $TiCl_4$ and co-catalyst concentrations into the more stable α-anomer.

Comparing the results of our present kinetic measurements with those of earlier [3] experiments carried out in abs. nitromethane solution in the absence of co-catalyst, it can be seen that the k values are of an identical order of magnitude. There, nitromethane itself acted as a co-catalyst, by preventing, as a strong donor present in large excess, the formation of stable complex associates by $TiCl_4$ with TAL, making thereby the ring cleavage reaction sterically possible.

Iron-halide catalysts

It is interesting that among the metal halides of Lewis acid character only $TiCl_4$ reacts with TAL, whereas the others, e.g. $FeCl_3$, do not. On the other hand, CsűRÖS *et al.* [5] described earlier that ring cleavage takes place in the presence of iron powder and acid bromides, the product being the corresponding 6-O-acyl derivative. Thus, α-acetobromoglucose has been prepared with acetyl bromide, 6-butyryl-2,3,4-triacetyl-α-D-glucopyranosyl bromide with butyryl bromide, and 6-benzoyl-2,3,4-triacetyl-α-D-glucopyranosyl bromide (in a poor yield) with benzoyl bromide. The reactions take place in dilute solutions at room temperature, in 3—7 days. The interaction of acetyl bromide and TAL has been re-investigated in our experiments. The process was followed by IR spectroscopy and thin-layer chromatography. We have found that the reaction proceeds in 48 hours instead of 72 hours, if the recommended [5] quantity of acetyl bromide is increased by 50%.

The role of iron in the reaction has been investigated in greater detail. It was assumed that iron was converted partly into $FeBr_3$ into the reaction mixture, and this was responsible for the catalytic effect. Since $FeCl_3$ was available but $FeBr_3$ was not, in our further experiments the reaction of TAL with acetyl chloride was studied. In this case, the product is 2,3,4,6-tetraacetyl-α-D-glucopyranosyl chloride (α-acetochloroglucose). Following the reaction by thin-layer chromatography, it could be established that the reaction occurred

considerably quicker in the presence of anhydrous $FeCl_3$, than in that of iron powder. Thus, it has been proved that $FeCl_3$ is the catalyst of the reaction. Evidently, the $< 1, 6 >$ ring cleavage takes place here according to a mechanism other than in the case of $TiCl_4$, since no "minimum amount" of the catalyst is needed, even a trace quantity is sufficient. This can be obviously traced back to the complexing properties of $FeCl_3$ being different from that of $TiCl_4$. $FeCl_3$ is only sparingly soluble in chloroform, and the IR spectra of the dilute solutions unfortunately did not show the shift of the carbonyl band either in TAL, or in the acid halide. Thus, no proof could be found for complex formation, or for the possible formation of acylium cations.

By the reaction of TAL and benzoyl chloride, 2,3,4-triacetyl-6-benzoyl-α-D-glucopyranosyl chloride, a new compound not yet described in the literature, has been prepared in a yield of 53%. This compound (and method) may attain a role in the synthesis of 2,3,4-triacetyl-6-acylglucosides.

Experimental

The preparation and method of testing of the complexes have been described earlier [1].

Diethoxytitanium dichloride was prepared according to NESMEYANOV *et al.* [6] by the reaction of tetraethoxytitanium and $TiCl_4$ in a mixture of benzene and petroleum ether m.p. 45—55 °C (lit. m. p. 40—50 °C).

Calcd Cl 33.98; Ti 22.97. Found Cl 32.81; Ti 22.12%.

Tetraethoxytitanium was prepared from sodium ethoxide and $TiCl_4$ [7].

Calcd Ti 21.05. Found Ti 21.34%.

Propoxytitanium trichloride was made from propanol and $TiCl_4$ [8]; m. p. 64 °C (lit. m. p. 65—67 °C).

Calcd Cl 49.86; Ti 22.45. Found Cl 49.55; Ti 22.61%.

Butoxytitanium trichloride was synthesized from butanol and $TiCl_4$ [9]; m. p. 55.65 °C (lit. m.p. 50—60 °C).

Calcd Cl 46.79; Ti 21.07. Found Cl 46.74; Ti 20.46%.

Phenoxytitanium trichloride was prepared from phenol and $TiCl_4$ in chloroform solution [10].

Calcd Cl 43.01; Ti 19.37. Found Cl 41 37; Ti 19.21%.

The TAL-phenoxytitanium trichloride complex of 1 : 2 molar ratio is a wine-red, powdery substance, sensitive to atmospheric moisture.

Calcd Cl 27.18; Ti 12.24. Found Cl 22.88; Ti 12.06%.

Preparation of 2,3,4,6-tetraacetyl-α-D-glucopyranosyl chloride from acetyl chloride

(*a*) In the presence of iron powder catalyst 2.9 g (0.01 mole) of TAL and 2 ml (2.21 g; 0.284 mole) of acetyl chloride were dissolved in 100 ml of dry chloroform, and 0.2 g of iron powder was added to the solution. After standing for 45 hrs at room temperature, the reaction mixture was washed with distilled water, calcium chloride and active carbon were added to the organic phase, which was then filtered. Chloroform was evaporated under reduced pressure, and the residual syrup was crystallized from a mixture of ether and petroleum ether. The colourless crystals obtained by filtration were dried in a vacuum desiccator over paraffin flakes and phosphorus pentoxide to yield 2.7 g (74%) of the product, m. p. 70—72 °C; $[\alpha]_D^{20}$ + 163° (in chloroform). Lit. m p. of 2,3,4-tetraacetyl-α-D-glucopyranosyl chloride [11] 75—76 °C; $[\alpha]_D^{20}$ + 166.2°.

Calcd Cl 9.66.

Found Cl 9.16%.

Recrystallization from ether–petroleum ether gave m. p. 74—75 °C; $[\alpha]_D^{20}+166°$.

(*b*) In the presence of $FeCl_3$ catalyst

2.9 g (0.01 mole) of TAL and 1.4 ml 1.55 g (0.197 mole) of acetyl chloride were dissolved in 100 ml of dry chloroform. 0.2. g (0.012 mole) of anhydrous iron(III) chloride was added to the solution. The reaction mixture was allowed to stand for 24 hrs at room temperature. The reaction mixture in chloroform was then washed, in the given order, with 5% HCl solution, 10% $NaHCO_3$ solution and distilled water, and then processed further as described under (*a*). Weight of the raw product: 3.25 g (88%); m.p. 73—75 °C; $[\alpha]_D^{20}+165°$.

Preparation of 2,3,4-triacetyl-6-benzoyl-α-D-glucopyranosyl chloride

2.9 g (0.01 mole) of TAL and 2.35 ml 2.81 g (0.02 mole) of benzoyl chloride were dissolved in 100 ml of dry chloroform, and 0.2 g (0.0012 mole) of anhydrous $FeCl_3$ was added to the solution. The reaction mixture was allowed to stand for 24 hrs at room temperature then washed with 5% HCl, 10% $NaHCO_3$ and water, dried over anhydrous Na_2SO_4 and clarified with activated carbon. The chloroform filtrate was evaporated at reduced pressure. The syrup which remained was crystallized from ether–petroleum ether to yield 2.34 g (53.5%) of the product; m.p. 124 °C; $[\alpha]_D^{20}$ 174.3 °C.

$C_{19}H_{21}O_9Cl$ (438.45). Calcd C 53.22; H 4.94; Cl 8.27.
Found C 53.37; H 5.32; Cl 8.24%.

The IR spectrum has the band of the acetyl group at 1755 cm^{-1}, the band of the benzoyl group at 1715 cm^{-1} and the ν C—Cl vibration at 610 cm^{-1}.

Thin-layer chromatography was carried out on Kieselgel G layer, with a 95 : 5 ether–petroleum ether solvent mixture. Phenol–sulfuric acid was used for detection.

REFERENCES

[1] FENICHEL, L., DEÁK, GY., HOLLY, S., BAKÓ, P., CSŰRÖS, Z.: Acta Chim. (Budapest), **85,** 299 (1975).
[2] CSŰRÖS, Z., DEÁK, GY., FENICHEL, L., HOLLY, S., PÁLINKÁS, J.: Acta Chim. (Budapest) **80,** 193 (1974)
[3] CSŰRÖS, Z., DEÁK, GY., HARASZTHY-PAPP, M.: Acta Chim. Acad. Sci. Hung. **21,** 193 (1959).
[4] LEMIEAUX, R. U.: Advances in Carbohydrate Chem. **9,** 1 (1954)
[5] CSŰRÖS, Z., DEÁK, GY., HARASZTHY-PAPP, M.: Acta Chim. Acad. Sci. Hung. **29,** 227 (1961)
[6] NESMEYANOV, A. N., BRAYTINA, E. M., FREYDLINA, R. H.: Dokl. Akad. Nauk USSR **94,** 249 (1954)
[7] JENNINGS, J. S., WARDLAW, W., WAY, W. R. J.: J. Chem. Soc. **1963,** 637
[8] NESMEYANOV, A. N., FREYDLINA, R. H., NOGINA, A. W.: Izv. Akad. Nauk. USSR **1952,** 1037
[9] MIRAMI, I.: J. Chem. Soc. Japan **61,** 66 (1958): C. A. **53,** 18850i (1959)
[10] LUTSCHINSKY, G. P., ALTMANN, E. S.: Z. anorg. Chem. **225,** 321 (1935)
[11] BRAUNS, D. H.: J. Am. Chem. Soc. **47,** 1280 (1925)

László FENICHEL; 1111 Budapest, Műegyetem rkp. 3. Hungary
Gyula DEÁK; 1083 Budapest, Szigony u. 143. Hungary
Péter BAKÓ; 1111 Budapest, Műegyetem rkp. 3. Hungary
Sándor HOLLY; 1025 Budapest, Pusztaszeri u 57—69. Hungary
Zoltán CSŰRÖS; 1111 Budapest, Műegyetem rkp. 3. Hungary.

Acta Chimica Academiae Scientiarum Hungaricae, Tomus 85 (3), pp. 327—332 (1975)

REMOVAL OF THE NITRO GROUP FROM NITROARGININE AND NITROARGININE PEPTIDES

A. TURÁN, A. PATTHY and S. BAJUSZ

(Research Institute for Pharmaceutical Chemistry, Budapest)

Received May 17, 1974

It has been found that reductive cleavage of the nitro group from nitroarginine and nitroarginine-containing peptides with zinc is frequently associated with the formation of by-products like aminoarginine and ornithine derivatives. The formation of amino-arginine-containing compounds can be suppressed by using trifluoracetic acid as the medium. In this case removal of the Boc and OBu^t protecting groups can be combined with that of the nitro group.

N^{ω}-nitroarginine has been used for peptide synthesis since its first application reported by BERGMANN and ZERVAS [1] in 1934, although removal of the nitro protecting group is accompanied by difficulties. For this reaction hydrogenolytic cleavage [1], electrolytic reduction [2], acidolysis with hydrogen fluoride [3], and reduction with zinc in acidic medium [4] have been suggested. None of these deblocking methods give perfect results. Hydrogenolysis of nitroarginine located in a larger peptide chain is generally slow and a number of side reactions have been observed affecting the guanidino group [5] or the aromatic amino acid residues if being present in the peptide (*e.g.* saturation of the phenylalanine [6] and tryptophan [7] side chain). The application of electrolytic reduction can be problematical in the preparation of peptides on a larger scale, and acidolysis with hydrogen fluoride may lead to partial decomposition of arginine to ornithine [8]. The reduction of nitroarginine with zinc in an acid, as recommended by PLESS and GUTMANN [4] on the basis of THIELE's [9] studies, seemed to be a promising method, due to the short reaction time and the simple conditions required. The possibility of its general application in the synthesis of arginin-containing peptides had, however, to be investigated for two reasons. Firstly, according to THIELE's paper mentioned above, the reaction of nitroguanidine proceeds in two directions, namely, besides aminoguanidine more or less guanidine by-products are also formed; secondly, the reduction of protected bradykinin, *i.e.* removal of the *p*-nitrobenzyl ester and two nitro protecting groups from the nonapeptide bradykinin, with zinc/HCl [4] afforded a product which possessed lower activity than that obtained by hydrogenolytic deblocking.

This paper describes our results obtained during a search for the optimal conditions of the reductive cleavage of the nitro protecting group with zinc in an acid.

For investigating this problem, first the deprotection of nitroguanidine was studied. The compositions of the reaction mixtures were examined and estimated by paper electrophoresis at pH 3.6.

It was found (Table I) that reduction in the presence of one equivalent of acetic acid — under the conditions given for the preparation of aminoguanidine in Organic Syntheses [10] — yielded aminoguanidine and guanidine in a ratio of about 60 to 40. It is noted in Organic Syntheses that by increasing the amount

Table I

Reduction of nitroguanidine with zinc in different acids

Medium	Products*		
	Guanidine	Amino-guanidine	Acetamido-guanidine
1 eq. AcOH in water	++	+++	
AcOH	+++	(+)	++
1*N* HCl	+++	++	
HCOOH	+++++		

* Estimated by paper electrophoresis: +about 20%, (+) less than 10%

of acetic acid the yield of aminoguanidine is decreased. Furthermore, acidic medium is recommended in the literature [4] for splitting off the nitro group of peptides containing nitroarginine. Consequently, it might be supposed that in acidic solution the formation of aminoguanidine would be repressed in favour of the guanidine. Nevertheless, it was found that reduction of nitroguanidine in acetic acid also led to an about 1 : 1 mixture of guanidine and a further product, which was acetylaminoguanidine, since aminoguanidine is spontaneously acetylated in acetic acid solution. In hydrochloric acid the reduction proceeded similarly in two directions but, naturally, aminoguanidine was formed as by-product instead of the acetyl derivative. Formic acid was the only medium wherein the reduction of nitroguanidine with zinc led to guanidine alone and no aminoguanidine could be detected on the electrophoretogram.

The reduction of N^{ω}-nitroarginine, Arg(NO_2), with zinc was studied in the same acids as used in the case of nitroguanidine and in aqueous trifluoroacetic acid, sulfuric acid, and phosphoric acid as well. The compositions of reaction mixtures were examined by paper electrophoresis and in an amino acid analyser. It was found that the proportion of arginine as well as the nature of the formed by-products depended strongly on the acid used. Based on the results obtained in the reduction of nitroguanidine it was presumed that N^{ω}-aminoarginine, Arg(NH_2), and/or N^{ω}-acetamido-arginine, Arg(NH—Ac)

were formed as the main by-products in this case. Therefore, both compounds were synthesized. Arg(NH_2) was prepared from ornithine and S-methylisothiosemicarbazide and isolated as crystalline flavianate. Arg(NH—Ac) was obtained from Arg(NH_2) by keeping its acetic acid solution in the presence of HCl. By means of these reference compounds, the composition of the reaction mixtures could be estimated as given in Table II.

Table II

Reduction of nitroarginine with zinc in different acids and by hydrogenolysis

Medium		Products, %				
		Arg	Arg(NH_2)	Arg(NH-Ac)	Orn	?
1 AcOH	85%	37.0	—	60.0	0.5	2.5
2 H_3PO_4	2*N*	60.6	33.6	—	5.7	—
3 HCOOH	95%	84.7	—	6.5*	1.8	6.8
4 HCl	2*N*	94.7	3.3	—	0.8	—
5 H_2SO_4	2*N*	98.0	1.1	—	0.9	—
6 TFA	80%	91.3	2.7	—	5.9	—
7 TFA	2*N*	95.9	2.4	—	1.7	—
8 H_2/Pd in water + 2.5 eq. AcOH		91.0	7.5	—	0.2	1.1
9 H_2/Pd in 80% AcOH		92.9	3.5	2.5	1.1	—

* Ac = formyl

It can be seen that in acetic acid (1) the main product is Arg(NH—Ac), which has also been isolated from the reaction mixture by ion-exchange chromatography. In phosphoric acid (2) Arg(NH_2) was the by-product. Formic acid (3) did not prove as useful a medium as in the experiment with nitroguanidine. The elution time in the amino acid analyzer of the main impurity (6.5%) was similar to that of Arg(NH—Ac), consequently it might be Arg(NH-For). Of other acidic media 2*N* H_2SO_4 (5) and 2*N* TFA (7) were found to be the best giving arginine in yields of 98 and 95.9%, respectively. It is worth mentioning that in concentrated TFA, which is used for the removal of Boc and OBu^t groups, ornithine was formed as a by-product (6%). Hydrogenolytic reduction of Arg(NO_2) effected either in water containing 2.5 eq. AcOH (similar to that given in Ref. [6]) or in 80% AcOH (8.9) resulted in mixtures, the compositions of which were quite similar to those obtained by zinc reductions in HCl, H_2SO_4 or TFA. The ratio of Arg(NH_2) to its acetyl derivative depends on the amount of acetic acid present during the catalytic reductions.

The reduction of Arg(NO_2) built in a peptide chain was studied on the tetrapeptide amide Leu-Arg(NO_2)-Pro-Gly-NH_2. In this case the reduction

products obtained were hydrolyzed in the usual manner and the resulting mixture was analyzed. The sum of basic components (with the exception of ammonia) of the hydrolysate were taken as 100% (the ratio of natural amino acids was 1 : 1).

The data obtained this way (Table III) indicate that the reduction of Arg(NO_2) built in a peptide chain gives in some cases arginine and the by-products in a different ratio from that obtained with Arg(NO_2) itself (Table II).

Table III

Basic components derived from arginine in the hydrolysate of Leu-Arg(NO_2)-Pro-Gly-NH_2 after reduction with Zn in different acids

Medium		Products, %			
		Arg	Arg(NH_2)	Arg(NH-Ac)	Orn
1 AcOH	85%	89.5	—	10.5	—
2 HCl	2*N*	84.0	8.7	—	7.3
3 H_2SO_4	2*N*	74.4	16.0	—	9.3
4 HCOOH	95%	93.4	—	—	6.6
5 TFA	80%	93.4	—	—	6.6
6 TFA	2*N*	96.0	—	—	4.0
7 H_2/Pd in 85% AcOH		96.4	—	—	3.6

For instance, in acetic acid the proportion of arginine formed from the tetrapeptide and from Arg(NO_2) were 89.5 and 37%, respectively. In sulfuric acid, however, the reduction of tetrapeptide was less successful than that of Arg(NO_2); the corresponding yields were 74.5 and 98%. The figures in Table III may not reflect the real situation quite truly, since some of the arginine content of the hydrolysate may originate from the transformation of by-products as shown in Table IV.

Formic acid and trifluoroacetic acid (Nos 4—6 in Table III) seemed to be the best media for the reduction of Arg(NO_2)-containing peptides with zinc. Moreover, in TFA no alteration in the yields of arginine were found (*cf.* Nos 6, 7, in Table II). In the experiments with TFA the tetrapeptide was used as its Boc derivative and the removal of this protecting group was combined with that of NO_2. Hydrogenolytic cleavage of the NO_2 group of the tetrapeptide amide (No. 7 in Table III) was quite successful, as ornithine could be detected as the only by-product in a yield of 3.6%. For complete deblocking, however, 48 hrs were required.

From these facts it can be concluded that the reductive cleavage of the nitro group of arginine derivatives with zinc is frequently accompanied by

Table IV

Transformation of N^G derivatives of Arg during acid hydrolysis (6N HCl, 115 °C, 24 hrs)

N^G-derivative	Products, %			
	Arg	Arg(NH_2)	Arg(NH-Ac)	Orn
1. Arg(NH—Ac) · AcOH*	—	2.5	88.2	9.3
2. Arg(NH—Ac) · AcOH	1.1	74.7	21.2	9.3
3. Arg(NH—Ac) · Fl**	8.0	76.0	—	16.0
4. Arg(NH_2) · Fl	9.2	77.8	—	13.0
5. Arg$(NO)_2$	77.6	2.7	—	19.7

* Hydrolyzed in AcOH — 12*N* HCl (1 : 1)

** Fl stands for flavianic acid

the formation of by-products like aminoarginine and ornithine derivatives. The formation of aminoarginine containing compounds can be suppressed by using trifluoroacetic acid as medium. In this case removal of the Boc and OBu^t protecting groups can be combined with that of the nitro group.

Experimental

Reduction of nitroguanidine derivatives with zinc

One mmole of a nitroguanidine compound was suspensed or dissolved in 4 ml of acetic, formic, or trifluoroacetic acid, or 10 ml of 2*N* hydrochloric, sulfuric, phosphoric or trifluoroacetic acid. To the stirred and cooled ($t \leq 30$ °C) mixture 0.4 g of wet, freshly activated zinc dust (Note 1) was added. Stirring was continued for 2 hrs. Unchanged zinc and the precipitated zinc salts were filtered off and washed with the acid in use. The combined filtrates were evaporated, except when using acetic acid (Note 2). The residue was dissolved in water, applied to a column of Amberlite AG 1×2 (acetate cycle), and was then eluted with water. The eluate was saturated with H_2S; the precipitated zinc sulfide was removed by centrifugation. The composition of the supernatant was determined either by electrophoresis (Note 3) or in an amino acid analyser (Note 4). When neccessary, the supernatant was evaporated and the remaining reduced material was isolated in the usual way.

Notes

1. Zinc dust was succesively washed with 1*N* HCl, water and ethanol in the wet state; its contact with air was prevented. It was used as a suspension; 0.4 g of wet zinc corresponded to about 0.3 g of dry material (about 9 meq.).

2. When using acetic acid, evaporation of the filtrate and washings were omitted. A typical reaction is described in the preparation of acetamido arginine.

3. Paper electrophoresis at pH 3.6 in pyridine–acetate buffer (30V/cm), run for 1—2 hrs, was used for qualitative determination of the reduction products of nitroguanidine.

4. JLC-5AH amino acid analyser was used. Analyses were performed on AMINEX A-5 resin at 30 °C, in 0.35*N* sodium citrate buffer (pH 5.28) at a flow rate of 100 ml/hr. The elution times (in min) were: ornithine (36), acetamidoarginine (39), formamidoarginine (41), ammonia (50), aminoarginine (78), arginine (102).

5. The composition of the mixture obtained on reduction of Leu-Arg(NO_2)-Pro-Gly-NH_2 was determined as follows: The solution obtained after the removal of zinc sulfide was evaporated and the residue dissolved in 6*N* HCl and hydrolyzed at 115 °C for 24 hrs. When using acetic acid as the medium, evaporation was omitted; the solution was diluted with an equal volume of 12*N* HCl and hydrolyzed as given above. After neutralization the composition of amino acids was determined. The sum of the basic components was arbitrarily set as 1 or 100%. Details are given in Table III.

N^G-Aminoarginine flavianate

Ornithine hydrochloride (1.68 g; 10 mmoles) and S-methylisothiosemicarbazide hydrochloride (2.33 g; 10 mmoles) were dissolved in 1*N* sodium hydroxide (20 ml) and kept at 40 °C for 30 hrs. To the mixture 2*N* hydrochloric acid (10 ml) and flavianic acid (3.14 g; 10 mmoles) dissolved in warm water (5 ml) were added. The mixture was cooled and the yellow crystals which separated were filtered off, washed with water and ethanol and dried; yield 3.1 g (61.5%), m.p. 218 °C.

$C_{16}H_{21}O_{10}N_7S$ (503.45). Calcd C 38.2; H 4.2; N 19.5; S 6.35. Found C 38.23; H 4.1; N 19.51; S 6.56%.

N^G-acetoamidoarginine flavianate

To a suspension of nitroarginine (2.2 g; 10 mmoles) in acetic acid (40 ml) wet zinc dust (4 g) was added; the mixture was cooled to below 30 °C and stirred for 2 hrs. Unreacted zinc and the separated zinc acetate were filtered off and washed with acetic acid. The combined filtrates were saturated with H_2S and zinc sulfide was removed by centrifugation. The supernatant (apart from a sample which was used in the amino acid analyser to determine the composition of the reaction mixture) was evaporated and applied to a column of Dowex 50×2 (H^+-cycle) and eluted with 0·1*N* ammonium acetate (pH 7). The fractions containing acetamidoarginine (detected by amino acid analysis) were pooled and evaporated. The residue was dissolved in hot ethanol and treated with an ethanolic solution (5 ml) of flavianic acid (2 g). Yellow crystals separated, which were filtered off, washed with ethanol and dried to obtain 2.2 g (40%), of the product, m.p. 215 °C.

$C_{18}H_{23}O_{11}N_7S \cdot H_2O$ (563.50). Calcd C 38.36; H 4.47; N 17.40; S 5.70. Found C 38.48; H 4.40; N 17.20; S 5.79%.

From Arg(NH_2): Aminoarginine flavianate (0.1 g) was dissolved by warming in acetic acid (10 ml) containing 1 drop of 1*N* HCl. After standing at room temperature overnight, the solution was evaporated and the residue triturated with ethanol. The yellow crystals were filtered off, washed with ethanol and dried to yield 0.09 g (90%) of the product, m.p. 215 °C.

REFERENCES

[1] Bergmann, M., Zervas, L.: Physiol. Chem. **224,** 40 (1934)
[2] Scopes, P. M., Walshaw, K. B., Welford, M., Young, G. T.: J. Chem. Soc. **1965,** 782
[3] Sakakibara, S., Shimonshi, Y., Kishida, Y., Okada, M., Susihara, H.: Bull. Chem. Soc. Japan **40,** 2164 (1967)
[4] Pless, J., Guttmann, St.: Peptides 1966, Proceedings of the 8th European Peptide Symposium, Ed. H. C. Beyerman *et al.*, p. 50. North Holland, Amsterdam, 1967
[5] Iselin, B. M.: Peptides 1963, Proceedings of the 6th European Peptide Symposium, Ed. L. Zervas, p. 27. Pergamon Press, Oxford, 1966
[6] Schafer, D. J., Young, G. T., Elliott, D. F., Wade, R.: J. Chem. Soc. (C) **1971,** 46
[7] Bajusz, S., Turán, A., Fauszt, I., Juhász, A.: Peptides 1972, Proceedings of the 12th European Peptide Symposium, Ed. H. Hanson and H-D. Jakubke, p. 93. North Holland, Amsterdam, 1973
[8] Yamashiro, D., Blake, J., Li, C. H.: J. Am. Chem. Soc. **94,** 2855 (1972)
[9] Thiele, J.: Ann. **270,** 23 (1892)
[10] Organic Syntheses, Coll. Vol. III, p. 73. J. Wiley and Sons, New York, 1967

András Turán
A. Patthy
Sándor Bajusz
1325 Budapest, POB. 82, Szabadságharcosok u. 47—49.
Hungary

Acta Chimica Academiae Scientiarum Hungaricae Tomus 85 (3), pp. 333—338 (1975)

REACTION OF α,β-UNSATURATED KETONES WITH *BIS*-NUCLEOPHILIC REACTANTS

FURTHER STUDIES WITH POLYOLEFINIC ($\alpha, \beta, \gamma, \delta$-UNSATURATED) KETONES AND β-HETEROARYL (FURYL AND THIENYL) α, β-UNSATURATED KETONES

O. H. HANKOVSZKY, K. HIDEG, K. POLGÁR and D. LLOYD*

*(Central Laboratory of Chemistry, University of Pécs, Hungary, and *Department of Chemistry, Purdie Building, University of St. Andrews, St. Andrews, Great Britain)*

Received August 16, 1974

The products obtained from the reactions of 1,2-diaminoethane with cinnamylideneacetone, furylideneacetone or β-ionone in refluxing cyclohexane-ether were *bis* (dienimines) **(7, 14, 10)**, but were probably formed by an indirect route rather than by direct condensation reactions. Thenylideneacetone gave a dimethyldithienyl-diazacyclotetradecadiene **(13)** under proper conditions, but in refluxing chloroform a *bis* (dienimine) was obtained. The cyclic product was also converted into this *bis* (dienimine) when heated.

α, β-unsaturated ketones are ambient electrophiles; in a previous paper [1] we have discussed their reactions with bifunctional nucleophiles, *viz.* 1,2-diaminoethane, 1,3-diaminopropane and ethane-1,2-dithiol. The nature of the products depended on the identity of both the enone and the nucleophile. For example, when diaminoethane was refluxed in a mixture of cyclohexane and ether (2 : 1), in the presence of anhydrous potassium carbonate, with mesityl oxide, benzylideneacetone or benzylideneacetophenone, the products were, respectively, a heterocyclic seven-membered ring compound **(1)** a fourteen-membered ring **(2)**, and the acyclic adduct **(3)**.

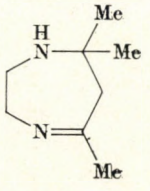

(1)

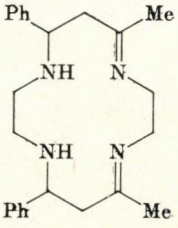

(2)

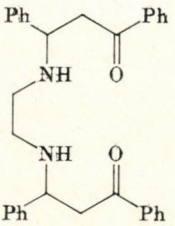

(3)

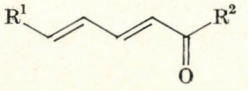

(4)

This work has now been extended to the reactions, under identical conditions, of dinaminoethane with polyolefinic carbonyl compounds **(4)**.

Reaction might now take place at the carbonyl group and/or at the β- or δ-carbon atoms. Previous studies [2] have shown that the site of reaction appears to be under thermodynamic control, with conjugate addition rather than condensation being the preferred path. The presence of δ-phenyl substituents promotes reaction at the β-position, presumably, because phenyl-vinyl conjugation is thereby retained.

When cinnamylideneacetone **(5)** reacted with diaminoethane the product was, however, the biscondensation product **(7)**, and not an adduct.

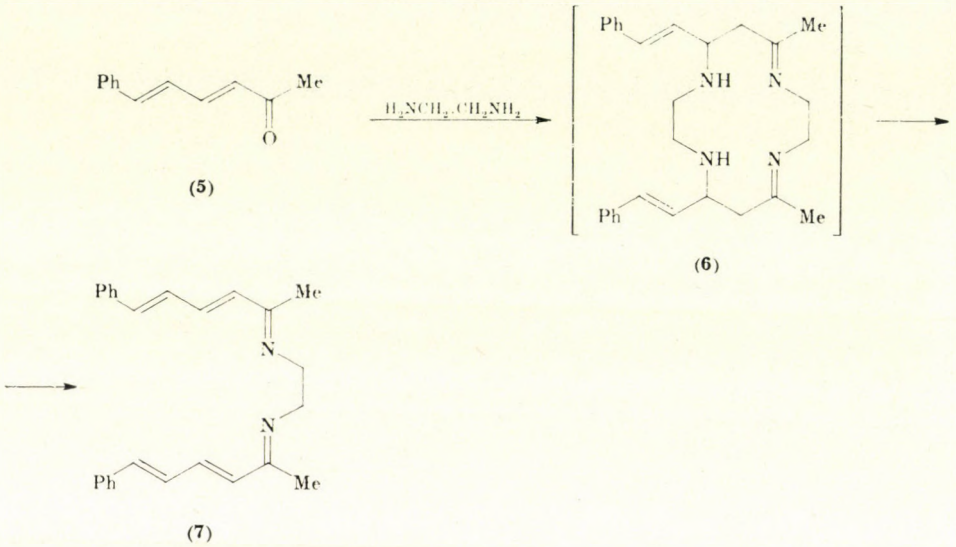

The structure of this product follows from its elemental analysis (C + H + N = 100%), IR spectrum (no NH band, but a C=N band at 1600 cm^{-1}) and its NMR spectrum, which has no sp^3 CH, except the methyl groups and the methylene groups derived from diaminoethane.

Benzylideneacetone reacts with diaminoethane to give the product **2** but, when heated in ethanol or chloroform, this product readily dissociates by a reverse Michael reaction into diamine and a bisenimine **(8)** [3]. It is tempting, therefore, to suggest that an analogous path may be followed by the dienone **5**, and that, like other δ-phenyldienones, it first undergoes β-addition to give a bis-adduct which reacts with another equivalent of diaminoethane to form a heterocycle (6), but this compound then dissociates to provide the isolated product **(7)**.

Cinnamylideneacetophenone (**4**; $R^1=R^2=Ph$) apparently did not react with diaminoethane under identical conditions. The adduct (3) formed from benzylideneacetophenone did not cyclize, presumably because of the low reactivity of the benzoyl-carbonyl groups. Similarly, any β-adduct from **4**,

($R^1=R^2=Ph$) would not cyclize to give an analogue of **6** (and hence of **7**) and it appears that the equilibrium between **4** ($R^1=R^2=Ph$) and its possible adducts lies on the side of the dienone, presumably because the latter is stabilized by conjugation.

It would thus appear that the driving force towards addition to the δ-phenyldienone system is small and the formation of **7** could be governed by the ready dissociation of the intermediate **6**.

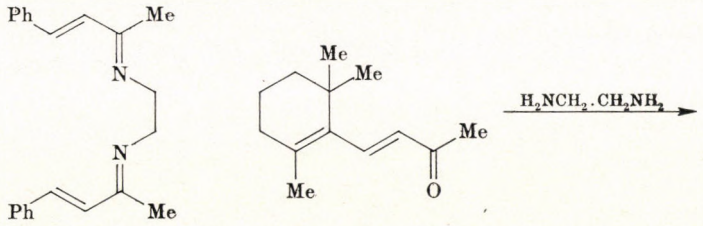

(8) **(9)**

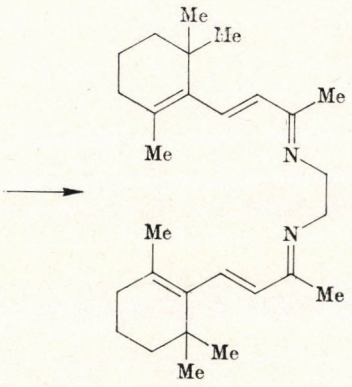

(10)

When the dienone used was β-ionone **(9)**, a product **(10)** analogous to **7** was again isolated. Although δ-methyldienones frequently give δ-adducts [2], this can be inhibited in the case of β-ionone for steric reasons. The structure of **10** follows from its IR spectrum, which indicates the presence of a conjugated azomethine group, and its NMR spectrum, which shows an AB quartet due to the olefinic protons.

Since furylideneacetone (11) and thenylideneacetone (12) might be considered either as polyenones or as the heterocyclic analogues of benzylideneacetone, it was of interest to investigate their reactions with diaminoethane.

From furylideneacetone only the product **14** (X=O) was obtained, but thenylideneacetone gave the cyclic product **13** (X=S), whose structure follows from its molecular weight and its IR and NMR spectra.

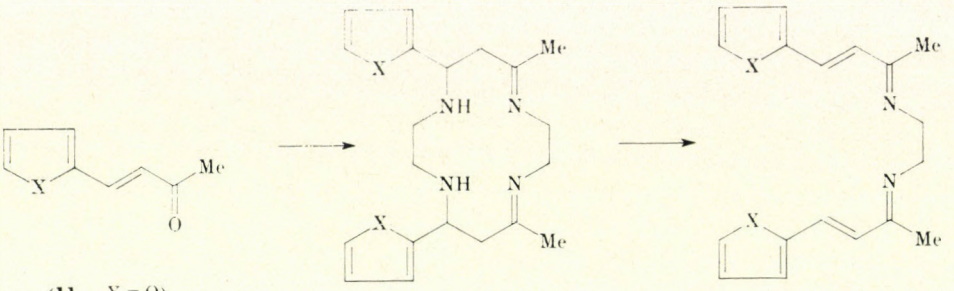

(**11**, X = O)
(**12**, X = S)

(**13**)

(**14**)

With Cu(II) salts it gave an intense lilac colour, owing to complex formation. This difference in behaviour between **11** and **12** is consistent with the much greater cyclic delocalisation of electrons in the thiophene ring compared with the furan ring, which results in the latter reacting similarly to other dienones, whereas the former reacts like a β-arylenone.

When compound 13 (X=S) was refluxed in chloroform, cleavage of the ring ensued and the bisenimine 14 (X=S) was formed. The latter product was also obtained when thenylideneacetone and diaminoethane were heated together in chloroform instead of in cyclohexane–ether mixture.

This stepwise formation of **14** (X=S), in which the cyclic compound **13** (X=S) is isolated, also provides evidence for the suggested formation of **7** from **5** *via* **6** as a transient intermediate.

Experimental

M.p.'s. were determined with a Büchi SMP-20 instrument, and are uncorrected. IR spectra were recorded with a Perkin-Elmer 257 instrument and NMR spectra with a Perkin-Elmer R-12 instrument, using tetramethylsilane as reference compound.

5,10-Dimethyl-1,14-diphenyl-6,9-diazatetradeca-1,3,5,9,11,13-hexaene (7)

Cinnamylideneacetone **(5)** (8.6 g, 0.05 mole) and 1.2-diaminoethane (3.0 g, 0.05 mole) were heated for 6 hrs in a stirred mixture of cyclohexane and ether (2 : 1) in the presence of potassium carbonate (5 g). After filtration, the solvent was evaporated and the residual oil dissolved in ethanol (50 ml), filtered and kept overnight. The light yellow product which precipitated was filtered off (10 g, 88%) and washed with ether. After crystallization from a mixture of ethanol and ether it had m.p. 126–128 °C.

$C_{26}H_{28}N_2$ (368.52). Calcd C 84.74; H 7.66; N 7.60. Found C 84.85; H 7.46; N 7.69%.

^1H–NMR (TFA): $\delta = 2.05$ (*s*, 6H, $2CH_3$); 3.80 (*t*, 4H, $=N-CH_2-CH_2-N=$); 6.55–7.60 (m, 18H, olefinic and aromatic).

1,10-Bis(2,6,6-trimethylcyclohex-1-ene-1-yl) 3,8-dimethyl-4,7-diazadeca-1,3,7,9-tetraene (10)

β-Ionone **(9)** (9.6 g, 0.05 mole) and 1,2-diaminoethane (3,0 g, 0.05 mole) were heated in ether (80 ml) in the presence of potassium carbonate (5 g). After 3 hrs, the mixture was filtered and the filtrate evaporated to half volume. The crystals which precipitated after a week were

filtered off and washed with ether to obtain a crude product (12.0 g, 52%), which was recrystallized from ether: m.p. 105—108 °C.

$C_{28}H_{44}N_2$ (408.67). Calcd C 82.30; H 10.85; N 6.85. Found C 82.15; H 10.45; N 6.96%.

IR (KBr) ν_{max}= 1640, 1580 cm^{-1} (C=N, C=C conj.).

^1H—NMR (CCl_4): δ = 1.05 (s, 12H, 2 $C(CH_3)_2$); 1.45 (m, 8H, 2 $-CH_2-CH_2-C$); 1.72 (s, 6H, 2 $C=C-CH_3$); 2.05 (s, 6H, 2 $CO-CH_3$); 2.24 (t, 4H, 2 $CH_2-C=$), 3.78 (s, 4H, $=N-CH_2-CH_2-N=$): 6.12 (d, 2H, $-CH=CH-$, J = 15.6 Hz): 8.73 ppm (d, 2H, $-CH=CH-$, J=15.6Hz).

1,10-Di(2-furyl)-3,8-dimethyl-4,7-diazadeca-1,3,7,9-tetraene (14: X = 0)

4-(2-Furyl)-3-butene-2-one **(11)** (6.7 g, 0.05 mole) and 1,2-diaminoethane (3.0 g, 0.05 mole) were dissolved in ether and the solution was heated in the presence of potassium carbonate (5 g). After 3 hrs, the mixture was filtered, the filtrate evaporated to half volume, and filtered again. The crystals which precipitated after standing overnight were filtered off and washed with ether. After recrystallization from ether, 12 g of the product (84%). m.p. 145—146 °C was obtained.

$C_{18}H_{20}N_2O_2$ (296.40). Calcd C 72.95; H 6.80; N 9.45; Found C 73.03; H 6.87; N 9.54%.

^1H—NMR ($CDCl_3$) : δ = 2.08 (s, 6H 2 CH_3); 3.82 (s, 4H, $=N-CH_2-CH_2-N=$); 6.4—7.5 ppm (compl., 10H, olefinic and furyl).

5,14-Dimethyl-7,12-di(2-thienyl)-1,4,8,11-tetraaza-cyclotetradeca-4,14-diene (13; X = S)

When 4-(2-thienyl)-3-butene-2-one **(12)** (4.56 g, 0.03 mole) and 1,2-diaminoethane (1.8 g, 0.03 mole) reacted as in the previous experiment, 4.35 g of product (75%) was obtained, m.p. 97—99 °C.

$C_{20}H_{28}N_4S_2$ (388.60). Calcd C 61.82; H 7.26; N 14.42. Found C 61.49; H 7.12; N 14.58%.

IR (KBr) ν_{max}=3310 (NH), 1670(C=N) cm^{-1}.

^1H—NMR ($CDCl_3$): δ = 1.8 (s, 6H, 2 CH_3); 2.6—2.9 (m, 8H, $-N-CH_2-CH_2-N-$ and 2 $-CH_2-C=N$); 3.10—3.50 (m, 4H, $=N-CH_2-CH_2-N=$); 3.4—3.6 (m, 2H 2 NH); 4.3—4.6 (compl., 2H, 2 $-N-CH$); 6.9—7.4 ppm (m, 6H, thienyl).

1,10-Di(2-thienyl)-3,8-dimethyl-4,7-diazadeca-1,3,7,9-tetraene (14; X = S)

(*a*) Compound **13** (X=S) (3.88 g, 0.01 mole) was dissolved in 20 ml of anhydrous chloroform and refluxed for 2 hrs. The cooled solution was evaporated to dryness in vacuum and the residue dissolved in a small volume of ether. The cream-coloured crystals which precipitated from the ethereal solution on storage in a refrigerator were filtered off (2.95 g, 90%), m.p 123—124 °C.

$C_{18}H_{20}N_2S_2$ (328.50). Calcd C 65.81; H 6.14; N. 8.53; S 19.52. Found C 65.78; H. 6.26; N 8.42; S 19.68%.

^1H—NMR ($CDCl_3$): δ = 2.10 (s, 6H, 2 CH_3); 3.80 (s, 4H, $=N-CH_2-CH_2-N=$); 6.80—7.40 ppm (compl., 10H, olefinic and thienyl).

(*b*) 4-(2-Thienyl)-3-butene-2-one **(12)** (4.56 g, 0.03 mole) and 1,2-diaminoethane (0.9 g, 0.015 mole) were dissolved in chloroform (30 ml) and refluxed for 2 hrs in the presence of anhydrous potassium carbonate (1 g). The filtrate was worked up in the way described under (*a*). The product was compound **14** (4.20 g, 85%), m.p. 123—124 °C, completely identical with the product obtained by the method described under (*a*).

*

The authors express their thanks to technicians Mrs. A. Halász, Mrs. M. Ott and Miss T. Huszár (Univ. Pécs) for their technical assistance and for the microanalyses.

REFERENCES

[1] HIDEG, K., LLOYD, D.: Chem. Comm. **1970,** 929; J. Chem. Soc. (C) **1971,** 3441
[2] INGOLD, C. K.: Structure and Mechanism in Organic Chemistry, 2nd Ed., p. 1020. Cornell Univ. Press. Ithaca, N. Y. 1969
[3] HANKOVSZKY, O. H., HIDEG, K., LLOYD, D., MCNAB, H.: Chem. Comm. **1974,** 378

Olga H. HANKOVSZKY
Kálmán HIDEG
Kinga POLGÁR
Central Laboratory of Chemistry, University of Pécs, 7643 Pécs, Szigeti út 12, Hungary

Douglas LLOYD; Department of Chemistry, Purdie Building, University of St. Andrews, St. Andrews, Fife KY16 9ST, Great Britain.

Acta Chimica Academiae Scientiarum Hungaricae, Tomus 85 (3) pp. 339—346 (1975)

STUDY OF THE TRANSFORMATIONS OF DIOLS AND CYCLIC ETHERS, XXXVII*

ISOMERIZATION OF OXETANES TO UNSATURATED ALCOHOLS ON GC COLUMNS

M. BARTÓK and K. FELFÖLDI

(Institute of Organic Chemistry, A. József University, Szeged)

Received September 16, 1974

The isomerization of oxetane, 2-methyloxetane, and cis-7-oxabicyclo[4.2.0]-octane to β, γ-unsaturated alcohols on a thermolite-supported GC charge containing tricresyl phosphate and poly(ethyleneglycol) was studied under the usual gas chromatographic conditions, between 130 and 170 °C. Both the isomerization of 2-methyloxetane to allyl carbinol, and that of cis-7-oxabicyclo[4.2.0]-octane to 3-oxymethylcyclohexene took place with very high selectivity. On the basis of our experiments, the isomerization at the electrophilic active centers of the column charge result from intramolecular proton migration involving a six-membered intermediate. The main evidence for this mechanism is the absence of isomerization in the case of oxetane; lack of the formation of α, β-unsaturated alcohols with substituted oxetanes. If the oxetanes are readily available, the experimental observation can also be utilized preparatively.

The isomerization of four-membered cyclic ethers to unsaturated alcohols was first observed by YURIEV and LEVI [1] oxacyclobutane isomerized on alumina to allyl alcohol and propionaldehyde. Recently, PORTNYAGIN and PAVEL [2] reported that under the influence of sulfuric acid, 2,2-disubstituted oxetanes isomerize mainly to β, γ-unsaturated alcohols. This procedure is interpreted by an intermolecular mechanism: proton addition is followed by the formation of a carbonium cation; this is stabilized by elimination of a proton, with the formation of the corresponding β, γ-unsaturated alcohol.

During the study of the transformations of oxacycloalkanes, the above isomerization has been observed with a number of oxacyclobutane derivatives under different experimental conditions [3—5]. It has been proved in our investigations that the isomerization is due to the electrophilic centers of the catalysis.

We have noticed during these experiments that the oxetanes are capable of isomerizing with very high selectivity on a thermolite charge containing the partition liquid, even under gas-chromatographic conditions. The following is an account of these investigations.

* Part XXXVI: Acta Chim. (Budapest), **78** 305 (1973).

Results and discussion

The isomerizations of oxacyclobutane **(1)**, 2-methyloxacyclobutane **(2)** and *cis*-7-oxacyclo [4.2.0]-octane **(3)** have been studied by an impulse microreactor technique on 1 ml thermolite (T) or kieselguhr (KG) supports, and also on T and KG charges containing tricresyl phosphate (TCP) or poly(ethylene glycol) 20 *M* (PEG) as partition liquids. Investigations were made between 250 and 400 °C on the supports, and between 130 and 170 °C on the column charges, in hydrogen and nitrogen as carrier gases and, additionally, on a charge pretreated with ammonia.

The chemical processes are shown in the following schemes:

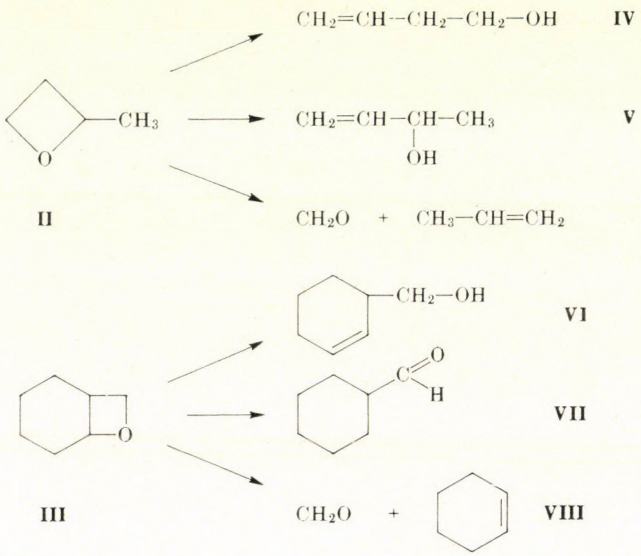

The experimental results and conclusions are as follows.

1. The KG support and the charges with KG proved inactive in the isomerization of oxetanes within the temperature range investigated. The pyrolysis of oxetanes on the support commences already at 300 °C.

2. On T, 46% of 2-methyloxetane **(2)** was transformed 250 °C: 10 to butyraldehyde, 20 to allyl carbinol **(4)**, and 16% to pyrolysis products of lower molecular weight.

3. Oxetane did not isomerize even on charges with T supports.

4. **2** isomerized on a TCP/T charge already at 130 °C, turning predominantly into **4**; some **5** was also formed, besides slight thermal decomposition (Figs 1 and 2). Formation of the isomers crotyl alcohol, butyraldehyde and methyl ethyl ketone was not observed. Peak 4 in the Figure could not be identified.

5. On the charges with T supports, the isomerization of **3** takes place predominantly to the corresponding β,γ-unsaturated alcohol **(6)** together with the formation of some **7** and **8** (Figs 3—5). Under the same conditions, **6** failed to isomerize to **7**, consequently, **6** cannot be an intermediate in the formation of **(7)**.

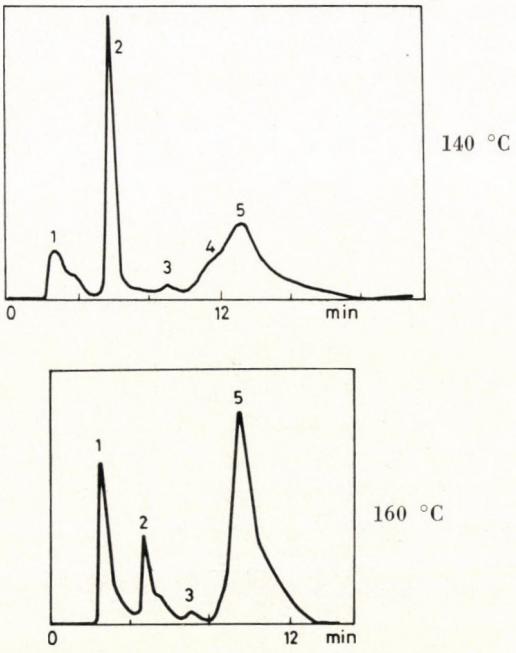

Figs 1—2. Isomerization of 2-methyloxetane on a charge of TCP/T (1: pyrolysis product; 2: 2-methyloxetane; 3: methyl vinyl carbinol; 4: unknown; 5: allyl carbinol)

6. The experimental data obtained in the case of nitrogen as carrier gas agreed with the results obtained with hydrogen. On the basis of these findings, the hydrogen carrier gas does not take part in the chemical process.

7. The isomerization of oxetanes failed to occur on a column charge pretreated with ammonia. Accordingly, it can be concluded that the T support contains electrophilic centers capable of isomerizing oxetanes under relatively mild experimental conditions, this is accompanied by the formation of β, γ-unsaturated alcohols.

In the case of **2** and **3**, the most probable mechanism of formation of β, γ-unsaturated alcohols is shown in the schemes below. At the same time, the mechanism of formation of isomeric unsaturated alcohols not included among the reaction products is also outlined. The aim was to prove the mechanism of the isomerization process, which is relatively selective, by the differences in

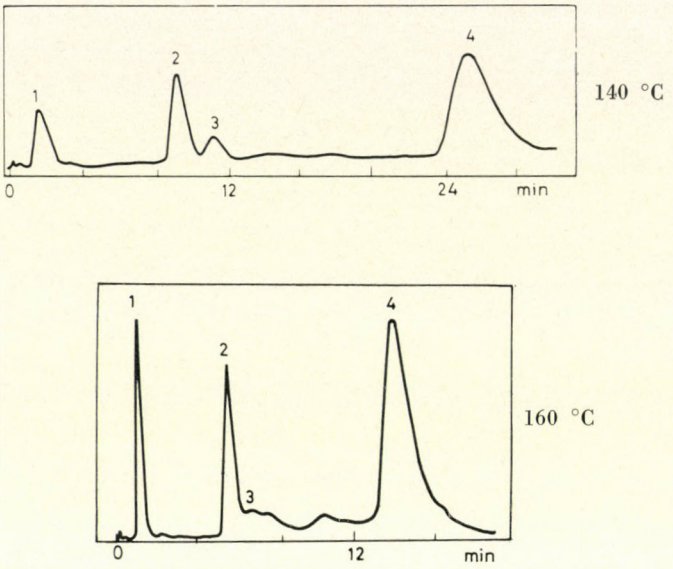

Figs 3—4. Isomerization of cis-7-oxabicyclo[4.2.0]-octane on a charge of TCP/T (1: cyclohexene; 2: formylcyclohexene; 3: *cis*-7-oxabicyclo[4.2.0]octane; 4: 3-hydroxy-methylcyclohexene)

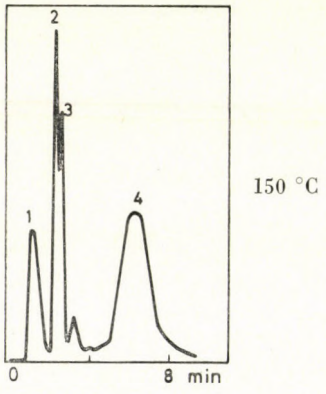

Figs 5. Isomerization of *cis*-7-oxabicyclo[4.2.0]-octane on a charge of PEG/T (symbols: see Figs 3—4)

the mechanisms. It can be seen from the reaction schemes that the isomerization accompanied by the formation of unsaturated alcohols can be interpreted by both inter- and intramolecular mechanisms (the reaction routes accepted by us are indicated by thick arrows).

Isomerization of 2-methyloxetane **(2)**

K = electrophilic active center of the column charge

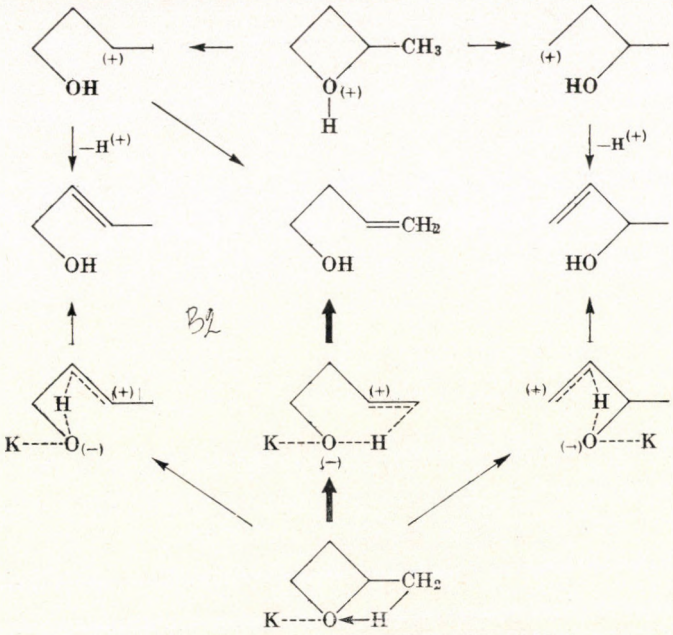

The intramolecular mechanisms are, in effect, proton migrations, taking place through 4-, 5-, or 6-membered intermediates. Since there is a chance of isomerization via the intermolecular mechanism for both oxetane and its substituted derivatives, but no isomerization is observed with oxetane, the isomerization mechanism must be intramolecular. It is not the hydrogen atoms of the oxacyclobutane skeleton that take part in the process, but a hydrogen atom of one of the carbon atoms bound to the 4-membered ring which, because of its favourable steric position, is capable of forming a 6-membered intermediate. This conclusion is supported not only by the greater stability of the 6-membered intermediate, but also by the experimental fact that the formation of α,β-unsaturated alcohols is insignificant compared to that of β,γ-unsaturated alcohols. The α,β-unsaturated alcohols would form by an intermolecular reaction, or by an intramolecular mechanism through a 4- or 5-membered intermediate, requiring the hydrogen of a 4-membered ring. This can be seen in the schemes.

Isomerization of *cis*-7-oxabicyclo[4,2,0]octane **(3)**

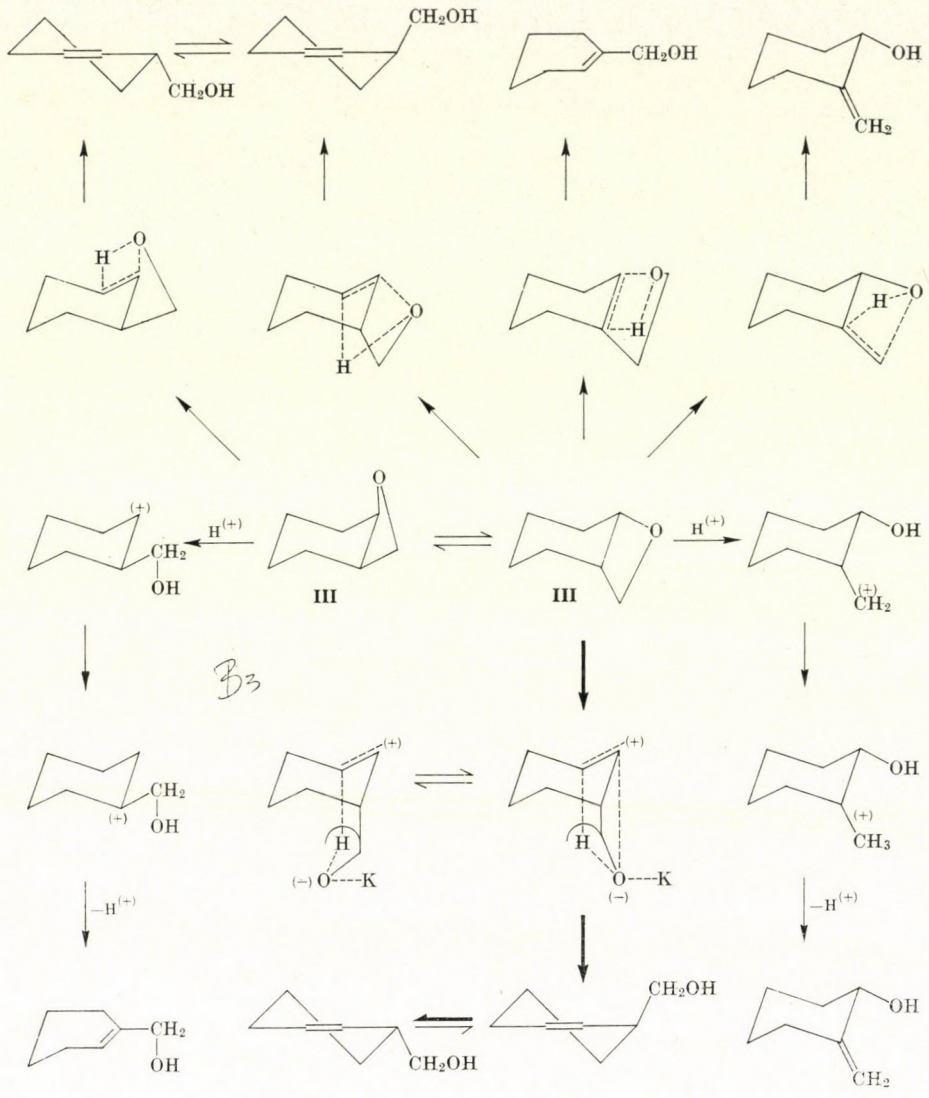

Apart from supporting the above conclusion concerning the mechanism of isomerization, the data of the experiments performed with **3** allowed investigation of the stereochemical conditions of the isomerization process, as shown in the scheme.

It is clear in the latter reaction scheme that the formation of the three unsaturated alcohol isomers could be interpreted either by an intramolecular mechanism through similar 4-membered intermediates or by the intermolecular

mechanism starting with proton attack. The reality of the latter would be supported by the possibility of formation of the stable tertiary carbonium cation, as a result of which the corresponding α,β-unsaturated alcohol would form. The failure of the formation of α,β-unsaturated alcohols, however, proves that the condition of formation of β,γ-unsaturated alcohols is the formation of a 6-membered intermediate requiring the participation of an axial hydrogen. The formation of **7** as another isomerization product of **3** can be interpreted by 1,3-migration within the molecule:

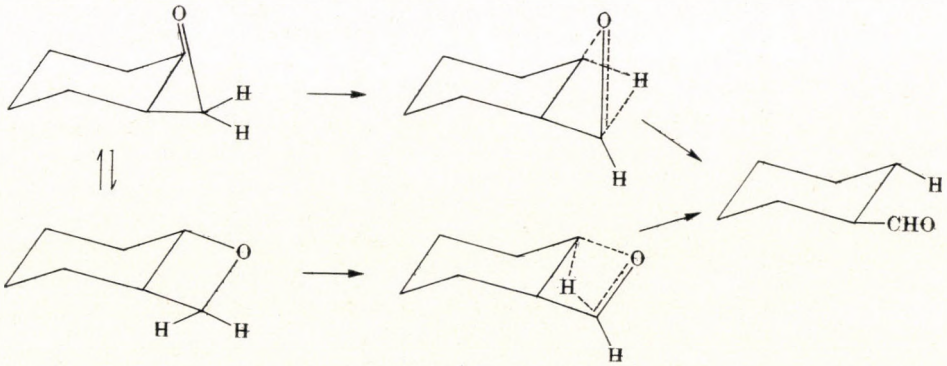

Experimental

Preparation of oxetanes.

The preparation of oxetane **(1)** and 2-methyloxetane **(2)** was performed as described earlier [6, 7.] *Cis*-7-oxabicyclo **[4.2.0]**-octane **(3)** was prepared from cis-2-chloromethyl-cyclohexanol with potassium hydroxide. This preparation will be described in detail later. (Bp. 750 mm Hg: 164 °C; n_D^4: 1.4630)

Supports and partition liquids used in GC investigations

Thermolite: a support of diatomaceous earth type developed by the MÁFKI (Hungarian Oil and Gas Research Institute) 8. Grain size: 0.2—0.3 mm. Before use, the support was boiled repeatedly with hydrochloric acid on a water bath and then washed until free of chloride ion.

Kieselguhr: a support with a grain size of 0.2—0.3 mm (Merck) was used.

Partition liquids: TCP and PEG 20 M (Carlo Erba) were used. The column charge was made in the usual way: 20% partition liquid + support.

Description of the investigations

As usual in gas chromatography, the investigations were carried out on the analytical arm of the Carlo Erba Fractovap Model P, with variations of the column charge, the temperature and the carrier gas.

Thermostat temperature: 130—170 °C;
Carrier gas: 40—60 ml/min of hydrogen or nitrogen;
Detector current: 175 mA;
Quantity of sample injected: 0.01 ml;
Columns: Investigation I—2 m TCP/T + 4 m PEG/KG

Investigation II — a) 2 TCP/T +
+4 m PEG/KG
b) 2 m TCP/KG
c) 2 m PEG/KG

Investigation III — a) 2 m TCP/T
b) 4 m PEG/T

The chromatogram peaks were identified, using the authentic substances.

REFERENCES

[1] YURIEV, YU. K., LEVI, I. S.: Zh. Obsch. Khim., **23,** 2047 (1953)
[2] PORTNYAGIN, YU. M., PAVEL, T. M.: Zh. Org. Khim., **9,** 890 (1973)
[3] BARTÓK, M., KOZMA, B., KOVÁCS, K.: Acta Chim. Acad. Sci. Hung., **55,** 49, 61 (1968)
[4] FREIDLIN, L. KH., SHARF, V. Z., BARTÓK, M., NAZARYAN, A. A.: Izv. Akad. Nauk SSSR, Ser. Khim., 310 (1970)
[5] BARTÓK, M., TÖRÖK, I., SZABÓ, I.: Acta Chim. (Budapest), **76,** 417 (1973)
[6] BARTÓK, M., APJOK, J.: Acta Phys. et Chem. Szeged, **8,** 133 (1962)
[7] BARTÓK, M., GILDE, A. S.: Acta Phys. et Chem. Szeged, **9,** 25 (1963)
[8] SZEPESY, L.: Gas Chromatography, p. 78. Műszaki Könyvkiadó, Budapest 1963

Mihály BARTÓK
Károly FELFÖLDI } 6720 Szeged, Dóm tér 8. Hungary.

INDEX

ANALYTICAL CHEMISTRY — ANALYTISCHE CHEMIE — АНАЛИТИЧЕСКАЯ ХИМИЯ

PAKSY, L., LAKATOS, I.: Effect of the Axial Injection of Argon on an Analytical Light Source, II. Comparative Study of Self-absorption 233

PAKSY, L., LAKATOS, I.: Effect of the Axial Injection of Argon on an Analytical Light Source, III. Variation of Self-absorption in the Electrode Space and with the Gas Rate and Concentration 249

GAÁL, J., INCZÉDY J.: Investigations on Metal Complexes Containing Optically Active Ligands, I. Complexes of D- and L-*threo*-1-(*p*-nitrophenyl) 2-amino-propanediol-1,3 formed with Palladium(II) ions 261

PHYSICAL AND INORGANIC CHEMISTRY — PHYSIKALISCHE UND ANORGANISCHE CHEMIE — ФИЗИЧЕСКАЯ И НЕОРГАНИЧЕСКАЯ ХИМИЯ

ANANTHAKRISHNAN, T. R., ARULDHAS, G.: Parametric Approach to the Analysis of Infrared Intensities 269

NAGY, S., LÉVAY, B. and VÉRTES, A.: Investigations on the Correlation between the Optimum Thickness of Mössbauer Absorbents and Certain Experimental Parameters 273

CSER, F., PÁRKÁNYI, L., and HENCSEI, P.: Lattice Dynamics Study of Crystalline Tetraphenylsilane 289

ORGANIC CHEMISTRY — ORGANISCHE CHEMIE — ОРГАНИЧЕСКАЯ ХИМИЯ

FENICHEL, L., DEÁK, GY., HOLLY, S., BAKÓ, P. and CSŰRÖS, Z.: Preparation and Investigation of Lewis Acid Complexes, X. Investigation of the Titanium Tetrachloride and Ethoxytitanium Trichloride Complexes of Triacetyllevoglucosan 299

FENICHEL, L., DEÁK, GY., BAKÓ, P., HOLLY, S. and CSŰRÖS, Z.: Preparation and Investigation of Lewis Acid Complexes, XI. Investigation of the Mechanism of the Ring Cleavage Reaction of Triacetyllevoglucosan 313

TURÁN, A., PATTHY, A., and BAJUSZ, S.: Removal of the Nitro Group from Nitroarginine and Nitroarginine Peptides 327

HANKOVSZKY, O. H., HIDEG, K., POLGÁR, K. and LLOYD, D.: Reaction of α, β-Unsaturated Ketones with *bis*-Nucleophilic Reactants. Further Studies with Polyolefinic (α, β, γ, δ-unsaturated) Ketones and β-Heteroaryl (furyl and thienyl) α, β-unsaturated Ketones 333

BARTÓK, M. and FELFÖLDI, K.: Study of the Transformations of Diols and Cyclic Ethers, XXXVII. Isomerization of Oxetanes to Unsaturated Alcohols on GC Columns 339

Printed in Hungary

A kiadásért felel az Akadémiai Kiadó igazgatója — Műszaki szerkesztő: Zacsik Annamária

A kézirat nyomdába érkezett: 1975. II. 28. — Terjedelem: 10,50 (A/5) ív, 74 ábra

75.1521 Akadémiai Nyomda, Budapest — Felelős vezető: Bernát György

ACTA CHIMICA

ТОМ 85—ВЫП. 3

РЕЗЮМЕ

Влияние вдува аргонного газа вдоль оси источника света анализатора, II

Исследование самоабсорбции (сравнительные исследования)

Л. ПАКШИ и И. ЛАКАТОШ

В качестве начала подробного изучения уменьшения самоабсорбции, наблюдаемого при продольном вдуве аргонного газа, были проведены фундаментальные исследования сравнительного характера. В ходе этих исследований было показано, что под влиянием аргона воздух вытесняется из плазмы и уменьшение самоабсорбции, независимо от условий возбуждения и характера спектральных полос, всегда наступает. Изменение самоабсорбции не сопровождается однозначным изменением характера спектра.

В ходе исследований были использованы спектрально чистые магниевые и алюминиевые электроды. Аргон вдували в дугу или на искру, горящие в атмосфере воздуха, через верхний просверленный электрод, без использования газовой ячейки. Изменение самоабсорбции исследовалось как в случае атомных, так и ионных полос вышеупомянутых элементов.

Влияние вдува аргонного газа вдоль оси источника света анализатора, III

Исследование самоабсорбции (исследование пространственного изменения, а также зависимости от скорости газа и концентрации)

Л. ПАКШИ и И. ЛАКАТОШ

Под влиянием продольного вдува аргонного газа, в любой части пространства между электродами, значительно уменьшается самоабсорбция атомных полос как в системе собственного, так и в системе инородного вспомогательного электрода. Согласно экспериментальным результатам, уменьшение самоабсорбции зависит от применяемой скорости вдува газа и не зависит от характера возбуждения (искра или дуга). Поведение ионных полос совершенно подобно поведению атомных полос, однако, степень уменьшения самоабсорбции в случае ионных полос меньше, чем в случае атомных полос. Уменьшение самоабсорбции под влиянием аксиального вдува аргона с практической точки зрения позволяет измерение спектральных полос порядка 10%, склонных к сильной самоабсорбции, в дуге переменного тока.

Исследование комплексов металлов с оптически активными лигандами, I

Комплексы D- и L-трео-1-(п-нитрофенил)-2-аминопропандиода-1,3 с ионами палладия(II)

Й. ГАЛ и Й. ИНЦЕДИ

Константы стабильности комплексов D- и L-трео-1-(п-нитрофенил)-2-аминопропандиола-1,3 с ионами палладия(II) были определены методом pH-метрического титрования. Твердое вещество $Na_2[Pd_2L_3Cl_6]$ было приготовлено, используя рацемическую смесь трео-1-(п-нитрофенил)-2-аминопропандиола-1,3; $[Pd\ L_2]Cl_2 \cdot 2{,}5H_2O$ был приготовлен, используя D- и L-трео-1-(п-нитрофенил)-2-аминопропандиол-1,3.

Параметрическое приближение в анализе интенсивностей ИК полос

Т. Р. АНАНТАКРИШНАН и Г. АРУЛДАС

Абсолютные интенсивности ИК полос полиатомных молекул относятся к ортогональной матрице параметров A через уравнение формы $\vec{\mu}_Q \cdot \tilde{\vec{\mu}}_Q \approx \tilde{A}KA$, где $\vec{\mu}_Q$ является столбцевой матрицей, содержащей производные дипольных моментов по нормальным координатам, и K является симметрической матрицей, включающей геометрию молекулы и производные дипольных моментов по внутренним координатам симметрии. Анализ вышеприведенного уравнения, уделяя особое внимание колеблющимся частицам второго порядка, приводит к интересным результатам, а именно, что должно существовать два силовых поля, соответствующих данным по интенсивности.

Исследование оптимальной толщины слоя абсорбента Мёссбауэра и зависимости между некоторыми экспериментальными параметрами

Ш. НАДЬ, Б. ЛЕВАИ и А. ВЕРТЕШ

Была исследована оптимализация толщины слоя абсорбента, используемого в спектроскопии Мёссбауэра. Оптимальной считали такую толщину слоя, при которой измеряемый за самое короткое время эффект является таковым, что по порядку хотя бы в к-раз больше статистического разброса основной полосы.

Было показано, что поскольку концентрация мёссбауэровских атомов не известна, наилучшую оценку оптимальной толщины слоя представляет собой $2/\mu$, где μ – масс-абсорбционный параметр абсорбента.

Исследование динамики решетки кристаллического тетрафенилсилана

Ф. ЧЕР, Л. ПАРКАНИ и П. ХЕНЧЕИ

Были произведены расчеты конформаций и энергии кристаллической решетки молекулы тетрафенилсилана, основанные на данных рентгено-структурных измерений и квантово-химических расчетов. Были сформулированы основные характеристики термического движения в решетке. Рассчитанная величина энергии решетки (—177,78 кдж/моль, т. е. —43,49 ккал/моль) находится в хорошем согласии с величиной, полученной из экспериментальных данных (—182,63 кдж/моль = —43,65 ккал/моль). Термические параметры рентгеновских исследований были связаны с изменениями в конформации и энергии решетки, протекающими за счет движений молекулы в кристаллической решетке.

Приготовление и исследование комплексов кислот Льюиса, X

Исследование комплексов триацетиллевоглюкозана с четыреххлористым титаном и этоксититантрихлоридом

Л. ФЕНИХЕЛ, ДЬ. ДЕАК, Ш. ХОЛЛИ, П. БАКО и З. ЧЮРЁШ

Реакция триацетиллевоглюкозана с четыреххлористым титаном была изучена путем исследования их комплексных соединений. Было показано, что <1,6>-кислородный мостик триацетиллевоглюкозана раскрывается в ходе реакции и продукт реакции оказывается одинаковым с комплексом между 2,3,4-триацетил-α-D-глюкопиранозилхлоридом и 2 молями четыреххлористого титана.

Было установлено, что реакция катализируется не только соединениями, содержащими активный водород, но и этоксититантрихлоридом.

Приготовление и исследование комплексов кислот Льюиса, XI

Исследование механизма реакции раскрытия кольца триацетиллевоглюкозана

Л. ФЕНИХЕЛ, ДЬ. ДЕАК, П. БАКО, Ш. ХОЛЛИ и З. ЧЮРЁШ

Реакция триацетиллевоглюкозана с $TiCl_4$ была изучена путем исследования их комплексных соединений.

Было установлено, что в данной реакции пропокси-, бутокси- и феноксititантрихлориды оказывают сокаталитическое влияние. На основе кинетических измерений предлагается возможный механизм реакции.

Исследуя реакцию триацетиллевоглюкозана с ацилгалогенидами, катализированную $FeCl_3$, был синтезирован 2,3,4-триацетил-6-бензоил-α-D-глюкопиранозилхлорид, еще не описанный в литературе.

Удаление нитрогрупп из нитроергинина и пептидов нитроаргинина

А. ТУРАН, А. ПАТИ и Ш. БАЮС

Было найдено, что восстановительное отщепление нитрогрупп от нитроаргинина и пептидов, содержащих нитроаргинин, с помощью цинка часто сопровождается образованием побочных продуктов, подобных производным аминоаргинина и орнитина. Образование соединений, содержащих аминоаргинин, было подавлено использованием трифторуксусной кислоты в качестве среды. В этом случае удаление защитных гчупп Boc и OBu^t может быть совмещено с удалением нитрогрупп.

Взаимодействие α, β-ненасыщенных кетонов с бис-нуклеофильными реагентами

Дальнейшие исследования с полиолефиновыми (α, β, γ, δ-ненасыщенными) кетонами и β-гетероарильными (фурил и тиенил) α, β-ненасыщенными кетонами

О. Х. ХАНКОВСКИ, К. ХИДЕГ, К. ПОЛГАР и Д. ЛЛОЙД

Продукты, образующиеся в реакции 1,2-диаминоэтана с циннамилиденацетоном фурилиденацетоном или β-иононом в кипящей смеси циклогексана с эфиром, оказались бис(диениминами) (4, 14, 10). Они, скорее всего, образуются каким-то косвенным путем, нежели в непосредственной реакции конденсации. Тенилиденацетон, в соответствующих условиях, дает диметилдитиенил-диазациклотетрадекадиен (13), а в кипящем ацетоне был получен бис(диенимин). При нагревании циклический продукт может быть также превращен в этот бис-(диенимин).

Изучение превращений диолов и циклических эфиров, XXXVII

Изомеризация оксетанов в ненасыщенные спирты на хроматографических колоннах

М. БАРТОК и К. ФЕЛФЁЛЬДИ

Изомеризация оксетана, 2-метилоксетана и *цис*-7-оксабицикло [4.2.0] — октана была исследована на ГХ наполнителе, содержащем трикезилфосфат и полиэтиленгликоль, с термолитным носителем, в условиях обычной газовой хроматографии и в интервале температур 130—170°С. 2-Метилоксетан изомеризуется в аллилкарбинол, а *цис*-7-оксабицикло [4.2.0] октан — в 3-оксиметилциклогексен; изомеризация протекает с большой селективностью.

Изомеризация, которая протекает на активных центрах наполнителя электрофильного характера, согласно исследованиям, представляет собой межмолекулярную миграцию протона, протекающую через шестичленное переходное состояние.

Quantitative STRUCTURE-ACTIVITY *Relationships*

Proceedings of the Conference on Chemical Structure-Activity Relationships. Quantitative approaches

Edited by M. TICHY

The participants of the Conference held in June 1973 discussed the interrelationships between biology, mathematics, chemistry, and physics. The researchers attempted to quantitatively measure the effect of various foreign substances on biological systems; they then used the methods and the models to produce such compounds the biological effect of which exactly correspond to the required effect. The therapeutic effects as well as the harmful side-effects of the medicines produced in this way could be measured accurately, therefore these research results are of vital importance in further pharmacological and toxicological researches.

In English · Approx · 240 pages · Cloth

A co-edition, distributed in the socialist countries by Kultura, Budapest, ISBN 963 05 05495, in all other countries by Birkhäuser Verlag, Basel—Stuttgar

---

AKADÉMIAI KIADÓ
Budapest

ELSEVIER PUBLISHING Co.
Amsterdam

Dielectric Spectroscopy of Polymers

by P. Hedvig

In this book the dielectric spectra of polymers, copolymers, polymeric compounds and blends are discussed and compared with dynamic mechanical, dilatometric and thermal analytic data. Recent analogue and digital experimental methods are discussed together with such related techniques as the nuclear magnetic resonance (NMR) spin echo method, dilatometry, dynamic mechanical relaxation and differential thermal analysis. Separate chapters are devoted to the study of dielectric spectra during degradation and cross-linking reactions. Ample examples are given to illustrate the possibilities of using the time domain (Fourier transform) method together with the dielectric depolarization method.

Relaxation maps of typical polymers are given in the Appendix.

In English · Approx · 380 pages · 240 figures · 11 tables · Cloth

A co-edition, distributed in the socialist countries by Kultura, Budapest, ISBN 963 05 04812, in all other countries by Adam Hilger Ltd., London

AKADÉMIAI KIADÓ
Budapest

ADAM HILGER LTD.
London

Advances in Epitaxy and Endotaxy

Selected Chemical Problems

edited by H. G. Schneider, V. Ruth and Teréz Kormány

This monograph summarizes the large number of research results achieved recently in the fields of epitaxy and endotaxy. A team of internationally renowned authors contributes to the understanding of this whole complex question. The volume consists of five chapters. The first chapter emphasizes the determinative part played by the technology of growing epitaxial and endotaxial layers in the production of solid state devices and of integrated circuits. In the second chapter the authors review the main theories concerning the chemical vapor deposition. The third chapter discusses the diffusion phenomena of vaporization, while the theme of the fourth chapter deals with the growth of semi-conductor thin layers from the melt. In the fifth chapter the theory of the chemistry of epitaxial and endotaxial layer growth, and within this the experimental proof of these theories is dealt with.

In English · Approx. 280 pages · Cloth

A co-edition — distributed in the socialist countries by Kultura, Budapest, ISBN 963 05 0482 0, in all other countries by Elsevier Publishing Co., Amsterdam

AKADÉMIAI KIADÓ
BUDAPEST

ELSEVIER PUBLISHING Co.
AMSTERDAM

TOPICS IN FLAVONOID CHEMISTRY AND BIOCHEMISTRY

Proceedings of the Fourth Hungarian Bioflavonoid Symposium Keszthely, September 20-22, 1973

Edited by L. FARKAS, M. GÁBOR and F. KÁLLAY

Names well-known in natural product chemistry hall-mark this book; leading scientists of the field from Budapest, Birmingham, Debrecen, Dublin, Frankfurt, Hannover, Heidelberg, Lyon, München, Paris, Rome, Sheffiield and Szeged present their recent research results on the chemistry, new methods of investigation and biochemistry of flavonoid compounds. The material includes topics of current interest, such as prenylated flavonoids, isoflavonoids, isoflavans, neoflavonoids, natural 2,5-dihydroxyflavanones, proanthocyanidines, new synthetic flavonoid glycosides, etc. Papers on the use of ^{13}C-NMR- and mass spectroscopy in flavonoid research illustrate the new techniques in structure elucidation. Up-to-date biochemical research on the metabolism, biological actions and antioxidant effect of flavonoids is reported.

In English · Approx. 240 pages · Cloth
ISBN 963 05 0479 0

AKADÉMIAI KIADÓ
Publishing House of the Hungarian Academy of Sciences
Budapest

The Acta Chimica publish papers on chemistry, in English, German, French and Russian.

The Acta Chimica appear in volumes consisting of four parts of varying size, 4 volumes being published a year.

Manuscripts should be addressed to

Acta Chimica
Budapest 112/91 Műegyetem

Correspondence with the editors should be sent to the same address.

The rate of subscription is $ 32,00 a volume.

Orders may be placed with "*Kultúra*" Foreign Trade Company for Books and Newspapers (1389 Budapest 62, P.O.B. 149 Account No. 218 10990) or with representatives abroad.

Les Acta Chimica paraissent en français, allemand, anglais et russe et publient des mémoires du domaine des sciences chimiques.

Les Acta Chimica sont publiés sous forme de fascicules. Quatre fascicules seront réunis en un volume (4 volumes par an).

On est prié d'envoyer les manuscrits destinés à la rédaction à l'adresse suivante:

Acta Chimica
Budapest 112/91 Műegyetem

Toute correspondance doit être envoyée à cette même adresse.

Le prix de l'abonnement est de $ 32,00 par volume.

On peut s'abonner à l'Entreprise pour le Commerce Extérieur de Livres et Journaux «*Kultúra*» (1389 Budapest 62, P.O.B. 149 Compte-courant No. 218 10990) ou à l'étranger chez tous les représentants ou dépositaires.

«*Acta Chimica*» издают трактаты из области химической науки на русском, французском, английском и немецком языках.

«*Acta Chimica*» выходят отдельными выпусками разного объема. 4 выпуска составляют один том. 4 тома публикуются в год.

Предназначенные для публикации рукописи следует направлять по адресу:

Acta Chimica
Budapest 112/91 Műegyetem

По этому же адресу направлять всякую корреспонденцию для редакции.

Подписная цена — $ 32,00 за том.

Заказы принимает предприятие по внешней торговле книг и газет «*Kultúra*» (1389 Budapest 62, P.O.B. 149 Текущий счет № 218 10990) или его заграничные представительства и уполномоченные.

Reviews of the Hungarian Academy of Sciences are obtainable at the folloving addresses:

AUSTRALIA

C. B. D. Library and Subscription Service
Box 4886, G. P. O.
Sydney N. S. W. 2001

Cosmos Bookshop
145 Acland St.
St. Kilda 3182

AUSTRIA

Globus
Höchstädtplatz 3
A—1200 Wien XX

BELGIUM

Office International de Librairie
30 Avenue Marnix
1050—Bruxelles

Du monde Entier
162 Rue du Midi
1000—Bruxelles

BULGARIA

Hemus
Bulvar Ruszki 6
Sofia

CANADA

Pannonia Books
P. O. Box 1017
Pstal Station "B"
Toronto, Ont. M5T 2T8

CHINA

C N P I C O R
Periodical Department
P. O. Box 50
Peking

CZECHOSLOVAKIA

Mad'arská Kultura
Národní třida 22
115 66 Praha

PNS Dovoz tisku
Vinohradská 46
Praha 2

PNS Dovoz tlače
Bratislava 2

DENMARK

Ejnar Munksgaard
Nörregade 6
DK—1165 Copenhagen K

FINLAND

Akateeminen Kirjakauppa
P. O. Box 128
SF-00101 Helsinki 10

FRANCE

Office International de Documentation et Librairie
48, Rue Gay Lussac
Paris 5

Librairie Lavoisier
11 Rue Lavoisier
Paris 8

Europeriodiques S. A.
31 Avenue de Versailles
78170 La Celle St. Cloud

GERMAN DEMOCRATIC REPUBLIC

Haus der Ungarischen Kultur
Karl-Liebknecht-Strasse 9
DDR—102 Berlin

Deutsche Post
Zeitungsvertriebsbamt
Strasse der Parisier Kommüne 3—4
DDR—104 Berlin

GERMAN FEDERAL REPUBLIC

Kunst und Wissen
Erich Bieber
Postfach 46
7 Stuttgart S

GREAT BRITAIN

Blackwell's Periodicals
P. O. Box 40
Hythe Bridge Street
Oxford OX1 2EU

Collet's Holdings Ltd.
Denington Estate
London Road
Wellingborough Northants NN8 2QT

Bumpus Haldane and Maxwell Ltd.
5 Fitzroy Square
London W1P 5AH

Dawson and Sons Ltd.
Cannon House
Park Farm Road
Folkestone, Kent

HOLLAND

Swets and Zeitlinger
Heereweg 347b
Lisse

Martinus Nijhoff
Lange Voorhout 9
The Hague

INDIA

Hind Book House
66 Babar Road
New Delhi 1

India Book House
Subscription Agency
249 Dr. D. N. Road
Bombay 1

ITALY

Santo Vanasia
Via M. Macchi 71
20124 Milano

Libreria Commissionaria Sansoni
Via Lamarmora 45
50121 Firenze

JAPAN

Kinokuniya Book-Store Co. Ltd.
826 Tsunohazu 1-chome
Shinjuku-ku
Tokyo 160—91

Maruzen and Co. Ltd.
P. O. Box 5050
Tokyo International 100—31

Nauka Ltd.-Export Department
2—2 Kanda
Jinbocho
Chiyoda-Ku
Tokyo 101

KOREA

Chulpanmul
Phenjan

NORWAY

Tanum-Cammermeyer
Karl Johansgatan 41—43
Oslo 1

POLAND

Węgierski Instytut Kultury
Marszalkowska 80
Warszawa

BKWZ Ruch
ul. Wronia 23
00—840 Warszawa

ROUMANIA

D. E. P.
Bucureşti

Romlibri
Str. Biserica Amzei 7
Bucureşti

SOVIET UNION

Sojuzpechatj — Import
Moscow

and the post offices in each town

Mezhdunarodnaya Kniga
Moscow G—200

SWEDEN

Almqvist and Wiksell
Gamla Brogatan 26
S—101 20 Stockholm

A. B. Nordiska Bokhandeln
Kunstgatan 4
101 10 Stockholm 1 Fack

SWITZERLAND

Karger Libri AG.
Arnold-Böcklin-Str. 25
4000 Basel 11

USA

F. W. Faxon Co. Inc.
15 Southwest Park
Westwood, Mass. 02090

Stechert-Hafner Inc.
Serials Fulfillment
P. O. Box 900
Riverside N. J. 08075

Fam Book Service
69 Fifth Avenue
New York N. Y. 10003

Maxwell Scientific International Inc.
Fairview Park
Elmsford N. Y. 10523

Read More Publications Inc.
140 Cedar Street
New York N. Y. 10006

VIETNAM

Xunhasaba
32, Hai Ba Trung
Hanoi

YUGOSLAVIA

Jugoslovenska Knjiga
Terazije 27
Beograd

Forum
Vojvode Mišića 1
21000 Novi Sad

24. VII. 1975. Index: 26.007

ACTA CHIMICA

ACADEMIAE SCIENTIARUM HUNGARICAE

ADIUVANTIBUS

V. BRUCKNER, GY. DEÁK, K. POLINSZKY,
E. PUNGOR, G. SCHAY, Z. G. SZABÓ

REDIGIT

B. LENGYEL

TOMUS 85 FASCICULUS 4

AKADÉMIAI KIADÓ, BUDAPEST

1975

ACTA CHIM. (BUDAPEST) ACASA 2 85 (4) 347–472 (1975)

ACTA CHIMICA

A MAGYAR TUDOMÁNYOS AKADÉMIA KÉMIAI TUDOMÁNYOK OSZTÁLYÁNAK IDEGEN NYELVŰ KÖZLEMÉNYEI

SZERKESZTI

LENGYEL BÉLA

TECHNIKAI SZERKESZTŐK

DEÁK GYULA és HARASZTHY-PAPP MELINDA

Az Acta Chimica német, angol, francia és orosz nyelven közöl értekezéseket a kémiai tudományok köréből.

Az Acta Chimica változó terjedelmű füzetekben jelenik meg, egy-egy kötet négy füzetből áll. Évente átlag négy kötet jelenik meg.

A közlésre szánt kéziratok a szerkesztőség címére (Budapest 112/91 Műegyetem) küldendők.

Ugyanerre a címre küldendő minden szerkesztőségi levelezés. A szerkesztőség kéziratokat nem ad vissza.

Megrendelhető a belföld számára az „Akadémiai Kiadó"-nál (1363 Budapest Pf 24. Bankszámla 215 11488), a külföld számára pedig a „Kultúra" Könyv- és Hírlap Külkereskedelmi Vállalatnál (1389 Budapest 62, P. O. B. 149. Bankszámla: 218 10990) vagy annak külföldi képviseleteinél és bizományosainál.

Die Acta Chimica veröffentlichen Abhandlungen aus dem Bereich der chemischen Wissenschaften in deutscher, englischer, französischer und russischer Sprache.

Die Acta Chimica erscheinen in Heften wechselnden Umfanges. Vier Hefte bilden einen Band. Jährlich erscheinen 4 Bände.

Die zur eröffentlichung bestimmten Manuskripte sind an folgende Adresse zu senden:

Acta Chimica
Budapest 112/91 Műegyetem

An die gleiche Anschrift ist auch jede für die Redaktion bestimmte Korrespondenz zu richten. Abonnementspreis pro Band: $ 32.00.

Bestellbar bei dem Buch- und Zeitungs-Außenhandels-Unternehmen »*Kultúra*« (1389 Budapest 62, P. O. B. 149 Bankkonto Nr. 218 10990) oder bei seinen Auslandsvertretungen und Kommissionären.

Acta Chimica Academiae Scientiarum Hungaricae, Tomus 85 (4), pp. 347–359 (1975)

THERMODYNAMISCHE BERECHNUNG VON REAKTIONSGLEICHGEWICHTEN ALIPHATISCHER STICKSTOFFVERBINDUNGEN

C. RÜGER, K. SCHWETLICK und H. KAMMER
(Sektion Chemie der Technischen Universität Dresden, DDR)

Eingegangen am 10. Januar 1974

Es werden die thermodynamischen Stoffdaten für Methyl- und Äthylisocyanat, N-Methylformamid, Acetamid und N,N'-Dimethylharnstoff im idealen Gaszustand mit Hilfe der statistischen Thermodynamik berechnet bzw. aus Inkrementen abgeschätzt.

Das thermodynamische Gleichgewicht und dessen Temperaturabhängigkeit werden im Bereich von 298 bis 1000 K für 9 Reaktionen aliphatischer Stickstoffverbindungen zu Isocyanaten untersucht.

Die Berechnungen zeigen, daß insbesondere:

a) die Carbonylierung von Nitroverbindungen
b) die Pyrolyse von Harnstoffen bei Temperaturen über 900 K und
c) die Dehydrierung von Formamiden bei Temperaturen über 800 K

die thermodynamisch begünstigten phosgenfreien Reaktionen zur Darstellung von Isocyanaten sind.

Zur Charakterisierung des Reaktionsablaufs wurde das thermodynamische Gleichgewicht von 10 möglichen Simultan- bzw. Folgereaktionen untersucht.

1. Problemstellung

Wir berechneten die thermodynamischen Gleichgewichtskonstanten für die folgenden Reaktionen in der Gasphase, die unter Isocyanatbildung verlaufen könnten:

$$CH_3NH_2 + COCl_2 \rightleftharpoons CH_3NCO + 2\,HCl \quad (1)$$

$$CH_3NO_2 + 3\,CO \rightleftharpoons CH_3NCO + 2\,CO_2 \quad (2)$$

$$CH_3NH_2 + CO \rightleftharpoons CH_3NCO + H_2 \quad (3)$$

$$CH_3NH_2 + CO_2 \rightleftharpoons CH_3NCO + H_2O \quad (4)$$

$$CH_3CN + H_2 + CO \rightleftharpoons CH_3CH_2NCO \quad (5)$$

$$CH_3NHCHO \rightleftharpoons CH_3NCO + H_2 \quad (6)$$

$$CH_3CONH_2 \rightleftharpoons CH_3NCO + H_2 \quad (7)$$

$$CH_2{=}CH_2 + NH_3 + CO \rightleftharpoons CH_3CH_2NCO + H_2 \quad (8)$$

$$CH_3NHCONHCH_3 \rightleftharpoons CH_3NCO + CH_3NH_2 \quad (9)$$

Zur Charakterisierung des Reaktionsablaufs untersuchten wir weiterhin das thermodynamische Gleichgewicht möglicher Simultan- bzw. Folgereaktionen:

$$CH_3NH_2 + CO \rightleftharpoons CH_3NHCHO \quad (10)$$

$$2\,CH_3NH_2 + CO \rightleftharpoons CH_3NHCONHCH_3 + H_2 \quad (11)$$

$$CH_3NHCHO \rightleftharpoons CH_3NH_2 + CO \quad (12)$$
$$CH_3NHCHO \rightleftharpoons CH_3CN + H_2O \quad (13)$$
$$2\ CH_3NHCHO \rightleftharpoons CH_3NHCONHCH_3 + H_2 + CO \quad (14)$$
$$CH_3CONH_2 \rightleftharpoons CH_3CN + H_2O \quad (15)$$
$$2\ CH_3NH_2 + CO_2 \rightleftharpoons CH_3NHCONHCH_3 + H_2O \quad (16)$$
$$CH_3NO_2 + 2\ CO + H_2 \rightleftharpoons CH_3NH_2 + 2\ CO_2 \quad (17)$$
$$CH_3NH_2 + CO \rightleftharpoons CH_3CN + H_2O \quad (18)$$
$$CH_3NCO + CH_3NH_2 \rightleftharpoons CH_3NHCONHCH_3 \quad (19)$$

2. Berechnung der thermodynamischen Funktionen

Die thermodynamischen Stoffdaten für organische Stickstoffverbindungen sind aus der Literatur nur vereinzelt bekannt. Deshalb schätzten wir die Standardbildungsenthalpien für N-Methylformamid, N,N'-Dimethylharnstoff, Methyl- und Äthylisocyanat aus Inkrementen ab und berechneten die Standardentropien und die Molwärmen bei konstantem Druck dieser Verbindungen statistisch.

Die thermodynamischen Funktionen von Methyl-, Äthylisocyanat, N-Methylformamid, Acetamid und N,N'-Dimethylharnstoff wurden nach dem Modell »harmonischer Oszillator-starrer Rotator« berechnet [1]. Für die praktische Berechnung der thermodynamischen Funktionen ergeben sich nach diesem Modell die in Tabelle I zusammengestellten Gleichungen.

Zur Berechnung der thermodynamischen Funktionen werden die Massen, die zentralen Hauptträgheitsmomente, die Symmetriezahlen und die Frequenzen der Normalschwingungen der Moleküle benötigt. Die zentralen Hauptträgheitsmomente wurden nach bekannten Methoden berechnet [2], wobei folgende Vereinfachungen vorgenommen wurden:

1. das Molekül wurde als eben und
2. die $-CH_3$, $-CH_2-$, $-NH_2$ und $-NH$-Gruppen wurden als Punktmassen betrachtet.

Die räumliche Struktur der Verbindungen wurde der Literatur entnommen, bzw. auf der Basis der POPLE'schen Standardgeometrie abgeleitet [3].

Die unter diesen Vereinfachungen berechneten zentralen Hauptträgheitsmomente, die verwendete räumliche Struktur und die daraus abgeleiteten Symmetriezahlen sind in Tabelle II zusammengefaßt.

Die zur Berechnung der Schwingungszustandssumme benötigten Frequenzen der Grundschwingungen der Moleküle wurden, soweit vorhanden, der Literatur entnommen.

Für Methyl- und Äthylisocyanat wurde auf die von HIRSCHMANN [8] bestimmten Fundamentalschwingungen zurückgegriffen. Für Acetamid wurden die von SPINNER [9] angegebenen Schwingungsfrequenzen benutzt, und

Tabelle I

Gleichungen für die praktische Berechnung der thermodynamischen Funktionen

Funktion	Gleichung
Reduzierte freie Energie	$\frac{F-E_0}{T} = R\left(-\frac{3}{2}\ln M - 4\ln T - \frac{1}{2}\ln J_A J_B J_C + \ln p + \ln\sigma - 130{,}52\right) + \left(\frac{F}{T}\right)_{\text{Schw}}$ (1.1)
Reduzierte freie Enthalpie	$\frac{G-H_0}{T} = R\left(-\frac{3}{2}\ln M - 4\ln T - \frac{1}{2}\ln J_A J_B J_C + \ln p + \ln\sigma - 129{,}52\right) + \left(\frac{F}{T}\right)_{\text{Schw}}$ (1.2)
Energie	$E - E_0 = 3\ RT + E_{\text{Schw}}$ (1.3)
Enthalpie	$H - H_0 = 4\ RT + H_{\text{Schw}}$ (1.4)
Entropie	$S = R\left(\frac{3}{2}\ln M + 4\ln T + \frac{1}{2}\ln J_A J_B J_C + \ln p - \ln\sigma - 133{,}52\right) + S_{\text{Schw}}$ (1.5)
Molwärme bei konstantem Volumen	$C_v = 3\ R + C_{\text{Schw}}$ (1.6)
Molwärme bei konstantem Druck	$C_p = 4\ R + C_{\text{Schw}}$ (1.7)

Tabelle II

Zentrale Hauptträgheitsmomente, räumliche Struktur und Symmetriezahl der berechneten Moleküle

Molekül	J_A	J_B	J_C	Symm.-gruppe	Symm.-zahl	Geometrie
	$10^{40}\text{g}^{-1}\text{cm}^{-2}$					
CH_3NCO	6,84	99,04	106,00	C_s	1	[4]
C_2H_5NCO	34,60	190,02	224,64	C_s	1	[4]
CH_3CONH_2	41,50	43,60	88,15	C_s	1	[5]
CH_3NHCHO	21,00	183,00	199,00	C_s	1	[6]
$(CH_3NH)_2CO$	79,72	125,45	205,17	C_{2v}	2	[7]

für N-Methylformamid wurden die spektroskopischen Untersuchungen von JONES [10] herangezogen.

Da für N,N'-Dimethylharnstoff kein geeignetes Spektrum aus der Literatur bekannt war, wurde von dieser Verbindung ein IR-Spektrum in Tripen und Nujol aufgenommen (Tabelle III).

Tabelle III

Auswertung des IR-Spektrum von $(CH_3NH)_2CO$

$\tilde{\nu}$/cm^{-1}	Zuordnung	Entartung	$\tilde{\nu}$/cm^{-1}	Zuordnung	Entartung
3350	$\nu_{as}NH$	2 · 2	1280	Amid III	2 · 1
3180	$\nu_{s}NH$	2 · 2	1190	ωCH_3[1]	2 · 1
2955	$\nu_{as}CH_3$[1]	2 · 2	1050	ωCH_3[1]	2 · 2
2910	$\nu_{s}CH_3$	2 · 1	940	$\nu_{as}CN$	2 · 2
1630	Amid	2 · 1	782	$\nu_{s}CN$	2 · 2
1550	Amid II	2 · 1	680	Amid IV	2 · 1
1460	$\delta_{as}CH_3$[1]	2 · 2	525	γ NH	2 · 1
1430	$\delta_{s}CH_3$[1]	2 · 1			

[1] Aus Tripen-Spektrum.

Zur Berechnung der Schwingungsanteile für die Bestimmung der thermodynamischen Funktionen wurde eine Tabelle der Einstein-Funktionen von SHERMAN und EWELL [11] benutzt. Die interpolierten Werte wurden auf die 4. Stelle abgerundet.

In Tabelle IV sind die auf dieser Grundlage für 218 K, 500 K, 800 K und 1000 K berechneten Schwingungsbeiträge H_{Schw}/T, S_{Schw} und C_{Schw} enthalten.

Ausgehend von den Gleichungen (1.1) bis (1.7) in Tabelle I wurden die reduzierte freie Enthalpie, die reduzierte Enthalpie, die Entropie und die Molwärme bei konstantem Druck für die obigen Verbindungen im idealen Gaszustand berechnet. Die bei 298 K, 500 K, 800 K und 1000 K bei einem Druck von 1 atm berechneten thermodynamischen Funktionen sind in Tabelle V zusammengestellt. Zum Vergleich sind in Tabelle V die Ergebnisse für eine Berechnung der thermodynamischen Funktionen von HNCO durch LUFT [12] und für CH_3CONH_2 nach ANTONOV [13] aufgenommen worden.

Die deutliche Abweichung der Ergebnisse von ANTONOV gegenüber unseren Resultaten ist darauf zurückzuführen, daß in den Berechnungen von ANTONOV das Acetamid unter Einbeziehung der inneren Rotation betrachtet wurde.

Die molaren Standardbildungsenthalpien $\Delta_B H_T^{\ominus}$ wurden aus Inkrementen abgeschätzt. Mit Hilfe der in Tabelle VI enthaltenen Gruppenbeiträge wurde für die molare Standardbildungsenthalpie von CH_3NHCHO und $(CH_3NH)_2CO$ gefunden:

$$CH_3NHCHO \quad \Delta_B H_{298}^{\ominus} = -44{,}1 \text{ kcal mol}^{-1}$$

$$CH_3NHCONHCH_3 \quad \Delta_B H_{298}^{\ominus} = -56{,}9 \text{ kcal mol}^{-1}$$

Tabelle IV

Schwingungsbeiträge der Zustandssumme

Molekül	T K^{-1}	$\frac{H_{Schw}}{T}$ [1]	$\frac{G_{Schw}}{T}$ [1]	S_{Schw} [1]	C_{Schw} [1]
CH_3NCO	298	1,721	0,683	2,403	5,137
	500	4,211	2,189	6,399	9,657
	800	7,808	4,928	12,736	15,959
	1000	9,588	6,856	16,444	17,647
C_2H_5NCO	298	2,403	0,919	3,323	7,315
	500	6,028	3,006	9,034	15,286
	800	11,244	7,004	18,248	23,915
	1000	14,195	9,842	24,037	27,857
CH_3CONH_2	298	1,736	0,562	2,298	6,121
	500	5,209	2,210	7,419	14,273
	800	10,298	5,710	16,008	22,571
	1000	13,127	8,470	21,597	26,232
CH_3NHCHO	298	1,479	0,443	1,922	5,278
	500	4,958	1,992	6,950	14,423
	800	10,299	5,507	15,806	23,268
	1000	13,537	8,189	21,726	27,718
$(CH_3NH)_2CO$	298	1,875	0,582	2,456	6,821
	500	5,977	2,474	8,451	17,112
	800	12,518	6,719	19,237	28,978
	1000	16,395	9,969	26,363	34,746

[1] In cal $K^{-1}mol^{-1}$

Die Standardbildungsenthalpie von CH_3NHO und C_2H_5NCO konnte zunächst nicht aus Inkrementen abgeschätzt werden, da in der Literatur bisher noch keine Gruppenbeiträge für die —N=C=O-Gruppe bekannt sind.

Wir waren deshalb gezwungen, die molare Standardbildungsenthalpie für Methyl- bzw. Äthylisocyanat im gasförmigen Zustand über einen Umweg zu berechnen.

Für C_6H_5NCO gab LAIDLER [17] eine molare Standardbildungsenthalpie $\Delta_B H^{\ominus}_{298}$ von 3,5 kcal mol^{-1} im flüssigen Zustand an. Aus der Literatur ist ebenfalls die Temperaturabhängigkeit des Dampfdruckes für Phenylisocyanat bekannt [18]. Nach der bekannten CLAUSIUS—CLAPEYRON'schen Gleichung errechnet sich für die molare Verdampfungswärme

$$\Delta_V H = 9{,}13 \text{ kcal mol}^{-1}.$$

Tabelle V

Statistisch berechnete thermodynamische Daten

Molekül	T K^{-1}	$\frac{G-H_0^{\ominus}}{T}$ [1]	$\frac{H-H_0^{\ominus}}{T}$ [1]	$S_T^{\ominus}$ [1]	$C_p^{\ominus}$ [1]
	298	48,14	8,78	56,92	10,73
HNCO[2]	500	52,98	10,08	63,06	13,12
	800	58,08	11,64	69,72	15,19
	1000	60,77	12,45	73,22	16,12
	298	51,93	9,67	61,60	13,09
CH_3NCO	500	57,55	12,16	69,71	17,60
	800	63,02	15,76	79,78	23,91
	1000	67,73	17,54	85,26	25,60
	298	55,83	10,35	66,18	15,26
C_2H_5NCO	500	61,99	13,98	76,01	23,23
	800	69,72	19,19	88,96	31,86
	1000	74,33	22,14	96,52	35,81
	298	52,69	9,68	62,37	14,07
CH_3CONH_2	500	58,45	13,16	71,60	22,22
	800	65,68	18,25	83,93	30,59
	1000	70,22	21,08	91,29	34,18
	298	57,77	11,15	68,92	15,57
CH_3CONH_2[3]	500	64,30	14,70	79,00	23,60
	800	73,27	18,84	92,11	32,60
	1000	78,35	21,54	99,89	37,18
	298	54,14	9,43	63,57	13,23
CH_3NHCHO	500	59,78	12,91	72,70	22,37
	800	67,05	18,33	85,38	31,58
	1000	71,51	21,49	92,99	35,67
	298	50,44	9,82	60,30	14,77
$(CH_3NH)_2CO$	500	56,46	13,93	70,41	25,06
	800	64,42	20,47	84,93	36,93
	1000	69,46	24,34	93,83	42,69

[1] In cal mol^{-1}K^{-1},
[2] LUFT [12].
[3] ANTONOV [13].

Tabelle VI

Gruppenbeiträge zur Berechnung von $\Delta_B H^{\Theta}_{298}$ organischer Stickstoffverbindungen

Gruppe	$\Delta_B H^{\Theta}_{298}$ [1]	Lit.	Gruppe	$\Delta_B H^{\Theta}_{298}$ [1]	Lit.
CH_3-	−10,12	[14]	$(H_2N)_2=O$	−57,80	[15]
$-CH_2-$	−4,93	[14]			
C_6H_5-	22,07	[14]			
$-NCO$	−6,14[2]		$(H)(H_2N)C=O$	−44,50	[15]
$-C(=O)NH_2$	−49,00	[15]			
			C—N[3]	9,30	[16]
			N—H	−2,60	[16]
			C—H	−3,83	[16]

[1] In kcal mol^{-1}
[2] Zur Berechnung siehe Abschnitt 3.4
[3] Bindungsbeiträge der Standardbildungsenthalpie.

Bei der Umrechnung der molaren Standardbildungsenthalpie für den flüssigen in die für den gasförmigen Zustand, ist neben der molaren Verdampfungswärme noch die Arbeit zu berücksichtigen, die geleistet werden muß, um das Gas isotherm vom Druck bei 298 K auf 760 mm Hg zu komprimieren. Aus [18] folgt für den Dampfdruck bei 298 K gleich 2,6 mm Hg.

$$\text{Nach } \Delta_B H^{\Theta}_{298}(g) = \Delta_B H^{\Theta}_{298}(l) + \Delta_V H + W$$
$$\text{folgt mit } \Delta_B H^{\Theta}_{298}(l) = 3{,}5 \text{ kcal mol}^{-1}$$
$$\Delta_B H^{\Theta}_{298}(g) = 15{,}93 \text{ kcal mol}^{-1}.$$

Für die Phenylgruppe wird in der Literatur ein Inkrement für $\Delta_B H^{\Theta}_{298}(g)$ von 22,07 kcal mol^{-1} [14] angegeben. Damit folgt für die —NCO-Gruppe ein Beitrag von −6,14 kcal mol^{-1}.

Mit den in Tabelle VI enthaltenen Beiträgen für die Gruppenbeiträge der Methyl- bzw. Äthylgruppe berechnet man die molare Standardbildungsenthalpie für den gasförmigen Zustand bei 298 K zu $\Delta_B H^{\Theta}_{298}(g) = -16{,}26$ kcal mol^{-1} für CH_3NCO und $\Delta_B H^{\Theta}_{298}(g) = -21{,}19$ kcal mol^{-1} für C_2H_5NCO. Die Temperaturabhängigkeit der Standardbildungsenthalpie wurde über die gebräuchliche thermodynamische Beziehung aus der statistisch berechneten Molwärme bei konstantem Druck ermittelt. Dabei wurden die in Tabelle VII zusammengestellten Temperaturabhängigkeiten der Molwärmen bei konstantem Druck verwendet.

Tabelle VII

Temperaturabhängigkeit der Molwärme bei konstantem Druck

Molekül	C_p(T) cal^{-1}mol K
CH_3NCO	$-11{,}31 + 1{,}04 \cdot 10^{-2}\,T \quad -3{,}40 \cdot 10^{-6}\,T^2$
C_2H_5NCO	$-22{,}99 + 3{,}56 \cdot 10^{-2}\,T \quad -2{,}45 \cdot 10^{-6}\,T^2$
CH_3CONH_2	$-25{,}65 + 4{,}54 \cdot 10^{-2}\,T \quad -2{,}69 \cdot 10^{-6}\,T^2$
CH_3NHCHO	$-28{,}84 + 5{,}47 \cdot 10^{-2}\,T \quad -3{,}19 \cdot 10^{-6}\,T^2$
$(CH_3NH)_2CO$	$-41{,}53 + 4{,}69 \cdot 10^{-2}\,T \quad -2{,}46 \cdot 10^{-6}\,T^2$

3. Berechnung und Diskussion der Reaktionsgleichgewichte

Nach der bekannten Beziehung

$$\ln K_p = -\frac{\Delta_R H_T^\ominus}{RT} + \frac{\Delta_R S_T^\ominus}{R}$$

wurden die Gleichgewichtskonstanten der Reaktionen (1) bis (19) für den idealen Gaszustand berechnet, wobei auf die in Tabelle V zusammengestellten thermodynamischen Stoffdaten zurückgegriffen wurde. Für alle übrigen Moleküle wurden die thermodynamischen Daten der Literatur entnommen [19].

Die für die Reaktionen (1) bis (8) bzw. (10) bis (19) berechneten Gleichgewichtskonstanten sind in Tabelle VIII zusammengestellt. Des weiteren wurde die Temperaturabhängigkeit der Gleichgewichtskonstanten der unter Isocyanatbildung verlaufenden Reaktionen in Abb. 1 graphisch dargestellt.

Von GISBIER [20] wurden die Gleichgewichtskonstanten einiger vergleichbarer Reaktionen unter Anwendung der ULICH-Funktion berechnet, die gut in Größenordnung und Trend mit unseren Ergebnissen übereinstimmen.

Abb. 1 zeigt, daß neben der Phosgenierung der Amine (1), deren Gleichgewichtskonstante nur eine geringe Temperaturabhängigkeit zeigt, vor allem die Carbonylierung der Nitroverbindung zu Isocyanaten thermodynamisch begünstigt ist. Auch das thermodynamische Gleichgewicht der Pyrolyse von Harnstoffen (9) bei Temperaturen über 750 K und der Dehydrierung von Formamiden (6) bei Temperaturen über 900 K liegt bei positiven lg K_p-Werten.

Carbonylierung von Nitroverbindungen

In der letzten Zeit sind viele Veröffentlichungen und Patente zur Carbonylierung von Nitroverbindungen [21] erschienen, bei denen Isocyanatausbeuten bis zu 70% erreicht wurden. Diese Reaktion ist jedoch stets an die

Tabelle VIII

Gleichgewichtskonstanten der Reaktionen (1) bis (19) bei 298 K, 500 K, 800 K und 1000 K

Reaktion	lg K_p 298 K	500 K	800 K	1000 K
1	7,008	6,435	6,178	5,886
2	71,252	37,253	19,667	13,879
3	−14,471	−9,506	−6,772	−5,861
4	−18,185	−11,620	−7,373	−5,995
5	−3,879	−8,760	−11,660	−12,520
6	−14,015	−5,600	−0,843	0,596
7	−23,817	−11,329	−4,074	−2,090
8	−13,688	−4,993	0,380	2,285
10	−0,909	−4,400	−6,135	−6,275
11	−0,783	−4,513	−7,152	−8,146
12	0,909	4,400	6,135	6,275
13	4,060	6,146	6,950	7,261
14	−0,029	0,816	1,144	0,966
15	−4,590	−0,083	3,480	4,538
16	−5,686	−9,176	−11,311	−12,081
17	83,279	46,761	26,439	19,654
18	3,147	1,746	0,815	0,986
19	13,688	4,993	−0,280	−2,285

Anwesenheit eines Katalysators gebunden und verläuft nur unter genau definierten Reaktionsbedingungen. Da das thermodynamische Gleichgewicht der Reaktion (2) vollständig auf der Seite der Reaktanten liegt, sollten vor allem kinetische Effekte einen Einfluß auf den Reaktionsablauf besitzen. Die in [22] berechnete Lage des thermodynamischen Gleichgewichts der Carbonylierung von Nitromethan zu Methylisocyanat stimmt qualitativ mit unseren Resultaten überein.

Von CALDERAZZO wurde festgestellt [23], daß die Carbonylierung von Nitroverbindungen bei Anwesenheit von Wasserstoff immer zu Aminen führt. Betrachtet man die thermodynamische Gleichgewichtskonstante der diesbezüglichen Reaktion (17), so zeigt Abb. 2, daß die Bildung der Amine bei Anwesenheit von Wasserstoff gegenüber der Isocyanatbildung thermodynamisch begünstigt ist.

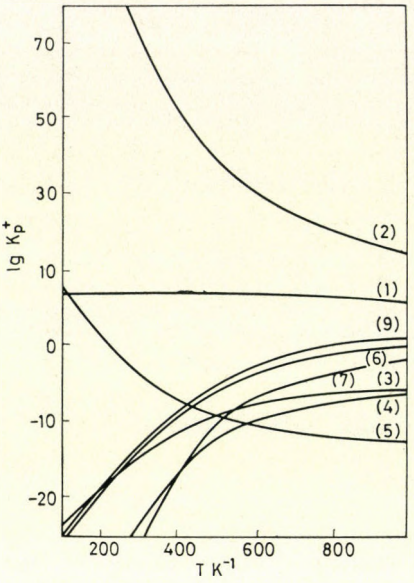

Abb. 1. Temperaturabhängigkeit der thermodynamischen Gleichgewichtskonstanten für die Reaktionen (1) bis (9) zwischen 200 K und 1000 K

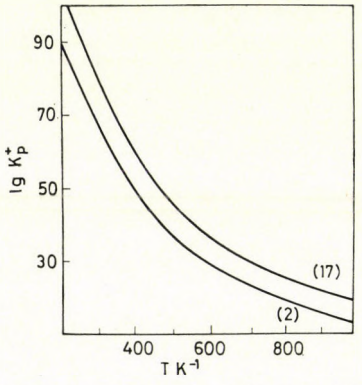

Abb. 2. Temperaturabhängigkeit der thermodynamischen Gleichgewichtskonstanten für die Reaktionen (2) und (17) zwischen 200 K und 1000 K

Dehydrierung von N-Methylformamid bzw. von Acetamid

Daß die Dehydrierung von Formamiden bei hohen Temperaturen unter Isocyanatbildung verläuft, wurde von SCHWETLICK und KRETZSCHMAR [24] praktisch bestätigt. Man erhielt durch katalytische Wasserstoffabspaltung aus N-Formamid in 20%iger Ausbeute Phenylisocyanat. In Abb. 3 ist die Gleichgewichtskonstante für die Dehydrierungsreaktion und möglicher Kon-

kurrenzreaktionen dargestellt. Daraus ist ersichtlich, daß die Reaktionen von N-Methylformamid zu Nitrilen (13) und zu Aminen (12) thermodynamisch begünstigt sind. KRETZSCHMAR erhielt als Nebenprodukte neben Nitrilen vor allem Harnstoffe (14). Abb. 1 macht jedoch deutlich, daß bei diesen Temperaturen eine Pyrolyse des Harnstoffs nach (9) thermodynamisch begünstigt ist.

Das nach (6) und (9) entstandene Isocyanat sollte jedoch mit dem aus (12) und (9) entstandenen Amin nach dem Verlassen der Kontaktzone nach (19) zu Harnstoffen reagieren.

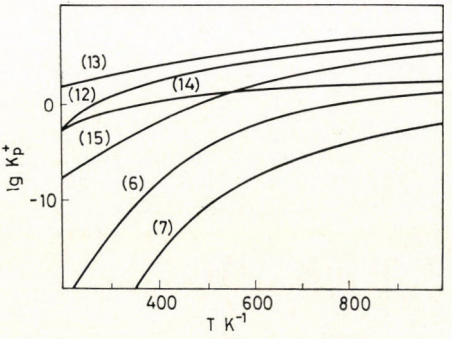

Abb. 3. Temperaturabhängigkeit der thermodynamischen Gleichgewichtskonstanten für die Reaktionen (6), (7) und (12) bis (15) zwischen 200 K und 1000 K

Die Dehydrierung von Acetamid zu Isocyanat (7) verläuft nach Abb. 1 thermodynamisch ungünstiger als die Dehydrierung der Formamide und ist in der Praxis auch noch nicht realisiert worden. Wie Abb. 3 deutlich zeigt, wird die Dehydratisierung zum Nitril (15) thermodynamisch begünstigt.

Carbonylierung von Aminen

Die Carbonylierung der Amine zu Isocyanaten verläuft thermodynamisch sehr ungünstig (Abb. 1). Eine direkte Carbonylierung von Aminen zu Isocyanaten mit katalytischen Mengen eines Katalysators ist in der Literatur noch nicht bekannt. STERN und SPECTOR gelang allerdings in Gegenwart von molaren Mengen Palladiumchlorid die Darstellung von Isocyanaten [25]. Bei der katalytischen Carbonylierung von Aminen ist die Bildung von N-Methylformamid begünstigt [26]. Auch die Bildung von Harnstoffen wurde beobachtet [27]. FUCHS stellte die Bildung von Nitrilen bei der Carbonylierung von Aminen fest [28]. Die durchgeführten thermodynamischen Betrachtungen zeigen, daß bei der Carbonylierung von Aminen die Reaktionen zum N-Methylformamid, zum N,N'-Dimethylharnstoff und vor allem aber zum Acetonitril

thermodynamisch gegenüber der Isocyanatbildung begünstigt sind. Diese Verhältnisse spiegeln sich in Abb. 4 wider. Thermodynamische Berechnungen von BELIK [22] zeigen, daß die Carbonylierungsreaktionen von sekundären und tertiären Aminen gegenüber der Carbonylierung primärer Amine thermodynamisch begünstigt sind.

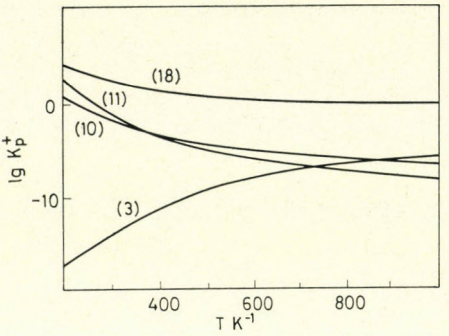

Abb. 4. Temperaturabhängigkeit der thermodynamischen Gleichgewichtskonstanten für die Reaktionen (3), (10), (11) und (18) zwischen 200 K und 1000 K

Hydrocarbonylierung der Nitrile

Die Hydrocarbonylierung der Nitrile führt nicht zu Isocyanaten. Die Reaktion weicht stets unter Bildung von Aminen aus [29]. Aus Abb. 1 folgt, daß das thermodynamische Gleichgewicht der Reaktion vor allem bei hohen Temperaturen auf der Seite der Ausgangsprodukte liegt. Im Gegensatz dazu liegt das von GISBIER [20] berechnete thermodynamische Gleichgewicht der Oxidation von Blausäure zu Isocyansäure eindeutig auf der Seite des Endproduktes.

LITERATUR

[1] GODNEW, I. N.: Berechnung thermodynamischer Funktionen aus Moleküldaten. VEB DVW Berlin (1963)
[2] HIRSCHFELDER, J. O.: J. chem. Physics **8,** 431 (1940)
[3] POPLE, J. P., GORDON, M.: J. Amer. chem. Soc. **89,** 4253 (1967)
[4] EYSTER, E. H., BROCKWAY, L. O., GILETTE, R. H.: J. Amer. chem. Soc. **62,** 3236 (1940)
[5] KIMURA, M., AOKI, M.: Bull. chem. Soc. Japan **26,** 429 (1953)
[6] JONES, R. L.: J. molecular Spectroscopy **11,** 411 (1963)
[7] WARSHAM, J. E., LARRY, H. A., PETERSON, S. W.: Acta crystallogr. **10,** 319 (1957)
[8] HIRSCHMANN, R. P., FASSEL, V. A., KNISELEY, R. N.: Spectrochim. Acta **21,** 2125 (1965)
[9] SPINNER, E.: Spectrochim. Acta **15,** 101 (1959)
[10] JONES, R. L.: J. molecular Spectroscopy **2,** 581 (1958)
[11] SHERMAN, J., EWELL, R. B.: J. physic. Chem. **46,** 641 (1942)
[12] LUFT, N. W., KARABANDA, O. P.: J. chem. Physics **22,** 956 (1954)
[13] ANTONOV, A. A.: Z. obscest. Chim. **34,** 2340 (1964)
[14] BENSON, S. W.: Chem. Rev. **3,** 302 (1969)
[15] LEHMANN, H., RUSCHITZKY, E.: Chem. Techn. **21,** 231 (1969)

[16] JANZ, G. J.: Thermodynamic Properties of Organic Compounds. Academic Press New York, 1967
[17] LAIDLER, K. J., LOVERING, E. G.: Canad. J. Chem. **40,** 26 (1962)
[18] CAROTHERS, W. H.: J. Amer. chem. Soc. **92,** 3856 (1970)
[19] STRULL, D. R., WESTRUM, E. F., SINKE, G. C.: The Chemical Thermodynamics of Organic Compounds. Wiley, New York, 1969
[20] GISBIER, J.: Z. Chem. **11,** 394 (1971)
[21] SCHNABEL, W. J.: F. P. Nr. 1564753
[22] BELIK, P. N., MOGILANSKI, A. I.: Ž. Vses. Chim. obščest. **18,** 238 (1973)
[23] CALDERAZZO, F.: J. inorg. nuclear Chem. **9,** 342 (1970)
[24] KRETZSCHMAR, F., SCHWETLICK, K.: Z. Chem. **14,** 152 (1974)
[25] STERN, E. W., SPECTOR, M. L.: J. org. Chem. **31,** 596 (1966)
[26] ROMANOVA, J. B., ALIEW, Y. Y.: Acad. Nauk Turk. SSR **1963,** 204
[27] DURAND, D., LASSAN, C.: Tetrahedron Letters **1969,** 2329
[28] FUCHS, W., GLASER, F.: Chem. Ing. Techn. **28,** 689 (1956)
[29] ROSENTHAL, A., GERVAY, J.: Chem. and Ind. **1963,** 1623

C. RÜGER
K. SCHWETLICK
H. KAMMER
8027 Dresden, Bergstraße 66c. DDR.

Acta Chimica Academiae Scientiarum Hungaricae, Tomus 85 (4), pp. 361—382 (1975)

MASS-SPECTROMETRIC STUDY OF ELECTRON-IMPACT AND HETEROGENEOUS PYROLYTIC DECOMPOSITION OF METHYL BROMIDE

O. KAPOSI, M. RIEDEL and G. Roberto SÁNCHEZ

(Department of Physical Chemistry and Radiology, L. Eötvös University, Budapest)

Received April 28, 1974

An MI 13—11 mass spectrometer was used to study the decomposition of CH_3Br as a result of electron impact, and as a function of the temperature on the surface of an incandescent tungsten filament.

From the low-resolution mass spectrum of CH_3Br and from the determined ionization and appearance potentials, conclusions were drawn as to the most probable decomposition pathways, and the activation energy of decomposition of the molecular ion was calculated.

It was demonstrated that the heterogeneous pyrolysis of CH_3Br proceeds according to a radical mechanism, and the low time constant reactors employed were suitable for the detection of the radicals produced in small amounts. The pyrolytic decomposition of CH_3Br begins at around 700 K, and the most important decomposition products are HBr, Br and CH_2 radicals. By the determination of the ionization potentials of the radicals formed in the pyrolysis, in the knowledge of the appearance potentials, the dissociation energies of the bonds most important from the aspect of the pyrolytic decomposition were determined. The activation energy of the heterogeneous decomposition indicates that on a carbonized tungsten filament methyl bromide decomposes in a catalyzed process.

The halogenated hydrocarbons added to the gas used to fill halogen lamps [1, 2] can decompose at the operating temperature, in both homogeneous and heterogeneous reactions. Heterogeneous decomposition proceeds on the incandescent tungsten filament, and homogeneous decomposition in the gas space of the lamp due to thermal and photoenergy. The gas-phase thermal decomposition of brominated methane derivatives, most frequently used as the source of halogen for filling lamps, can be studied in a tube reactor, on a mixture with a similar gas composition to that in the lamps; the equilibrium pyrolysis products in the temperature interval 400—1000° are analyzed by infrared spectrophotometry [3]. Decomposition reactions on the incandescent filament can be followed by a mass spectrometer [4, 5] under conditions where the homogeneous part of the reaction can be practically eliminated.

In the present paper we report our experimental results relating to the pyrolytic decomposition of methyl bromide on a tungsten filament. The results obtained on methylene bromide [4, 5] and methyl bromide prove that the mass-spectrometric method is not only of importance as regards the elucidation of the mechanism of heterogeneous decomposition in halogen lamps, but also

provides a possibility for the acquisition of other important physico-chemical informations. Thus, conclusions may be drawn as to the relative stabilities of the individual brominated methane derivatives from their fragmentation on electron impact [6], as to the strengths of the individual bonds from measurement of the appearance potentials of the fragments and the ionization potentials of the radicals formed in the pyrolysis and from the bond-dissociation energies calculated from these, and as to the most probable fragmentation pathways from the measured and calculated appearance potentials. The above data can be used to determine the activation energies of decomposition of the molecular ions resulting from the electron impact. From the activation energy calculated from the temperature-dependence of the pyrolytic decomposition conclusions may be drawn as to the mechanism of heterogeneous thermal decomposition.

Experimental method

Measurements were made on the mass spectrometer described earlier [4, 5]. The methyl bromide used (a product of Fluka) was shown mass-spectrometrically to contain methyl alcohol and dimethyl ether as impurities. It was purified as follows: The methyl bromide vapour at 700 torr was passed through baked-out Union Carbide 4*a* zeolite, which adsorbed the methyl alcohol. Purification from dimethyl ether and possible other impurities was achieved by distillation. The distillation column had a theoretical plate number of ca. 100, the equilibrium pressure was ca. 600 torr, and the vapour extraction was ca. 10%. The receiver ampoules were evacuated to ca. 3 torr, frozen with liquid air, and sealed. The ampoule was connected to the inlet system of the mass spectrometer, with the incorporation of a 'rotaflo' type tap fitted with viton sealing. After the freezing-out of the methyl bromide with liquid air, the ampoule was opened with a magnetic breaker and then subjected to high vacuum. After closing of the 'rotaflo' tap, the methyl bromide was brought to room temperature (where its vapour pressure is ca. 4 atm); fine regulation of the tap permitted the establishment of a methyl bromide vapour pressure of 5—10 torr in the ampoule of the inlet system, and by the further expansion of this amount a pressure of 10^{-2} torr was produced in the 5 dm^3 inlet bulb of the mass spectrometer.

In some of the heterogeneous pyrolytic examinations use was made of the closed reactor type reported earlier [4, 5] in connection with the investigation of methylene bromide, incorporated into the ion-source of the mass spectrometer. In order to study the dependence of the pyrolysis mechanism on the reactor geometry, we also carried out experiments in reactors in which the decomposition filament was situated outside the glass bulb, opposite the capillary (open reactor, Fig. 1). The gas pressure of the substance under examination was very low in the reactor: in the closed type it was 10^{-2} torr, and in the open type even less than this, at times being almost the same as the pressure of 10^{-6} torr in the ion source. In accordance with the Knudsen flow rules, collisions in the gas space in the reactor are negligible compared to the number of those on the tungsten filament, and thus decomposition can occur only in a heterogeneous reaction. The reactors were placed in the direct vicinity of the ionization chamber and their time constants (particularly with the open type, similar to the reactor used by LE GOFF [6]) were very small; this permitted the detection of unstable, very reactive particles (atoms, radicals) too.

The tungsten filament built into the reactor was identical to the filament used in 12 V halogen lamps. In pyrolytic studies on molybdenum the filament was of the same size (⌀ 0.3 mm) as in the case of tungsten. The preparation of the reactors for measurement (conditioning of the filaments) was carried out as described earlier [4, 5]. The filaments were made available by the Tungsten Laboratory, Technical Physics Research Institute of the Hungarian Academy of Sciences.

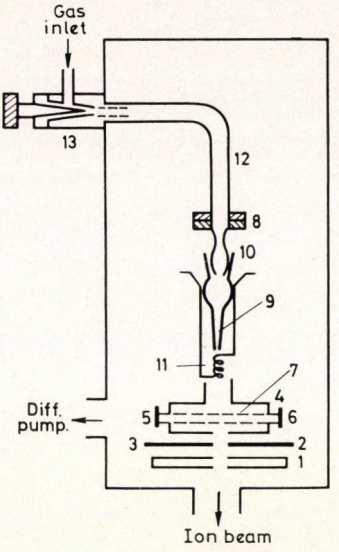

Fig. 1. Schematic diagram of the open pyrolysis cell and the ion source. 1. Accelerating electrode; 2. extracting electrode; 3. focusing electrode; 4. ionization cell; 5. cathode; 6. electron collector; 7. electron beam; 8. connection with teflon gasket; 9. capillary; 10. ground-glass fitting; 11. W or Mo filament; 12. stainless steel gas inlet tube; 13. needle valve

Experimental results

An account is first given of those mass-spectrometric measurements performed under conditions such that the filament of the reactor was not heated. In this way the methyl bromide decomposes only upon the action of the ionizing electrons, disregarding the unavoidable thermal decomposition on the electron-emitting incandescent cathode. In the case of the operation of pyrolyzing reactors, however, in addition to this also the thermal decomposition is significant, and thus the conditions are more complex.

I. Study of the decomposition of methyl bromide as a result of electron impact

1. *Low-resolution mass spectrum of methyl bromide*

Evaluation of the pyrolysis measurements demands above all a knowledge of the mass spectrum of methyl bromide.

Table I contains low-resolution mass spectra of methyl bromide at electron energies of 70 and 20 eV. The relative intensities are referred to the m/e 94 peak ($CH^{81}Br^+ + CH_3{}^{79}Br^+$), and are also given as a percentage of the total ion current.

Table I

Low-resolution mass spectra of methyl bromide at electron energies of 20 and 70 eV

Mass number	Ion	20 eV		70 eV	
		total ion current %	base peak %	total ion current %	base peak %
12	C^+	0.455	1.29	0.77	3.25
13	CH^+	0.882	2.49	1.29	5.43
14	CH_2^+	1.83	5.18	2.78	11.7
15	CH_3^+	16.05	45.38	23.8	100.6
79	$^{79}Br^+$	1.41	3.98	5.90	24.9
80	$H^{79}Br^+$	0.485	1.37	0.94	3.96
81	$^{81}Br^+$	1.55	4.37	5.8	24.6
82	$H^{81}Br^+$	0.510	1.44	0.91	3.9
91	$C^{79}Br^+$	1.04	2.92	2.2	9.3
92	$CH^{79}Br^+$	0.515	1.46	1.11	4.76
93	$C^{81}Br^+$ $CH_2{}^{79}Br^+$	3.22	9.12	5.4	22.8
94	$CH^{81}Br^+$ $CH_3{}^{79}Br^+$	35.36	100.0	23.7	100.0
95	$CH_2{}^{81}Br^+$	2.53	7.14	3.47	14.6
96	$CH_3{}^{81}Br^+$	34.17	96.64	21.9	92.6

In the case of measurements with the same apparatus, under the same experimental conditions, the extent of the fragmentation in the ion source depends on the electron energy and on the strengths of the bonds in the compound [7]. Information on the relative stability of methyl bromide can be obtained by investigating the extent of fragmentation on ionization with electrons of different energies.

For comparison of the fragmentation conditions of brominated methane derivatives we used the molecular ion decomposition probability (W_z) introduced by PAHL [8, 9] and defined by the following relation:

$$W_z = \frac{\Sigma I_f}{\Sigma I_f + \Sigma I_m} \tag{1}$$

where ΣI_f is the sum of the relative intensities of the fragment ions, and ΣI_m is the sum of the relative intensities of the isotope peaks of the undecomposed molecular ions (in the present case the sum of the relative ion currents of $CH_3{}^{79}Br^+$ and $CH_3{}^{81}Br^+$).

The values calculated for methyl bromide from equation (1) are given in Table II, from which it can be seen that the probability of decomposition of the molecule increases with the increase of the electron energy.

Table II

Variation of the decomposition probability (W_z) of the methyl bromide molecular ion with the electron energy

Electron energy [eV]	W_z
20	0.310
25	0.409
30	0.466
70	0.555

For comparison of the stabilities of the various compounds PAHL [8] introduced the mean fragmentation quotient (Q_B):

$$Q_B = \frac{\Sigma I_f}{Z \cdot \Sigma I_m} \tag{2}$$

where Z is the number of bonds in the molecule.

With the use of our earlier results [4, 5] for the comparison of the stabilities of methyl bromide and methylene bromide, the values of W_z and Q_B are presented in Table III. It can be seen from the tabulated data that under identical conditions methylene bromide undergoes a greater degree of fragmentation than methyl bromide; in other words, the molecular-ion CH_3Br^+ is more stable than the $CH_2Br_2^+$ ion. At the same time, the value of Q_B is smaller for methyl bromide than for methylene bromide, in agreement with the fact that Q_B is an inverse measure of the average stability per bond of the molecular-ion.

Table III

W_z and Q_B values of CH_3Br and CH_2Br_2, calculated from the experimental data measured at 70 eV

Compound	W_z	Q_B
CH_3Br	0.555	0.311
CH_2Br_2	0.663	0.348

2. *Determination of the fragmentation processes of methyl bromide as a result of electron impact*

The fragment ions formed in the decomposition of methyl bromide can arise from a very large number of fragmentation processes. As was shown in the case of methylene bromide [4, 5], determination of the appearance (AP) and ionization (IP) potentials leads to the possibility of selecting the most probable decomposition pathways. The principle of the procedure is that we determine the appearance potentials of all of the fragments, and the ionization potentials of the radicals formed in the pyrolysis. All possible AP values are

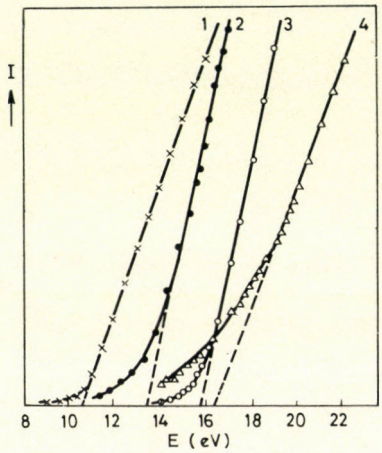

Fig. 2. Ionization efficiency curves of (1) $CH_3{}^{81}Br^+$, (2) $CH_2{}^{81}Br^+$, (3) $^{40}Ar^+$, and (4) $CH^{79}Br^+$. The values on the electron energy scale are corrected against $^{40}Ar^+$

calculated from the normal heat of formation data ($\Delta H^0(R^+)$) in the literature, and of the possible processes which are accepted as most probable for which the calculated AP value is closest to the measured value.

The ionization efficiency curves were recorded by the procedure employed in the case of methylene bromide [4, 5]. The curves were evaluated by the method of linear extrapolation [10, 11]. In some cases the evaluation was checked with the more exact MORRISON method [12]; the results obtained by the two methods agreed within the limits of error.

The electron energy scale was calibrated by the internal standard method [7]. The calibrating gas was argon, the IP value of which is known with high accuracy. Measured by the photoionization method [13], its value is $15.76 \pm \pm 0.01$ eV, which lies among the AP values of the fragments measured here. In the measurements the argon was admitted into the ion source together with the methyl bromide by means of a double inlet system, at such a partial pressure that ion currents of similar intensity should be obtained for the ions CH_3Br^+ and $^{40}Ar^+$. Figure 2 shows the ionization efficiency curves of

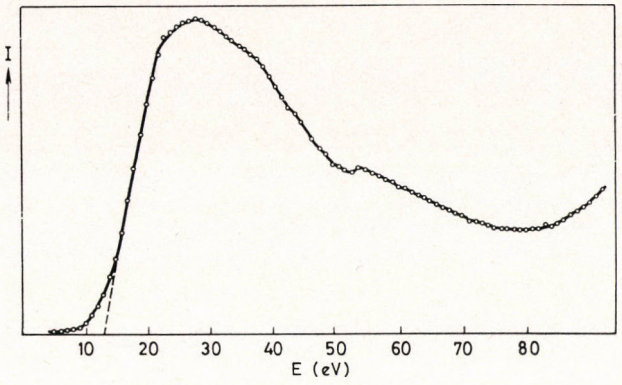

Fig. 3. Variation of the ion current of CH^+ in arbitrary units as a function of the corrected electron energy

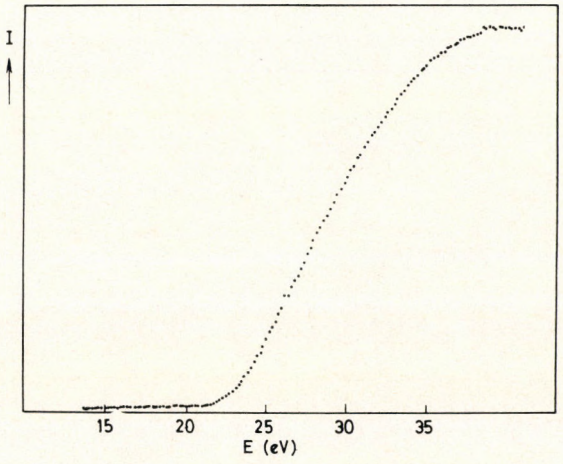

Fig. 4. Ionization efficiency curve of C^+

$CH_3{}^{81}Br^+$, appearing with high intensity, of $CH_2{}^{81}Br^+$, with medium intensity, of $CH^{79}Br^+$, measured at low intensity, and of $^{40}Ar^+$, in the range of about 5 eV.

Figure 3 depicts the ionization efficiency curve of CH^+ in the whole ionization electron energy range, and Fig. 4 that of C^+ in the interval 15—40 eV. It can be seen from Fig. 4 that the low-intensity ionization efficiency curve of C^+ is linear over a fairly wide interval, and thus the function can reasonably safely be extrapolated to the zero ion current value. This too proves the applicability of linear extrapolation in our case, and the superfluousness of the substantially more complex Morrison method.

The ionization efficiency curve of CH_2^+ is presented in Fig. 5. The plot reveals two break points, and from extrapolation of the linear sections AP val-

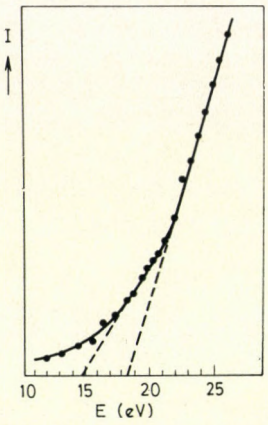

Fig. 5. Ionization efficiency curve of CH_2^+

ues of 18.2 and 14.7 eV are obtained. This indicates that the ion CH_2^+ is formed in at least two decomposition processes. It is clear from Table IV that the two values agree very well with the corresponding literature values. In contrast to the Figures given in this paper, for the evaluation of the ionization efficiency curves we used scales where the electron energy could be determined with an accuracy of ± 0.1 eV. The *AP* and *IP* values obtained from the ionization

Table IV

Measured AP and IP values of fragments formed in decompositions of Data referring to CH_2Br_2 and denoted by * are our earlier experi-

Radical	ΔH^0 [kcal/mole]		Ion	ΔH^0 [kcal/mole]	
	lit.	measd.		lit.	measd.
H	52.1	—			
H_2	0.0	—			
$C_{(g)}$	170.9	—	C^+	431.0	—
$Br_{(g)}$	26.7	—	Br^+	300.0	—
CH	142.0	—	CH^+	399.0	—
CH_2	91.0	–	CH_2^+	333.0	—
CH_3	33.2	—	CH_3^+	260.0	—
HBr	−7.8	—	HBr^+	262.8	—
CBr	145.3	—	CBr^+	388.0	—
CHBr	94*	96	$CHBr^+$	364*	367
CH_2Br	40* 46.3	48	CH_2Br^+	243*	249
CH_3Br	−8.4	—	CH_3Br^+	234	—

efficiency curves are listed in Table IV, together with the corresponding literature AP, IP and ΔH^0 data, and the values obtained previously for methylene bromide. It can be seen from the Table that the values for the high-intensity ions could be determined with an error of at most ± 0.3 eV, while the corresponding error for the low-intensity ions was ± 0.5 eV.

In the interest of making the possible decomposition processes of methyl bromide more easy to survey, it is practical to employ the earlier introduced [4, 5] fragmentation mechanism matrix. The elements of the matrix are the stoichiometric coefficients of the components of all the possible decomposition reactions (Table V). The construction and use of the fragmentation matrix, and the calculation of the theoretical AP are given in references [4, 5].

If the AP values calculated for the individual decomposition routes are compared with those found experimentally, the most probable decomposition processes can be selected. The measured values and the selected calculated values approximating most closely to them are listed in Table VI. It is clear from the tabulated values that, with the exception of Br^+ and CBr^+, the AP values for all the ions agree within the limits of error with one or an other of the theoretically calculated values, and that the measured values are somewhat higher, as a sign that in this case the assumption of the ground state is not strictly valid [14]. On this basis, the most probable decomposition processes

CH_3Br and CH_2Br_2, and literature AP, IP and ΔH^0 data
mental results [4, 5]; other literature data are from [7]

IP [eV]			*AP* [eV]		
lit.	CH_2Br_2*	measd.	lit.	CH_2Br_2*	measd.
11.1±0.5	—	—	—	22.7±0.5	22.9±0.5
11.85	12.2±0.3	—	16.6	—	15.8±0.5
11.13	—	—	21.4	22.0±0.5	21.7±0.3
11.9	—	—	14.9 18.1	17.1±0.3	14.7±0.5 18.2±0.5
9.82	—	9.6±0.3	13.0	—	12.8±0.3
11.69	11.9±0.3	—	—	18.2±0.2	15.9±0.3
—	12.2±0.5	—	—	19.6±0.3	18.8±0.3
—	11.7±0.5	—	—	16.0±0.5	16.3±0.5
8.34 9.20	8.7±0.3	—	13.6	11.1±0.2	13.4±0.3
10.6	—	10.5±0.2	10.6	—	10.5±0.2

Table V

Stoichiometric matrix of electron-impact fragmentation of methyl bromide
The positions of the zero elements are denoted by dots

Calculated *AP* [eV]	CH_3Br^+	CH_2Br^+	$CHBr^+$	CBr^+	HBr^+	CH^+	CH_2^+	CH^+	Br^+	C^+	CH_3Br	CH_2Br	CHBr	CBr	HBr	CH_3	CH_2	CH	Br	H_2	H	C	
26.9	.	.	.	.	.	.	.	.	.	1	−1	.	.	.	.	.	.	.	1	.	3	.	
22.4	.	.	.	.	.	.	.	.	.	1	−1	.	.	.	.	.	.	.	1	1	1	.	C^+
18.6	.	.	.	.	.	.	.	.	.	1	−1	.	.	.	1	.	.	.	.	1	.	.	
20.9	.	.	.	.	.	.	.	.	.	1	−1	.	.	.	1	.	.	.	.	.	2	.	
27.6	.	.	.	.	.	.	.	.	1	.	−1	.	.	.	.	.	.	.	.	.	3	1	
23.1	.	.	.	.	.	.	.	.	1	.	−1	.	.	.	.	.	.	.	.	1	1	1	
24.1	.	.	.	.	.	.	.	.	1	.	−1	.	.	.	.	.	.	1	.	.	2	.	Br^+
19.6	.	.	.	.	.	.	.	.	1	.	−1	.	.	.	.	.	.	1	.	1	.	.	
19.6	.	.	.	.	.	.	.	.	1	.	−1	.	.	.	.	.	1	.	.	.	1	.	
15.0	.	.	.	.	.	.	.	.	1	.	−1	.	.	.	.	1	.	.	.	.	.	.	
18.9	.	.	.	.	.	.	.	1	.	.	−1	.	.	.	.	.	.	.	1	1	.	.	
23.4	.	.	.	.	.	.	.	1	.	.	−1	.	.	.	.	.	.	.	1	.	2	.	CH^+
19.7	.	.	.	.	.	.	.	1	.	.	−1	.	.	.	1	.	.	.	.	.	1	.	
18.3	.	.	.	.	.	.	1	.	.	.	−1	.	.	.	.	.	.	.	1	.	1	.	
14.5	.	.	.	.	.	.	1	.	.	.	−1	.	.	.	1	.	.	.	.	.	.	.	CH_2^+
12.8	.	.	.	.	.	1	.	.	.	.	−1	.	.	.	.	.	.	.	1	.	.	.	CH_3^+
19.4	.	.	.	.	1	.	.	.	.	.	−1	.	.	.	.	.	.	.	.	1	.	1	
23.9	.	.	.	.	1	.	.	.	.	.	−1	.	.	.	.	.	.	.	.	.	2	1	HBr^+
20.4	.	.	.	.	1	.	.	.	.	.	−1	.	.	.	.	.	.	1	.	.	1	.	
15.7	.	.	.	.	1	.	.	.	.	.	−1	.	.	.	.	.	1	.	.	.	.	.	
19.3	.	.	.	1	.	.	.	.	.	.	−1	.	.	.	.	.	.	.	.	1	1	.	CBr^+
23.8	.	.	.	1	.	.	.	.	.	.	−1	.	.	.	.	.	.	.	.	.	3	.	
16.2	.	.	1	.	.	.	.	.	.	.	−1	.	.	.	.	.	.	.	.	1	.	.	$CHBr^+$
20.7	.	.	1	.	.	.	.	.	.	.	−1	.	.	.	.	.	.	.	.	.	2	.	
13.2	.	1	.	.	.	.	.	.	.	.	−1	.	.	.	.	.	.	.	.	.	1	.	CH_2Br^+
10.7	1	.	.	.	.	.	.	.	.	.	−1	.	.	.	.	.	.	.	.	.	.	.	CH_3Br^+

Table VI

Experimental AP values, and calculated AP values most closely approximating the measured ones

Ion	*AP* [eV]	
	calculated	measured
C^+	22.4	22.9
Br^+	15.0	15.8
CH^+	—	21.7
CH_2^+	18.2	18.2
CH_3^+	12.8	12.8
HBr^+	15.7	15.9
CBr^+	19.3	18.8
$CHBr^+$	16.2	16.3
CH_2Br^+	13.2	13.4
CH_3Br^+	10.7	10.5

Table VII

Probable ion-formation processes of methyl bromide in the case of electron-impact ionization

Ion	Reaction
C^+	$CH_3Br \xrightarrow{e} C^+ + Br + H_2 + H$
Br^+	$CH_3Br \xrightarrow{e} Br^+ + CH_3$
CH^+	$CH_3Br \xrightarrow{e} CH^+ + H_2 + Br$
CH_2^+	$CH_3Br \xrightarrow{e} CH_2^+ + H + Br$ $CH_3Br \xrightarrow{e} CH_2^+ + HBr$
CH_3^+	$CH_3Br \xrightarrow{e} CH_3^+ + Br$
HBr^+	$CH_3Br \xrightarrow{e} HBr^+ + CH_2$
CBr^+	$CH_3Br \xrightarrow{e} CBr^+ + H_2 + H$
$CHBr^+$	$CH_3Br \xrightarrow{e} CHBr^+ + H_2$
CH_2Br^+	$CH_3Br \xrightarrow{e} CH_2Br^+ + H$
CH_3Br^+	$CH_3Br \xrightarrow{e} CH_3Br^+$

are given in Table VII. In spite of the larger differences observed for Br^+ and CBr^+, the selection of the decomposition pathway was a clear-cut one. The value of 21.7 eV measured in the case of CH^+ could not be ascribed to any of the decomposition schemes. Also this value agrees within the limits of error with the literature value (21.41 eV) [15], and in accordance with these authors we also consider the most probable decomposition route to be:

$$CH_3Br \rightarrow CH^+ + H_2 + Br$$

The two AP values obtained for CH_2^+ also exhibit good agreement with the AP values calculated for the two fragmentation routes displayed in the Table.

3. *Activation energies of decomposition of the molecular ions*

In the foregoing, use was made of the fact [4, 5] that the AP of the fragment ion can be regarded as the heat of reaction of the ion-formation process, and the heat of formation of the ion can be determined from it. Since the molecular ion is formed in an isolated system (in the ion source of the mass spectrometer), its energy is taken over by the fragments produced from it. Conversely, if the decomposition requires energy, then the molecular ion acquires this from the impact electron. If the total energy necessary to induce the reaction is ΔH, and the heat of reaction is ΔH_R, then the activation energy of the process is given by:

$$\Delta H^{\ddagger} = \Delta H - \Delta H_R \tag{3}$$

Naturally, relation (3) is also true for an exothermic reaction.

Let the decomposition process be:

$$XY^+ = X^+ + Y \tag{4}$$

The sum (ΔH) of the heat of reaction and the activation energy for this reaction can be calculated as follows from the AP of the fragment ion appearing in the mass spectrum of the molecule XY:

$$\Delta H = AP(X^+) - IP(XY) \tag{5}$$

The heat of reaction is:

$$\Delta H_R = \Delta H(X^+) + \Delta H(Y) - \Delta H(XY^+) \tag{6}$$

Accordingly, the activation energy is:

$$\Delta H^{\ddagger} = AP(X^+) - IP(XY) - \Delta H(X^+) - \Delta H(Y) + \Delta H(XY^+) \tag{7}$$

Equation (7) was used, together with the IP and AP values measured by us and the literature ΔH data [7], to calculate the activation energies of the most important decomposition reactions of the molecular ion CH_3Br^+. The data are given in Table VIII, from which it can be seen that both CH_3Br^+ and $CH_2Br_2^+$ decompose in processes requiring little or no activation energy, with the production of Br and HBr. Naturally, a higher activation energy is required for the decomposition of neutral molecules of similar structure in a non-catalyzed process. In the literature [7] one can find values of 20 kcal/

mole for the reaction $CH_3Br^+ \rightarrow CH_2^+ + HBr$, and 7 kcal/mole for the similar decomposition of CH_3I^+; these values agree within an order of magnitude witk the data measured by us. It must be noted that the results are of only moderate accuracy because of the errors in the *AP* and *IP* measurements, and the error may be as much as $\pm 10\%$.

Table VIII

Activation energies of decompositions of the molecular ions

Reaction	ΔH [kcal/mole]	ΔH_R [kcal/mole]	$\Delta H^{\ddagger}$ [kcal/mole]
$CH_3Br \rightarrow CH_3^+ + Br$	53	54	−1
$CH_3Br^+ \rightarrow CH_2^+ + HBr$	99	91	8
$CH_2Br_2^+ \rightarrow CH_2Br^+ + Br$	14	24	−10
$CH_2Br_2^+ \rightarrow CHBr^+ + HBr$	126	115	11

II. Study of the heterogeneous pyrolysis of methyl bromide

1. *Dependence of the spectrum of methyl bromide on the temperature of the reactor filament*

The dependence of the spectrum of methyl bromide on the temperature of the tungsten filament when a closed type of reactor is used is shown in Figs 6—7. For the sake of greater clarity the spectral peaks appearing at

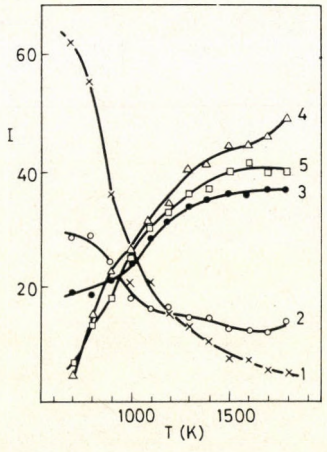

Fig. 6. Variation with temperature (T) of relative intensity (I) of (1) CH_3Br^+, (2) CH_3^+, (3) Br^+, (4) HBr^+, and (5) CH_2^+ originating from the pyrolytic decomposition of methyl bromide. Closed reactor, W filament, electron energy 70 eV

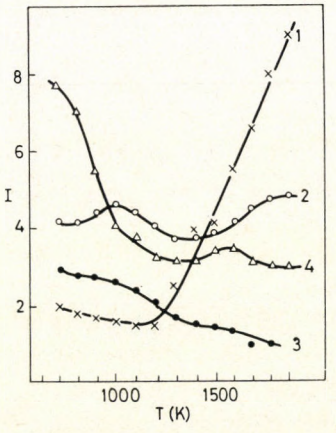

Fig. 7. Variation with temperature (T) of the relative intensity (I) of the peaks (1) $C^+ + CH^+$, (2) CBr^+, (3) $CHBr^+$, and (4) CH_2Br^+ originating from the pyrolytic decomposition of methyl bromide. Closed reactor, W filament, electron energy 70 eV

high and low intensities are plotted on separate diagrams. The relative ion currents are given in arbitrary, but identical units.

In the case of the open reactor the residence time of the substance under examination is substantially lower, and thus the number of collisions on the spiral also decreases considerably. The possibility of wall reactions and of the recombination of the labile reaction products similarly decreases. Experimental results for methyl bromide with this reactor type are presented in Figs 8 and 9.

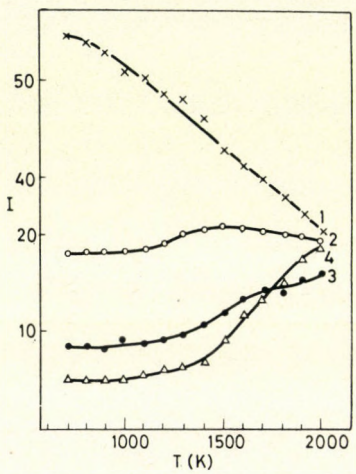

Fig. 8. Variation with temperature (T) of the relative ion current intensity (I) of (1) CH_3Br^+, (2) CH_3^+, (3) Br^+, and (4) HBr^+ originating from the pyrolytic decomposition of methyl bromide. Open reactor, W filament, electron energy 70 eV

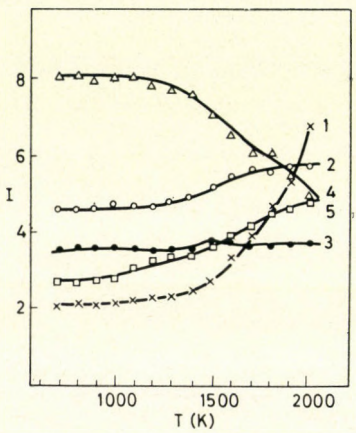

Fig. 9. Variation with temperature (T) of the relative intensity (I) of (1) $CH^+ + C^+$, (2) CBr^+, (3) $CHBr^+$, (4) CH_2Br^+, and (5) CH_2^+ formed in the decomposition of methyl bromide. Open reactor, W filament, electron energy 70 eV

The effect of the nature of the incandescent filament on the pyrolysis was examined with the open reactor type by exchanging the tungsten filament for a molybdenum one of the same size. The reason of this choice was not only the high-temperature incandescence and similar chemical structure of molybdenum, but also the fact that molybdenum is incoporated as a structural material in some halogen lamps. Experimental results obtained with this reactor are depicted in Figs 10 and 11.

The temperature-dependence of the pyrolysis was studied at an electron energy of 70 eV, and thus the fragmentation is due to both the electron energy and the thermal energy. The effect of the electrons can be eliminated if the ionizing electron energy is less than the appearance potential of the decomposition product investigated, but larger than the ionization potential of the radical. Naturally, therefore, the ion currents to be measured are very small,

being of the order of 10^{-15}—10^{-16} A at the applied ion-source pressure of 10^{-6} torr. The main reasons for this are as follows: (1) only part of the methyl bromide entering the reactor collides with the filament and is pyrolyzed (this proportion is lower in the case of the open reactor); (2) only part of the reaction products reach the ionization chamber (recombination is disregarded); (3) only a very small proportion of the gas molecules are ionized. In the present case this proportion is much lower even, because of the very low electron energy: (4) finally, as a result of the low transmission coefficient of the mass spectrometer only a part of the ions formed arrive to the collector. These causes

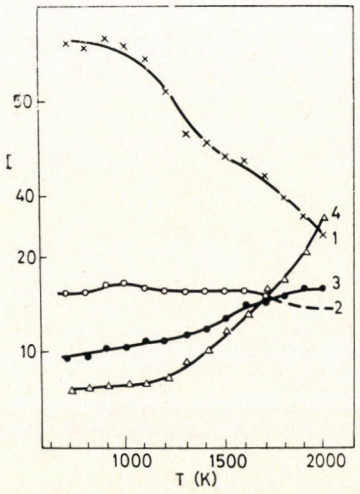

Fig. 10. Variation with temperature (T) of the relative intensity (I) of the ion currents of (1) CH_3Br^+, (2) Br^+, (3) CH_3^+, and (4) HBr^+ originating from the decomposition of methyl bromide. Open reactor, Mo filament, electron energy 70 eV

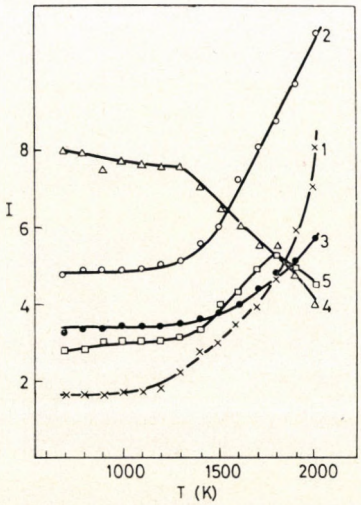

Fig. 11. Temperature (T) dependence of relative intensity (I) of (1) $C^+ + CH^+$, (2) CBr^+, (3) $CHBr^+$, (4) CH_2Br^+, and (5) CH_2^+ originating from the decomposition of methyl bromide. Open reactor, Mo filament, electron energy 70 eV

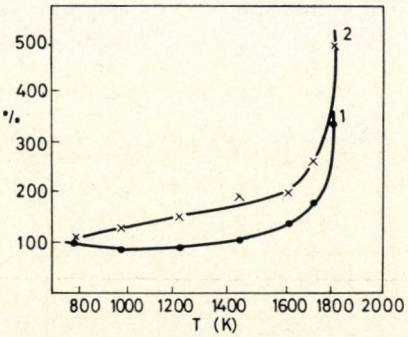

Fig. 12. Temperature dependence of the percentage increase of the peak heights of (1) Br^+ and (2) HBr^+ formed in the pyrolysis of methyl bromide. Electron energy 13 eV

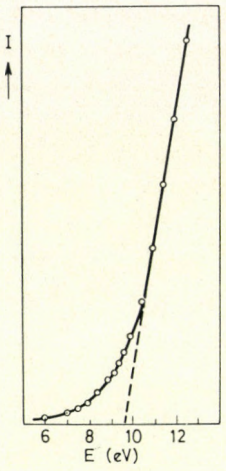

Fig. 13. Ionization efficiency curve of the methyl radical formed by pyrolysis from methyl bromide at a filament temperature of 2000 °K. The electron energy scale is corrected against $^{40}Ar^+$

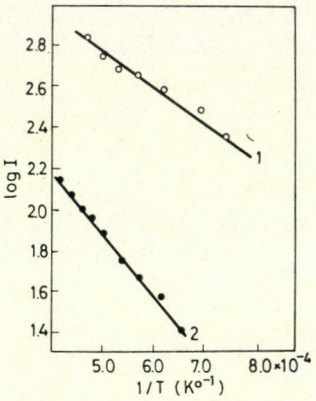

Fig. 14. Arrhenius plots of (1) HBr and (2) Br formed in the decomposition of methyl bromide on a W filament. Electron energy 70 eV

permit the measurement of very small, and moreover fluctuating ion currents. The ion currents of Br^+ and HBr^+ formed as main products of the thermal decomposition were measured as a function of temperature with an SI-03 ion-counter [4, 5]. The electron energy was 13 eV, which lies between the appearance potentials of these ions and the ionization potentials of Br and HBr (Fig. 12).

The ionization potentials of the radicals and atoms formed in the decomposition could be determined (recording of ionization efficiency curves 1). Figure 13 shows the ionization efficiency curve of the methyl radical formed at a filament temperature of 2000°K. The *IP* value obtained by linear extrapolation of the curve is 9.6 ± 0.3 eV, which agrees well with the literature value of 9.8 eV [16].

2. *Determination of the activation energy of the heterogeneous pyrolysis*

Several methods were attempted for the mass-spectrometric determination of the activation energy of the heterogeneous pyrolysis of methyl bromide. The most suitable of these proved to be the open reactor type, in which the possibility of recombination of the decomposition products could be avoided.

To avoid the fragmentation resulting from the action of the ionizing electrons, the neutral HBr and Br produced during pyrolysis were ionized with a low electron energy, and those processes were studied which provide

the main products of the pyrolysis, HBr and Br. However, the values calculated from the very small ion currents exhibited an extremely wide spread. Accordingly, the measurement was carried out also with an electron energy of 70 eV, and the ion current measured at room temperature, *i.e.* produced by the electrons, was deduced from the ion currents measured at the various temperatures. The logarithms of the ion currents corrected in this way, are shown for Br and HBr in Fig. 14 as a function of $1/T$.

3. *Interpretation of the experimental results on the pyrolysis of methyl bromide*

Before an interpretation of the experimental results, a brief account will be given of the factors controlling the operation of closed spherical reactors incorporated into the ion source of the mass spectrometer under conditions where the gas pressure inside the reactor is small enough for the Knudsen conditions to be realized [7]: The filament is situated at the centre of the reactor, and a capillary connects the reactor with the ionization chamber, where the gas pressure is 3 orders of magnitude lower than in the reactor. The number of molecules dn transformed in time dt during reaction on a solid surface is given by the product of ϱ, involving physical and geometric factors, and the impact efficiency factor γ characteristic of the chemical process:

$$dn = (\varrho \cdot \gamma)dt \tag{8}$$

Since the number of molecules decomposed, dn can be measured by the mass spectrometer, for the determination of γ characterizing the chemical process it is necessary to know the physical factor. It can be shown that the pressure of the ion source of the mass spectrometer is proportional to the pressure p in the reactor, the proportionality factor depending only on the reactor geometry, and being independent of the nature and temperature of the gas [17—20]. For a detailed description of the pressure conditions of the reactor–ion source system both in the stationary and transient case it is necessary to know two quantities: (1) the collision number, dependent on the reactor geometry:

$$\nu_i = \frac{A}{S} \tag{9}$$

which gives how many times a molecule collides with a filament of surface A if the cross-section of the outflow capillary of the reactor is S; (2) the time constant, in sec, characteristic of the transient stage:

$$\tau = 3.76 \times 10^{-4} \frac{V}{S} \sqrt{\frac{M}{T}} \tag{10}$$

where V is the volume of the reactor, M is the molecular weight of the gas, and T is its temperature. (9) and (10) require a knowledge of several quantities which in this case are not sufficiently well defined (the reactor volume, the gas temperature, the outflow rate, etc.). However, in the knowledge of the geometric data of the reactor and the capillary, and the surface of the filament used (0.66 cm^2), we can estimate how many times a molecule entering the reactor collides with the filament during its residence time. In the present case this is ca. 80. In an open reactor the collision number is much lower and is more difficult to estimate. For a similar set-up LE GOFF gives a collision number of 2.7 [6, 21].

From a study of the temperature dependence of the pyrolysis it can be stated that in addition to the earlier discussed fragmentation effect of the electron energy, another complicating factor is that the mass spectrum is temperature-dependent even regardless of the pyrolysis. This is manifested in the fact that if the temperature of the ion source increases, then (1) the specific intensities of all the ions decrease, and (2) the relative intensity of the molecular ion decreases.

It was demonstrated by STEVENSON [22] that the first effect can be traced back to two causes. With the increase of the temperature the rate of effusion of the molecules from the ion source increases, while with the increase of the kinetic energy of the molecules the efficiency of collection of the ions decreases. For these two reasons the ion current is proportional to $T^{-1/2}$. The reason why the relative intensities of the molecular ions decrease with the increase of temperature is that the vibrational energy of the molecular ions increases with the temperature [23], and thus there is a corresponding increase in the probability of their decomposition. The first effect can be neglected because of the square-root relation, and because of the plotting of the individual peaks as a percentage of the total ion current. Nor does the other effect give rise to a large error, as under the conditions of the ion source the temperature of the ionization chamber does not vary appreciably with the reactor temperature (under the high-vacuum conditions there is only thermal radiation, and the heat conduction can be neglected).

If all the above is taken into consideration, the following qualitative findings can be made with regard to the pyrolytic decomposition of methyl bromide on the basis of the temperature dependence of the mass spectrum: In the case of a tungsten filament the pyrolytic decomposition in a closed-type reactor (Figs 6—7) begins at 800 K; the ratio of the decomposed and undecomposed methyl bromide increases first rapidly and then more slowly with the temperature, and at 1800 K the ratio becomes constant with the decomposition of the bulk of the methyl bromide. In the case of open reactors (Figs 8—9) the temperature dependence of the relative intensities of the individual ion currents is much less, in accordance with the fact that in the re-

actor a much lower proportion of the methyl bromide molecules entering the ionization chamber collide with the incandescent filament, and far fewer times. As a consequence of this, the pyrolysis-caused temperature dependence of the mass spectrum in an open reactor is much less than in a closed reactor. In the two reactor types the decomposition proceeds by the same mechanism. The main decomposition products are HBr and the Br, CH_3 and CH_2 radicals. With the rise of temperature the increase in the relative intensity of HBr is larger than that for Br, while at the same time the intensity of CH_3 decreases and that of CH_2 increases. The latter process appears particularly distinctly in the case of the closed reactors, which ensure repeated collisions for the methyl bromide molecules; above 1500 K the relative intensities of the ions formed from the radicals CH and C increase. The relative intensities of the other carbon, hydrogen and bromine-containing ions appearing with low intensity decrease in the case of a closed reactor, and increase slightly compared to the amount of methyl bromide decomposed in an open reactor as a function of temperature. This means that these radicals are very labile and thus the probability of their detection is higher in the open reactor with its low time constant. On the other hand, the radicals CH_3 and CH_2 are fairly stable and may recombine to a small extent on the walls of the reactor capillary (in Fig. 6 the ion current of CH_2^+ increases strongly with temperature). This fact agrees with the observation of FABIAN and ROBERTSON [24], who showed that the impact efficiency factor of the propyl radical on a glass wall is very small: $\gamma = 4.5 \times 10^{-5}$.

The experimental results obtained with an open reactor containing a molybdenum filament did not differ substantially from those in experiments made under similar conditions, but with a tungsten filament. The only striking difference is that the relative ion currents of the low-intensity CBr^+, CH^+ and C^+ ions at high temperature increase more rapidly for the molybdenum filament than for the tungsten filament. This may be related to the fact that carbon is less soluble in molybdenum [25] than in tungsten [26], and the resulting molybdenum carbide is less stable than the tungsten carbides. From the similarity observed in the cases of molybdenum and tungsten it may be concluded that the brominated methane derivatives undergo pyrolysis in a similar manner on the two metals.

From the activation energy of the decomposition conclusions can be drawn on the mechanism of the heterogeneous pyrolytic decomposition. For the reasons mentioned, the temperature dependences of the ion currents of Br and HBr were determined with an electron energy of 70 eV (Fig. 14).

The activation energy can be calculated from the Arrhenius equation:

$$\Delta H^{\ddagger} = 2.303 \cdot 1.986 \frac{\Delta \log I}{\Delta\, 1/T} \cdot \qquad (11)$$

In our case the ion current I of a fragment is made up of two parts: a term $I_1(T)$ due to the pyrolysis and thus dependent on the temperature (T), and an ion current $I_2(E)$ resulting from the fragmentation caused by the electron impact (E) and independent of temperature:

$$I = I_1(T) + I_2(E) \tag{12}$$

I_2 can be determined from (12) by the method of mean values, and thus the temperature-dependent part of the ion current can be picked out separately. Fig. 14 shows the Arrhenius plots of the ion currents corrected in this way. From the temperature dependences of the ion currents resulting from the atomic Br and HBr, the following activation energies were obtained for the following processes:

$$CH_3Br \rightarrow CH_3 + Br \quad 15 \pm 3 \text{ kcal/mole}$$
$$CH_3Br \rightarrow CH_2 + HBr \quad 8 \pm 2 \text{ kcal/mole.}$$

The accuracy of the results is affected by two factors. It was mentioned earlier that the ion current varies a little with the temperature of the ion source, independently of the pyrolysis. In addition, as a consequence of the continuous carbonization–decarbonization the surface of the pyrolyzing tungsten filament varies, and other authors too [27] have demonstrated that this has an extremely large influence on the activation energy of the heterogeneous decomposition. The homogeneous thermal decomposition of brominated methane derivatives proceeds in a chain reaction by a radical mechanism [28]. With a toluene vapour technique SZWARC and SEBUM [29] obtained a value of 67.5 kcal/mole for the activation energy of the decomposition of CH_3Br. From the much lower activation energy of the heterogeneous pyrolysis it may be concluded that on tungsten the brominated methane derivatives decompose in a catalytic process according to a radical mechanism. Two parallel processes take place side by side: Br is produced *via* splitting of the C—Br bond, and HBr is eliminated from the molecule. This latter process requires less activation energy. In agreement with this, on the diagram depicting the temperature-dependence of the mass spectrum (Fig. 6) the increase of the relative ion current of HBr is much larger than that for Br. At the same time the activation energy of the decomposition of the molecular ion CH_3Br^+ formed in the electron-impact ionization is smaller in the direction of the Br-formation process than in the direction of the HBr-formation process (Table VIII). This result agrees with the data of the mass spectrum of methyl bromide recorded at room temperature: according to the data of Table I, the relative ion current of Br^+ is roughly five times as high as the ion current of HBr^+.

The energies required to split the bonds of most importance as regards the pyrolytic decompositions of CH_3Br and CH_2Br_2 [4, 5] were calculated

Table IX

Bond-dissociation energies calculated from the experimental data and from the literature heats of formation for the molecules CH_3Br and CH_2Br_2

Bond	Calcd. from exptl. data [kcal/mole]	From [7] [kcal/mole]
$Br-CH_3$	74 ± 4	68
$H-CH_2Br$	118 ± 5	108
$Br-CH_2Br$	65 ± 4	65
$H-CHBr_2$	111 ± 5	102

from the ionization potentials of the radicals formed in the pyrolysis and from the appearance potentials determined from the fragmentation in the course of the electron impact. The bond-dissociation energies for these same bonds were calculated from literature data [7]. The results are listed in Table IX. It can be seen that our measured values in general agree with the bond-dissociation energies calculated from the literature data within 10%. The experimental results show that the mass-spectrometric method is well applicable to the study of the fragmentation of brominated methane derivatives.

The data which can be calculated from the experimental results are important from both practical and theoretical aspects, and it thus appears worth while to extend the experiments described here to the remaining two members of this group of compounds ($CHBr_3$ and CBr_4).

REFERENCES

[1] Mosby, F. A., Schupp, L. J., Steiner, G. G., Zubler, E. G.: Illum. Eng. **62,** 198 (1967)
[2] Hangos, I., Deutsch, T.: Kém. Közlemények **37,** 459 (1972)
[3] Deutsch, T.: Thesis. L. Eötvös University, Budapest (1973)
[4] Kaposi, O., Riedel, M., Deutsch, T.: Magy. Kém. Folyóirat **79,** 505 (1973)
[5] Kaposi, O., Riedel, M., Deutsch, T.: Acta Chim. (Budapest) **81,** 43 (1974)
[6] Le Goff, P.: J. Chim. Phys. **53,** 359 (1956)
[7] Field, F. H., Franklin, J. L.: Electron Impact Phenomena, Acad. Press, New York, 1970
[8] Pahl, M.: Z. Naturforsch. **9b,** 188 (1954)
[9] Pahl, M.: Z. Naturforsch. **9b,** 418 (1954)
[10] Hurzeler, H., Inghram, M. G., Morrison, J. D.: J. Chem. Phys. **28,** 76 (1958)
[11] Collin, J. E.: The Determination of Ionization and Appearance Potentials. In: R. J. Reed: Mass Spectrometry, Acad. Press, London, 1965
[12] Morrison, J. D.: J. Appl. Phys. **28,** 1409 (1957)
[13] Dibeler, H., Reese, R. M., Krauss, M.: Adv. Mass Spectrometry **3,** 471 (1966)
[14] Stevenson, D. P.: Disc. Faraday Soc. **10,** 35 (1951)
[15] Reed, R. J., Snedden, W.: Trans. Faraday Soc. **55,** 876 (1959)
[16] Melton, C. E., Hamill, W. H.: J. Chem. Phys. **41,** 3464 (1964)
[17] Carter, G.: Vacuum **12,** 245 (1962)
[18] Ehrlich, G.: General Electric Rep. 63RL 3375M; Advan. Cat. **14,** 255 (1963)
[19] Redhead, P. A.: Vacuum **12,** 203 (1962)
[20] Robertson, A. J. B.: Adv. Mass Spectrometry **1,** 559 (1958)
[21] Le Goff, P.: J. Chim. Phys. **50,** 423 (1953)

[22] STEVENSON, D. P.: J. Chem. Phys. **17,** 101 (1949)
[23] REESE, R. M., DIBELER, V. H., MOHLER, F. L.: J. Research Natl. Bur. Standards **46,** 79 (1951)
[24] FABIAN, D. J., ROBERTSON, A. J. B.: Trans. Faraday Soc. **54,** 301 (1958)
[25] FEW, W. E., MANNING, G. K.: J. Metals N. Y. **413,** 271 (1952)
[26] GOLDSCHMIDT, H. J., BRAND, J. A.: J. Less-common Met. **5,** 181 (1963)
[27] DAWSON, P. H., ROBERTSON, A. J. B.: Trans. Faraday Soc. **60,** 157 (1964)
[28] BRAMFORD, C. H., TIPPER, C. F. H.: Decomposition and Inversation of Organic Compounds. In: SWINBORNE, E. S.: The Decomposition of Halogen Compounds. Elsevier, Amsterdam, 1972
[29] SZWARC, M., SEBUM, A. H.: J. Chem. Phys. **19,** 656 (1951)

Olivér KAPOSI
Miklós RIEDEL } 1088 Budapest, Puskin u. 11—13 Hungary.

G. Roberto SÁNCHEZ; C. N. I. C. Calle 25 No 258, Rpto Cubanacan, Habana, Cuba.

Acta Chimica Academiae Scientiarum Hungaricae, Tomus 85 (4), pp. 383—387 (1975)

STUDIES ON THE CALCINATION OF AMMONIUM URANATE WITH SPECIAL REFERENCE TO SURFACE AREA

M. Y. FARAH and S. A. EL-FEKEY

(Nuclear Chemistry Dept., Atomic Energy Establishment, Cairo, Egypt)

Received May 30, 1974

In revised form September 25, 1974

Thermal decomposition of thin layers of washed ammonium uranate of 0.3 cm thickness, up to 350°C leads to a rapid increase in the surface area of UO_3 powder; in thick layers self-reduction starts while surface area increases but to a lower extent. Above this temperature sintering leads in both cases to a reduction in surface area. However, washing prior to thermal decomposition using ethanol, acetone as also degassing of uranates, and further the temperature range of the calcination and thickness on trays are found to effect markedly surface areas of the powders formed.

Introduction

Uranium tri- and sesquioxides have been used as intermediary oxides in the preparation of UO_2 fuel. They are prepared either by the direct thermal decomposition of uranyl nitrate [1—5] or by the calcination of ammonium uranate [6—10]. Sintering characteristics of UO_2 powders are largely governed by their mode of preparation. Oxides made by thermal decomposition of nitrate usually have poor sintering characteristics and are used to produce uranium fluoride feed for diffusion plants [11]. Previous work in this laboratory [10, 12] showed that sinterable grades of UO_2 may be obtained, however, by the calcination of ammonium uranate.

In this investigation, the effects of washing and calcination on surface area of powders formed during thermal decomposition of ammonium uranates were studied between 25° and 800°C, in view of obtaining reproducible oxide and determining the temperature at which maximal and minimal surfaces occur. The thickness of uranates on the tray varied between 0.3 and 2.5 cm using static beds, to define its impact on the physico-chemical characterization of the prepared powders.

Experimental

Effect of uranate washing and bed thickness during calcination on the characteristics of the products and effect of calcination regime

Ammonium uranate was precipitated from nuclear pure uranyl nitrate solution (70 g uranium/litre), using air-diluted gaseous ammonia at 80°C to reach pH 8.0 after eleven minutes, under vigorous stirring of the tank for 15

minutes, and readjusting the pH value. After filtering, the uranate was divided into four portions. The first was unwashed, the second washed and the third degassed under vacuum for 10 days after being washed. The uranates were calcined in 0.3 or 2.5 cm thickness layers. The surface area was measured at the end, using continuous flow-BET method.

In view of establishing a procedure for obtaining reproducible surface area for intermediary oxides, a plan of experiments was elaborated, whereby samples of uranates precipitated at pH 8, filtered and washed, were calcined at the required temperature in one or two steps for different durations of time from 2 to 24 hours.

Results and discussion

I. Effect of washing of uranates and their thickness on trays during calcination

Fig. 1(a, b, c) shows the surface areas for 0.3 cm thickness of calcined samples. For unwashed sample (a) the BET values decrease to 6.6 m^2/g at 220°C, attain 33 m^2/g at 350°C and again decrease below 2.61 m^2/g at 700°C. For washed sample (b) there is no decrease at first but a gradual increase to 36 m^2/g at 350°C, followed by an identical sharp decrease to 3.34 m^2/g as for (a) when heated to 700°C. The degassed sample (c) indicates more or less similar behaviour to (b), with a 37.00 m^2/g optimum surface area at 350°C. It is apparent that this optimum is related to the decomposition of uranate, and ammonium departure leading to shattering and fining of the particles, while the decrease around 200°C for sample (a) is presumably related to partial contamination of surface by nitrates, that block the pores and retard ammonia departure. The subsequent decrease between 400°C and 800°C is presumably due to micro-sintering. The actual results contribute in throwing more light on the published antagonistic results, summarised by WOOLFREY [11] for different authors, who do not always quote the conditions of their preparations. It is believed that the thickness of layers during calcination is essentially responsible for variation in textures reported in the previous literature.

Fig. 2 reports BET values for sample (a) and sample (b). It is observed that the intermediate 16.1 m^2/g product obtained around 450°C in thick layer (2.5 cm), is practically completely formed of U_3O_8, owing to self-reduction of the UO_3 by the evolved ammonia.

II. Effect of calcination regime

A) The results of BET determination for one-step calcination at 200°, 400° or 600° for thin or thick layer uranate indicate that:

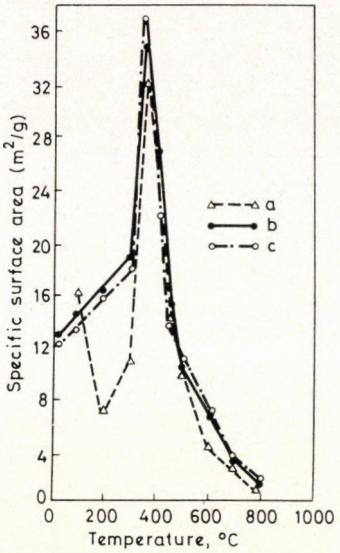

Fig. 1. Effect of calcination temperature upon the specific surface area of powders formed during the decomposition of ammonium uranates

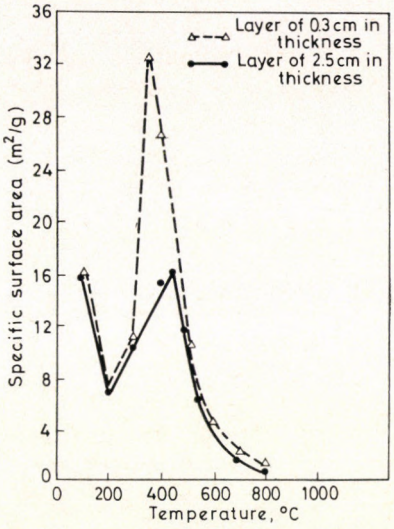

Fig. 2. Effect of calcination temperature upon the specific surface area of powders formed during the decomposition of different layers of ammonium uranate

1. Between 6 and 24 hours (Fig. 3) a thin layer calcined sample having 7.12 m^2/g surface decreased to 6.5 m^2/g at 200°C, and from 5.2 to 4.69 m^2/g at 600°C (Fig. 5), while BET at 400°C increased from 26.55 to 28.00 m^2/g (Fig. 4).

2. For thick layers (2.5 cm), the same general trend is also observed at 200° and 600°, but at 400°C there is, however, a fall in BET from 24.05 to 15.0 m^2/g indicating a parallel microsintering due to partial reduction by ammonia, whose departure being hindered in thick fixed bed. This phenomenon is absent in rotary furnaces or fluidised beds.

B) Fig. 6 reproduces the results of BET versus temperature for five calcined samples:

a) two hours at 350°C as a first step,

b) four hours at 400°, 500°, 600°, 700° and 800°C, respectively, as a second step.

According to Fig. 6, BET is shown to decrease, respectively, from 30.0 to 18.1, 5.4, 4.0 and 1.4 m^2/g. Thus it is advisable to avoid surpassing 600°C for the second calcination step, this result compares favourably with that of AINSCOUGH [13] in so far as BET is concerned. Two-step calcination at 600°C leads to an approximately constant reproducible BET value of 5.40 ± 0.04 m^2/g.

The fluctuating values of BET reported by many authors are believed to be due to i) the method of surface area measurement used: conventional

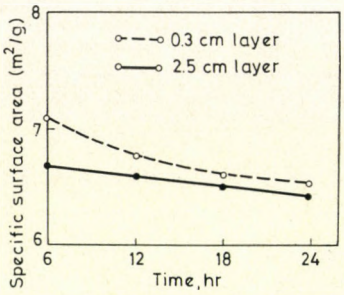

Fig. 3. Effect of duration of calcination at 200°C upon the specific surface area of powders, during the decomposition of different layers of ammonium uranate

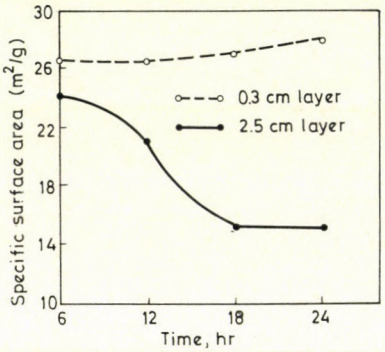

Fig. 4. Effect of duration of calcination at 400°C upon the specific surface area of UO_3 formed during the decomposition of different layers of ammonium uranate

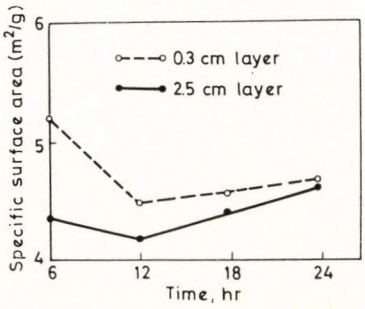

Fig. 5. Effect of duration of calcination at 600°C upon the specific surface area of U_3O_8 formed during the decomposition of different layers of ammonium uranate

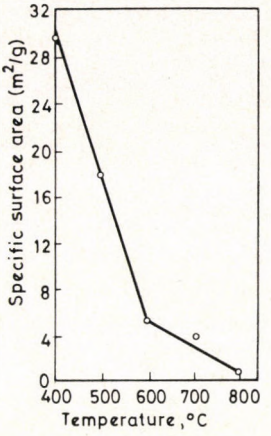

Fig. 6. Effect of calcination temperature, after 2 hours at 350°C, upon the specific surface area of powders formed during the decomposition of ammonium uranate

BET, continuous flow BET, or permeability; ii) washing of uranates before calcination and iii) variation in calcination schedules and thickness of layers in fixed-bed furnaces. One-step calcination in both thin or thick layers of ammonium uranates for up to 24 hours duration, fails to give a stable BET value, while two-step calcination leads to an approximately constant reproducible BET value.

REFERENCES

[1] AERE C/R 1874 and 2276 reports (1959)
[2] AES-tr-4939, 4941, 5072 and 5073 Reports (1959)
[3] DP-749 Reports (1962)
[4] Rodrigo Otero, A. *et al.*: Proceedings of the International Symposium on Fluidisation, Madrid (1967)
[5] Rodrigo Otero, A. *et al.*: Publicado en Anales de la Real Sociedad Espanola de Fisica Y Quimica, Quimia, Tomo LXVI Pag 399, Num 4 (1970)
[6] Ippolitova, E. A. *et al.*: ANL-trans-33, 114 (1961)
[7] Notz, K. J. *et al.*: TID-6228 (1960);
[8] Ukaji, R.: AEC-tr-4939 (1959)
[9] Margotin, P. *et al.*: Compt. Rend., **252,** 4005 (1961)
[10] El-Fekey, S. A.: Ph. D. Thesis, Cairo University (1972)
[11] Woolfrey, J. L.: AAEC/TM 476 (1968)
[12] Farah, M. Y., El-Fekey, S. A.: Recent Advances in Science and Technology of Material. Vol. 3. pp. 343—349, Plenum ed. New York (1974)
[13] Ainscough, J. B.: TID-7637 (1961)

M. Y. Farah
S. A. El-Fekey } Cairo 5, Rashdan St., DOKKI, Egypt.

Acta Chimica Academiae Scientiarum Hungaricae, Tomus 85 (4), pp. 389—394 (1975)

INTERACTION OF TRANSITION METALS WITH SOME ALKALOIDS, METAL COMPLEXES OF QUINALDINE, QUININE, BRUCINE AND CODEINE

Omar FAROOQ and Aneesudin MALIK*

(Inorganic Research Lab., Chemistry Department, Aligarh Muslim University, Aligarh, U. P. India)

Received June 21, 1974

Complexes of alkaloids such as quinaldine, quinine, brucine and codeine with some transition metals are reported. The complexes of codeine were synthesized with a large number of metal ions namely, Cu^{2+}, Ni^{2+}, Co^{2+}, Mn^{2+}, Ti^{3+}, Cr^{3+} and VO^{2+}(dioxovanadium(IV)). Unlike alkaloids, their complexes are in general highly soluble in water but almost insoluble in common organic solvents. The results of chemical analyses indicate a metal : ligand ratio of 1 : 2 for quinaldine and codeine and 1 : 1 for brucine and quinine complexes. Infrared spectra were studied in KBr pellets in the range 2.5—16 μ whereas, far infrared spectra were recorded with CsI using nujol to locate the pertinent site of coordination. Thermogravimetric studies in the range of 25—800°C, at a rate of 6°/min revealed that two water molecules are coordinated to the metal. Molar conductances of 1% aqueous solution are of the order 6.66×10^{-5} mhos cm^2 mol^{-1}, indicating thereby the non-electrolytic nature of these complexes in solution, most probably owing to bridging. Magnetic measurements by GOUY's method after applying PASCAL's correction at 25°C reveal a paramagnetism due to the tetrahedral arrangement in nickel(II) and cobalt(II) complexes of codeine. These compounds are coloured and have high melting points.

Introduction

A limited number of references are available on metal alkaloid complexes [1—4]. Complexes of alkaloids with Sb, Cd, Hg, Cu and Co have been reported, but these studies are limited to the composition and properties of the complexes. The present communication deals with the complexes of alkaloids such as quinaldine, quinine, brucine and codeine with some transition metals. Infrared spectral studies, thermogravimetric analysis, magnetic suspectability and molar conductance measurements have been carried out to determine the likely coordination sites in the alkaloid complexes.

Experimental

The quinaldine (B. D. H., England) was distilled. Quinine (B. D. H., England), brucine and codeine (E. Merck, Germany) vanadyl chloride, uranyl sulfate (B. D. H.), cupric chloride, chromium chloride, manganese chloride, cobalt chloride, nickel chloride (E. Merck) were used without purification. Titanium(III) chloride was prepared as described earlier [5].

The complexes reported here were synthesized by mixing solutions of the metal salt and the alkaloid in methanol. The compounds were coloured, hygroscopic, highly soluble in water and mineral acids, but insoluble in common organic solvents.

* Present address: Department of Metallurgy and Material Science, Liverpool University, Liverpool, England.

I. R. spectra of quinaldine, quinine, codeine and brucine were recorded with a Perkin—Elmer Model 21 spectrophotometer, using KBr discs in the range 2.5 to 16 μ while the far infrared spectra were recorded with a Beckman Model BK 56 (104 417) spectrophotometer, using nujol mull with CsI. TGA were done on Stanton Thermobalance, England, in the range 25—800°C at a heating rate of 6° per min. Molar conductances were recorded with a Philips Conductivity Bridge model PR 9500 in conjunction with a dip type cell and the magnetic measurements were performed by GOUY's method at 25°C. Microanalyses were done by I. I. T. Kanpur.

Results of elemental analysis

1. $Ti(QD)_2Cl_3.2\ H_2O$. Yellow product, d. p. 204—205°C. Calcd. for $C_{20}H_{18}N_2.TiCl_3.2\ H_2O$: C 50.40; H 4.61; N 5.88; Ti 10.68; Cl^- 22.35; Found C 49.48; H 4.74; N 5.78; Ti 10.60; Cl^- 22.21%.

2. $VO(QD)_2Cl_2^+.2\ H_2O$. Grey product, d. p. 149—150°C. Calcd. for $C_{20}H_{18}N_2.VOCl_2.2H_2O$: C 51.76; H 4.74; N 6.04; V 10.99; Cl^- 15.29. Found C 51.84; H 4.80; N 6.25; V 11.20; Cl^- 15.45%.

3. $UO_2(QD)_2SO_4$. Dark yellow, d. p. above 360°C. Calcd. for $C_{20}H_{18}N_2.UO_2SO_4$: C 36.78; H 2.76; N 4.26; U 36.41; SO_4^{2-} 14.71. Found C 36.94; H 2.88; N 4.32; U 36.63; SO_4^{2-} 14.91%.

4. $Ti(Q)CL_3 2\ .\ H_2O$. Mustard product, d. p. 242—243°C. Calcd. for $C_{20}H_{24}O_2N_2.TiCl_3.2\ H_2O$: C 46.67; H 5.44; Ti 9.28; Cl^- 9.28. Found C 48.02; H 5.60; N 5.50; Ti 9.40; Cl^- 9.39%.

5. $VO(Q)Cl_2 2\ .\ H_2O$. Steel grey product, d. p. 232—233°C. Calcd. for $C_{20}H_{18}N_2O_2.VOCl_2.2\ H_2O$: C 48.22; H 5.76; N 5.60; V 10.44; Cl^- 16.14. Found C 48.02; N 5.48; H 5.90; V 10.60; Cl^- 16.24%.

6. $Cu(Cod)_2Cl_2.2\ H_2O$. Mustard product, d. p. 156—157°C. Calcd. for $C_{36}H_{42}O_6N_2.CuCl_2.2\ H_2O$: C 56.36; H 5.90; N 3.60; Cu 8.25; Cl^- 9.25. Found C 56.90; N 3.60; Cu 8.02; Cl^- 9.54%.

7. $Co(Cod)_2Cl_2.2\ H_2O$. Bluish green product, d. p. 218—219°C. Calcd. for $C_{36}H_{42}O_6N_2.CoCl_2.2\ H_2O$: C 57.06; H 6.02; N 3.66; Co 7.74; Cl^- 9.49. Found C 56.90; H 6.30; N 3.60; Co 7.80; Cl^- 9.54%.

8. $Ti(Cod)_2Cl_3.2\ H_2O$. Dirty yellow product, d. p. 271—272°C. Calcd. for $C_{36}H_{42}O_6N_2.TiCl_3 2\ H_2O$: C 55.40; H 5.97; N 3.16; Ti 2.54; Cl^- 13.49. Found C 55.32; H 6.04; N 3.12; Ti 2.48; Cl^- 13.60%.

9. $VO(Cod)_2Cl_2.2\ H_2O$. Dark grey product, d. p. 149—150°C. Calcd. for $C_{36}H_{42}O_6N_2.VOCl_2.2\ H_2O$: C 55.98; H 6.60; N 3.60; V 6.59; Cl^- 9.18. Found C 55.88; H 6.42; N 3.56; V 6.72; Cl^- 9.30%.

10. $Ni(Cod)_2Cl_2.2\ H_2O$. Green product, d. p. 150—152°C. Calcd. for $C_{36}H_{42}O_6N_2.NiCl_2.2\ H_2O$: C 57.10; H 6.08; N 3.68; Ni 7.76; Cl^- 9.55, Found C 54.60; H 6.25; N 3.71; Ni 7.82; Cl^- 9.80%.

11. $Cr(Cod)_2Cl_3.2\ H_2O$. Light green product, m. p. above 360°C. Calcd. for $C_{36}H_{42}O_6N_2.CrCl_3.2\ H_2O$: C 54.53; H 5.81; N 3.66; Cr 6.56; Cl^- 13.42. Found C 54.60; H 6.25; N 3.71; Cr 6.77; Cl^- 13.56%.

12. $Mn(Cod)_2Cl_2.H_2O$. Pink product, d. p. 254—255°C. Calcd. for $C_{36}H_4\ O_6N_2.MnCl_2.2\ H_2O$: C 56.88; H 6.05; N 3.68; Mn 7.22; Cl^- 9.33. Found C 55.90; H 6.00; N 3.72; Mn 7.10; Cl^- 9.50%.

13. $VO(B)Cl_2.2\ H_2O$: Grey product, d. p. above 360°C. Calcd. for $C_{23}H_{26}O_4N_2.VOCl_2.2\ H_2O$: C 45.70; H 4.96; V 8.44; N 4.63; Cl^- 11.74. Found C 45.54; H 4.78; N 4.51; V 8.32; Cl^- 11.90%.

14. $Ti(B)Cl_3.2\ H_2O$. Light product, d. p. 280—282°C. Calcd. for $C_{23}H_{26}O_4N_2.TiCl_3.2\ H_2O$: C 47.24; H 5.14; N 4.79; Ti 8.18; Cl^- 18.30. Found C 47.36; H 4.69; N 5.27; Ti 8.25; Cl^- 18.50%.

15. $UO_2(B)SO_4.2\ H_2O$. Yellow product, d. p. above 360°C. Calcd. for $C_{23}H_{26}O_4N_2.UO_2SO_4.2\ H_2O$: C 41.31; H 4.49; N 4.19; U 35.57; SO_4^{2-} 14.37. Found C 41.50; H 5.15; N 4.22; U 35.70; SO_4^{2-} 14.50%.

Results and discussion

The alkaloids quinine and brucine form 1 : 1 complexes with Ti^{3+}, VO^{2+} and UO_2^{2+}, whereas quinaldine gives 1 : 2 adducts. Codeine forms 1 : 2 complexes with Cu^{2+}, Co^{2+}, VO^{2+}, Mn^{2+}, Ti^{3+} and Cr^{3+}.

* QD = $C_9H_6NCH_3$ (Quinaldine), Q — $C_{20}H_{24}N_2O_2$ (Quinine), Cod = $C_{18}H_{21}O_3N$ (Codeine) B = $C_{23}H_{26}O_4N_2$ (Brucine); the decomposition points are uncorrected.

Quinaldine complexes. On considering the spectra of the metal–quinaldine complexes, it can rightly be assumed that the heterocyclic nitrogen of quinaldine(I) would evidently be the only pertinent donor atom. In the presence of the coordinated heterocyclic amine, four regions, namely ca. 1650—1400 (CC,CN stretchings [6]), ca. 1300—1100 cm^{-1} (CH in-plane deformations [7]), ca. 1000 cm^{-1} (ring skeletal vibrations) and ca. 850—750 cm^{-1} (CH out-of-plane deformations [8]) have been found to be affected by coordination.

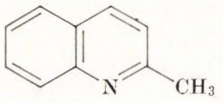

I

In the present studies on metal quinaldine complexes, the main information regarding coordination is obtained from the changes occurring in the regions of ring skeletal and CH out-of-plane deformation vibrations. The bands arising from ring skeletal and those from CH out-of-plane are shifted to higher wavenumbers together with increasing intensities. The changes in the above regions may be explained in terms of π-bonding through a vacant *d*-orbital of the metal and a delocalized π-orbital of heterocyclic nitrogen [9]. The bands at 930(m) and 1035 cm^{-1}(m) in UO_2^{2+} and VO^{2+} complexes, respectively, may be assigned to M—O stretches [10].

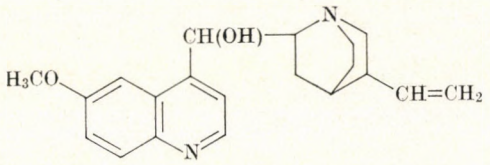

II

Quinine complexes. Quinine (II) has three possible donor atoms, [11] namely, nitrogen atoms of the 6-methoxyquinoline and quinuclidine ring and a secondary OH group. A possible reason for the shifts in OH [12] and CH stretching [13] is the involvement of heteroatomic nucleus of the substituted quinoline in coordination. Further evidence in favour of coordination through heterocyclic nitrogen is obtained on considering the changes occurring in the regions of ring CC,CN stretchings of 6-methoxy quinoline, ring skeletal vibrations of the heteroatomic ring and CH out-of-plane deformation vibrations. The bands in these regions are usually shifted to higher frequencies with an increase in the number of bands. There is not much evidence for the coordination through nitrogen of the quinuclidine ring. Besides the slight shifts in CN stretchings, there is a paucity of information in favour of coordination

through the more basic and reactive nitrogen of quinuclidine ring. The band at 1030 cm^{-1} is assigned to V—O stretching [10].

Codeine complexes. The alkaloid codeine (III) forms 1 : 2 complexes with Cu^{2+}, Co^{2+}, VO^{2+}, Mn^{2+}, Ti^{3+} and Cr^{3+}. There are only three possible coordination sites [14] in the alkaloid, namely, the secondary OH, the tertiary nitrogen attached to a methyl group and the oxygen of the furan ring.

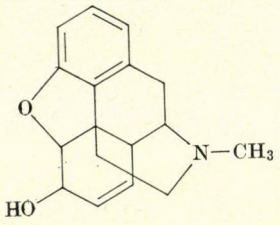

III

The IR spectrum of codeine shows a weak band at 2710 cm^{-1} (—NCH stretch). The spectra of the complexes indicate either no shift of these bands or shifting to the high side by 10 to 25 cm^{-1} in some cases. This does not give sufficient information regarding the possibility of coordination through this atom [15]. Similarly, only minor shifts occur in the bands attributed to the substituted furan ring [16] on coordination. Therefore, the possibility of coordination through the $-CH_3$ and the substituted furan ring is more or less excluded.

The medium intensity bands at 3600 cm^{-1} and 3460 cm^{-1} in the spectrum of codeine are assigned to secondary OH stretchings and to the intramolecular, hydrogen-bonded OH group, respectively [17]. In Ni^{2+}, Co^{2+} and Cu^{2+} complexes, the OH stretching band is shifted to much lower frequencies whereas in the spectra of Mn^{2+}, VO^{2+}, Ti^{3+} and Cr^{3+} there is no such band in the region 3600—3500 cm^{-1} or in its vicinity. It probably merges with the intramolecular hydrogen bonding frequency. The band arising from intramolecular hydrogen bonding appears in the form of a weak band at lower frequencies in the spectra of the complexes. The lowering is 10 to 20 cm^{-1}, the only plausible explanation of the appreciable changes in OH stretchings and intramolecular hydrogen bonding bands is the possibility of coordination through the hydroxyl group.

The medium intensity band 1640(VO^{2+}), 1635(Co^{2+}), 1630(Cr^{3+}), 1630(Cu^{2+}) and a broad at 1630—1640 cm^{-1} in Ti^{3+} complexes are assigned to coordinated water [20] (OH bonding modes). The medium band at 1065 cm^{-1} is attributed to V—O stretches [10] in the vanadyl complexes. The cobalt complex has a magnetic moment of 4.02 BM, indicating a paramagnetic character and a tetrahedral arrangement [18]. Thermogravimetric analysis also reveals that both water molecules are coordinated to the cobalt atom. Similarly,

the nickel complex is presumably a tetrahedral. The value of μ_{eff} is 2.85 exhibiting two unpaired electrons [19]. The loss of 2 water molecules in these complexes in the range of 120—210°C supports the above concept of coordination to the metal atom [20].

Brucine complexes

Brucine(IV) consists of several ring systems and various functional groups *viz.* pyrrocoline, hydroindole, ketopiperazine and 1-oxa-Δ-3-cycloheptane rings together with various functional groups such as $-OCH_3$, $-NCO$, $-N-$, etc.

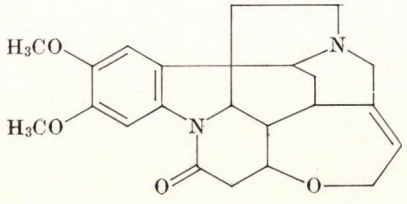

IV

It is not possible to give specific assignments to all the bands present in the spectrum of brucine. Three positions are susceptible to coordination in brucine, namely, the acylazole group, the oxygen of a 7-membered cyclic ether(oxepine) and the tertiary nitrogen of the CH_2-N-CH_2 group present in the 5/6 pyrrocoline ring. In the spectrum of brucine, the CO and CN stretching bands of the acylazole system [21] belonging to ketopiperazine appear at 1025, 1035 cm^{-1}, respectively. In the spectra of the complexes the bands arising from CN stretchings disappear, whereas that from CO is shifted to lower frequencies by 20 cm^{-1}. It may safely be assumed that in brucine complexes coordination takes place through the nitrogen of the acylazole system as is indicated by the disappearance of the CN stretching band and the lowering of the CO band in the spectra of the complexes.

The position of the bands arising from various other groups considered for possible coordination sites did not show any change as indicated by the spectra of brucine complexes. For example, the bands assigned to CH(3000 cm^{-1}), $-OCH_3$(1200 cm^{-1}) and C=C(1665 cm^{-1}) stretchings [22] in the spectrum of brucine remain almost unaltered in the spectra of the complexes. The bands at 1040 and 945 cm^{-1} in the spectra of vanadyl and uranyl brucine complexes are assigned to V—O and U—O stretches, respectively [10].

These complexes are practically non-electrolytes. The molar conductance of a 1% aqueous solution falls in the range of 6.66×10^{-5} mohs cm^2 mol^{-1},

indicating the probability of bridging in solution phase. The complexes undergo hydrolysis even in very dilute solution within a short period. Moreover, the insolubility in common organic solvents and the amorphous nature are in conformity with the above conclusion. In the present studies, the evidence regarding the coordination in metal-alkaloid complexes is inferred from certain physico-chemical studies. Although the results are not exhaustive, taking into account the paucity of information available regarding the structure of alkaloids, they seem convincing. Further studies are needed to explore this problem of medicinal importance. Similar work is in progress in our laboratory.

*

The authors offer their thanks to Prof. W. RAHMAN for providing facilities, to the Council of Scientific and Industrial Research, New Delhi, for award of a senior Fellowship to one of them (O. F.), to Dr. NASEER AHMAD for the infrared spectra and to Mrs. SHAKTI R. AHMAD for useful suggestions.

REFERENCES

[1] THOMSON, TH. SR.: Chem. Zentr., **1,** 1515 (1911)
[2] DEQUENOIS, P.: Anal. Chim. Acta, **1,** 50 (1947)
[3] BURROWS, G. H., TURNER, E. E.: J. Proc. Roy. Soc. N. S. Wales, **55,** 263 (1922)
[4] SUBBA RAO, N. V., SESHRADI, T. T.: Proc. Indian Acad. Sci., **11A,** 289 (1940)
[5] AHMAD, N., RAHMAN, S. M. F., MALIK, W. U.: J. Indian Chem. Soc., **40,** 515 (1963)
[6] KATRITZKY, A. R.: Physical Methods in Heterocyclic Chemistry, Vol. II, Academic Press, New York, 1963
[7] BELLAMY, L. J.: The Infrared Spectra of Complex Molecules. Methuen and Co., London 1958
[8] Ref. 6, p. 280
[9] GILL, N. S., SCAIFE, D. E., NUTTAL, R. H., SHARPE, D. W.: J. Inorg. nucl. Chem., **18,** 79 (1961)
[10] SELBIN, J.: Chem. Rev., **65,** 162 (1965)
[11] ALBERT, A.: Heterocyclic Chemistry, The Athanole Press, University of London 1959
[12] MARION, L., RAMSAY, D. A., JONES, R. N.: J. Amer. Chem. Soc., **73,** 305 (1951)
[13] RAO, C. N. R.: Chemical Applications of Infrared Spectroscopy pp. 296, 193. Academic Press Inc., New York
[14] BENTLEY, K. W.: The Alkaloids, pp. 96, Vol. I., Interscience Publishing Co., New York, 1957
[15] HILL, R. D., MEAKINS,: J. Chem. Soc., 761, (1958), 2927 (1960)
[16] Ref. 13, pp. 324—328
[17] Ref. 13, pp. 355—357
[18] BIRADAR, N. S., KULKARNI, N. H., SIRMOKADAMA: Indian J. Chem., **8,** 838 (1970)
[19] PAULING, L.: The Nature of Chemical Bond, pp. 168, III. ed. Oxford and IBH Publishing, New Delhi, 1963
[20] MATHUR, B. S., SRIVASTAVA, T. S.: J. Inorg. nucl. Chem., **32,** 3277 (1970)
[21] Ref. 6, p. 315
[22] Ref. 13, p. 148

Omar FAROOQ; Inorganic Research Lab., Chemistry Department, Aligarh Muslim University, Aligarh, U. P. India

Aneesudin MALIK; Department of Metallurgy and Material Science, Liverpool University, Liverpool, England.

Acta Chimica Academiae Scientiarum Hungaricae, Tomus 85 (4), pp. 395—398 (1975)

METAL–AMINO ACID INTERACTION, II

A STUDY OF THE COMPLEX COMPOUNDS OF TRIVALENT RARE EARTHS WITH GLUTAMIC ACID

Omar FAROOQ and Naseer AHMAD

(Inorganic Research Laboratory, Chemistry Department, Aligarh Muslim University, Aligarh, U. P. India)

Received July 10, 1974

The complexes of trivalent rare earths with glutamic acid are reported. The elemental analyses supported the formula (Glut-H)$_3$ R. E. 3 H_2O (where Glut = glutamic acid and R. E. = trivalent rare earths). Thermogravimetric studies revealed the presence of three coordinated water molecules. The magnetic moments in B. M. give the characteristic unequal double humped curve and infra-red spectra taken in the range between 2.5 and 16 μ in KBr pellets showed the coordination of rare earth ions through the ionized carboxylic group adjacent to the amino group. The comparable molar conductances of the rare earth salts and the complexes in aqueous solutions demonstrated greater ionic bonding between rare earths and amino acids.

Metal protein complexes have emerged as a central problem of bioinorganic chemistry. Amino acids being an integral part of proteins play an important role in the process of isolation and purification of proteins. A number of transition metal–amino acid complexes have been studied mainly with a view to affecting the separation and identification of amino acids [1—6]. The interaction of lanthanides with amino acids has been studied mostly in solution employing various physico-chemical methods [7—10], but very little attention has been paid to their isolation and elucidation of their structure. Recently a detailed study of this aspect of the problem was undertaken by the authors and the complex compounds of trivalent rare-earths with an essential amino acid, L-aspartic acid were reported [11]. The present communication deals with the isolation and characterisation of rare earths with glutamic acid. These studies are based upon elemental analysis, molar conductance, thermogravimetric analysis, i. r., decomposition temperature and magnetic measurement.

Experimental

Freshly precipitated carbonate, prepared from their oxides (A. R. Koch — Light, London), were treated with aqueous solution of glutamic acid (A. R. B. D. H. England) in stoichiometric proportions with a slight excess of the carbonate. The mixture was stirred for an hour, filtered and the filtrate concentrated, mixed with a slight excess of ethanol and left for slow evaporation to obtain crystalline compounds which were dried in vacuum at room temperature for several days over P_2O_5.

The i. r. spectra were taken in the NaCl region in KBr pellets with a Beckman Spectrophotometer, model BK 56 (U. S. A.) between 2.5 and 16 μ. Thermolysis curves were recorded with a Stanton Thermobalance (U. K.) from 25 to 900°C in air with a heating rate of 6° per

minute. The molar conductances were measured with a Philips Conductivity Bridge, model PRI 500 (India) in conjunction with a dip type cell (cell factor 1.48), and the magnetic measurements were carried out at 27°C employing Faraday's method. The analyses for C, H and N were done by the Microanalytical Service I. I. T., Kanpur (India). Rare earths were determined as their oxalates [12]. No melting was observed up to 360°C. These compounds are extremely hygroscopic, they do not dissolve in common organic solvents but have high solubility in water. Table I gives elemental analyses and some characterising data about these compounds.

Results and discussion

Elemental analyses for carbon, hydrogen, nitrogen and rare-earths and thermogravimetric studies supported the formula $M(glut\text{-}H)_3 . 3\ H_2O$. The dehydration occurs between 124 and 205°C in all of these compounds as is evident from 8—9% approximate weight loss. After 205°C, the decomposition of the hydrated compounds starts and leads to the evolution of probably both carbon dioxide and carbon monoxide. The formation of stable oxides of rare-earths starts from around 650°C (La, Pr to Lu except Pm). In the case of cerium glutamate there is direct conversion to stable oxide CeO_2 from about 350°C with a 73% weight loss. In case of yttrium, the formation of Y_2O_3 is complete at 700°C. The removal of water molecules in the range of 125—205°C shows that all the three water molecules are coordinated to metal ions [13].

The magnetic moments in B. M. calculated after applying the diamagnetic correction for glutamic acid and the water molecules give the characteristic unequal double humped curve [14]. The molar conductances of $2.0 \times \times 10^{-4}$ *M* aqueous solutions of these compounds were of the order of 0.38 ± 0.1 mhos cm^2 and those of the corresponding trichlorides of rare earths more or less of the same magnitude and order but about 2.7 times higher than the corresponding glutamates. This is perhaps due to the ionic bonding between the metal and the amino acid. The slightly larger value for the rare earth salts might be due to the high ionic mobility of the chlorides as compared to that of large amino acid anions.

The peaks on the i. r. spectra of these complexes were compared with those of glutamic acid. The bands which throw some light on active coordinating abilities of amino acids are NH_3^+ sym and asym [15], COO^- sym and asym [16], and CN stretchings [17]. The NH_3^+ asym stretching vibrations of free glutamic acid appear as medium intensity bands at 1620 and 1520 cm^{-1}, respectively. On complexation, these bands disappeared. The COO^- sym vibration which occurs at 1420 cm^{-1} as medium intensity band in free acid is lowered by 15—20 cm^{-1} as a strong band on complexation in all the cases. However, the COO^- asym band occurring at 1640 cm^{-1} as medium intensity is of reduced intensity and appears in the form of a shoulder at 1635—1630 cm^{-1} in these compounds. The CN stretching vibrations present as a medium sharp intensity band at 920 cm^{-1} in glutamic acid showed a lowering of 30 to 50 cm^{-1} in the complexes. It is quite difficult to select between COO^- and NH_3^+ stretchings

Table I

Some characterising data

Compound	Carbon	Hydrogen	Nitrogen	Rare earth	Magnetic moment (B. M.)	Molar conductance	Colour
$Y(Glut)_3{*}3H_2O$	30.98 (30.90)	5.16 (5.20)	7.23 (7.20)	15.13 (15.20)	Diamag	0.37	Light yellow
$La(Glut)_3 3H_2O$	28.95 (28.40)	4.76 (4.81)	6.66 (6.72)	22.08 (22.15)	-do-	0.38	White
$Ce(Glut)_3 3H_2O$	28.47 (28.50)	4.77 (4.90)	6.65 (6.73)	22.15 (22.02)	1.98	0.38	Light pink
$Pr(Glut)_3 3H_2O$	28.44 (28.56)	4.74 (4.82)	6.64 (6.70)	22.12 (22.20)	3.42	0.38	White
$Nd(Glut)_3 3H_2O$	28.27 (28.32)	4.71 (4.32)	6.60 (6.70)	6.60 (6.70)	3.54	0.37	Pinkish white
$Sm(Glut)_3 3H_2O$	28.02 (28.00)	4.67 (4.70)	6.54 (6.66)	22.45 (22.50)	1.90	0.37	Dirty white
$Eu(Glut)_3 3H_2O$	27.96 (28.01)	4.66 (4.60)	6.52 (6.50)	23.59 (23.70)	3.78	0.37	White
$Gd(Glut)_3 3H_2O$	27.73 (22.90)	4.62 (4.68)	6.46 (6.42)	24.22 (24.30)	7.80	0.37	Dirty white
$Tb(Glut)_3 3H_2O$	27.66 (27.70)	4.61 (4.59)	6.45 (6.49)	24.42 (24.51)	9.38	0.38	White
$Dy(Glut)_3 3H_2O$	27.51 (27.60)	4.58 (4.68)	6.42 (6.48)	24.83 (24.73)	10.18	0.39	White
$Ho(Glut)_3 3H_2O$	27.40 (27.50)	4.57 (4.67)	6.39 (6.40)	25.10 (25.19)	10.22	0.38	White
$Er(Glut)_3 3H_2O$	27.31 (27.40)	4.56 (4.60)	6.37 (6.40)	25.45 (25.55)	9.25	0.39	White
$Tm(Glut)_3 3H_2O$	27.22 (27.30)	4.54 (4.58)	6.35 (6.39)	25.54 (25.43)	7.58	0.39	White
$Yb(Glut)_3 3H_2O$	27.07 (27.17)	4.51 (4.55)	6.31 (6.38)	26.01 (26.20)	4.50	0.39	White
$Lu(Glut)_3 3H_2O$	26.99 (27.02)	4.49 (4.52)	6.29 (6.34)	26.16 (26.24)	Diamag	0.37	White

* Glut = Glutamic acid-H, $C_5H_9O_4N-H$.
The observed values are given in parentheses.

as pertinent sites of coordination but generally in amino acids, coordination through COO^- groups takes place with normal change in the NH_3^+ stretching vibrations [18]. Moreover, glutamic acid being a dicarboxylic acid is prone to lose a proton from COOH (pKa $\sim$ 4.0) rather than NH_3^+ group (pKa$\sim$9.80).

In view of the above facts, it may safely be assumed that glutamic acid retained its 'zwitter ion' character in its complexes and the possibility of its

coordination through nitrogen is ruled out. The following structure may be assigned

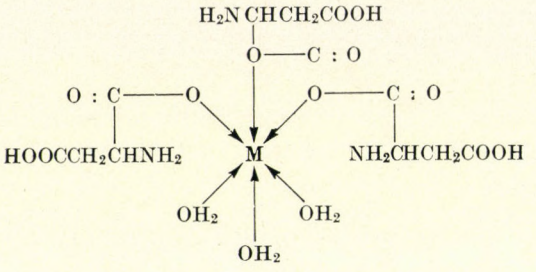

where M = rare earth ion.

*

The authors thank Prof. W. RAHMAN for providing facilities, to the C. S. I. R. New Delhi for the award of Senior Fellowship to one of them (O. F.) and to Prof. W. U. MALIK, Roorkee University, Roorkee for I. R. spectra.

REFERENCES

[1] PEIFFER, P., WARNER, H.: Z. Physiol. Chem., **246,** 212 (1937)
[2] LIFSCHITZ, I.: Proc. Acad. Sci. Amsterdam, **39,** 1192 (1937); *ibid.* Rec. Trans. Chim., **60,** 225 (1941)
[3] CHABERCK, S. Jr., MARTELL, A. E.: J. Am. Chem. Soc., **74,** 6021 (1952)
[4] LI, N. C., DOODY, E.: J. Am. Chem. Soc., **74,** 4184 (1952)
PERRIN, D. D.: J. Chem. Soc., **290** (1959)
[5] KROLL, H.: J. Am. Chem. Soc., **76,** 2034 (1954)
[6] VOLSHTEIN, L. M., MOTYAGVA, G. G., ANAKHOVA, L. S.: Zh. Neorgan Khim, **1,** 2328 (1956)
[7] RYBCHIKOV, D. I., TERENTEVA, E. A.: Izvest. Akad. Nauk S. S. S. R. Otdel Khim Nauk, **44,** (1944)
[8] BATYAEV, I. M., LARINOV, S. V., SHUL'MAN, V. M.: Zh. Neorgan. Khim., **6,** 53 (1961)
[9] CEFOLA, M., TOMPA, A. S., CELIANO, A. V., GENTILE, P. S.: Inorg. Chem., **1,** 290 (1962)
[10] KRISS, E. E.: Ukr. Khim Zh., **31,** 328 (1964)
[11] FAROOQ, O., AHMAD, N., MALIK, A. U.: Acta Chim. (Budapest) **83,** 343 (1974)
[12] SPENCER, J. F.: "The Metals of the Rare-Earths", p. 105 Longmans, London 1919
[13] MATHUR, B. S., SRIVASTAVA, T. S.: J. Inorg. Nucl. Chem., **32,** 3277 (1970)
[14] SELBIN, J., AHMAD, N., BHACCA, N.: Inorg. Chem. **10,** No. 7, 1383 (1971)
[15] BELLAMY, L. J.: "The Infrared Spectra of Complex Molecules", p. 238, Methuen, London 1954
[16] *ibid,* page 240
[17] KOEGEL, R. J., GREENSTEIN, J. P., WINITZ, M., BIRNBAUM, S. M., MCCALLUM, R. A.: J. Am. Chem. Soc., **77,** 5708 (1955)
[18] LENOMANT, H.: J. Chim. Phys., **43,** 327 (1946)
[19] NAKAMOTO, K.: "Infrared Spectra of Inorganic and Coordination Compounds", p. 156, Wiley, New York, 1963
[20] LUCCHESI, P. J., GLASSON, W. A.: J. Am. Chem. Soc., **78,** 1347 (1956)

Omar FAROOQ, Naseer AHMAD } Inorganic Research Laboratory, Chemistry Department, Aligarh Muslim University, Aligarh/U. P. India.

Acta Chimica Academiae Scientiarum Hungaricae, Tomus 85 (4), pp. 399—407 (1975)

INVESTIGATION OF ANODIC DISSOLUTION OF COPPER IN ANHYDROUS ACETIC ACID SOLUTIONS, III

THE COMBINED EFFECT OF CHLORIDE AND PERCHLORATE

L. KISS and M. L. VARSÁNYI

(Department of Physical Chemistry and Radiology, L. Eötvös University, Budapest)

Received July 10, 1974

The anodic dissolution of copper in anhydrous acetic acid containing chloride or chloride and perchlorate has been studied with rotating disc electrode.

Under the conditions described the anodic dissolution of copper proceeds in three steps, *viz.*:

1. $Cu + Cl^- \rightleftarrows CuCl_{ads} + e$
2. $CuCl_{ads} + Cl^- \rightleftarrows CuCl_{2(0)}^-$
3. $CuCl_{2(0)}^- \rightleftarrows CuCl_{2(\infty)}^-$

0 and ∞ refer to the surface of the electrode, respectively to the bulk of the solution. When the solvent contains only chloride reaction step 2 does not affect the process; when both chloride and perchlorate are present, it is reaction step 1 that is irrelevant.

In the previous communications [1, 2] we presented some results concerning the anodic dissolution of copper in anhydrous acetic acid containing lithium perchlorate (0.5 mole/dm^3), respectively lithium chloride (0.5 mole/dm^3). We have found that in both cases copper is oxidized to Cu(I) and that in the solvent which contains lithium perchlorate the rate of the process is determined by the diffusion of the Cu(I) ions, whereas in the presence of lithium chloride also transport polarization has its role. We have found, further, that in the solvent containing lithium chloride $CuCl_2^-$ complexes are formed.

No data could be found in the literature for the stability constants of these complexes formed in anhydrous acetic acid, so we have determined this constant. Further, we have studied the effect the variation of the concentration of chloride ions exerts upon the anodic dissolution of copper in anhydrous acetic acid. In this paper the results of these investigations are presented.

The experimental apparatus, the preparation of the electrode, the reagents, the dehydration of the solvent have been described in a previous paper [3]. The potentials given are referred to a calomel electrode in acetic acid [3]. Experiments were carried out at room temperature and in nitrogen atmosphere.

Determination of the stability constant

The known potentiometric method [4] was used for the determination of the stability constant K of the $CuCl_2^-$ complexes. K can be calculated from Eq. (1)

$$\Delta\varphi = \frac{RT}{zF} \ln K + \frac{n\,RT}{zF} \ln c_x \tag{1}$$

where

$$\Delta\varphi = \varphi_{M^{z+}/M} - \varphi_{MX_n/M} \tag{2}$$

$\varphi_{M^{z+}/M}$ is the equilibrium potential between the metal M and a solution containing the ion M^{z+} at a concentration of $c_{M^{z+}}$; $\varphi_{MX_n/M}$ is the equilibrium potential of metal M and a solution containing its complex MX_n at a concentration of c_{MX} and the ligand at a concentration of c_x when $c_{M^{z+}} = c_{MX}$ and c_x is in a large excess. According to Eq. (1), when plotted as a function of lg c_x $\Delta\varphi$ is a straight line the slope of which depends on the co-ordination number n for the given central ion of charge number z.

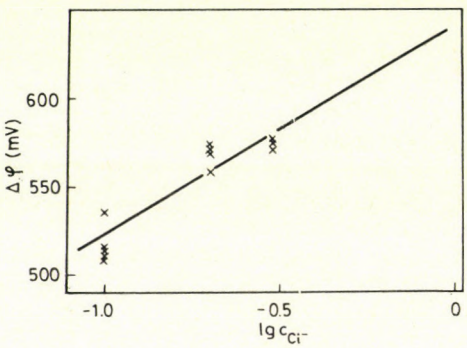

Fig. 1. The $\Delta\varphi$ *vs.* lg c_{Cl}-correlation, for solutions of c_{Cl}-mole/dm³ LiCl + (0.5 − c_{Cl^-}) mole/dm³ $LiClO_4$ in acetic acid

In our case $z = 1$, and, according to earlier studies [2], $n = 2$. To measure $\Delta\varphi$ a definite copper-ion concentration was produced, in a solution of 0.5 mole/dm³ $LiClO_4$ (no complexing agent present) respectively, in a solution of c_{Cl^-} mole/dm³ LiCl + (0.5 − c_{Cl^-}) mole/dm³ $LiClO_4$, by dissolving the copper electrode for a given time at a constant intensity of the electric current. In this case copper, as we found it also in separate measurements, dissolved as Cu(I). (The effective charge number is $n_e = 1$.) The equilibrium electrode potentials established by the copper ions gone into solution are easy to record, they do not change with time. $\Delta\varphi$ values were recorded for $c_{Cl^-} = 0.1$, 0.2, and 0.3; results are shown in Figure 1. The straight line is drawn with a slope of 118 mV, the value of constant a (the intersection with the ordinate) was determined according to the method of least squares. On the basis of the data in Fig. 1, lg $K = 10.85 \pm 0.2$ was found, this value can be made still more accurate by repeated measurements.

The effect of chloride ions on the anodic dissolution of copper

With a rotating copper disc electrode we studied the anodic dissolution of copper in anhydrous acetic acid containing c_{Cl^-} mole/dm^3 LiCl + (0.5 − − c_{Cl^-}) mole/dm^3 $LiClO_4$. c_{Cl^-} was varied between 0.05 and 0.4. The total electrolyte concentration has been kept constant to secure constant ion strength when chloride concentration is changed. First, polarization curves were plotted at various rotation speeds of the electrode. In Fig. 2, the correlation between

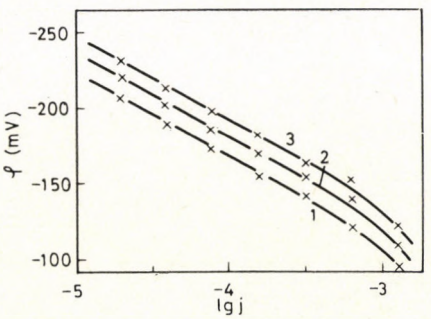

Fig. 2. Correlation between the potential of a rotating disc electrode and the logarithm of the anodic current density in solutions of 0.3 mole/dm^3 LiCl + 0.2 mole/dm^3 $LiClO_4$ in acetic acid. Rotation speeds of the electrode were 1. $f = 160$ min^{-1}, 2. $f = 610$ min^{-1}, 3. $f = 3070$ min^{-1}

electrode potential φ and current density j is shown, in the usual semi-logarithmic presentation, for three different r. p. m. of the electrode in a solution of 0.3 mole/dm^3 LiCl + 0.2 mole/dm^3 $LiClO_4$. $\varphi/\lg j$ is linear within two orders of magnitude of current density and with increasing speed of rotation the line is shifted towards more negative potentials. At higher current intensities deviations from the straight line occur, there is a shift of the values recorded towards more positive potentials. The foremost cause of this is the separation of CuCl on the surface, also a slight resistive potential drop may occur. Curves of this type were plotted in the solutions mentioned, at all the concentrations studied.

The Tafel-constant b for the straight section of the polarization curves was found between 55 and 65 mV, generally. This would suggest that the rate is determined by diffusion towards the solution of the Cu(I)-complex. Therefore we attempted the plotting of j as a function of $f^{1/2}$ at a constant electrode potential (f is the r. p. m. of the electrode) but then a straight line starting from the origin could not be obtained as expected for the case of diffusion overvoltage. Therefore, according to the method discussed in our previous paper [2], the experimental data were presented as a $\frac{1}{j}$ *vs.* $f^{-1/2}$ plot. Thus, as shown

in Fig. 3, the points give straight lines. When these lines, corresponding to various electrode potentials, are extrapolated to $f^{-1/2} = 0$ then $1/j$ values are pointed out by the intersections on the ordinate; on the basis of these values a polarization curve can be drawn, as shown earlier, and this curve does not show the effect of diffusion [2].

The φ *vs.* $\lg j_0$-functions corresponding to various chloride concentrations, when plotted in the manner just explained, give straight lines (*cf.* Fig. 4).

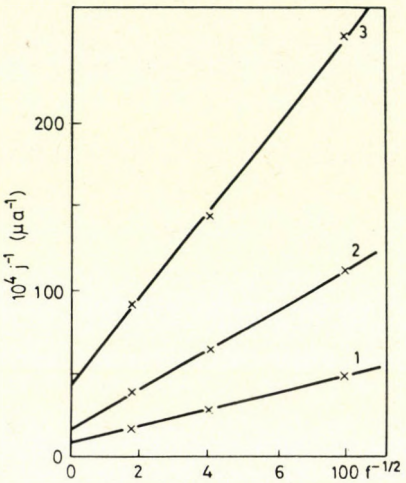

Fig. 3. Correlation between j^{-1} and $f^{-1/2}$ at a constant electrode potential, for solutions of 0.3 mole/dm^3 LiCl + 0.2 mole/dm^3 $LiClO_4$ in acetic acid. 1. $\varphi = -150$ mV, 2. $\varphi = -170$ mV, 3. $\varphi = -190$ mV

These are shifted towards negative potentials when chloride ion concentration is increased. From data in Fig. 4 the correlation between $\lg j_0$ and $\lg c_{Cl^-}$ corresponding to a given potential ($\varphi = -130$ mV) can be described. Fig. 5 contains the data thus arrived at, these give a straight line the slope of which indicates the order of reaction ν_{Cl^-} in respect to chloride. This slope, according to Fig. 5, is 2.28, *i.e.* $\nu_{Cl^-} \simeq 2$.

However, in the case of transfer polarization ($z = 1$, $\alpha = 0.5$) the slope of the polarization curves determined for solutions which contain LiCl and $LiClO_4$ (*cf.* Fig. 4) is 56 mV instead of 118 mV as expected.

We think the experimental results obtained can be explained by the following reactions:

$$1.\ Cu + Cl^- \underset{k_k}{\overset{k_a}{\rightleftharpoons}} CuCl_{(ads)} + e$$

$$2.\ CuCl_{(ads)} + Cl^- \underset{k_{r2}}{\overset{k_{r1}}{\rightleftharpoons}} CuCl^-_{2(0)}$$

$$3.\ CuCl^-_{2(0)} \longrightarrow CuCl^-_{2(\infty)}$$

where $CuCl_{(ads)}$ stands for CuCl adsorbed on the surface of the electrode: we suppose that only a slight part of the surface is covered (the straight section of the polarization curve). $CuCl_{2(0)}^-$ and $CuCl_{2(\infty)}^-$ are concentrations of the given complex on the surface of the electrode, and in the bulk of the solution respectively. Because LiCl exists in anhydrous acetic acid solvent largely undissociated, presumably as ionpairs, in all reactions Cl^- reprecents undissociated LiCl.

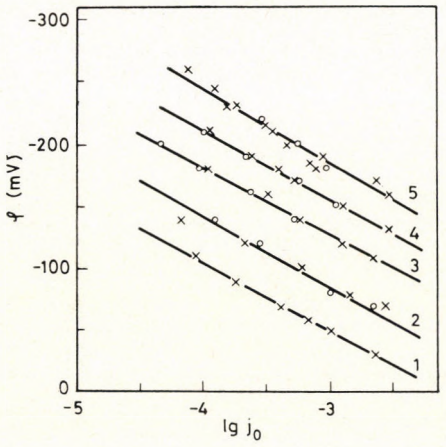

Fig. 4. Correlation between φ and $\lg j_0$ for solutions of c_{Cl^-} mole/dm³ LiCl + (0.5 − c_{Cl^-}) mole/dm³ $LiClO_4$ in acetic acid. j_0 is the current density belonging to $f^{-1/2} = 0$ 1. $c_{Cl^-} = 0.05$, 2. $c_{Cl^-} = 0.1$, 3. $c_{Cl^-} = 0.2$, 4. $c_{Cl^-} = 0.3$, 5. $c_{Cl^-} = 0.4$. The curve drawn in the broken line corresponds to $c_{Cl^-} = 0.5$ mole/dm³

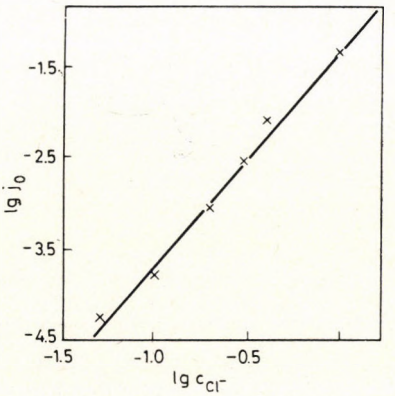

Fig. 5. Correlation between $\lg j_0$ values belonging to $\varphi = -130$ mV and the logarithm of the concentration of chloride ions

According to this, the first step is the electrochemical process proper, *i.e.* the charge transfer, the second is a chemical reaction, and the third is the diffusion. For these steps the relevant rate constants are noted.

When stationary state is reached the rate of the consecutive reactions will be the same, thus for the first, the electrochemical process we can write

$$j = k_a c_{Cl^-} - k_k c_{CuCl_{ads}} \tag{3}$$

where

$$k_a = k'_a \exp \frac{\alpha F \varphi}{RT} \tag{4}$$

$$k_k = k'_k \exp \left[- \frac{(1 - \alpha) F \varphi}{RT} \right] \tag{5}$$

k'_a and k'_k are constants; α is the anodic transfer coefficient, the other notations are as usual.

For the second, the chemical process we can write

$$j = k_{r_1} c_{\mathrm{CuCl_{ads}}} c_{\mathrm{Cl^-}} - k_{r_2} c_{\mathrm{CuCl_{2(0)}^-}} \tag{6}$$

and for the diffusion we have

$$j = X(c_{\mathrm{CuCl_{2(0)}^-}} - c_{\mathrm{CuCl_{2(\infty)}^-}}) \tag{7}$$

where, in the case of a rotating disc electrode

$$X = 0.62\ FD^{2/3}\nu^{-1/6}\omega^{1/2}. \tag{8}$$

D is the diffusion coefficient of the $CuCl_2^-$ complex, ω is the angular velocity of the rotating electrode, $\omega = \frac{2\pi}{60} f$, if f is the speed of rotation in min^{-1}; ν is the kinematic viscosity of the solution. c_i stands for the concentration of a given component i at the electrode surface, and in the solution, respectively.

In the course of our experiments the concentration of the complex in the solution was practically zero, or $c_{\mathrm{CuCl_{2(\infty)}^-}} = 0$. With this in mind, and based upon Eqs (3), (6) and (7), the non-measurable concentrations at the electrode surface may be eliminated and for current density the following equation can be written

$$j = \frac{\frac{k_a}{k_k} k_{r_1} c_{\mathrm{Cl^-}}^2}{1 + \frac{k_{r_1}}{k_k} c_{\mathrm{Cl^-}} + \frac{k_{r_2}}{X}}. \tag{9}$$

Therefrom

$$\frac{1}{j} = \frac{1 + \frac{k_{r_1}}{k_k} c_{\mathrm{Cl^-}}}{\frac{k_a}{k_k} k_{r_1} c_{\mathrm{Cl^-}}^2} + \frac{k_{r_2}}{\frac{k_a}{k_k} k_{r_1} c_{\mathrm{Cl^-}}^2} \frac{1}{X}. \tag{10}$$

According to Eq. (10), there is a linear correlation between $1/j$ and $f^{-1/2}$ when the reaction pathway consists of steps 1, 2 and 3, in this sequence (*cf.* Eq. (8)), and the intersection j_0 is determined by the first term of the right hand side of Eq. (10)

$$j_0 = \frac{k_a}{k_k} \frac{k_{r_1} c_{\mathrm{Cl^-}}^2}{1 + \frac{k_{r_1}}{k_k} c_{\mathrm{Cl^-}}}. \tag{11}$$

In consequence (*cf.* Eqs (4) and (5)) the correlation between φ and $\lg j_0$ will give a straight line with a slope $\sim$60 mV when $k_{r_1} \ll k_k$. The figure $\simeq$56 mV (*cf.* Fig. 4) is in good agreement with this. On the basis of the φ *vs.* $\lg j_0$ lines plotted for solutions which contain various amounts of chloride, the order of reaction (*cf.* Fig. 5) in respect to chloride is $\nu_{Cl^-} = 2$. Also this is possible only if $k_{r_1} \ll k_k$, and thus, according to Eq. (11), the order of reaction in respect to chloride is 2. This means at the same time that the rate (exchange current)

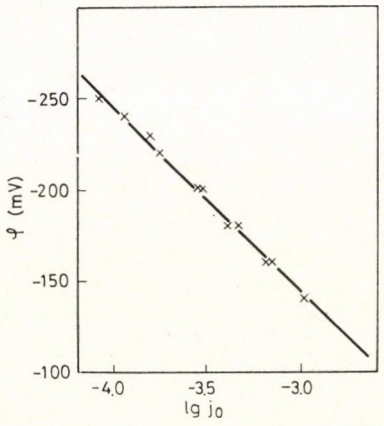

Fig. 6. Correlation between φ and $\lg j_0$ in solutions of 0.3 mole/dm^3 LiCl in acetic acid

of process 1 is great and that, practically, this step may be held as in equilibrium, and the rate of the process to be determined by the chemical reaction step 2. Consequently

$$j_0 = \frac{k'_a}{k'_k} k_{r_1} c^2_{Cl^-} \exp\left(\frac{F\varphi}{RT}\right). \tag{12}$$

According to data published in earlier papers [2], the slopes of straight lines plotted for φ *vs.* $\lg j_0$ in anhydrous acetic acid solutions of 0.5 mole/dm^3 LiCl was much greater (92 mV) than the figure found, and mentioned before, for solutions of LiCl + $LiClO_4$. Therefore we determined the correlation between φ and $\lg j_0$ in the case of a solution which contained only 0.3 mole/dm^3 of LiCl. Results of these tests are to be seen in Fig. 6. The slope also in this case is great (99 mV). From these two tests (with 0.5 mole/dm^3, and 0.3 mole/dm^3 of the chloride) an approximative, informative figure for the order of reaction of the chloride can be calculated, $\nu_{Cl^-} \simeq 1$. (Ion strength can change considerably in this case.) Therefrom, and from the slope of the φ *vs.* $\lg j_0$ curves we obtain that in the absence of ClO_4^- $k_{r_1} \gg k_k$, thus from Eq. (11) it follows that

$$j_0 = k_a c_{Cl^-} = k'_a c_{Cl^-} \exp\left(\frac{\alpha F\varphi}{RT}\right). \tag{13}$$

Our experimental findings thus suggest that $LiClO_4$ is not an indifferent electrolyte for anodic dissolutions in acetic acid containing LiCl, but that the addition of $LiClO_4$ decreases the rate constant k_{r_1} (or increases k_k). In Fig. 4 the broken line shows the correlation between φ and $\lg j_0$ in a 0.5 mole/dm^3 solution of LiCl.

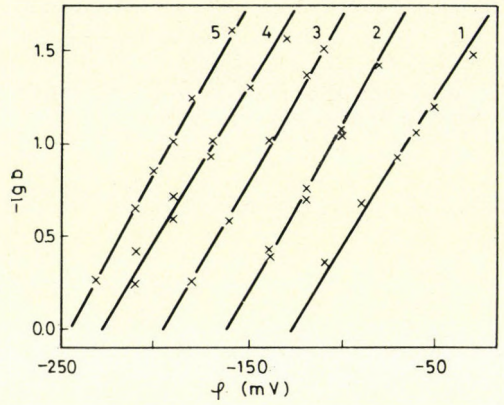

Fig. 7. Correlation between $-\lg b$ and φ at constant concentrations of chloride. 1. $c_{Cl^-} =$ $= 0.05$, 2. $c_{Cl^-} = 0.1$, 3. $c_{Cl^-} = 0.2$, 4. $c_{Cl^-} = 0.3$, 5. $c_{Cl^-} = 0.4$

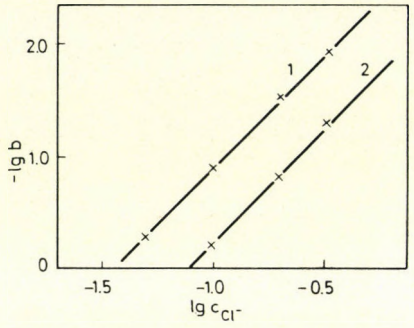

Fig. 8. Correlation between $-\lg b$ and $\lg c_{Cl^-}$ at constant electrode potentials. 1. $\varphi =$ $= -110$ mV, 2. $\varphi = -150$ mV

For a further comparison of Eq. (10) with the experimental data we studied how the slope b of the straight lines j^{-1} *vs.* $f^{-1/2}$ is affected by the potential, respectively by the concentration of the chloride. On the basis of Eq. (10)

$$-\lg b = A + 2 \lg c_{Cl^-} + \frac{2 \cdot 3 F \varphi}{RT} \tag{14}$$

where

$$A = \lg \frac{k'_{a_1} k_{r_1}}{k'_{k_1} k_{r_2}} 0.62 F D^{2/3} \nu^{-1/6} \left(\frac{2\pi}{60}\right)^{1/2}.$$

According to this, at a constant concentration of chloride, a linear correlation should exist between $-\lg b$ and φ, and at a constant potential a linear correlation should exist between $-\lg b$ and $\lg c_{Cl^-}$. Figures 7 and 8 show that, indeed, straight lines result, and that, in accord with Eq. (14),

$$\left(\frac{-\partial \lg b}{\partial \varphi}\right)_{c_{Cl^-}} \simeq + \frac{1}{60} \text{ mV}^{-1}$$

and

$$\left(\frac{-\partial \lg b}{\partial \lg c_{Cl^-}}\right)_{\varphi} \simeq 2.2.$$

When potentials are shifted towards the positive values the curve plotted for $-\lg b$ *vs.* $\lg c_{Cl^-}$ are shifted towards higher $-\lg b$ figures.

Thus, according to experimental findings, when copper is anodically dissolved in anhydrous acetic acid which contains chloride, or chloride and perchlorate, this dissolution proceeds along the pathway that consists of steps 1 to 3. If the solvent contains chloride only, the rate of diffusion is commensurable with that of step 1, when also perchlorate is present, the rate of diffusion is commensurable with that of the chemical process 2.

REFERENCES

[1] KISS, L., VARSÁNYI, M. L.: Magy. Kém. Foly., **80**, 29 (1974), Acta Chim. (Budapest) **81**, 61 (1974)
[2] KISS, L., VARSÁNYI, M. L.: Magy. Kém. Foly., **80**, 225 (1974), Acta Chim. (Budapest) **83**, 165 (1974)
[3[KISS, L., DO NGOC LIEN, VARSÁNYI, M, L.: Annales Univ. Sci. Budapestinensis, Sect. Chim., **12**, 145 (1971)
[4] KRAWTZOW, W. I.: Electrodnye Processi v Rastworach Komplexow Metallov. — Izd. LGU, 1969, p. 26

László KISS
L. Magda VARSÁNYI
1088 Budapest, Puskin u. 11—13. Hungary.

Acta Chimica Academiae Scientiarum Hungaricae, Tomus 85 (4), pp. 409—415 (1975)

O-HYDROXY-4-BENZAMIDOTHIOSEMICARBAZIDE AS A CHELATING REAGENT, IV

MAGNETOSPECTRAL STUDIES ON ITS Ti(III), V(IV), Fe(II), Pd(II), Ce(III) AND U(VI) COMPLEXES

M. P. SWAMI, P. C. JAIN*, V. B. RANA, S. K. SAHNI and A. K. SRIVASTAVA**
(School of Chemistry, Meerut College, Meerut, India)

Received June 31, 1974

Complexes of *o*-hydroxy-4-benzamidothiosemicarbazide with titanium(III), oxovanadium(IV), iron(II), palladium(II), cerium(III) and uranium(VI) have been isolated and characterized by analyses, conductometric, magnetic susceptibility, electronic and infrared spectral measurements. Uranium(VI) complex exhibits temperature independent paramagnetism. The explanation for a slightly lower value of magnetic moment for the vanadium(IV) complex has been sought in the possible presence of a metal-metal link in this complex. The i. r. studies reveal the tridentate nature of the ligand, bonding occurring through phenolic oxygen, thioketonic sulphur and amido nitrogen. The palladium(II) complex is square-planar while all other complexes possess octahedral stereochemistry.

Introduction

In the earlier communications [1—4], *o*-hydroxy-4-benzamidothiosemicarbazide (OH-BTSC) has been reported as a chelating reagent for many transition metal ions since it has amido nitrogen, thioketo sulphur and phenolic oxygen ideally situated for coordination. The present paper deals with isolation, magnetic, electronic and infrared spectral studies of the complexes of titanium(III), vanadium(IV), iron(II), palladium(II), cerium(III) and uranium(VI).

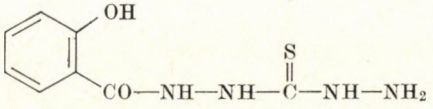

Experimental

The ligand was synthesized by the method of VARMA [5]. Analytical grade reagents were used throughout. Palladium(II) chloride was a Johnson Mathey product. Elemental analyses were done at the microanalytical division I. I. T. Kanpur-208016 (India). Magnetic measurements on powders of the complexes

* Address for correspondence — 729/1, Begum Bagh, Meerut-250001 (India).
** Instituto Di Chimica Universita Di Roma, Rome.

were made at room temperature employing Gouy's technique and using $Hg[Co(CNS)_4]$ as calibrant. Electronic spectral measurements were carried out on a Hilger-Uvispek spectrophotometer in ethanol solution. The infrared spectra were recorded on a Perkin Elmer spectrophotometer 137 B in KBr pellets. A Toshniwal conductivity bridge type CL01/01 using dip type electrodes was employed for conductance measurements. Elico pH meter model LI-100 was used for pH measurements.

Isolation of the complexes

For the preparation of the complexes titanium(III) chloride, vanadyl chloride, iron(II), chloride, palladium(II) chloride, cerium(III) ammonium nitrate and uranyl nitrate were used.

25 ml of an ethanol solution of (0.5 *M*) metal salt was added to 75 ml of an equimolar ethanol solution of OH-BTSC, coloured precipitates separated in all the cases, for palladium(II) and vanadium(IV) however, only at an appropriate pH. The precipitates were digested, filtered and washed with acetone and ether. They were dried at 70°C in an electrical oven.

In the case of vanadium(IV) a green colour was first obtained which later changed to blue. On refluxing the reaction mixture a greenish-blue mass separated which was treated similarly. Palladium(II) yielded a yellowish-brown precipitate on refluxing which was filtered off, washed separately with ethanol and ether and dried. pH of the isolation and colour of the final products are given in Table II. The percentage of water of crystallization in the complexes was determined by finding out the loss in their weights on heating at 110°C.

Results and discussion

The conductance measurements in dimethylformamide reveal non-electrolytic nature of all the complexes but of Ti(III) and Ce(III) complexes which are uni-univalent in character [6, 7].

Electronic spectral studies

All octahedral complexes of Ti(III) have an absorption band at 20 000 cm^{-1} assigned to $^2T_{2g} \rightarrow {}^2E_g$. Very often a shoulder on the low energy side of this band has been observed which is attributed to Jahn-Teller distortion affecting the ^2E_g excited state. The bands observed in the present complex at 15 820 cm^{-1} and 15 010 cm^{-1} have been assigned to the transition from $^2B_{2g}$ to $^2B_{1g}$ and to $^2A_{1g}$, respectively. The other band at 30 220 cm^{-1} may be a charge-transfer band.

Table I

Analytical, magnetic and conductance data

Complex	%	C	H	N	S	Cl/H_2O	Metal	$\Lambda_m X10^{-3}$ in DMF solution $Ohm^{-1}cm^{-1}$ $mole^{-1}$	μ_{eff} B. M.
$[Ti(C_8H_9N_4O_2S)_2]Cl$	F	34.50	3.28	20.20	11.78	6.52	17.46	85.2	1.70
	R	35.80	3.57	20.90	11.90	6.64	18.00		
$[(VO)_2(C_8H_9N_4O_2S)_2(OH)_2]H_2O$	F	30.40	3.27	16.98	9.80	2.74	15.88	37.4	1.40
	R	30.19	3.45	17.61	10.00	2.80	16.03		
$[Fe(C_8H_9N_4O_2S)_2].3H_2O$	F	33.80	4.10	19.87	11.10	9.52	9.87	34.7	4.80
	R	34.28	4.28	20.00	11.43	9.68	10.00		
$[Pd(C_8H_9N_4O_2S)(OH)].4H_2O$	F	22.84	4.51	13.04	7.48	16.80	24.87	43.2	Diamagnetic
	R	22.85	4.28	13.13	7.85	17.14	25.25		
$[Ce(C_8H_9N_4O_2S)_2](NO_3).H_2O$	F	28.10	2.79	18.62	9.18	2.68	20.45	81.5	2.21
	R	28.66	2.98	18.80	9.55	2.60	20.89		
$[UO_2(C_8H_9N_4O_2S)(NO_3)].2H_2O$	F	16.01	2.00	10.96	5.21	5.98	39.52	35.8	0.60
	R	16.18	2.19	11.78	5.39	5.07	40.03		

Table II

Electronic spectral bands and their assignments

Complex	pH	Colour	Bands	Assignments
$[Ti(O\text{-}BTSC)_2]$ Cl	4.0	Orange-brown	15010	$^2B_{2g} \rightarrow {}^2A_{1g}$
			15820	$\rightarrow {}^2B_{1g}$
			30220	charge-transfer
$[(VO)_2(O\text{-}BTSC)_2(OH)_2]H_2O$	9.0	Greenish-blue	13250	$e_g \rightarrow b_{2g}$
			16980	$\rightarrow a_{1g}$
			24950	$\rightarrow b_{1g}$
$[Fe(O\text{-}BTSC)_2] \cdot 3H_2O$	4.0	Brownish-red	10120	$^5T_{2g} \rightarrow {}^5E_g$
			9510	
$[Pd(O\text{-}BTSC)(OH)] \cdot 4H_2O$	9.5	Yellowish-brown	16400	$^1A_{1g} \rightarrow {}^1A_{2g}$
			18380	$\rightarrow {}^1B_{1g}$
			26540	$\rightarrow {}^1E_{1g}$
			35300	$\rightarrow {}^1A_{2u}$ charge-
			45000	$\rightarrow {}^1E_{2u}$ transfer
$[Ce(O\text{-}BTSC)_2]NO_3 \cdot N_2O$	3.9	Brownish	21720	$4f^2 \rightarrow 4f'5d'$
			23155	
			31745	
			45415	$^5F_{5/2} \rightarrow {}^2D_{3/2}$
			47590	$\rightarrow {}^2D_{5/2}$
$[UO_2(O\text{-}BTSC)(NO_3)] 2H_2O$	4.1	Brownish-yellow	32140	charge-transfer
			33450	
			40000	

In general, three absorption bands have been observed in the spectra of oxovanadium complexes in the spectral region 11 000—16 000 cm^{-1} (band I), 14 000—19 000 cm^{-1} (band II) and 21 000—30 000 cm^{-1} (band III) when the molecule is tetragonally distorted from regular octahedral symmetry [8]. The third band is not always observed, being often overlapped, by a charge-transfer band and whenever it has been observed it is generally a shoulder. The present complex shows three bands appearing at 13 250 cm^{-1} ($e_g \rightarrow b_{2g}$), 16 980 cm^{-1} ($e_g \rightarrow a_g$) and 24 950 cm^{-1} ($e_g \rightarrow b_{1g}$). The third band has, however, been obtained as a shoulder. Tetragonal radial parameters D*t* and D*s* have been evaluated to be −831 cm^{-1} and 3031 cm^{-1}, respectively. The value of 10 D*q* is 11 700 cm^{-1}. The negative value of D*t* refers to weak σ-donating ability but still more than π-donating ability since D*q* and D*s* both are positive.

Only one absorption band is expected in the electronic spectra of octahedral iron(II) complexes which has been assigned to $^5T_{2g} \rightarrow {}^5E_g$. In the present case, however, two bands at 10 120 cm^{-1} and 9510 cm^{-1} have been observed which are the splittings of double structure of the octahedral band.

This degeneracy of the ^5E_g state may possibly be due to Jahn-Teller distortion. For iron(II), the excited state is also orbitally degenerate and thus the doubling of the band is expected. The theoretical estimation of this splitting is a tough task even if several approximations are made. The doublet separation 8/3 $d\sigma$ and this qualitatively yields information about the differences in σ-antibonding effects of the ligands [9]. The value of $10Dq$ is 10 120 cm^{-1}.

The electronic spectrum of the palladium complex closely resembles that of $PdBr_4^{2-}$ which has a square-planar stereochemistry. Of the five bands, the first three are spin-allowed d–d transitions corresponding to one electron jumps:

$$b_{2g}(\pi^*) \rightarrow b_{1g}(\sigma^*) \ (^1A_{1g} \rightarrow {}^1A_{2g}) \ (16\,400\ cm^{-1})$$
$$a_{1g}(\sigma^*) \rightarrow b_{1g}(\sigma^*) \ (^1A_{1g} \rightarrow {}^1B_{1g}) \ (18\,380\ cm^{-1})$$
$$e_g(\pi^*) \rightarrow b_{1g}(\sigma^*) \ (^1A_{1g} \rightarrow {}^1E_g) \ (26\,040\ cm^{-1})$$

The other two bands at 35 300 cm^{-1} and 45 000 cm^{-1} may be due to charge-transfer. The theoretical model of GRAY and BALLHAUSEN [10] showed two distinct types of charge-transfer bands in square-planar complexes: ligand (π) → metal (type I), and metal → ligand a_{2u} (π-type II). The ligand (π) to metal type complexes will have two bands spaced by $\sim$10 000cm^{-1}, as observed in $PdBr_4^{2-}$ and $PdCl_4^{2-}$ where as M → L type will have three closely spaced transitions. Therefore, in any case the spacing of the two orbitally allowed charge-transfer bands can form the basis for the distinction between L → M or M → L transitions. The two allowed charge-transfer bands observed in the present complex, which are spaced by 9700 cm^{-1}, may be placed in type I.

$$b_2u(\pi) \rightarrow b_{1g}(\sigma^*) \ (^1A_{2g} \rightarrow A2u) \ (35\,300\ cm^{-1})$$
$$e_u(\pi^*) \rightarrow b_{1g}(\sigma^*) \ (^1A_{1g} \rightarrow {}^1E_u) \ (45\,000\ cm^{-1})$$

The utility of absorption spectra in ascertaining the nature of the band between the lanthanide ion and the surrounding donor group is limited. The observed bands are due to the transitions within the $4f$ levels, which are least affected by changes in the environment and, therefore, there is substantial identity on the absorption spectra of the ion whether it is solvated or associated with any chelating group. However, small splittings of the characteristic bands are due to crystal field effects on J levels of the central ion [11, 12]. Of the five bands observed in the spectra of Ce(III) complex three are Laporte-allowed transitions and can be assigned as $4f^2 \rightarrow 4f^15d^1$. The other two bands have been assigned as $^5F_{5/2} \rightarrow {}^2D_{3/2}$ and $^5F_{5/2} \rightarrow {}^2D_{5/2}$.

The absorption spectra of uranium(VI) complex exhibit three bands in the ultraviolet region all being charge-transfer bands from ligand to metal. No d–d transitions are expected in this case.

Magnetic studies

Ti(III) having electronic configuration $3d^1$ is expected to give the magnetic moment values of one unpaired electron. In present case the magnetic moment for Ti(III) complex was found to be 1.70 B. M. which is in fair agreement with other octahedral complexes of Ti(III). The normal magnetic moment for the oxovanadium(IV) complexes when the orbital contribution is completely quenched, as is the case with low symmetry fields, is 1.73 B. M. There are, however, a few exceptions [13, 14]. The value of the magnetic moment (1.40 B. M.) for the complex under study is sufficiently low and has been attributed to the possible metal-metal interaction besides several other causes [15, 16].

The magnetic moment of an iron(II) spin-free complex in an octahedral environment should be about 5.5 B. M. at 300°K. The magnetic moment for the present complex is 4.8 B. M. which may presumably be due to deviation from regular octahedral symmetry or the electron delocalization [17].

In the case of Ce(III) complex the observed magnetic moment (221 B. M.) being close to other cerium(III) complexes reported in literature [11]. The '*f*' electrons of lanthanide ions are shielded from the perturbing effect of the ligands by the outer lying *s* and *p* electrons. Therefore, a behaviour similar to the gaseous ion has been observed.

The magnetic measurements reveal a temperature independent paramagnetism in case of uranium(VI) complex ($\mu_{eff} = 0.60$ B. M.) which is in fair agreement with other complexes of uranium(VI) reported in the literature [18]. As anticipitated the palladium(II) complex is diamagnetic.

Infrared studies

The absorption band at 3560 cm^{-1} in OH-BTSC is obviously due to phenolic group of the ligand. This band has disappeared from the spectra of the complexes indicating thereby that phenolic oxygen is bonded to the metal ion.

The absorption peaks due to the amide group and NCO deformation have not undergone much change because these absorption bands are influenced by other vibrational modes too. However, the lowering that has occurred on complexation indicates the involvement of amido nitrogen in the bond formation.

It is very well established that the coordination of sulphur atom to the metal ion would result in the decrease of the stretching frequencies of C=S because of the weakening of C=S bond due to the drainage of electrons towards the metal ion. However, as the vibration is affected by other vibrational modes not much change is expected. The slight changes in the position and nature of the absorption bands at 1309 cm^{-1} and 771 cm^{-1} assigned to C=S have been

taken as evidence for coordination [19]. The bands observed in the i. r. spectra of vanadium(IV) and uranium(VI) complexes at 964 cm^{-1} and 939 cm^{-1}, respectively, may be considered diagnostic of the presence of V–O and U–O multiple bonds. The ionic nitrates usually show a weak forbidden vibration in the region of 1050 cm^{-1} besides other vibrational modes. This has been attributed to deformation of the ion in the field of the crystal [20, 21]. In cerium(III) complex a weak absorption band has been observed at 1057 cm^{-1} which may be assigned to this vibration.

The coordinated nitrato complexes show characteristic frequencies in the regions 1531—1481 (ν_4) 1290—1253 (ν_1), 1034—970 (ν_2) and 805—781 cm^{-1} (ν_6) [20, 21]. The frequency ν_2, corresponding to one of the frequencies of nitrate group, which is forbidden for the trigonally symmetric NO_3 ion, appears as a strong absorption in the nitrato complexes, as the symmetry is now reduced. The strong band appearing at 1027 cm^{-1} in the uranyl complex may be assigned to coordinated nitrato group. In the present case other vibrations *e.g.*, ν(CN), (NH) rock and ν(CS), also appear in the regions of ν_4, ν_1 and ν_6.

*

One of the authors (VBR) is thankful to U. G. C., New Delhi for financial assistance

REFERENCES

[1] SWAMI, M. P., RASTOGI, D. K., JAIN, P. C., SRIVASTAVA, A. K.: Israel J. Chem. 2, 653—58 (1971)
[2] *Idem*: Acta Chim. Hung. (in press)
[3] SWAMI, M. P., JAIN, P. C., SRIVASTAVA, A. K.: Curr. Sci. **42** (6), 199—200 (1973)
[4] *Idem*: Roezki Chemii. Ann. Soc. Chim. Polonurum (in press)
[5] VARMA, R. S.: J. Indian Chem. Soc. **43** (8), 558 (1966)
[6] SEARS, P. G., WILHOIT, E. D., DANSON, R. L.: J. Phys. Chem. **59,** 373 (1959)
[7] QUAGLIANO, J. V. *et al.*: J. Am. Chem. Soc. **83,** 3770 (1961)
[8] SELBIN, J., MORPURGO, L.: J. Inorg. Nucl. Chem. **27,** 673 (1965)
[9] LEVER, A. B. P.: Inorganic Electronic Spectroscopy, Elsevier (N. Y.) (1968)
[10] GRAY, H. B., BALLHAUSEN, C. J.: J. Am. Chem. Soc. **85,** 260 (1963)
[11] JORGENSEN, C. K.: Progress in Inorg. Chem. **4,** 73 (1962)
[12] *Idem*: Z. Naturf. **19**w, 424 (1964)
[13] ZELENTSOV, V. V.: Dokl. Akad. Nauk SSSR **139,** 1110 (1961)
[14] *Idem*: Russ. J. Inorg. Chem. **7,** 670 (1962)
[15] NIGAM, H. L., KANTH, K. M., PANDEYA, K. B.: Indian J. Chem. **11** (10), 1031 (1973)
[16] NAKAMOTO, K.: Infrared Spectra of Inorganic and Coordination Compounds. Wiley, N. Y. 1963
[17] COTTON, F. A.: Progress in Inorganic Chemistry Vol. 6. Intersience N. Y. 1964 p. 176
[18] NIGAM, H. L., MATHUR, V. K., SRIVASTAVA, S. C.: Bull. Chem. Soc. Japan **36** (12), 1658 (1963)
[19] YAMAGUCHI, A., PENDLAND, R. B., MIZUSHIMA, S., LAME, R. T. J., CURAN, C., QVAGLIANO, J. V.: J. Amer. Chem. Soc. **80,** 527 (1958)
[20] GATEHOUSE, B. M., LIVINGSTONE, S. E., NYHOLM, R. S.: J. Chem. Soc., **4222** (1957)
[21] *Idem*: J. Inorg. Nucl. Chem. **8,** 75 (1958)

M. P. SWAMI
P. C. JAIN
V. B. RANA
S. K. SAHII
A. K. SRIVASTAVA
729/1, Begum Bagh, Meerut-250001 (India).

Acta Chimica Academiae Scientiarum Hungaricae, Tomus 85 (4), pp. 417—435 (1975)

INFLUENCE OF CYCLIC STRUCTURE ON THE RADIOLYSIS OF HYDROCARBONS, III

RADIOLYSIS OF CYCLOPROPANE, CYCLOBUTANE AND CYCLOBUTENE

Zs. Horváth and G. Földiák

(Institute of Isotopes, Hungarian Academy of Sciences)

Received August 18, 1974

Except for a few recent papers, the radiation chemistry of cyclopropane, cyclobutane and cyclobutene has not been investigated.

The authors have established that the $G(H_2)$ values of cyclobutane and cyclobutene are extraordinarily low as compared with those of the corresponding aliphatic alkanes and higher cycloalkanes; their values are near to the $G(H_2)$ values of propene and butene, respectively, as well as to those of higher cycloalkenes.

The values of G(fragment) of cyclic C_3 and C_4 hydrocarbons are considerably higher than those of $G(H_2)$. A marked tendency to ring opening can be observed in three- and four-membered carbon rings as compared with higher cycloalkanes and cycloalkenes. Thus, owing to the high strain energy, a higher fraction of the radiation energy is used for ring fission than for hydrogen elimination. The results show that the molecular structure plays a decisive but complex role in radiation chemical reactivity; *e.g.* cyclobutane is more reactive than cyclobutene and cyclopropane although the latter compounds possess higher strain energies.

Introduction

Literature data show that until recently, the main subjects of studies on hydrocarbon radiolysis were aliphatic alkanes and alkenes. At the same time, of cyclic hydrocarbons, mainly C_5 and C_6 compounds have been investigated.

Our studies are part of a research project to be carried out in this Institute, the main purpose of which is to elucidate correlations between molecular structure (*e.g.* ring dimension) and radiation chemical processes, including the study of the influence of physico-chemical parameters such as bond energies, strain energies, etc.

1. Literature survey

Systematic investigations in the field of the radiolysis of hydrocarbons have been extended recently by Wojnárovits *et al.* [1, 2, 3] to the γ-radiolysis of practically all available aliphatic and cyclic C_5–C_{12} hydrocarbons which are liquids at room temperature. By determining the distribution of stable products, the ratio of C–H and C–C bond fissions was evaluated for individual hydrocarbons. It has been established that, while no appreciable

Table I/a

Values of G(product) from C_3 hydrocarbons

Starting hydrocarbon	Propane			
Reference	[5, 6]	[7]	[7]	[8]
Type of radiation	$^{60}Co, \gamma$	$^{60}Co, \gamma$	$^{60}Co, \gamma$	γ
Conditions of irradiation	gas, 25°C	gas, 35°C	liquid, 35°C	liquid
Dose, eV g^{-1}	$0.6-2\times10^{21}$	6.7×10^{19}	6.7×10^{19}	
Hydrogen	1.00			4.3
C_1 Methane	0.27	1.4	0.75	1.2
C_2 Ethane	0.32	2.2	0.50	0.9
Ethylene	0.04	1.0	0.66	
Acetylene		0.31	0.09	
C_3 Propane				
Propene	0.04	2.0	2.9	
Allene				
C_4 *n*-Butane	0.17	0.33	0.30	0.83
Isobutane		1.40	0.80	
1-Butene				
trans-2-Butene				
cis-2-Butene				
C_5 *n*-Pentane		0.07	0.07	0.62
Isopentane		0.29	0.13	
1-Pentene				
(Pentenes)	0.08			
Pentadiene				
3-Methyl-1-butene				
C_6 *n*-Hexane		0.07	0.15	
3-Methylpentane				
2-Methylpentane		0.48	0.85	
2,3-Dimethylbutane				
2,2-Dimethylbutane		1.70	1.4	
1-Hexene				
trans-2-Hexene	0.7			
cis-2-Hexene				
2-Methyl-1-pentene				
4-Methyl-1-pentene				
4-Methyl-2-pentene				
1,5-Hexadiene				

differences can be observed between the radiolysis of normal hydrocarbon homologues, the decomposition of cyclic compounds shows a strong dependence on the number of carbon atoms in the ring. The differences between the radiation chemical reactions of aliphatic and cyclic hydrocarbons as well as between those of cyclic compounds with different number of carbon atoms in the ring are in correlation with the differences in the thermodynamic characteristics of the parent compounds (strain energy, heat of dehydrogenation, etc.).

irradiated under different conditions

Propene		Cyclopropane			
[9]	[10]	[11]	[12]	[12]	[13]
Brems-strahlung	photolysis 185 nm	$^{60}Co, \gamma$	$^{60}Co, \gamma$	photolysis 147 nm	γ
liquid, −78°C	gas, 22°C	gas, 760 Torr	gas, 10 Torr	gas, 4.8 Torr	gas
2.26×10^{24}		6×10^{20}			7×10^{20}
0.6		1.36			1.12, 1.16
0.04	0.28	0.38			
	0.20		0.64	0.36	
	0.36	2.40	3.28	1.80	
	0.32		1.00	0.24	
	0.28	0.52			
		0.27	0.96	0.12	
	0.08	0.03	0.36	0.36	
0.02		0.37			
	0.40	0.03			
0.02	0.68			0.20	
		0.14			
0.02				0.12	
		0.10			
	0.02	0.03			
0.02					
0.02	0.08				
	0.06				
0.022		0.03			
		0.06			
0.080					
0.054	0.24	0.13			
0.14					
0.030					
0.022		0.07			
0.033					
0.375	0.64				
0.055					
0.17	0.24				

The reverse is also true: the differences in $G(H_2)$ values observed may serve as a basis for the estimation of certain thermodynamic characteristics [4].

As is obvious from the above introduction, the effect of cyclic structure on the radiolysis of hydrocarbons has not been investigated for substances containing 3 or 4 carbon atoms in the rings, except for a few papers which have appeared recently. This may be due to the difficult experimental technique as well as to problems concerning the preparation and purification of hydro-

Table I/b

Values of G(product) from C_4 hydrocarbons

Starting hydrocarbon	*n*-Butane			1-Butene	
Reference	[14]	[14]	[15]	[16]	[16]
Type of radiation	electrons 1.5 MeV	^{60}Co, γ	^{60}Co, γ	γ	γ
Conditions of irradiation	gas 100 Torr	liquid	liquid 0°C	gas 23°C	liquid 23°C
Dose, eV g^{-1}	2.5×10^{21}	3.7×10^{21}	1.67×10^{20}	2.53×10^{21}	2.53×10^{21}
Hydrogen	5.06	4.73		1.03	0.64
C_1 Methane	0.96	0.50	0.52	0.26	0.05
C_2 Ethane	1.89	1.29	0.99	0.43	0.13
Ethylene	0.59	0.58	0.78	4.30	0.21
Acetylene				2.92	0.30
C_3 Propane	2.12	0.29	0.16	0.22	0.06
Propene	0.18	0.16	0.20	0.13	0.13
Allene					
C_4 *n*-Butane				1.94	0.30
Isobutane					
1-Butene	0.23	0.88			
trans-2-Butene	0.64	0.50	1.80	0.52	0.16
cis-2-Butene	0.18	0.48	0.46	0.56	0.18
1,3-Butadiene					
Diacetylene					
Cyclobutene					
Vinylacetylene					
C_5-products	0.32	0.18			
C_6-products	0.38	0.38			
C_7-products	0.09	0.05			0.2
C_8-products	0.26	0.38		0.17	1.72

carbons with small rings. All G(product) values available in the literature for our model compounds have been listed in Table I, together with the corresponding experimental conditions. G-values for photolysis have been calculated using quantum yields as given in the corresponding references.

In addition to G(product) values, the papers reviewed deal, as a rule, with the mechanism of formation of certain main products, using mass spectrometric or scavenger evidences.

As far as we know, no data at all have been reported on hydrogen or hydrocarbon yields from the radiolysis of mixtures of C_3 and C_4 cyclic hydrocarbons.

irradiated under different conditions

Cyclobutane		Cyclobutene		Isobutane	
[17]	[18]	[19]		[20]	[21]
^{60}Co, γ	γ	photolysis 123.6 nm	photolysis 147 nm	^{60}Co, γ	^{137}Co, γ
gas 20 Torr	gas	gas 5 Torr	gas 1 Torr	liquid	gas 150°C
1.2×10^{21}				5.8×10^{19}	1.29×10^{20}
1.86		47*		4.16	
0.06	0.34	traces	22*	1.98	5.69
0.10	0.23				
1.41	3.81	118*	115*		
0.45	1.02	100*	100*		
0.12				0.68	2.66
	0.53			1.62	1.01
0.10	0.12				
	0.08			1.67	
0.07	0.079				
0.26	0.096				
0.30	0.256				
0.12	0.185	128*	92*		
0.18					
0.07		39*	37*		
0.10					
0.36					
0.99					
0.10					

* Instead of G-values, relative yields have been given: acetylene ≡ 100

At the same time this problem is of considerable theoretical interest since chemical transformations of hydrocarbons with small rings are particularly influenced by their rigid structure. They are, therefore, inclined to some special reactions in contrast to cycloalkanes and cycloalkenes with larger rings: *e.g.* in many respects cyclopropane behaves similarly to propene rather than to propane.

The subject of the present work was to investigate the radiolysis of normal, branched and cyclic C_3 and C_4 alkanes and alkenes. Product compositions produced under identical conditions were compared; the effect of strained

small ring on the radiation chemical decomposition of saturated and unsaturated compounds has been evaluated in terms of physico-chemical data on the molecules (bond energies, strain energies, etc.).

2. Experimental

Some of the hydrocarbons irradiated were commercial products: cyclopropane, *n*-butane, 1-butene and isobutane were supplied by FLUKA, propane and propene by the Hungarian Oil and Gas Research Institute. Cyclic C_4 hydrocarbons were synthesized by ourselves. Two reaction routes were selected to obtain cyclobutane and cyclobutene (Fig. 1); both of these represent modifications of the methods described in the literature [22].

The purity of hydrocarbons was, as a rule, higher than 98.5% (including those prepared by ourselves), nevertheless, attempts were made to remove the remaining impurities. By preparative gas chromatography the amount of impurities could be reduced to a level as low as 0.01—0.1%.

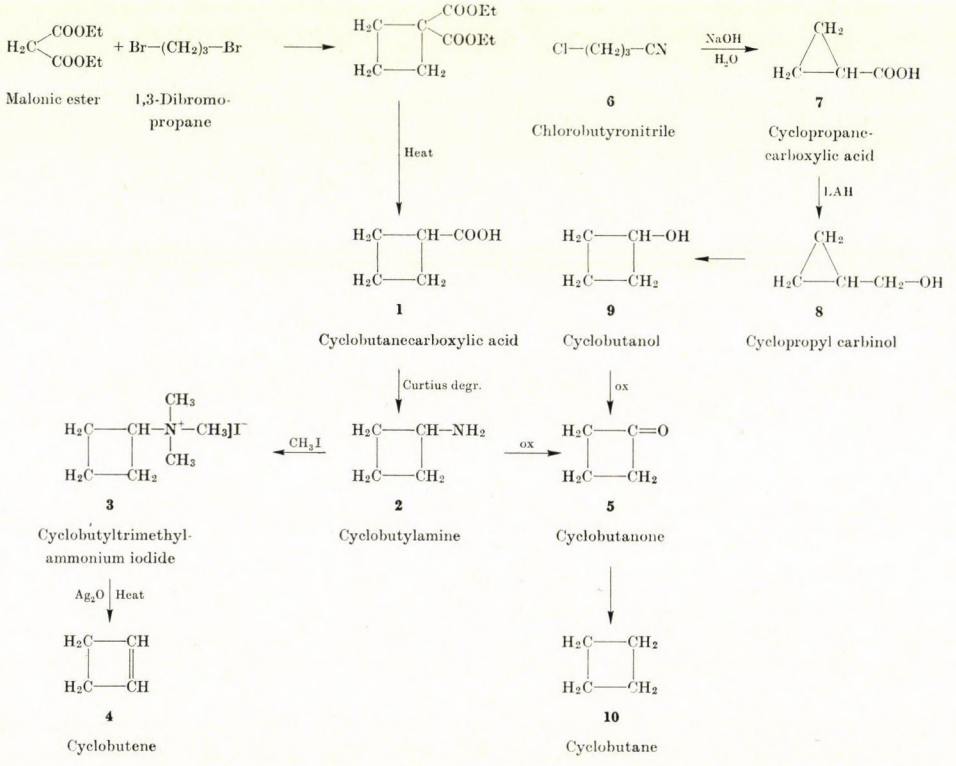

Fig. 1. General scheme of cyclobutane and cyclobutene synthesis

Irradiations have been carried out under pressure, in liquid phase, in Rasotherm glass ampoules with a volume of 0.4 cm^3. The ampoules were filled using an apparatus designed and constructed by us; this allowed to measure exactly the amounts of hydrocarbons to be irradiated either in pure form or in mixtures; air was excluded during handling of the samples (Fig. 2).

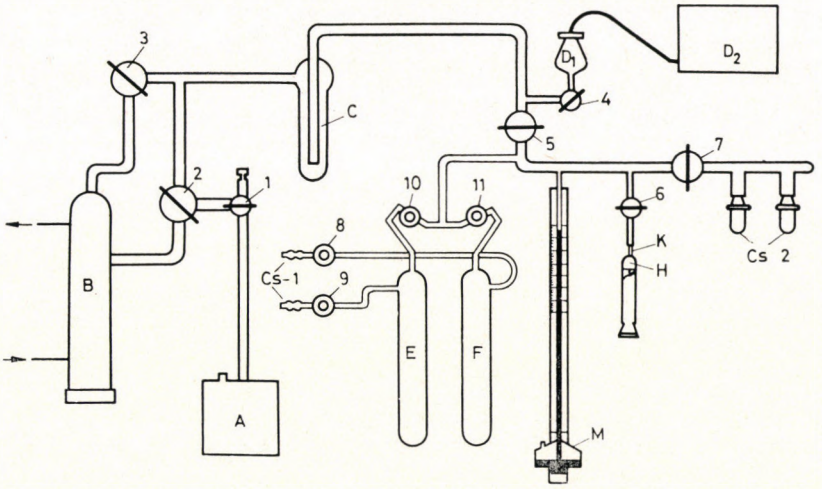

Fig. 2. Apparatus for charging and closing the ampoules: 1—7 glass vacuum stopcocks; 9—11 pressure and vacuum-tight metal stopcocks

A rotation pump
B mercury diffusion pump
C freezing trap
D_1, D_2 ionization manometer
E, F gas storage vessels
H irradiation ampoule
K capillary
M mercury manometer
Cs-1 and Cs-2 joints for charging

Ampoules with hydrocarbon samples were irradiated in the ^{60}Co facility of this Institute [23]. Experiments were carried out at 30—35°C, with an integral dose as high as 6.23×10^{20} eV g^{-1} (9.36 Mrad). The average dose rate was equal to 9.58×10^{19} eVg^{-1} h^{-1} (1.44 Mrad h^{-1}). The differences between dose rates for ampoules placed in different positions were less than 5%. Alcoholic chlorobenzene dosimetry was used [24].

Qualitative and quantitative analyses of H_2 and of the C_1–C_5 products formed during irradiation were carried out by performing three gas chromatographic analyses for each sample. Hydrogen yield was measured at room temperature, by a home-made gas chromatograph, with a katharometer, using a column containing alumina. Hydrocarbon products were analyzed using two separate Type Chrom-31 gas chromatographs provided with a flame ion-

ization detector. One of them contained a column packed with activated alumina and was programme operated from 60°C up to 160°C; an open tubular column coated with squalane was in the other chromatograph operated at 27°C. All samples were analyzed on both gas chromatographs; thus, most C_1–C_5 hydrocarbon products could be identified and their amounts evaluated.

3. Results

First of all, the yields of hydrogen, of fragmentation products (*i.e.* hydrocarbons having fewer carbon atoms than the parent hydrocarbon) and of products with identical carbon number to that of the parent compounds were evaluated. Yields of these products formed during irradiation of cyclic and open chain alkanes and alkenes have been listed in Tables II and III.

The hydrogen yields from cycloalkanes are strongly influenced by the number of carbon atoms in the ring, as opposed to normal alkanes, where $G(H_2)$ is almost independent of the carbon number. $G(H_2)$ values from cyclopropane and cyclobutane are remarkably small as compared with the corresponding aliphatic alkanes as well as higher cycloalkanes (*e.g.* cyclopentane:

Table II

Values of G(product) from C_3 hydrocarbons

Product	Hydrocarbon irradiated		
	Propane	Propene	Cyclo-propane
Hydrogen	3.60	0.80	0.91
C_1 Methane	1.11	—	0.22
C_2 Ethane	0.44	—	0.12
Ethylene	0.58	0.21	1.50
Acetylene	0.18	0.51	0.32
C_3 Propane	—	—	0.27
Propene	2.41	—	0.70
Allene	—	0.33	0.25
C_4 Methylcyclopropane	—	—	0.08
Isobutane	0.18	—	—
n-Butane	0.13	—	—
1-Butene + 1,3-Butadiene	—	0.13	0.13
cis- and *trans*-2-Butene	—	0.09	0.53

Table III

Values of G(product) from C_4 hydrocarbons

Product	Hydrocarbon irradiated				
	n-Butane	Isobutane	1-Butene	Cyclobutane	Cyclobutene
Hydrogen	4.03	3.27	0.73	1.70	0.55
C_1 Methane	0.56	2.25	0.10	0.060	0.020
C_2 Ethane	1.30	0.11	0.066	0.44	—
Ethylene	0.74	0.096	0.22	4.93	1.27
Acetylene	0.085	0.049	0.24	0.29	1.62
C_3 Propane	0.21	1.60	0.055	0.004	—
Propene	0.17	1.55	0.012	0.050	0.004
Cyclopropane	0.35	—	—	0.15	—
Allene	—	—	0.067	—	—
C_4 *n*-Butane	—	—	—	0.070	—
1-Butene + 1,3-Butadiene	0.66	—	—	0.48	—
Isobutene	—	2.12	—	—	—
trans-2-Butene	—	—	0.065	0.070	—
cis-2-Butene	—	0.32	0.21	0.13	—
1,2-Butadiene + Cyclobutene	—	—	0.15	0.72	—
1-Butene-3-yne	—	—	—	—	0.13
C_5 Saturated	~0.56	~0.31	~0.075	—	—
Unsaturated	~0.17	~0.11	~0.030	—	~0.09

5.1, cyclohexane: 5.3*) their values are nearer to the $G(H_2)$ values of the corresponding monoalkenes and higher cycloalkenes (*e.g.* cyclopentene: 1.27, cyclohexene: 1.26). Cyclobutene produced a lower hydrogen yield than did 1-butene.

The data in the Tables show the presence of products which may have been formed with the rupture of more than one C – C bond. The yields of C_2 hydrocarbons from cyclopropane, cyclobutane and cyclobutene are higher than those from the corresponding alkenes, *i.e.* propene and 1-butene, respectively. The C_2 fraction consists mostly of ethylene in the case of cycloalkanes, and of ethylene and acetylene in the case of cyclobutene.

On comparing the values of G(fragment) from cyclic C_3 and C_4 hydrocarbons with those from C_5–C_6 cycloalkanes, a marked tendency to ring fission

* If not otherwise stated, data concerning the radiolysis of higher than C_4 hydrocarbons have been taken from works carried out in this laboratory by other authors, under conditions nearly identical to those of ours [3, 25].

Table IV

Values of G (fragment) from irradiated alkanes and alkenes

Cycloalkanes	G	Cycloalkenes	G	Alkanes	G	Alkenes	G
Cyclopropane	2.16			Propane	2.31	Propene	0.72
Cyclobutane	5.92	Cyclobutene	2.90	*n*-Butane	3.42	1-Butene	0.76
Cyclopentane	1.09*	Cyclopentene	0.38*	*n*-Pentane	2.37*		
Cyclohexane	0.22*	Cyclohexene	0.29*	*n*-Hexane	2.05*	1-Hexene	0.58*

* Taken from Refs. [3, 25].

can be observed (Table IV). The bond energies of cycloalkanes and cycloalkenes are influenced by their higher free enthalpy of formation relative to the corresponding open chain hydrocarbons, *i.e.* they possess a surplus energy called strain energy. The high strain energy of C_3 and C_4 cycles may be attributed mainly to the distortion of the C–C valence angles. When the hydrocarbon ring is opened, this surplus energy is liberated, thus decreasing the energy requirement of C–C bond fission processes (Figs 3a, b).

The energy requirement of dehydrogenation of cyclic hydrocarbons decreases almost monotonically with increasing carbon number, as shown by Fig. 3c.

Figure 3d shows WOJNÁROVITS's *j*-values [3] characteristic of the ratio of C–C and C–H bond fissions in cycloalkane molecules activated by irradiation:

$$j \equiv \frac{G(C\text{–}C)}{G(C\text{–}H)} \,. \tag{1}$$

Here G(C–H) was taken equal to $G(H_2)$. This may be accepted as a first approximation since, as a rule, one molecule of hydrogen requires that one molecule be activated by irradiation. The G(C–C) value characteristic of the number of molecules activated by irradiation and subsequently undergoing C–C bond fission can be calculated on the basis of the overall G-values of all products whose formation involves some sort of C–C bond fission, with appropriate weighing by stoichiometric factors.

Fig. 3d evidences that the *j*-values of C_3–C_4 cycloalkanes are extraordinarily large by comparison with higher cycloalkanes, indicating that the extent of C–C bond fission processes in lower cycloalkanes is much higher than C–H bond fission. On this basis, the general conclusion can be drawn that, of the competing processes of C–H and C–C bond fission, the rate of reactions leading to hydrogen evolution increases with increasing number of carbon atoms in the ring, provided that irradiations occur under identical conditions.

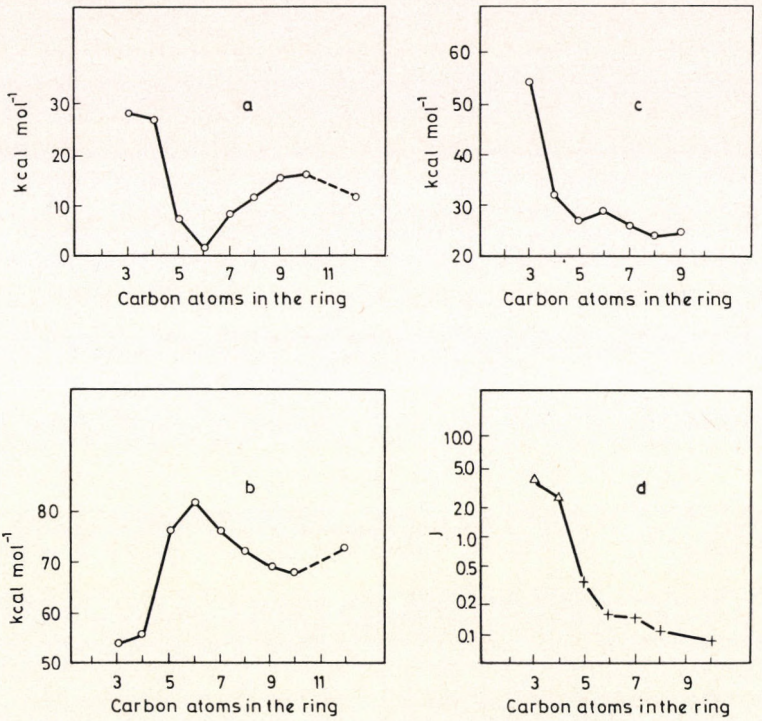

Fig. 3. Characteristics of cycloalkanes as a function of the ring size
a: overall strain energy; b: energy of C–C bond rupture; c: energy of dehydrogention; d: *j*-values. △ — data from the present authors; + — data from other authors under identical conditions [3]; ○ — calculated values

Whereas the irradiation of propane and propene produces a single C_3 product in each case (by the formation of an additional double bond), propane, propene and allene can be found among the products of irradiated cyclopropane. The order of the overall yields of C_3 products is: propane [$G(C_3) = 2.41$] > >cyclopropane [$G(C_3) = 1.22$] > propene [$G(C_3) = 0.33$]. According to the literature, the formation of hydrocarbon products higher than the parent compounds may be attributed to radical combination processes; thus, the formation of C_4 from C_3 products, shown in Table II, may be due to the combination of alkyl and cycloalkyl radicals with methyl radicals, at least as a first approximation.

On evaluating the overall yields of C_4 products from irradiated C_4 hydrocarbons, the following order can be observed: cyclobutane [$G(C_4) = 1.47$] > > *n*-butane [$G(C_4) = 0.66$] > 1-butene [$G(C_4) = 0.43$] > cyclobutene [$G(C_4) =$ $= 0.13$]. It can be seen from Table III that the C_4 products are mostly unsaturated, except for the low *n*-butane yield from cyclobutane.

On comparing the yields of fragments and of hydrocarbons with carbon numbers identical to those of the parent compounds, it may be established that cyclobutane is much less stable in the liquid phase γ-radiolysis than is cyclopropane (*cf.* Table IV). This does not contradict the fact that the j-value of cyclopropane is lower since this value only shows that there are more C–H fission processes than C–C bond fission reactions as seen from the hydrogen yields discussed above. Whereas the $G(H_2)$ value of cyclopropane is nearly equal to that of propene, the $G(H_2)$ of cyclobutane is about 2.5 times higher than that of 1-butene.

Table III also shows the product composition obtained from irradiated isobutane with a branched chain. The exceedingly high yields of CH_4, C_3 products and of isobutene show that the reactions of methyl radicals are of decisive importance in determining the overall direction of transformations.

4. Discussion

On the basis of data listed in Tables II and III as well as of the correlations recognized, it will be attempted to develop a uniform interpretation for the mechanisms of processes occurring during γ-radiolysis of cyclic C_3 and C_4 hydrocarbons in the liquid phase.

4.1. *Radiation chemical reactions of cyclopropane*

$$\text{cyclo-}C_3H_6 \xrightarrow{\sim\sim} \text{cyclo-}C_3H_6^+ + e^- \tag{2}$$

$$\text{cyclo-}C_3H_6 \xrightarrow{\sim\sim} \text{cyclo-}C_3H_6^* \tag{3}$$

According to mass-spectrometric data [26], cyclo-$C_3H_6^+$ produced in primary process (2) may react with cyclopropane, *e.g.*, in the following ion-molecule reactions:

$$\text{cyclo-}C_3H_6^+ + \text{cyclo-}C_3H_6 \begin{cases} \nearrow C_3H_7^+ + C_3H_5^\cdot & (4a) \\ \searrow C_4H_7^+ + C_2H_5^\cdot & (4b) \end{cases}$$

Further reactions of ions and radicals produced in processes (4), involving the abstraction of a hydrogen atom or a hydride ion lead to stable products:

$$C_2H_5^\cdot \xrightarrow{+H} C_2H_6 \tag{5}$$

$$C_3H_5^\cdot \xrightarrow{+H} C_3H_6 \tag{6}$$

$$C_3H_7^+ \xrightarrow{+H^-} C_3H_8 \quad G(\text{propane}) = 0.27 \tag{7}$$

The decomposition of the excited cyclopropane molecule produced in the primary process may occur by following scheme, *via* a supposed biradical intermediate:

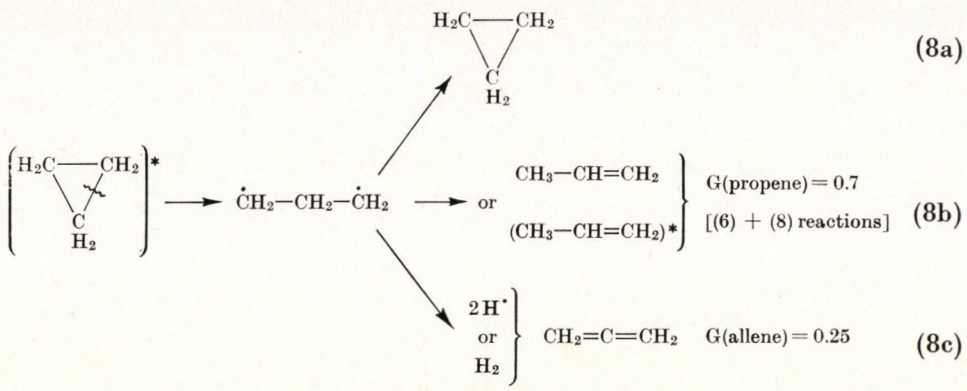

The relatively high yield of C_2 products supports the suggestion that the ring may decompose with a 'simultaneous' rupture of two C–C bonds, whic means that both ruptures occur before thermalization of the molecule:

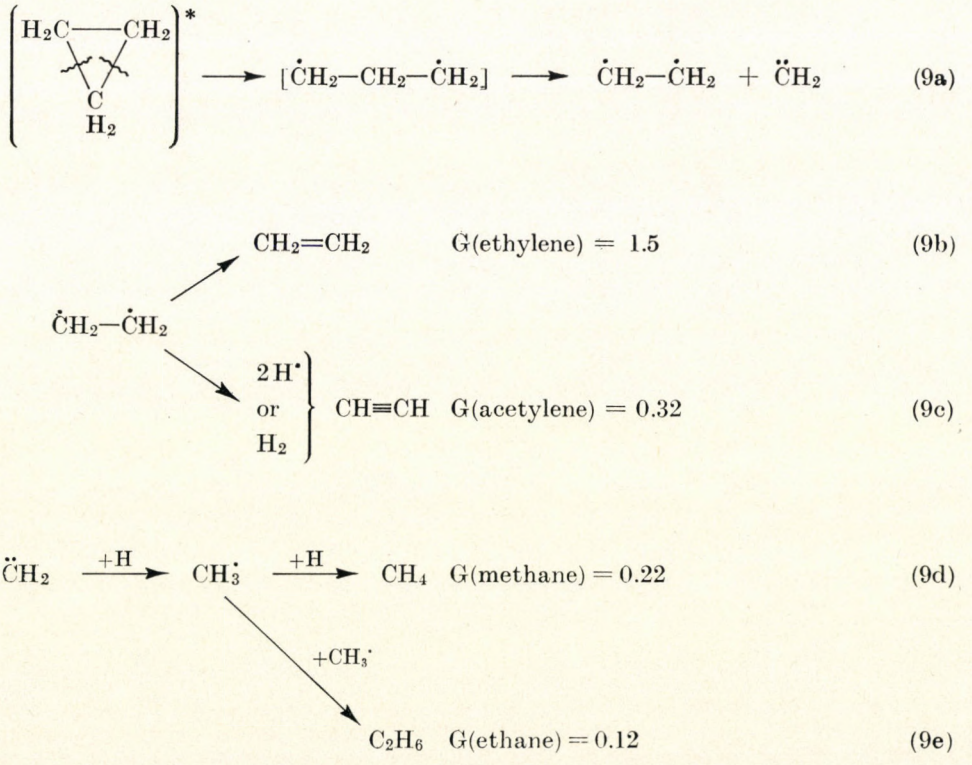

On comparing the yields of processes (9b) and (9c), it is obvious that the probability of ethylene formation is about 5 times higher than that of acetylene. The low methane yield relative to that of C_2 products may be due to the rapid unimolecular rearrangement of dimethylene biradicals formed upon ring decomposition as opposed to bimolecular processes of methylene radicals. Of the latter ones, methyl radicals and, subsequently, methane are formed with lower efficiency (9d); another process is radical combination resulting in ethane [Reaction (9e)] or higher alkanes. It is known that some of the methylene radicals may take part in insertion reactions; if a methylene group is inserted into a C–H or a C–C bond, the result is a product containing one CH_2 group more than the reacting molecule.

Reaction of methylene radicals with cyclopropane gives excited methylcyclopropane; its deactivation by collision gives methylcyclopropane, or, after rearrangement, 1-butene or 2-butene:

$$\ddot{C}H_2 + \text{cyclo-}C_3H_6 \longrightarrow \text{cyclo-}C_3H_5{-}CH_3^* \qquad (10a)$$

$$\text{cyclo-}C_3H_5{-}CH_3^* \longrightarrow \begin{cases} \text{cyclo-}C_3H_5{-}CH_3 & G(\text{methylcyclopropane}) = 0.08 \quad (10b) \\ CH_2{=}CH{-}CH_2{-}CH_3 & G(\text{1-butene}) = 0.13 \quad (10c) \\ CH_3{-}CH{=}CH{-}CH_3 & G(\textit{cis}\text{- and }\textit{trans}\text{-2-butene}) = 0.53 \quad (10d) \end{cases}$$

By summarizing the yields of stable decomposition products of radicals produced in equivalent amounts in Reaction (9a), it can be shown that methylene radicals react in other processes with a yield of $G = 0.74 - 0.86$; probably, these processes lead to the formation of higher molecular weight products:

$$G(\dot{C}H_2{-}\dot{C}H_2) = 1.82 \quad [\text{Reactions (9b), (9c)}]$$

$$\underline{G(\ddot{C}H_2) = 1.08} \quad [\text{Reactions (9d), (9e), (10b), (10c), (10d)}]$$

$$\Delta G_I = 0.74$$

assuming that the total amount of ethane has been produced in Reaction (9e):

$$\Delta G_{II} = \Delta G_I + G(C_2H_6) = 0.86$$

Several papers deal with the formation of different cycloalkyl products in the radiolysis of higher cycloalkanes, on the basis of direct ESR investigations of C_3–C_8 compounds [27, 28] or pulse radiolysis studies [29]:

$$\text{cyclo-}C_nH_{2n}^* \rightarrow \text{cyclo-}C_nH_{2n-1}^{\cdot} + H^* \qquad (11)$$

$$H^* + \text{cyclo-}C_nH_{2n} \rightarrow H_2 + \text{cyclo-}C_nH_{2n-1}^{\cdot} \qquad (12)$$

$$2\ \text{cyclo-}C_nH_{2n-1} \begin{cases} \nearrow\ \text{cyclo-}C_nH_{2n-2} + \text{cyclo-}C_nH_{2n} & (13a) \\ \searrow\ (\text{cyclo-}C_nH_{2n})_2 & (13b) \end{cases}$$

If these reactions also occur during the radiolysis of cyclopropane, their stable products will increase the yields of hydrogen, cyclopropane and C_6 compounds. No cyclopropene and C_6 hydrocarbons could, however, be detected under our conditions. Literature data suggest that cyclopropene is unstable at room temperature [30, 31]; thus, even if it had been produced in minor amounts during irradiation, it must have transformed into other products by the time of analysis. Nevertheless, the difference between the actual hydrogen yield (Table II) and that predicted on the basis of Reactions (8c) and (9c) [$\Delta G = 0.91 - (0.25 + 0.32) = 0.34$)] indicates that Reactions (11)—(13) may actually take place.

4.2. *Radiation chemical reactions of cyclobutane*

$$\text{cyclo-}C_4H_8 \xrightarrow{\sim\sim} \text{cyclo-}C_4H_8^+ + e^- \qquad (14)$$

$$\text{cyclo-}C_4H_8 \xrightarrow{\sim\sim} \text{cyclo-}C_4H_8^* \qquad (15)$$

The primary process (15) leads, with a high probability, to the formation of an energy-rich biradical *via* C–C bond fission and the opening of the ring. This biradical reacts further with C–C bond fission:

$$\begin{bmatrix} CH_2{-}CH_2 \\ \vdots\quad\vdots \\ CH_2{-}CH_2 \end{bmatrix}^* \longrightarrow [\dot{C}H{-}CH_2{-}CH_2{-}\dot{C}H_2] \longrightarrow CH_2{=}CH_2 + (CH_2{=}CH_2)^* \qquad (16)$$

$$(CH_2{=}CH_2)^* \longrightarrow H_2 + CH{\equiv}CH \qquad [G(\text{acetylene}) = 0.29] \qquad (17a)$$

$$(CH_2{=}CH_2)^* + M \longrightarrow CH_2{=}CH_2 \qquad (17b)$$

Most of the ethylene ($G = 4.93$) has been formed in processes (16) and (17b).

The cyclopropane found among the products suggests that another type of ring decomposition with a 'simultaneous' rupture of two C–C bonds of the excited molecule may also occur. As judged from the yields, the probability of this reaction is lower by about an order of magnitude than that of process (16)

Further possible reactions of methylene radicals are analogous to those discussed for cyclopropane. This is supported also by the extremely low yield of methane from irradiated cyclobutane: $G(CH_4) = 0.06$.

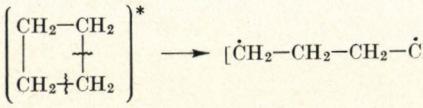

$$\dot{C}H_2-CH_2-CH_2-\dot{C}H_2] \longrightarrow \ddot{C}H_2 + \dot{C}H_2-CH_2-\dot{C}H_2 \qquad (18a)$$

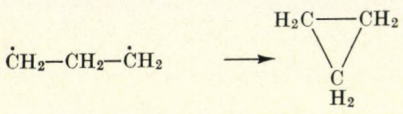

(18b)

The scheme of the further possible reactions of cyclo-$C_4H_8^+$ produced in reaction (14) has been proposed on the basis of mass spectrometric data [26, 32], in correspondence with the actual yields:

$$\text{cyclo-}C_4H_8^+ \longrightarrow \begin{cases} C_2H_4^+ + C_2H_4 & (19a) \\ C_2H_5^+ + CH_3^\cdot & (19b) \\ C_3H_5^+ + CH_3^\cdot & (19c) \end{cases}$$

Ions produced in reactions (19) may react further with cyclobutane in electron transfer or hydride ion transfer processes:

$$C_2H_4^+ + \text{cyclo-}C_4H_8 \rightarrow C_4H_8^+ + C_2H_4 \qquad (20)$$

$$C_2H_5^+ + \text{cyclo-}C_4H_8 \rightarrow C_4H_7^+ + C_2H_6 \qquad (21)$$

$$C_3H_5^+ + \text{cyclo-}C_4H_8 \rightarrow C_4H_7^+ + C_3H_6 \qquad (22)$$

$$C_4H_8^+ + e^- \rightarrow C_4H_8^* \qquad (23)$$

$$C_4H_7^+ + e^- \rightarrow (C_4H_7)^* \qquad (24)$$

Further decomposition of the excited molecules originating from neutralization reaction (23) leads to the following stable products:

$$C_4H_8^* \longrightarrow \begin{cases} CH_3-CH=CH-CH_3 & G(\textit{cis}\text{- and }\textit{trans}\text{-2-butene}) = 0.20 & (25a) \\ CH_2=CH-CH_2-CH_3 & G(\text{1-butene and 1,3-butadiene}) = 0.48 & (25b) \\ H_2+CH_2=CH-CH=CH_2 & & (25c) \end{cases}$$

The yields shown indicate that all three processes denoted by (25) have nearly the same probabilities.

The fraction of molecules that have preserved their C_4 cycle after reaction (23) and the molecules that have been directly excited and have avoided C–C bond rupture may form cyclobutene after elimination of a hydrogen molecule:

$$\text{cyclo-}C_4H_8^* \rightarrow H_2 + \text{cyclo-}C_4H_6 \quad G(\text{1,2-butadiene+cyclobutene}) = 0.72 \qquad (26)$$

Excited (cyclo-$C_4H_7^{\cdot}$)* produced in process (24) may react further as follows:

$$(\text{cyclo-}C_4H_7^{\cdot})^* \longrightarrow \begin{cases} \dot{C}H_2-CH_2-CH=CH_2 & (27a) \\ C_2H_3^{\cdot} + C_2H_4 & (27b) \\ \text{cyclo-}C_4H_5^{\cdot} + H_2 & (27c) \end{cases}$$

Analogously to photochemical reactions, it may be assumed that energy-rich hydrogen atoms also lead to ring opening:

$$H^* + \text{cyclo-}C_4H_8 \rightarrow n\text{-}C_4H_9^{\cdot} \qquad (28)$$

The resulting n-$C_4H_9^{\cdot}$ may abstract another hydrogen atom to form n-butane; since G(n-butane) = 0.07, it follows that reaction (28) actually occurs but with a low probability.

Radicals produced in the system (including hydrogen atoms) may react in different ways, *e.g.* they may abstract hydrogen from cyclobutane or may combine with alkenes or other radicals formed upon radiolysis:

$$R^{\cdot} + \text{cyclo-}C_4H_8 \rightarrow RH + \text{cyclo-}C_4H_7^{\cdot} \qquad (29)$$

$$R^{\cdot} + CH_2=CH_2 \rightarrow R-CH_2-\dot{C}H_2 \qquad (30)$$

$$R_1^{\cdot} + R_2^{\cdot} \rightarrow \text{products} \qquad (31)$$

Similarly to the radiolysis of C_3, C_5 and C_6 cycloalkanes [2], it may be assumed that the following radical combination reactions also occur:

$$CH_3^{\cdot} + \text{cyclo-}C_4H_7^{\cdot} \rightarrow \text{cyclo-}C_4H_7-CH_3 \qquad (32)$$

$$C_4H_9^{\cdot} + \text{cyclo-}C_4H_7^{\cdot} \rightarrow \text{cyclo-}C_4H_7-C_4H_9 \qquad (33)$$

Finally, although we have no accurate data on the distribution of C_{n+1}—C_{2n} products, it may be attempted to evaluate the hydrogen balance on the basis of the reactions mentioned. In reaction (17a) equivalent amounts of acetylene and hydrogen are produced; since no other way for acetylene production has been assumed, this means that G(H_2) = G(acetylene) = 0.29. Similarly, reaction (25c) produces equivalent amounts of 1,3-butadiene and hydrogen; assuming equal probabilities for reactions (25b) and (25c), we obtain G(H_2) = 0.24. In an analogous way, in reaction (26) a value of G(H_2) = = 0.72 may be obtained. On adding these contributions, G(H_2) = 0.29 + + 0.24 + 0.72 = 1.25, as compared with the actual G(H_2) = 1.70, which means a deficite as low as G(H_2) = 0.45 between the measured and calculated

values. Since it seems realistic to assume that a smaller fraction of the total hydrogen (1/3—1/4 of the total value) has been formed in radical processes like (27c) and (29), the proposed scheme is probably correct.

4.3. *Radiation chemical reactions of cyclobutene*

The main radiolysis products of cyclobutene are ethylene and acetylene together with hydrogen and vinylacetylene (1-butene-3-yne), the yields of the latter two compounds being by about an order of magnitude lower than those of the main products. The yields can be interpreted in terms of a biradical type intermediate:

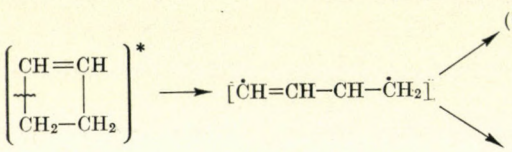

(34a)

(34b)

Excited ethylene and acetylene molecules produced in processes (34a) and (34b) are stabilized by collisional deactivation. According to stoichiometric equations ethylene and acetylene must be formed in identical amounts actually, the yield of acetylene is higher, the difference being $\Delta G =$ $=$ G(acetylene) $-$ G(ethylene) $= 1.62-1.27 = 0.35$. On this basis the following additional processes have been assumed:

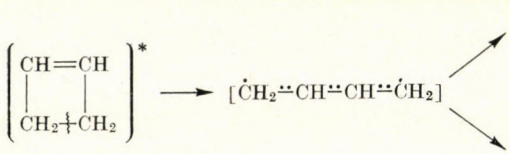

(35a)

(35b)

The actual yields show that the probabilities of processes (35a) and (35b) are nearly equal since ΔG(acetylene)/2 $= 0.35/2 \approx 0.17$ and G(vinylacetylene) $= 0.13$.

Considerable amounts of 1,3-butadiene were also found due to thermal isomerization [33] and photochemical decomposition [19] of gaseous cyclobutene:

$$\text{cyclo-}C_4H_6 + H^* \rightarrow (C_4H_7^{\cdot})^* \tag{36}$$

$$(C_4H_7^{\cdot})^* \rightarrow 1,3\text{-}C_4H_6 + H^{\cdot} \tag{37a}$$

$$(C_4H_7^{\cdot})^* \rightarrow C_4H_7^{\cdot} \tag{37b}$$

The addition of a hydrogen atom to cyclobutene is an exothermic process and, in absence of collisional deactivation, the energy-rich product formed may transform into 1,3-butadiene. In liquid phase, however, collisional deactivation may occur at an appreciable rate, and this may be the reason why no 1,3-butadiene has been detected in cyclobutene irradiated under the conditions described.

This seems to be supported also by the results of DeLeon and Doepker [19] who have found a decreasing 1,3-butadiene yield with increasing cyclobutene pressure.

REFERENCES

[1] Wojnárovits, L., Földiák, G.: Acta Chim. (Budapest): **82,** 285 (1974)
[2] Wojnárovits, L.: Thesis, Budapest 1973
[3] Földiák, G., Cserép, Gy., Horváth, Zs., Wojnárovits, L.: Proc. Symposium on the Mechanism of Hydrocarbon Reactions, P-41. Siófok, 1973
[4] Földiák, G., Cserép, Gy., György, I., Horváth, Zs., Wojnárovits, L.: Hung. J. Ind. Chem. (Veszprém), **2,** Suppl., 277 (1974)
[5] Yang, K. P., Manno, P.: J. Amer. Chem. Soc., **81,** 3507 (1959)
[6] Birdwell, B. F., Crawford, G. W.: J. Chem. Phys., **33,** 928 (1960)
[7] Koob, R. D., Kevan, L.: Trans. Faraday Soc., **64,** 428 (1968)
[8] So, M. T., Huang, S. R.: J. Chem. Phys., **47,** 4896 (1967)
[9] Wagner, C. D.: Tetrahedron, **14,** 164 (1961)
[10] Borell, P., Cervenka, A., Turner, J. W.: J. Chem. Soc. No 12 (B), 2293 (1971)
[11] Tanaka, J., Hatano, Y., Shida, S.: Bull. Chem. Soc. Japan, **44,** 2860 (1971)
[12] Scala, A., Ausloos, P.: J. Chem. Phys., **49,** 2282 (1968)
[13] Yang, K.: J. Phys. Chem., **65,** 42 (1961)
[14] Miyazaki, T., Arai, S., Shida, S., Suhohara, S.: Bull. Chem. Soc. Japan, **37,** 1332 (1964)
[15] Fujisaki, N., Shida, S., Hatano, Y., Tanno, K.: J. Phys. Chem., **75,** 2854 (1971)
[16] Kaufman, P. C.: J. Phys. Chem., **67,** 1671 (1963)
[17] Heckel, R., Hanrahan, R. J.: Int. J. Radiat. Phys. Chem., **5,** 271 (1973)
[18] Doepker, R. D., Ausloos, P.: J. Chem. Phys., **44,** 1641 (1966)
[19] DeLeon, A., Doepker, R. D.: J. Phys. Chem., **75,** 3656 (1971)
[20] Tanno, K., Shida, S.: J. Phys. Chem., **72,** 3496 (1968)
[21] Miyazaki, T.: J. Phys. Chem., **71,** 4282 (1967)
[22] Horváth, Zs., Gruber, L., Földiák, G.: Proc. 3rd Tihany Symposium on Radiation Chemistry (Ed.: J. Dobó and P. Hedvig) Akadémiai Kiadó, Budapest, 1972
[23] Hirling, J., Stenger, V.: Energia és Atomtechnika, **22,** 466 (1969)
[24] Horváth, Zs., Bányai, É., Földiák, G.: Radiochim. Acta **13,** 150 (1970)
[25] Wojnárovits, L., Földiák, G.: Proc. 3rd Tihany Symposium on Radiation Chemistry (Ed.: J. Dobó and P. Hedvig) Akadémiai Kiadó, Budapest, 1972
[26] American Petroleum Institute Research Project, **44,** Catalog of Mass Spectra Data
[27] Corvaja, C., Giocometti, G., Brustolon, M.: Z. Phys. Chem. Neue Folge, **82,** 272 (1972)
[28] Kuwota, K., Kotake, Y., Inada, K., Ono, M.: J. Phys. Chem., **76,** 2061 (1972)
[29] Ebert, M., Kun, S. P., Land, E. S., Swallow, A. S.: Proc. Roy. Soc. **287A,** 1 (1965)
[30] Closs, G. L.: J. Amer. Chem. Soc., **85,** 99 (1963)
[31] Closs, G. L., Krautz, K. D.: J. Org. Chem., **31,** 638 (1966)
[32] Hughes, B. M., Tiernan, T. O.: J. Chem. Phys., **51,** 4373 (1969)
[33] Cooper, W., Walters, W. D.: J. Amer. Chem. Soc., **80,** 4220 (1958)

Zsuzsanna Horváth
Gábor Földiák
H-1525 Budapest, P. O. B. 77. Hungary.

Acta Chimica Academiae Scientiarum Hungaricae, Tomus 85 (4), pp. 437—443 (1975)

ИЗМЕНЕНИЕ СОСТАВА ТВЕРДЫХ СТЕКОЛ ПОД ВЛИЯНИЕМ СОЛЕВЫХ РАСПЛАВОВ

З. БОКШАИ и Г. БУКЭ

Кафедра Общей и Неорганической Химии Университета им. Л. Этвеша Будапешт

И. М. БУШУЕВА

Кафедра Физической Химии ЛГУ, Ленинград

1974. X. 15

При обработке натриево—кальциевых силикатных стекол расплавом нитрата щелочного металла при температуре 355°C вблизи поверхности уменьшается содержание щелочного окисла в стекле, а под влиянием ставшего основным за счет Na_2CO_3 расплава — увеличивается. Эти изменения в составе модифицируют механическую прочность стекла и его химическую устойчивость. Т. к. потерю щелочного окисла и приобретение его нельзя представить без диффузии ионов кислорода, а также, в связи с тем, что вероятным кажется образование кислородных ионов при температуре обработки, то, согласно предложенному механизму диффундирующий кислород всегда присоединяется хотя бы к одному атому кремния.

Исходная цель исследований

За последние 10—15 лет, с целью повышения прочности стекол, были проведены исследования влияния солевых расплавов на твердые стекла. Изменение механических свойств обычно объясняют напряжению, появляющимся вследствие ионообмена между двумя фазами (1—8). Вполне вероятным кажется и то, что ионообмен одновременно оказывает влияние и на химическую устойчивость стекла. Продолжая наши исследования по коррозии стекла, мы собирались изучать зависимость между степенью ионного обмена и химической устойчивостью. Мы также рассчитывали и на то, что исследование процесса ионосбмена поможет улучшить понимание поведения стеклянных электродов в солевых расплавах. Первые результаты оказались, однако, весьма неожиданными и подняли целый ряд важных вопросов. Поэтому исходные цели были модифицированы и дальнейшие исследования уже проводились с целью выяснения новых наблюдаемых явлений.

Экспериментальная часть

Исследования проводились на образцах стекла, использованного нами уже ранее, а именно на стекле типа Дола с составом 21,41 мол.% Na_2O, 6,47 мол.% CaO и 72,11 мол.% SiO_2. Плавление стекла проводили при температуре 1350 ± 20°C, в течение 16 часов, с аналитически чистыми реагентами и в платиновом тигле. Из расплава были приготовлены стеклянные палочки с длиной 4—5 см и диаметром 0,3 см. Для аналитической проверки состава и

гомогенности образцов, повторной обработкой (всего 5 раз) HF снимали с поверхности слой толщиной 1,5 μм. Вслед за этим, образцы промывались вначале разбавленным аммиачным раствором, а затем водой, высушивались при температуре 120°C и, наконец, помещались в солевой расплав. Для удаления воды, перед плавлением соль была высушена при температуре 200°C. С целью обеспечения благоприятных и постоянных условий, в 50 г расплава при 355°C помещали лишь 2 образца, и для каждого эксперимента приготовляли новый расплав. По истечении времени обработки, образцы вынимали из еще теплого расплава и на поверхности их затвердевал тонкий слой соли. Для удаления последнего образцы подвергали промывке (25 сек) дестиллированной водой.

С целью определения состава, изменившегося вследствие взаимодействия, постепенно вытравляли поверхностный слой. На одной ступени частичного растворения было использовано 10 мл 0,2%-ого раствора HF; последний, при постоянном перемешивании, соприкасался с образцом при температуре 25 $\pm$ 0,2°C, в течение 7 минут. Концентрация ионов натрия и калия была определена с помощью чувствительного пламенного фотометра, а концентрация кремния была определена на основе цветной реакции с молибденовым сияим (9). Толщина поверхностных фракций была рассчитана, исходя из содержания кремния во фракции и принимая в расчет поверхность образца и плотность стекла.

Взаимодействие стекла с расплавами нитрата калия

Распределение ионов калия, проникнувших в стекло, и оставшихся ионов натрии вблизи поверхности представлено на рис. 1. Их концентрация (C_K, C_{Na}), деленная на исходную концентрацию щелочи в стекле (C_O), представляет собой величину(C_K/C_O, C_{Na}/C_O), не зависящую от единиц измерения. На рисунке эти относительные концентрации представлены в зависимости от расстояния.

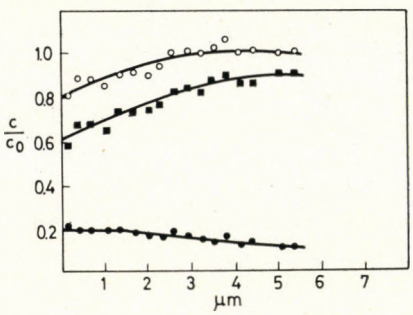

Рис. 1. Распределение щелочных ионов в поверхностном слое стекла, обработанного KNO_3, при 355°C и в течение 6 часов. ■ Относительная концентрация ионов натрия, ● Относительная концентрация ионов калия; ⊙ Сумма относительных концентраций ионов натрия и калия

В согласии с наблюдениями других авторов, концентрация натрия монотонно возрастает, пока не достигает величины, соответствующей граничному значению. Градиент же концентрации иона калия в первом слое толщиной 1,2 μм практически равен нулю. В то же время нет никаких оснований полагать какое-либо равновесие или весьма быструю диффузию для данного слоя. Наиболее интересным, однако, является ход кривой суммы концентраций, на участке которой, соответствующей 2,5 μм, наблюдается значительная нехватка щелочи. В связи с тем, что авторы до сих пор опубликованных сообщений не сомневались — по-крайней мере согласно написанному — в том что происходит обмен эквивалентного числа ионов, то необходимым казалось повторное проведение экспериментов. Как оказалось, поведение это было характерным и всегда одним и тем же. Принимая во внимание закон электронейтральности, наблюдаемые явления можно объяснить лишь тем, что наряду с ионами натрия и калия также и другой ион переходит из одной фазы в другую. Принципиально возможны два случая:

1) из расплава в стекло переходит какой-либо катион, не принятый нами ранее во внимание,

2) отрицательно заряженные ионы выходят из фазы стекла.

Если нехватка щелочи вызвана появлением неизвестного катиона, то, согласно рис. 1, его подвижность должна быть меньше, чем иона калия. Поэтому протон, который диффундирует быстро, не может быть причиной данного эффекта. Т. к. нехватка щелочи весьма значительна, то появление инородных ионов лишь тогда может служить объяснением, если их концентрация, относящаяся к расплаву, значительно превышает величину, соответствующую примеси KNO_3. В связи с тем, что диффузию кислорода удалось обнаружить в самых различных стеклах [11—13], то принципиально вероятным может быть и то, что ионы кислорода проникают через поверхность стекла из более глубоко лежащих слоев в расплав нитрата калия. Не принимая во внимание литературные данные для стёкол не содержащих щёлочных ионов получаем для энергии активации диффузии кислорода величину около 70 ккал/моль [11—14], или 12 ккал/моль [15]. Последная величина была измерена авторами (Шеффером и Оэльем [15]) в калиево-свинцово-силикатном стекле между 275 и 425 °C. Для наших исследований, из-за низкой температуры следовало бы, предположить конечно, какой то процесс с меншей энергией активации однако из-за различии в составе стекол совсем не обязательно, что механизм наблюдённой нами диффузии кислорода имеет такой же атомный характер как это предпологается на основе соображений о структуре, опубликованных в литературе. Во всяком случае нам ещё нужно будет вернуться к вопросу механизма для того, чтобы согласовать диффузию кислорода с транспортом отрицательного заряда.

Во всяком случае, на основе предположения что кислородный ион выходит из стекла, диффузия двух щелочных ионов находится в полном со-

гласии с их пространственным распределением. Между силикатными анионами сетки, движение щелочных ионов происходит намного быстрее по сравнению с миграцией отрицательных зарядов. Таким образом, за любым изменением концентрации отрицательных групп следует, без опозданий, изменение в пространственном распределении катионов. Если в такой системе протекает взаимодиффузия — что и имеем в настоящем случае —, то скорость ее опре-

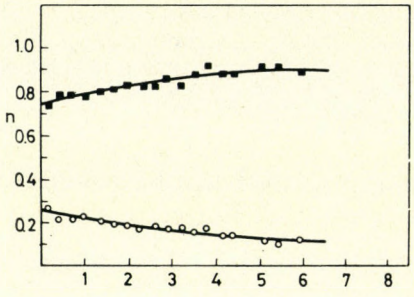

Рис. 2. Изменение молярной доли ионов натрия (■) и ионов калия (●) после обработки KNO_3 в зависимости от расстояния от поверхности

деляется не просто концентрацией, а градиентом молярной доли подвижных ионов. Молярная доля ионов натрия и калия, относимая к системе щелочных ионов,

$$n_{Na} = C_{Na}/(C_{Na} + C_K) \quad \text{и} \quad n_K = C_K/(C_{Na} + C_K)$$

представлена на рис. 2 в зависимости от расстояния от поверхности. В данном случае уже не наблюдается аномалий, характерных для рис. 1.

Причина диффузии кислорода и ее возможный механизм

Для исследования формирования нехватки щелочи независимо от катионного обмена, была произведена обработка и расплавом нитрата натрия. Результат оказался подобным изложенному выше, хотя и был получен меньший эффект. Согласно нашему предположению, отсутствующие ионы натрия и в настоящем случае переходят в фазу расплава с эквивалентным количеством кислородных ионов, т. е., в сущности, содержание окиси натрия в стекле уменьшается. Теоретически условием протекания этого процесса является то, что химический потенциал окиси натрия в расплаве должен быть меньше, чем в стекле. Для проверки данной гипотезы, в последующем мы попробовали изменить знак разницы химических потенциалов в стекле и в расплаве, и тем самым, вызвать изменение состава в обратном направлении. Как и ожидалось, при обработке эвтектической смесью $NaNO_3$ и Na_2CO_3 концентрация окиси

натрия вблизи поверхности стекла действительно увеличилась. Распределение щелочных ионов представлено на рис. 3, на котором, для сравнения, представлено также и состояние после обработки нитратом натрия.

Исходя из того факта, что кислородные ионы переходят из одной в другую, еще вовсе не следует, что и внутри фазы стекла происходит миграция кислородных ионов, обладающих двумя отрицательными зарядами. Однако правда, что высокая энергия активации диффузии, сообщаемая в литературе, находится в согласии с образованием и диффузией кислородных ионов. Используя же приводимые константы и формулы [11], при экстраполяции

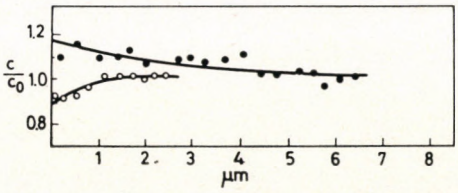

Рис. 3. Относительная концентрация ионов натрия в поверхностном слое стекла, обработанного расплавами солей

○ в стекле, обработанном $NaNO_3$
● в стекле, обработанном эвтектическим расплавом $NaNO_3$ и Na_2CO_3

диффузионных постоянных к температурам измерений получаем величины, которые на целый порядок ниже величины, необходимой для наблюдения какого-либо эффекта. (Коэффициент диффузии иона кислорода в стекле с составом 16% Na_2O, 12% CaO и 72% SiO_2 при 355°C равен 10^{-20}см^2/сек.) Таким образом, маловероятным кажется, чтобы механизм наблюдаемого явления совпадал бы с механизмом диффузии кислорода, описанным в литературе.

Образование и диффузия кислородных ионов протекает, вероятно, согласно такому механизму, когда один диффундирующий ион кислорода (атом кислорода) всегда присоединяется хотя бы к одному атому кремния. На основе стереохимии кремния можно полагать механизм типа S_N2, с помощью которого нам уже удалось интерпретировать взаимодействие стекла с гидроксильными ионами [16]. Это — реакция какой-либо части силикатного каркаса с гидроксильным ионом:

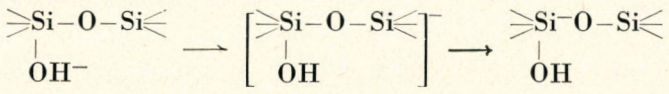

Характерным для механизма — действительность которого будет распространена и на диффузию иона кислорода — является то, что атакуемый кремний в промежуточном состоянии является пентаковалентным. При

взаимодействии с солевыми расплавами, конечный атом кислорода (т. е. немостиковый ион кислорода, $\geqslant Si-O^-$) играет ту же самую роль, что и гидроксильный ион в предыдущем примере. Кислородный ион образуется и реагирует с каркасом на поверхности согласно следующему уравнению:

$$\underset{\text{стекло}}{\geqslant Si-O^-} + \underset{\text{стекло}}{\geqslant Si-O^-} \rightleftharpoons \underset{\text{стекло}}{\geqslant Si-O-Si\leqslant} + \underset{\text{расплав}}{O^{-2}}$$

Сам же процесс транспорта является более сложным; представим его на минимальном числе групп:

$$\geqslant Si^1-O^- + Si^2-\overset{*}{O}^- + Si^3-O-Si^4\leqslant \rightarrow$$

$$\rightarrow \geqslant Si^1-O^- + Si^2-\overset{*}{O}-Si^3 + {}^-O-Si^4\leqslant \rightarrow$$

$$\rightarrow \geqslant Si^1-O- Si^2 + {}^-\overset{*}{O}-Si^3 + {}^-O-Si^4\leqslant .$$

Кислород, обозначенный звездочкой, в двух ступенях полностью переходит от 2-ого атома кремния к 3-ему атому. Дольнейшую же миграцию можно представить так, что он переходит к такому атому кремния, который и не представлен на нашем упрощенном каркасе с двумя измерениями. Следует заметить, что данный атом кислорода образует в промежуточном состоянии (второй ряд) мостик с атомом кремния и, в противоположность двум другим состояниям, здесь не имеет ионного заряда. Скорость сдвига заряда больше, чем скорость атомов кислорода, а направление их одинаково. Откуда удаляется заряд, там, на месте двух конечных кислородов, образуется по одному кислородному мостику (на нашей схеме между атомами кремния 1 и 2), что, между прочим, вытекает и из стехиометрических зависимостей, независимо от механизма.

При обработке чистым нитратным расплавом, вблизи поверхности возрастает доля мостиковых атомов кислорода. Т. к. механическая прочность гомогенного стекла тем больше, чем больше число мостиковых атомов кислорода и чем меньше число конечных атомов кислорода, то встает вопрос о том, какая доля изменения прочности образцов, обработанных расплавом нитрата калия, вызвана ионным обменам, а какая потерей щёлочного стекла. Хотя ответ на этот вопрос может быть получен, в первую очередь, экспериментально, однако, и сейчас кажется совсем очевидным, что потеря окиси натрия сама по себе может вызвать увеличение твердости стекла.

Согласно нашим измерениям, химическая устойчивость слоя с изменившимся составом также изменяется; возрастание содержания щелочного

Таблица 1

Относительная концентрация натрия, экстраполированная к поверхности, и скорость растворения стеклянных образцов в различном состоянии

Состояние стекла	Относительная концентрация ионов натрия C_{Na}/C_0	Толщина слоя, растворенного за 1 минуту при 25 °C под действием 0,2 %-ого раствора HF (μм/мин)
Необработанное	1,00	0,042
Обработанное $NaNO_3$	0,90	0,032
Обработанное эвтектической смесью $NaNO_3$ и Na_2CO_3	1,15	0,049

окисла увеличивает скорость взаимодействия с раствором HF а потеря щелочного окисла уменьшает эту скорость. Этот эффект наиболее сильно проявляется в непосредственной близости с поверхностью, и здесь наименьшей является погрешность измерений. В таблице 1 приводятся величины скоростей, относящихся к обработанному и необработанному стеклам, а также величины относительных концентраций иона натрия, экстраполированные к поверхности.

Summary

Upon the treatment of sodium-calcium glasses with molten nitrates at 355°C, the alkali oxide content decreases in the vicinity of the surface, whereas it increases upon the addition of molten Na_2CO_3. These changes in the composition modify the mechanical strength and chemical resistance of the glass. The loss and gain of alkali oxides cannot be assumed without oxide ion diffusion and their formation is likely under the conditions of the treatment, therefore, according to the suggested mechanism, diffusing oxygen always becomes bonded to at least one silicon atom.

ЛИТЕРАТУРА

[1] Burggraaf, A. J., Cornelissen, J.: Phys. Chem. Glass, **5,** 123, 1964
[2] Burggraaf, A. J.: Philips Res. Rep. Suppl., No 3, 106, 1966
[3] Kistler, S. S.: J. Am. Ceram. Soc., **45,** 59, 1962
[4] Aclogue, P., Tochon, J.: Symposium sur la résistance mécanique du verre et les moyens de l'améliorer, p. 687 Florence 1961
[5] Höhnert, M., Hinz, W.: Silikattechnik, **18,** 377, 1967
[6] Hager, J., Zsabrev, A.: XI. Siliconf., Budapest 55, 1973
[7] Urnes, S.: J. Am. Ceram. Soc., **56,** 514, 1973
[8] Schröder, H., Gliemeroth, G.: Naturwissenschaften **57,** 533, 1970
[9] Csákvári, B., Boksay, Z., Bouquet, G.: Anal. Chim. Acta, **56,** 279, 1971
[10] Boksay, Z., Varga, M., Bouquet, G.: XI. Szilikátipari Konferencia, Budapest, 1973
[11] Kingery, W. D., Lecron, J. A.: Physics Chem. Glasses, **1,** 87, 1960
[12] Doremus, R. H.: J. Am. Ceram. Soc., **43,** 655, 1960
[13] Sucov, E. W.: J. Am. Ceram. Soc., **46,** 14, 1963
[14] Douglas, R. W., Isard, M. A.: J. Soc. Glass Tech. **33,** 289, 1949
[15] Schaeffer, H. A., Oel, H. J.: Glastechn. ber. **42,** 493, 1969
[16] Budd, S. M.: Phys. Chem. Glass **2,** 111, 1961

Zoltán Boksay
Gusztáv Bouquet } H-1088 Budapest, Múzeum körút 6—8. Hungary.

I. M. Busujeva; Leningrad V—4 Szrednij pr. 41. USSR.

Acta Chimica Academiae Scientiarum Hungaricae, Tomus 85 (4), pp. 445—454 (1975)

POLAROGRAPHIC BEHAVIOUR OF URANYL ION IN CITRATE SOLUTIONS

I. M. ISSA, M. A. GHANDOUR, A. M. HAMMAN and M. K. HASSAN

(Chemistry Department, Assiut University, Assiut, A. R. E. Egypt)

Received November 18, 1974

The polarographic behaviour of U(VI) in citrate solution was investigated. Two waves were observed: the limiting currents and half-wave potentials of which depend on pH. At pH < 3, the first wave corresponds to the reduction of the uranyl citrate complex, into a mixture of U(IV) and U(V) citrate complexes. The second wave which is very small at higher concentrations of citrate (>0.1 *M*) corresponds to the reduction of free U(V). Between pH 3 and 6, the two waves, originating from the splitting of the principal wave (first wave), are attributed to the existence of two uranyl citrate species both of which are reduced to U(V), followed by dismutation of U(V) into U(IV) and U(VI). The two waves coalesce into one at higher U(VI) concentrations. The electrode reduction processes proceed reversibly and mainly under diffusion control with partial kinetic component.

Introduction

The polarographic behaviour of uranium, particularly those of higher oxidation states, have been extensively examined. However, little attention has been paid to the polarography of hexavalent uranium in organic acid media [1—12]. 0.1 *M* citric acid of different pH (between 2 and 8), in presence of 0.1 *M* KCl as supporting electrolyte, was used for electroreduction of 2×10^{-4} *M* $UO_2(NO_3)_2$ on a dropping mercury electrode by NEUMAN et al. [1]. Citric acid, among other acids, in conjunction with hydrazine was also used as base electrolyte by HOLA and OKAC [13].

In the present investigation, the effects of U(VI) and citric acid concentrations and pH of the base electrolyte on the electroreduction of U(VI) have been examined.

Experimental

Chemicals and solutions

2 *M* citric acid was prepared from a twice recrystallised sample (Feinchemie K. G. Sebnitz, C. P. Product) using bidistilled water. This solution, after proper dilution, was standardised against a standard alkali solution. Every few days a new solution was prepared in order to minimize bacterial decomposition. Uranyl perchlorate prepared by repeated evaporation of uranyl nitrate (G. R. Merck) with perchloric acid, was dissolved in 100 ml to give ~0.02 *M* solution. The exact uranium concentration of the solution was determined gravimetrically as U_3O_8 [14]. Other chemicals used in this investigation were of A. R. grade.

Nitrogen used for deoxygenating solutions was purified, 0.1% Triton X-100 was used to suppress the maxima whenever it was desired.

Procedure

Appropriate volume of uranyl solution to produce the desired concentration at final dilution was added to the proper quantity of supporting electrolyte. The solution was brought to a volume of 10 ml and mixed in the polarographic cell which was basically the same as that used by ISSA and THARWAT [15].

The solution was deoxygenated with purified nitrogen for 15 minutes then passing the gas above the solution during the electrolysis. It was polarographed using an LP 60 polarograph at full scale sensitivity of 20 μA and a polarisation rate of 200 mV/min. The limiting currents were determined graphically using the average of the recorded trace swings after correction for the residual currents. The half-wave potentials were evaluated from the log-analysis graphs of the waves.

The pH of the solution was adjusted by the addition of carbonate-free sodium hydroxide or perchloric acid and determined using a WG PYE model 290 pH meter.

The capillary characteristics of the dropping mercury electrode measured in 0.1 *M* KCl (open circuit) at a mercury height of 43.5 cm, were $m = 1.77$ mg sec^{-1} and $t = 3.52$ sec. The temperature for all experiments was maintained at 30°C$\pm$0.2°C.

Results and discussion

Preliminary experiments were carried out using citric acid alone as indifferent electrolyte. This was done to investigate the polarographic behaviour in citric acid without addition of another supporting electrolyte. The polarograms of 1 m*M* $UO_2(ClO_4)_2$ in different concentrations of citric acid ranging from 0.05 up to 2 *M* were recorded and represented graphically in Fig. 1. As can be seen from Fig. 1, each polarogram consists of two waves. The half-wave potentials, limiting currents, reciprocal of the slopes of logarithmic analysis and slopes of log *h vs.* log *i* plots are listed in Table I.

The height of the first wave increases gradually on increasing the acid concentration up to 0.2 *M* when the limiting current is equal to 4.6 μA. Above 0.4 *M* citric acid concentration, the limiting current decreases and reaches a value of 3.6 μA at 2 *M* acid. On the other hand, the height of the 2nd wave

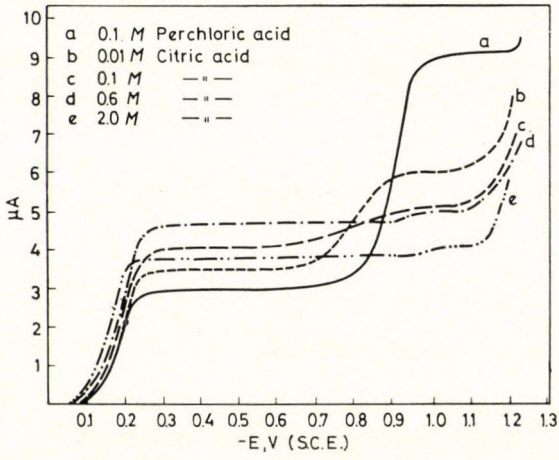

Fig. 1. Polarograms of 1 m*M* $UO_2(ClO_4)_2$

Table I

Limiting currents, half-wave potentials, reciprocal slope of log analysis and slope of log h vs log i plots for polarograms of 1 mM $UO_2(ClO_4)_2$ at different concentrations of citric acid

Citric acid *M*	i_l, μA		$0.061/\alpha n_a$		$-E_{1/2}$		log $h \sim$ log i slope	
	1st wave	2nd wave	1st wave	2nd wave	1st wave	2nd wave	1st wawe	2nd wave
0.05	4.2	2.3	0.060	0.09	0.184	0.841	0.40	0.40
0.1	4.5	1.4	0.058	0.11	0.182	0.825	0.40	0.43
0.2	4.6	1.1	0.066	—	0.180	—	0.41	—
0.4	4.6	0.6	0.066	—	0.179	—	0.40	—
0.6	4.4	0.5	0.066	—	0.158	—	0.43	—
0.8	4.2	0.3	0.060	—	0.149	—	0.42	—
1.0	4.0	0.3	0.060	—	0.149	—	0.43	—
1.5	3.8	0.2	0.060	—	0.141	—	0.44	—
2.0	3.6	0.2	0.060	—	0.137	—	0.45	—

decreases on increasing the acid concentration. It becomes very small, and ill-defined. The half-wave potentials of both waves shift towards less negative potentials on increasing the acid concentration indicating that hydrogen ions are participating in the electroreduction mechanism.

In order to elucidate this behaviour, the polarograms were recorded in the presence of 0.1 *M* $HClO_4$ as supporting electrolyte, to which citric acid was added in different concentrations. In 0.1 *M* $HClO_4$, two waves were observed (*c.f.* Fig. 1), the height of the second wave was twice that of the first wave, which indicate that U(VI) is reduced to U(V) (first wave) and subsequent reduction of U(V) into U(III) in one step (second wave). The addition of citric acid increases the limiting current of the first wave and decreases that of the second. Thus the limiting currents of the first wave and of the second wave for 1 m*M* U(VI) are 2.8 and 5.8 μA at zero citric acid concentration. In the presence of 0.1 *M* citric acid the corresponding values are 4.5 and 1.4 μA, respectively.

It is known that citrate forms complexes with many different ions including uranium [16, 17]. Therefore, the first step indicates the reduction of uranyl citrate species into lower oxidation states of uranium. The latter states are more stable towards polarographic reduction in the presence of excess of citric acid and hence their reduction wave was obliterated.

NEUMAN *et al.* [1] suggested that the first wave in 0.1 *M* citric acid containing 0.1 *N* KCl as supporting electrolyte corresponds to the reduction of UO_2^{2+}–citrate complex into tetravalent uranium. However, in the present investigation, the limit of increase of the first wave amounts to $\sim$1.6 μA (in 0.1 *M* citric acid) if it is compared with the one electron height (2.8 μA)

observed in citric acid-free 0.1 *M* $HClO_4$. Furthermore, the increase in current starts to diminish on increasing the acid concentration. This behaviour was also observed if $NaClO_4$ or KCl solutions was used instead of $HClO_4$. Thus, one can assume that the increase in current may be due to the interference of U(VI) citrate complexes which is reduced to U(V) species, and the disproportionation of pentavalent uranium. Numerous investigations verified the dismutation of pentavalent uranium [18—20]:

$$2U(V) \rightleftharpoons U(IV) + U(VI)$$

The equilibrium is dependent on pH, concentration of uranyl ion and dropping time of the capillary electrode [21]. The disproportionation rate is reported to be negligibly small between pH 2 and 2.5 in perchlorate media [22, 23]. However, the increase in the wave height can be observed not only with increasing hydrogen ion concentration, but also in the presence of other inorganic ions and organic acids [24]. Assuming that U(V) complexes are rather unstable the addition of citric acid may enhance the rate of disproportionation, since the tendency of U(IV) towards complexation is greater than that of UO_2^{2+} [25], *i.e.* the equilibrium is shifted to right hand side. In the presence of large excess of citric acid, *viz*: ~1 *M*, viscosity of the solution, in addition to the increased stability of the uranyl citrate species will counteract the increase in the limiting current.

From the log analysis graphs of the first wave it is apparent that the electroreduction of UO_2^{2+} in citric acid medium proceeds reversibly since the reciprocal of the slope is 0.058—0.066 which is close to the theoretical value of 0.061 which corresponds to one reversible electron process at 30°C.

NEUMAN *et al.* [1] reported that the second wave was ill-defined and cannot be assigned with certainty. However, from the present investigation, this wave did not appear at all if the concentration of UO_2^{2+} was less than 1 m*M* in 2 *M* citric acid concentration. It began to appear at concentration of 1 m*M* UO_2^{2+} as a very small wave with a height of 0.3 μA and maintains this value at higher concentration of the depolarizer. Therefore, one can suggest that the second wave may correspond to the electroreduction of uncomplexed U(V) into U(IV), since no reduction wave of U(IV) was obtained by NEUMAN *et al.* [1].

For the second wave, the reciprocal of the slopes of the analysis is ~{0.09—0.11) indicating that the process is irreversible assuming that the second step involves one electron for U(V) reduction.

From the slopes of log h — log i plots, it can be assumed that the two reduction steps are mainly diffusion controlled with partial kinetic component. This may be visualised from the effect of changing the depolarizer concentration from 2.5×10^{-4} to 2×10^{-3} *M*, on the limiting current of the first and

second waves. In the case of the first wave, i_l/C amounts to 4.0 μA/mM in 1.0 M citric acid whereas in 0.1 M citric acid it equals 4.6 ± 0.2 μA/M. A constant value of 1.4 μA/mM was observed for the second wave in 0.1 M acid and for the concentration range 2.5×10^{-4}—7.5×10^{-4} U(VI). At higher concentration of the acid, the second wave height is small and no constant value of i_d/C could be obtained. Therefore, 0.1 M citric acid may be recommended as supporting electrolyte for the polarographic determination of U(VI), making use of the first wave.

Effect of pH

The polarograms recorded for 1 mM $UO_2(ClO_4)_2$ in 0.1 M citric acid and 0.1 M $NaClO_4$ at different pH between 2.35 and 12 are shown in Fig. 2. At pH 2.35 two waves are observed, the first one with $E_{1/2} = -0.21$ V corresponds to

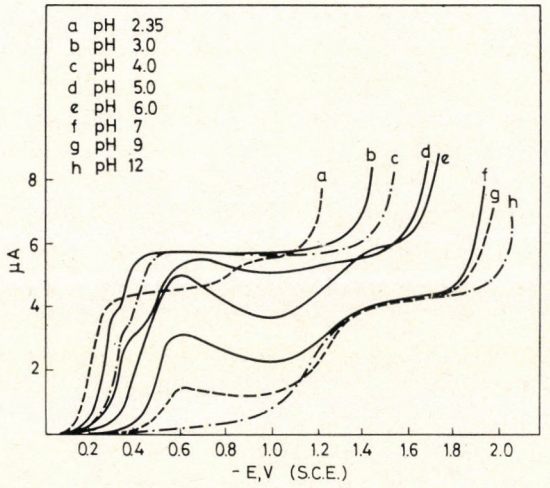

Fig. 2. Effect of pH: 1 mM UO_2^{2+}, 0.1 M citric acid + 0.1 M $NaClO_4$

the first wave in 0.1 M citric acid and represents the reduction of U(VI) into a mixture of U(V) and U(IV). The second wave whose half-wave potential is −0.84 V may correspond to the reduction of uncomplexed U(V). On further rising the pH of the solution through the addition of NaOH, the limiting current of the first wave, *i.e.* the principal wave, increases while that of the second wave remains constant and the two waves intermingle at pH 3. In the meantime splitting of the principal wave into two waves of unequalheight also occurs. The half wave potentials and limiting currents of the two waves are listed in Table II. The $E_{1/2}$ of waves shift to more negative potentials with rise of pH. At pH 6, the two waves merge and a minimum is appeared. On further increasing the pH of the base electrolyte, the limiting currents and the mi-

Table II

Limiting currents and half wave potentials at different pH, 0.1 M citric acid, 0.1 M $NaClO_4$, 1 mM UO_2^{2+}

pH	1st wave		2nd wave	
	i_l	$-E_{1/2}$	i_l	$-E_{1/2}$
2.35	4.2	0.21	1.3	0.86
3.05	3.7	0.24	1.8	0.36
4.10	3.0	0.30	2.5	0.44
4.98	2.2	0.45	2.3	0.49

nima decrease gradually indicating that two waves may be obtained between pH 6 and 12, but the minimum vitiates the first wave. The half wave potential of the second wave amounts to −1.25 V at pH between 9 and 12. This is due to the progressive hydrolysis of hydrated uranyl ion (perhaps, $UO_2^{2+} \cdot 6\ H_2O$) on increasing pH. Also complicated uranyl compounds, such as $U_2O_5^{2+}$ and $U_3O_8(OH)_4^{2-}$ may form [16, 26]. When coordinating anions are present in the solution, the situation becomes even more confusing.

It is evident that the limiting currents decrease and half-wave potentials shift towards more negative values on adding gelatin or Triton X-100. It was also observed that the polarograms were affected with time of contact between the depolarizer and supporting electrolyte, at higher pH, before recording the polarograms. Spectrophotometrically, a change in optical density with time was also observed which is in agreement with the previous work of NEUMAN and FELDMAN [27]. Therefore, the behaviour observed at higher pH may be attributed to the hydrolysis and slow equilibrium attainment between the complex species. The discussion will be limited to the polarographic behaviour of U(VI) in citrate media at pH < 6.

NEUMAN *et al.* [1] suggested that between pH 3 and 6 in citrate media, the first wave was due to a 2-electron reduction of a dimeric complex:

$$(\text{U(VI)} : \text{citrate})_2 + m\ \text{H}^+ + 2e = 2(\text{U(V)}: \text{citrate})$$

and the second wave was attributed to the following reaction:

$$\text{U(V)} : \text{citrate} + n\ \text{H}^+ + e = \text{U(IV)} : \text{citrate}$$

Consequently, a total 2-electron reduction mechanism is involved. Those authors [1] mentioned that the first wave has a reciprocal slope of 0.034 when $\log i^2/i_{l-i}$ was plotted against potential indicating a reversible 2-electron reduction for a dimer. The same slope was also obtained in the present work, but the analysis of both waves as $\log i/i_{d-i}$ *vs* E gave linear plots with reciprocal

slopes close to the theoretical value of reversible one-electron reduction *viz*: (0.055—0.066) within the pH range studied. Therefore, one can assume that the first wave may correspond to the electroreduction of two species, the dimer U_2L_2 and monomer UL which are present in admixture and simultaneously reduced at the same potential.

$E_{1/2}$ of the first and second waves amounting to —0.32 and —0.46 V, respectively, at pH 4.6 agree with —0.30 and —0.45 reported by NEUMAN *et al.* [1]. However, since it is well-established that U(V) is reduced at nearly —0.86 V *vs.* S.C.E. in moderately acid solutions [28], it is improbable that the second wave corresponds to the reduction of U(V)-citrate complex to U(IV).

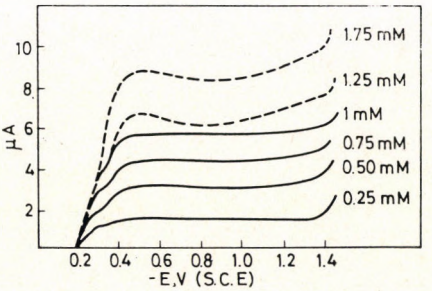

Fig. 3. Effect of $[UO_2^{2+}]$ at pH 3.1 *M* citric acid

NEUMAN *et al.* [1] reported that U(IV)-citrate did not give an anodic wave, indicating that the system as a whole was irreversible irrespective of the reversibility tests. Furthermore, from the unequality of the heights of the two waves at pH < 5, it is concluded that the two waves represent the reduction of two uranyl citrate species, both of which are reduced to U(V)-citrate complexes followed by disproportionation of the reduction products into U(VI) and U(IV). This may find support from experiments which were carried out at different concentrations of citrate anions while keeping the pH constant at 4.6. It was found that the limiting current of the second wave decreases on increasing the citric acid concentrations and that the wave was completely vitiated and merged with the first wave in $\sim$0.5 *M* citrate. The total limiting current of the single wave observed is higher than the height of the first wave before the merging of the waves. It is, therefore, concluded that the second wave is not corresponding to the reduction of U(V)-citrate but to the reduction of another U(VI)-citrate complex species.

In addition to the effects of pH and total ligand concentrations, so far discussed, on the splitting of the principal wave, it was found that the concentration of U(VI) had an effect too. Complete polarograms were recorded for different concentrations of the depolarizer at the same pH and the same concentration of citrate. As can be seen on Fig. 3, an increase in the uranyl

concentration led to the intermingling of the waves. For each pH, a certain UO_2^{2+} concentration was needed for the occurrence of this phenomenon. It was found that the lower the pH the lower the concentration of the depolarizer needed for merging of the two waves. Thus, it can be assumed that the two waves are corresponding to the presence of two species of citrate complexes, the stability and structure of which depend on the U(VI) concentration and that only one of them prevails in the electrode reaction. Consequently a single wave appears at higher concentration of U(VI).

From $E_{1/2}$-pH plots of the waves, recorded in 0.1 *M* citric acid, shown in Fig. 4, it is apparent that each consists of three linear sections covering the

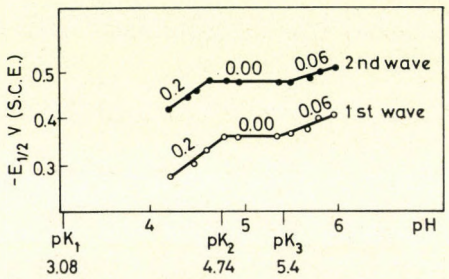

Fig. 4. $E_{1/2}$ — pH plot

pH ranges 4.2—4.7, 4.7—5.4 and 5.4—5.9. The slopes of the linear sections are 0.2, 0 and 0.06 for the three pH ranges, respectively.

The $E_{1/2}$-pH plot at lower pH is not linear (not represented in the graph). At pH 5.4—6, one H^+-ion is involved in the electroreduction step, whereas the horizontal section indicates a pH independent reduction step. This pH-independent region lies between pK_2, 4.74, and pK_3, 5.40, of citric acid whereas pK_1 of citric acid is 3.08.

From definition,

$$pH = pK_1\ (= 3.08) + \log\ H_2cit^-/H_3cit,$$
$$pH = pK_2\ (= 4.74) + \log\ H\ cit^{2-}/H_2cit^- \text{ and}$$
$$pH = pK_3\ (= 5.4) + \log\ cit^{3-}/H\ cit^{2-}$$

it is assumed that at intersection of two lines of pH $-E_{1/2}$ plots, *i.e.* at pK_2 and pK_3, two ligand species are present in equal concentrations and at pH $> pK_i$ of the acid (i, referred to as the ith dissociation constant of a polybasic acid), one species predominates. On this basis, at pH 4.7 *e.g.*, mainly two species are present in equal concentrations, $Hcit^{2-}$ and H_2cit^- which may be responsible for the appearance of the two waves. At pH < 3 only H_2cit^- undergoes

chelation whereas the undissociated acid H_3cit does not, and one wave is observed. Also, at pH $>$ 6, cit^{3-} exists in a large amount compared to others and the two waves coalesce into one step.

From the log h — log i plots for the polarograms obtained at pH 3—5, it was found that the electroreduction process is mainly diffusion controlled with partial kinetic component.

The separate limiting currents of both waves are not proportional to the concentration of the depolarizer from 2.5×10^{-4} to 1×10^{-3} M, but the total limiting current is (at pH 3), and the value of i_l/c is equal to 5.6 μA/mM. This is attributed to the fact that the rate of disproportion of U(V) depends on the concentration. The proportionality of limiting currents to the concentration of depolarizer does not hold when either the pH or the concentration of U(VI) is increased above 1 mM. In the latter case a minimum appears at the plateau of the second wave and is not removed by Triton. However, the depth and width of the minimum increase with increasing pH of the solution. Furthermore, the separation of the two waves was found to be difficult when the concentration of UO_2^{2+} increased. This behaviour may support the mechanism hitherto discussed.

Composition of the complex

Spectrophotometry

Uranyl ions and citrate ions combine to form 1 : 1 and 2 : 1 complexes. In the presence of higher concentrations of citrate, the former is more stable, and actually exists alone. The latter is highly dissociated, and exists only when the concentration of metal ion exceeds that of the citrate. The results are identical with those obtained by NEUMAN and FELDMAN [27].

Amperometry

Amperometric titration of 0.5 ml 0.05 M $UO_2(ClO_4)_2$ with 0.01 M sodium citrate at a potential of —0.25 V *vs* S.C.E. gave L-shape graph throughout the pH range studied. A reversed L-shape graph is obtained if citrate is titrated with UO_2^{2+}. From these studies it is concluded that a 1 : 1 metal–ligand complex is formed. The complex is stable at pH 4—5.

Effect of citrate concentration

At pH 4.6 and 1×10^{-3} M $UO_2(ClO_4)_2$ the half-wave potentials of both reduction waves are independent of the citrate ion concentration when the U/citrate mole ratio was varied from 1 : 5 to 1 : 1000. This verified the fact that at this pH no complexes are formed containing more than one mole of citrate per mole of uranium. It also indicated that there is no change in the

number of citrate molecules associated with uranium during its reduction to the lower valency state. However, the presence of large excess of citrate gave rise to one wave. This may be due to a slow equilibrium attainment between the complex species and despite their presence, only one of them is reduced in the dropping mercury electrode.

REFERENCES

[1] Neuman, W. F., Havill, J. R., Feldman, I.: J. Am. Chem. Soc. **73,** 3593 (1951)
[2] Minereuski, J., Sabkowska, A.: Acta Chim. Acad. Sci. Hung., **27,** 143 (1961)
[3] Polfi, E., Hadabas, B.: Acta Chim. Acad. Sci. Hung., **27,** 155 (1961)
[4] Davis, D.: Anal. Chem. **33,** 492 (1961)
[5] Hola, J.: Coll. Czech. Chem. Commun. **29,** 905 (1964)
[6] Lai, T., Hsieh, C.: Inorg. Nucl. Chem. **26,** 1215 (1964)
[7] Lai, T., Ching, T.: Anal. Chim. Acta **37,** 253 (1967)
[8] Dosanka, S., Milenko, S.: Coll. Czech. Chem. Commun. **36** 935 (1971)
[9] Mánok, F., Várhelyi, Cs.: Minerva Galatcanu-Titieni; Rev. Roum. Chim. **17** 675 (1972)
[10] Lai, T., Wey, S.: Anal. Chem. Acta **33,** 324 (1965)
[11] Athavale, V., Dhaneshwan, R., Padwanabha, C.: Indian J. Chem. **5** 313—15 (1967)
[12] Hola, J., Okac, A.: Coll. Czech. Chem. Commun,. **27,** 1697 (1961)
[13] Hola, J., Okac, A.: Coll. Czech. Chem. Commun., **5,** 424 (1967)
[14] Vogel, A. I.: "A Text-Book of Quantitative Inorganic Analysis", 3rd ed. Longmans, London, 1968, p. 539
[15] Issa, I. M., Tharwat, M.: Electrochim. Acta **17,** 343 (1972)
[16] Rabinowitz, E., Belford, R. L.: "Spectroscopy and Photochemistry of Uranyl Compounds", Pergamon Press Inc., London 1964, pp. 136—139
[17] Jorgensen, C. K.: "Inorganic Complexes", Academic Press Inc., London 1963, p. 97
[18] Herasymenko, P.: Trans. Faraday Soc. **24,** 272 (1928)
[19] Kern, D. M. H., Orlemann, E. F.: J. Am. Chem. Soc., **71,** 2102 (1949)
[20] Orlemann, E. F., Kern, D. M. H.: J. Am. Chem. Soc. **75,** 3058 (1953)
[21] Koutecky, J., Koryta, J.: Chem. Listy **48,** 996 (1954); Coll. Czech. Chem. Commun. **19,** 945 (1954)
[22] Nelson, F., Kraus, K. A.: J. Am. Chem. Soc., **71,** 2517 (1949)
[23] Nelson, F., Kraus, K. A.: J. Am. Chem. Soc., **73,** 2157 (1951)
[24] Sobkowska, A., Minczewski, J.: Nukleonika, **10,** 311 (1965)
[25] Cordfunke, E. H. P.: "The Chemistry of Uranium", Elsevier Publishing Co., 1969, p. 105
[26] Harwitz, A., Atkinson, G.: J. Phys. Chem. **71,** 4142 (1967)
[27] Neuman, W. F., Feldman, I.: J. Am. Chem. Soc., **73,** 2312 (1951)
[28] Kolthoff, I. M., Lingane J. J.: "Polarography". Interscience Publishers, New York 2nd ed. 1952

I. M. Issa
M. A. Ghandour
A. M. Hamman
M. K. Hassan

Chemistry Department, Assiut University,
Assiut, A.R.E. Egypt.

Acta Chimica Academiae Scientiarum Hungaricae, Tomus 85 (4), pp. 455—470 (1975)

MICHAEL REACTION WITH β-*p*-TOLUOYL- AND *p*-CHLOROBENZOYLACRYLIC ACIDS AND THEIR AMIDES

A. SAMMOUR, A. A. AFIFY, M. M. ABD-ALLAH and E. A. SOLIMAN
(Faculty of Science, Ain Shams University, Cairo, Egypt)

Received April 28, 1974; in revised form November 8, 1974

β-*p*-Toluoyl- and *p*-chlorobenzoylacrylic acids react under Michael conditions with diethyl malonate, dimethyl succinate, diisobutyl ketone, ethyl phenylacetate, ethyl acetoacetate, benzyl methyl ketone, ethyl methyl ketone, methyl isopropyl ketone and acetonylacetone to give cyclic or normal Michael addition products depending on the nature of the active methylene compound.

In continuation of our recent studies [1, 2], in this work Michael reactions with β-aroylacrylic acids have been investigated.

The olefinic double bond in β-aroylacrylic acids is activated by the adjacent carbonyl and carboxyl groups. The polarization of the olefinic double bond by the ketone group outweighs that caused by the carboxyl group. The keto group gives a more stable carbonium ion than the carboxyl group, *i.e.* the α-carbon atom will accept nucleophiles (the components in Michael condensation) more readily than the β-carbon atom.

β-Aroylacrylic acids are thus expected to resemble α, β-unsaturated ketones in their mode of addition.

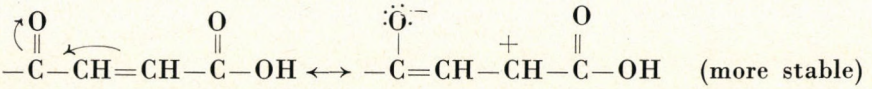

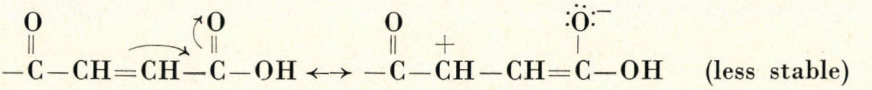

The object of the present work has been to study whether β-aroylacrylic acids behave as α, β-unsaturated acids or as α, β-unsaturated ketones in the Michael addition with compounds containing active methylene groups.

It has been found that the addition of diethyl malonate (*cf.* [3]), dimethyl succinate (*cf.*[4]), diisobutyl ketone, and ethyl phenylacetate to β-*p*-toluoyl- and *p*-chlorobenzoylacrylic acids **Ia** and **b** in sodium methoxide afforded the normal Michael adducts **IIa**—h.

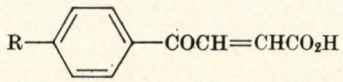

I

a R = CH_3, *b* R = Cl

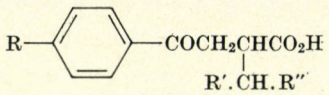

II

	R	R′	R″
a,	CH_3	$CO_2C_2H_5$	$CO_2C_2H_5$
b,	Cl	$CO_2C_2H_5$	$CO_2C_2H_5$
c,	CH_3	CO_2CH_3	$CH_2CO_2CH_3$
d,	Cl	CO_2CH_3	$CH_2CO_2CH_3$
e,	CH_3	$CH(CH_3)_2$	$COCH_2CH(CH_3)_2$
f,	Cl	$CH(CH_3)_2$	$COCH_2CH(CH_3)_2$
g,	CH_3	C_6H_5	$CO_2C_2H_5$
h,	Cl	C_6H_5	$CO_2C_2H_5$

The NMR spectrum of **IIc** shows bands at τ values 2.00, 2.05, 2.15, 2.50 and 2.60 (4H of disubstituted aryl group), 5.50 (2H of $-\underline{CH}-COOH$ and $-\underline{CH}-COOCH_3$), 6.45 (9H of three CH_3 groups), and 6.65 (4H of $CH-\underline{CH_2}-CO-Ar$ and $-CH-\underline{CH_2}-COOCH_3$) [5].

Alkaline hydrolysis of **IIa**, **c** and **g** in boiling 5% alcoholic potassium hydroxide led to the formation of the dibasic acids **IIIa—c**, respectively.

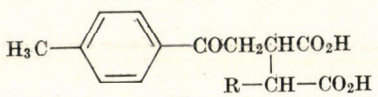

III

a, R = H **d,** R = CH_3 **c,** R = C_6H_5

When **IIa** and **c** were treated with boiling acetic anhydride, the 3,4-dihydro-α-pyrone derivatives **IVa** and **b** were obtained.

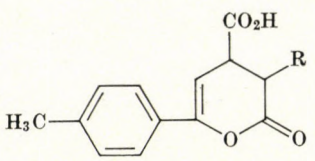

IV

a, R = $CO_2C_2H_5$ **b,** R = $CH_2CO_2CH_3$

Claisen condensation of **IIa** and **b** with benzaldehyde or anisaldehyde gave the tricarboxylate derivatives **Va** and **b.**

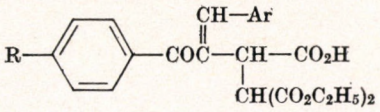

V

	R	Ar
a,	CH_3	C_6H_5
b,	Cl	$C_6H_4OCH_3-(p-)$

The NMR spectrum of **Va** has bands at τ values 2.10, 2.20 (4H of disubstituted phenyl group), 2.55, 2.65 (5H of phenyl group), 5.95—6.19 (4H of $-\overset{\overset{O}{\|}}{C}-O-\underline{CH_2}$-group), 6.30 ($CH_3$ of $Ar-CH_3$ and two CH_3 of ethyl ester), 6.45 (1H of $-\overset{\overset{O}{\|}}{C}-\underline{CH}-\overset{\overset{O}{\|}}{C}-$), 6.60 (1H of $-\underline{CH}-COOH$) and 6.80 (1H of $-CH.Ph$).

When the acid **Ia** was allowed to react with diethyl succinate (molar ratio 1 : 2) in the presence of sodium methoxide, 3,3', 4,4'-tetrahydro-2,2'-dioxo-6-6'-di-*p*-tolyl-3,3'-bi-2H-pyran-4,4'-dicarboxylic acid (**VI**) was obtained.

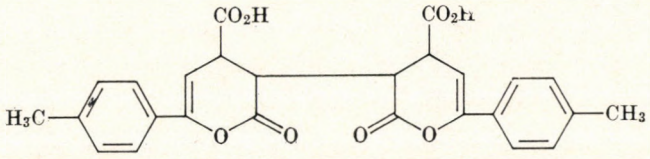

VI

On the other hand, the addition of ethyl acetoacetate, benzyl methyl ketone, ethyl methyl ketone, methyl isopropyl ketone and acetonylacetone under the same conditions led to the formation of the 3-cyclohexene-1-carboxylic acid derivatives **VIIa—i**.

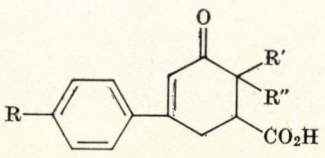

VII

	R	R′	R″
a,	CH_3	$CO_2C_2H_5$	H
b,	Cl	$CO_2C_2H_5$	H
c,	CH_3	C_6H_5	H
d,	Cl	C_6H_5	H
e,	CH_3	CH_3	H
f,	Cl	CH_3	H
g,	CH_3	CH_3	CH_3
h,	Cl	CH_3	CH_3
i,	CH_3	CH_2COCH_3	H

The NMR spectrum of **VIId** has bands at δ values 7.80, 7.71, 7.54, 7.51 (4H of disubstituted aryl group), 7.31, 7.27 (5H of phenyl group), 6.51 (1H of H—C(—C=O)=), 4.07 (1H of —CH—COOH), 3.98 (1H of —CH—Ph) and 2.30 (2H of $-CH_2$).

Decarbethoxylation of (**VIIa** and **b**) with alcoholic potassium hydroxide gave the 3-cyclohexene-1-carboxylic acid derivatives **VIIIa** and **b**.

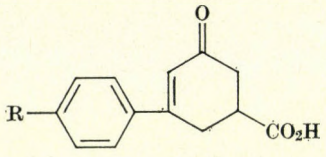

VIII

a, R = CH_3 **b,** R = Cl

Further, we investigated the reaction of the β-aroyl-N-arylacrylamides **IXa—e** with diethyl malonate under the same Michael conditions as above, to obtain ethyl-3,4-dihydro-6-aryl-4-(arylcarbamoyl)-2H-pyran-3-carboxylates **Xa—e**.

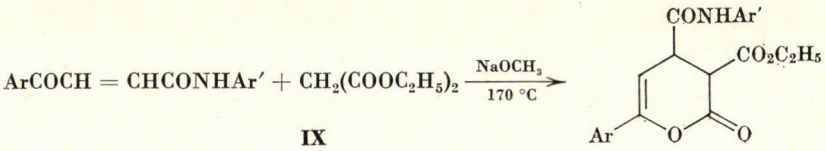

IX **X**

	Ar	Ar′
a,	$C_6H_4CH_3$—*p*	C_6H_5
b,	$C_6H_5CH_3$—*p*	C_6H_4—CH_3—*p*
c,	C_6H_4—Cl—*p*	C_6H_5
d,	$C_{10}H_{11}$—2	C_6H_5
e,	$C_{10}H_{11}$—2	C_6H_4—CH_3—*p*

Hydrolysis of **Xa** with a mixture of boiling hydrochloric acid and acetic acid and 5% alcoholic potassium hydroxide gave **XI** and **XII**, respectively.

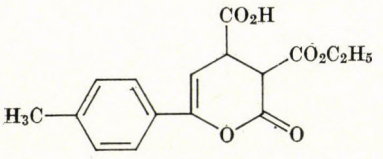

XI

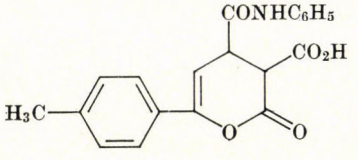

XII

The cyclohexene derivatives **VII** condensed with hydrazine hydrate or phenylhydrazine in boiling ethanol to give the hydrazone derivatives (**XIIIa—h**).

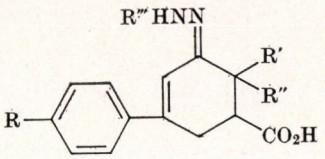

XIII

	R	R′	R″	R‴
a,	CH_3	$CO_2C_2H_5$	H	H
b,	Cl	$CO_2C_2H_5$	H	H
c,	CH_3	C_6H_5	H	H
d,	CH_3	CH_3	H	H
e,	Cl	CH_3	H	H
f,	CH_3	CH_3	CH_3	H
g,	CH_3	CH_3	H	C_6H_5
h,	CH_3	CH_3	CH_3	C_6H_5

Interestingly, **VIIa** and **b** reacted with phenylhydrazine in boiling ethanol to give the phenylhydrazones **XIVa** and **b** with elimination of the carbethoxyl group.

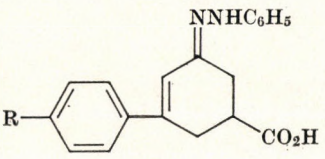

XIV

a, R = CH_3 **b,** R = Cl

The NMR spectrum of **XIVa** shows bands at τ values 0.7 (1H of —COOH), 2.55, 2.65, 2.81, 2.89, 3.30, 3.40 (9H of phenyl and disubstituted phenyl groups), 3.45 (1H of NH), 7.25, 7.55 (1H and 4H of $C\underline{H}_2-C\underline{H}-C\underline{H}_2$) and 7.72 (3H of $Ar-CH_3$).

On the other hand, the condensation of **VIa** with phenylhydrazine in glacial acetic acid afforded 3,3*a*, 4,5-tetrahydro-3-oxo-2-phenyl-6-*p*-tolyl-2H-indazole-4-carboxylic acid (**XV**).

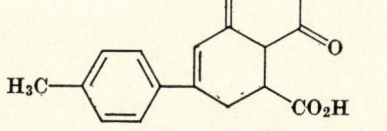

XV

The reaction of **VIIa** and **b** with hydroxylamine hydrochloride gave the oximes **XVIa** and **b** with elimination of the carbethoxyl group.

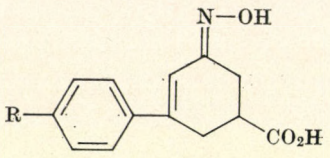

XVI

a, $R = CH_3$ **b,** $R = Cl$

The reaction of **IIa** with piperidine or benzylamine in boiling benzene yield **XVIIa** and **b**, respectively.

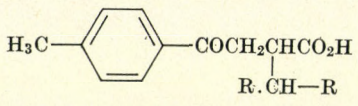

XVII

a, $R = CONHC_5H_{10}$ **b,** $R = CONHCH_2C_6H_5$

On the other hand, **IIc** and **d** reacted with benzylamine in boiling benzene to give methyl 1-benzyl-4-carboxy-6-aryl-1,2,3,4-tetrahydro-2-oxo-3-pyridyl-acetate (**XVIIIa** and **b**).

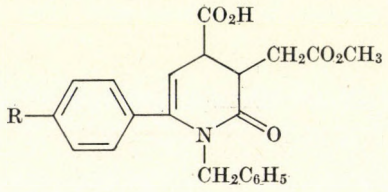

XVIII

a, $R = CH_3$ **b,** $R = Cl$

Furthermore, 5-aryl-2-methyl-3-morpholino- or piperidino-3-cyclohexa-2,4-diene-1-carboxylic acids (**XIXa—d**) were obtained *via* the reaction of the Michael adducts **VIIe** and **f** with morpholine or piperidine in boiling benzene.

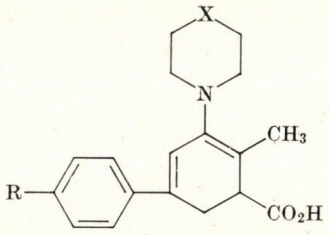

XIX

	R	X
a,	CH_3	O
b,	CH_3	CH_2
c,	Cl	O
d,	Cl	CH_2

Experimental

The IR spectra were obtained with a Unicam SP 1200 spectrophotometer using the KBr wafer technique. The NMR spectra were recorded with a Varian A60 spectrophotometer. All m. p.'s are uncorrected.

Base-catalyzed addition of active methylene compounds to β-aroylacrylic acids (Ia and b) and their amides (IXa—e). Formation of IIa—h, VI, VIIa—i and Xa—e

A mixture of the β-aroylacrylic acid or its amide (0.01 mole), the active methylene compound (0.01 mole), and sodium methoxide solution (0.015 mole) was heated at 170°C for 10 hrs. The reaction mixture was poured into water, then extracted with ether to get rid of any unreacted organic materials. The aqueous layer was acidified with ice-cold dilute hydrochloric acid. The oil which separated was triturated with light petrol (b.p. 80—100°C). The solid obtained was crystallized from a suitable solvent to give the colourless Michael adducts (**IIa—h**, **VI**, **VIIa—i** and **Xa—e**, respectively) (*cf.* Table I).

Alkaline hydrolysis of IIa, c and g, VIIa and b and Xa. Formation of IIIa—c, VIIIa and b and XII

An alcoholic solution of **IIa**, **c** or **g**, **VIIa** or **b**, or **Xa** (2 g) was treated with aqueous potassium hydroxide solution (5%, 10 ml), and the reaction mixture was refluxed for 8 hrs. The cold mixture was acidified with dilute hydrochloric acid. The solid obtained was crystallized from a suitable solvent to give the dibasic acid derivatives **IIIa—c**, **VIIIa** and **b** and **XII**, respectively, as colourless crystals (*cf.* Table II).

Ring closure of IIa and c. Formation of IVa and b

A solution of **IIa** or **c** (0.01 mole) in acetic anhydride (20 ml) was refluxed for 6 hrs The solid obtained after concentration and cooling was crystallized from a proper solvent to give pale yellow crystals (**IVa** or **b**) (*cf.* Table III).

Condensation of IIa and b with aldehydes. Formation of Va and b

A mixture of **IIa** or **b** (0.01 mole), benzaldehyde or anisaldehyde (0.01 mole) ethyl alcohol (20 ml) and a few drops of piperidine was refluxed for 6 hrs. The solid product obtained on evaporation of most of the solvent and cooling was crystallized from benzene to give the butene derivatives **Va** and **b**, respectively, as colourless crystals (*cf.* Table IV).

Acid hydrolysis of Xa. Formation of XI

A solution of **Xa** (2 g) in a mixture of glacial acetic acid (10 ml) and conc. hydrochloric acid (10 ml) was refluxed 4 hrs. The reaction mixture was poured into ice. The solid which separated was filtered off and crystallized from benzene to give pale yellow crystals, m. p. 186°C; Yield: 95%.

$C_{16}H_{16}O_6$ (304). Calcd. C 63.1; H 5.2. Found C 63.4; H 5.2%.

Condensation of VII with hydrazine hydrate or phenylhydrazine. Formation of XIIIa—h, XIV and XV

A mixture of **VII** (0.01 mole), hydrazine hydrate or phenylhydrazine (0.01 mole) and ethanol or glacial acetic acid (15 ml), was refluxed for 6 hrs. The solid product formed after concentration and cooling was crystallized from a proper solvent to give the hydrazone derivatives **XIIIa—b**, **XVI** and **XV**, respectively, as yellow crystals (*cf.* Table V).

Table I

Michael adducts **IIa—h, VI, VIIa—i** *and* **Xa—e**

Compd.	M.p., °C	Solvent; Yield, %	Formula (Mol. wt.)		Analysis, % Found	Analysis, % Calcd.	Infrared Spectrum: ν of groups (KBr, cm⁻¹)		
IIa	149—150	E	$C_{18}H_{22}O_7$	C,	61.3	61.7	OH (acid) 3440	$-CH_2$ 2950	CO (ester) 1760
		92	(350)	H,	6.5	6.3	CO (acid) 1720	CO (aroyl) 1680	C=C 1610
IIb	147—8	B	$C_{17}H_{19}ClO_7$	C,	55.7	55.1			
		94	(370.5)	H,	5.3	5.1			
IIc	80—1	P	$C_{17}H_{20}O_7$	C,	60.7	60.7	OH (acid) 3440	$-CH_2$ 2940	CO (ester) 1750
		86	(336)	H,	5.6	5.9	CO (acid) 1720	CO (aroyl) 1680	C=C 1610
IId	85—6	P	$C_{16}H_{17}ClO_7$	C,	54.0	53.8			
		82	(356.5)	H,	4.8	4.7			
IIe	162—3	P	$C_{20}H_{28}O_4$	C,	72.0	72.2			
		87	(332)	H,	8.2	8.4			
IIf	222—3	B	$C_{19}H_{25}ClO_4$	C,	64.2	64.6	OH (acid) 3400	$-CH_2$ 2960	CO (acid) 1730
		95	(352.5)	H,	7.8	7.9	CO (aroyl) 1680	C=C 1600	
IIg	237—8	B	$C_{21}H_{22}O_5$	C,	70.7	71.1			
		95	(354)	H,	5.9	6.2			
IIh	213—4	T	$C_{20}H_{19}ClO_5$	C,	64.5	64.6			
		91	(374.5)	H,	5.2	5.0			

VI	238—9	E 88	$C_{26}H_{22}O_8$ (342)	C, H,	65.0 6.2	65.1 6.4	OH (acid) 3230 C=C 1620	CO (acid) 1745	CO (pyrone) 1690
VIIa	128—9	B 90	$C_{17}H_{18}O_5$ (302)	C, H,	67.5 5.9	67.5 6.0	OH (acid) 3230 CO (cyclo- hexene) 1660	CO (ester) 1740 C=C 1610	CO (acid) 1720
VIIb	167—8	B 90	$C_{16}H_{15}ClO_5$ (322.5)	C, H,	59.0 4.5	59.5 4.6			
VIIc	167—8	B/E 82	$C_{20}H_{18}O_3$ (306)	C, H,	78.2 5.9	78.4 5.8			
VIId	183—4	B/E 98	$C_{19}H_{15}ClO_3$ (326.5)	C, H,	69.3 4.7	69.8 4.5	OH (acid) 3480 CO (cyclo- hexene) 1650	$-CH_2$ 3030 C=C 1600	CO (acid) 1720
VIIe	217—8	B/E 75	$C_{15}H_{16}O_3$ (244)	C, H,	73.2 6.1	73.7 6.5	OH (acid) 3420 C=C 1610	CO (acid) 1720	CO (cyclo- hexene) 1640
VIIf	225—6	B/E 95	$C_{14}H_{13}ClO_3$ (264.5)	C, H,	63.2 4.9	63.3 4.8			
VIIg	237	Bu 84	$C_{16}H_{18}O_3$ (258)	C, H,	74.4 6.8	74.4 6.9	—OH (acid) 3500 C=C 1615	CO (acid) 1720	CO (cyclo- hexene) 1680
VIIh	228—9	E 90	$C_{15}H_{15}ClO_3$ (278.5)	C, H,	64.6 4.9	64.6 5.3			

(Table I continued)

Compd.	M.p., °C	Solvent; Yield, %	Formula (Mol. wt.)		Analysis, % Found	Analysis, % Calcd.	Infrared Spectrum ν of groups (KBr, cm^{-1})		
VIIi	179—180	T 77	$C_{17}H_{18}O_4$ (286)	C, H,	71.1 6.2	71.3 6.3	OH (acid) 3400 C=C 1610	CO (acid) 1720	CO (cyclo-hexene) 1690
Xa	180—1	E 92	$C_{22}H_{21}NO_5$ (379)	C, H, N,	69.3 5.4 3.5	69.6 5.6 3.6	NH (amide) 3520 CO (amide) 1640	CO (ester) 1740 $-CH_2$ 2950	CO (pyrone) 1710
Xb	145—6	E 94	$C_{23}H_{23}NO_5$ (393)	C, H, N,	70.2 5.6 3.5	70.2 5.8 3.5			
Xc	193	E 88	$C_{21}H_{18}ClNO_5$ (339.5)	C, H, N,	63.2 4.3 3.2	63.0 4.5 3.5	NH (amide) 3520 CO (amide) 1640	CO (ester) 1740 $-CH_2$ 2915	CO (pyrone) 1720
Xd	132—3	E 91	$C_{25}H_{25}NO_5$ (419).	C, H, N,	69.6 6.3 2.8	69.6 6.6 3.0			
Xe	118—9	B 92	$C_{26}H_{27}NO_5$ (433)	C, H, N,	72.2 5.9 3.2	72.0 6.2 3.2	NH (amide) 3480 CO (amide) 1670	CO (ester) 1730 $-CH_2$ 2920	CO (pyrone) 1710

B ≡ benzene, Bu = butanol, E = ethanol, P = light petrol, T = toluene

Table II

The dibasic acids **IIIa—c**, **VIIIa** *and* **b** *and* **XII**

Compd.	M.p., °C	Solvent; Yield, %	Formula (Mol. wt.)		Analysis, % Found	Analysis, % Calcd.	Infrared spectrum ν of group (KBr, cm^{-1})		
IIIa	173—4	T 67	$C_{13}H_{14}O_5$ (250)	C, H,	62.3 5.7	62.4 5.6			
IIIb	133	B 71	$C_{14}H_{16}O_5$ (246)	C, H,	64.0 5.8	63.6 6.0	OH (acid) 3480 CO (aroyl) 1680	$-CH_2$ 2950 C=C 1600	CO (acid) 1725
IIIc	177—8	B 72	$C_{19}H_{18}O_5$ (326)	C, H,	70.1 5.8	69.9 5.5			
VIIIa	216—7	T 60	$C_{14}H_{14}O_3$ (230)	C, H,	73.4 6.0	73.0 6.1	OH (acid) 3450 $-CH_2$ 3030, 2920	CO (acid) 1720 C=C 1610	CO (cyclo-hexene) 1680
VIIIb	206—7	E 66	$C_{13}H_{11}ClO_3$ (250.5)	C, H,	62.7 4.2	62.3 4.3			
XII	205	E 66	$C_{20}H_{17}NO_5$ (351)	C, H,	68.1 4.6	68.3 4.8	OH or NH 3420 CO (amide) 1680	CO (acid) 1710 C=C 1615	CO (pyrone) 1700

B = benzene, E = ethanol, T = toluene

Table III

The α-pyrone derivatives **IVa** *and* **b**

Compd.	M.p., °C	Solvent; Yield, %	Formula (Mol. wt.)		Analysis, % Found	Analysis, % Calcd.	Infrared spectrum: ν of group (KBr, cm^{-1})		
IVa	185—6	B 68	$C_{16}H_{16}O_6$ (304)	C, H,	— 63.4 5.2	63.1 5.2	OH (acid) 3460 CO (acid) 1720	$-CH_2$ 2940 CO (aroyl) 1670	CO (ester) 1740 C = C 1610
IVb	165	P 72	$C_{16}H_{16}O_6$ (304)	C, H,	62.9 5.1	63.1 5.2	OH (acid) 3510 CO (acid) 1720	$-CH_2$ (acid) 2920 CO (aroyl) 1680	CO (ester) 1760 C = C 1610

B = benzene, P = light petrol

Table IV

The butene derivatives **Va** *and* **b**

Compd.	M.p., °C	Yield, %	Formula (Mol. wt.)		Analysis, % Found	Analysis, % Calcd.	Infrared spectrum ν of group (KBr, cm^{-1})		
Va	150—1	80	$C_{25}H_{26}O_7$ (438)	C,	68.1	68.4	OH (acid) 3940	$-CH_2$ 2960	CO (ester) 1740
				H,	5.7	5.9	CO (acid) 1720	CO (aroyl) 1680	C = C 1600
Vb	146—7	81	$C_{25}H_{25}ClO_8$ (488.5)	C,	60.9	61.4			
				H,	5.1	5.1			

Mixed melting point of **Va** with **Vb** was 125°C

Table V

The hydrazone derivatives **XIIIa—h, XIV** *and* **XV**

Compd.	M.p., °C	Solvent; Yield, %	Formula (Mol. wt.)		Analysis, % Found	Analysis, % Calcd.	Infrared spectra: ν of group (KBr, cm^{-1})		
XIIIa	136—7	T 75	$C_{17}H_{20}N_2O_4$ (316)	C, H, N,	64.5 6.4 8.9	64.0 6.2 8.5	OH or NH 3340 C=C 1600	$-CH_2$ 2920	CO or CN 1730
XIIIb	219—220	E 72	$C_{16}H_{17}ClN_2O_4$ (336.5)	C, H,	57.6 5.3	57.5 5.0			
XIIIc	>250	A 68	$C_{20}H_{20}N_2O_2$ (320)	C, H,	75.5 6.0	75.0 6.2			
XIIId	122—3	E 66	$C_{15}H_{18}N_2O_2$ (258)	C, H, N,	69.2 7.0 11.0	69.7 6.9 10.8			
XIIIe	128—9	B 72	$C_{14}H_{15}ClN_2O_2$ (278.5)	C, H,	59.9 5.2	60.3 5.4	OH or NH 3430 C = C 1600	$-CH_2$ 2950	CO or CN 1720
XIIIf	>250	B/E 72	$C_{16}H_{20}N_2O_2$ (272)	C, H,	70.2 7.1	70.5 7.3			
XIIIg	185	B 74	$C_{21}H_{22}N_2O_2$ (334)	C, H, N,	75.3 6.3 8.2	75.4 6.5 8.3			
XIIIh	190	B 66	$C_{22}H_{24}N_2O_2$ (348)	C, H,	75.5 6.6	75.8 6.8			
XIVa	187—8	E 62	$C_{20}H_{20}N_2O_2$ (320)	C, H, N,	74.5 6.3 8.7	75.0 6.2 8.9	OH or NH 3290 C=C 1600	$-CH_2$ 2910, 2860	CO or CN 1710, 1660
XIVb	218—9	T 78	$C_{19}H_{17}ClN_2O_2$ (340.5)	C, H, N,	67.0 4.8 8.2	66.9 4.9 8.2			
XV	>270	A 75	$C_{21}H_{18}N_2O_3$ (346)	C, H, N,	73.0 5.3 7.8	72.8 5.2 8.0	OH (acid) 3450 CN (indazole) 1725	CH_2 3000, 2980 C=C 1610	CO (acid) 1720

A = acetic acid, B = benzene, Bu = butanol, E = ethanol, T = toluene

Table VI

The oxime derivatives **XVIa** *and* **b**

Compd.	M.p., °C	Solvent; Yield, %	Formula (Mol. wt.)		Analysis, % Found	Analysis, % Calcd.	Infrared spectra ν of group (KBr, cm^{-1})		
XVIa	214—5	B 50	$C_{14}H_{15}NO_3$ (245)	C, H, N,	68.5 6.2 5.8	68.5 6.1 5.7	OH (acid) 3460 C = C 1600	CH_2 2920	CN (oxime) 1680
XVIb	200—1	T 50	$C_{13}H_{12}ClNO_3$ (265.5)	C, H,	58.5 4.7	58.7 4.5			

Table VII

The amine derivatives **XVIIa** *and* **XVIIIa** *and* **b** *and* **XIXa—d**

Compd.	M.p., °C	Solvent; Yield, %	Formula (Mol. wt.)		Analysis, % Found	Analysis, % Calcd.	Infrared spectra ν of group (KBr, cm^{-1})		
XVIIa	182—3	E 65	$C_{24}H_{34}N_2O_5$ (430)	C, H, N,	67.5 7.3 6.4	66.9 7.9 6.5			
XVIIb	203	B 68	$C_{28}H_{28}N_2O_5$ (472)	C, H, N,	71.5 5.8 5.7	71.1 5.9 5.9	OH or NH 3300 C=C 1610	$-CH_2$ 2930	CO 1680, 1660
XVIIIa	178—9	E 78	$C_{23}H_{23}NO_5$ (393)	C, H,	70.5 5.6	70.2 5.8	OH (acid) 3480 C = C 1610	$-CH_2$ 2920	CO 1720, 1680
XVIIIb	170—1	Bu 72	$C_{22}H_{20}ClNO_5$ (413.5)	C, H,	63.3 5.3	63.8 4.8			
XIXa	174—5	B 65	$C_{19}H_{23}NO_3$ (313)	C, H, N,	72.5 7.1 4.3	72.8 7.3 4.4			
XIXb	192—3	E 64	$C_{20}H_{25}NO_2$ (311)	C, H,	77.2 7.8	77.1 8.0			
XIXc	202—3	E 78	$C_{18}H_{20}ClNO_3$ (333.5)	C, H,	64.5 5.7	64.7 5.9	OH (acid) 3400 C=C 1600	$-CH_2$ 2980	CO 1700
XIXd	177—8	B 76	$C_{19}H_{22}ClNO_2$ (331.5)	C, H, N,	68.5 6.5 4.2	68.7 6.6 4.2			

Condensation with hydroxylamine hydrochloride

A mixture of **VIIa** and **b** (0.01 mole), hydroxylamine hydrochloride (0.01 mole), sodium acetate (2 g), ethanol (20 ml) and a few drops of water was refluxed for 8 hrs. The solid product formed after concentration and cooling was crystallized from a suitable solvent to give yellow crystals of **XVIa** and **b** (*cf.* Table VI).

Reaction of IIa, IIc, IId, VIIe and VIIf with amines. Formation of XVIIa and b, XVIIIa and b and XIXa—d, respectively

A mixture of **IIa**, **IIc**, **IId**, **VIIe** or **VIIf** (0.01 mole), piperidine, benzylamine and/or morpholine (0.01 mole) and benzene (20 ml) was refluxed for 6 hrs. The solid product obtained after concentration and cooling was crystallized from a proper solvent to give colourless crystals of **XVIIa** and **b**, **XVIIIa** and **b**, and **XIXa—d**, respectively (*cf.* Table VII).

REFERENCES

[1] Sammour, A., Selim, M. I. B., Soliman, E. A.: U. A. R. J. Chem. **16,** 312 (1972)
[2] Sammour, A., El Hashash, M. A.: J. Pract. Chem. **314,** 906 (1972)
[3] Harnik, M.: Israel J. Chem. **3,** 1 (1965); C. A. **63,** 1748d (1965)
[4] Sammour, A., Raouf, A., Elkassaby, M., Ibrahim, M. A.: Acta Chim. (Budapest) **78,** 399 (1973)
[5] Schwarz, J. C. P.: "Physical Methods in Organic Chemistry", pp. 173, 174. Oliver and Boyd, Edinburgh, 1964

A Sammour
A. A. Afify
M. M. Abd-Allah
E. A. Soliman

Ain Shams University Abbassia, Cairo, Egypt.

INDEX

PHYSICAL AND INORGANIC CHEMISTRY – PHYSIKALISCHE UND ANORGANISCHE CHEMIE – ФИЗИЧЕСКАЯ и НЕОРГАНИЧЕСКАЯ ХИМИЯ

RÜGER, C., SCHWETLICK, K. und KAMMER, H.: Thermodynamische Berechnung von Reaktionsgleichgewichten aliphatischer Stickstoffverbindungen (Thermodynamic Computation of Reaction Equilibria of Aliphatic Nitrogen Compounds) 347

KAPOSI, O., RIEDEL, M., ROBERTO SÁNCHEZ, G.: Mass-spectrometric Study of Electron-impact and Heterogeneous Pyrolytic Decomposition of Methyl Bromide 361

FARAH, M. Y. and EL-FEKEY, S. A.: Studies on the Calcination of Ammonium Uranate with Special Reference to Surface Area 383

FAROOQ, O. and MALIK, A.: Interaction of Transition Metals with Some Alkaloids, Metal Complexes of Quinaldine, Quinine, Brucine and Codeine 389

FAROOQ, O. and AHMAD, N.: Metal–Amino Acid Interaction, II. A Study of the Complex Compounds of Trivalent Rare Earths with Glutamic Acid 395

KISS, L. and VARSÁNYI, M. L.: Investigation of Anodic Dissolution of Copper in Anhydrous Acetic Acid Solutions, III. The Combined Effect of Chloride and Perchlorate 399

SWAMI, M. P., JAIN, P. C., RANA, V. B., SAHNI, S. K. and SRIVASTAVA, A. K.: *o*-Hydroxy-4-benzamidothiosemicarbazide as a Chelating Reagent, IV. Magnetospectral Studies on its Ti(III), V(IV), Fe(II), Pd(II), Ce(III) and U(VI) Complexes 409

HORVÁTH, Zs. and FÖLDIÁK, G.: Influence of Cyclic Structure on the Radiolysis of Hydrocarbons, III. Radiolysis of Cyclopropane, Cyclobutane and Cyclobutene 417

З. Бокшаи, Г. Букз и И. М. Бушуева: Изменение состава твердых стекол под влиянием солевых расплавов. (BOKSAY, Z., BOUKQUET, G. and BUSHUEVA, I. M.: Variation of the Composition of Glasses Under the Effect of Molten Salts) 437

ISSA, I. M., GHANDOUR, M. A., HASSAN, M. K. and HAMMAN, A. M.: Polarographic Behaviour of Uranyl Ion in Citrate Solutions 445

ORGANIC CHEMISTRY – ORGANISCHE CHEMIE – ОРГАНИЧЕСКАЯ ХИМИЯ

SAMMOUR, A., AFIFY, A. A., ABD-ALLAH, M. M. and SOLIMAN, E. A.: Michael Reaction with *β*-*p*-Toluoyl- and *p*-Chlorobenzoyl-acrylic Acids and their Amides 455

Printed in Hungary

A kiadásért felel az Akadémiai Kiadó igazgatója. Műszaki szerkesztő: Zacsik Annamária

A kézirat nyomdába érkezett: 1973. III. 7. — Terjedelem: 11,2 (A/5) ív

75.1619 Akadémiai Nyomda, Budapest — Felelős vezető: Bernát György

ACTA CHIMICA

ТОМ 85—ВЫП. 4

РЕЗЮМЕ

Термодинамический расчет равновесий алифатических соединений азота

Ц. РЮГЕР, К. ШВЕТЛИК и Х. КАММЕР

С помощью статистической термодинамики были вычислены или определены из инкрементов термодинамические параметры для метил- и этилизоцианатов, N-метилформамида, ацетамида и N,N'-диметилмочевины в идеальном газовом состоянии.

Были исследованы термодинамические равновесия и их зависимость от температуры для девяти превращений алифатических соединений азота в изоцианаты, в интервале температур 298 ÷ 1000°К. Расчеты показывают, что термодинамически благоприятным бесфосгенным птуем получения изоцианатов являются

а) карбонилирование нитросоединений,

б) пиролиз мочевин выше 900°К и

в) дегидрирование формамидов выше 800°К.

Для характеристики хода протекания реакции были исследованы термодинамические равновесия для 10 возможных параллельных и последовательных процессов.

Исследование разложения метилбромида в следствии электронных столкновений и гетерогенного пиролиза с помощью масс-спектрометра

О. КАПОШИ, М. РИДЕЛЬ и Р. Г. САНЧЕЗ

С помощью масс-спектрометра MI 13—11 было исследовано разложение CH_3Br под влиянием электронных столкновений, а также на поверхности вольфрамовой спирали в зависимости от температуры спирали.

Исходя из масс-спектра CH_3Br низкого разрешения и определенных потенциалов ионизации и появления, были сделаны заключения относительно наиболее вероятных путей разложения, а также была рассчитана энергия активации разложения молекулярного иона.

Было показано, что гетерогенный пиролиз CH_3Br протекает согласно радикальному механизму и, что применяемые реакторы с низкой постоянной времени были пригодны для обнаружения радикалов, образующихся в небольших количествах. Пиролитическое разложение CH_3Br начинается приблизительно при 700°К и наиболее важными продуктами разложения являются HBr, Br и CH_2-радикалы. На основе определенных ионизационных потенциалов радикалов, образующихся при пиролизе, и зная потенциалы появления, были определены энергии диссоциации связей наиболее важных с точки зрения пиролиза. Величина энергии активации гетерогенного разложения указывает на то, что на карбонизированной W спирали CH_3Br разлагается по каталитическому механизму.

Исследование обжига ураната аммония до три- и сесквиоксида и влияние поверхности

М. Й. ФАРАХ и С. А. ЭЛЬ-ФЕКЕИ

Термическое разложение тонкого слоя ураната аммония толщиной 0,3 см вплоть до 350°С приводит к быстрому увеличению поверхности порошка VO_3; в толстом слое помимо этого наблюдается самовосстановление, что приводит к пониженному увеличению поверхности. Выше этой температуры окаливание в обоих случаях приводит к восста-

новлению в поверхностном слое. Было найдено, что значительный эффект на величину поверхности образующихся порошков оказывает также предварительная промывка уранатов этанолом или ацетоном и дегазирование их, а также режим обжига и толщина слоя на корытах.

Взаимодействие переходных металлов с алкалоидами. Комплексы хинальдина, хинина, бурцина и кодеина

О. ФАРУҚ и А. МАЛИҚ

Описываются комплексы алкалоидов таких, как хинальдин, хинин, бурцин и кодеин, с некоторыми переходными металлами. В частности, комплексы кодеина были синтезированы с большим числом ионов металлов такими, как Cu^{+2}, Ni^{+2}, Co^{+2}, Mn^{+2}, Ti^{+3}, Cr^{+3} и VO^{+2} (диоксованадий/IV/). В отличие от алкалоидов, их комплексы обычно хорошо растворимы в воде, но почти нерастворимы в органических растворителях. Результаты химического анализа указывают на то, что комплексы хинальдина и кодеина обладают составом 1 : 2 (металл : лигадн), а комплексы бруцина и хинина — составом 1 : 1. ИҚ спектры этих соединений были сняты в таблетках KBr в области 2,5—16 μ, а далекие ИҚ спектры были сняты с CSI, используя нуёл с целью локализации мест координации. Термогравиметрические исследования в области 25—800°C, проводимые со скоростью 6°/мин, указывают на то, что две молекулы воды координированы с металлом. Молярная электропроводность 1%-ого водного раствора является порядка 6,66. 10^{-5} $ом^{-1}см^2моль^{-1}$, что указывает на неэлектролитную природу этих комплексов в фазе растворов, вероятно, вследствие образования мостиков. Магнитные измерения, после применения поправки Паскаля при 25°C, основанные на методе Гуя, указывают на парамагнетизм вследствие тетраэдрической ориентации в комплексах никеля(II) и кобальта(II) с кодеином. Это окрашенные вещества с высокой температурой плавления.

Взаимодействия между металлами и аминокислотами, II

Исследование комплексов между трехвалентными редкоземельными металлами и глутаминовой кислотэй

О. ФАРУҚ и Н. АХМАД

Описываются комплексы трехвалентных редкоземельных металлов с глутаминовой кислотой. Элементарный анализ подтверждает формулу (Глут-H)$_3$. РМ. $3H_2O$ (где Глут — глутаминовая кислота и РМ — редкоземельный металл). На основе термогравиметрических исследований было обнаружено присутствие трех координированных молекул воды. Магнитные моменты в В. М. дают характерную неравную кривую с двойным горбом, а ИҚ исследования в таблетках KBr, в области 2,5—16 μ указывают на координацию ионов редкоземельных металлов через ионизированную карбоксильную группу, соседнюю с аминогруппой. Сравнение молярной проводимости солей редкоземельных металлов и их комплексов в водных растворах демонстрирует более сильную ионную связь между редкоземельными металлами и аминокислотами.

Изучение анодного растворения меди в уксуснокислых растворах, III

Взаимное влияние ионов хлорида и перхлората

Л. КИШ и Л. М. ВАРШАНИ

Изучалось анодное растворение меди в безводных уксуснокислых растворах, содержащих ионы хлорида и перхлората, с помощью вращающегося дискового электрода. Экспериментальные результаты указывают на то, что в применяемых условиях анодное растворение меди происходит согласно следующему механизму:

1. $Cu + Cl^- \rightleftharpoons CuCl_{адс} + e$
2. $CuCl_{адс} + Cl^- \rightleftharpoons CuCl^-_{2(0)}$
3. $CuCl^-_{2(0)} \rightleftharpoons CuCl^-_{2(\infty)}$

(Индексы (o) и (∞) относятся к веществу, находящемуся на поверхности электрода и в растворе, соответственно.) Если раствор содержит только хлорид, то реакция 2. не влияет на кинетику суммарного процесса, а в случае раствора, содержащего помимо хлорида также и перхлорат, реакция 1. оказывается той, которая не влияет на кинетику суммарного процесса.

О-Гидрокси-4-бензамидотиосемикарбазид как хелатный реагент, IV

Магнетоспектральное исследование его комплексов с Ti(III), V(IV), Fe(II), Pd(II), Ce(III) и U(VI)

М. П. СВАМИ, П. С. ДЖЕЙН, В. Б. РАНА, С. К. САХНИ и А. К. СРИВАСТАВА

Комплексы О-гидрокси-4-бензамидотиосемикарбазида с титаном(III), оксованадием(IV), железом(II), палладием(II), церием(III) и ураном(VI) были изолированы и охарактеризованы на основе их анализа, кондуктометрических измерений и измерений магнитной воспримчивости, а также на основе исследований их электронных и ИК сьектров. Комплексы урана(VI) обладают парамагнетизмом, не зависящим от температуры. Более низкую величину магнитного момента комплекса ванадия(IV) пытались объяснить возможным присутствием связи металл-металл в данном комплексе. ИК исследования указывают на трехфункциональную природу лиганда, где связывание происходит через фенольный кислород, тиокетоновую серу и амидный азот. Комплекс палладия(II) является квадратно-планарным, в то время как все другие комплексы обладают октаэдрической конфигурацией.

Влияние циклической структуры на радиолиз углеводородов, III

Радиолиз циклопропана, циклобутана и циклобутена

ЖУЖАННА ХОРВАТ и Г. ФЕЛЬДИАК

Несмотря на несколько новых статей, радиационная химия циклопропана, циклобутана и циклобутена еще не исследовалась.

Авторы установили, что значения $G(H_2)$ циклобутана и циклобутена являются чрезвычайно низкими по сравнению с значениями соответствующих алифатических алканов и высших циклоалканов; они находятся вблизи к значениям $G(H_2)$ пропана и бутена, а также высших циклоалкенов.

Значения G(осколков циклических C_3 и C_4 углеводородов значительно превышают значения $G(H_2)$. Обнаруживается повышенное открытие кольца 3- и 4-членных циклов в сравнении с высшими циклоалканами и циклоалкенами. Таким образом, в следствии высокой энергии натяжения, большая доля энергии излучения превращается в размыкание кольца чем в отцепление водорода. Результаты показывают на то, что структуа молекулы играет решающую, но комплексную роль в радиационно-химической реактивности; например циклобутан оказывается более реактивным циклобутену и циклопропану, хотя последние соединения имеют более высокие энергии натяжения.

Полярографическое поведение уранильного иона в цитратных растворах

И. М. ИССА, М. А. ГАНДУР, М. К. ХАССАН и А. М. ХАММАМ

Было исследовано полярографическое поведение цитратных растворов U(VI). Наблюдаются две полосы: лимитирующий ток и потенциалы полуволны которых зависят от pH. При $pH < 3$ первая полоса соответствует восстановлению уранил-цитратного комплекса до смеси цитратных комплексов U(IV) и U(V). Вторая полоса, которая очень мала при более высоких концентрациях цитрата (< 0,1 М), соответствует восстановлению свободного U(V). При $pH = 3 \div 6$ две полосы, образующиеся за счет расщепления основной полосы (1-ая полоса), приписываются присутствию двух видов уранилцитратных частиц,

оба из которых восстанавливаются до U(V) с последующим превращением U(V) в U(IV) и U(VI). Две волны объединяются в одну волну при более высоких концентрацияс U(VI). Процессы электродного восстановления протекают обратимо и в основном контролируются диффузией с частичным кинетическим компонентом.

Реакция Михаэля с β-п-толуоил и п-хлорбензоилакриловыми кислотами и их амидами

А. САММУР, А. А. АФИФИ, М. М. АБД-АЛЛАХ и Е. А. СОЛИМАН

β-п-Толуоил и п-хлорбензоилакриловые кислоты реагируют в усовиях реакции Михаэля с диэтилмалонатом, диметилсукцинатом, диизобутилкетоном, этилфенилацетатом, диметилсукцинатом, диизобутилкетоном, этилфенилацетатом, этилацетатом, бензилметилкетоном, этилметилкетоном, метилизопропилкетоном и ацетонилацетоном, давая циклические или нормальные продукты присоединения Михаэля, зависящие от природы активного метиленового соединения.

The Acta Chimica publish papers on chemistry, in English, German, French and Russian.

The Acta Chimica appear in volumes consisting of four parts of varying size, 4 volumes being published a year.

Manuscripts should be addressed to

Acta Chimica
Budapest 112/91 Műegyetem

Correspondence with the editors should be sent to the same address.

The rate of subscription in $ 32.00 a volume.

Orders may be placed with "*Kultúra*" Foreign Trade Company for Books and Newspapers (1389 Budapest 62, P. O. B. 149. Account No. 218 10990) or with representatives abroad.

Les Acta Chimica paraissent en français, allemand, anglais et russe et publient des mémoires du domaine des sciences chimiques.

Les Acta Chimica sont publiés sous forme de fascicules. Quatre fascicules seront réunis en un volume (4 volumes par an).

On est prié d'envoyer les manuscrits destinés à la rédaction à l'adresse suivante:

Acta Chimica
Budapest 112/91 Műegyetem

Toute correspondance doit être envoyée à cette même adresse.

Le prix de l'abonnement est de $ 32,00 par volume.

On peut s'abonner à l'Entreprise pour le Commerce Extérieur de Livres et Journaux «*Kultúra*» (1389 Budapest 62, P. O. B. 149 Compte-courant No. 218 10990) ou à l'étranger chez tous les représentants ou dépositaires.

«*Acta Chimica*» издают трактаты из области химической науки на русском, французском, английском и немецком языках.

«*Acta Chimica*» выходят отдельными выпусками разного объема. 4 выпуска составляют один том. 4 тома публикуются в год.

Предназначенные для публикации рукописи следует направлять по адресу:

Acta Chimica
Budapest 112/91 Műegyetem

По этому же адресу направлять всякую корреспонденцию для редакции.

Подписная цена — $ 32,00 за том.

Заказы принимает предприятие по внешней торговле книг и газет «*Kultúra*» (1389 Budapest 62, P. O. B. 149. Текущий счет № 218 10990) или его заграничные представительства и уполномоченные.

Reviews of the Hungarian Academy of Sciences are obtainable at the following addresses:

AUSTRALIA

C. B. D. Library and Subscription Service
Box 4886, G. P. O.
Sydney N. S. W. 2001

Cosmos Bookshop
145 Acland St.
St. Kilda 3182

AUSTRIA

Globus
Höchstädtplatz 3
A—1200 Wien XX

BELGIUM

Office International de Librairie
30 Avenue Marnix
1050—Bruxelles

Du Monde Entier
162 Rue du Midi
1000—Bruxelles

BULGARIA

Hemus
Bulvar Ruszki 6
Sofia

CANADA

Pannonia Books
P. O. Box 1017
Postal Station "B"
Toronto, Ont. M5T 2T8

CHINA

C N P I C O R
Periodical Department
P. O. Box 50
Peking

CZECHOSLOVAKIA

Mad'arská Kultura
Národní třida 22
115 66 Praha

PNS Dovoz tisku
Vinohradská 46
Praha 2

PNS Dovoz tlače
Bratislava 2

DENMARK

Ejnar Munksgaard
Nörregade 6
DK—1165 Copenhagen K

FINLAND

Akateeminen Kirjakauppa
P. O. Box 128
SF-00101 Helsinki 10

FRANCE

Office International de Documentation et Librairie
48, Rue Gay-Lussac
Paris 5

Librairie Lavoisier
11 Rue Lavoisier
Paris 8

Européridiques S. A.
31 Avenue de Versailles
78170 La Celle St. Cloud

GERMAN DEMOCRATIC REPUBLIC

Haus der Ungarischen Kultur
Karl-Liebknecht-Strasse 9
DDR—102 Berlin

Deutsche Post
Zeitungsvertriebsamt
Strasse der Pariser Kommüne 3—4
DDR-104 Berlin

GERMAN FEDERAL REPUBLIC

Kunst und Wissen
Erich Bieber
Postfach 46
7 Stuttgart S

GREAT BRITAIN

Blackwell's Periodicals
P. O. Box 40
Hythe Bridge Street
Oxford OX1 2EU

Collet's Holdings Ltd.
Denington Estate
London Road
Wellingborough Northants NN8 2QT

Bumpus Haldane and Maxwell Ltd.
5 Fitzroy Square
London W1P 5AH

Dawson and Sons Ltd.
Cannon House
Park Farm Road
Folkestone, Kent

HOLLAND

Swets and Zeitlinger
Heereweg 347b
Lisse

Martinus Nijhoff
Lange Voorhout 9
The Hague

INDIA

Hind Book House
66 Babar Road
New Delhi 1

India Book House
Subscription Agency
249 Dr. D. N. Road
Bombay 1

ITALY

Santo Vanasia
Via M. Macchi 71
20124 Milano

Libreria Commissionaria Sansoni
Via Lamarmora 45
50121 Firenze

JAPAN

Kinokuniya Book-Store Co. Ltd.
826 Tsunohazu 1-chome
Shinjuku-ku
Tokyo 160—91

Maruzen and Co. Ltd.
P. O. Box 5050
Tokyo International 100—31

Nauka Ltd.—Export Department
2—2 Kanda
Jinbocho
Chiyoda-ku
Tokyo 101

KOREA

Chulpanmul
Phenjan

NORWAY

Tanum-Cammermeyer
Karl Johansgatan 41—43
Oslo 1

POLAND

Węgierski Instytut Kultury
Marszalkowska 80
Warszawa

BKWZ Ruch
ul. Wronia 23
00—840 Warszawa

ROUMANIA

D. E. P.
Bucureşti

Romlibri
Str. Biserica Amzei 7
Bucureşti

SOVIET UNION

Sojuzpechatj — Import
Moscow
and the post offices in each town

Mezhdunarodnaya Kniga
Moscow G—200

SWEDEN

Almqvist and Wiksell
Gamla Brogatan 26
S—101 20 Stockholm

A. B. Nordiska Bokhandeln
Kunstgatan 4
101 10 Stockholm 1 Fack

SWITZERLAND

Karger Libri AG.
Arnold-Böcklin-Str. 25
4000 Basel 11

USA

F. W. Faxon Co. Inc.
15 Southwest Park
Westwood, Mass. 02090

Stechert-Hafner Inc.
Serials Fulfillment
P. O. Box 900
Riverside N. J. 08075

Fam Book Service
69 Fifth Avenue
New York N. Y. 10003

Maxwell Scientific International Inc.
Fairview Park
Elmsford N. Y. 10523

Read More Publications Inc.
40 Cedar Street
New York N. Y. 1000

VIETNAM

Xunhasaba
32, Hai Ba Trung
Hanoi

YUGOSLAVIA

Jugoslovenska Knjiga
Terazije 27
Beograd

Forum
Vojvode Mišića 1
21000 Novi Sad

The Acta Chimica publish papers on chemistry, in English, German, French and Russian.

The Acta Chimica appear in volumes consisting of four parts of varying size, 4 volumes being published a year.

Manuscripts should be addressed to

Acta Chimica
Budapest 112/91 Műegyetem

Correspondence with the editors should be sent to the same address.

The rate of subscription in $ 32.00 a volume.

Orders may be placed with "*Kultúra*" Foreign Trade Company for Books and Newspapers (1389 Budapest 62, P. O. B. 149. Account No. 218 10990) or with representatives abroad.

Les Acta Chimica paraissent en français, allemand, anglais et russe et publient des mémoires du domaine des sciences chimiques.

Les Acta Chimica sont publiés sous forme de fascicules. Quatre fascicules seront réunis en un volume (4 volumes par an).

On est prié d'envoyer les manuscrits destinés à la rédaction à l'adresse suivante:

Acta Chimica
Budapest 112/91 Műegyetem

Toute correspondance doit être envoyée à cette même adresse.

Le prix de l'abonnement est de $ 32,00 par volume.

On peut s'abonner à l'Entreprise pour le Commerce Extérieur de Livres et Journaux «*Kultúra*» (1389 Budapest 62, P. O. B. 149 Compte-courant No. 218 10990) ou à l'étranger chez tous les représentants ou dépositaires.

«*Acta Chimica*» издают трактаты из области химической науки на русском, французском, английском и немецком языках.

«*Acta Chimica*» выходят отдельными выпусками разного объема. 4 выпуска составляют один том. 4 тома публикуются в год.

Предназначенные для публикации рукописи следует направлять по адресу:

Acta Chimica
Budapest 112/91 Műegyetem

По этому же адресу направлять всякую корреспонденцию для редакции.

Подписная цена — $ 32,00 за том.

Заказы принимает предприятие по внешней торговле книг и газет «*Kultúra*» (1389 Budapest 62, P. O. B. 149. Текущий счет № 218 10990) или его заграничные представительства и уполномоченные.

Reviews of the Hungarian Academy of Sciences are obtainable at the following addresses:

AUSTRALIA

C. B. D. Library and Subscription Service
Box 4886, G. P. O.
Sydney N. S. W. 2001

Cosmos Bookshop
145 Acland St.
St. Kilda 3182

AUSTRIA

Globus
Höchstädtplatz 3
A—1200 Wien XX

BELGIUM

Office International de Librairie
30 Avenue Marnix
1050—Bruxelles

Du Monde Entier
162 Rue du Midi
1000—Bruxelles

BULGARIA

Hemus
Bulvar Ruszki 6
Sofia

CANADA

Pannonia Books
P. O. Box 1017
Postal Station "B"
Toronto, Ont. M5T 2T8

CHINA

C N P I C O R
Periodical Department
P. O. Box 50
Peking

CZECHOSLOVAKIA

Mad'arská Kultura
Národní třida 22
115 66 Praha

PNS Dovoz tisku
Vinohradská 46
Praha 2

PNS Dovoz tlače
Bratislava 2

DENMARK

Ejnar Munksgaard
Nörregade 6
DK—1165 Copenhagen K

FINLAND

Akateeminen Kirjakauppa
P. O. Box 128
SF-00101 Helsinki 10

FRANCE

Office International de Documentation et Librairie
48, Rue Gay-Lussac
Paris 5

Librairie Lavoisier
11 Rue Lavoisier
Paris 8

Europériodiques S. A.
31 Avenue de Versailles
78170 La Celle St. Cloud

GERMAN DEMOCRATIC REPUBLIC

Haus der Ungarischen Kultur
Karl-Liebknecht-Strasse 9
DDR—102 Berlin

Deutsche Post
Zeitungsvertriebsamt
Strasse der Pariser Kommüne 3—4
DDR-104 Berlin

GERMAN FEDERAL REPUBLIC

Kunst und Wissen
Erich Bieber
Postfach 46
7 Stuttgart S

GREAT BRITAIN

Blackwell's Periodicals
P. O. Box 40
Hythe Bridge Street
Oxford OX1 2EU

Collet's Holdings Ltd.
Denington Estate
London Road
Wellingborough Northants NN8 2QT

Bumpus Haldane and Maxwell Ltd.
5 Fitzroy Square
London W1P 5AH

Dawson and Sons Ltd.
Cannon House
Park Farm Road
Folkestone, Kent

HOLLAND

Swets and Zeitlinger
Heereweg 347b
Lisse

Martinus Nijhoff
Lange Voorhout 9
The Hague

INDIA

Hind Book House
66 Babar Road
New Delhi 1

India Book House
Subscription Agency
249 Dr. D. N. Road
Bombay 1

ITALY

Santo Vanasia
Via M. Macchi 71
20124 Milano

Libreria Commissionaria Sansoni
Via Lamarmora 45
50121 Firenze

JAPAN

Kinokuniya Book-Store Co. Ltd.
826 Tsunohazu 1-chome
Shinjuku-ku
Tokyo 160—91

Maruzen and Co. Ltd.
P. O. Box 5050
Tokyo International 100—31

Nauka Ltd.—Export Department
2—2 Kanda
Jinbocho
Chiyoda-ku
Tokyo 101

KOREA

Chulpanmul
Phenjan

NORWAY

Tanum-Cammermeyer
Karl Johansgatan 41—43
Oslo 1

POLAND

Węgierski Instytut Kultury
Marszalkowska 80
Warszawa

BKWZ Ruch
ul. Wronia 23
00—840 Warszawa

ROUMANIA

D. E. P.
București

Romlibri
Str. Biserica Amzei 7
București

SOVIET UNION

Sojuzpechatj — Import
Moscow
and the post offices in each town

Mezhdunarodnaya Kniga
Moscow G—200

SWEDEN

Almqvist and Wiksell
Gamla Brogatan 26
S—101 20 Stockholm

A. B. Nordiska Bokhandeln
Kunstgatan 4
101 10 Stockholm 1 Fack

SWITZERLAND

Karger Libri AG.
Arnold-Böcklin-Str. 25
4000 Basel 11

USA

F. W. Faxon Co. Inc.
15 Southwest Park
Westwood, Mass. 02090

Stechert-Hafner Inc.
Serials Fulfillment
P. O. Box 900
Riverside N. J. 08075

Fam Book Service
69 Fifth Avenue
New York N. Y. 10003

Maxwell Scientific International Inc.
Fairview Park
Elmsford N. Y. 10523

Read More Publications Inc.
40 Cedar Street
New York N. Y. 1000

VIETNAM

Xunhasaba
32, Hai Ba Trung
Hanoi

YUGOSLAVIA

Jugoslovenska Knjiga
Terazije 27
Beograd

Forum
Vojvode Mišića 1
21000 Novi Sad

1. IX. 1975

Index: 26.007